REPORT NO.
UCB/EERC-89/04
JULY 1989

EARTHQUAKE ENGINEERING RESEARCH CENTER

EARTHQUAKE ANALYSIS AND RESPONSE OF INTAKE-OUTLET TOWERS

by

ALOK GOYAL

ANIL K. CHOPRA

A Report on Research conducted under
Grants CEE-8401439 and CES-8719296
from the National Science Foundation

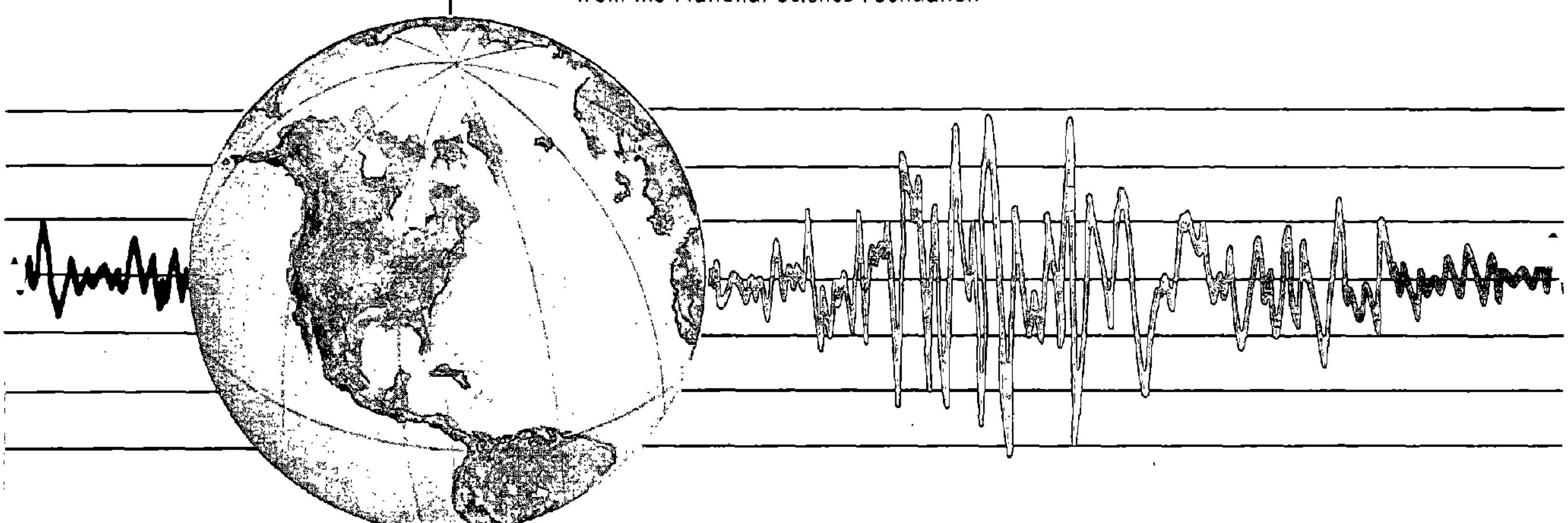

COLLEGE OF ENGINEERING

UNIVERSITY OF CALIFORNIA AT BERKELEY

i.b

For sale by the National Technical Information Service, U.S. Department of Commerce, Springfield, Virginia 22161

See back of report for up to date listing of EERC reports.

50272-101

REPORT DOCUMENTATION PAGE	1. REPORT NO. NSF/ENG-89023	2.	PB91-229286
4. Title and Subtitle Earthquake Analysis and Response of Intake-Outlet Towers			5. Report Date July 1989
			6.
7. Author(s) A. Goyal and A.K. Chopra			8. Performing Organization Rept. No. UCB/EERC-89/04
9. Performing Organization Name and Address Earthquake Engineering Research Center University of California, Berkeley 1301 S 46th St. Richmond, CA 94804			10. Project/Task/Work Unit No.
			11. Contract(C) or Grant(G) No. (C) (G) CEE 8401439 CES 8719296
12. Sponsoring Organization Name and Address National Science Foundation 1800 G. St. NW Washington, DC 20550			13. Type of Report & Period Covered
			14.

15. Supplementary Notes

16. Abstract (Limit: 200 words)

The available procedure for earthquake analysis of axisymmetric intake-outlet towers is extended to towers of arbitrary geometry, but with two axes of plan symmetry, and to include the effects of tower-foundation-soil interaction. For the time being, rigorous treatment of tower-foundation-soil interaction effects has been restricted to towers with a circular foundation supported near the surface of a viscoelastic halfspace. However, an approximate treatment of non-circular foundations is also included.

Using the analytical procedure the responses of idealized intake-outlet towers to harmonic ground motion are presented for a range of parameters characterizing the tower geometry, surrounding and inside water, and foundation-soil system. On the basis of these response functions, the effects of tower-water interaction and tower-foundation-soil interaction on the response of towers are identified and shown to be significant in many cases.

A simplified procedure is developed to determine the maximum earthquake forces in intake-outlet towers directly from the design earthquake spectrum without the need for a response history analysis. All the significant effects of tower-water interaction and tower-foundation-soil interaction are included in the analysis. An equivalent single-degree-of-freedom system is developed to consider approximately the effects of tower-foundation-soil interaction in the fundamental mode response of towers, and standard data are presented to conveniently determine the effective natural period and damping of the interacting system.

17. Document Analysis a. Descriptors

b. Identifiers/Open-Ended Terms

c. COSATI Field/Group

18. Availability Statement:	19. Security Class (This Report)	21. No. of Pages
Release Unlimited	unclassified	449
	20. Security Class (This Page) unclassified	22. Price

(See ANSI-Z39.18) See Instructions on Reverse

OPTIONAL FORM 272 (4-77)
(Formerly NTIS-35)
Department of Commerce

EARTHQUAKE ANALYSIS AND RESPONSE

OF INTAKE-OUTLET TOWERS

by

Alok Goyal

Anil K. Chopra

A Report on Research Conducted Under
Grants CEE-8401439 and CES-8719296
from the National Science Foundation

Report No. UCB/EERC-89/04
Earthquake Engineering Research Center
University of California
Berkeley, California

July 1989

i.a

ABSTRACT

Reliable analytical procedures to predict the earthquake response of intake-outlet towers are necessary in order to design earthquake resistant towers and to evaluate the seismic safety of existing towers. The objectives of this investigation are : (1) to develop reliable and efficient techniques for analyzing the earthquake response of intake-outlet towers of arbitrary geometry but with two axes of plan symmetry, including tower-water interaction and tower-foundation-soil interaction; (2) to investigate the significance of these interaction effects on the earthquake response of towers; (3) to develop a simplified analysis procedure for the preliminary phase of design and safety evaluation of towers that provides sufficiently accurate estimates of the design forces directly from the earthquake design spectrum; and (4) to develop the necessary techniques, tables, and charts for convenient implementation of the simplified analysis procedure.

The available procedure for earthquake analysis of axisymmetric intake-outlet towers is extended to towers of arbitrary geometry, but with two axes of plan symmetry, and to include the effects of tower-foundation-soil interaction. The total system is represented as four substructures: tower, surrounding water, contained water, and the foundation supported on flexible soil. The substructure representation of the system permits use of the most effective idealization for each substructure. The tower is idealized as an assemblage of one-dimensional beam elements, including bending and shear deformations as well as rotatory inertia. The fluid domain outside the tower but within a fictitious, circular cylinder having an appropriately selected radius is discretized by three-dimensional finite elements, and the effects of the unbounded extent of the fluid outside the fictitious cylinder are treated by the boundary integral procedures utilizing classical solutions for domains exterior to a circular cylinder. The water contained within a hollow tower, being a bounded domain, is simply discretized by the standard finite element method. For the time being, rigorous treatment of tower-foundation-soil interaction effects has been restricted to towers with a circular foundation supported near the surface of a viscoelastic halfspace. However, an approximate

treatment of non-circular foundations is also included.

Utilizing the analytical procedure the responses of idealized intake-outlet towers to harmonic ground motion are presented for a range of parameters characterizing the tower geometry, surrounding and inside water, and foundation-soil system. Based on these frequency response functions, the effects of tower-water interaction and tower-foundation-soil interaction on the response of towers are identified and shown to be significant in many cases.

The dynamic response of Briones Dam Intake Tower to Taft ground motion is presented for various cases: rigid or flexible foundation rock, and with or without water. Study of these response results demonstrates that the earthquake response of this tower is increased because of hydrodynamic effects and decreased as a result of tower-foundation-soil interaction. It is also demonstrated that the earthquake response of this tower can be computed to a satisfactory degree of accuracy by considering the contributions of only the first two natural vibration modes. This observation provides a basis for developing a simplified analysis procedure suitable for practical application.

Such a simplified procedure is developed to determine the maximum earthquake forces in intake-outlet towers directly from the design earthquake spectrum without the need for a response history analysis. All the significant effects of tower-water interaction and tower-foundation-soil interaction are included in the analysis. It is demonstrated that the hydrodynamic effects can be approximated by added mass functions for outside and inside water. It is also shown that the added mass associated with surrounding water or inside water can be determined to a useful degree of accuracy without requiring rigorous three-dimensional analysis of the two fluid domains. An equivalent single-degree-of-freedom system is developed to consider approximately the effects of tower-foundation-soil interaction in the fundamental mode response of towers, and standard data are presented to conveniently determine the effective natural period and damping of the interacting system. The simplified response spectrum analysis procedure utilizes convenient methods for computing the first two natural frequencies and modes of vibration of the tower and the above mentioned simplified representation of hydrodynamic and foundation interaction effects. This procedure is demonstrated to be accurate enough for preliminary design and safety evaluation of towers.

ACKNOWLEDGEMENTS

This research investigation was supported by the National Science Foundation under Grants CEE-8401439 and CES-8719296. The authors are grateful for this support.

The report is an expanded and revised version of Alok Goyal's doctoral dissertation submitted to the University of California at Berkeley in March 1988. The dissertation committee consisted of Professors Anil K. Chopra (Chairman), Bruce A. Bolt and Ray W. Clough. The authors are thankful to Professors Bolt and Clough for reviewing the dissertation manuscript.

The authors are also grateful to graduate student Tsung-Li Tai who assisted with the final preparation of the report.

Table of Contents

1. INTRODUCTION

Earthquake analysis of cantilever tower structures, such as intake-outlet towers, requires special considerations which do not arise in structures on land. Any procedure for analysis of earthquake response of these structures must recognize the interaction forces and modifications in the vibration properties caused by the surrounding as well as the contained water. Similarly, the analysis procedure must be general enough to consider the modifications in the vibration properties and effective damping due to deformability of the supporting foundation rock or soil. Thus, just like in the case of concrete gravity dams, structure-water and structure-foundation-soil interaction effects should be considered in developing methods for analysis of intake-outlet towers. The advances that have been made in the analysis of concrete dams [10,19,22] can be used to advantage in the development.

The significance of tower-foundation-soil interaction effects is not clear because of two competing factors that can be identified based on the research on buildings [45,46]: On the one hand, these tower structures tend to be relatively flexible long-period structures which suggests that soil-structure interaction effects are likely to be small; and on the other hand, many of these tower structures are slender with a large height-to-radius ratio and the soil-structure interaction effects become increasingly significant for slender structures. For tall chimneys, these effects have been shown to be significant under certain situations [35]. Thus the influence of tower-foundation-soil interaction needs to be investigated in earthquake response of intake-outlet towers.

Earlier research on the earthquake analysis, response and design of axisymmetric (circular plan with radius varying arbitrarily over height) intake-outlet towers culminated in (i) a general procedure for linear response analysis considering hydrodynamic effects by neglecting tower-foundation-soil interaction effects [32-34] ; (ii) the computer program EATSW [32] to implement this procedure which has been widely used in practice ; (iii) improved understanding of how the surrounding water influences the vibration properties and earthquake response of towers [33,34] ; (iv) correlation of analytical results with experimental data from forced vibration field tests [41] ; and (v) a procedure for earthquake resistant design of intake-outlet towers [11,13]. The U.S. Army Corps of Engineers adopted this design procedure in their standard practice [38].

Thus much of the existing work that rigorously considers tower-water interaction effects is restricted to axisymmetric towers, i.e. towers of circular plan with radius varying arbitrarily over height supported on rigid foundation rock. This work is aimed at relaxing both of these restrictions.

In order to analyze the earthquake response of intake-outlet towers having non-circular plans with dimensions varying along the height, the tower must be idealized as a discretized system, utilizing, say, the finite element method. Three-dimensional shell elements have been used to discretize hollow prismatic structures partially submerged in water [8]. However, this idealization seems unnecessarily complex unless the cross-sections of the tower are expected to undergo significant in-plane distortions. Such distortions generally do not develop in reinforced-concrete intake-outlet towers. Therefore, such a structure can be effectively idealized as an assemblage of one-dimensional beam elements, including bending and shear deformations as well as rotatory inertia [28]. The shear deformations are included to permit accurate analysis of squat towers. A simpler version of such an approach has been utilized in the dynamic response analysis of tall chimneys [35].

The hydrodynamic terms in the finite element equations for the tower are determined by solving appropriate boundary value problems for the surrounding fluid and the contained fluid. Because surface wave and water compressibility effects have been shown to be negligible in the dynamic response of towers [33], the hydrodynamic terms will be determined by solving the simpler Laplace equation over three-dimensional idealizations of the fluid domains subject to appropriate boundary conditions. The fluid domain outside the tower (of arbitrary plan) but within a fictitious, circular cylinder having an appropriately selected radius is discretized by three-dimensional finite elements, and the effects of the unbounded extent of the fluid outside the fictitious cylinder are treated by the boundary integral procedures utilizing classical solutions for domains exterior to a circular cylinder [33]. The water contained within a hollow tower, being a bounded domain, is simply discretized by the standard finite element method.

The above mentioned analysis procedure is extended in this work to include tower-foundation-soil interaction effects. For the time being, rigorous treatment of these effects has been restricted to towers with a circular foundation supported near the surface of a viscoelastic halfspace. However, an approximate treatment of non-circular foundations is also included.

The objectives of this investigation are : (a) to develop reliable and efficient techniques for analyzing the response of intake-outlet towers of arbitrary geometry, but with two axes of plan symmetry, to earthquake ground motion, including the effects of tower-water interaction and tower-foundation soil interaction ; (b) to develop an efficient hydrodynamic analysis procedure for the unbounded fluid domain exterior to the tower (c) to investigate the significance of various interaction effects on the earthquake response of intake-outlet towers; (d) to develop a simplified analysis procedure appropriate for the preliminary phase of design and safety evaluation of intake-outlet towers that provides sufficiently accurate estimates of of design forces directly from the earthquake design spectrum ; and (e) to develop necessary techniques, tables and charts for convenient implementation of the simplified analysis procedure.

A general procedure for the earthquake response analysis of intake-outlet towers including tower-water interaction and tower-foundation soil interaction is presented in Chapter 3. The general analytical procedure is based on the substructure method, wherein each substructure -- the tower, the foundation and supporting soil, the surrounding water domain, and the inside water domain -- is idealized, as mentioned earlier, in a manner appropriate to its properties and dynamic behavior. Presented in Chapter 4 are numerical methods for the efficient evaluation of various terms appearing in the equations of motion. These include the mass, stiffness and damping terms for the tower structure, added hydrodynamic mass and excitation terms associated with surrounding water as well as inside water, and foundation impedance functions.

The objective of Chapter 5 is then to investigate how the response of towers is affected by tower-water interaction and by tower-foundation-soil interaction for a wide range of basic parameters characterizing the tower geometry, surrounding and inside water, and foundation soil. For a number of towers with different geometries in plan as well as along the height, the response to harmonic ground motion is presented in the form of frequency response functions. Based on these response results, the effects of tower-water interaction and tower-foundation soil interaction on the response of towers are investigated.

Chapter 6 presents the displacement responses and envelope of maximum shear forces and bending moments along the height of the Briones Dam Intake Tower to Taft ground motion for various assumptions for the water and the foundation soil. Based on the results from these analyses, the effects of tower-water interaction and tower-foundation-soil interaction on the displacements, maximum shear forces and bending moments are investigated. It is shown that hydrodynamic effects significantly influence the earthquake response of towers but the influence of tower-foundation-soil interaction is relatively small.

In Chapter 7, the more important factors influencing the dynamic response of towers are incorporated in a simplified analysis procedure that is intended for the preliminary phase of earthquake resistant design and safety evaluation of intake-outlet towers. In this simplified procedure, the hydrodynamic effects are represented by the added hydrodynamic mass evaluated from the analysis of a rigid tower [13], the tower-foundation-soil interaction effects are included using concepts similar to those developed for building foundation systems [45,46] and concrete gravity dams [20,21], and the maximum response considering the first two vibration modes of the tower [11] is computed directly from the earthquake design spectrum.

Chapter 8 presents simplified methods for evaluation of the added hydrodynamic mass associated with water surrounding the tower or contained within a hollow tower. Figures and tables of appropriate data are presented for convenient computation of the added mass.

A step-by-step summary of the simplified analysis procedure for intake-outlet towers is presented in Chapter 9, wherein the concepts developed in Chapters 7 and 8 are combined. Also included is a simplified procedure for evaluating the frequencies and shapes of the first two vibration modes of the tower. Additionally, the simplified procedure is shown to be sufficiently accurate for the preliminary phase of design and safety evaluation of intake-outlet towers.

Finally, the conclusions of this investigation regarding the effects of tower-water interaction, and tower-foundation-soil interaction on the response of intake-outlet towers to horizontal earthquake ground motion are presented in Chapter 10.

2. SYSTEM AND GROUND MOTION

The system considered consists of a hollow reinforced concrete intake-outlet tower partially submerged in water and supported through a rigid foundation on the horizontal surface of flexible soil (Figure 2.1). The surrounding water is idealized by a fluid domain of constant depth, extending to infinity in radial directions. The hollow tower is also partially filled with water. The tower may be of arbitrary cross-section having two axes of symmetry. This restriction allows the hydrodynamic pressures on the inside and outside surfaces of the tower, caused by the horizontal components of the earthquake ground motion along the planes of symmetry, to be represented as equivalent lateral forces and external moments distributed over the tower height acting along these planes. The system is analyzed under the assumption of linear behavior for the tower concrete, the surrounding and inside water, and the foundation soil.

The tower is idealized as a one-dimensional Timoshenko beam including the effects of rotatory inertia and shear deformations [44], the latter included to permit accurate analysis of squat towers. Because surface wave and water compressibility effects have been shown to be negligible in the dynamic response of towers for a wide range of slenderness ratios [32,33], the lateral hydrodynamic forces and external hydrodynamic moments are determined by solving the Laplace equation over three-dimensional fluid domains (both inside and outside) subject to appropriate boundary conditions. The part of the foundation above the ground level is treated as a part of the tower and the remaining part of the foundation below the ground level is idealized as a rigid footing of infinitesimal thickness supported on the surface of a homogeneous viscoelastic halfspace. The latter assumption is reasonable because the embedment is usually shallow. Perfect bonding between the foundation and the foundation soil is assumed, i.e. the effect of transient partial separation of the foundation from soil is not considered.

The earthquake excitation for the tower-water-foundation-soil system is defined by two horizontal components of the free-field ground acceleration. The vertical component of the

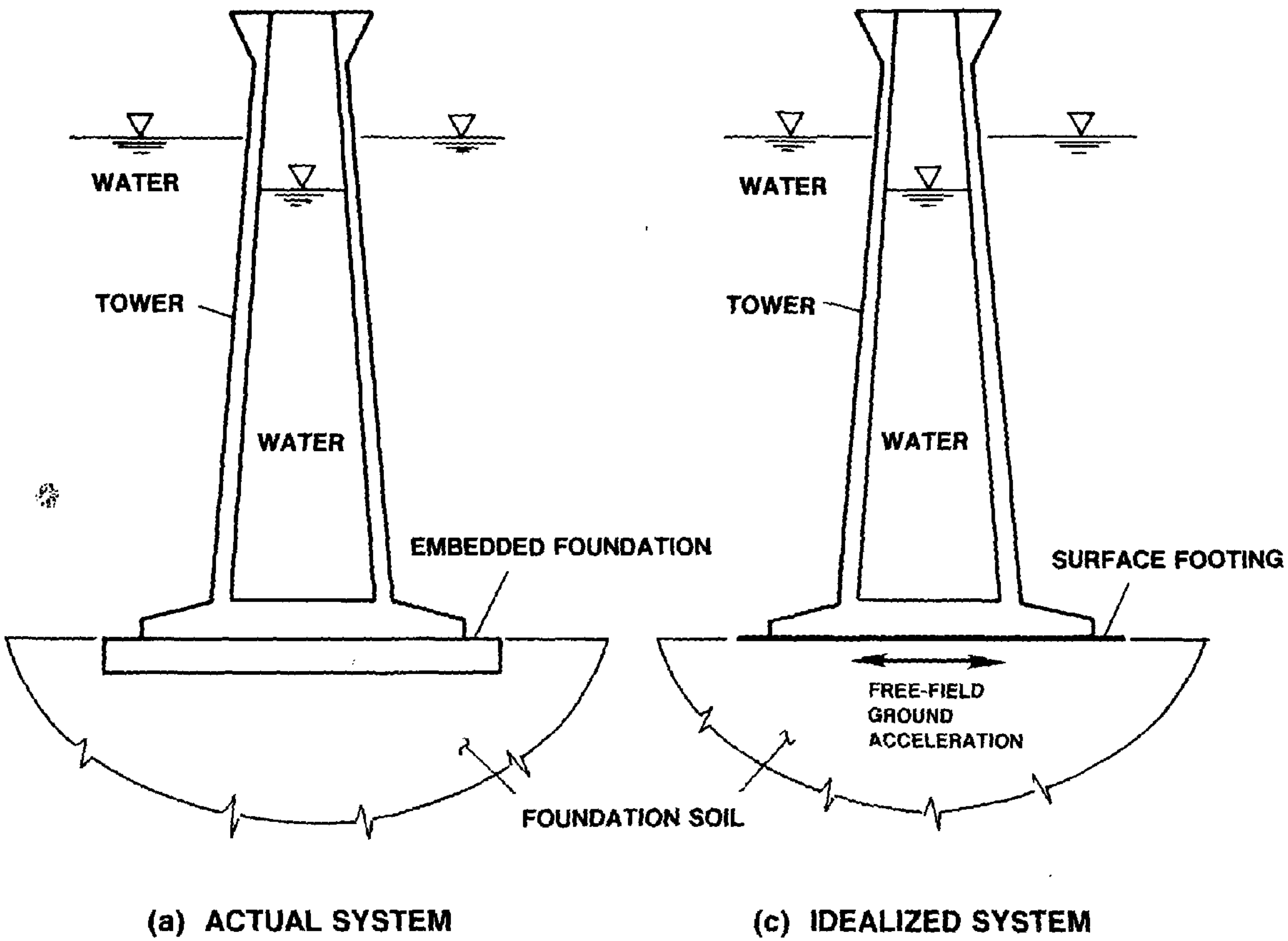

Figure 2.1 Tower-Water-Foundation-Soil System

ground motion is expected to have little influence on the response of towers and is therefore not considered in this investigation. The ground motion is assumed to be identical at all points on the horizontal base of the tower. The analysis procedure is presented for one component of horizontal ground motion in a plane of symmetry. The dynamic response of the tower for each horizontal component of ground motion can be evaluated separately and the responses to the two components superimposed to determine the total response.

3. GENERAL ANALYTICAL PROCEDURES

3.1 Introduction

The governing equations of motion for the tower including the effects of tower-water interaction and tower-foundation-soil interaction are conveniently written in the Fourier transformed frequency domain because the impedance functions for the foundation on a halfspace depend on the excitation frequency. The system consists of four substructures : the tower, the foundation and supporting soil, the surrounding water domain, and the inside water domain (Figure 3.1). The governing equations for these substructures are presented next in the frequency domain followed by a general analytical procedure based on the substructure method.

3.2 Frequency Domain Equations

3.2.1 Tower Substructure

The equations of motion for planar vibrations of a tower idealized as a Timoshenko beam and subject to harmonic ground acceleration $\ddot{u}_g(t) = e^{i\omega t}$ (Figure 3.2) are written in frequency domain as two coupled partial differential equations :

$$m_s(z)\, \overline{\ddot{u}^t}(z,\omega) - (1+i\eta_s)\frac{\partial}{\partial z}\left[G_s k(z) A(z) \left[\frac{\partial}{\partial z}\bar{u}(z,\omega) - \bar{\theta}(z,\omega) \right] \right]$$

$$= -\bar{f}^{\,o}(z,\omega) - \bar{f}^{\,i}(z,\omega) \tag{3.1a}$$

$$I_s(z)\, \overline{\ddot{\theta}^t}(z,\omega) - (1+i\eta_s)\left[\frac{\partial}{\partial z}\left[E_s I(z) \frac{\partial}{\partial z}\bar{\theta}(z,\omega)\right] + G_s k(z) A(z) \left[\frac{\partial}{\partial z}\bar{u}(z,\omega) - \bar{\theta}(z,\omega)\right] \right]$$

$$= -\overline{m}^{\,o}(z,\omega) - \overline{m}^{\,i}(z,\omega) \tag{3.1b}$$

in which $m_s(z)$ and $I_s(z)$ are the mass and rotatory inertia per unit of height of the tower ; η_s is the constant hysteretic damping factor for the tower ; and $G_s k(z) A(z)$ and $E_s I(z)$ are the

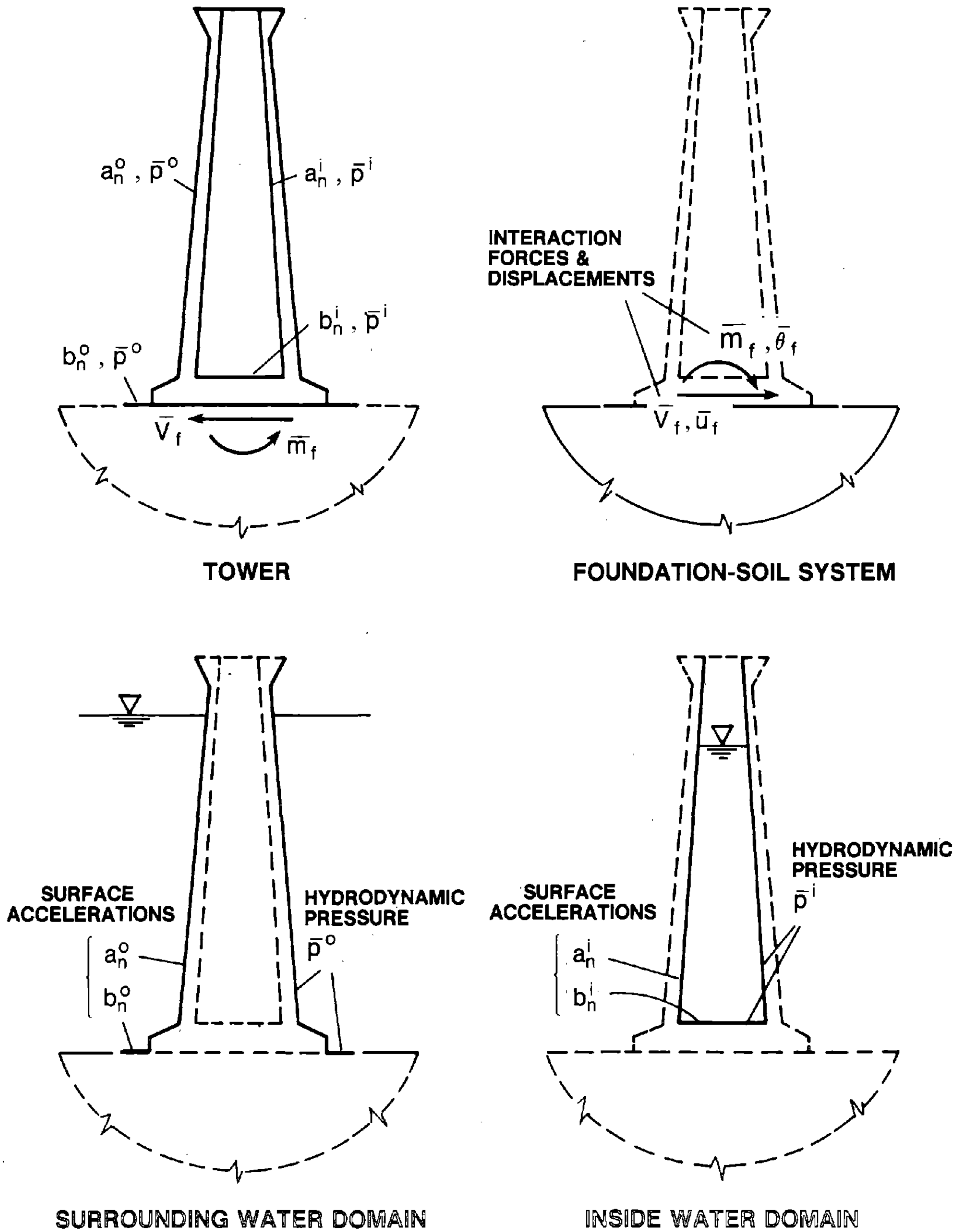

Figure 3.1 Substructure Representation of the Tower-Water-Foundation-Soil System

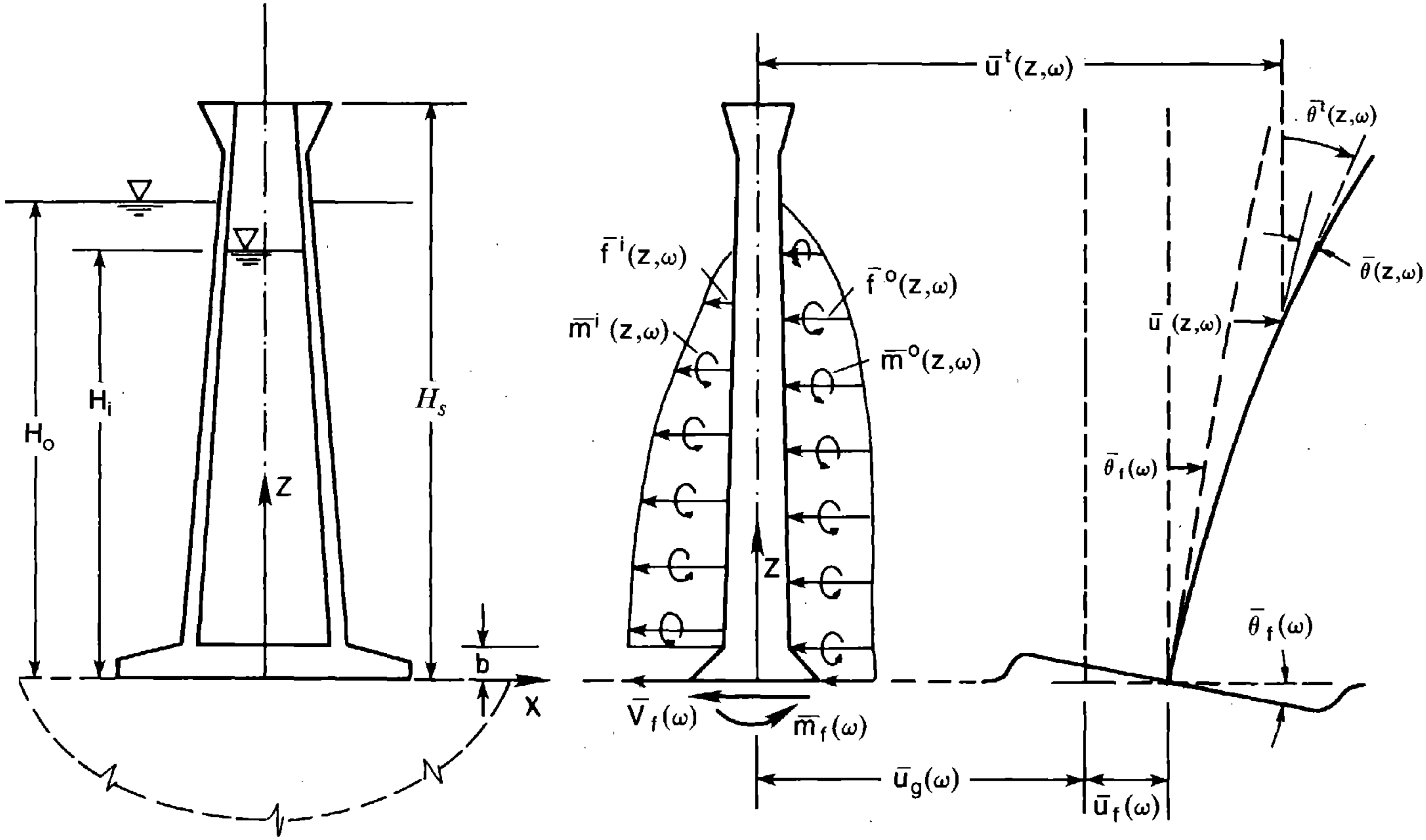

(a) TOWER SUBSTRUCTURE **(b) FORCES (HYDRODYNAMIC AND FOUNDATION) AND DISPLACEMENTS**

Figure 3.2 One-Dimensional Idealization, Interaction Forces and Displacements for the Tower cross-sectional stiffnesses for the tower in pure shear and pure bending at a location z above the base, respectively. In these equations, $\bar{u}(z,\omega)$ is the complex frequency response function for the lateral displacement due to bending plus shear deformations of the tower and $\bar{\theta}(z,\omega)$ is the similar function for the bending slope of the tower axis ; and $\overline{\ddot{u}^t}(z,\omega)$ and $\overline{\ddot{\theta}^t}(z,\omega)$ are the response functions for total (beam deformation plus base translation and rotation) lateral and rotational accelerations, respectively. In equation (3.1), $\bar{f}^o(z,\omega)$ and $\overline{m}^o(z,\omega)$ are the response functions for equivalent lateral forces and external moments acting along the height of the tower in its plane of vibration due to hydrodynamic pressure on the outside surface ; and $\bar{f}^i(z,\omega)$ and $\overline{m}^i(z,\omega)$ are the corresponding functions due to hydrodynamic pressure on the inside surface. The response functions for external hydrodynamic moments, $\overline{m}^o(z,\omega)$ and $\overline{m}^i(z,\omega)$, are non-zero only for non-uniform towers.

In addition to equation (3.1), the total equilibrium of horizontal forces leads to the following equation :

$$\int_0^{H_s} [\, m_s(z)\, \overline{\ddot{u}^t}(z,\omega) + \bar{f}^o(z,\omega) + \bar{f}^i(z,\omega) \,]\, dz + \bar{V}_f(\omega) = 0 \tag{3.2}$$

Similarly, total equilibrium of moments about the base of the tower leads to the following equation:

$$\int_0^{H_s} z\, [\, m_s(z)\, \overline{\ddot{u}^t}(z,\omega) + \bar{f}^o(z,\omega) + \bar{f}^i(z,\omega) \,]\, dz$$

$$+ \int_0^{H_s} [\, I_s(z)\, \overline{\ddot{\theta}^t}(z,\omega) + \overline{m}^o(z,\omega) + \overline{m}^i(z,\omega) \,]\, dz + \overline{m}_f(\omega) = 0 \tag{3.3}$$

In these equilibrium equations, $\bar{V}_f(\omega)$ and $\overline{m}_f(\omega)$ are the frequency response functions for shear force and bending moment, respectively, at the base of the tower, and H_s is the height of the tower.

Assuming small displacements and rotations, the frequency response functions for total lateral and rotational accelerations along the height can be expressed in the following form (Figure 3.2):

$$\overline{\ddot{u}^{t}}(z,\omega) = 1 - \omega^2\, \bar{u}(z,\omega) - \omega^2\, \bar{u}_f(\omega) - \omega^2\, z\, \bar{\theta}_f(\omega) \tag{3.4a}$$

$$\overline{\ddot{\theta}^{t}}(z,\omega) = -\, \omega^2\, \bar{\theta}(z,\omega) - \omega^2\, \bar{\theta}_f(\omega) \tag{3.4b}$$

where $\bar{u}_f(\omega)$ and $\bar{\theta}_f(\omega)$ are the complex frequency response functions for the lateral displacement and rotation of the foundation, respectively, relative to the free field ground motion.

The natural frequencies and mode shapes of the tower without water on fixed base are given by solutions of the associated eigen value problem for equation (3.1) [26,27]. The n-th mode shape is completely defined by two functions $\phi_n(z)$ and $\psi_n(z)$ describing the lateral displacements and rotations of the tower axis [27]. The numerical procedure to evaluate these functions by solving the associated eigen value problem is presented in Chapter 4. The lateral displacements and rotations of the tower, $\bar{u}(z,\omega)$ and $\bar{\theta}(z,\omega)$, can be expressed as a linear combination of its fixed-base natural modes of vibration :

$$\bar{u}(z,\omega) = \sum_{n=1}^{\infty} \phi_n(z)\, \bar{Y}_n(\omega) \tag{3.5a}$$

$$\bar{\theta}(z,\omega) = \sum_{n=1}^{\infty} \psi_n(z)\, \bar{Y}_n(\omega) \tag{3.5b}$$

where $\bar{Y}_n(\omega)$ is the frequency response function for the generalized (modal) coordinate associated with the n-th mode of vibration.

The equations of motion for the tower are transformed to modal coordinates by substituting equations (3.4) and (3.5) into equation (3.1), using the principle of virtual work and the orthogonality properties of normal modes. Similarly, the total equilibrium equations for horizontal forces and moments are transformed to modal coordinates by substituting equations (3.4) and (3.5) into equations (3.2) and (3.3), and using the orthogonality properties of normal modes. This leads to :

$$M_n \left[-\omega^2 + (1+i\eta_s)\omega_n^2\right] \bar{Y}_n(\omega) - \omega^2 L_n^h \bar{u}_f(\omega) - \omega^2 L_n^r \bar{\theta}_f(\omega) = -L_n - \bar{l}_n^o(\omega) - \bar{l}_n^i(\omega) \tag{3.6a}$$

$$-\omega^2 \sum_{n=1}^{\infty} L_n^h \bar{Y}_n(\omega) - \omega^2 m_t \bar{u}_f(\omega) - \omega^2 L_0^r \bar{\theta}_f(\omega) = -m_t - \bar{l}_h^o(\omega) - \bar{l}_h^i(\omega) - \bar{V}_f(\omega) \tag{3.6b}$$

$$-\omega^2 \sum_{n=1}^{\infty} L_n^r \bar{Y}_n(\omega) - \omega^2 L_0^r \bar{u}_f(\omega) - \omega^2 I_t \bar{\theta}_f(\omega) = -L_0^r - \bar{l}_r^o(\omega) - \bar{l}_r^i(\omega) - \overline{m}_f(\omega) \tag{3.6c}$$

in which ω_n represents the natural frequency for the n-th mode of vibration of the fixed-base tower without water. The generalized mass M_n, generalized excitation term L_n, and generalized excitation terms L_n^h and L_n^r associated with base translation and rotation, respectively, are given by :

$$M_n = \int_0^{H_s} m_s(z) \left[\phi_n(z)\right]^2 dz + \int_0^{H_s} I_s(z) \left[\psi_n(z)\right]^2 dz \tag{3.7}$$

$$L_n = L_n^h = \int_0^{H_s} m_s(z)\, \phi_n(z)\, dz \tag{3.8}$$

$$L_n^r = \int_0^{H_s} z\, m_s(z)\, \phi_n(z)\, dz + \int_0^{H_s} I_s(z)\, \psi_n(z)\, dz \tag{3.9}$$

Similarly, the total mass of the tower, m_t, is :

$$m_t = \int_0^{H_s} m_s(z)\, dz \tag{3.10}$$

the total mass moment of inertia of the tower about its base, I_t, is:

$$I_t = \int_0^{H_s} z^2\, m_s(z)\, dz + \int_0^{H_s} I_s(z)\, dz \tag{3.11}$$

and the mass coupling between the lateral and rotational motions of the foundation is represented by :

$$L_0^r = \int_0^{H_s} z\, m_s(z)\, dz \tag{3.12}$$

For a rigid tower supported on deformable soil through a rigid foundation, m_t, I_t and L_0^r can be interpreted as generalized mass terms for lateral and rotational motions of the foundation.

The hydrodynamic terms in equation (3.6) are given by :

$$\bar{l}_n^\alpha(\omega) = \int_0^{H_\alpha} \phi_n(z)\, \bar{f}^\alpha(z,\omega)\, dz + \int_0^{H_\alpha} \psi_n(z)\, \overline{m}^\alpha(z,\omega)\, dz \quad ; \quad \alpha = o,i \tag{3.13}$$

$$\bar{l}_h^\alpha(\omega) = \int_0^{H_\alpha} \bar{f}^\alpha(z,\omega)\, dz \quad ; \quad \alpha = o,i \tag{3.14}$$

$$\bar{l}_r^\alpha(\omega) = \int_0^{H_\alpha} z\, \bar{f}^\alpha(z,\omega)\, dz + \int_0^{H_\alpha} \overline{m}^\alpha(z,\omega)\, dz \quad ; \quad \alpha = o,i \tag{3.15}$$

in which $\alpha = o$ and i, are used to identify the terms for outside and inside water, respectively; H_o (H_α , $\alpha=o$) and H_i (H_α , $\alpha=i$) are the outside and inside water depths.

The frequency response functions $\bar{f}^o(z,\omega)$ and $\overline{m}^o(z,\omega)$ of hydrodynamic forces due to pressures on the outside surface of the tower will be expressed later in terms of accelerations of the modal coordinates $\bar{Y}_n(\omega)$, the lateral displacement $\bar{u}_f(\omega)$ and of the rotation $\bar{\theta}_f(\omega)$ of the foundation by analysis of the surrounding water domain substructure. Similarly, corresponding functions $\bar{f}^i(z,\omega)$ and $\overline{m}^i(z,\omega)$ for inside water will be expressed in terms of $\bar{Y}_n(\omega)$, $\bar{u}_f(\omega)$ and $\bar{\theta}_f(\omega)$ by the analysis of the inside water domain. Also, the response functions for the tower-foundation-soil interaction forces, $\bar{V}_f(\omega)$ and $\overline{m}_f(\omega)$, will be expressed in terms of response functions for interaction displacements $\bar{u}_f(\omega)$ and $\bar{\theta}_f(\omega)$ by analysis of the foundation supported on a viscoelastic halfspace.

It is well known that the magnitude of L_n, L_n^h and L_n^r decreases with mode number n, which implies that the contribution of higher vibration modes in the response of towers subjected to horizontal ground motion tends to be small. As a result, only the first N modes of the tower need to be considered in the dynamic response of the tower. Therefore, in what follows, equation (3.6a) is included only for $n=1,2, \ldots, N$ and only N terms are included in the infinite summations in equations (3.6b,c). For a particular excitation frequency ω, equation (3.6) represent $N+2$ simultaneous complex algebraic equations in the unknowns $\bar{Y}_n(\omega)$, $n=1,2, \ldots, N$; $\bar{u}_f(\omega)$ and $\bar{\theta}_f(\omega)$.

3.2.2 Foundation-Soil Substructure

The governing equations for the rigid foundation subjected to free-field ground motion $\ddot{u}_g(t) = e^{i\omega t}$ and harmonic interaction forces $V_f(t) = \bar{V}_f(\omega)\, e^{i\omega t}$ and $m_f(t) = \overline{m}_f(\omega)\, e^{i\omega t}$ (Figure 3.3) are:

$$-\omega^2\, m_f\, \bar{u}_f(\omega) + K_{VV}(\omega)\, \bar{u}_f(\omega) + K_{VM}(\omega)\, \bar{\theta}_f(\omega) = -\, m_f + \bar{V}_f(\omega) \tag{3.16a}$$

$$-\omega^2\, I_f\, \bar{\theta}_f(\omega) + K_{MV}(\omega)\, \bar{u}_f(\omega) + K_{MM}(\omega)\, \bar{\theta}_f(\omega) = \overline{m}_f(\omega) \tag{3.16b}$$

in which m_f is the mass and I_f is the rotatory inertia of the foundation. $K_{VV}(\omega)$, $K_{MM}(\omega)$ and $K_{VM}(\omega)$ [$K_{MV}(\omega) = K_{VM}(\omega)$ by reciprocity theorem] are the impedance functions which may be obtained from the solutions of two boundary value problems for the foundation-soil domain, arising from the application of a harmonic horizontal force and a harmonic moment separately to the rigid foundation. Available solutions for these problems will be summarized in Section 4.2. Inherent in the evaluation of these impedance functions is the assumption that the hydrodynamic pressures on the surface of the foundation soil outside the foundation have negligible influence.

3.2.3 Tower-Foundation-Soil System

Substitution of equation (3.16) for $\bar{V}_f(\omega)$ and $\overline{m}_f(\omega)$ into equations (3.6b,c) leads to

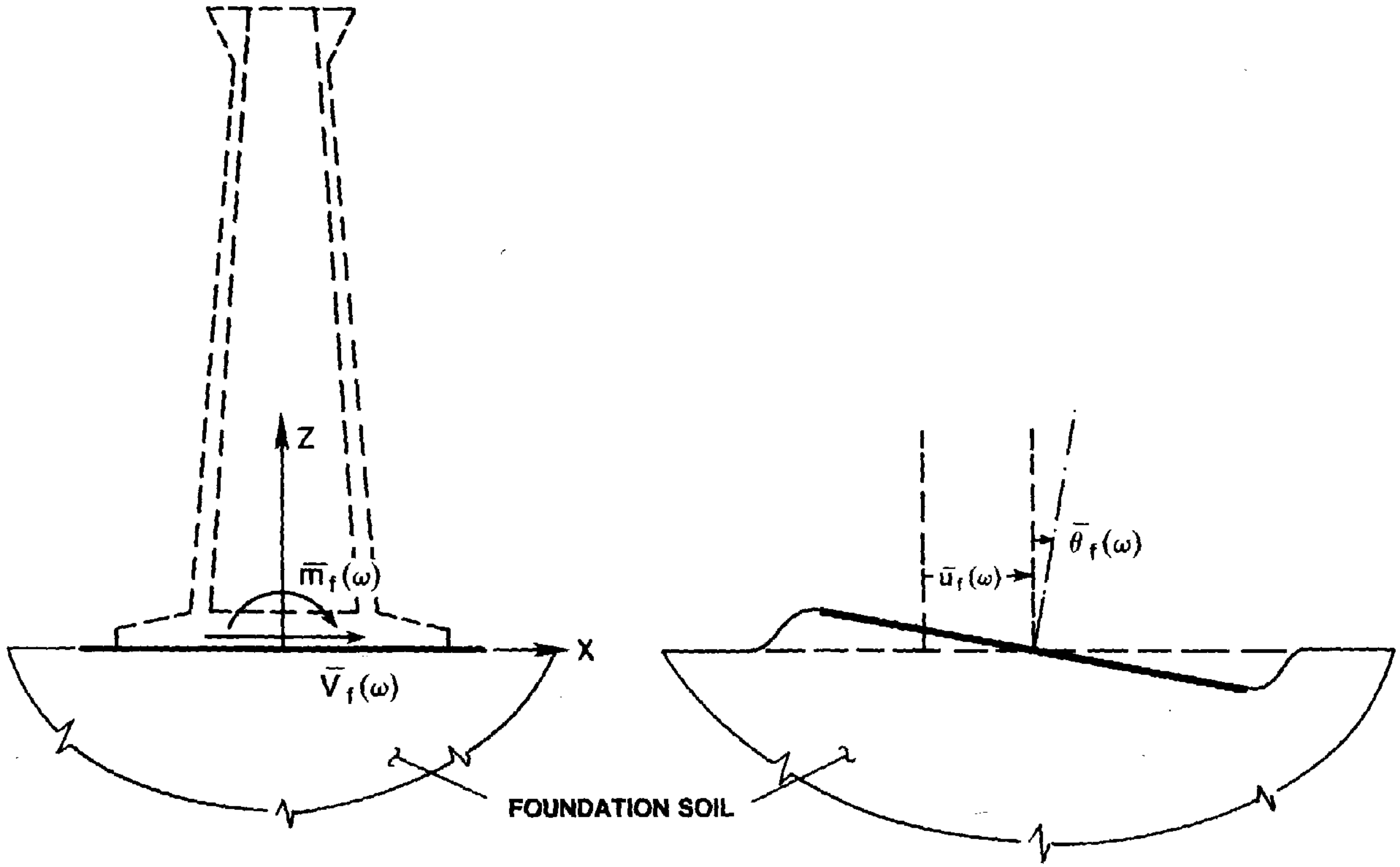

(a) INTERACTION FORCES

(b) INTERACTION DISPLACEMENTS

Figure 3.3 Interaction Forces and Displacements of the Foundation-Soil System

$N+2$ complex simultaneous equations for the tower-foundation-soil system :

$$M_n \, [\, - \, \omega^2 + (1+i\eta_s) \, \omega_n^2 \,] \, \overline{Y}_n(\omega) - \omega^2 \, L_n^h \, \overline{u}_f(\omega) - \omega^2 \, L_n^r \, \overline{\theta}_f(\omega)$$

$$= - \, L_n - \overline{l}_n^o(\omega) - \overline{l}_n^i(\omega) \quad ; \quad n=1,2, \ldots, N \tag{3.17a}$$

$$- \, \omega^2 \sum_{n=1}^{N} L_n^h \, \overline{Y}_n(\omega) - \omega^2 \, (\, m_t + m_f \,) \, \overline{u}_f(\omega) - \omega^2 \, L_0^r \, \overline{\theta}_f(\omega) + K_{VV}(\omega) \, \overline{u}_f(\omega)$$

$$+ \, K_{VM}(\omega) \, \overline{\theta}_f(\omega) = - \, (\, m_t + m_f \,) - \overline{l}_h^o(\omega) - \overline{l}_h^i(\omega) \tag{3.17b}$$

$$- \, \omega^2 \sum_{n=1}^{N} L_n^r \, \overline{Y}_n(\omega) - \omega^2 \, L_0^r \, \overline{u}_f(\omega) - \omega^2 \, (\, I_t + I_f \,) \, \overline{\theta}_f(\omega) + K_{MV}(\omega) \, \overline{u}_f(\omega)$$

$$+ \, K_{MM}(\omega) \, \overline{\theta}_f(\omega) = - \, L_0^r - \overline{l}_r^o(\omega) - \overline{l}_r^i(\omega) \tag{3.17c}$$

These equations have the same structure as developed earlier [12] for building-foundation systems. The additional terms appearing in equation (3.17) because of hydrodynamic pressures on towers are evaluated from the analysis of fluid domain substructures described in the next two sections.

3.2.4 Surrounding Water Domain Substructure

Boundary Value Problem-- The frequency response functions of unknown hydrodynamic forces $\overline{f}^o(z,\omega)$ and $\overline{m}^o(z,\omega)$, which appear in equations (3.13) to (3.15), can be expressed in terms of accelerations of the outside surface by analysis of the surrounding (outside) water domain. Assuming water to be incompressible and neglecting its internal viscosity, the small amplitude, irrotational motion of water is governed by the three-dimensional Laplace equation :

$$\frac{\partial^2 \overline{p}^o}{\partial x^2} + \frac{\partial^2 \overline{p}^o}{\partial y^2} + \frac{\partial^2 \overline{p}^o}{\partial z^2} = 0 \tag{3.18}$$

where $\bar{p}^o(\vec{x},\omega)$ is the frequency response function for hydrodynamic pressure (in excess of hydrostatic pressure); i.e. the hydrodynamic pressure $p^o(\vec{x},t)$, where $\vec{x} = (x,y,z)$ defines the coordinate vector of a point, due to harmonic ground acceleration $\ddot{u}_g(t) = e^{i\omega t}$ is given by $p^o(\vec{x},t) = \bar{p}^o(\vec{x},\omega)\, e^{i\omega t}$. The hydrodynamic pressure in the water surrounding the tower is generated by acceleration of the outside surface of the tower and vertical acceleration of the reservoir bottom. The motion of these boundaries is related to the hydrodynamic pressure by the boundary conditions in equations (3.19) and (3.22) which are presented using the notations of Figure 3.4.

For horizontal ground acceleration $\ddot{u}_g(t) = e^{i\omega t}$ in a plane of symmetry for the tower, the boundary condition at the tower-water interface, Γ_t^o, becomes :

$$\frac{\partial}{\partial n^o}\bar{p}^o(\vec{x},\omega) = -\,\rho_w\, a_n^o(\vec{x},\omega) \tag{3.19}$$

in which ρ_w is the mass density of water ; n^o represents the direction of the normal to the surface ; and $a_n^o(\vec{x},\omega)$ is the spatial distribution of the acceleration of the outside surface in its normal direction. For ground acceleration applied in the x direction, $a_n^o(\vec{x},\omega)$ at the tower-water interface Γ_t^o is related to the total lateral and rotational accelerations of the tower axis by the following equation :

$$a_n^o(\vec{x},\omega) = n_x^o(\vec{x})\,\overline{\ddot{u}^t}(z,\omega) - x\, n_z^o(\vec{x})\,\overline{\ddot{\theta}^t}(z,\omega) \tag{3.20}$$

where $n_x^o(\vec{x})$ and $n_z^o(\vec{x})$ are the direction cosines of the normal at a point $\vec{x}$ on the outside surface with respect to x and z axes respectively. Expanding $\overline{\ddot{u}^t}(z,\omega)$ and $\overline{\ddot{\theta}^t}(z,\omega)$ by equation (3.4) and using equation (3.5), the equation (3.20) becomes :

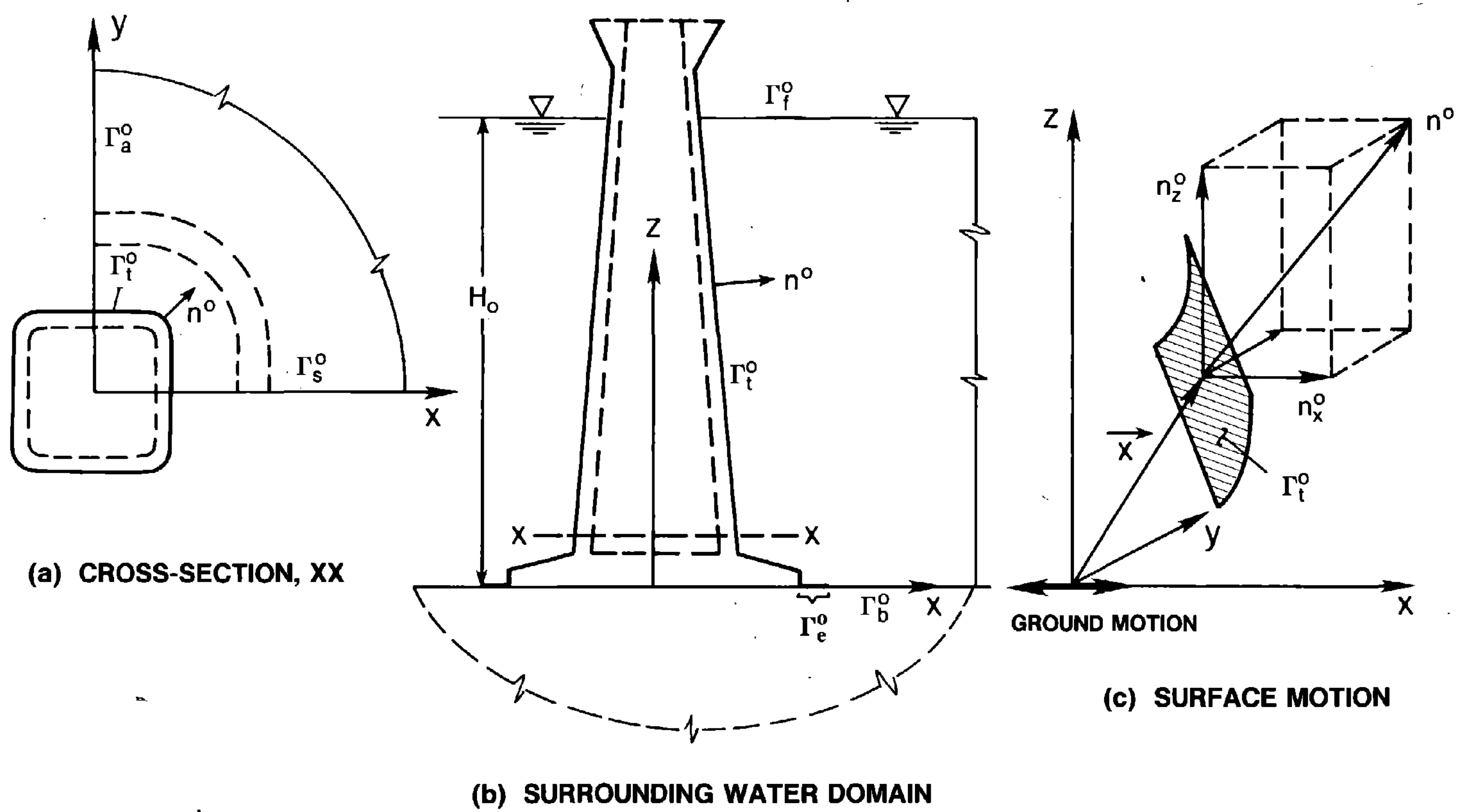

Figure 3.4 Notations and Definitions for Surrounding Water Domain

$$\frac{\partial}{\partial n^o}\bar{p}^o(\vec{x},\omega) = -\rho_w\, n_x^o(\vec{x})\,[\,1 - \omega^2 \sum_{j=1}^{N} \phi_j(z)\,\bar{Y}_j(\omega) - \omega^2\,\bar{u}_f(\omega) - \omega^2\, z\,\bar{\theta}_f(\omega)\,]$$

$$+\rho_w\, x\, n_z^o(\vec{x})\,[\,-\omega^2 \sum_{j=1}^{N} \psi_j(z)\,\bar{Y}_j(\omega) - \omega^2\,\bar{\theta}_f(\omega)\,] \qquad (3.21)$$

Since vertical ground motion is not considered, the vertical acceleration of the reservoir bottom is caused only by the rotation of the foundation, which may be partially exposed to the water surrounding the tower. If Γ_e^o represents the exposed part of the foundation at reservoir bottom Γ_b^o, then the boundary condition at the reservoir bottom Γ_b^o becomes:

$$\frac{\partial}{\partial z}\,\bar{p}^o(\vec{x},\omega) = \begin{cases} \rho_w\, x\,[\,-\omega^2\,\bar{\theta}_f(\omega)\,] & \vec{x}\,\epsilon\Gamma_e^o \\ 0 & otherwise \end{cases} \qquad (3.22)$$

In this equation, the vertical acceleration of the reservoir bottom caused by its deformation due to rotation of the foundation is assumed equal to zero away from the foundation only for simplicity in the numerical solution. The errors introduced by this simplification are insignificant because these vertical accelerations of the reservoir bottom are small and rapidly decrease with increasing radial distance from the foundation, [36], and the hydrodynamic forces due to vertical acceleration of the reservoir bottom away from the tower are small [18].

Neglecting the effects of surface waves which are known to be small [32,33], the boundary condition at the free surface, Γ_f^o , is :

$$\bar{p}^o(\vec{x},\omega) = 0 \qquad (3.23)$$

The frequency response function $\bar{p}^o(\vec{x},\omega)$ for the hydrodynamic pressure in the water surrounding the tower is the solution of equation (3.18) subject to boundary conditions in equations (3.21) to (3.23). In addition to these boundary conditions, $\bar{p}^o(\vec{x},\omega)$ should remain bounded at all distances in radial directions of the unbounded fluid domain.

Solution for Hydrodynamic Pressure-- The linear form of the governing equation and boundary conditions allow $\bar{p}^o(\vec{x},\omega)$ to be expressed as :

$$\bar{p}^o(\vec{x},\omega) = p_0^o(\vec{x}) - \omega^2 \sum_{j=1}^{N} p_j^o(\vec{x})\, \bar{Y}_j(\omega) - \omega^2 p_h^o(\vec{x})\, \bar{u}_f(\omega) - \omega^2 p_r^o(\vec{x})\, \bar{\theta}_f(\omega) \tag{3.24}$$

In equation (3.24), the hydrodynamic pressure $p_0^o(\vec{x})$ due to the horizontal free-field ground acceleration of a rigid tower is the solution of equation (3.18) subject to the following boundary conditions :

$$\frac{\partial}{\partial n^o}\,\bar{p}^o(\vec{x}) = -\rho_w\, n_x^o(\vec{x}) \qquad \vec{x} \in \Gamma_t^o \tag{3.25a}$$

$$\frac{\partial}{\partial z}\,\bar{p}^o(\vec{x}) = 0 \qquad \vec{x} \in \Gamma_b^o \tag{3.25b}$$

$$\bar{p}^o(\vec{x}) = 0 \qquad \vec{x} \in \Gamma_f^o \tag{3.25c}$$

The hydrodynamic pressure function $p_j^o(\vec{x})$ due to horizontal acceleration $\phi_j(z)$ and rotational acceleration $\psi_j(z)$ of the tower axis that correspond to the j-th mode of vibration, with no motion at the tower base, is the solution of equation (3.18) subject to the following boundary conditions :

$$\frac{\partial}{\partial n^o}\,\bar{p}^o(\vec{x}) = -\rho_w\,[\, n_x^o(\vec{x})\, \phi_j(z) - x\, n_z^o(\vec{x})\, \psi_j(z)\,] \qquad \vec{x} \in \Gamma_t^o \tag{3.26a}$$

$$\frac{\partial}{\partial z}\,\bar{p}^o(\vec{x}) = 0 \qquad \vec{x} \in \Gamma_b^o \tag{3.26b}$$

$$\bar{p}^o(\vec{x}) = 0 \qquad \vec{x} \in \Gamma_f^o \tag{3.26c}$$

The pressure function $p_h^o(\vec{x})$ due to horizontal, interaction acceleration of the foundation with a rigid tower is the solution of equation (3.18) with the boundary conditions of equation (3.25). Thus $p_h^o(\vec{x}) = p_0^o(\vec{x})$. The pressure function $p_r^o(\vec{x})$ due to rotational, interaction acceleration of the foundation with a rigid tower is the solution of equation (3.18) with the following boundary conditions :

$$\frac{\partial}{\partial n^o}\,\bar{p}^o(\vec{x}) = -\,\rho_w\,[\,n_x^o(\vec{x})\,z - n_z^o(\vec{x})\,x\,] \qquad \vec{x}\in\Gamma_t^o \tag{3.27a}$$

$$\frac{\partial}{\partial z}\,\bar{p}^o(\vec{x}) = \begin{Bmatrix} \rho_w\,x & \vec{x}\in\Gamma_e^o \\ 0 & otherwise \end{Bmatrix} \qquad \vec{x}\in\Gamma_b^o \tag{3.27b}$$

$$\bar{p}^o(\vec{x}) = 0 \qquad \vec{x}\in\Gamma_f^o \tag{3.27c}$$

An efficient analysis procedure, which uses the finite element method coupled with boundary integral procedures, is presented in Chapter 4 to solve the above-defined boundary value problems and determine the pressure functions $p_0^o(\vec{x})$, $p_j^o(\vec{x})$, $p_h^o(\vec{x})$ and $p_r^o(\vec{x})$.

Hydrodynamic Forces-- Due to symmetry of the tower with respect to the vertical plane in the direction of applied ground motion, the hydrodynamic pressures on the outside surface of the tower can be replaced by equivalent lateral forces and external moments acting in this plane along the height of the tower. Similar to equation (3.24) for hydrodynamic pressures, the frequency response functions for hydrodynamic forces $\bar{f}^o(z,\omega)$ and moments $\overline{m}^o(z,\omega)$, appearing in equations (3.13) to (3.15), can be expressed as :

$$\bar{f}^o(z,\omega) = f_0^o(z) - \omega^2\sum_{j=1}^{N} f_j^o(z)\,\bar{Y}_j(\omega) - \omega^2 f_h^o(z)\,\bar{u}_f(\omega) - \omega^2 f_r^o(z)\,\bar{\theta}_f(\omega) \tag{3.28a}$$

$$\overline{m}^o(z,\omega) = m_0^o(z) - \omega^2\sum_{j=1}^{N} m_j^o(z)\,\bar{Y}_j(\omega) - \omega^2 m_h^o(z)\,\bar{u}_f(\omega) - \omega^2 m_r^o(z)\,\bar{\theta}_f(\omega) \tag{3.28b}$$

These forces and moments are evaluated at any location z along the height by integrating their corresponding pressure functions along the perimeter of the tower-water interface Γ_t^o pertaining to that location by the following equations :

$$f_\beta^o(z) = \int_{\Gamma_t^o} n_x^o(\vec{x})\,p_\beta^o(\vec{x})\,ds_1^o \qquad ; \qquad \beta = 0,1,2,\ldots,N,h,r \tag{3.29a}$$

$$\mathcal{m}_\beta^o(z) = - \int_{\Gamma_i^o} x \; n_z^o(\vec{x}) \; p_\beta^o(\vec{x}) \; ds_1^o \; - \; \delta(z) \int_{\Gamma_e^o} x \; p_\beta^o(\vec{x}) \; d\Gamma \quad ; \quad \beta = 0,1,2, \ldots, N,h,r \tag{3.29b}$$

in which s_1^o defines the local coordinate along the perimeter of the outside surface for any fixed location z along the height (Figure 3.4) and $\delta(z)$ is the Dirac delta function. The second term in equation (3.29b) for external hydrodynamic moments represents a concentrated external moment at the base of the tower due to hydrodynamic pressures on the exposed surface of the foundation.

Introducing $\phi_h(z) = 1$ and $\psi_h(z) = 0$ as the rigid body lateral displacement and rotation of the tower axis associated with the unit lateral displacement of the foundation and $\phi_r(z) = z$ and $\psi_r(z) = 1$ as the corresponding functions associated with the rotation of the foundation, the functions $f_\beta^o(z)$ and $\mathcal{m}_\beta^o(z)$, $\beta = 0,1,2, \ldots, N,h,r$ can be shown (Appendix A) to have the following reciprocity property :

$$\int_0^{H_o} \phi_\beta(z) \, f_\gamma^o(z) \, dz + \int_0^{H_o} \psi_\beta(z) \, \mathcal{m}_\gamma^o(z) \, dz = \int_0^{H_o} \phi_\gamma(z) \, f_\beta^o(z) \, dz + \int_0^{H_o} \psi_\gamma(z) \, \mathcal{m}_\beta^o(z) \, dz \tag{3.30}$$

in which $\beta,\gamma = 0,1,2, \ldots, N,h,r$ and H_o is the depth of water surrounding the tower.

Generalized Forces -- Substitution of equation (3.28) into equations (3.13) to (3.15) and the reciprocity property of hydrodynamic forces [equation (3.30)] allows the response functions for generalized hydrodynamic forces appearing in equation (3.17) to be expressed as :

$$\bar{l}_n^o(\omega) = - \, \omega^2 \sum_{j=1}^{N} M_{nj}^o \, \bar{Y}_j(\omega) - \omega^2 \, L_n^{ho} \, \bar{u}_f(\omega) - \omega^2 \, L_n^{ro} \, \bar{\theta}_f(\omega) + L_n^o \; ; \; n=1,2, \ldots, N \tag{3.31a}$$

$$\bar{l}_h^o(\omega) = - \, \omega^2 \sum_{n=1}^{N} L_n^{ho} \, \bar{Y}_n(\omega) - \omega^2 \, m_l^o \, \bar{u}_f(\omega) - \omega^2 \, L_0^{ro} \, \bar{\theta}_f(\omega) + m_l^o \tag{3.31b}$$

$$\bar{l}_r^o(\omega) = - \, \omega^2 \sum_{n=1}^{N} L_n^{ro} \, \bar{Y}_n(\omega) - \omega^2 \, L_0^{ro} \, \bar{u}_f(\omega) - \omega^2 \, I_l^o \, \bar{\theta}_f(\omega) + L_0^{ro} \tag{3.31c}$$

where

$$M_{nj}^{o} = \int_{0}^{H_o} \phi_n(z)\, f_j^o(z)\, dz + \int_{0}^{H_o} \psi_n(z)\, m_j^o(z)\, dz \qquad j,n = 1,2, \ldots, N \tag{3.32}$$

$$L_n^o = L_n^{ho} = \int_{0}^{H_o} \phi_n(z)\, f_0^o(z)\, dz + \int_{0}^{H_o} \psi_n(z)\, m_0^o(z)\, dz \qquad n = 1,2, \ldots, N \tag{3.33}$$

$$L_n^{ro} = \int_{0}^{H_o} \phi_n(z)\, f_r^o(z)\, dz + \int_{0}^{H_o} \psi_n(z)\, m_r^o(z)\, dz \qquad n = 1,2, \ldots, N \tag{3.34}$$

Comparison of equation (3.31) with equation (3.6) and equations (3.32) to (3.34) with equations (3.7) to (3.9) suggests that M_{nj}^o and L_n^o can be interpreted as generalized added mass and added excitation associated with the hydrodynamic pressure on the outside surface. Similarly, L_n^{ho} and L_n^{ro} can be interpreted as the coefficients of the associated generalized added excitation due to translation and rotation, respectively, of the base of the tower.

In equation (3.31), the constants m_t^o, I_t^o and L_0^{ro} are given by the following equations:

$$m_t^o = \int_{0}^{H_o} f_h^o(z)\, dz \tag{3.35}$$

$$I_t^o = \int_{0}^{H_o} z\, f_r^o(z)\, dz + \int_{0}^{H_o} m_r^o(z)\, dz \tag{3.36}$$

$$L_0^{ro} = \int_{0}^{H_o} z\, f_h^o(z)\, dz + \int_{0}^{H_o} m_h^o(z)\, dz \tag{3.37}$$

Similar to m_t, I_t, and L_0^r for the tower [equations (3.10) to (3.12)], m_t^o, I_t^o, and L_0^{ro} represent the inertial influence of surrounding water due to lateral and rotational motions of the foundation. For a rigid tower supported on deformable soil, m_t^o, I_t^o, and L_0^{ro} can be interpreted as the generalized added hydrodynamic mass terms of the surrounding water associated with lateral and rotational motions of the foundation.

3.2.5 Inside Water Domain Substructure

Parallel to the analysis of surrounding water domain substructure, the frequency response functions of unknown hydrodynamic lateral forces $\bar{f}^{\,i}(z,\omega)$ and moments $\overline{m}^{\,i}(z,\omega)$, acting on the inside surface of the tower, are expressed in terms of inside surface accelerations, $a_n^i(\vec{x},\omega)$. For ground acceleration acting in the x direction, $a_n^i(\vec{x},\omega)$ at the tower-water interface Γ_t^i is related to the total lateral and rotational acceleration of the tower axis by the following equation :

$$a_n^i(\vec{x},\omega) = n_x^i(\vec{x})\ \overline{\ddot{u}^t}(z,\omega) - x\ n_z^i(\vec{x})\ \overline{\ddot{\theta}^t}(z,\omega) \tag{3.38}$$

where $n_x^i(\vec{x})$ and $n_z^i(\vec{x})$ are the direction cosines of the normal at a point $\vec{x}$ on the inside surface with respect to x and z axes respectively (Figure 3.5). The frequency response function for hydrodynamic pressure for inside water domain, $\bar{p}^i(\vec{x},\omega)$, also satisfies the Laplace equation [equation (3.18)], and therefore, similar to equation (3.21) for surrounding water domain, the boundary condition relating hydrodynamic pressure to acceleration of tower-water interface Γ_t^i (Figure 3.5) can be expressed as:

$$\frac{\partial}{\partial n^i}\ \bar{p}^i(\vec{x},\omega) = -\ \rho_w\ n_x^i(\vec{x})\ [\ 1 - \omega^2 \sum_{j=1}^{N} \phi_j(z)\ \bar{Y}_j(\omega) - \omega^2\ \bar{u}_f(\omega) - \omega^2\ z\ \bar{\theta}_f(\omega)\ ]$$

$$+\ \rho_w\ x\ n_z^i(\vec{x})\ [\ -\ \omega^2 \sum_{j=1}^{N} \psi_j(z)\ \bar{Y}_j(\omega) - \omega^2\ \bar{\theta}_f(\omega)\ ] \tag{3.39}$$

in which n^i represents the direction of the normal to the inside surface. The vertical acceleration of the bottom boundary Γ_b^i (Figure 3.5) of the water domain inside the tower due to rotation of the foundation is related to the hydrodynamic pressure on the boundary Γ_b^i by the following equation which is similar to the first part of equation (3.22) for surrounding water :

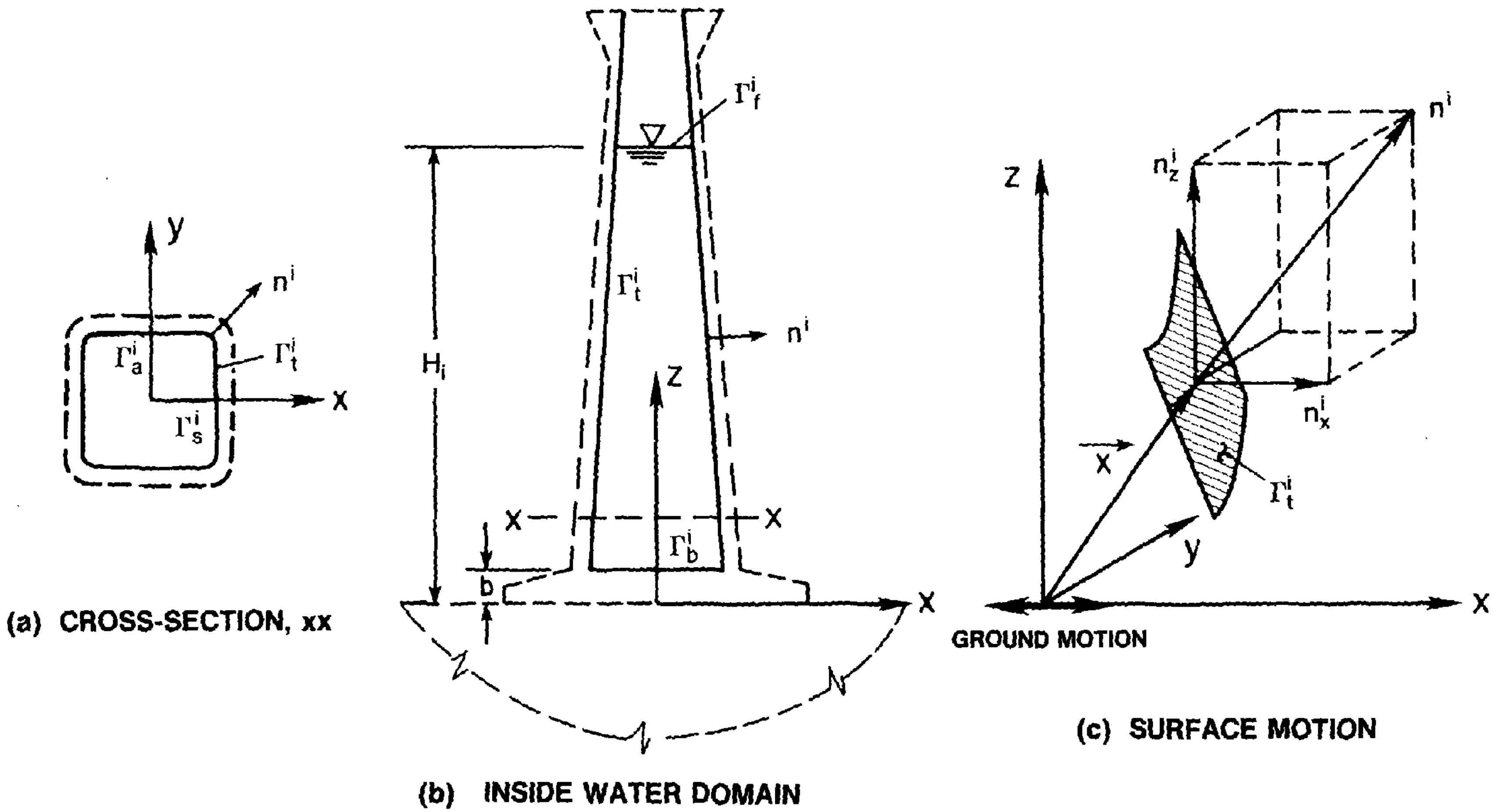

Figure 3.5 Notations and Definitions for Inside Water Domain

$$\frac{\partial}{\partial z}\,\bar{p}^{\,i}(\vec{x},\omega) = \rho_w\, x\, [\, -\,\omega^2\,\bar{\theta}_f(\omega)\,] \tag{3.40}$$

In addition to the boundary conditions of equations (3.39) and (3.40), the hydrodynamic pressure for inside water domain, $\bar{p}^{\,i}(\vec{x},\omega)$, also satisfies the free surface boundary condition, equation (3.23).

Similar to equations (3.24), (3.28a) and (3.28b) for surrounding water domain, the linear form of the governing equation and boundary conditions allow $\bar{p}^{\,i}(\vec{x},\omega)$, $\bar{f}^{\,i}(z,\omega)$ and $\overline{m}^{\,i}(z,\omega)$ to be expressed as :

$$\bar{p}^{\,i}(\vec{x},\omega) = p_0^i(\vec{x}) - \omega^2 \sum_{j=1}^{N} p_j^i(\vec{x})\,\bar{Y}_j(\omega) - \omega^2\, p_h^i(\vec{x})\,\bar{u}_f(\omega) - \omega^2\, p_r^i(\vec{x})\,\bar{\theta}_f(\omega) \tag{3.41}$$

$$\bar{f}^{\,i}(z,\omega) = f_0^i(z) - \omega^2 \sum_{j=1}^{N} f_j^i(z)\,\bar{Y}_j(\omega) - \omega^2\, f_h^i(z)\,\bar{u}_f(\omega) - \omega^2\, f_r^i(z)\,\bar{\theta}_f(\omega) \tag{3.42}$$

$$\overline{m}^{\,i}(z,\omega) = m_0^i(z) - \omega^2 \sum_{j=1}^{N} m_j^i(z)\,\bar{Y}_j(\omega) - \omega^2\, m_h^i(z)\,\bar{u}_f(\omega) - \omega^2\, m_r^i(z)\,\bar{\theta}_f(\omega) \tag{3.43}$$

Parallel to the definitions for surrounding water domain, in equations (3.41) to (3.43), $p_0^i(\vec{x})$, $f_0^i(z)$ and $m_0^i(z)$ are the hydrodynamic pressure, resultant lateral force and external hydrodynamic moment on the inside surface when the tower is rigid and excited by unit horizontal acceleration at the base (boundary conditions similar to equation (3.25) for outside water domain); $p_j^i(\vec{x})$, $f_j^i(z)$ and $m_j^i(z)$ are the corresponding functions when the tower is excited in its j-th mode and there is no motion of its base [c.f. equation (3.26)]; $p_h^i(\vec{x})$, $f_h^i(z)$ and $m_h^i(z)$ are the corresponding functions due to unit horizontal, interaction acceleration of the foundation with a rigid tower [c.f. equation (3.25)]; and $p_r^i(\vec{x})$, $f_r^i(z)$ and $m_r^i(z)$ are similar functions for a rigid tower excited by a unit rotational acceleration at the base [c.f. equation (3.27)]. A numerical procedure to solve the boundary value problems governing $p_0^i(\vec{x})$, $p_j^i(\vec{x})$, $p_h^i(\vec{x})$, and $p_r^i(\vec{x})$ is presented in Chapter 4.

The hydrodynamic force and moment functions are evaluated at any location z along the height by integrating their corresponding pressure functions along the perimeter of the inside surface Γ_t^i pertaining to that location by the following expressions :

$$f_\beta^i(z) = \int_{\Gamma_t^i} n_x^i(\vec{x})\, p_\beta^i(\vec{x})\, ds_1^i \quad ; \quad \beta = 0,1,2,\ldots,N,h,r \tag{3.44a}$$

$$m_\beta^i(z) = -\int_{\Gamma_t^i} x\, n_z^i(\vec{x})\, p_\beta^i(\vec{x})\, ds_1^i - \delta(z-b)\int_{\Gamma_b^i} x\, p_\beta^i(\vec{x})\, d\Gamma \quad ; \quad \beta=0,1,2,\ldots,N,h,r \tag{3.44b}$$

in which s_1^i defines the local coordinate along the perimeter of the inside surface at location z above the base and b represents the distance of the bottom boundary for inside water domain from the assumed ground level (Figure 3.5). The second term in equation (3.44b) for hydrodynamic moments represents a concentrated external moment due to hydrodynamic pressures at the bottom boundary of the inside water domain. However, this term contributes only to those hydrodynamic terms which are associated with the rotation of the foundation [equation (3.15)].

Since the reciprocity property of hydrodynamic forces for surrounding water [equation (3.30)] also applies for inside water [Appendix A, Section A.2], the frequency response functions for generalized hydrodynamic forces appearing in equation (3.17), namely $\bar{l}_n^i(\omega)$, $\bar{l}_h^i(\omega)$ and $\bar{l}_r^i(\omega)$, are expressed, in a form similar to equation (3.31) for surrounding water:

$$\bar{l}_n^i(\omega) = -\omega^2 \sum_{j=1}^{N} M_{nj}^i\, \bar{Y}_j(\omega) - \omega^2 L_n^{hi}\, \bar{u}_f(\omega) - \omega^2 L_n^{ri}\, \bar{\theta}_f(\omega) + L_n^i \quad ; \quad n=1,2,\ldots,N \tag{3.45a}$$

$$\bar{l}_h^i(\omega) = -\omega^2 \sum_{n=1}^{N} L_n^{hi}\, \bar{Y}_n(\omega) - \omega^2 m_t^i\, \bar{u}_f(\omega) - \omega^2 L_0^{ri}\, \bar{\theta}_f(\omega) + m_t^i \tag{3.45b}$$

$$\bar{l}_r^i(\omega) = -\omega^2 \sum_{n=1}^{N} L_n^{ri}\, \bar{Y}_n(\omega) - \omega^2 L_0^{ri}\, \bar{u}_f(\omega) - \omega^2 I_t^i\, \bar{\theta}_f(\omega) + L_0^{ri} \tag{3.45c}$$

The added hydrodynamic mass and excitation terms M_{nj}^i, L_n^i, L_n^{hi}, and L_n^{ri} are given by equations (3.32) to (3.34) ; and the generalized mass terms m_t^i, I_t^i, and L_0^{ri} due to horizontal and rotational, interaction accelerations of the foundation by equations (3.35) to (3.37) with the following modifications : (i) the integration limit is the height H_i (i.e. up to the free surface) from the assumed ground level (Figure 3.5) and (ii) $f_\beta^o(z)$ and $m_\beta^o(z)$ are replaced by $f_\beta^i(z)$ and $m_\beta^i(z)$, respectively. Parallel to their counterparts for surrounding water, all these terms carry similar physical interpretation for inside water.

3.2.6 Tower-Water-Foundation-Soil System

Substitution of equations (3.31) and (3.45) into equation (3.17) and retaining only the first N natural vibration modes leads to :

$$- \omega^2 \sum_{j=1}^{N} \tilde{M}_{nj} \, \bar{Y}_j(\omega) + (1+i\eta_s) \, M_n \, \omega_n^2 \, \bar{Y}_n(\omega) - \omega^2 \, \tilde{L}_n^h \, \bar{u}_f(\omega) - \omega^2 \, \tilde{L}_n^r \, \bar{\theta}_f(\omega)$$

$$= - \tilde{L}_n \quad ; \quad n=1,2, \ldots, N \tag{3.46a}$$

$$- \omega^2 \sum_{n=1}^{N} \tilde{L}_n^h \, \bar{Y}_n(\omega) - \omega^2 \, (\tilde{m}_t + m_f) \, \bar{u}_f(\omega) - \omega^2 \, \tilde{L}_0^r \, \bar{\theta}_f(\omega) + K_{VV}(\omega) \, \bar{u}_f(\omega)$$

$$+ K_{VM}(\omega) \, \bar{\theta}_f(\omega) = - (\tilde{m}_t + m_f) \tag{3.46b}$$

$$- \omega^2 \sum_{n=1}^{N} \tilde{L}_n^r \, \bar{Y}_n(\omega) - \omega^2 \, \tilde{L}_0^r \, \bar{u}_f(\omega) - \omega^2 \, (\tilde{I}_t + I_f) \, \bar{\theta}_f(\omega) + K_{MV}(\omega) \, \bar{u}_f(\omega)$$

$$+ K_{MM}(\omega) \, \bar{\theta}_f(\omega) = - \tilde{L}_0^r \tag{3.46c}$$

where

$$\tilde{M}_{nj} = M_n \, \delta_{nj} + M_{nj}^o + M_{nj}^i \quad ; \quad n,j=1,2, \ldots, N \tag{3.47a}$$

$$\tilde{L}_n^h = \tilde{L}_n = L_n + L_n^o + L_n^i \quad ; \quad n=1,2,\ldots,N \tag{3.47b}$$

$$\tilde{L}_n^r = L_n^r + L_n^{ro} + L_n^{ri} \quad ; \quad n=1,2,\ldots,N \tag{3.47c}$$

$$\tilde{m}_t = m_t + m_t^o + m_t^i \tag{3.47d}$$

$$\tilde{I}_t = I_t + I_t^o + I_t^i \tag{3.47e}$$

$$\tilde{L}_0^r = L_0^r + L_0^{ro} + L_0^{ri} \tag{3.47f}$$

Equation (3.46) contains the effects of tower-water interaction and tower-foundation-soil interaction. The surrounding water introduces the added hydrodynamic mass terms M_{nj}^o and added excitation terms L_n^o, and the inside water contributes corresponding terms M_{nj}^i and L_n^i. The translation $\bar{u}_f(\omega)$ and rotation $\bar{\theta}_f(\omega)$ of the foundation permitted by the deformability of the underlying soil introduce two additional equations which are coupled to the modal equations of the tower through inertia terms L_n and L_n^r. In these two additional equations, the lateral and rotational motions of the foundation result in the generalized mass terms m_t, I_t, and L_0^r associated with the mass of the tower ; m_t^o, I_t^o, and L_0^{ro} associated with the inertial influence of the surrounding water ; and m_t^i, I_t^i, L_0^{ri} associated with the inertial influence of the inside water. The lateral and rotational motions of the foundation also lead to added excitation terms (which are also the coupling terms between motions of the foundation and the modal coordinates) L_n^o and L_n^{ro} due to the surrounding water, and L_n^i and L_n^{ri} due to the inside water. It should be noted that equation (3.46) is identical to equation (5) in Reference [12] for building-foundation systems except for added hydrodynamic mass and excitation terms associated with the effects of outside and inside water.

These equations represent $N+2$ complexed valued equations in the frequency response functions for the modal coordinates $\bar{Y}_j(\omega)$, $j=1,2,\ldots,N$, corresponding to the first N

vibration mode shapes of the tower without water on fixed base, and the frequency response functions $\bar{u}_f(\omega)$ and $\bar{\theta}_f(\omega)$ for interaction displacement and rotation of the foundation, respectively. For each excitation frequency of interest, these simultaneous equations are to be solved to give $\bar{Y}_j(\omega)$. Repeated solution for the excitation frequencies covering the range over which the earthquake ground motion and structural response have significant components leads to the complete frequency response functions for the modal coordinates.

3.3 Response to Arbitrary Ground Motion

The response of the tower to arbitrary ground motion can be computed once the frequency response functions $\bar{Y}_j(\omega)$, $j=1,2,\ldots,N$, for the modal coordinates have been obtained from the solution of equation (3.46) for excitation frequencies in the range of interest. The response time histories of modal coordinates are given by the Fourier integral as a superposition of responses to individual harmonic components of the ground motion :

$$Y_j(t) = \frac{1}{2\pi} \int_{-\infty}^{+\infty} \bar{Y}_j(\omega)\, \bar{\ddot{u}}_g(\omega)\, e^{i\omega t}\, d\omega \tag{3.48}$$

where $\bar{\ddot{u}}_g(\omega)$ is the Fourier transform of the specified free-field ground acceleration $\ddot{u}_g(t)$:

$$\bar{\ddot{u}}_g(\omega) = \int_0^d \ddot{u}_g(t)\, e^{-i\omega t}\, dt \tag{3.49}$$

in which d is the duration of the ground motion. The Fourier integrals in equations (3.48) and (3.49) are computed in their discrete forms using the Fast Fourier Transform (FFT) algorithm [6,23]. The lateral displacements and bending slopes of the tower axis are obtained by superposing modal responses [equation (3.5)]:

$$u(z,t) = \sum_{j=1}^{N} \phi_j(z)\, Y_j(t) \tag{3.50a}$$

$$\theta(z,t) = \sum_{j=1}^{N} \psi_j(z)\; Y_j(t) \tag{3.50b}$$

The shear force $Q(z,t)$ and bending moment $\mathcal{M}(z,t)$ along the height of the tower can be determined by the static force-displacement relationship using the cross-sectional stiffnesses $G_s k(z) A(z)$ in shear and $E_s I(z)$ in bending :

$$Q(z,t) = \sum_{n=1}^{N} Q_n(z)\; Y_n(t) \tag{3.51a}$$

$$\mathcal{M}(z,t) = \sum_{n=1}^{N} \mathcal{M}_n(z)\; Y_n(t) \tag{3.51b}$$

where

$$Q_n(z) = G_s\; k(z)\, A(z) \left[\frac{d}{dz}\, \phi_n(z) - \psi_n(z) \right] \tag{3.52a}$$

$$\mathcal{M}_n(z) = E_s\, I(z)\, \frac{d}{dz}\, \psi_n(z) \tag{3.52b}$$

In equation (3.52), $Q_n(z)$ and $\mathcal{M}_n(z)$ represent the height-wise distribution of shear forces and bending moments associated with deflections of the tower in the n-th vibration mode described by lateral displacements $\phi_n(z)$ and bending slopes $\psi_n(z)$ of the tower axis. Instead of equation (3.52) which involves the derivatives of mode shape functions $\phi_n(z)$ and $\psi_n(z)$, the elastic forces can be expressed in terms of the mass of the tower [14]. This leads to :

$$Q_n(z) = \omega_n^2 \int_z^{H_s} m_s(\xi)\, \phi_n(\xi)\, d\xi \tag{3.53a}$$

$$\mathcal{M}_n(z) = \omega_n^2 \left[\int_z^{H_s} (\,\xi - z\,)\, m_s(\xi)\, \phi_n(\xi)\, d\xi + \int_z^{H_s} I_s(\xi)\, \psi_n(\xi)\, d\xi \right] \tag{3.53b}$$

where ω_n is the natural frequency of the n-th vibration mode of the fixed-base tower without water. A complete derivation of equation (3.53) is presented in Appendix B. Once $Q_n(z)$

and $m_n(z)$ are computed using equation (3.53), then at any instant of time, the shear force and bending moment at any location along the height can be evaluated from equation (3.51).

In practical applications, it would be necessary to analyze the tower for two components of the horizontal ground motion applied along the planes of symmetry. In that case, the response of the tower to each component of the ground motion can be computed individually by the above-mentioned procedure utilizing the tower properties appropriate for vibration along the direction of the ground motion component. The analysis will result in forces (shears and bending moments) acting in two mutually perpendicular planes.

4. NUMERICAL EVALUATION PROCEDURES

The procedure presented in Chapter 3 to analyze the earthquake response of intake-outlet towers requires the evaluation of natural vibration frequencies and mode shapes of the tower, the foundation impedance functions, and the added hydrodynamic mass and excitation terms in the equations of motion [equation (3.46)]. In this chapter, efficient numerical solution procedures are developed for evaluating these quantities separately for each of the four substructures : tower, foundation-soil system, fluid domain surrounding the tower, and the fluid domain contained within the tower.

4.1 Tower Vibration Properties

4.1.1 Eigen Value Problem

The eigen value problem governing the undamped free vibrations of the tower (with fixed base and no water) can be derived from equation (3.1) by expressing the lateral displacements $u(z,t)$ due to bending and shear deformations, and bending slopes $\theta(z,t)$ along the height of the tower axis in the following form :

$$u(z,t) = \phi(z)\, e^{i\omega t} \tag{4.1a}$$

$$\theta(z,t) = \psi(z)\, e^{i\omega t} \tag{4.1b}$$

which results in two coupled differential equations in two unknown functions, $\phi(z)$ and $\psi(z)$, for the deflection curve of the tower axis corresponding to lateral displacements and bending slopes, respectively [28]:

$$-\omega^2 m_s(z)\,\phi(z) - \frac{d}{dz}\left[G_s k(z) A(z)\left[\frac{d}{dz}\phi(z) - \psi(z)\right]\right] = 0 \tag{4.2a}$$

$$-\omega^2 I_s(z)\,\psi(z) - \frac{d}{dz}\left[E_s I(z)\,\frac{d}{dz}\psi(z)\right] - G_s k(z) A(z)\left[\frac{d}{dz}\phi(z) - \psi(z)\right] = 0 \tag{4.2b}$$

in which ω is the natural frequency of vibration of the tower; $m_s(z)$, $I_s(z)$ represent the mass and rotatory inertia along the height; and $G_s k(z) A(z)$, $E_s I(z)$ are the cross-sectional stiffnesses of the tower in pure shear and pure bending, respectively, at a location z above the base. The boundary conditions associated with equation (4.2) can be expressed in terms of variables $\phi(z)$ and $\psi(z)$ as follows :

(i) The deflection at the tower base vanishes :

$$\left[\phi(z) \right]_{z=0} = 0 \tag{4.3a}$$

(ii) The slope, due to bending only, vanishes at the tower base :

$$\left[\psi(z) \right]_{z=0} = 0 \tag{4.3b}$$

(iii) The bending moment at the top of the tower vanishes :

$$\left[E_s I(z) \frac{d}{dz} \psi(z) \right]_{z=H_s} = 0 \tag{4.3c}$$

(iv) The shear force at the top of the tower vanishes :

$$\left[G_s k(z) A(z) \left[\frac{d}{dz} \phi(z) - \psi(z) \right] \right]_{z=H_s} = 0 \tag{4.3d}$$

Equations (4.2) and (4.3) constitute the strong formulation of the eigen value problem. Its analytical solutions are available only for simple cases, e.g. towers of uniform cross-section and constant material properties along the height [28]. In order to analyze towers of arbitrary geometry considered here, a weak formulation of the eigen value problem is obtained by multiplying equations (4.2a) and (4.2b) respectively by variation functions $\bar{\phi}(z)$ and $\bar{\psi}(z)$, adding them together, integrating by parts over the height and using the boundary conditions of equation (4.3). This leads to :

$$\int_0^{H_s} E_s I(z) \frac{d}{dz}\bar{\psi}(z) \frac{d}{dz}\psi(z)\, dz + \int_0^{H_s} G_s k(z) A(z)\, \bar{\psi}(z)\, \psi(z)\, dz$$

$$+ \int_0^{H_s} G_s k(z) A(z) \frac{d}{dz}\bar{\phi}(z) \frac{d}{dz}\phi(z)\, dz$$

$$- \int_0^{H_s} G_s k(z) A(z) \frac{d}{dz}\bar{\phi}(z)\, \psi(z)\, dz - \int_0^{H_s} G_s k(z) A(z)\, \bar{\psi}(z) \frac{d}{dz}\phi(z)\, dz$$

$$= \omega^2 \left[\int_0^{H_s} m_s(z)\, \bar{\phi}(z)\, \phi(z)\, dz + \int_0^{H_s} I_s(z)\, \bar{\psi}(z)\, \psi(z)\, dz \right] \tag{4.4}$$

This integral form permits approximate solutions of natural vibration frequencies and mode shapes by the finite element method.

4.1.2 Finite Element Approximation

The tower structure is idealized by a one-dimensional finite element system with N_S nodal points. Let ϕ_i, ψ_i, $i = 1,2, \ldots, N_S$ be the unknown values of functions $\phi(z)$, $\psi(z)$, at N_S nodal points and $N_i(z)$, $i = 1,2, \ldots, N_S$ be the locally supported one-dimensional continuous interpolation functions of class C_0 corresponding to each nodal point, then the functions $\phi(z)$ and $\psi(z)$ are approximated by :

$$\phi(z) \approx \sum_{i=1}^{N_S} N_i(z)\, \phi_i \tag{4.5a}$$

$$\psi(z) \approx \sum_{i=1}^{N_S} N_i(z)\, \psi_i \tag{4.5b}$$

in which all interpolation functions satisfy the following condition at nodal points to maintain the global continuity of functions $\phi(z)$ and $\psi(z)$:

$$N_i(z_j) = \delta_{ij} \qquad ; \qquad i,j = 1,2, \ldots, N_S \tag{4.6}$$

where z_j represents the coordinate for the j-th node and δ_{ij} is the Kronecker delta function. Corresponding to $2N_S$ unknowns, namely ϕ_i's and ψ_i's, the $2N_S$ different set of variation functions $\bar{\phi}(z)$ and $\bar{\psi}(z)$ are defined by the Galerkin method [53] :

$$\begin{aligned} \bar{\phi}(z) &= N_i(z) \\ \bar{\psi}(z) &= 0 \end{aligned} \qquad i = 1,2, \ldots, N_S \tag{4.7a}$$

and

$$\begin{aligned} \bar{\phi}(z) &= 0 \\ \bar{\psi}(z) &= N_i(z) \end{aligned} \qquad i = 1,2, \ldots, N_S \tag{4.7b}$$

Let $\boldsymbol{\phi}$ be a vector of order $2N_S$ defined as :

$$\boldsymbol{\phi}^T = [\, \phi_1 \,, \psi_1 \,, \phi_2 \,, \psi_2 \,, \ldots , \phi_{N_S} \,, \psi_{N_S} \,] \tag{4.8}$$

then substituting equation (4.5) into equation (4.4), and using equations (4.7a) and (4.7b) alternatively for each nodal point to define the variation functions, leads to standard matrix form of the eigen value problem :

$$\boldsymbol{K}_s \, \boldsymbol{\phi} = \omega^2 \, \boldsymbol{M}_s \, \boldsymbol{\phi} \tag{4.9}$$

in which $\boldsymbol{K}_s$ and $\boldsymbol{M}_s$ are the symmetric stiffness and mass matrices, respectively, of order $2N_S \times 2N_S$. The elements of the stiffness matrix $\boldsymbol{K}_s$ are related to the cross-sectional stiffness properties of the tower and the interpolation functions :

$$(\, \boldsymbol{K}_s \,)_{2i-1,2j-1} = \int_0^{H_s} G_s k(z) A(z) \, \frac{d}{dz} N_i(z) \, \frac{d}{dz} N_j(z) \, dz \tag{4.10a}$$

$$(\, \boldsymbol{K}_s \,)_{2i,2j} = \int_0^{H_s} E_s I(z) \, \frac{d}{dz} N_i(z) \, \frac{d}{dz} N_j(z) \, dz + \int_0^{H_s} G_s k(z) A(z) \, N_i(z) \, N_j(z) \, dz \tag{4.10b}$$

$$(\, \boldsymbol{K}_s \,)_{2i-1,2j} = - \int_0^{H_s} G_s k(z) A(z) \, \frac{d}{dz} N_i(z) \, N_j(z) \, dz \tag{4.10c}$$

$$(\, \boldsymbol{K}_s \,)_{2i,2j-1} = - \int_0^{H_s} G_s k(z) A(z) \, N_i(z) \, \frac{d}{dz} N_j(z) \, dz \tag{4.10d}$$

where $i,j = 1,2,\ldots,N_S$. Similarly, in terms of the cross-sectional inertial properties of the tower (i.e. mass and rotatory inertia distributions of the tower) and the interpolation functions, the elements of mass matrix $\boldsymbol{M}_s$ are:

$$(\boldsymbol{M}_s)_{2i-1,2j-1} = \int_0^{H_s} m_s(z)\, N_i(z)\, N_j(z)\, dz \tag{4.11a}$$

$$(\boldsymbol{M}_s)_{2i,2j} = \int_0^{H_s} I_s(z)\, N_i(z)\, N_j(z)\, dz \tag{4.11b}$$

$$(\boldsymbol{M}_s)_{2i-1,2j} = (\boldsymbol{M}_s)_{2i,2j-1} = 0 \tag{4.11c}$$

where $i,j = 1,2,\ldots,N_S$. Since $N_i(z)$, $i = 1,2,\ldots,N_S$ are locally supported interpolation functions, integration in equations (4.10) and (4.11) is not performed over the full height of the tower for each term but only over the height of each one-dimensional finite element to obtain the element stiffness and mass matrices. These element matrices are assembled by standard procedures [53] to yield global stiffness and mass matrices, $\boldsymbol{K}_s$ and $\boldsymbol{M}_s$, respectively.

Many numerical techniques are available to solve the eigen value problem of equation (4.9). The procedure used here is inverse iteration with Gram-Schmidt orthogonalization to obtain the first N mode shapes, $\boldsymbol{\phi}_n$, in vector form, and then compute the corresponding frequency ω_n from the Rayleigh Quotient [2]. The mode shape functions $\phi_n(z)$ and $\psi_n(z)$ are then evaluated from $\boldsymbol{\phi}_n$ by equation (4.5), which have the following orthogonality properties [27]:

$$\int_0^{H_s} m_s(z)\, \phi_n(z)\, \phi_m(z)\, dz + \int_0^{H_s} I_s(z)\, \psi_n(z)\, \psi_m(z)\, dz = 0 \qquad if\ \omega_n \neq \omega_m \tag{4.12a}$$

$$\int_0^{H_s} G_s k(z) A(z) \left[\frac{d}{dz}\phi_n(z) - \psi_n(z) \right] \left[\frac{d}{dz}\phi_m(z) - \psi_m(z) \right] dz$$

$$+ \int_0^{H_s} E_s I(z)\, \frac{d}{dz}\psi_n(z)\, \frac{d}{dz}\psi_m(z)\, dz = 0 \qquad if\ \omega_n \neq \omega_m \tag{4.12b}$$

As is well known, it is due to these orthogonality properties that the modal equations for the tower alone [equation (3.6a)] are not coupled through the generalized mass and stiffness terms.

The effects of shear deformations and rotatory inertia on the vibration properties of tower are examined by evaluating the natural vibration frequencies of circular cylindrical towers with inside and outside radii ratio equal to 0.8 by two methods, resulting in ω_n from the weak formulation of the Timoshenko beam theory and ω_{bn} from the analytical solutions of the classical Euler's beam theory [14] which includes only bending deformations and neglects rotatory inertia. The frequency ratio ω_n/ω_{bn} for circular cylindrical towers is plotted against the average radius-to-tower-height ratio, r_a/H_s, for the first two natural modes of vibration of the fixed-base tower without water (Figure 4.1). These results demonstrate the well known results that the influence of shear deformations and rotatory inertia on the vibration frequencies increases for increasing mode number and for decreasing slenderness ratio, i.e. increasing r_a/H_s, and that more than three-fourths of the change in frequencies because of these two effects is due to shear deformations [14,28]. Therefore, in the dynamic analysis of towers considering only one or two modes of vibration, while the contributions of shear deformations should be included in the analysis of squat towers, the influence of rotatory inertia may be neglected.

4.2 Foundation Impedance Functions

4.2.1 System Idealization

The foundation is idealized as a rigid, massless footing of infinitesimal thickness with shape and size of the actual foundation (Figure 2.1). The foundation is supported on the surface of a linear viscoelastic halfspace, which is idealized as a constant hysteretic solid characterized by its shear modulus of elasticity, G_f, the mass density, ρ_f, Poisson's ratio, ν_f, and the specific loss factor, $\Delta W/W$. For a viscoelastic solid in harmonic motion, ΔW is the area of the elliptical hysteresis loop in the stress-strain relationship and W is the strain

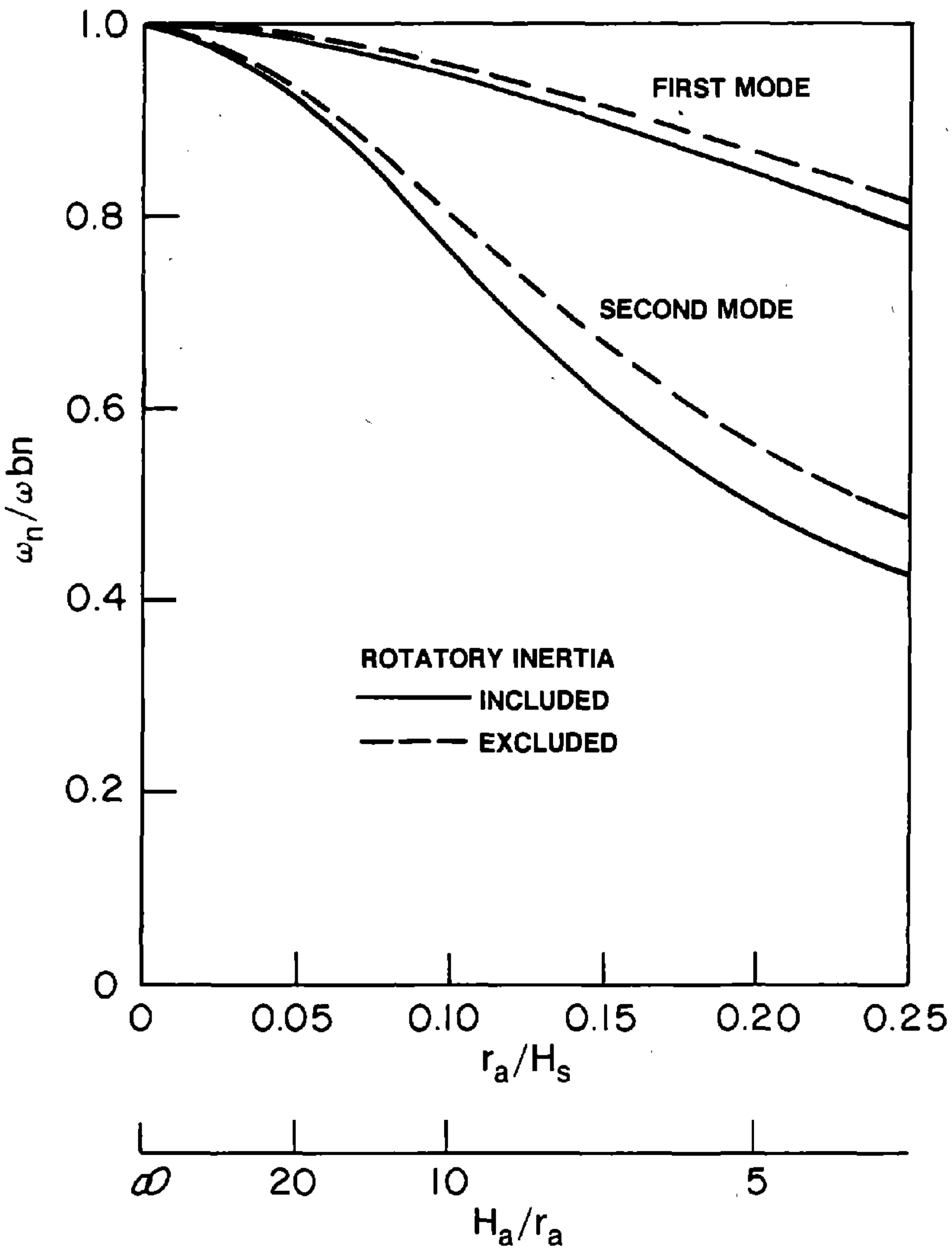

Figure 4.1 Effects of Shear Deformations on Natural Frequencies of Circular Cylindrical Towers

energy stored in a linear elastic material which is subjected to the same amplitudes of stress and strain as the viscoelastic material (Figure 4.2). For a linear material $\Delta W = 0$. For a constant hysteretic solid, $\Delta W / W$ is independent of the excitation frequency, and can expressed as

$$\frac{\Delta W}{W} = 2 \pi \eta_f \tag{4.13}$$

where η_f is the damping factor. The effective shear modulus for a constant hysteretic solid undergoing harmonically varying stresses and strains is

$$\tilde{G}_f = G_f (1 + i \eta_f) \tag{4.14}$$

Laboratory tests [43] on soils indicate that generally the stress-strain loop is not an ellipse, i.e. soils are not perfect viscoelastic solids, and $\Delta W / W$ is essentially independent of the vibration frequency but a function of the strain amplitude. In this investigation, it is presumed that, provided the values of $\Delta W / W$ for the soil and the viscoelastic solid are taken equal, the viscoelastic model considered adequately simulates the actual behavior of soils.

Under these assumptions, the impedance functions $K_{VV}(\omega)$, $K_{MM}(\omega)$ and $K_{VM}(\omega)$ [$K_{MV}(\omega) = K_{VM}(\omega)$ by reciprocity theorem], which appear in the equations of motion for tower-water-foundation-soil system [equation (3.46)], are obtained from the solution of two boundary value problems for a viscoelastic halfspace, arising from the application of a harmonic horizontal force and a harmonic moment separately to the rigid foundation. These solutions can be obtained by the application of the correspondence principle [5] to analytical approximations of numerically obtained solutions for the corresponding elastic problem [47]. This approach may be used if (i) the solutions of the impedance functions for the corresponding elastic problem are available, and (ii) they do not fluctuate strongly with frequency, thus permitting analytical approximations. Numerical values of the impedance functions have been reported for circular and rectangular foundations supported on the

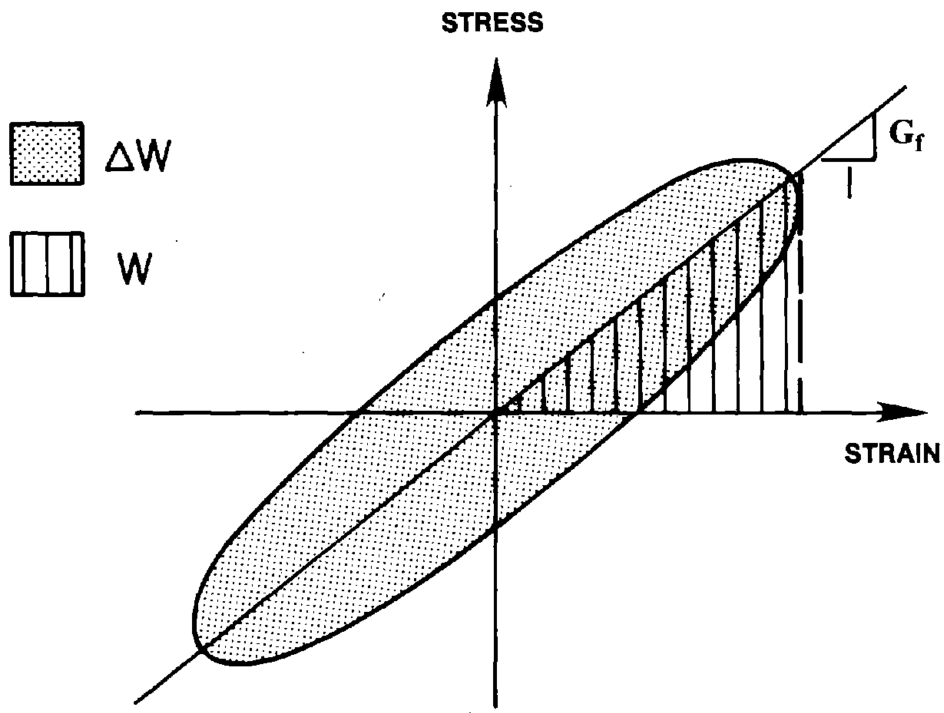

Figure 4.2 Stress-Strain Ellipse for Viscoelastic Material (Adapted from Reference [47])

surface of an elastic halfspace [48,51]. For other foundation geometries, the impedance functions can be obtained by discrete methods [50]. Utilizing the procedures of Reference [47], the impedance functions are derived next for a circular foundation supported on the surface of a viscoelastic halfspace.

4.2.2 Circular Foundation on Elastic Halfspace

The impedance functions for a rigid circular foundation supported on the surface of an elastic halfspace can be represented in the following form :

$$K_{VV}(\omega) = [\ k_{VV}(a_f,\nu_f) + i\ a_f\ c_{VV}(a_f,\nu_f)\ ]\ K_x \tag{4.15a}$$

$$K_{MM}(\omega) = [\ k_{MM}(a_f,\nu_f) + i\ a_f\ c_{MM}(a_f,\nu_f)\ ]\ K_\theta \tag{4.15b}$$

$$K_{VM}(\omega) = [\ k_{VM}(a_f,\nu_f) + i\ a_f\ c_{VM}(a_f,\nu_f)\ ]\ K_x\ r_f \tag{4.15c}$$

in which k's and c's are the dimensionless real-valued coefficients that depend on Poisson's ratio ν_f and the frequency parameter :

$$a_f = \frac{\omega\ r_f}{C_s} \tag{4.16}$$

where r_f is the radius of the foundation, and $C_f = \sqrt{(G_f/\rho_f)}$ is the shear wave velocity in the halfspace. In equation (4.15), the symbols K_x and K_θ represent the static stiffness of the foundation in horizontal and rotational directions; they are defined as :

$$K_x = \frac{8\ G_f\ r_f}{(\ 2 - \nu_f\ )} \tag{4.17a}$$

$$K_\theta = \frac{8\ G_f\ r_f^3}{3\ (\ 1 - \nu_f\ )} \tag{4.17b}$$

The real parts of the impedance functions represent force components in phase with the displacements, and may be therefore be interpreted as dynamic stiffness coefficients for the foundation-soil system. The imaginary parts, on the other hand, are force components in phase with the velocities and when positive, are indicative of energy dissipation by radiation of waves away from the foundation into the halfspace, and may therefore be interpreted as damping coefficients.

The coefficients k_{VV}, c_{VV}, k_{MM} and c_{MM}, which appear in equation (4.15) have been obtained by solving the two boundary value problems mentioned above and tabulated [48]. In the present investigation, these coefficients are approximated by the following semi-empirical expressions [47] :

$$k_{VV}(a_f,\nu_f) \approx 1 - \gamma_1 \frac{[\ \gamma_2\ a_f\ ]^2}{1 + [\ \gamma_2\ a_f\ ]^2} - \gamma_3\ a_f^2 \tag{4.18a}$$

$$c_{VV}(a_f,\nu_f) \approx \gamma_4 + \gamma_1\ \gamma_2 \frac{[\ \gamma_2\ a_f\ ]^2}{1 + [\ \gamma_2\ a_f\ ]^2} \tag{4.18b}$$

$$k_{MM}(a_f,\nu_f) \approx 1 - \beta_1 \frac{[\ \beta_2\ a_f\ ]^2}{1 + [\ \beta_2\ a_f\ ]^2} - \beta_3\ a_f^2 \tag{4.19a}$$

$$c_{MM}(a_f,\nu_f) \approx \beta_4 + \beta_1\ \beta_2 \frac{[\ \beta_2\ a_f\ ]^2}{1 + [\ \beta_2\ a_f\ ]^2} \tag{4.19b}$$

where γ_i and β_i are numerical coefficients which depend on Poisson's ratio, ν_f. An iterative numerical scheme was used to determine these coefficients in order for the semi-empirical expressions to provide a "best" fit to the "exact" data.

The numerical values of impedance functions for an elastic halfspace presented in Reference [48] are used in this investigation as "exact" data to evaluate coefficients γ_i and β_i. The resulting coefficients presented in Table 4.1 differ from those originally suggested in Reference [47]. The stiffness coefficients k_{VV}, k_{MM} and damping coefficients c_{VV} and c_{MM} evaluated from equations (4.18) and (4.19) using two sets of numerical values for coefficients γ_i and β_i, one from Table 4.1 and the other from Reference [47], are presented in Figure 4.3 along with their "exact" values [48]. It is apparent that the coefficients of Table 4.1 are preferable to those of Reference [47] as the former provide a better approximation. Since the coupling terms k_{VM} and c_{VM} show strong fluctuations with frequency [48], they are not

Table 4.1 -- Values of γ_i and β_i in Equations (4.18) and (4.19)

Quantity	$\nu_f=0$	$\nu_f=1/3$	$\nu_f=0.45$	$\nu_f=1/2$
γ_1	0.19 (0.00)*	0.16 (0.00)	0.06 (0.00)	0.00 (0.00)
γ_2	0.44 (0.00)	0.44 (0.00)	0.16 (0.00)	0.00 (0.00)
γ_3	0.00 (0.00)	0.00 (0.00)	0.00 (0.00)	0.00 (0.00)
γ_4	0.70 (0.775)	0.59 (0.65)	0.59 (0.60)	0.59 (0.60)
β_1	0.72 (0.525)	0.69 (0.50)	0.53 (0.45)	0.40 (0.40)
β_2	0.60 (0.80)	0.60 (0.80)	0.73 (0.80)	0.78 (0.80)
β_3	-0.003 (0.00)	-0.001 (0.00)	0.020 (0.00)	0.029 (0.00)
β_4	0.00 (0.00)	0.00 (0.00)	0.00 (0.00)	0.00 (0.00)

* Values in ( ) are from Reference [47]

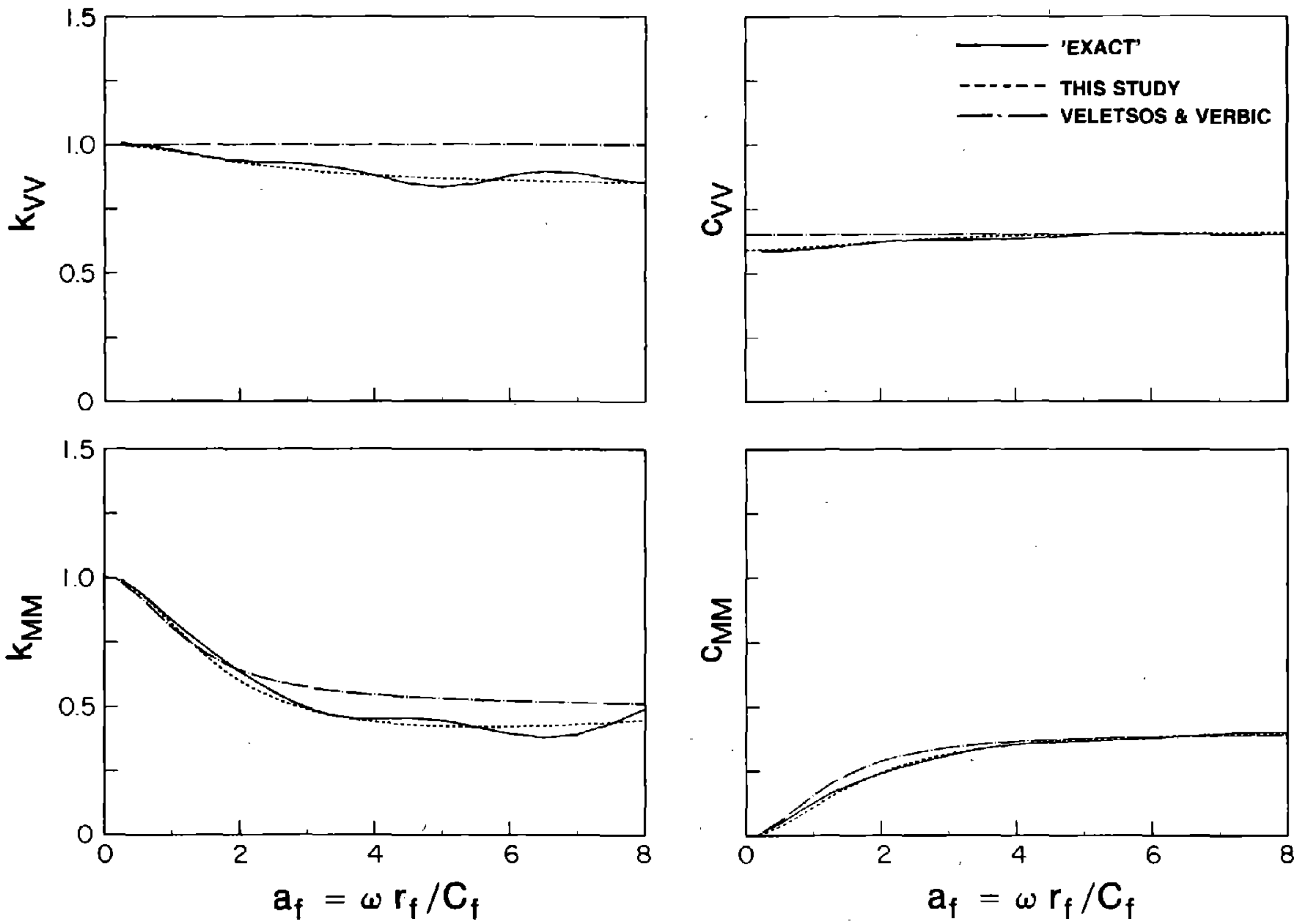

Figure 4.3 Functions k_{VV} , k_{MM} , c_{VV} and c_{MM} for Circular Footing on Elastic Halfspace with $\nu_f = 1/3$

approximated by expressions like equation (4.18) or (4.19).

4.2.3 Circular Foundation on Viscoelastic Halfspace

The impedance functions for the foundation on a viscoelastic halfspace are determined from equation (4.15) by application of the correspondence principle [5] merely by replacing the real-valued shear modulus G_f by the complex modulus $\tilde{G}_f$. Implicit in this statement is the assumption that Poisson's ratio for the viscoelastic material is a real-valued quantity equal to that for the material in the corresponding elastic problem. It should be noted that G_f enters in equation (4.15) both directly in the expressions for a_f, K_x and K_θ [equations (4.16) and (4.17)], and indirectly, through the dependence of k's and c's on a_f [equations (4.18) and (4.19)]. Application of the correspondence principle to equation (4.15) leads to :

$$K_{VV}(\omega) = [\ k_{VV}(\tilde{a}_f,\nu_f) + i\ \tilde{a}_f\ c_{VV}(\tilde{a}_f,\nu_f)\ ]\ \tilde{K}_x \tag{4.20a}$$

$$K_{MM}(\omega) = [\ k_{MM}(\tilde{a}_f,\nu_f) + i\ \tilde{a}_f\ c_{MM}(\tilde{a}_f,\nu_f)\ ]\ \tilde{K}_\theta \tag{4.20b}$$

$$K_{VM}(\omega) = [\ k_{VM}(\tilde{a}_f,\nu_f) + i\ \tilde{a}_f\ c_{VM}(\tilde{a}_f,\nu_f)\ ]\ \tilde{K}_x\ r_f \tag{4.20c}$$

where

$$\begin{aligned} \tilde{K}_x &= K_x\ (\ 1 + i\ \eta_f\ ) \\ \tilde{K}_\theta &= K_\theta\ (\ 1 + i\ \eta_f\ ) \\ \tilde{a}_f &= a_f \ /\ \sqrt{1 + i\eta_f} \end{aligned} \tag{4.21}$$

Equations (4.20a) and (4.20b) can be evaluated directly by substituting equations (4.18) and (4.19) with a_f replaced by $\tilde{a}_f$. Since analytical expressions are not available for the coupling terms, the numerically obtained values of corresponding elastic problem [48] are used directly for the viscoelastic problem :

$$k_{VM}(\tilde{a}_f,\nu_f) = k_{VM}(a_f,\nu_f) \qquad (4.22a)$$

$$c_{VM}(\tilde{a}_f,\nu_f) = c_{VM}(a_f,\nu_f) \qquad (4.22b)$$

The errors introduced due to this approximation should be negligible for most engineering purposes because the coupling terms are relatively small and usually not even considered [46].

Using equations (4.18) to (4.22) and separating the real and imaginary parts, equation (4.20) which defines the impedance functions for viscoelastic halfspace can be rewritten in the following form :

$$K_{VV}(\omega) = [\ k^v_{VV} + i\ a_f\ c^v_{VV}\ ]\ K_x \qquad (4.23a)$$

$$K_{MM}(\omega) = [\ k^v_{MM} + i\ a_f\ c^v_{MM}\ ]\ K_\theta \qquad (4.23b)$$

$$K_{VM}(\omega) = [\ k^v_{VM} + i\ a_f\ c^v_{VM}\ ]\ K_x\ r_f \qquad (4.23c)$$

where k^v's and c^v's are real-valued functions of a_f, ν_f, and η_f and the v superscript refers to viscoelastic problem. For fixed values of Poisson's ratio ν_f and hysteretic damping constant η_f, comparison of equation (4.23a) to equation (4.20a) after substitution of equation (4.18) yields the following expressions for k^v_{VV} and c^v_{VV} :

$$k^v_{VV} = 1 - \frac{\gamma_1\ [\ R + \sqrt{1/2(R-1)}\ (\ \gamma_2 a_f)\ ]\ (\ \gamma_2 a_f\ )^2}{R + 2\sqrt{1/2(R-1)}\ (\ \gamma_2 a_f) + (\ \gamma_2 a_f\ )^2} - \sqrt{1/2(R-1)}\ \gamma_4\ a_f - \gamma_3\ a_f^2 \qquad (4.24a)$$

$$c^v_{VV} = \sqrt{1/2(R+1)}\ \gamma_4 + \frac{\gamma_1\ \gamma_2\sqrt{1/2(R+1)}\ (\ \gamma_2 a_f\ )^2}{R + 2\sqrt{1/2(R-1)}\ (\ \gamma_2 a_f) + (\ \gamma_2 a_f\ )^2} + \frac{\eta_f}{a_f} \qquad (4.24b)$$

where $R = \sqrt{1 + \eta_f^2}$. Similarly, comparison of equation (4.23b) to equation (4.20b) after substitution of equation (4.19) leads to the following expressions for k^v_{MM} and c^v_{MM} :

$$k^v_{MM} = 1 - \frac{\beta_1 \, [\, R + \sqrt{½(R-1)} \, (\beta_2 a_f) \,] \, (\beta_2 a_f)^2}{R + 2\sqrt{½(R-1)} \, (\beta_2 a_f) + (\beta_2 a_f)^2} - \sqrt{½(R-1)} \, \beta_4 \, a_f - \beta_3 \, a_f^2 \tag{4.25a}$$

$$c^v_{MM} = \sqrt{½(R+1)} \, \beta_4 + \frac{\beta_1 \, \beta_2 \sqrt{½(R+1)} \, (\beta_2 a_f)^2}{R + 2\sqrt{½(R-1)} \, (\beta_2 a_f) + (\beta_2 a_f)^2} + \frac{\eta_f}{a_f} \tag{4.25b}$$

and comparison of equation (4.23c) to equation (4.20c) gives the following expressions for the coupling terms k^v_{VM} and c^v_{VM} :

$$k^v_{VM} = k_{VM} - a_f \sqrt{½(R-1)} \, c_{VM} \tag{4.26a}$$

$$c^v_{VM} = \sqrt{½(R+1)} \, c_{VM} + \frac{\eta_f}{a_f} \, k_{VM} \tag{4.26b}$$

Equation (4.26) is limited in the sense that it provides k^v_{VM} and c^v_{VM} for only those values of a_f for which k_{VM} and c_{VM} are available. Therefore, linear interpolation should be used for other values of a_f. For $\nu_f = 1/3$, the functions k^v_{VV}, c^v_{VV}, k^v_{MM}, c^v_{MM}, k^v_{VM} and c^v_{VM} have been evaluated over a range of frequency parameter a_f for various values of hysteretic damping coefficient η_f (Figure 4.4).

4.2.4 General Foundations

The analytical procedure presented in Chapter 3 is applicable to towers of arbitrary cross-section with surface supported or embedded foundations of general shape supported on a homogeneous or non-homogeneous viscoelastic halfspace. Solutions to two boundary value problems for the halfspace, arising from the application of a harmonic horizontal force and a harmonic moment applied separately to the mat foundation, are required to define the impedance functions $K_{VV}(\omega)$, $K_{MM}(\omega)$ and $K_{VM}(\omega)$, which appear in the equations of motion for the tower [equation (3.46)]. Such solutions were obtained for a circular foundation supported on the surface of a viscoelastic halfspace, as described in Sections 4.2.2 and 4.2.3. Using available procedures, the impedance functions may be determined for surface-

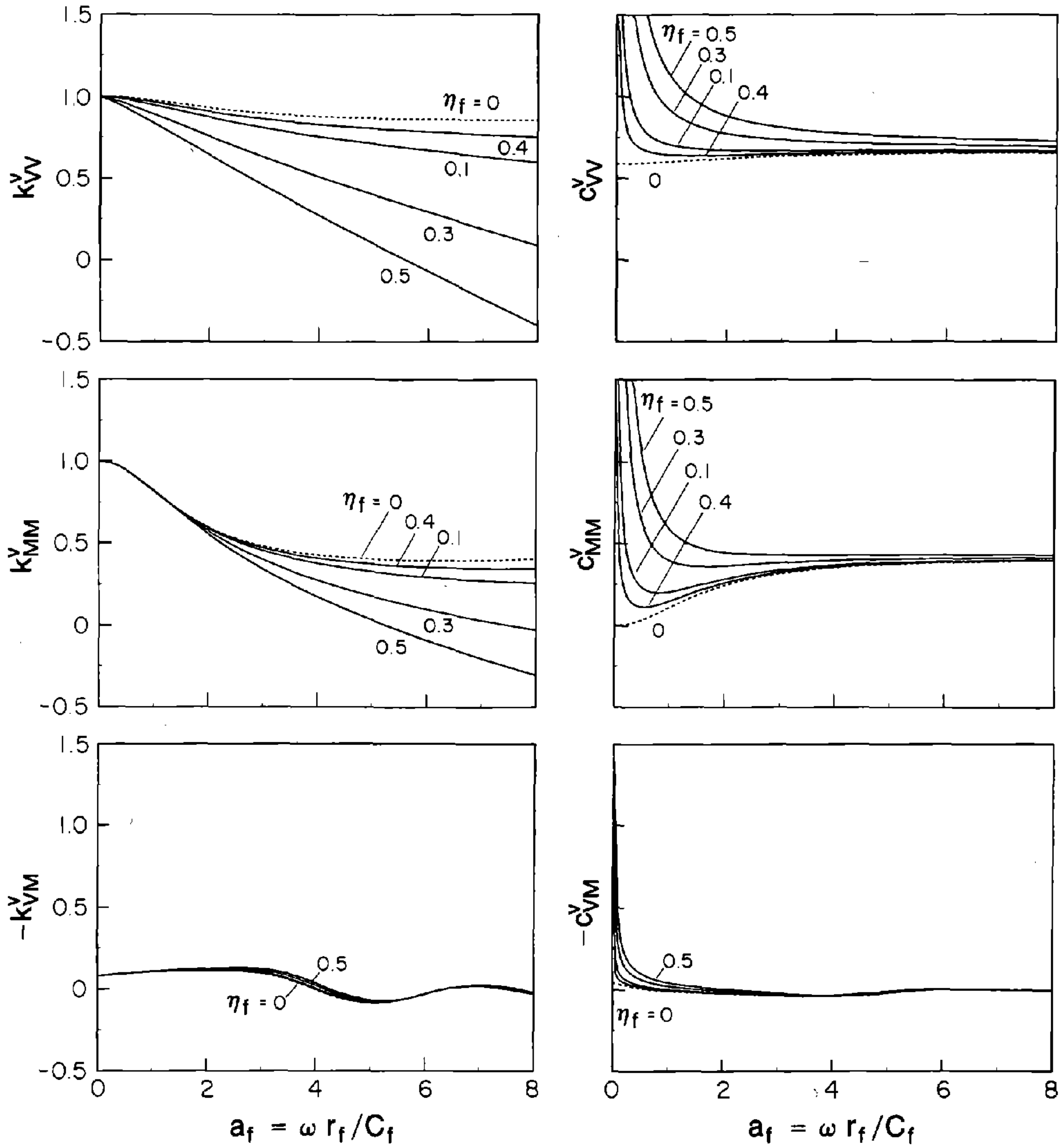

Figure 4.4 Functions k_{VV}^{v} , c_{VV}^{v}, k_{MM}^{v}, c_{MM}^{v} , k_{VM}^{v}, and c_{VM}^{v} for Circular Footing on Viscoelastic Halfspace with $\nu_f = 1/3$

supported or embedded foundations of arbitrary shape [3,42,50], and utilized in the computer program implementing the tower analysis procedure.

However, the present version of the computer program includes an approximate treatment of non-circular foundations supported on the surface of a viscoelastic halfspace. This approach is, in part, based on ATC-3 design recommendations for buildings [55] and is expected to be accurate enough for many practical applications. The information for circular foundations presented in Sections 4.2.2 and 4.2.3, incorporated in the computer program, is applied to mat foundations of arbitrary shapes with the following changes :

1. The radius r_f in the expressions for K_x and a_f that enters in equations (4.15a) and (4.15c) is replaced by the quantity :

$$r_x = \sqrt{\frac{A_f}{\pi}} \tag{4.27a}$$

   which represents the radius of a circular foundation that has the area, A_f, of the actual foundation.

2. The radius r_f in the expressions for K_θ and a_f that enters in equation (4.15b) is replaced by the quantity :

$$r_\theta = \left[\frac{4I_o}{\pi} \right]^{\frac{1}{4}} \tag{4.27b}$$

   which represents the radius of a circular foundation that has the moment of inertia I_o of the actual foundation. It is of interest to note that for nearly square foundations, $r_x \approx r_\theta$.

4.3 Hydrodynamic Solutions for Surrounding Water

4.3.1 Boundary Value Problems

The hydrodynamic lateral forces $f_\beta^o(z)$ and external moments $m_\beta^o(z)$, $\beta = 0,1,2,\ldots,N,h,r$, associated with the hydrodynamic pressures $p_\beta^o(\vec{x})$ acting on the outside surface of the tower [equation (3.29)] enter into the equations of motion in the frequency domain [equation (3.46)] through added hydrodynamic mass and excitation terms. As mentioned in Section 3.2.4, $p_\beta^o(\vec{x})$ are solutions of the three-dimensional Laplace equation:

$$\frac{\partial^2 p^o}{\partial x^2} + \frac{\partial^2 p^o}{\partial y^2} + \frac{\partial^2 p^o}{\partial z^2} = 0 \tag{4.28}$$

for the $N+2$ sets of boundary conditions given by equation (3.25) for $p_0^o(\vec{x})$ [or $p_h^o(\vec{x})$, since $p_h^o(\vec{x}) = p_0^o(\vec{x})$], by equation (3.26) for $p_j^o(\vec{x})$, $j = 1,2,\ldots,N$, and by equation (3.27) for $p_r^o(\vec{x})$. These boundary conditions can be collectively written in generalized form :

$$\frac{\partial}{\partial n^o}\, p^o(\vec{x}) = -\,\rho_w\, a_n^o(\vec{x}) \qquad \vec{x} \in \Gamma_t^o \tag{4.29a}$$

$$\frac{\partial}{\partial z} p^o(\vec{x}) = \begin{cases} -\,\rho_w\, b_n^o(\vec{x}) & \vec{x} \in \Gamma_e^o \\ 0 & \textit{otherwise} \end{cases} \qquad \vec{x} \in \Gamma_b^o \tag{4.29b}$$

$$p^o(\vec{x}) = 0 \qquad \vec{x} \in \Gamma_f^o \tag{4.29c}$$

in which $a_n^o(\vec{x})$ represents the spatial distribution of the acceleration of the tower-water interface Γ_t^o along its normal direction n^o; function $b_n^o(\vec{x})$ represents the distribution of vertical acceleration on the exposed surface Γ_e^o of the footing, which is also a part of reservoir bottom, Γ_b^o; and Γ_f^o defines the free surface of water. The boundary conditions of equation (4.29) are equivalent to equations (3.25), (3.26) and (3.27) if the functions $a_n^o(\vec{x})$ and $b_n^o(\vec{x})$

are defined by equations (4.30), (4.31) and (4.32), respectively :

$$a_n^o(\vec{x}) = n_x^o(\vec{x}) \qquad \vec{x} \in \Gamma_t^o \tag{4.30a}$$

$$b_n^o(\vec{x}) = 0 \qquad \vec{x} \in \Gamma_e^o \tag{4.30b}$$

$$a_n^o(\vec{x}) = n_x^o(\vec{x})\, \phi_j(z) - x\, n_z^o(\vec{x})\, \psi_j(z) \qquad \vec{x} \in \Gamma_t^o \tag{4.31a}$$

$$b_n^o(\vec{x}) = 0 \qquad \vec{x} \in \Gamma_e^o \tag{4.31b}$$

$$a_n^o(\vec{x}) = n_x^o(\vec{x})\, z - x\, n_z^o(\vec{x}) \qquad \vec{x} \in \Gamma_t^o \tag{4.32a}$$

$$b_n^o(\vec{x}) = -\,x \qquad \vec{x} \in \Gamma_e^o \tag{4.32b}$$

where $n_x^o(\vec{x})$ and $n_z^o(\vec{x})$ are the direction cosines of the normal at a point $\vec{x}$ on the tower-water interface with respect to x and z axes, respectively; and functions $\phi_j(z)$ and $\psi_j(z)$ characterize the shape of the deflection curve of the tower in the j-th mode of vibration. In addition to the boundary conditions of equation (4.29), the pressure function $p^o(\vec{x})$ should remain bounded at all distances in the radial direction of the fluid domain which is assumed to extend to infinity.

The symmetry of the tower geometry about the vertical plane Γ_s^o (Figure 3.4) along which the horizontal ground motion is applied leads to an additional requirement :

$$\frac{\partial}{\partial y} p^o(\vec{x}) = 0 \qquad \vec{x} \in \Gamma_s^o \tag{4.33}$$

Similarly, the symmetry of tower geometry about the vertical plane Γ_a^o (Figure 3.4) in the direction normal to the applied ground motion requires that :

$$p^o(\vec{x}) = 0 \qquad \vec{x} \in \Gamma_a^o \tag{4.34}$$

Equation (4.28) together with appropriate boundary conditions at various boundaries -- the tower-water interface [equation (4.29a)], the reservoir bottom [equation (4.29b)] and the free surface of water [equation (4.29c)] -- define the complete boundary value problem for the surrounding water domain. The symmetry and antisymmetry conditions of equations (4.33) and (4.34) only restrict the form of possible solutions.

4.3.2 General Solution

If there is no vertical acceleration of the reservoir bottom [i.e. $b_n^o(\vec{x}) = 0$], the general solution $p^o(\vec{x})$ of the three-dimensional Laplace equation in cylindrical co-ordinates $\vec{x} = (r,z,\theta)$ for the surrounding water domain subject to the boundary conditions of equations (4.29b), (4.29c), (4.33) and (4.34) is of the form:

$$p^o(\vec{x}) = \sum_{m=1}^{\infty} \sum_{n=1}^{\infty} A_{mn} K_{2n-1} (\alpha_m r/H_o) \cos(2n-1)\theta \cos(\alpha_m z/H_o) \qquad (4.35)$$

where $\alpha_m = (2m-1)\pi / 2$, H_o represents the depth of the surrounding water, and K_n is the modified Bessel function of order n of the second kind. The unknown coefficients A_{mn} are determined to satisfy the boundary condition at the tower-water interface [equation (4.29a)]. This boundary condition and the geometry of the tower dictate the choice of procedure to be used in evaluating the coefficients A_{mn}.

These coefficients have been analytically evaluated for circular-cylindrical towers [33,40] using the orthogonality of $\cos(2n-1)\theta \cos(\alpha_m z/H_o)$ functions over the tower surface. However, it is usually necessary to use numerical methods in order to evaluate these coefficients if the geometry of the tower is more complex or if the effects of the vertical acceleration of the reservoir bottom are to be considered. Using boundary integral procedures [25] directly on the tower-water interface involves rapidly changing behavior of Bessel functions for small r/H_o values [1] resulting in poor convergence of the series solution. On the other hand, the conventional finite element method which gives directly the hydrodynamic pressure functions instead of the coefficients in equation (4.35), would involve a large number of elements and excessive computational requirements, and even then, the complete fluid domain may not be modeled accurately [54]. To overcome these difficulties, the idea of combining numerical and analytical methods [7,24,52], known as mixed approach, is adopted here with some modifications while maintaining the symmetry of matrices. The method presented is similar, in principle, to the method presented for the analysis of two-dimensional harbor oscillations [7] but is developed specially for the three-dimensional hydrodynamic analysis of symmetric intake-outlet towers. A variational principle is derived which makes it possible to localize the numerical computations within a small region of the fluid domain and gives directly the values of hydrodynamic pressure on the outside surface of the tower and on the exposed surface of the footing.

4.3.3 The Variational Principle

Let the surrounding-water domain τ^o be divided into two sub-domains τ_A^o and τ_B^o by the hypothetical circular-cylindrical surface Γ_c^o which has radius r_c and contains the tower as well as the portion Γ_e^o of the reservoir bottom which may undergo vertical acceleration (Figure 4.5). The choice of a cylindrical surface is advantageous because it allows the use of general analytical solutions given in equation (4.35) as the set of trial functions for the boundary integral procedure for domain τ_B^o. Because the radius r_c of this hypothetical surface Γ_c^o can be made reasonably small and the tower plan has two axes of symmetry, only a very small portion of the fluid domain τ_A^o need be discretized into finite elements (Figure 4.5). The hydrodynamic pressure in domain τ_B^o is represented by the linear combination of trial functions of equation (4.35) with unknown coefficients which must be determined by matching it with the pressure and pressure gradient in τ_A^o along Γ_c^o:

$$p_A^o(\vec{x}) = p_B^o(\vec{x}) \qquad \vec{x} \in \Gamma_c^o \tag{4.36a}$$

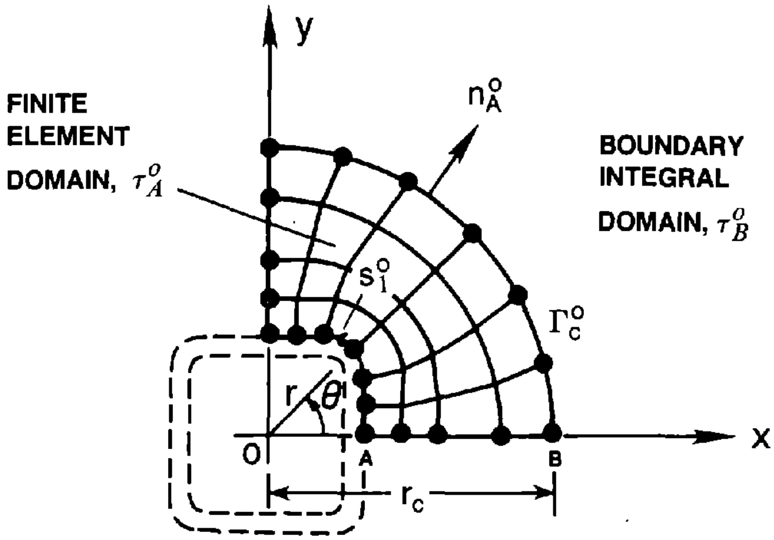

(a) FINITE ELEMENT SYSTEM IN x-y PLANE AT xx

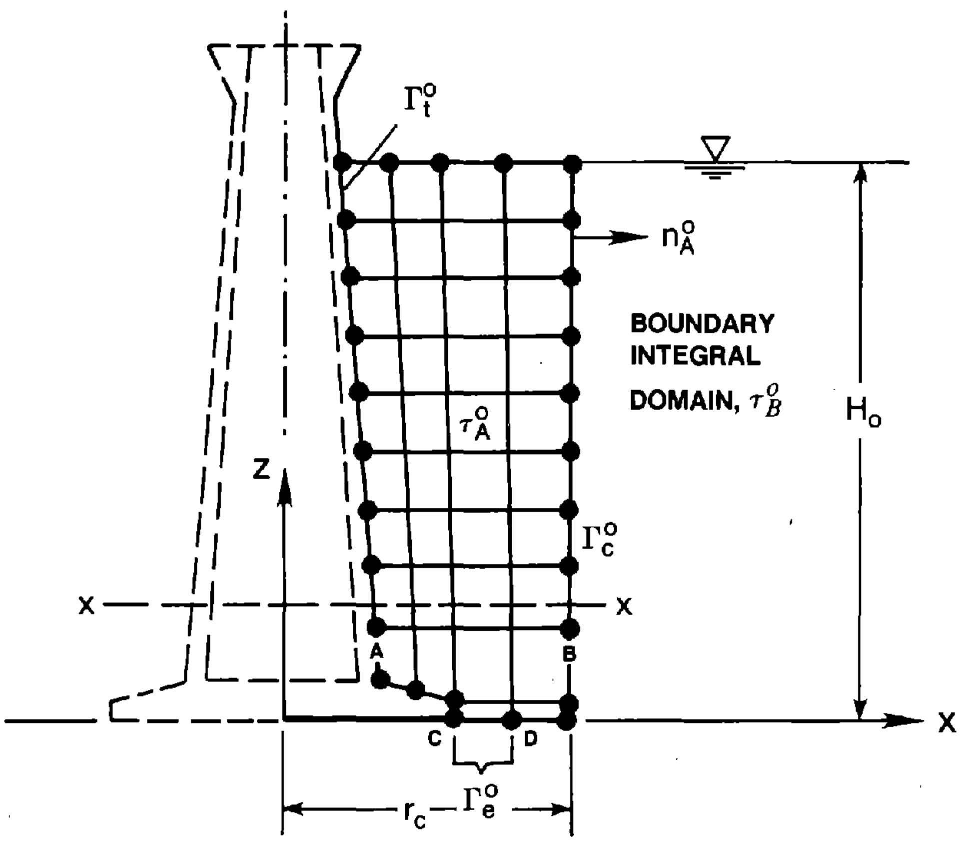

(b) FINITE ELEMENT SYSTEM IN x-z PLANE

Figure 4.5 Three-Dimensional Finite Element System for Surrounding Water Domain

$$\frac{\partial}{\partial n_A^o} p_A^o(\vec{x}) = \frac{\partial}{\partial n_A^o} p_B^o(\vec{x}) \qquad \vec{x} \in \Gamma_c^o \tag{4.36b}$$

where n_A^o represents the unit normal to the surface Γ_c^o pointing outward from region τ_A^o; and p_A^o, p_B^o represent the values of hydrodynamic pressure in regions τ_A^o and τ_B^o respectively. Due to the special structure of p_B^o, the infinite extent of the fluid domain is exactly represented in this formulation.

According to the well known Euler's theorem [37], the function $p^o(\vec{x})$ which minimizes the functional :

$$\Pi(p) = \frac{1}{2}\int_{\tau_A^o} \nabla p \cdot \nabla p \; d\tau + \frac{1}{2}\int_{\tau_B^o} \nabla p \cdot \nabla p \; d\tau + \int_{\Gamma_c^o} \frac{\partial p_B^o}{\partial n_A^o} [\, p_B^o - p_A^o \,] \, d\Gamma$$

$$- \rho_w \int_{\Gamma_t^o} p_A^o \, a_n^o(\vec{x}) \, d\Gamma - \rho_w \int_{\Gamma_e^o} p_A^o \, b_n^o(\vec{x}) \, d\Gamma \tag{4.37}$$

satisfies equation (4.28) and boundary conditions of equations (4.29), (4.33), and (4.34). The first two terms defined as volume integrals represent the potential energy of the sub-domains τ_A^o and τ_B^o respectively. The third surface integral term in this functional is a constraint to match the pressure and its gradient across the hypothetical surface Γ_c^o. The last two terms defined as surface integrals on the tower-water interface Γ_t^o and on the portion of reservoir bottom inside the hypothetical cylinder, Γ_e^o, produce forcing terms.

The application of Green's identity to the second integral of equation (4.37) with appropriate boundary conditions for τ_B^o leads to :

$$\frac{1}{2}\int_{\tau_B^o} \nabla p \cdot \nabla p \; d\tau = \int_{\Gamma_c^o} p_B^o \, [\, - \frac{\partial p_B^o}{\partial n_A^o} \,] \, d\Gamma \tag{4.38}$$

Substitution of equation (4.38) into equation (4.37) and further simplification of terms lead to the following localized functional:

$$\Pi(p) = \frac{1}{2} \int_{\tau_A^o} \nabla p \cdot \nabla p \, d\tau + \frac{1}{2} \int_{\Gamma_c^o} p_B^o \left[\frac{\partial p_B^o}{\partial n_A^o} \right] d\Gamma + \int_{\Gamma_c^o} p_A^o \left[- \frac{\partial p_B^o}{\partial n_A^o} \right] d\Gamma$$

$$- \rho_w \int_{\Gamma_t^o} p_A^o \, a_n^o(\vec{x}) \, d\Gamma - \rho_w \int_{\Gamma_e^o} p_A^o \, b_n^o(\vec{x}) \, d\Gamma \qquad (4.39)$$

Thus, with p_B^o restricted to the form of equation (4.35), no numerical calculation is required beyond the hypothetical surface Γ_c^o, in contrast to the conventional variational principle which would involve only the first integral with τ_A^o extending to infinity and the last two surface integral terms. The function $p^o(\vec{x})$ which renders this localized functional stationary, satisfies the governing equation for hydrodynamic pressure (equation 4.28), the associated boundary conditions of equations (4.29), (4.33), (4.34), and the required constraint of equation (4.36) [Appendix C]. The numerical procedure developed to evaluate the pressure function $p^o(\vec{x})$ is presented next.

4.3.4 Finite Element Approximation

The hydrodynamic pressure on the tower surface is numerically evaluated by minimizing the functional of equation (4.39). For this purpose, the fluid domain τ_A^o is idealized as an assemblage of three-dimensional finite elements with N_A nodal points and consequently, the surfaces Γ_t^o, Γ_c^o and Γ_e^o get discretized into a number of subdivisions as shown in Figure 4.5. Let p_i, $i=1,2, \ldots, N_A$ be the unknown pressures at the N_A nodal points and $N_i(\vec{x})$, $i=1,2, \ldots, N_A$ be the locally-supported continuous interpolation functions of class C_0 corresponding to each nodal point, then the pressures in domain τ_A^o are approximated by

:

$$p_A^o(\vec{x}) \approx \sum_{i=1}^{N_A} N_i(\vec{x})\, p_i \qquad \vec{x} \in \tau_A^o \tag{4.40}$$

in which all interpolation functions satisfy the following condition at nodal points to maintain the global continuity of pressure function p_A in domain τ_A^o:

$$N_i(\vec{x}_j) = \delta_{ij} \quad ; \quad i,j = 1,2,\ldots,N_A \tag{4.41}$$

where $\vec{x}_j$ represents the coordinate for the j-th node in domain τ_A^o and δ_{ij} is the Kronecker delta function.

Similarly, the pressures in domain τ_B^o are represented by the linear combination of the first N_B normalized functions in the general solution [equation (4.35)] :

$$p_B^o(\vec{x}) \approx \sum_{i=1}^{N_B} M_i(\vec{x})\, q_i \qquad \vec{x} \in \tau_B^o \tag{4.42}$$

in which q_i's are the unknown coefficients and in cylindrical co-ordinates, $M_i(\vec{x})$ are defined as:

$$M_i(\vec{x}) = \frac{K_{2n-1}(\alpha_m r/H_o)}{K_{2n-1}(\alpha_m r_c/H_o)} \cos(2n-1)\theta \cos(\alpha_m z/H_o) \tag{4.43}$$

where $m=1,2,\ldots,M_z$; $n=1,2,\ldots,N_\theta$; $N_B=M_z \times N_\theta$; $i=(n-1)M_z+m$; M_z and N_θ are the number of terms included in the first and second series, respectively, in equation (4.35). Due to the cylindrical geometry of the hypothetical surface Γ_c^o, its outward normal always satisfies the following equation :

$$\frac{\partial}{\partial n_A^o} = \frac{\partial}{\partial r} \qquad along\ \Gamma_c^o \tag{4.44}$$

Therefore, due to the special structure of $M_i(\vec{x})$, the pressures $p_B^o(\vec{x})$ and their gradients on surface Γ_c^o can be represented in the following form using equation (4.44) and substituting

$r = r_c$ in equation (4.43) :

$$p_B^o(\vec{x}) \approx \sum_{i=1}^{N_B} M_i^\Gamma(\vec{x})\, q_i \qquad \vec{x} \in \Gamma_c^o \tag{4.45}$$

$$\frac{\partial}{\partial n_A^o}\, p_B^o(\vec{x}) \approx \sum_{i=1}^{N_B} B_i\, M_i^\Gamma(\vec{x})\, q_i \qquad \vec{x} \in \Gamma_c^o \tag{4.46}$$

in which functions $M_i^\Gamma(\vec{x})$ and constants B_i are defined as :

$$M_i^\Gamma(\vec{x}) = \cos(2n-1)\theta \cos(\alpha_m z/H_o) \tag{4.47}$$

$$B_i = -\frac{1}{2}\frac{\alpha_m}{H_o}\frac{K_{2n}(\alpha_m r_c/H_o) + K_{2n-2}(\alpha_m r_c/H_o)}{K_{2n-1}(\alpha_m r_c/H_o)} \tag{4.48}$$

where $m=1,2,\ldots,M_z$; $n=1,2,\ldots,N_\theta$; $N_B = M_z \times N_\theta$; $i=(n-1)M_z+m$.

Substitution of equations (4.40), (4.45), and (4.46) into equation (4.39) leads to a functional in vectors $\boldsymbol{p}$ and $\boldsymbol{q}$ containing the unknowns p_i, $i = 1,2,\ldots,N_A$, and q_i, $i = 1,2,\ldots,N_B$, respectively:

$$\Pi(\boldsymbol{p},\boldsymbol{q}) = \frac{1}{2}\,\boldsymbol{p}^T\boldsymbol{K}_I\,\boldsymbol{p} + \frac{1}{2}\,\boldsymbol{q}^T\boldsymbol{K}_{III}\,\boldsymbol{q} + \frac{1}{2}\,[\,\boldsymbol{p}^T\boldsymbol{K}_{II}\,\boldsymbol{q} + \boldsymbol{q}^T\boldsymbol{K}_{II}^T\,\boldsymbol{p}\,] - \boldsymbol{p}^T\boldsymbol{Q}_I - \boldsymbol{p}^T\boldsymbol{Q}_{II} \tag{4.49}$$

in which $\boldsymbol{K}_I$ is $N_A \times N_A$ symmetric matrix with its jk-element given by :

$$(\,\boldsymbol{K}_I\,)_{j,k} = \int_{\tau_A^o} \nabla N_j(\vec{x})\cdot\nabla N_k(\vec{x})\, d\tau \quad ; \quad j,k=1,2,\ldots,N_A \tag{4.50}$$

The zero pressure boundary condition on surfaces Γ_f^o and Γ_a^o is satisfied by assigning zeros to the rows and columns in the matrix $\boldsymbol{K}_I$ corresponding to the nodes on these surfaces. Since M_i^Γ, $i=1,2,\ldots,N_B$ is a set of orthogonal functions on surface Γ_c^o, the matrix $\boldsymbol{K}_{III}$ in equation (4.49) is a diagonal matrix of order N_B with its jj-element given by :

$$(\boldsymbol{K}_{III})_{j,j} = B_j \int_{\Gamma_e^o} M_j^\Gamma(\vec{x}) \cdot M_j^\Gamma(\vec{x}) \, d\Gamma \quad ; \quad j = 1,2, \ldots, N_B \tag{4.51}$$

If the nodal points in the finite element mesh for domain τ_A^o are numbered in a special way, assigning the first N_T numbers to the tower-water interface and the last N_C numbers to the hypothetical surface between domains τ_A^o and τ_B^o, the matrix $\boldsymbol{K}_{II}$ defining the coupling between the pressures in domains τ_A^o and τ_B^o is of size $N_C \times N_B$ and its jk-element is given by :

$$(\boldsymbol{K}_{II})_{j,k} = - B_k \int_{\Gamma_e^o} N_j(\vec{x}) \cdot M_k^\Gamma(\vec{x}) \, d\Gamma \quad ; \quad j = N_A - N_C + 1, \ldots, N_A \; ; \; k = 1,2, \ldots, N_B \tag{4.52}$$

The vectors $\boldsymbol{Q}_I$ and $\boldsymbol{Q}_{II}$ appearing in the functional [equation (4.49)] are of order N_A and their j-th terms are given by :

$$(\boldsymbol{Q}_I)_j = \int_{\Gamma_t^o} N_j(\vec{x}) \cdot a_n^o(\vec{x}) \, d\Gamma \quad ; \quad j = 1,2, \ldots, N_A \tag{4.53}$$

$$(\boldsymbol{Q}_{II})_j = \int_{\Gamma_e^o} N_j(\vec{x}) \cdot b_n^o(\vec{x}) \, d\Gamma \quad ; \quad j = 1,2, \ldots, N_A \tag{4.54}$$

In vector $\boldsymbol{Q}_I$, only first N_T terms are non-zero which correspond to the nodes on the tower-water interface. Similarly, in matrix $\boldsymbol{Q}_{II}$ only those terms which correspond to the nodes on the exposed portion of the foundation footing surface in contact with water are non-zero.

Only matrix $\boldsymbol{K}_{III}$ can be evaluated analytically and, therefore, all other matrices are estimated by numerical integration. Since the interpolation functions $N_i(\vec{x})$, $i = 1,2, \ldots, N_A$ are locally supported, integration is not performed over the full domain or the entire surface for each element of these matrices. The domain τ_A^o is discretized into volume elements and surfaces Γ_t^o, Γ_c^o and Γ_e^o into surface elements. Integration in equations (4.50) to (4.54) is done at the element level and the element matrices are assembled by standard procedures [53].

Returning to equation (4.49), stationarity of the functional $\Pi(\boldsymbol{p},\boldsymbol{q})$ implies :

$$\frac{\partial \Pi}{\partial p_i} = 0 \quad ; \quad i=1,2,\ldots,N_A \tag{4.55a}$$

$$\frac{\partial \Pi}{\partial q_i} = 0 \quad ; \quad i=1,2,\ldots,N_B \tag{4.55b}$$

which leads to a system of linear algebraic equations

$$\boldsymbol{K}\,\boldsymbol{r} = \boldsymbol{Q} \tag{4.56}$$

in $N_A + N_B$ unknowns :

$$\boldsymbol{r}^T = [\,\boldsymbol{p}^T\,,\,\boldsymbol{q}^T\,] = (\,p_1,p_2,\ldots,p_{N_A}\,,\,q_1,q_2,\ldots,q_{N_B}\,) \tag{4.57}$$

The structure of matrix $\boldsymbol{K}$ and vector $\boldsymbol{Q}$ is shown in Figure 4.6. These equations can be condensed to give :

$$\boldsymbol{K}_o\,\boldsymbol{p} = \boldsymbol{Q}_o \tag{4.58}$$

where

$$\boldsymbol{K}_o = \boldsymbol{K}_I - \boldsymbol{K}_{II}\,\boldsymbol{K}_{III}^{-1}\,\boldsymbol{K}_{II}^T \tag{4.59a}$$

$$\boldsymbol{Q}_o = \boldsymbol{Q}_I + \boldsymbol{Q}_{II} \tag{4.59b}$$

The unknown hydrodynamic pressure vector $\boldsymbol{p}$ is evaluated by solving these simultaneous equations and its analytical representation $p^o(\vec{x})$ is then estimated by using equation (4.40), the symmetric properties of pressure functions along surface Γ_s^o, and the anti-symmetric properties along surface Γ_a^o. This analysis procedure is repeated $N+2$ times to evaluate the complete set of pressure functions $p_\beta^o(\vec{x})$, $\beta = 0,1,2,\ldots,N,h,r$, using different values of functions $a_n^o(\vec{x})$ and $b_n^o(\vec{x})$ given by equations (4.30) to (4.32). Once the pressures are known, the height-wise distributions of resultant hydrodynamic lateral forces and

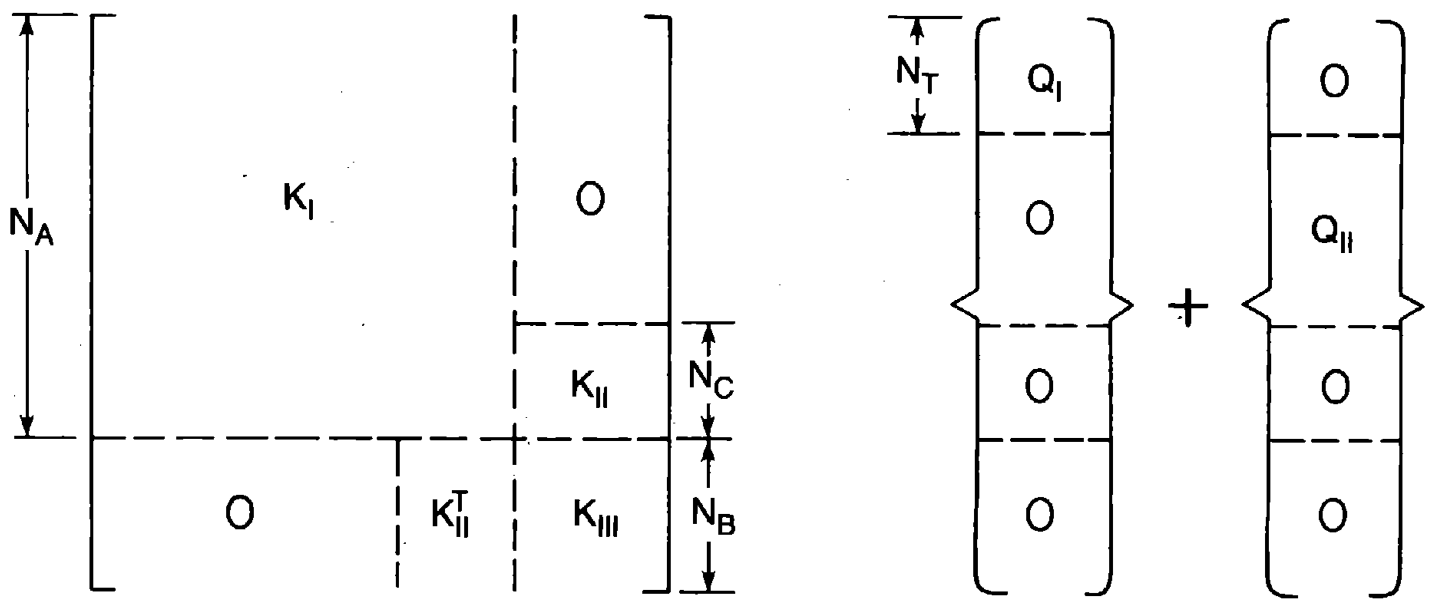

(a) MATRIX K

(b) VECTOR Q

Figure 4.6 The Structure of Matrix **K** and Vector **Q** moments are evaluated by integrating the components of these pressures along the perimeter of the outside surface of the tower using equation (3.29).

4.3.5 Semi-Analytical Process for Axisymmetric Towers

The finite element approximation within sub-domain τ_A^o coupled to the continuum solution for domain τ_B^o through the boundary integral procedures has been shown in the preceding sections to be capable of solving the Laplace equation over three-dimensional fluid domains exterior to a tower. This general procedure can be simplified for axisymmetric towers because spatially-varying surface motions of axisymmetric towers can be expressed as a Fourier series in the circumferential coordinate θ, and therefore, the orthogonality of trigonometric functions can be exploited to replace the three-dimensional problem by a series of uncoupled two-dimensional problems. The complete solution then is the superposition of all the two-dimensional solutions.

For axisymmetric towers, the direction cosines of the outward normal to the tower-water interface at a point $\vec{x}$ -- $n_x^o(\vec{x})$ with respect to the horizontal direction of excitation and $n_z^o(\vec{x})$ with respect to the vertical direction along the height -- can be represented in terms of their corresponding functions $\bar{n}_x^o(r,z)$ and $\bar{n}_z^o(r,z)$ defined along the surface of the tower in the $r-z$ plane at $\theta=0$:

$$n_x^o(\vec{x}) = \bar{n}_x^o(r,z)\cos\theta \tag{4.60a}$$

$$n_z^o(\vec{x}) = \bar{n}_z^o(r,z) \tag{4.60b}$$

Using this geometric property, the linear structure of the boundary conditions [equation (4.29)], and the relationship $x = r\cos\theta$ between the cartesian and cylindrical coordinate systems, the distributions of acceleration $a_n^o(\vec{x})$ on the tower-water interface and $b_n^o(\vec{x})$ on the reservoir bottom can be redefined in terms of their corresponding functions $\bar{a}_n^o(r,z)$ and

$\bar{b}_n^o(r,z)$ evaluated along the surface of the tower in the $r-z$ plane at $\theta=0$ i.e.

$$a_n^o(\vec{x}) = \bar{a}_n^o(r,z)\cos\theta \tag{4.61a}$$

$$b_n^o(\vec{x}) = \bar{b}_n^o(r,z)\cos\theta \tag{4.61b}$$

Because of the orthogonality of trigonometric functions, the hydrodynamic pressures associated with acceleration distributions of equation (4.61) also vary as $\cos\theta$ in the circumferential direction i.e.

$$p^o(\vec{x}) = \bar{p}^o(r,z)\cos\theta \tag{4.62}$$

Thus only the first term in both the Fourier expansions of tower-surface acceleration and reservoir bottom acceleration are relevant for the analysis at hand [32,34], and only one two-dimensional problem need be solved.

To obtain the hydrodynamic pressures in the form of equation (4.62), the functions $p_A^o(\vec{x})$ and $p_B^o(\vec{x})$ must also vary as $\cos\theta$:

$$p_A^o(\vec{x}) = \bar{p}_A^o(r,z)\cos\theta \approx \sum_{i=1}^{N_A} \overline{N_i}(r,z)\cos\theta\, p_i \tag{4.63}$$

$$p_B^o(\vec{x}) = \bar{p}_B^o(r,z)\cos\theta \approx \sum_{i=1}^{N_B} \overline{M_i}(r,z)\cos\theta\, q_i \tag{4.64}$$

where

$$\overline{M_i}(r,z) = \left[\frac{K_1(\alpha_i\, r/H_o)}{K_1(\alpha_i\, r_c/H_o)}\right]\cos(\alpha_i\, z/H_o) \quad ; \quad i=1,2,\ldots,N_B \tag{4.65}$$

In equation (4.63), $\overline{N_i}(r,z)$, $i=1,2,\ldots,N_A$ are the two-dimensional interpolation functions in the r-z plane and $\overline{M_i}(r,z)\cos\theta$ equals $M_i(\vec{x})$ in equation (4.43) for $m=i$ and $n=1$.

Substitution of equations (4.61), (4.63), and (4.64) into the functional of equation (4.39) and integration along θ direction leads to a two dimensional functional in the r-z plane:

$$\Pi(p) = \frac{1}{2} \int_{\Omega_A^o} \left[\frac{\partial p}{\partial r} \cdot \frac{\partial p}{\partial r} + \frac{\partial p}{\partial z} \cdot \frac{\partial p}{\partial z} \right] r\, dr\, dz + \frac{1}{2} \int_{\Omega_A^o} \frac{1}{r}\, p \cdot p\, dr\, dz$$

$$+ \frac{1}{2} \int_{\Lambda_c^o} \bar{p}_B^o \left[\frac{\partial \bar{p}_B^o}{\partial r} \right] r\, dz - \int_{\Lambda_c^o} \bar{p}_A^o \left[\frac{\partial \bar{p}_B^o}{\partial r} \right] r\, dz$$

$$- \rho_w \int_{\Lambda_t^o} \bar{p}_A^o\, \bar{a}_n^o(r,z)\, r\, d\Lambda - \rho_w \int_{\Lambda_e^o} \bar{p}_A^o\, \bar{b}_n^o(r,z)\, r\, d\Lambda \qquad (4.66)$$

wherein the area domains Ω_A^o and Ω_B^o in the $r-z$ plane appear instead of the volume domains τ_A^o and τ_B^o in equation (4.39), and the contours Λ_t^o , Λ_c^o and Λ_e^o in the $r-z$ plane appear instead of the surface domains Γ_t^o , Γ_c^o and Γ_e^o (Figure 4.7).

Applying the numerical procedure presented in Section 4.3.4 to axisymmetric fluid domains [see Appendix D for details], the functional of equation (4.66) can be minimized to obtain $\bar{p}^o(r,z)$. The procedure is implemented for the $N+2$ different distributions of acceleration on the tower-water interface and the reservoir bottom [equations (4.30) to (4.32)], specialized for axisymmetric towers through equation (4.61) :

$$\bar{a}_n^o(r,z) = \bar{n}_x^o(r,z) \qquad (r,z) \in \Lambda_t^o \qquad (4.67a)$$

$$\bar{b}_n^o(r,z) = 0 \qquad (r,z) \in \Lambda_e^o \qquad (4.67b)$$

$$\bar{a}_n^o(r,z) = \bar{n}_x^o(r,z)\, \phi_j(z) - r\, \bar{n}_z^o(r,z)\, \psi_j(z) \qquad (r,z) \in \Lambda_t^o \qquad (4.68a)$$

$$\bar{b}_n^o(r,z) = 0 \qquad (r,z) \in \Lambda_e^o \qquad (4.68b)$$

$$\bar{a}_n^o(r,z) = \bar{n}_x^o(r,z)\, z - r\, \bar{n}_z^o(r,z) \qquad (r,z) \in \Lambda_t^o \qquad (4.69a)$$

$$\bar{b}_n^o(r,z) = -\, r \qquad (r,z) \in \Lambda_e^o \qquad (4.69b)$$

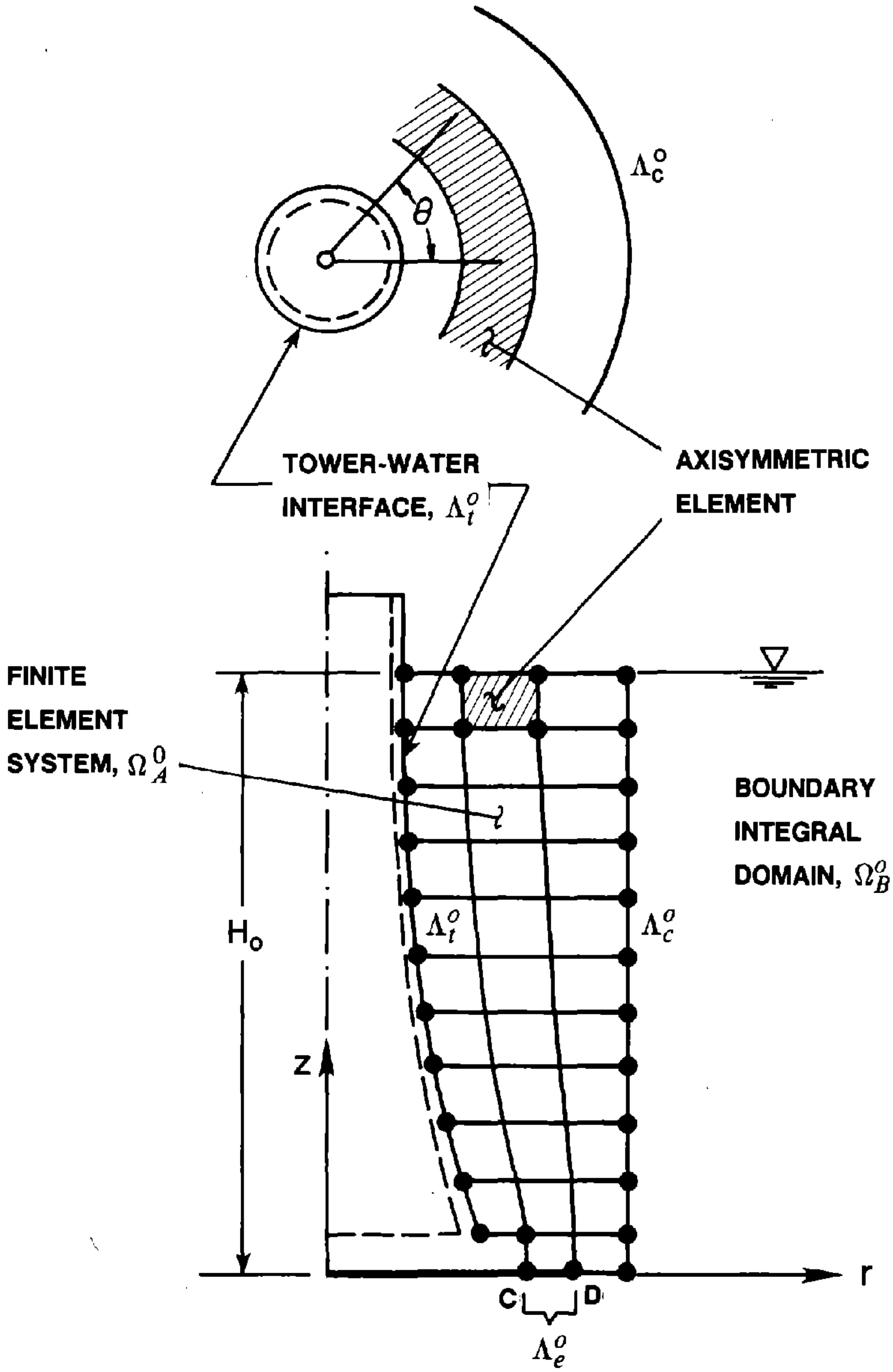

Figure 4.7 Axisymmetric Finite Element System for Surrounding Water Domain

This would result in the complete set of pressure functions $\bar{p}^o_\beta(r,z)$, $\beta = 0,1,2,\ldots,N,h,r$. The resultant lateral hydrodynamic force and moments per unit of height, acting on the tower surface in the vertical plane of ground motion, are then evaluated by a special case of equation (3.29) which is obtained by utilizing equation (4.62):

$$f^o_\beta(z) = \Big[\pi\, r\, \bar{n}^o_x(r,z)\, \bar{p}^o_\beta(r,z)\Big]_{r=r_o(z)} \tag{4.70a}$$

$$m^o_\beta(z) = \Big[\pi\, r^2\, \bar{n}^o_z(r,z)\, \bar{p}^o_\beta(r,z)\Big]_{r=r_o(z)} - \pi\, \delta(z) \int_{\Lambda^o_e} r\, \Big[\bar{p}^o_\beta(r,z)\Big]_{z=0}\, dr \tag{4.70b}$$

where $r_o(z)$ defines the radius of the outside surface at a location z along the height.

By exploiting the orthogonality of trigonometric functions along with the geometric properties of axisymmetric towers, what was originally a three-dimensional problem has now been transformed to a two-dimensional one and, consequently, the computational effort is substantially reduced.

4.3.6 Evaluation of the Procedure

Convergence -- The computational effort required for an accurate representation of the hydrodynamic pressure p^o_B in domain τ^o_B is directly proportional to M_z and N_θ, the number of terms to be included in equation (4.35) corresponding to $\cos(\alpha_m z/H_o)$ and $\cos(2n-1)\theta$ functions, respectively. Therefore, it is necessary to establish the smallest values for M_z and N_θ sufficient to achieve the desired degree of accuracy.

The smallest value of M_z that yields sufficiently accurate results can be estimated by analyzing an axisymmetric tower for increasing values of M_z. An axisymmetric tower is chosen because, as shown in Section 4.3.5, only the $N_\theta = 1$ term is necessary in equation (4.35) which makes it convenient to evaluate the dependence on M_z. The axisymmetric finite element system used to discretize the subdomain τ^o_A to determine the lateral hydrodynamic force $f^o_0(z)$ is presented in Figure 4.8. Determined by the procedure of Section

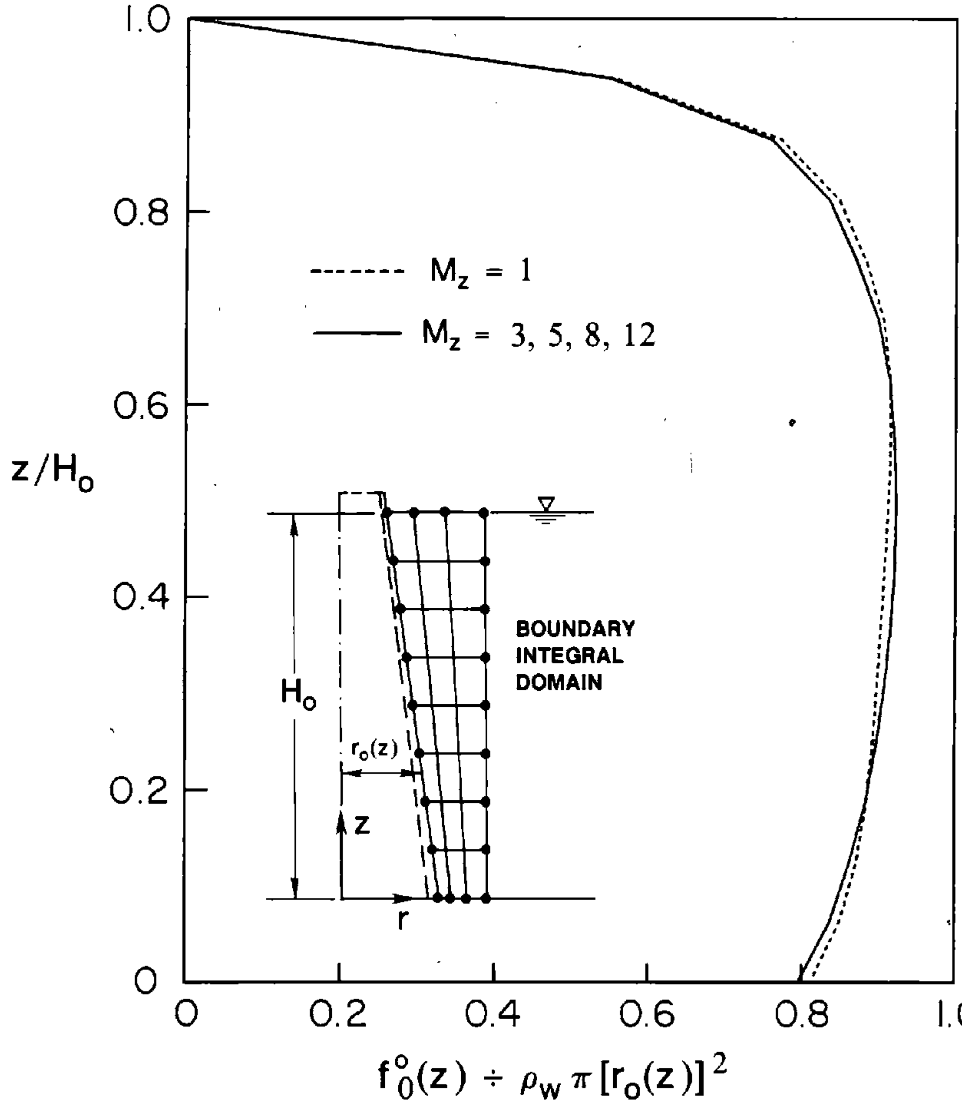

Figure 4.8 Lateral Hydrodynamic Forces $f_0^o(z)$ on Axisymmetric Tower for Different Values of M_z

4.3.5, the results are also summarized in Figure 4.8 for a rigid, tapered axisymmetric tower [with $H_o/r_o(0) = 5$ and $r_o(0)/r_o(H_o) = 2$] subjected to unit harmonic, horizontal ground acceleration for different values of M_z. It is apparent that $M_z \geq 3$ is sufficient for accurate results.

In order to estimate N_θ, the number of circumferential functions necessary to obtain accurate results, the lateral hydrodynamic force $f_0^o(z)$ on a rigid, uniform tower of non-circular cross-section subjected to unit harmonic, horizontal ground acceleration has been computed by the procedure of Section 4.3.4 using $M_z = 12$ and different values of N_θ. By discretizing the subdomain τ_A^o with the finite element system shown in Figure 4.9, the height-wise distribution of lateral hydrodynamic force $f_0^o(z)$ is obtained by using various values of N_θ. The results presented for a tower with $H_o/b_o = 10$ indicate that analysis using $N_\theta \geq 2$ provides sufficiently accurate results. Conservative values of $M_z = 12$ and $N_\theta = 6$ are used for all subsequent analyses so that the results are sufficiently accurate for all flexible towers of arbitrary geometries.

Accuracy -- The accuracy of the finite element method coupled with the boundary integral procedures presented in Sections 4.3.4 and 4.3.5 is demonstrated by comparing the numerical results from this approach with the analytical, infinite series solution for circular cylindrical towers [32,33]. The fluid domain exterior to a rigid circular cylinder subjected to unit harmonic, horizontal ground acceleration can be numerically analyzed by solving (i) a two-dimensional axisymmetric problem by the methods of Section 4.3.5, or (ii) a general three-dimensional problem by the methods of Sections 4.3.3 and 4.3.4. It is apparent from Figure 4.10, wherein the finite element idealizations of subdomains τ_A^o in each case are also shown, that the two sets of numerical results for the distribution of lateral hydrodynamic force $f_0^o(z)$ are essentially identical to analytical results. Therefore, the hydrodynamic analysis procedures presented in Sections 4.3.3 to 4.3.5 will lead to accurate values for the

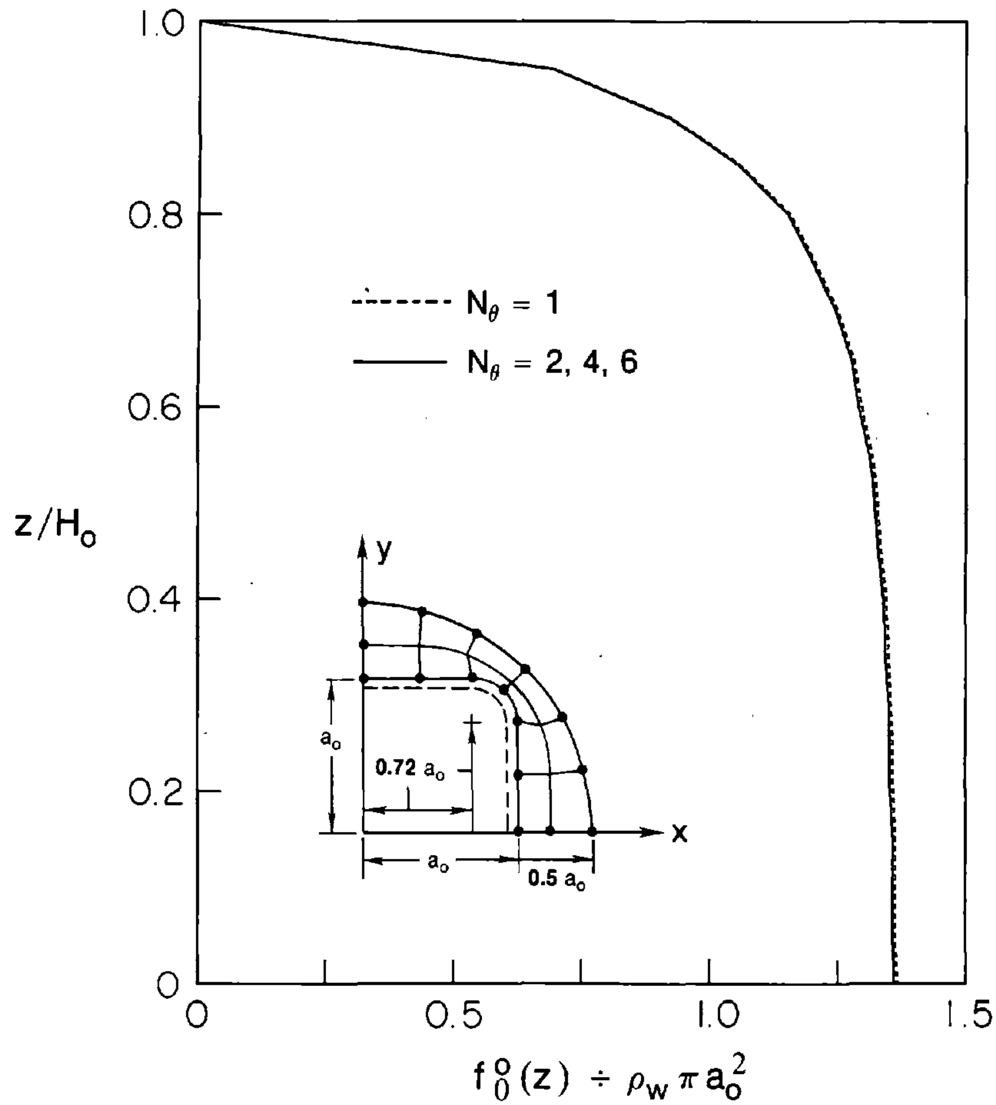

Figure 4.9 Lateral Hydrodynamic Forces $f_0^o(z)$ on Uniform Tower for Different Values of N_θ

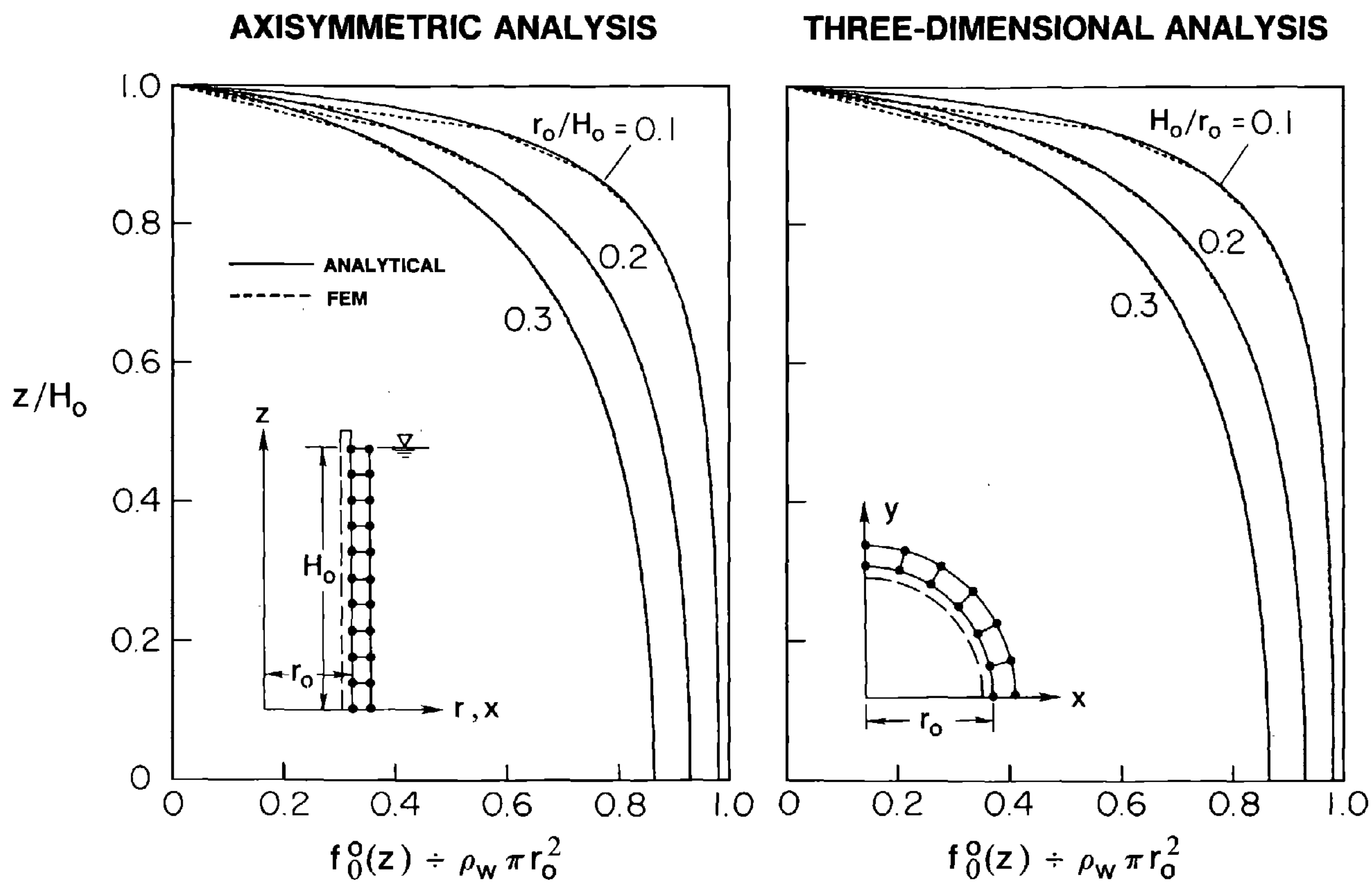

Figure 4.10 Lateral Hydrodynamic Forces due to Surrounding Water on Rigid Cylindrical Towers from Two Finite Element Analyses; Comparison with Analytical Results

hydrodynamic terms required in equation (3.46) for earthquake analysis of towers.

Efficiency -- In the conventional finite element method (FEM), the subdomain τ_B^o (Figure 4.5) would not exist and the subdomain τ_A^o must extend far enough to obtain an accurate representation of the unbounded fluid domain with the pressure gradient assumed to be zero at the outside surface Γ_c^o of the subdomain τ_A^o [34]. In order to compare the computational effort required by conventional FEM and the procedure presented in Sections 4.3.3 to 4.3.5, a rigid, tapered, axisymmetric tower subjected to unit harmonic, horizontal ground acceleration has been analyzed by both methods. The conventional finite element analysis is repeated for several values of the radial dimension r_c of the finite element system, characterized by the ratio r_c/r_o where r_o represents the radius of the outside surface of the tower at the base. It is apparent from the numerical results (Figure 4.11) for the lateral hydrodynamic force $f_0^o(z)$ that, in order to obtain accurate results by the conventional FEM, the dimension r_c of the finite element system should exceed $8r_o$. On the other hand, accurate results are obtained by the procedure presented in Section 4.3.5 using a finite element system with $r_c = 1.5\, r_o$ coupled with boundary integral procedures for the subdomain τ_B^o. The CPU time required on an IBM 3090 main-frame computer in the conventional FEM with $r_c = 8\, r_o$ is approximately three times of what is required in the coupled finite element-boundary integral procedure, a comparison that demonstrates the efficiency of the latter.

4.4 Hydrodynamic Solutions for Inside Water

4.4.1 Boundary Value Problems

Similar to the analysis for surrounding water domain, the hydrodynamic lateral forces $f_\beta^i(z)$ and external moments $m_\beta^i(z)$, $\beta = 0,1,2,\ldots,N,h,r$, associated with the hydrodynamic pressures $p_\beta^i(\vec{x})$ acting on the inside surface of the tower [equation (3.44)] enter into the equations of motion in frequency domain [equation (3.46)] through the added

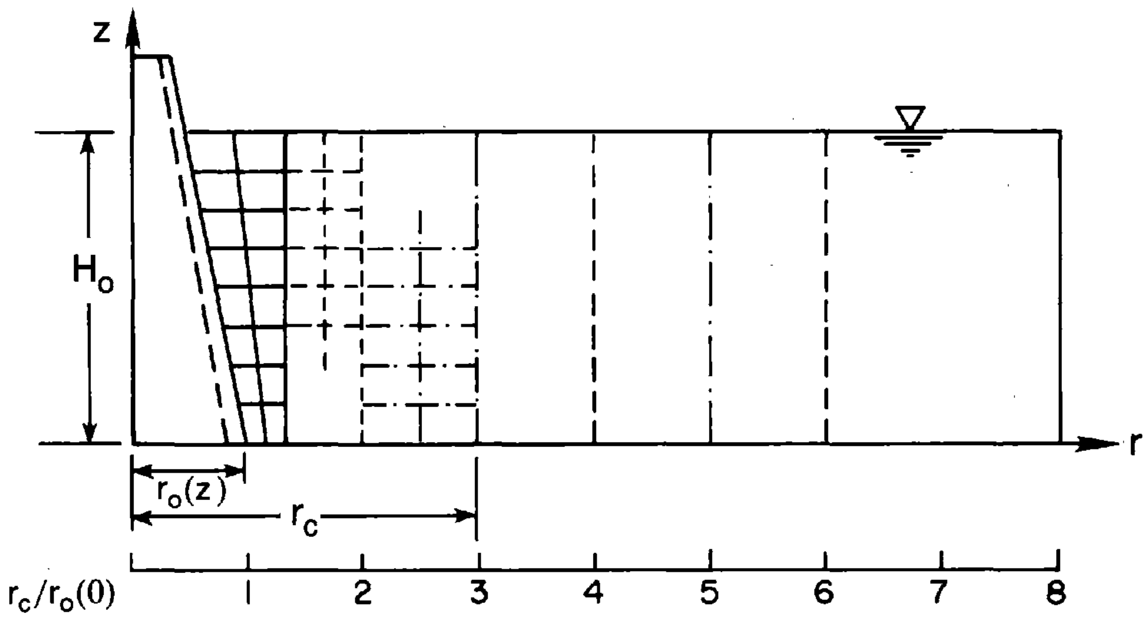

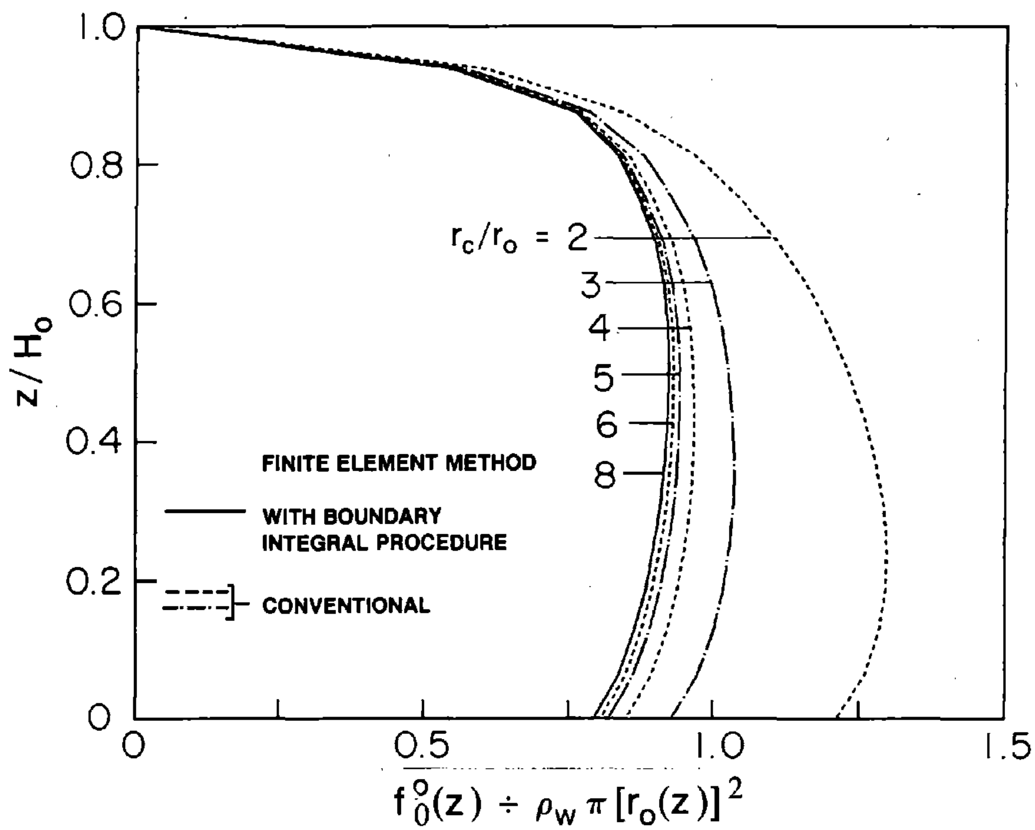

Figure 4.11 Lateral Hydrodynamic Forces Computed by Conventional FEM with Various Radial Dimensions $r_c/r_o(0)$ and Compared with Coupled FEM and boundary Integral Procedure

hydrodynamic mass and excitation terms. As mentioned in Section 3.2.5, $p^i_\beta(\vec{x})$ are solutions of the three-dimensional Laplace equation:

$$\frac{\partial^2 p^i}{\partial x^2} + \frac{\partial^2 p^i}{\partial y^2} + \frac{\partial^2 p^i}{\partial z^2} = 0 \tag{4.71}$$

subjected to the $N+2$ sets of boundary conditions collectively written in a generalized form:

$$\frac{\partial}{\partial n^i}\, p^i(\vec{x}) = -\,\rho_w\, a^i_n(\vec{x}) \qquad \vec{x} \in \Gamma^i_t \tag{4.72a}$$

$$\frac{\partial}{\partial z} p^i(\vec{x}) = -\,\rho_w\, b^i_n(\vec{x}) \qquad \vec{x} \in \Gamma^i_b \tag{4.72b}$$

$$p^i(\vec{x}) = 0 \qquad \vec{x} \in \Gamma^i_f \tag{4.72c}$$

in which $a^i_n(\vec{x})$ represents the spatial distribution of the acceleration of the tower water interface, Γ^i_t, along its normal direction, n^i ; function $b^i_n(\vec{x})$ represents the distribution of vertical acceleration of the reservoir bottom, Γ^i_b; and Γ^i_f defines the free surface of water. The boundary conditions of equation (4.72) apply to $p^i_0(\vec{x})$ [or $p^i_h(\vec{x})$ since $p^i_0(\vec{x}) = p^i_h(\vec{x})$], $p^i_j(\vec{x})$, and $p^i_r(\vec{x})$ if the functions $a^i_n(\vec{x})$ and $b^i_n(\vec{x})$ are defined by equations (4.73), (4.74) and (4.75), respectively :

$$a^i_n(\vec{x}) = n^i_x(\vec{x}) \qquad \vec{x} \in \Gamma^i_t \tag{4.73a}$$

$$b^i_n(\vec{x}) = 0 \qquad \vec{x} \in \Gamma^i_b \tag{4.73b}$$

$$a^i_n(\vec{x}) = n^i_x(\vec{x})\, \phi_j(z) - x\, n^i_z(\vec{x})\, \psi_j(z) \qquad \vec{x} \in \Gamma^i_t \tag{4.74a}$$

$$b^i_n(\vec{x}) = 0 \qquad \vec{x} \in \Gamma^i_b \tag{4.74b}$$

$$a_n^i(\vec{x}) = n_x^i(\vec{x})\, z - x\, n_z^i(\vec{x}) \qquad \vec{x} \in \Gamma_t^i \tag{4.75a}$$

$$b_n^i(\vec{x}) = -\, x \qquad \vec{x} \in \Gamma_b^i \tag{4.75b}$$

in which $n_x^i(\vec{x})$ and $n_z^i(\vec{x})$ are the direction cosines of the normal at a point $\vec{x}$ on the tower-water interface with respect to x and z axes respectively ; and functions $\phi_j(z)$ and $\psi_j(z)$ characterize the shape of the deflection curve of the tower in the j-th mode of vibration. In addition to the boundary conditions of equation (4.72), the symmetry of the tower geometry about the vertical plane Γ_s^i, along which the horizontal ground motion is applied, and about the vertical plane Γ_a^i in the direction normal to the applied ground motion (Figure 3.5) results in two additional requirements :

$$\frac{\partial}{\partial y} p^i(\vec{x}) = 0 \qquad \vec{x} \in \Gamma_s^i \tag{4.76}$$

$$p^i(\vec{x}) = 0 \qquad \vec{x} \in \Gamma_a^i \tag{4.77}$$

If there is no vertical acceleration of the bottom boundary of the inside water domain [i.e. $b_n^i(\vec{x}) \neq 0$], the hydrodynamic pressure functions $p_\beta^i(\vec{x})$ for circular cylindrical towers can be obtained from available analytical solutions [29,40]. However, it is usually necessary to use numerical methods in order to evaluate $p_\beta^i(\vec{x})$ if the geometry of the tower is more complex or if the effects of the vertical acceleration of the bottom boundary of the inside water domain are to be considered. For a bounded water domain inside a tower of arbitrary geometry, a numerical procedure based on the variational principle and conventional finite element method is presented next which gives directly the hydrodynamic pressures on the tower-water interface and on the inside reservoir bottom.

4.4.2 Finite Element Approximation

According to Euler's theorem [37], the function $p^i(\vec{x})$ which minimizes the functional :

$$\Pi(p) = \frac{1}{2} \int_{\tau^i} \nabla p \cdot \nabla p \; d\tau - \rho_w \int_{\Gamma_t^i} p \; a_n^i(\vec{x}) \; d\Gamma - \rho_w \int_{\Gamma_b^i} p \; b_n^i(\vec{x}) \; d\Gamma \tag{4.78}$$

satisfies equation (4.71) and boundary conditions of equations (4.72), (4.76), and (4.77) [Appendix C, Section C.2]. The first volume integral term in equation (4.78) represents the potential energy of the inside water domain τ^i and the last two terms, defined as surface integrals on the tower-water interface Γ_t^i and on the reservoir bottom Γ_b^i, produce forcing terms.

The hydrodynamic pressure on the tower surface is numerically evaluated by minimizing the functional of equation (4.78). For this purpose, the fluid domain τ^i is idealized as an assemblage of three-dimensional finite elements with N_A nodal points and consequently, the surfaces Γ_t^i and Γ_b^i get discretized into a number of sub-divisions as shown in Figure 4.12. Similar to equation (4.40) for the surrounding water domain, pressure in domain τ^i is expressed in terms of the unknown pressures p_i at i-th node for N_A nodal points by the following equation:

$$p^i(\vec{x}) \approx \sum_{1=1}^{N_A} N_i(\vec{x}) \, p_i \qquad \vec{x} \in \tau^i \tag{4.79}$$

where $N_i(\vec{x})$ represents the locally supported continuous interpolation functions of class C_0 corresponding to i-th nodal point. Substitution of equation (4.79) into equation (4.78) leads to a functional in vector $\boldsymbol{p}$ containing the unknowns p_i, $i = 1,2, \ldots, N_A$:

$$\Pi(\boldsymbol{p}) = \frac{1}{2} \boldsymbol{p}^T \boldsymbol{K}_I \, \boldsymbol{p} - \boldsymbol{p}^T \boldsymbol{Q}_I - \boldsymbol{p}^T \boldsymbol{Q}_{II} \tag{4.80}$$

in which $\boldsymbol{K}_I$ is $N_A \times N_A$ symmetric matrix with its jk-element given by:

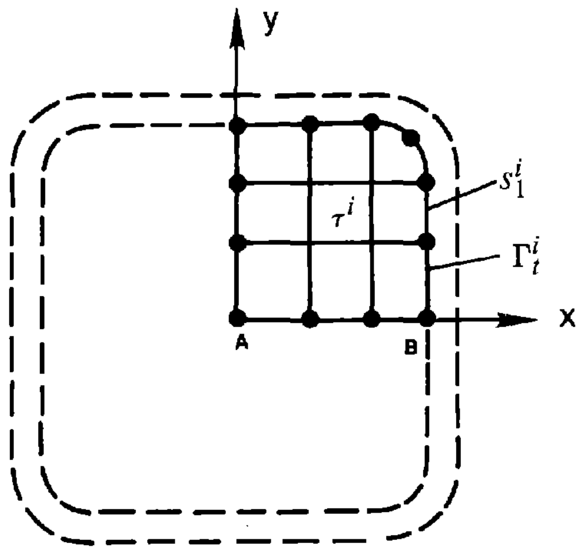

(a) FINITE ELEMENT SYSTEM IN x-y PLANE AT XX

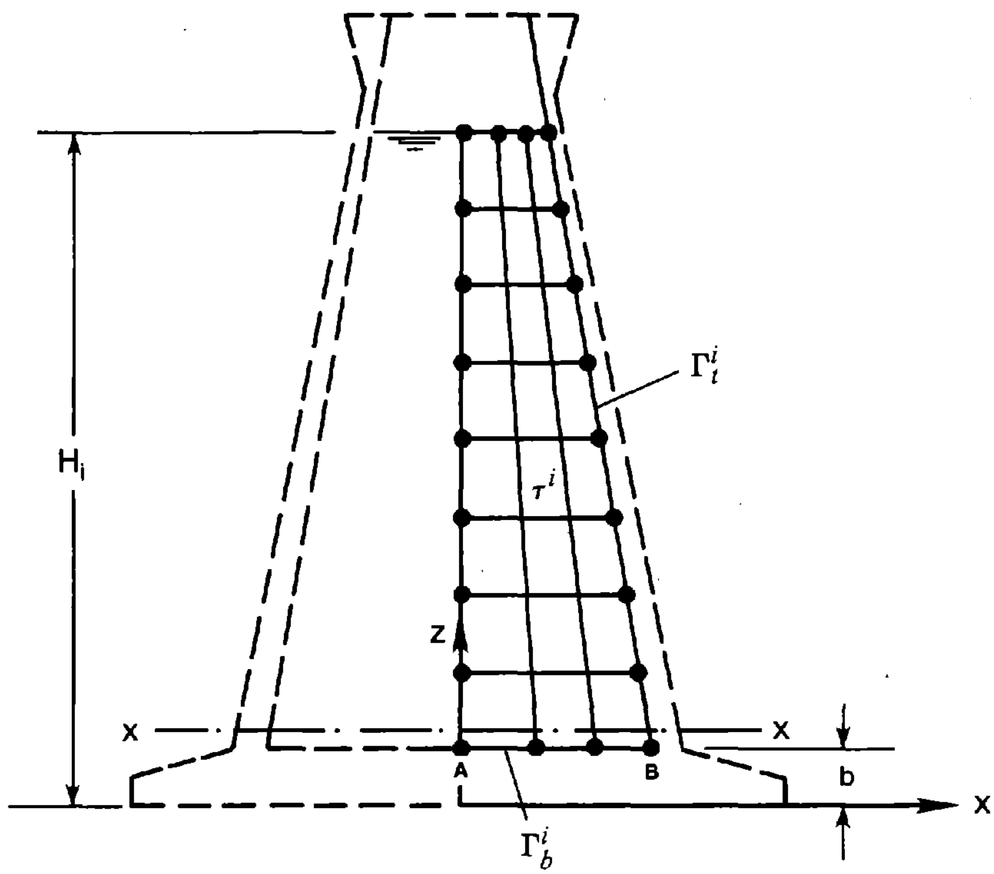

(b) FINITE ELEMENT SYSTEM IN x-z PLANE

Figure 4.12 Three-Dimensional Finite Element System for Inside Water Domain

$$(\boldsymbol{K}_I)_{j,k} = \int_{\tau^i} \nabla N_j(\vec{x}) \cdot \nabla N_k(\vec{x})\, d\tau \quad ; \quad j,k = 1,2, \ldots, N_A \tag{4.81}$$

The zero pressure boundary condition on surfaces Γ_f^i and Γ_a^i is satisfied by assigning zeros to the rows and columns in the matrix $\boldsymbol{K}_I$ corresponding to the nodes on these surfaces. Similarly, the vectors $\boldsymbol{Q}_I$ and $\boldsymbol{Q}_{II}$ appearing in the functional [equation (4.78)] are of order N_A and their j-th elements are given by:

$$(\boldsymbol{Q}_I)_j = \int_{\Gamma_i^i} N_j(\vec{x}) \cdot a_n^i(\vec{x})\, d\Gamma \quad ; \quad j = 1,2, \ldots, N_A \tag{4.82}$$

$$(\boldsymbol{Q}_{II})_j = \int_{\Gamma_e^o} N_j(\vec{x}) \cdot b_n^i(\vec{x})\, d\Gamma \quad ; \quad j = 1,2, \ldots, N_A \tag{4.83}$$

In matrix $\boldsymbol{Q}_I$, only those terms are non-zero which correspond to the nodes on the tower-water interface. Similarly, only the terms corresponding to the nodes on the reservoir bottom, are non-zero in matrix $\boldsymbol{Q}_{II}$.

Since the interpolation functions $N_i(\vec{x})$, $i = 1,2, \ldots, N_A$ are locally supported, integration is not performed over the full domain or the entire surface to determine elements of these matrices. Similar to the procedure used for surrounding water domain, integration in equations (4.81), (4.82) and (4.83) is done at element level and the matrices are assembled by standard procedures [53].

Minimization of the functional of equation (4.80) with respect to p_i, $i = 1,2, \ldots, N_A$ leads to a system of linear, algebraic equations in N_A unknowns :

$$\boldsymbol{K}_i\, \boldsymbol{p} = \boldsymbol{Q}_i \tag{4.84}$$

in which $\boldsymbol{K}_i = \boldsymbol{K}_I$ and $\boldsymbol{Q}_i = \boldsymbol{Q}_I + \boldsymbol{Q}_{II}$. The unknown hydrodynamic pressure vector $\boldsymbol{p}$ is evaluated by solving these simultaneous equations and its analytical representation $p^i(\vec{x})$ is then estimated by using equation (4.79), the symmetric properties of pressure functions along surface Γ_s^i, and the anti-symmetric properties along surface Γ_a^i. This analysis procedure is repeated $N+2$ times to evaluate the complete set of pressure functions $p^i_\beta(\vec{x})$, $\beta = 0,1,2, \ldots, N,h,r$ using different values of functions $a^i_n(\vec{x})$ and $b^i_n(\vec{x})$ given by equations (4.73) to (4.75). Once the pressures are known, the height-wise distributions of resultant hydrodynamic lateral forces and external moments are evaluated by integrating the components of these pressures along the perimeter of the inside surface of the tower using equation (3.44).

4.4.3 Semi-Analytical Process for Axisymmetric Towers

Similar to equation (4.61) for the surrounding water domain, acceleration $a^i_n(\vec{x})$ on the tower-water interface and $b^i_n(\vec{x})$ on the reservoir bottom can be redefined in terms of their corresponding functions $\bar{a}^i_n(r,z)$ and $\bar{b}^i_n(r,z)$ evaluated along the surface of the tower in the $r-z$ plane at $\theta=0$ i.e.

$$a^i_n(\vec{x}) = \bar{a}^i_n(r,z) \cos\theta \tag{4.85a}$$

$$b^i_n(\vec{x}) = \bar{b}^i_n(r,z) \cos\theta \tag{4.85b}$$

Using the orthogonality property of trigonometric functions, it has been shown [40] that the hydrodynamic pressures associated with acceleration distribution of equation (4.85) also varies as $\cos\theta$ in the circumferential direction i.e.

$$p^i(\vec{x}) = \bar{p}^i(r,z) \cos\theta \tag{4.86}$$

Thus, as for the surrounding water domain, only one two-dimensional problem needs to be solved. Therefore, to obtain the hydrodynamic pressures in the form of equation (4.86), the function $p^i(\vec{x})$ appearing in the functional of equation (4.78) must be of the following form:

$$p^i(\vec{x}) = \bar{p}^i(r,z) \cos\theta \approx \sum_{i=1}^{N_A} \overline{N_i}(r,z) \cos\theta \, p_i \tag{4.87}$$

in which $\overline{N_i}\ (r,z)$, $i=1,2, \ldots, N_A$ are the two-dimensional interpolation functions in the r-z plane.

Substitution of equation (4.87) into the functional of equation (4.78) and integration along θ direction leads to a two dimensional functional in the r-z plane:

$$\Pi(p) = \frac{1}{2}\int_{\Omega^i}\left[\frac{\partial p}{\partial r}\cdot\frac{\partial p}{\partial r} + \frac{\partial p}{\partial z}\cdot\frac{\partial p}{\partial z}\right] r\, dr\, dz + \frac{1}{2}\int_{\Omega^i}\frac{1}{r}\, p\cdot p\, dr\, dz$$

$$- \rho_w \int_{\Lambda_t^i} \bar{p}^{i}\, \bar{a}_n^i(r,z)\, r\, d\Lambda - \rho_w \int_{\Lambda_b^i} \bar{p}^{i}\, \bar{b}_n^i(r,z)\, r\, d\Lambda \tag{4.88}$$

wherein, parallel to Section 4.3.5, the volume domain τ^i has been replaced by area domain Ω^i in the $r-z$ plane and the surface domains Γ_t^i and Γ_b^i by contours Λ_t^i and Λ_b^i , also in the $r-z$ plane (Figure 4.13). Applying the numerical procedure presented in Section 4.4.2 to axisymmetric fluid domains [see Appendix D, Section D.2 for details], the functional of equation (4.88) can be minimized to obtain $\bar{p}^i(r,z)$. The procedure is implemented for the $N+2$ different distributions of acceleration on the tower-water interface and the reservoir bottom [equations (4.73) to (4.75)], specialized for axisymmetric towers through equation (4.85):

$$\bar{a}_n^i(r,z) = \bar{n}_x^i(r,z) \qquad (r,z) \in \Lambda_t^i \tag{4.89a}$$

$$\bar{b}_n^i(r,z) = 0 \qquad (r,z) \in \Lambda_b^i \tag{4.89b}$$

$$\bar{a}_n^i(r,z) = \bar{n}_x^i(r,z)\, \phi_j(z) - r\, \bar{n}_z^i(r,z)\, \psi_j(z) \qquad (r,z) \in \Lambda_t^i \tag{4.90a}$$

$$\bar{b}_n^i(r,z) = 0 \qquad (r,z) \in \Lambda_b^i \tag{4.90b}$$

$$\bar{a}_n^i(r,z) = \bar{n}_x^i(r,z)\, z - r\, \bar{n}_z^i(r,z) \qquad (r,z) \in \Lambda_t^i \tag{4.91a}$$

$$\bar{b}_n^i(r,z) = -\, r \qquad (r,z) \in \Lambda_b^i \tag{4.91b}$$

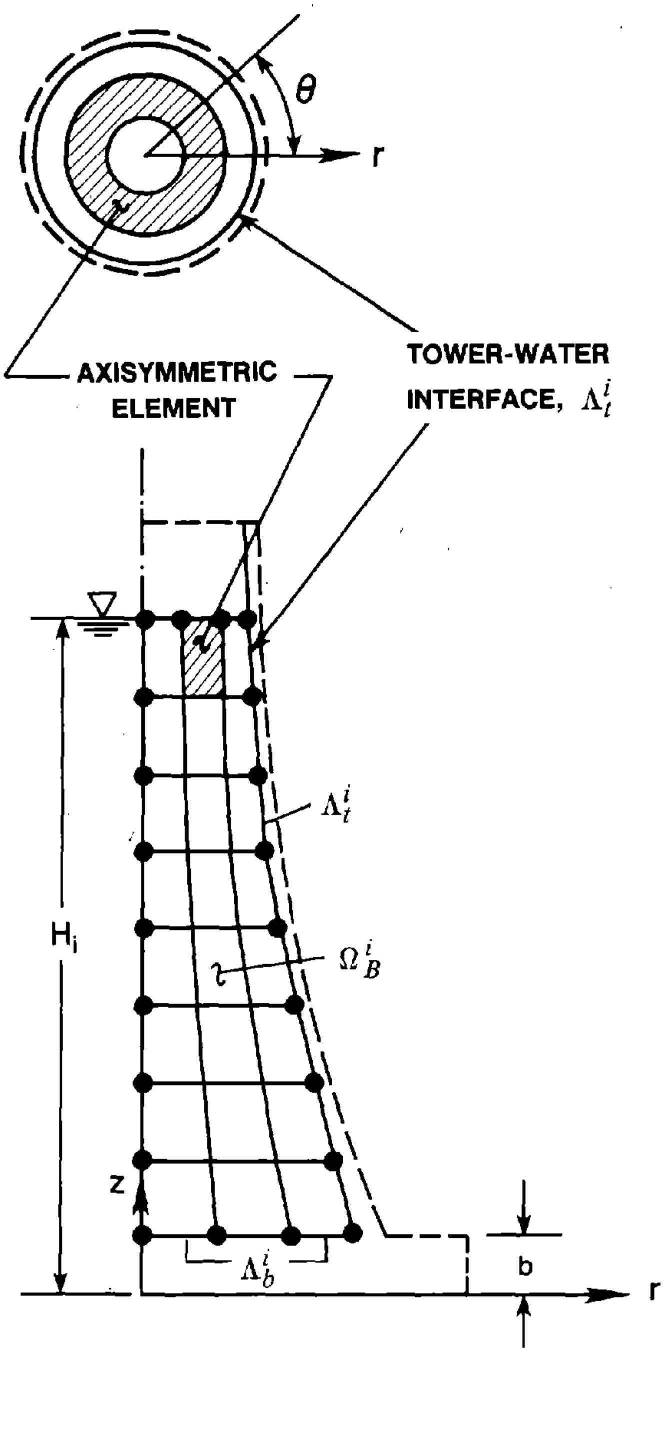

Figure 4.13 Axisymmetric Finite Element System for Inside Water Domain

This would result in the complete set of pressure functions $\bar{p}_\beta^i(r,z)$, $\beta = 0,1,2, \ldots, N,h,r$. The resultant lateral hydrodynamic force and moments per unit of height on the tower surface in the vertical plane of ground motion are then evaluated by a special case of equation (3.44)which is obtained by utilizing equation (4.86):

$$f_\beta^i(z) = \Big[\pi \, r \, \bar{n}_x^i(r,z) \, \bar{p}_\beta^i(r,z) \Big]_{r=r_i(z)} \tag{4.92a}$$

$$m_\beta^i(z) = \Big[\pi \, r^2 \, \bar{n}_z^i(r,z) \, \bar{p}_\beta^i(r,z) \Big]_{r=r_i(z)} - \pi \, \delta(z-b) \int_{\Lambda_e^i} r \, \Big[\bar{p}_\beta^i(r,z) \Big]_{z=b} \, dr \tag{4.92b}$$

where $r_i(z)$ defines the radius of the inside surface at a location z along the height; and b represents the z-coordinate of bottom boundary for the inside water domain. The computational effort required for an axisymmetric analysis is substantially lower compared to a three-dimensional analysis of the inside water domain.

4.4.4 Evaluation of the Procedure

The accuracy of the finite element method presented in the preceding sections is demonstrated by comparing the numerical results by this approach with analytical, infinite series solution for circular cylindrical towers [40]. The fluid domain interior to a rigid circular cylinder subjected to unit harmonic horizontal ground acceleration can be numerically analyzed by solving (i) a two-dimensional axisymmetric problem by the methods of Section 4.4.3, or (ii) a general three-dimensional problem by the method of Section 4.4.2. It is apparent from Figure 4.14 that the two sets of numerical results for the distribution of lateral hydrodynamic force $f_0^i(z)$ are essentially identical to analytical results. Therefore, the hydrodynamic analysis procedures using the finite element method presented in Sections 4.4.2 and 4.4.3 will lead to accurate values for the hydrodynamic terms required in equation (3.46) for earthquake analysis of towers of arbitrary geometry.

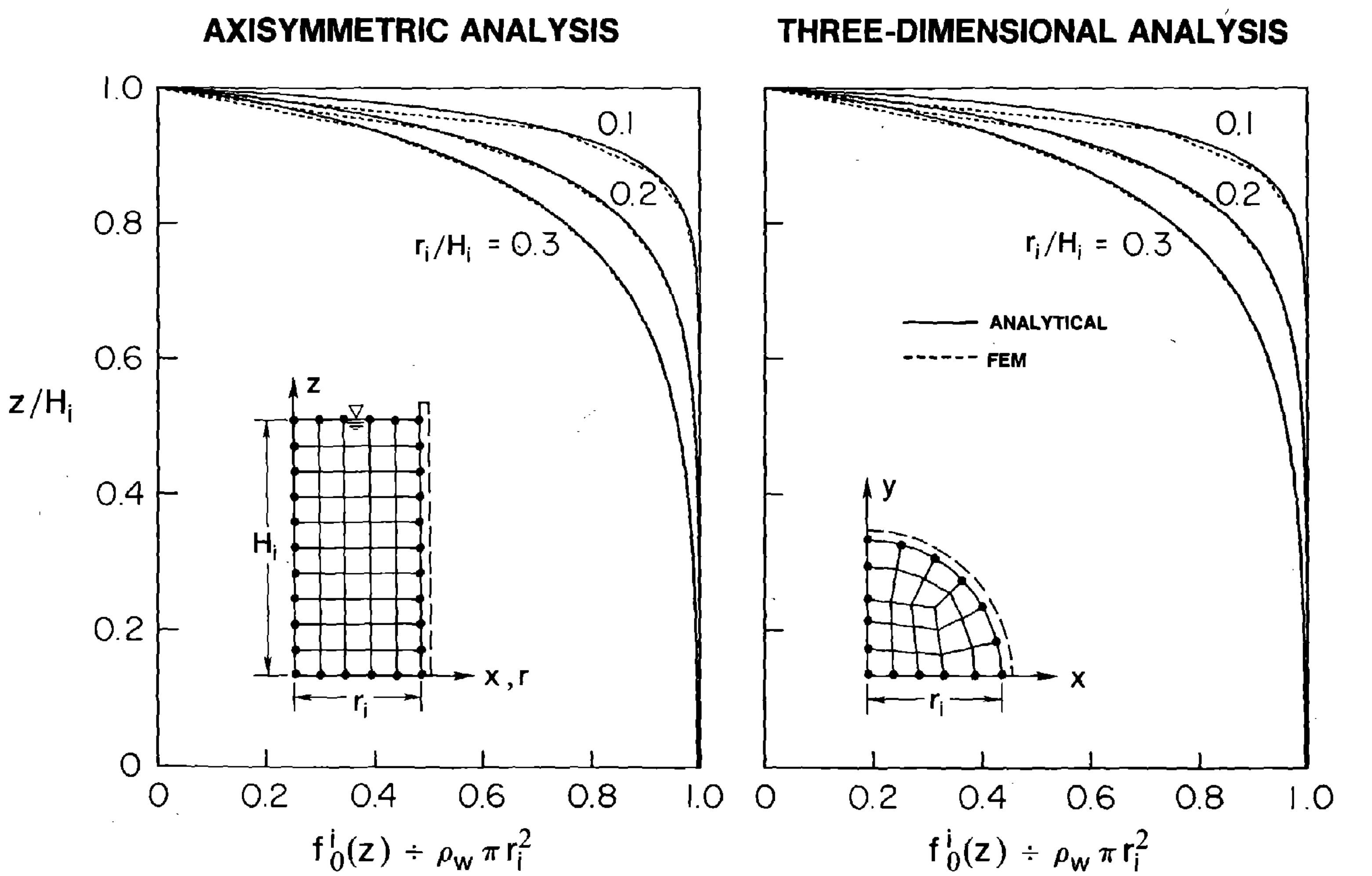

Figure 4.14 Lateral Hydrodynamic Forces due to Inside Water on Rigid Circular Cylindrical Towers from Two Finite Element Analyses; Comparison with Analytical Results

4.5 Computer Program

The response analysis procedure presented in Chapter 3 is implemented in two series of computer programs, 'TOWERRZ' series for axisymmetric towers and 'TOWER3D' series for towers of arbitrary cross-sections having two axes of symmetry, to numerically evaluate the earthquake response of intake-outlet tower systems described in Chapter 2. The effects that arise from the interaction between the tower and surrounding water, the tower and contained water, and the tower-foundation-soil interaction are included in the analysis. Efficient computational procedures described in Sections 4.1 to 4.4 have been incorporated into the computer program to make it an effective tool to compute the earthquake responses of intake-outlet towers of arbitrary geometry.

A 3-node, one-dimensional, Timoshenko beam element is included in the computer program to model the tower. Two different elements -- an 8-node, axisymmetric element and a 20-node, three-dimensional element are included to model the fluid domains. The numerical values of impedance functions for a circular foundation supported on the surface of a viscoelastic halfspace are evaluated by this program using the expressions derived in Section 4.2.3. However, an approximate treatment of non-circular foundations supported on the surface of a viscoelastic halfspace, presented in Section 4.2.4, is adopted in these programs. Alternatively, the user may provide the foundation impedance functions for the particular foundation-soil system being analyzed. The FFT algorithm used to evaluate the Fourier integrals in equations (3.49) and (3.50) recognizes that ground acceleration records and response histories are real-valued functions to reduce the computational time and storage requirements [23].

The input for the computer program consists of various system control parameters, geometric and material properties of the tower, control parameters to generate finite element meshes for the fluid domains, the number of natural vibration modes of the tower to be included, the FFT parameters, and the horizontal component of free-field ground acceleration. The output from the computer program consists of the complex-valued frequency response functions for the modal coordinates, the complete response-history of displacements, and the maximum values of shear force and bending moment at specified locations along the height of the tower.

The user's guide for the 'TOWERRZ' series of programs is presented in Appendix K of this report along with a numerical example. Similarly, the user's guide for the 'TOWER3D' series of programs is presented in Appendix L of this report along with a numerical example.

5. FREQUENCY RESPONSE FUNCTIONS

5.1 Introduction

The response of idealized intake-outlet towers to harmonic horizontal ground motion is presented in this chapter in the form of frequency response functions. The response results are computed using the general analytical procedure developed in Chapter 3 and the efficient numerical evaluation procedures presented in Chapter 4. The response results are presented for a wide range of important parameters that characterize the dynamic response of the tower-water-foundation-soil system. Based on the frequency response functions, the effects of tower-water interaction and tower-foundation-soil interaction on the dynamic response of towers are investigated.

5.2 Systems and Soil-Structure Interaction Parameters

5.2.1 Tower-Water-Foundation-Soil Systems

The response results are computed for towers with three different geometries : circular cylindrical towers, circular tapered towers, and non-circular uniform towers. For a circular cylindrical tower (Figure 5.1a), three different values for the ratio of tower height to average radius, H_s/r_a= 20, 10, and 5 are considered. The first one is typical of many slender towers, whereas the last one is selected as a rather extreme example for squat towers. The ratio of the inside and outside radii, r_i/r_o, is selected equal to 0.8, i.e. the wall thickness t_w = 0.2 r_o, a value typical of many towers. For a tapered tower with a circular cross-section (Figure 5.1b), the inside and outside radii at the top of the tower are taken equal to half of what they are at the base. The inside and outside radii decrease linearly along the height but their ratio $r_i(z)/r_o(z)$ at any location z above the base remains 0.8. Three values of the ratio of the tower height to its average radius r_a at the base, H_s/r_a= 20, 10 and 5, are considered. The responses of a uniform tower with the non-circular cross-section shown in Figure 5.1c, and with H_s/r_a = 20, are computed for ground motion applied separately along x and y

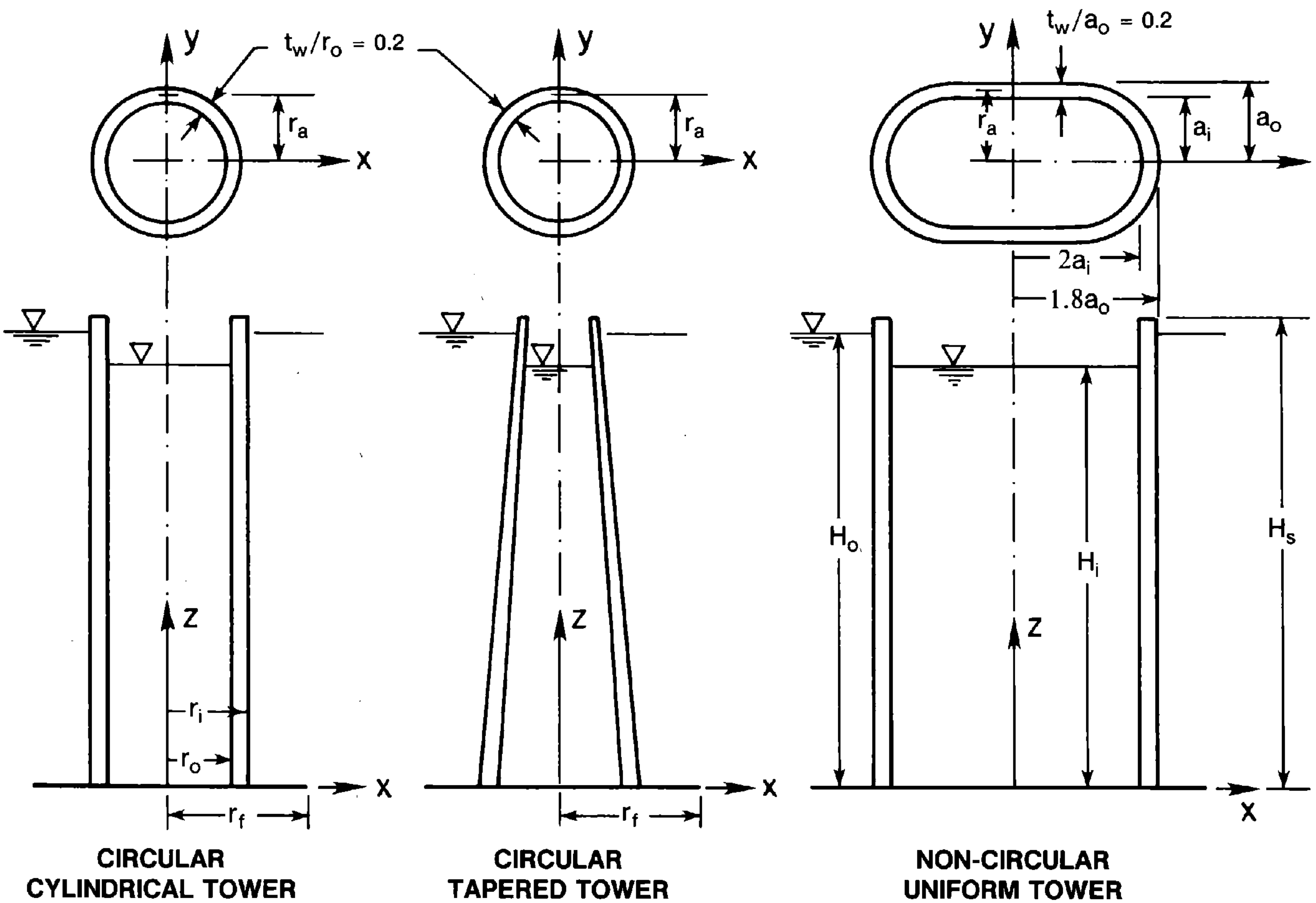

Figure 5.1 Three Idealized Towers

axes.

All towers are assumed to be homogeneous and isotropic with linear elastic properties for the concrete : Poisson's ratio = 0.17, unit weight = 155 lb/ft^3 and the Young's modulus of elasticity E_s = 4.5 million psi. The modification in the effective modulus of elasticity due to reinforcing steel is not considered. Energy dissipation in the tower concrete is represented by constant hysteretic damping factor of η_s = 0.10. This value corresponds to a viscous damping ratio of 0.05 in all natural vibration modes of the tower without water on rigid foundation soil.

Tower-foundation-soil interaction effects are investigated only for circular (both cylindrical and tapered) towers. In both cases, the tower structure is assumed to be supported through a rigid circular foundation on the surface of deformable soil idealized as a homogeneous, isotropic, viscoelastic halfspace. The following material properties of the foundation soil or rock are kept constant : Poisson's ratio ν_f = 1/3, and the ratio of the soil mass density to concrete mass density, ρ_f/ρ_s, = 1. Similarly, the ratio of the mass of the foundation to the mass of the superstructure, m_f/m_t, and the ratio of the rotatory inertia of the foundation to the total rotatory inertia of the tower structure about the base, I_f/I_t, are taken equal to 1.0 and 0.2, respectively. The selected values for m_f/m_t and I_f/I_t are more or less representative of many existing towers. They need not be varied because, within the ranges of values that are of interest in practical applications, the response of the structure is generally insensitive to variations in these particular ratios [45]. Energy dissipation in the flexible foundation soil is represented by constant hysteretic damping with damping factor η_f = 0.10.

The interpretation of tower-foundation-soil interaction effects is facilitated by three dimensionless parameters suggested, in part, by earlier research on buildings [46] : (i) The wave parameter $\sigma = C_f T_1 / r_a$ which is a measure of the relative stiffness of foundation soil and the tower, where C_f is the shear wave velocity in the foundation soil, T_1 is the fixed base natural period of vibration of the tower without water, and r_a is the average radius of the tower cross-section at the base; (ii) the ratio H_s/r_f of the height of the tower to the radius of the foundation footing; and (iii) the mass distribution parameter $\gamma = I_t/(\rho_s \pi r_a^2 H_s^3)$. To cover the wide range of tower properties and foundation soils, the wave parameter σ is varied from 20 to ∞, where the latter value represents rigid foundation soil ; the ratio H_s/r_f is varied from 2 to 8 ; and two values of parameter γ are considered : 0.15 for circular cylindrical towers (Figure 5.1a), and 0.06 for circular tapered towers (Figure 5.1b). This particular choice of dimensionless parameters for the tower-foundation-soil systems is discussed in Section 5.2.2. All the dimensionless parameters affecting tower-foundation-soil interaction are listed in Table 5.1 along with the range in which they are varied.

The water surrounding (outside) the tower is idealized as a fluid domain of constant depth extending to infinity in radial directions. The unit weight of water is taken equal to 62.4 lb/ft^3. Two values of inside water depth, H_i, and surrounding water depth, H_o, are considered : no water ($H_o/H_s = 0$, $H_i/H_s = 0$), and full water level ($H_o/H_s = 1$, $H_i/H_s = 1$). The hydrodynamic effects in the earthquake response of towers are influenced by the slenderness ratio H_s/r_a, in addition to H_o/H_s and H_i/H_s.

5.2.2 Soil-Structure Interaction Parameters

Two of the more significant parameters controlling tower-foundation-soil interaction effects are : σ and H_s/r_f. Because $H_s/r_f = (H_s/r_a)\cdot(r_a/r_f)$, it would be useful to determine whether interaction effects depend individually on the slenderness ratio H_s/r_a and the ratio r_f/r_a of the footing and tower radii or only on the combined parameter H_s/r_f. For this purpose, the ratio $\tilde{T}_1^f/T_1$, where $\tilde{T}_1^f$ is the fundamental resonant period of the tower-foundation-soil system, is computed for three circular cylindrical towers (Figure 5.1a), all with $\gamma = 0.15$ but varying slenderness ratio $H_s/r_a = 20$, 10 and 5, while keeping σ and H_s/r_f constant by adjusting C_f and ratio r_f/r_a. These computations are repeated for different combinations of σ and H_s/r_f. Similar computations are also performed for three circular

Table 5.1 -- Dimensionless Parameters for

Tower-Foundation-Soil Systems

Description	Definition	Value, this study
Wave parameter	$\sigma = C_f \cdot \frac{T_1}{r_a}$	Variable, 20 to ∞
Height to footing radius ratio	$\frac{H_s}{r_f}$	Variable, 2 to 8
Mass distribution parameter	$\gamma = \frac{I_t}{\rho_s \pi r_a^2 H_s^3}$	Variable, 0.15 and 0.06
Damping factor for soil	η_f	Fixed, 0.10
Footing mass ratio	$\frac{m_f}{m_t}$	Fixed, 1.0
Rotatory inertia ratio	$\frac{I_f}{I_t} = 0.10\,(1 + \frac{m_f}{m_t})$	Fixed, 0.2
Mass density ratio	$\frac{\rho_f}{\rho_s}$	Fixed, 1.0
Poisson's ratio	ν_f	Fixed, 1/3

tapered towers (Figure 5.1b), all with $\gamma = 0.06$ but varying slenderness ratio $H_s/r_a = 20$, 10 and 5. These results are summarized in Figure 5.2, wherein T_1^f/T_1 is plotted as a function of $1/\sigma$ for three different values of H_s/r_f for circular cylindrical towers (Figure 5.2a) and for circular tapered towers (Figure 5.2b). It is apparent that the period ratio T_1^f/T_1 is essentially independent of the individual values of ratios H_s/r_a and r_f/r_a, so long as H_s/r_f is kept constant. Therefore, the dimensionless parameters σ, H_s/r_f, and γ, are appropriate to characterize the effects of tower-foundation-soil interaction.

5.3 Cases Analyzed and Response Quantities

5.3.1 Cases Analyzed

The response results for the idealized tower-water-foundation-soil systems listed in Table 5.2 are presented in this chapter. These systems are defined by the geometry of the tower structure, direction of ground motion, and the chosen values for the important system parameters : H_s/r_a, H_o/H_s, H_i/H_s, σ, H_s/r_f, and γ. The response results for various cases and their interpretations are organized to understand the effects of various parameters on tower-water interaction, on tower-foundation-soil interaction, and ultimately on tower response.

5.3.2 Response Quantities

The complex-valued frequency response functions presented here are dimensionless response factors that represent the amplitude of the acceleration at the top of the tower, excluding the rigid body motions of the tower associated with translation and rotation of the foundation, due to unit harmonic free-field horizontal ground acceleration.

The frequency response functions, describing the response to harmonic horizontal ground motion, are computed for the excitation frequency ω varied over a relevant range of interest. Five fixed-base modes of the tower are included in the response computations for all cases. With these modal coordinates, the resulting frequency response functions are

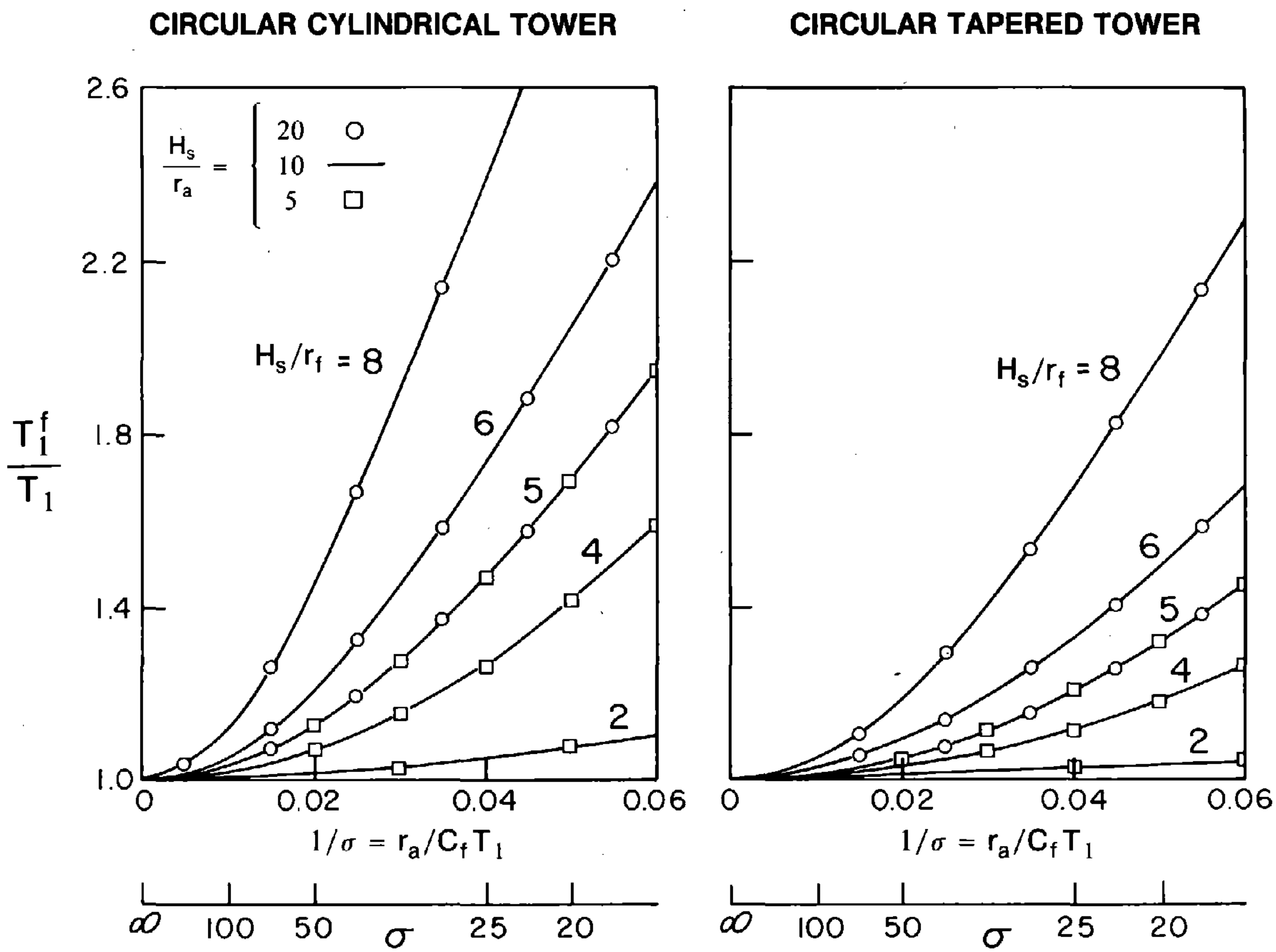

Figure 5.2 Ratio of Vibration Periods of a Tower (Without Water) on Flexible and Rigid Foundation Soils; Results are Presented for a Range of σ, H_s/r_f and H_s/r_a

Table 5.2 -- Cases of the Idealized

Tower-Water-Foundation-Soil Systems Analyzed

Case	Tower	Foundation Rock			Surrounding Water		Inside Water	
	H_s/r_a	Condition	σ	H_s/r_f	Condition	H_o/H_s	Condition	H_i/H_s
CIRCULAR CYLINDRICAL TOWERS $\gamma = 0.15$								
1	10	rigid	∞	-	none	0	none	0
2	10	rigid	∞	-	full	1	none	0
3	10	rigid	∞	-	none	0	full	1
4	10	rigid	∞	-	full	1	full	1
5	20	rigid	∞	-	partial	0 to 1	partial	0 to 1
6	10	rigid	∞	-	partial	0 to 1	partial	0 to 1
7	5	rigid	∞	-	partial	0 to 1	partial	0 to 1
8	10	flexible	40	5	none	0	none	0
9	10	flexible	20	5	none	0	none	0
10	10	flexible	60	5	none	0	none	0
11	10	flexible	40	3	none	0	none	0
12	10	flexible	40	7	none	0	none	0
13	20	flexible	20 to ∞	8	none	0	none	0
14	10	flexible	20 to ∞	5	none	0	none	0
15	5	flexible	20 to ∞	2	none	0	none	0
16	10	flexible	40	5	full	1	full	1
AXISYMMETRIC TAPERED TOWERS $\gamma = 0.06$								
17	10	rigid	∞	-	none	0	none	0
18	10	rigid	∞	-	full	1	none	0
19	10	rigid	∞	-	none	0	full	1
20	10	rigid	∞	-	full	1	full	1
21	20	flexible	20 to ∞	8	none	0	none	0
22	10	flexible	20 to ∞	5	none	0	none	0
23	5	flexible	20 to ∞	2	none	0	none	0
24	10	flexible	40	5	none	0	none	0
25	10	flexible	40	5	full	1	full	1
NON-CIRCULAR UNIFORM TOWERS GROUND MOTION ALONG X-AXIS								
26	20	rigid	∞	-	none	0	none	0
27	20	rigid	∞	-	full	1	none	0
28	20	rigid	∞	-	none	0	full	1
NON-CIRCULAR UNIFORM TOWERS GROUND MOTION ALONG Y-AXIS								
29	20	rigid	∞	-	none	0	none	0
30	20	rigid	∞	-	full	1	none	0
31	20	rigid	∞	-	none	0	full	1

accurate for excitation frequencies up to approximately six times the fundamental natural frequency ω_1 of the tower on rigid foundation soil with no water.

For each case in Table 5.2, the modulus of the complex-valued frequency response function for acceleration is plotted against the excitation frequency parameter ω/ω_1. When presented in this dimensionless form, the response results apply to all towers, which have the same geometry and the chosen values of Poisson's ratio, H_s/r_a, H_o/H_s, H_i/H_s, σ, H_s/r_f, and γ, irrespective of their actual height and elastic modulus or unit weight.

5.4 Tower-Water Interaction Effects

5.4.1 Principal Effects of Interaction

The effects of interaction between the tower and the water (both surrounding and inside) on the response of towers to horizontal ground motion are shown in Figure 5.3 where the results from analyses of cases 1 to 4 and 17 to 20 (Table 5.2) are plotted. The response of a tower without water (Case 1 or 17) is characteristic of a multi-degree of freedom system with frequency-independent mass, stiffness and damping properties. The response of the tower with surrounding and inside water, however, is affected by the hydrodynamic terms appearing in the equations of motion (Chapter 3) which can be interpreted as modifying the dynamic properties of the tower by introducing an added mass and an added force.

The results presented in Figure 5.3 reveal that water, inside or outside, has two principal effects : (i) the fundamental resonant frequency of the tower decreases because of the added hydrodynamic mass ; and (ii) the amplitude of the fundamental resonant peak increases in part due to the added hydrodynamic force. This amplitude increase is less than reported earlier [34] because the effective damping at the reduced resonant frequency is unchanged with the frequency-independent constant hysteretic damping assumed in this study, but is reduced in Reference [34] because of the frequency-dependent viscous damping model, leading to larger resonant response.

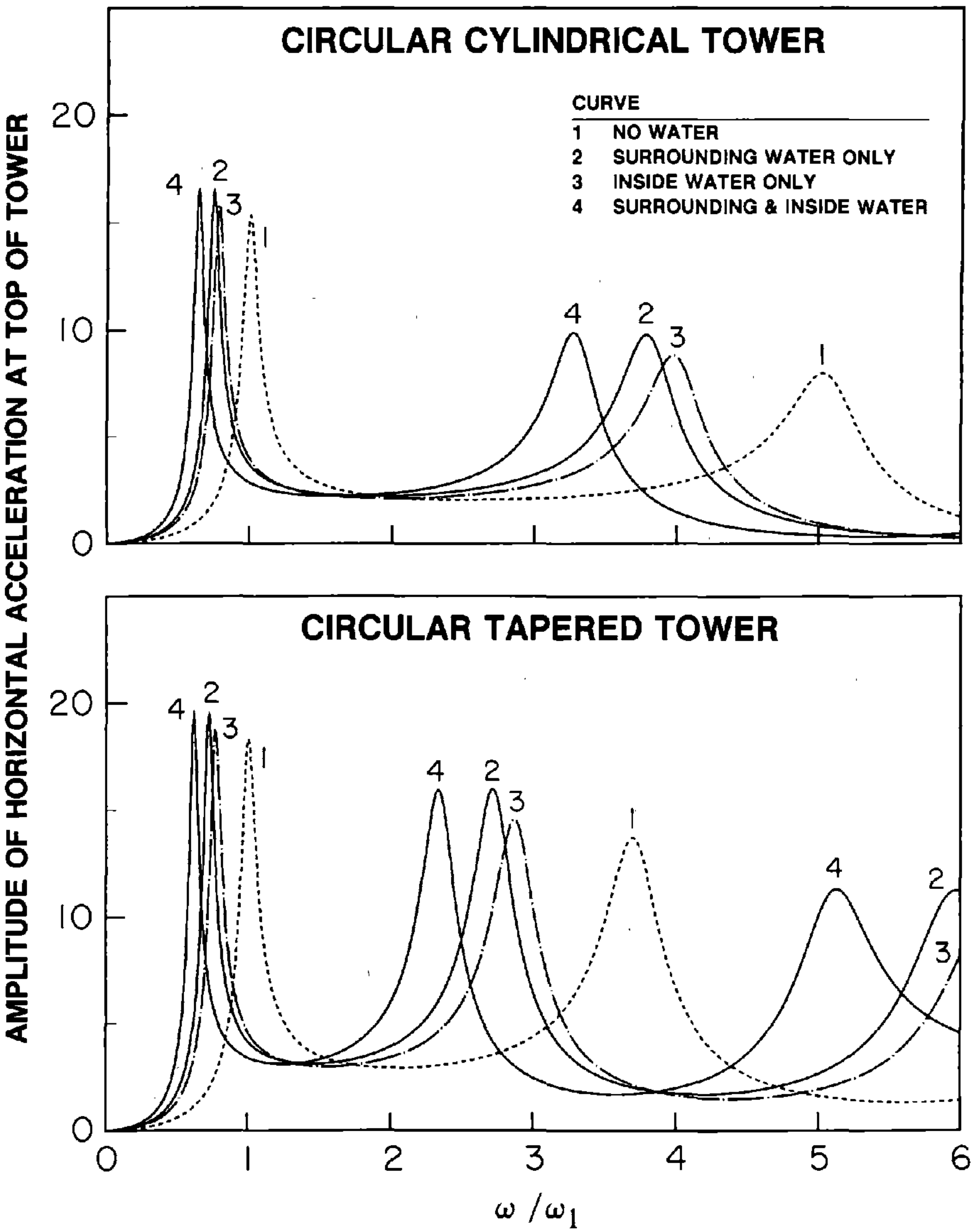

Figure 5.3 Hydrodynamic Effects in Response of Towers due to Harmonic Ground Motion. Results Presented for Various Assumptions of Surrounding and Inside Water (Cases 1 to 4 and 17 to 20 of Table 5.2)

It is apparent from Figure 5.3 that the resonant frequencies of the tapered towers are more closely spaced than those of the uniform tower and that the amplitudes of the resonant peaks without water are larger for the tapered towers. However, the tower-taper has very little influence on the percentage decrease in the fundamental resonant frequency, and the percentage increase in the amplitude of the fundamental resonant peak, due to surrounding or inside water.

The values of T_n^o/T_n and T_n^i/T_n are presented for the first two resonant peaks ($n=$ 1, 2) in Figure 5.4 as functions of the ratio of water depth to tower height, H_o/H_s for surrounding water and H_i/H_s for inside water, for three different values of H_s/r_a (Cases 5, 6, and 7 of Table 5.2). In these period ratios, T_n is the n-th natural vibration period of the tower on rigid foundation soil without water, which is increased to T_n^o due to the surrounding water, and to T_n^i due to the inside water, Since these results demonstrate the qualitative similarity between the effects of surrounding water and of the inside water, the following observations are valid for both cases : (i) Water lengthens the fundamental vibration period with this effect being very small for H_o/H_s or H_i/H_s less than 0.5, but increases rapidly at greater water depths; (ii) The lengthening of vibration period for the second resonant peak is very small for H_o/H_s or H_i/H_s less than 0.2, increases rapidly for water depth ratios up to 0.6, but the rate of increase slows down between water depth ratios of 0.6 to 0.8. This particular behavior is closely related to the variation of generalized added hydrodynamic mass with water depth which in turn depends on the second mode shape and the added mass distribution ; (iii) For full reservoir (i.e. H_o/H_s = 1 or H_i/H_s = 1), the percentage lengthening of the first two vibration periods is about the same ; however, for partially filled reservoir, specially when $0.2 \le H_o/H_s \; or \; H_i/H_s \le 0.8$, the percentage increase in the second vibration period is substantially larger than that in the fundamental vibration period ; and (iv) Vibration periods of slender towers (i.e. large H_s/r_a values) are lengthened to a greater degree than for squat towers.

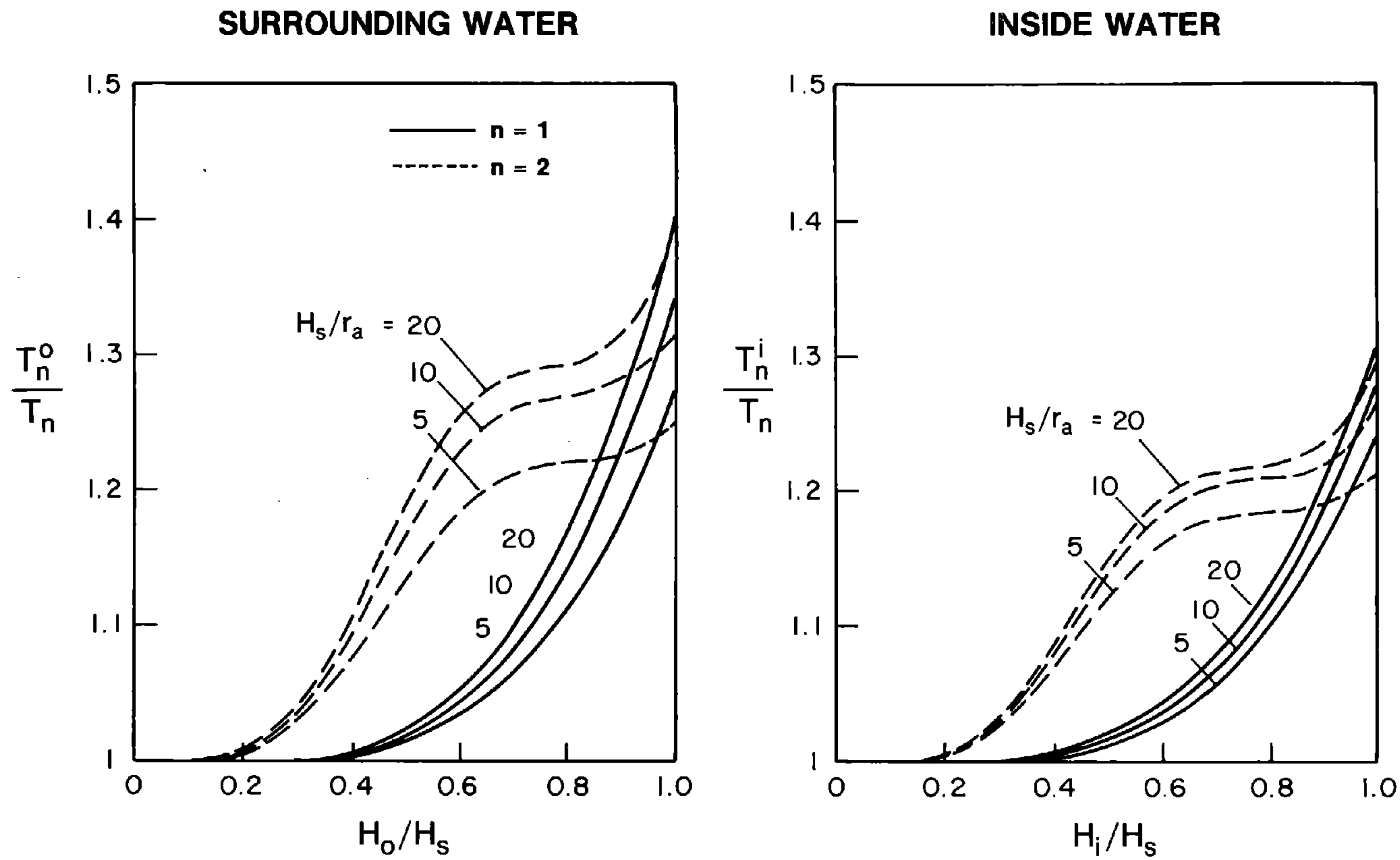

Figure 5.4 Ratio of Vibration Periods of a Tower (on Rigid Foundation Soil) with and without Water; Results are Presented for Fundamental and Second Vibration Period and for Surrounding and Inside Water

As expected, the reductions in resonant frequencies (or increases in resonant periods) due to surrounding and inside water are cumulative (Figure 5.3). By considering the free vibration of a tower supported on rigid foundation soil and constrained to vibrate in its n-th mode shape on fixed base without water, it can be shown that [Appendix E] :

$$\left[\frac{T_n^r}{T_n}\right]^2 = \left[\frac{T_n^o}{T_n}\right]^2 + \left[\frac{T_n^i}{T_n}\right]^2 - 1 \tag{5.1}$$

in which T_n^r is the effective n-th natural vibration period of the tower on rigid foundation soil due to combined effects of surrounding and inside water. Based on the above mentioned numerical results it can be verified that, although equation (5.1) is not exact when coupling of the natural vibration modes of the tower caused by the added hydrodynamic mass is considered, it is an excellent approximation for the fundamental vibration mode but errors tend to increase with increasing mode number.

5.4.2 Direction of Ground Motion

The frequency response function for a tower of circular cross-section, with or without water, is independent of the orientation of the horizontal ground motion. However, this may not be the case for other cross-sections. In order to examine this matter, frequency response functions are presented in Figure 5.5 for a uniform tower with non-circular cross-section (Figure 5.1c) subjected to excitations in two different directions along the planes of symmetry (Cases 26 to 31, Table 5.2). In order to facilitate interpretation of the response, the height-wise distribution of lateral hydrodynamic forces $f_0^o(z)$ and $f_0^i(z)$ on a rigid tower due to the surrounding and the inside water, respectively, associated with the two directions of excitation are also presented in Figure 5.6. The hydrodynamic forces are presented in their normalized form, i.e. $f_0^o(z)$ has been normalized by the mass of the displaced water per unit of height of the tower, $\rho_w A_o$, and $f_0^i(z)$ by the mass of the water contained in the tower per unit of its height, $\rho_w A_i$. An added mass, equivalent to the hydrodynamic force

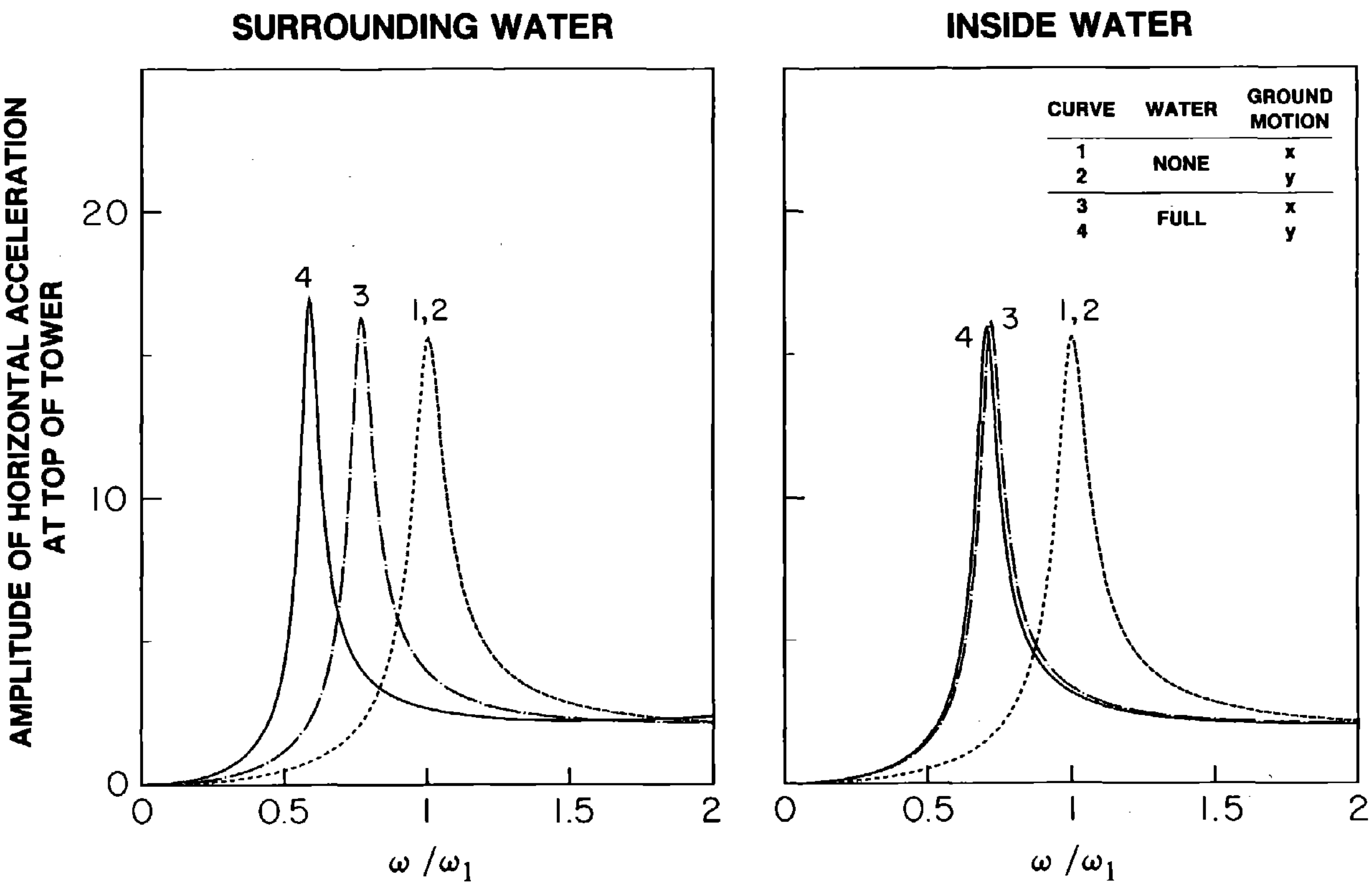

Figure 5.5 Influence of Direction of Ground Motion on Response of Towers with Non-Circular Cross Section (Cases 26 to 31, Table 5.2)

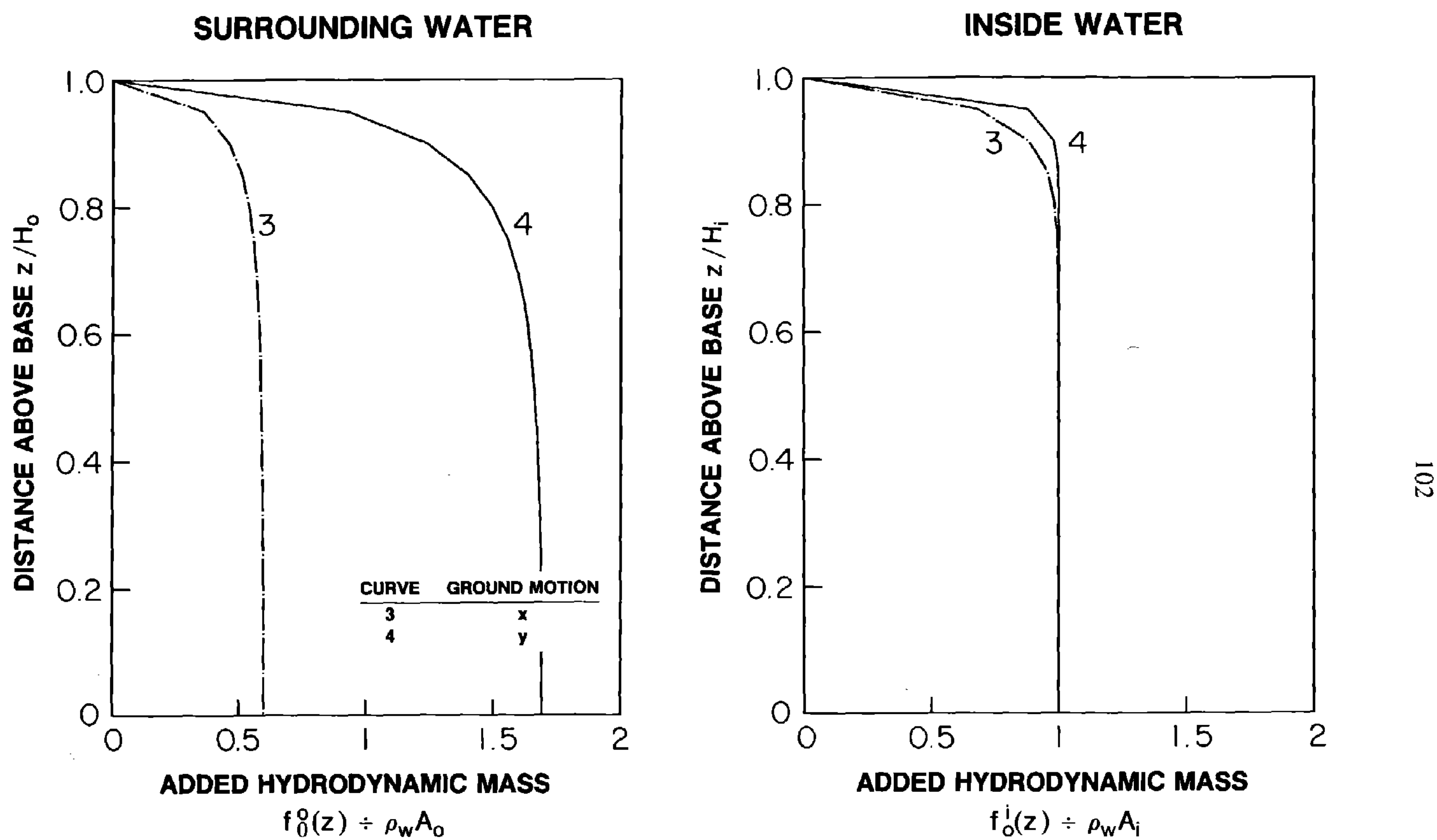

Figure 5.6 Influence of Direction of Ground Motion on the Added Hydrodynamic Mass (Cases 27,28,30 and 31 of Table 5.2)

assumed to be moving with the tower, adequately represents the hydrodynamic interaction effects in the fundamental mode response of towers [33].

The response results presented in Figure 5.5 indicate that, as expected, the frequency response functions of the tower by itself (no water) are essentially independent of the direction of ground motion (Cases 26 and 29 in Table 5.2). In fact, the two responses would be identical if the effects of shear deformations and rotatory inertia were neglected. Although these effects were included, they are small for slender towers like the one considered here. However, the dynamic response of towers with surrounding water, in particular the reduction in the fundamental resonant frequency due to surrounding water, is strongly influenced by the direction of ground motion (Figure 5.5) because the magnitude of the added hydrodynamic mass strongly depends on the direction of ground motion (Figure 5.6a). For a tower of particular cross-section, one of the parameters governing the magnitude of added hydrodynamic mass is the cross-sectional dimension perpendicular to the direction of ground motion, which is quite different for the tower of Figure 5.1(c) in the two directions. On the contrary, the frequency response functions for the tower with inside water, in particular the decrease in the fundamental resonant frequency due to inside water, is essentially independent of the direction of excitation (Figure 5.5) because most of the water contained in the hollow tower moves as a rigid mass for either direction of ground motion (Figure 5.6b). When presented in the normalized form of Figure 5.5, the amplitude of the fundamental resonant peak is essentially unaffected by the direction of ground motion because, as will be shown in Chapter 8, the distribution of added hydrodynamic mass is about the same.

5.5 Tower-Foundation-Soil Interaction Effects

5.5.1 Principal Effects of Interaction

The effects of tower-foundation-soil interaction on the response of towers are demonstrated in Figure 5.7 where the response results from analyses of cases 1, 8, 9, 10, 11, and 12 are plotted. Tower-foundation-soil interaction reduces the fundamental resonant frequency

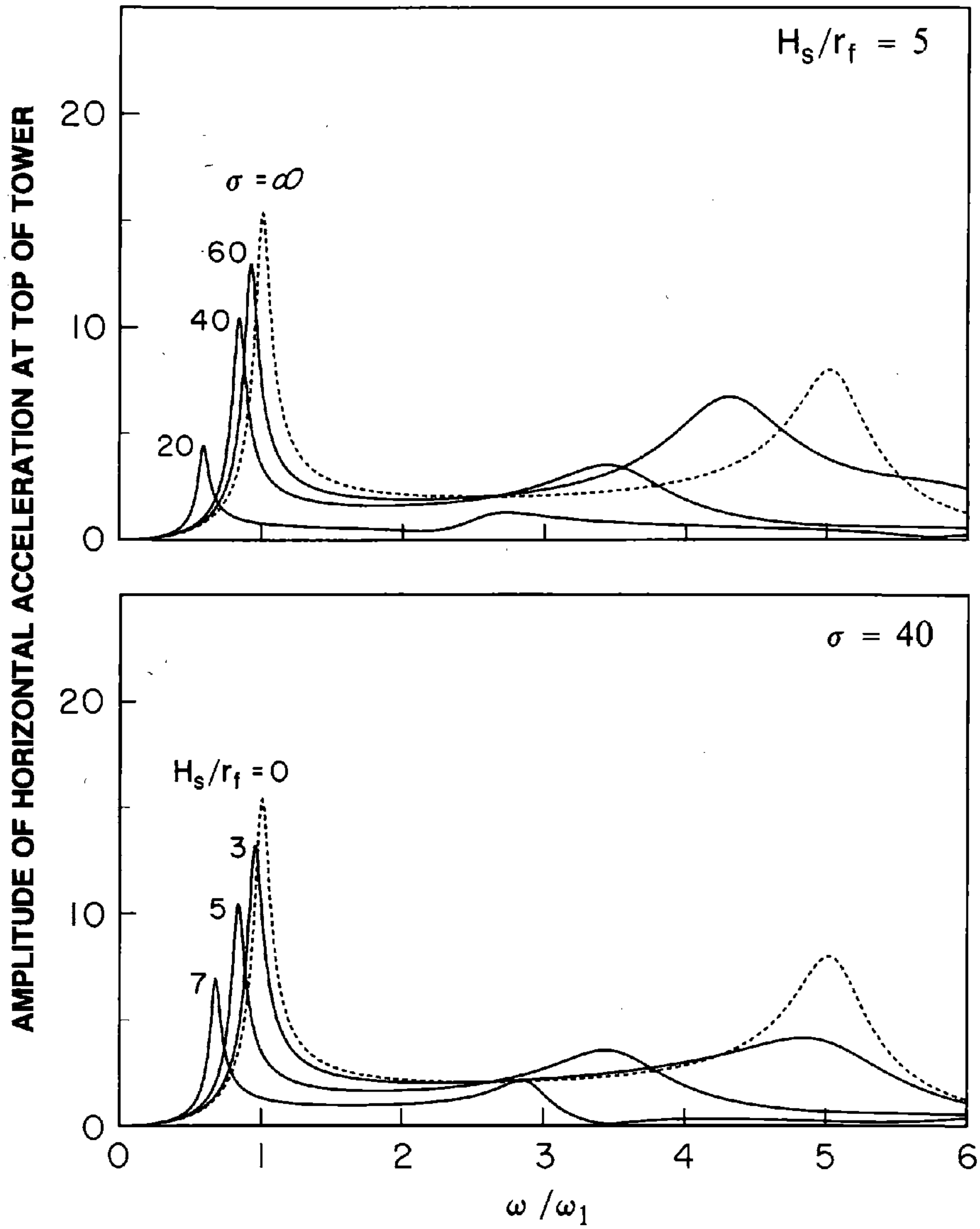

Figure 5.7 Influence of Wave Parameter σ and Ratio H_s/r_f on Response of Towers to Harmonic Ground Motion, $\ddot{u}_g(t) = e^{i\omega t}$; Response Results Presented for Circular Cylindrical Towers (Cases 1, and 8 to 12, Table 5.2)

of the tower, reduces the amplitude of the fundamental resonant peak, and increases the bandwidth at resonance because of the radiation and material damping in the foundation soil region. Similarly, the higher resonant frequencies are reduced, although to a lesser degree than the fundamental resonant frequency, and the amplitudes of the higher resonant peaks are substantially reduced. The second resonant frequency of bending beams, such as the towers considered, is affected more than the shear beams [46] because the interaction forces, base shear and moment, due to the second mode are more significant in the former case. The larger reduction in the amplitudes of higher resonant peaks is the result of the increased radiation damping in the foundation soil at high excitation frequencies.

The response results presented in Figure 5.7 (Cases 1, 8, 9, and 10, 11, and 12) show the dependence of tower-foundation-soil interaction effects on the dimensionless wave parameter $\sigma = C_f\, T_1/r_a$, and the ratio of tower-height to foundation radius, H_s/r_f. For more flexible foundation soils (lower shear wave velocity C_f) or for a stiff structure (lower fundamental vibration period T_1), the wave parameter σ is smaller and the interaction effects are larger, i.e. larger reductions of the fundamental resonant frequency and amplitudes of the fundamental resonant peak are observed. Similarly, for larger values of H_s/r_f, the interaction effects are larger. For lower values of σ and higher values of H_s/r_f, the higher amplitudes of the rocking motion at the fundamental resonant frequency generate stress waves of higher amplitudes propagating away from the structure-foundation interface which dissipate more energy through radiation and material damping. Consequently, the apparent damping of the structure increases causing lower amplitudes of resonant peaks and wider bandwidths at resonance.

For systems characterized by constant values of shear wave velocity, C_f, and the ratio of footing-radius to tower-radius, r_f/r_a, the influence of the slenderness ratio of the tower, H_s/r_a, is not clear because of two competing factors : On the one hand, towers with large H_s/r_a ratio are usually relatively flexible long-period structures leading to a larger value of wave parameter σ which suggests that the structure-foundation interaction effects are likely to be small (Figure 5.7a); and on the other hand, larger H_s/r_a ratio usually leads to larger ratio of tower-height to footing-radius, H_s/r_f, for which the structure-foundation interaction effects become increasingly significant (Figure 5.7b). Since the response results presented in terms of σ and H_s/r_f for a fixed value of γ are independent of H_s/r_a (Section 5.2.2), the influence of the ratio H_s/r_a on the tower-foundation-soil interaction effects can be investigated by simply comparing the dependence of σ and H_s/r_f on H_s/r_a. Using bending theory for uniform towers, it can be shown that T_1 is proportional to H_s^2/r_a. Therefore, for fixed C_f, the wave parameter σ, which by definition is proportional to T_1/r_a, is proportional to the square of H_s/r_a. For fixed r_f/r_a, however, the ratio H_s/r_f is proportional to H_s/r_a only. Therefore, with increasing value of H_s/r_a, the influence of tower-foundation-soil interaction on the response of the towers is reduced because the increase in the value of σ is much greater than the increase in the value of ratio H_s/r_f. This is the primary reason that the tower-foundation-soil interaction effects are likely to be more significant in the response of squat towers than in the response of slender towers even though the latter have larger tower-height to footing-radius ratio.

The influence of mass distribution parameter γ (Table 5.1) on the tower-foundation-soil interaction effects is demonstrated by plotting the ratio T_1^f/T_1, where T_1 is the fundamental resonant period of the fixed-base tower which is increased to T_1^f due to soil flexibility, in Figure 5.8 as a function of $1/\sigma$ and H_s/r_f for two different families of towers : circular cylindrical towers (Cases 13 to 15) and circular tapered towers (Cases 21 to 23). As demonstrated in Figure 5.8, soil flexibility has less influence on the fundamental vibration period for lower values of γ. Because the parameter γ for tapered towers is smaller than for uniform towers, for the same values of σ and H_s/r_f, tower-foundation-soil interaction therefore has less influence on the response of tapered towers. Physically, for the same total mass and height, the overturning moment at the base tends to be smaller for tapered towers resulting in reduced rocking motion of the footing and associated interaction effects.

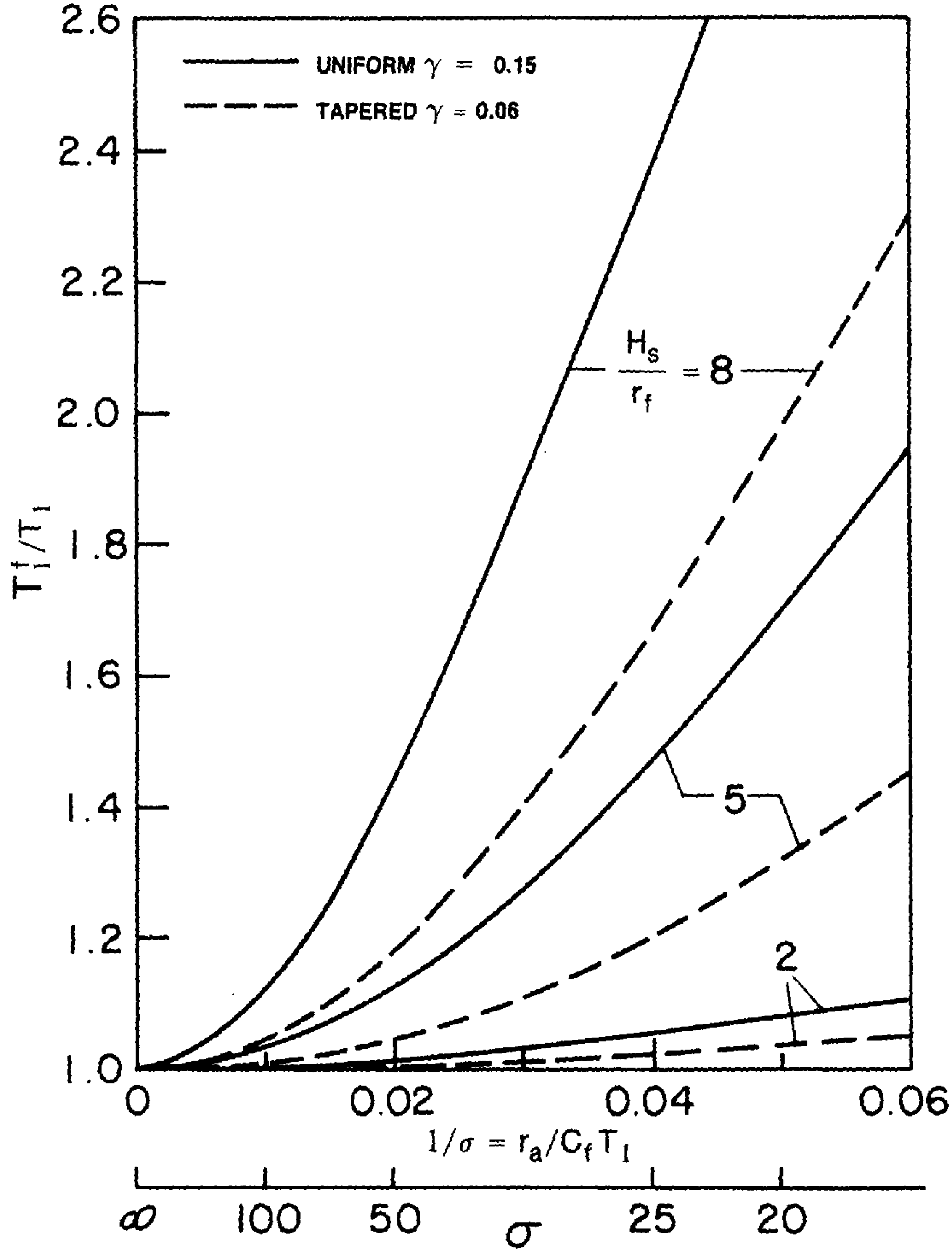

Figure 5.8 Influence of Mass Distribution Parameter on Period Ratio T_1^f/T_1 ; Response Results Presented for Cases 13 to 15 and 21 to 23

5.5.2 Influence of Hydrodynamic Interaction

The simultaneous effects of tower-water interaction and of tower-foundation-soil interaction on the dynamic response of axisymmetric towers (both cylindrical and tapered) can be observed from the response functions presented in Figure 5.9 for four systems : towers on rigid foundation soil with no water (Case 1 and 17); towers on flexible foundation soil with no water (Case 8 and 20); towers on rigid foundation soil with full water (Case 4 and 24); and towers on flexible foundation soil with full water (Case 16 and 25).

The response results demonstrate that the effects of tower-foundation-soil interaction on the frequency and amplitude of the fundamental resonant peak are qualitatively similar whether the hydrodynamic interaction effects are included in the analysis or neglected. Additionally, the percentage increase in the fundamental resonant period (or reduction of fundamental resonant frequency) due to tower-foundation-soil interaction is almost independent of hydrodynamic interaction effects. This observation leads to the following approximation:

$$\frac{\tilde{T}_1}{T_1} \approx \frac{T_1^r}{T_1} \cdot \frac{T_1^f}{T_1} \tag{5.2}$$

where T_1 is the fundamental vibration period of the tower on rigid foundation soil without water, which increases to T_1^r due to tower-water interaction, to T_1^f due to tower-foundation-soil interaction, and to $\tilde{T}_1$ due to both types of interaction simultaneously. Similarly, the percentage decrease in the amplitude of the fundamental resonant peak resulting from the increase in effective damping due to tower-foundation-soil interaction effects remains practically independent of the hydrodynamic interaction effects.

The response results presented in the previous section suggest that hydrodynamic interaction should reduce the effects of tower-foundation-soil interaction on the frequency and amplitude of the fundamental resonant peak but the response results of Figure 5.9 do not support this suggestion. Because water lengthens the fundamental vibration period of

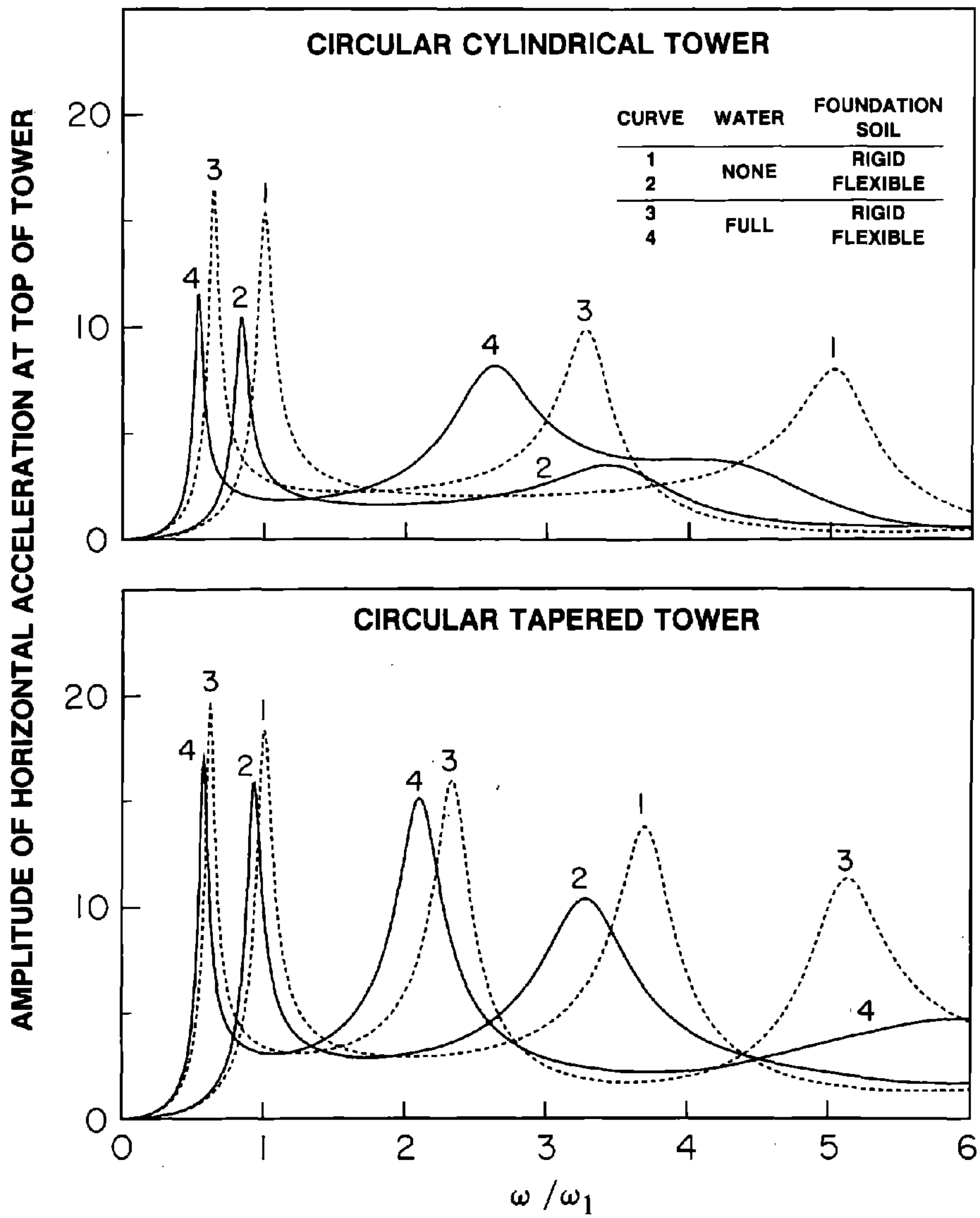

Figure 5.9 Response of Towers due to Harmonic Ground Motion for Four Conditions: Tower on Rigid Soil with No Water (Cases 1 and 7); Tower on Flexible Soil with No Water (Cases 8 and 24); Tower on Rigid Soil with Full Water (Cases 4 and 20); and Tower on Flexible Soil with Full Water (Cases 16 and 25)

the tower leading to an increase in the effective value of the wave parameter σ, the results of Figure 5.7 would indicate reduced effects of tower-foundation-soil interaction. It appears that this reduction is compensated by the increase in tower-foundation-soil interaction effects due to increased overturning moment (or due to higher value of γ) caused by the added hydrodynamic mass.

The influence of tower-foundation-soil interaction on the higher resonant peaks is, however, smaller in the presence of water. For towers vibrating in higher vibration modes, the added hydrodynamic mass produces small overturning moments which are not large enough to compensate for the reduction in interaction effects resulting from the lengthening of the higher vibration periods due to water.

6. EARTHQUAKE RESPONSE OF BRIONES DAM INTAKE TOWER

6.1 Introduction

The earthquake response of Briones dam intake tower to Taft ground motion is presented in this chapter. The analytical and numerical procedures developed in Chapters 3 and 4, are used to compute the response of the intake tower under various assumptions for the impounded water and the foundation rock. Based on the results from these analyses, the effects of tower-water interaction and tower-foundation-soil interaction on the tower responses are investigated. Certain aspects of practical earthquake analysis for intake-outlet towers are also discussed.

6.2 Briones Dam Intake Tower and Ground Motion

6.2.1 Briones Dam Intake Tower

This reinforced concrete intake tower, located east of San Francisco Bay, is approximately 230 ft high, has a hollow circular cross-section of outside diameter of 22.67 ft near the base and tapering to a diameter of 11.5 ft at the top. The wall thickness is 1.33 ft at the base, decreasing to 1.06 ft near the top. The tower is supported on a 13 ft high solid concrete block which has a diameter of 60 ft at the ground level (Figure 6.1a). The one-dimensional finite element idealization of the intake tower consists of 15 three-node elements with 31 nodal points (Figure 6.1b), resulting in 60 degrees of freedom if the foundation soil is assumed to be rigid and 62 degrees of freedom if the flexibility of foundation soil is considered. The solid concrete block supporting the hollow tower is treated as rigid.

The concrete in the intake tower is assumed to be a homogeneous, isotropic, linear elastic solid with the following properties : Young's modulus of elasticity E_s = 4.5 million psi, unit weight = 155 lb/ft^3, and Poisson's ratio = 0.17. The effects of reinforcing steel on the elastic modulus, which are expected to be small, are neglected. Energy dissipation in the tower is represented by a constant hysteretic damping factor of η_s = 0.10. This damping

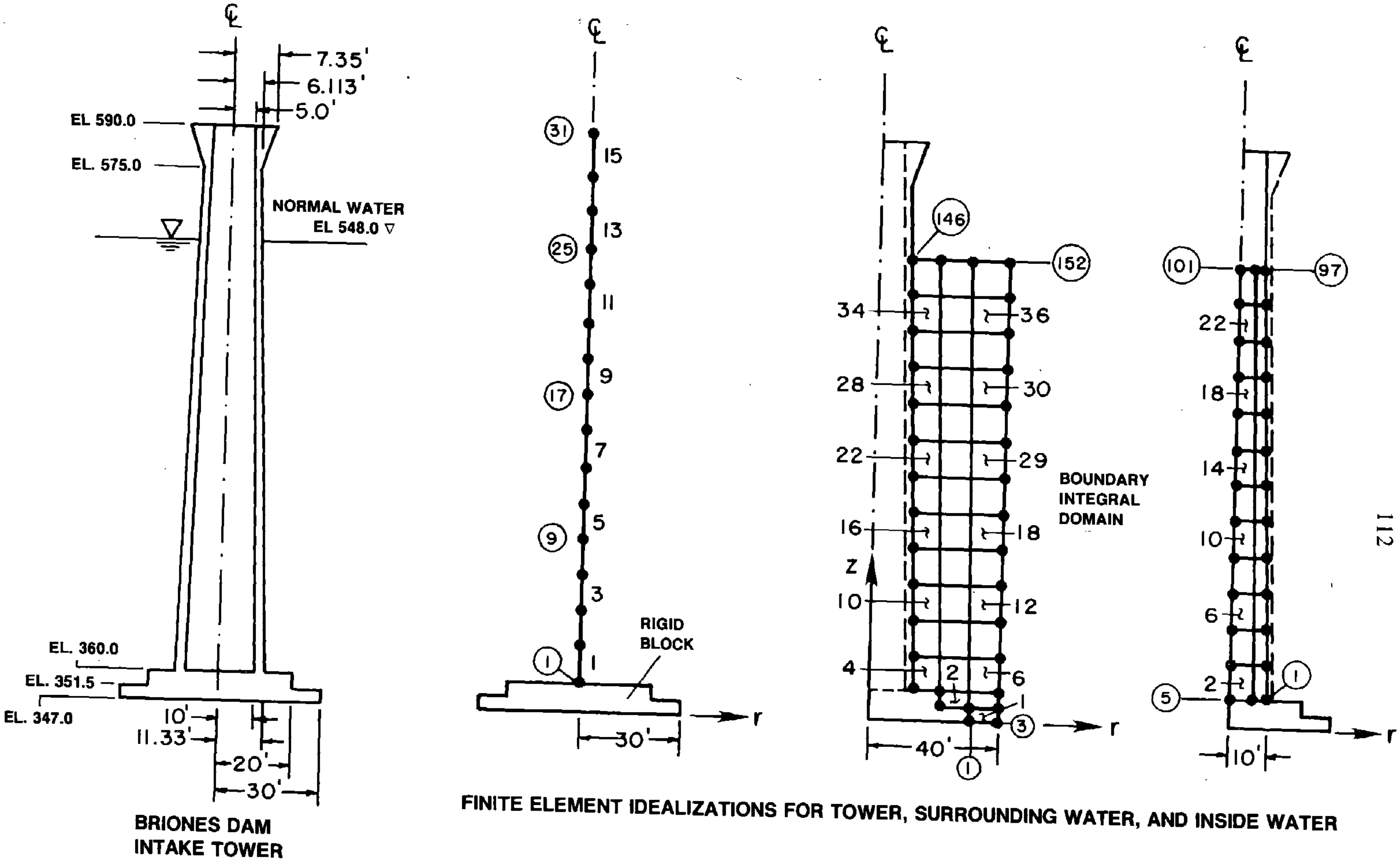

Figure 6.1 Finite Element Idealizations for Analysis of Briones Dam Intake Tower

factor corresponds to a viscous damping ratio of 5% in all the natural vibration modes of the tower (on rigid foundation soil without water) which is greater than 2% to 3% measured in forced vibration tests [41] because of much larger motions and higher stresses expected during strong earthquake ground motion.

The tower structure, including the foundation block, is idealized as supported through a massless, rigid foundation of radius r_f equal to 30 ft on a homogeneous, isotropic, viscoelastic half space. The material properties of the foundation soil are assumed to be : shear wave velocity C_f = 1000 ft/sec ; unit weight = 165 lb/ft^3, Poisson's ratio = 1/3, and a constant hysteretic damping factor of η_f = 0.10.

The water in the reservoir surrounding the tower is idealized as a fluid domain that extends to infinity in all radial directions and has a constant depth of 201 ft. Because water level inside operating intake-outlet towers is typically within a few feet of the elevation of surrounding water, the elevation of the inside and surrounding water is kept the same which results in a depth equal to 188 ft for the water contained inside the hollow tower (Figure 6.1). As mentioned in Chapter 3, water is treated as incompressible ; and its unit weight is taken as 62.4 lb/ft^3. The added hydrodynamic mass and excitation terms in the equations of motion for the tower are calculated from numerical solutions of the Laplace equation using procedures presented in Sections 4.3.5 and 4.4.3. The selected finite element idealizations for the fluid domains, using eight-node quadrilateral axisymmetric elements, are shown in Figure 6.1c for the outside water and in Figure 6.1d for the inside water. Twelve analytical functions are used to express the hydrodynamic pressures [Equation (4.64), Section 4.3.5)] in the boundary integral domain (Figure 6.1c) for analysis of the surrounding water domain.

The properties selected for the tower and foundation soil in this response analysis have not been determined from field, laboratory or design data. Thus the computed response results should not be used directly to evaluate the seismic safety of this tower.

6.2.2 Ground Motion

The ground motion recorded at Taft Lincoln School Tunnel during the Kern County, California, earthquake of July 21, 1952 is selected as the free-field ground motion for the analysis of Briones Dam Intake Tower. Only one component of the ground motion acting in the horizontal plane, defined by the S69E component of the Taft ground motion (Figure 6.2), is used in this study. Since the Briones Dam Intake Tower is essentially axisymmetric (except for openings along its height), the response results are independent of the orientation of the horizontal ground motion. This ground motion is much less intense than is expected at the site if a major earthquake were to occur on the nearby Hayward fault. Thus the presented results should not be used directly to evaluate the safety of this tower.

6.3 Response Results

With the objective of evaluating the effects of tower-water interaction and tower-foundation-soil interaction, the Briones Dam Intake Tower is analyzed for the six sets of assumptions and conditions listed in Table 6.1. For each case, the earthquake response of the tower is computed under the assumption of linear behavior of the tower-water-foundation-soil system. The displacement history is obtained by Fourier synthesis of the complex-valued frequency response functions for the modal coordinates. These response functions for Briones Dam Intake Tower are computed for the excitation frequency range 0 to 25 Hz, which includes all the significant responses. To represent accurately the response of the tower in this frequency range, five modes on fixed base (ω_1 = 1.08 Hz to ω_5 = 31.36 Hz) are included in the analyses for all cases. In the Fourier synthesis for the response history, 2048 time steps of 0.02 seconds are used, of which the last-half number of steps form a "quiet zone" to reduce the aliasing error inherent in the discrete Fourier transform.

The fundamental resonant period and the effective damping ratio at that period determined by the half-power bandwidth method, both obtained from the frequency response function, are listed in Table 6.1 for each case, along with the corresponding ordinates

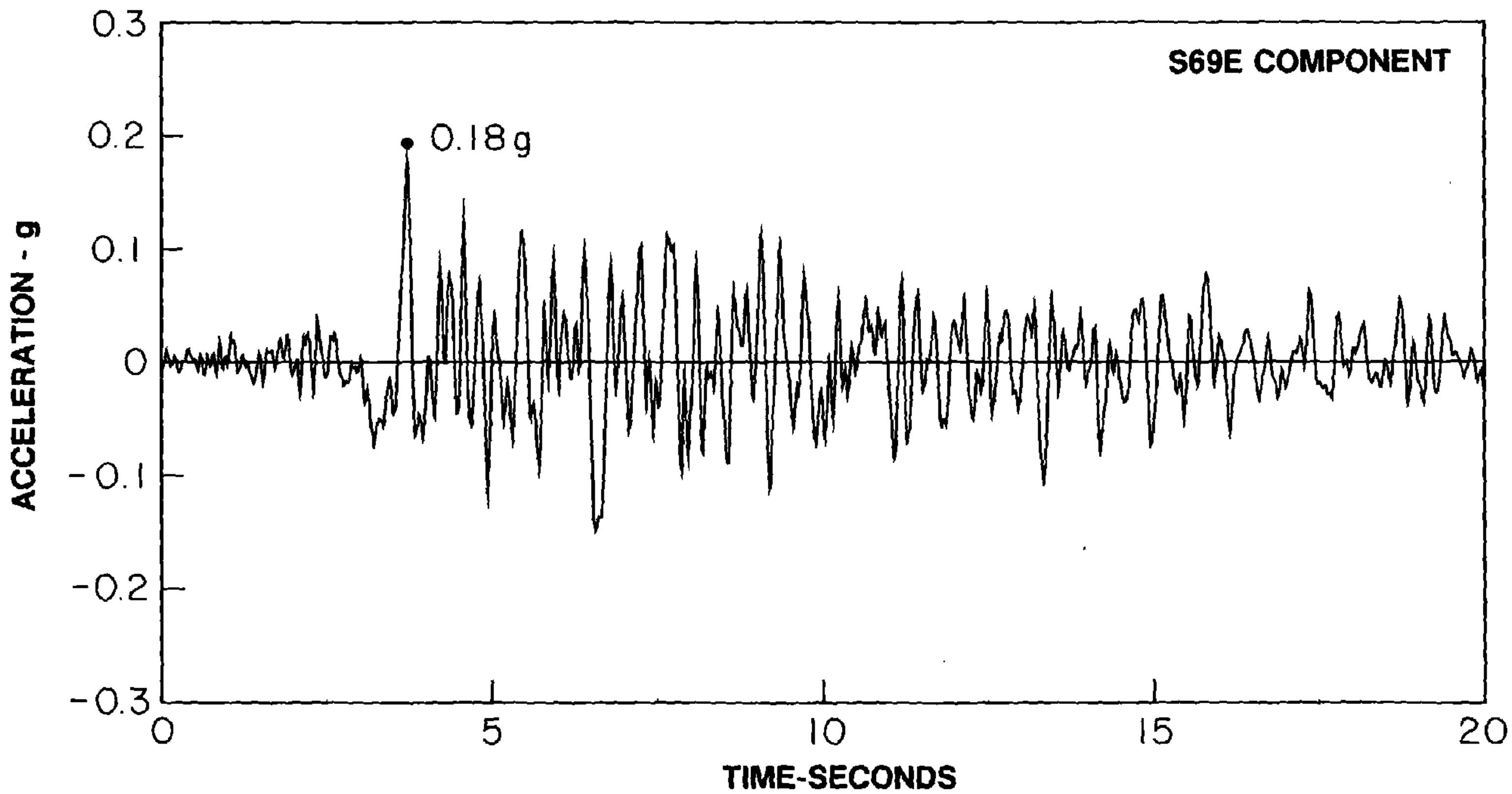

Figure 6.2 Ground Motion Recorded at Taft Lincoln School Tunnel, Kern County, California, Earthquake, July 21, 1952

Table 6.1 -- Cases of Briones Dam Intake Tower Analyzed, Periods of Vibration, Damping Ratios, and Response Spectrum Ordinates for S69E Component of Taft Ground Motion

Case	Foundation Soil	Surrounding Water	Inside Water	Fundamental Mode Properties				Second Mode Properties			
				Resonant Period in seconds	Damping Ratio, as a percentage	$S_a(T,\xi)$ in g's	$S_d(T,\xi)$ in inches	Resonant Period in seconds	Damping Ratio, as a percentage	$S_a(T,\xi)$ in g's	$S_d(T,\xi)$ in inches
1	rigid	none	none	0.927	5.0	0.196	1.647	0.214	5.0	0.440	0.197
2	rigid	normal	none	1.173	5.0	0.151	2.032	0.292	5.0	0.362	0.302
3	rigid	none	normal	1.130	5.0	0.148	1.849	0.280	5.0	0.360	0.276
4	rigid	normal	normal	1.324	5.0	0.124	2.126	0.331	5.0	0.516	0.553
5	flexible	none	none	0.970	5.4	0.166	1.528	0.232	7.2	0.367	0.193
6	flexible	normal	normal	1.415	5.5	0.121	2.370	0.358	6.6	0.349	0.438

$S_a(T,\xi)$ and $S_d(T,\xi)$ of the pseudo-acceleration and deformation spectra for the S69E component of Taft ground motion. Similar data for the second vibration mode of the tower is also presented in Table 6.1. Because energy dissipation in the tower is modeled by hysteretic damping, which is independent of excitation frequency, the damping ratio is not affected by the shift in resonant frequency due to hydrodynamic effects (Cases 1 to 4).

The results of the computer analysis consist of the response history of horizontal displacements (in the direction of the ground motion) at the nodal points and the shear forces and bending moments along the height of the tower. Due to the axisymmetric geometry of the tower, the weight of the tower and hydrostatic pressures on the outside and inside surface of the tower do not cause lateral displacements, shear forces or bending moments. Only a small portion of the response results are presented here to highlight the important effects. The maximum horizontal displacement at the top of the tower (nodal point 31) and maximum shear force and bending moment at the tower base (nodal point 1) are summarized in Table 6.2 for each case. Presented are the dynamic responses of the tower on rigid foundation soil, including the frequency response function for the modal accelerations (Figure 6.3), the time history of horizontal displacement at the top of the tower (Figure 6.4) and the distribution of envelope values of the maximum horizontal displacements, shear forces and bending moments along the height of the tower (Figures 6.5 and 6.6). Similar response results considering tower-foundation-soil interaction are presented in Figures 6.7 to 6.10.

6.4 Tower-Water and Tower-Foundation-Soil Interaction Effects

6.4.1 Tower-Water Interaction Effects

Interaction between the tower and the water, surrounding or inside the tower, introduces hydrodynamic terms into the equations of motion that affect the dynamic response of the tower. As described in Chapter 3, the hydrodynamic terms can be interpreted as an added mass and an added force. Tower-water interaction reduces the resonant frequencies (or lengthens the resonant periods) due to added hydrodynamic mass and magnifies the

Table 6.2 -- Maximum Responses of Briones Dam Intake Tower to Taft Ground Motion

Case	Surrounding Water	Inside Water	Horizontal Displacement at Top of Tower in inches	Forces at Base	
				Shear Force in kips	Bending Moment in kips-ft
(a) Tower on Rigid Foundation Soil					
1	none	none	2.91	347	36632
2	normal	none	4.34	562	55596
3	none	normal	3.71	477	50590
4	normal	normal	4.59	1069	88726
(b) Tower on Flexible Foundation Soil					
5	none	none	2.55	296	30491
6	normal	normal	4.90	1028	81805

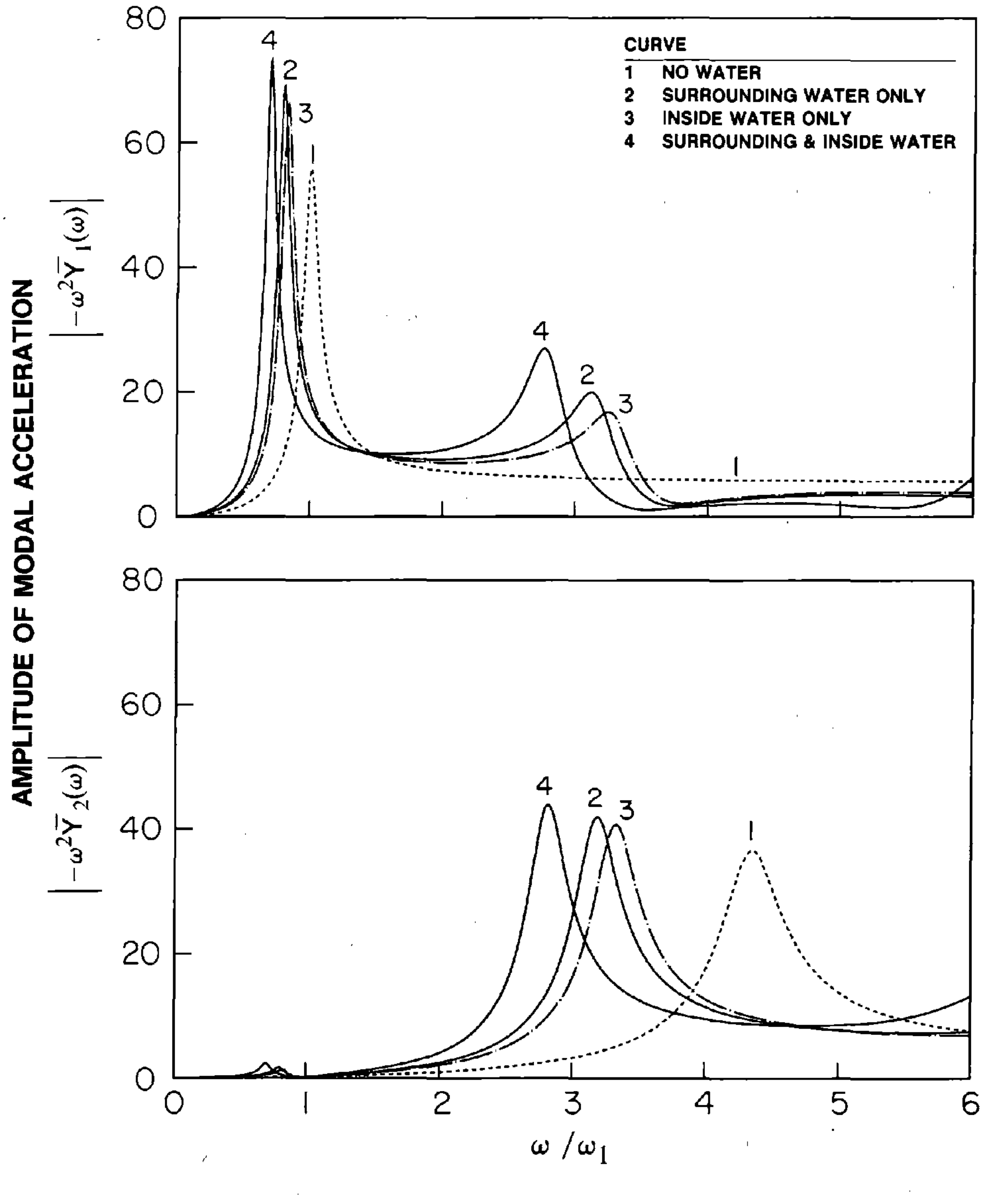

Figure 6.3 Response of Briones Dam Intake Tower on Rigid Foundation Soil due to Harmonic Ground Acceleration Results Presented are for Responses in $\bar{Y}_1(\omega)$ and $\bar{Y}_2(\omega)$ Modal Coordinates

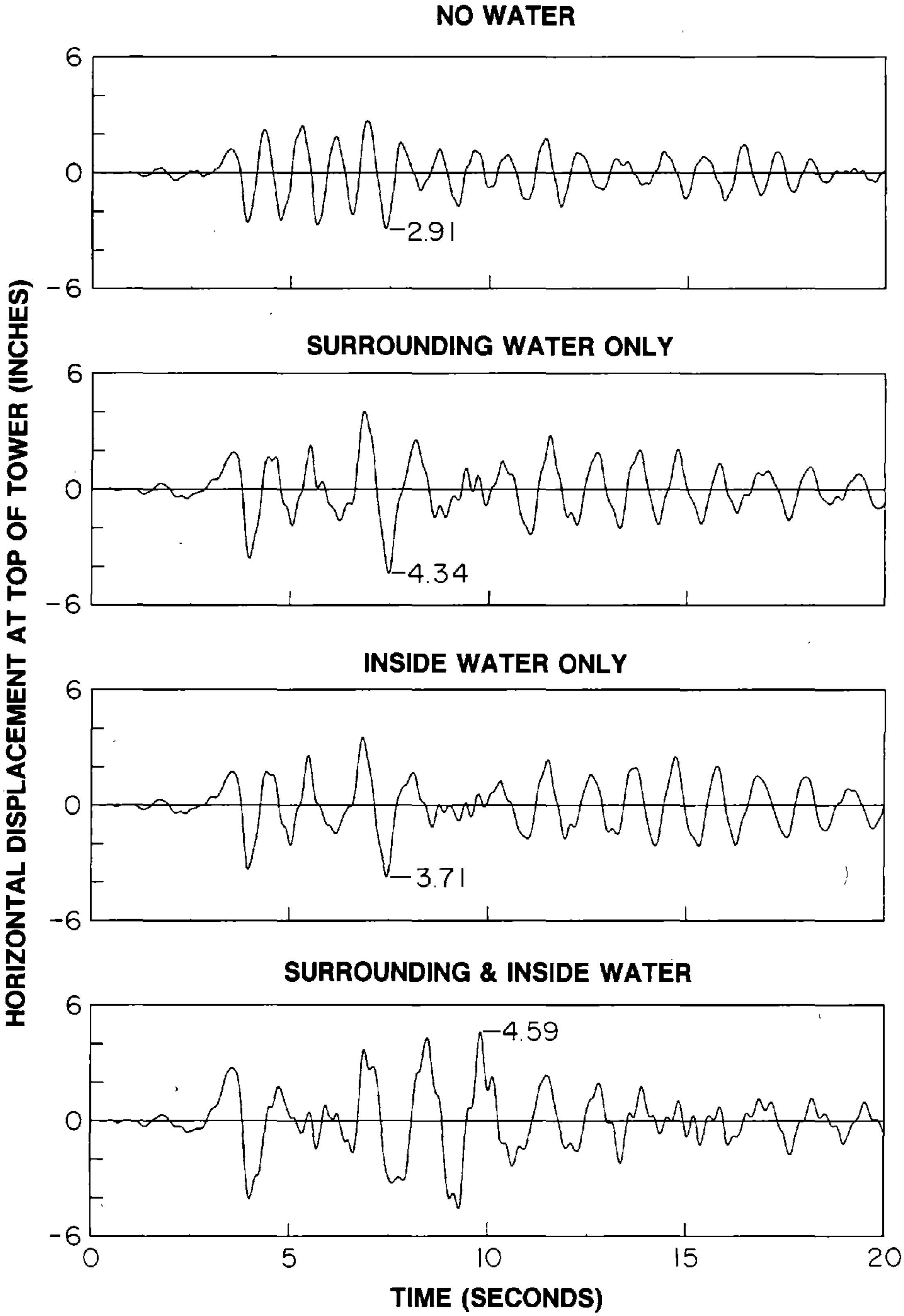

Figure 6.4 Displacement Response at the Top of Briones Dam Intake Tower on Rigid Foundation Soil due to S69E Component of Taft Ground Motion

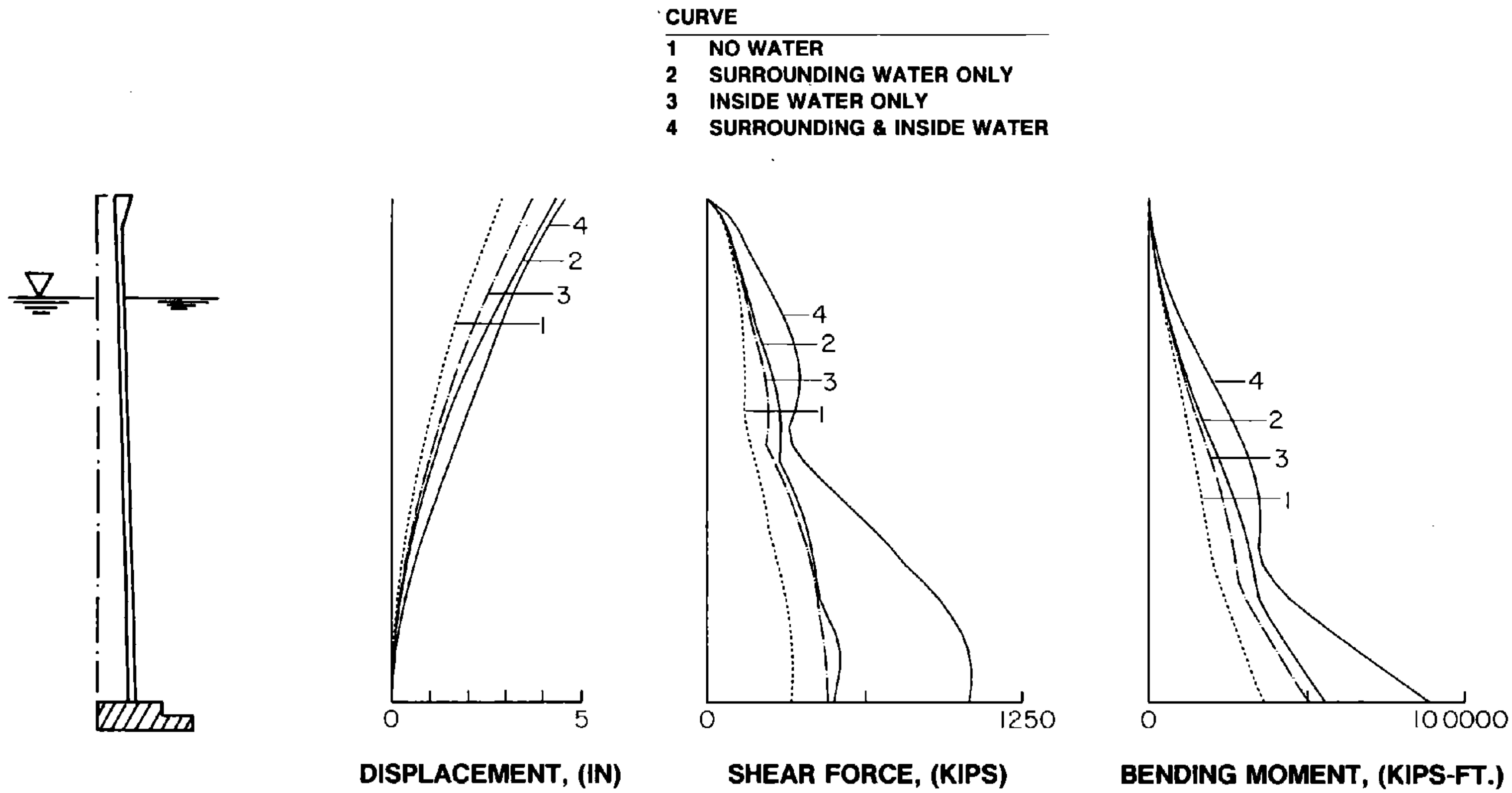

Figure 6.5 Envelope Values of Maximum Responses of Briones Dam Intake Tower on Rigid Foundation Soil due to S69E Component of Taft Ground Motion

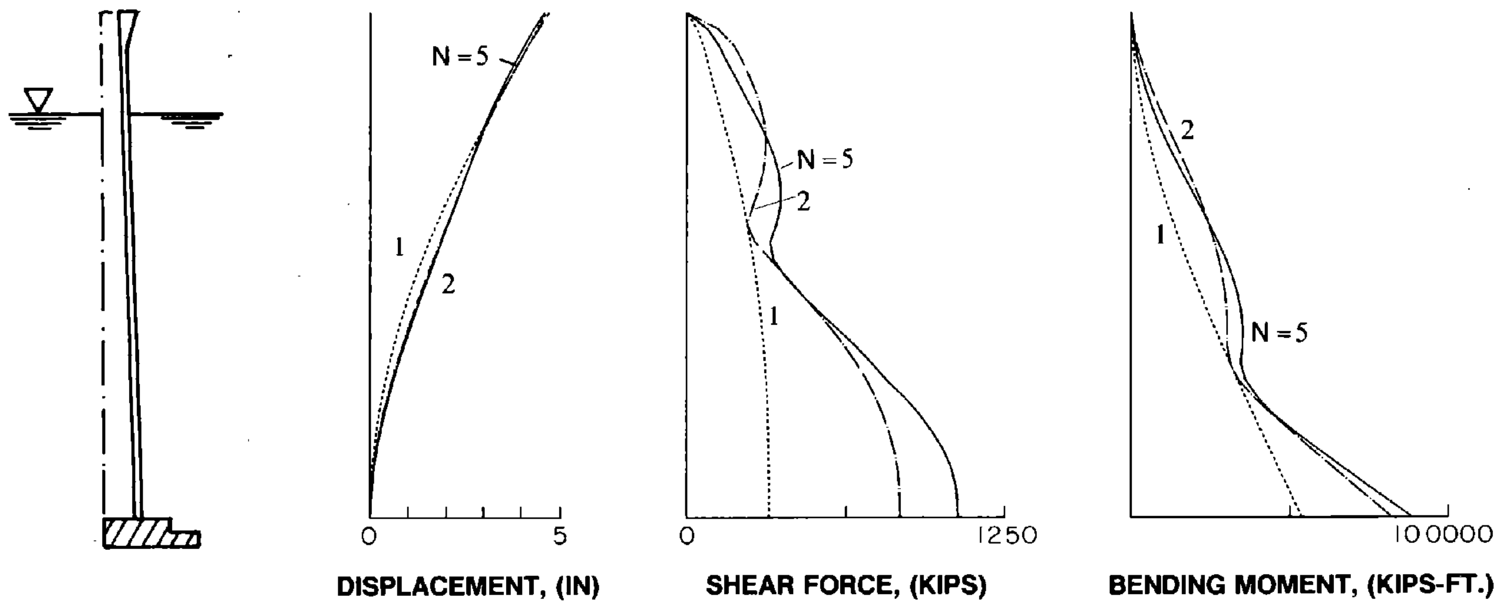

Figure 6.6 Influence of the Number, N, of Vibration Modes of the Tower Included in the Analysis of Case 4 of Table 6.1

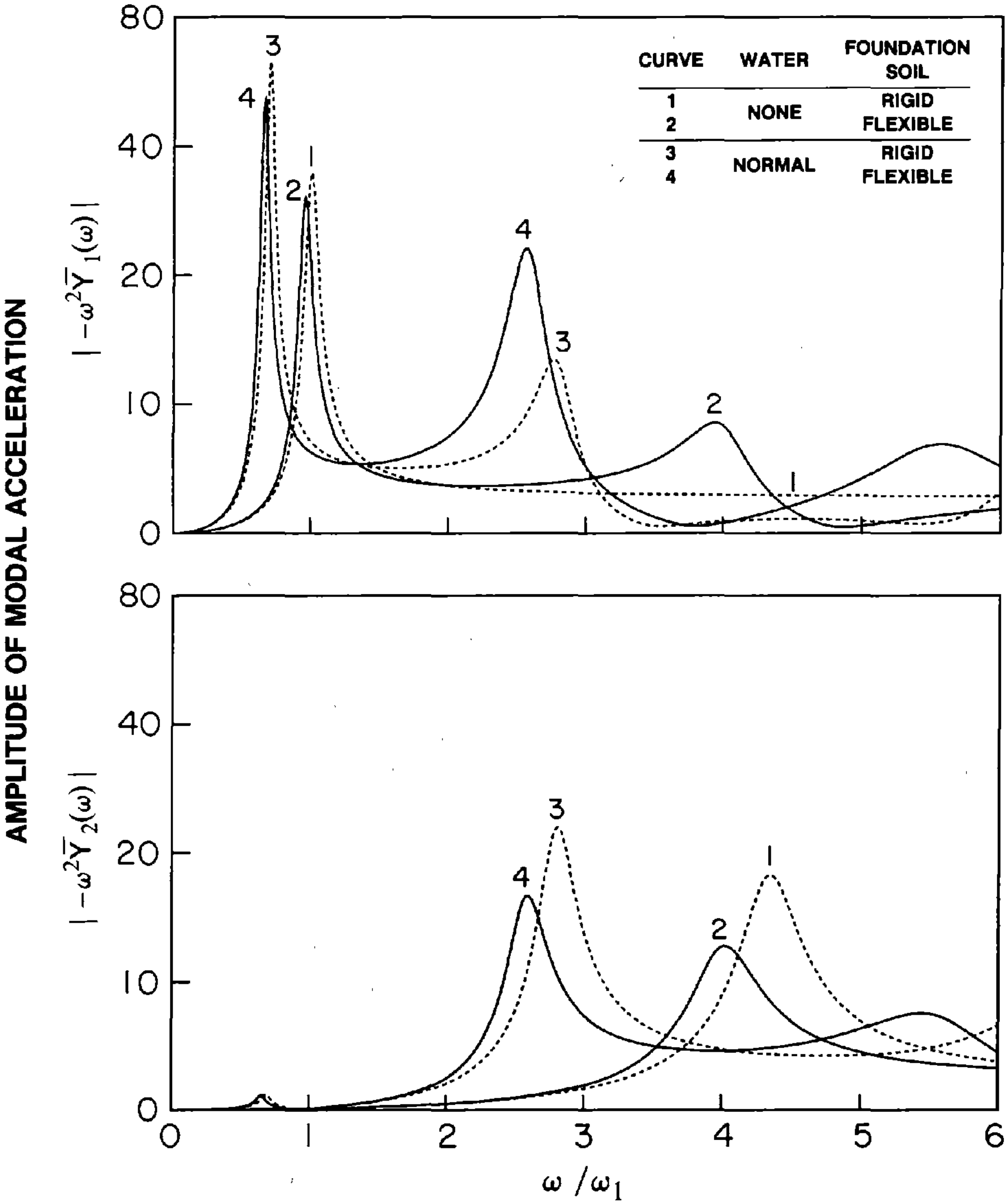

Figure 6.7 Response of Briones Dam Intake Tower on Rigid Foundation Soil due to Harmonic Ground Acceleration, Results Presented are for Responses in $\overline{Y}_1(\omega)$ and $\overline{Y}_2(\omega)$, the First Two Modal Coordinates

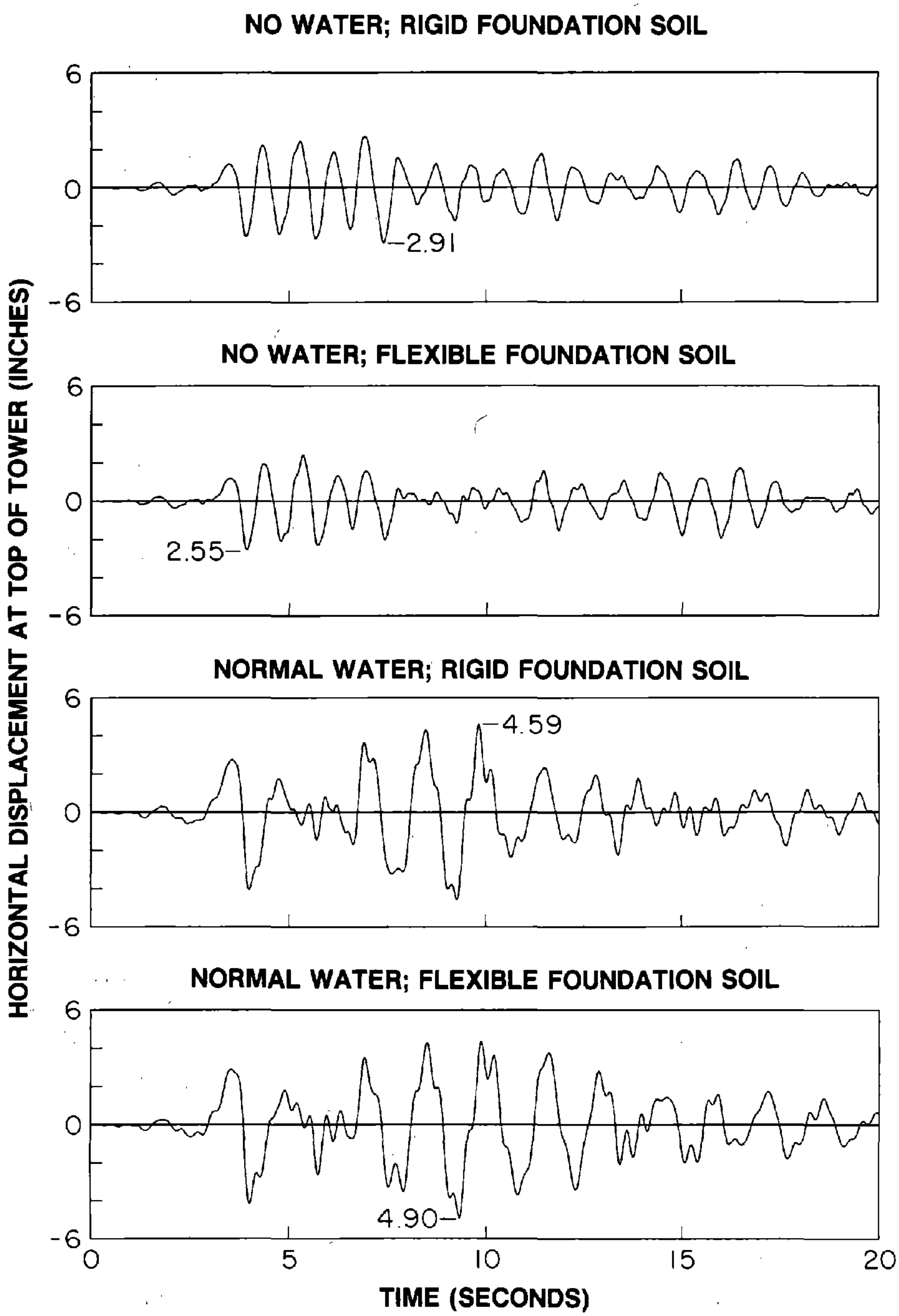

Figure 6.8 Displacement Response at the Top of Briones Dam Intake Tower due to S69E Component of Taft Ground Motion

CURVE	WATER	FOUNDATION SOIL
1	NONE	RIGID
2		FLEXIBLE
3	NORMAL	RIGID
4		FLEXIBLE

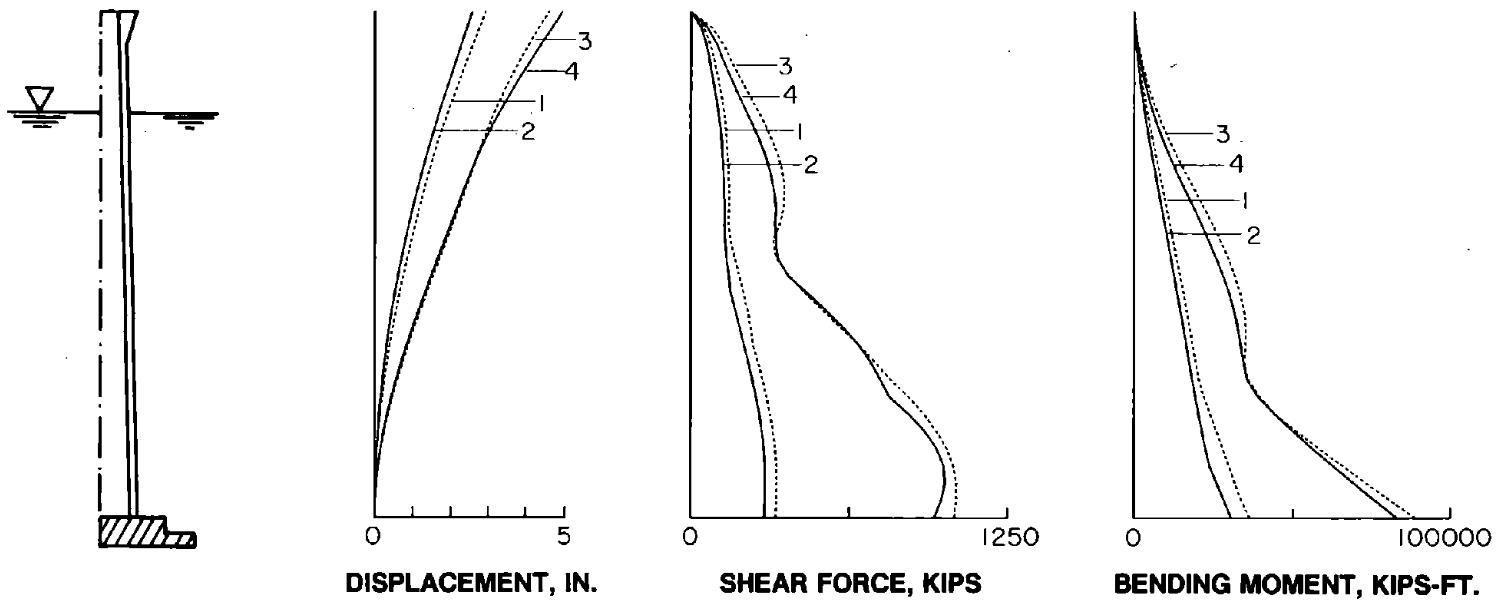

Figure 6.9 Envelope Values of Maximum Responses of Briones Dam Intake Tower due to S69E Component of Taft Ground Motion

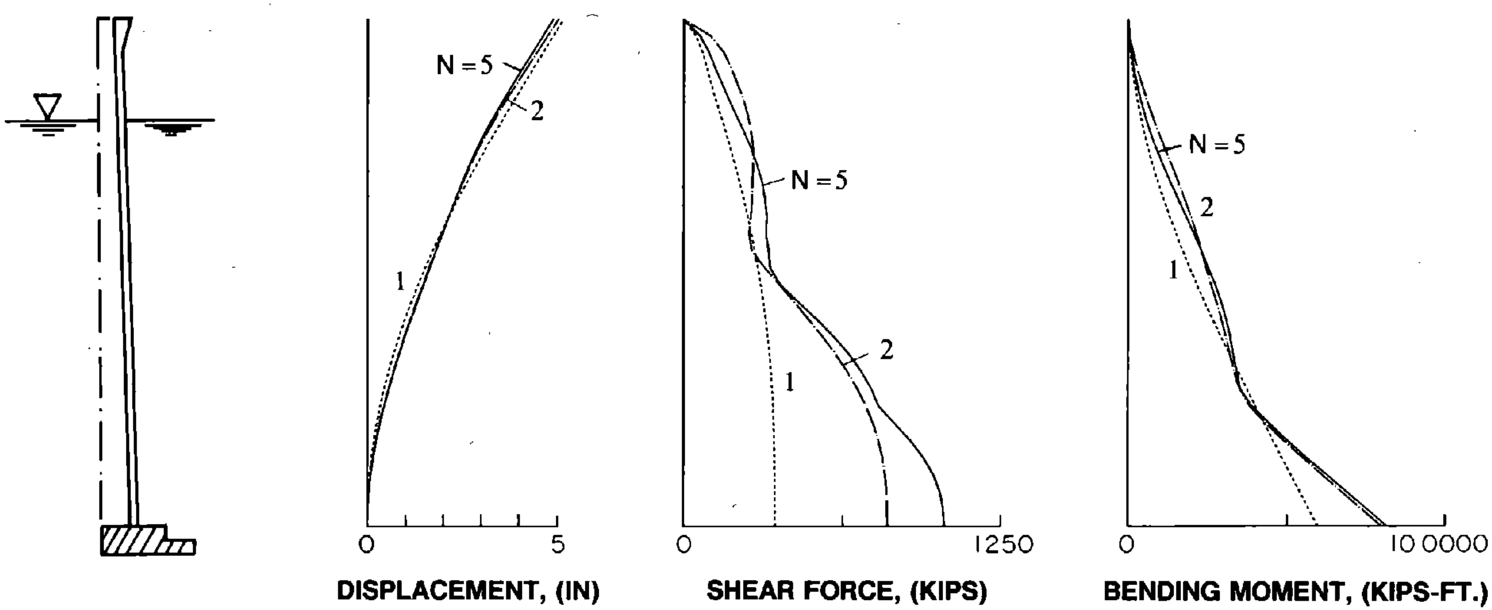

Figure 6.10 Influence of the Number, N, of Vibration Modes of the Tower Included in the Analysis of Case 6 of Table 6.1

amplitudes of resonant peaks due to added hydrodynamic force (Figure 6.3). The fundamental vibration period of the tower lengthens from 0.927 sec to 1.173 sec due to the effects of water surrounding the tower, to 1.130 sec due to the effects of inside water, and to 1.324 sec due to the combined effects of surrounding and inside water (Table 6.1). Similarly, the second vibration period of the tower lengthens from 0.214 sec to 0.292 sec due to the effects of water surrounding the tower, to 0.280 sec due to the effects of inside water, and to 0.331 sec due to the combined effects of surrounding and inside water.

The hydrodynamic interaction effects on the response of a tower to a specified earthquake ground motion are controlled by (1) the change in the response spectrum ordinates (Table 6.1) corresponding to the change in the fundamental and second (and higher) resonant periods, and (2) by the change in the frequency response functions, in particular the amplitudes of the resonant peaks (Figure 6.3). As a combined result of these two factors, the maximum displacement at the top of the tower increases from 2.91 in. to 4.34 in. due to the effects of surrounding water, to 3.71 in. due to the effects of inside water, and to 4.59 in. due to the effects of both surrounding and inside water (Figure 6.4). This increase in displacements is accompanied by larger increases in maximum shear forces and bending moments along the height of the tower (Figure 6.5) because the higher vibration modes contribute more to shears and moments than to displacements.

The relative contributions of the various vibration modes to the response of the tower with both surrounding and inside water (Case 4) are demonstrated in Figure 6.6 where the envelope values of the maximum lateral displacements, shear forces and bending moments along the height of the tower are presented, obtained from three different analyses considering one, two and five modes. It is apparent that, for this particular tower-water system and ground motion, the second mode response contribution is significant because the ordinate of the pseudo-acceleration response spectrum associated with the second vibration mode is larger compared to that for the fundamental vibration mode (Table 6.1). It is also apparent that the first two vibration modes are sufficient to predict the response of this tower to the selected earthquake. The relative contributions of the various vibration modes to response of the towers depend, of course, on the vibration periods of the towers and the shape of the earthquake response spectrum. This matter will be addressed further in Chapter 7.

6.4.2 Tower-Foundation-Soil Interaction Effects

Interaction between the tower and the foundation supported on flexible soil reduces the resonant frequencies as well as the amplitudes of resonant peaks (Figure 6.7). Tower-foundation-soil interaction lengthens the fundamental resonant period of Briones Dam Intake Tower from 0.927 sec to 0.970 sec because of foundation-soil flexibility and increases the effective damping from 5.0% to 5.4% at that period because of material damping and the radiation of waves in the foundation-soil region (Table 6.1). Similarly, tower-foundation-soil interaction lengthens the second vibration period from 0.214 sec to 0.232 sec and increases the effective damping from 5% to 7.2% (Table 6.1). This larger increase in effective damping for the second vibration mode comes from the increased radiation damping at higher frequencies. The tower-foundation-soil interaction effects are small in the response of Briones Dam Intake Tower, which is consistent with the results of Chapter 5 where it is shown that these effects are small for long-period, slender towers.

Tower-foundation-soil interaction reduces the maximum displacement at the top of the tower from 2.91 in. to 2.55 in. (Figure 6.8). Similar reductions are also observed in the maximum shear forces and bending moments along the height of the tower (Figure 6.9). These reductions in the response of a tower to a specified ground motion are controlled, in part, by the change in the response spectrum ordinate due to lengthening of the fundamental vibration period and increased damping. In this particular case, the reductions in responses due to tower-foundation-soil interaction are much smaller than the response increases due to hydrodynamic effects.

As noted earlier, the fundamental resonant period of the tower is lengthened because of tower-water interaction and also because of tower-foundation-soil interaction. Simultaneous consideration of the two sources of interaction results in a fundamental resonant period of the tower that is longer than the period including either interaction effect individually (Table 6.1). In particular, tower-water interaction lengthens the fundamental resonant period by approximately the same percentage whether the foundation soil is rigid or flexible. Similar to the observations from earlier results presented in Chapter 5, hydrodynamic interaction reduces the influence of tower-foundation-soil interaction effects on the second vibration mode, e.g. the increase in damping ratio for the second vibration mode from 5% to 7.2% due to tower-foundation-soil interaction is reduced to an increase from 5% to 6.6% when hydrodynamic interaction effects are also included (Table 6.1).

Because the increase in effective damping due to tower-foundation-soil interaction is larger in the higher vibration modes, their contributions to the tower response should be reduced when foundation flexibility is considered in the analysis. For this particular tower, however, the contributions of higher modes, specially the second vibration mode, to the response of tower remain significant (Figure 6.10), in part, because the effects of tower-foundation-soil interaction are small to start with and they are further reduced, as mentioned above, because of hydrodynamic interaction effects. Tower-foundation-soil interaction, when considered with hydrodynamic interaction effects, slightly increases the maximum displacements at the top of the tower (Figure 6.9a) but reduces the maximum shear forces and bending moments over most of the tower height (Figures 6.9b and 6.9c). These different effects on the various response quantities result from the fact that the second vibration mode contributes differently to various response quantities (Figure 6.10).

6.5 Practical Earthquake Analysis of Intake-Outlet Towers

The analytical and numerical procedures, which were developed in Chapters 3 and 4, and used to compute the earthquake response results presented in this chapter, are very efficient and hence useful in the design of new intake-outlet towers and in the safety evaluation of existing towers. In practical applications, the analysis should be performed for each of the two components of the horizontal ground motion, applied along the planes of symmetry of the tower, to obtain the maximum shear forces and bending moments acting along the height of the tower in two mutually perpendicular planes. The effects of static loads should be considered simultaneously with the dynamic response to two horizontal components of ground motion considering tower-water interaction and tower-foundation-soil interaction. Dynamic response analysis performed including the first five vibration modes of the tower should provide sufficiently accurate estimates of maximum responses.

The computational time required to obtain a complete response history of displacements and forces in Briones Dam Intake Tower (including the solution of associated eigen value problem and fast Fourier transforms) is shown in Table 6.3 for six cases mentioned earlier. Although each of the interaction effects significantly complicate the analysis, the additional computational time required to include them is modest, demonstrating the efficiency of the numerical procedures presented in Chapter 4 for the evaluation of various terms in the equations of motion. The overall efficiency of the analytical procedure, as demonstrated by the data in Table 6.3, lies in the use of the substructure method along with the transformation of displacements to generalized coordinates.

Table 6.3 -- Computation Times for Complete Analysis of Briones Dam Intake Tower to S69E Component of Taft Ground Motion

Case	Foundation Soil	Surrounding Water	Inside Water	No. of Generalized Coordinates	Central Processor Time* in seconds
1	rigid	none	none	5	4.9
2	rigid	normal	none	5	6.8
3	rigid	none	normal	5	6.1
4	rigid	normal	normal	5	8.3
5	flexible	none	none	5	5.6
6	flexible	normal	normal	5	9.4

* IBM 3090 Computer

7. SIMPLIFIED REPRESENTATION OF HYDRODYNAMIC AND FOUNDATION INTERACTION EFFECTS

7.1 Introduction

A general analytical procedure for computing the complete response-history of an intake-outlet tower subjected to specified earthquake ground motion has been presented in Chapters 3 and 4. The procedure is intended for the final design analysis of a new tower, and for the final safety-evaluation analysis of an existing tower. For the preliminary phase of design or safety-evaluation of intake-outlet towers, it would be useful to develop a simplified version of the analysis procedure, which is easier to implement and provides sufficiently accurate estimates of the maximum earthquake forces directly from the design earthquake spectrum without the need for a response history analysis. Utilizing the response results and conclusions of Chapters 5 and 6, such a simplified analysis procedure is developed in this chapter that includes all the significant effects of tower-water interaction and tower-foundation-soil interaction influencing the earthquake response of towers.

7.2 System and Ground Motion

The system considered consists of a hollow reinforced concrete intake-outlet tower partially submerged in water and supported on the horizontal surface of flexible foundation soil (Figure 7.1). The hollow tower is also partially filled with water. The tower may be of arbitrary cross-section having two axes of symmetry. This restriction allows the hydrodynamic pressures on the inside and outside surfaces of the tower, caused by the horizontal components of the earthquake ground motion along the planes of symmetry, to be represented as equivalent lateral forces and moments distributed over the tower height acting along these planes. The part of the tower foundation which is above the ground level is treated as a rigid part of the tower and the remaining part of the foundation below the ground level is idealized as a rigid foundation of infinitesimal thickness supported on the surface of a

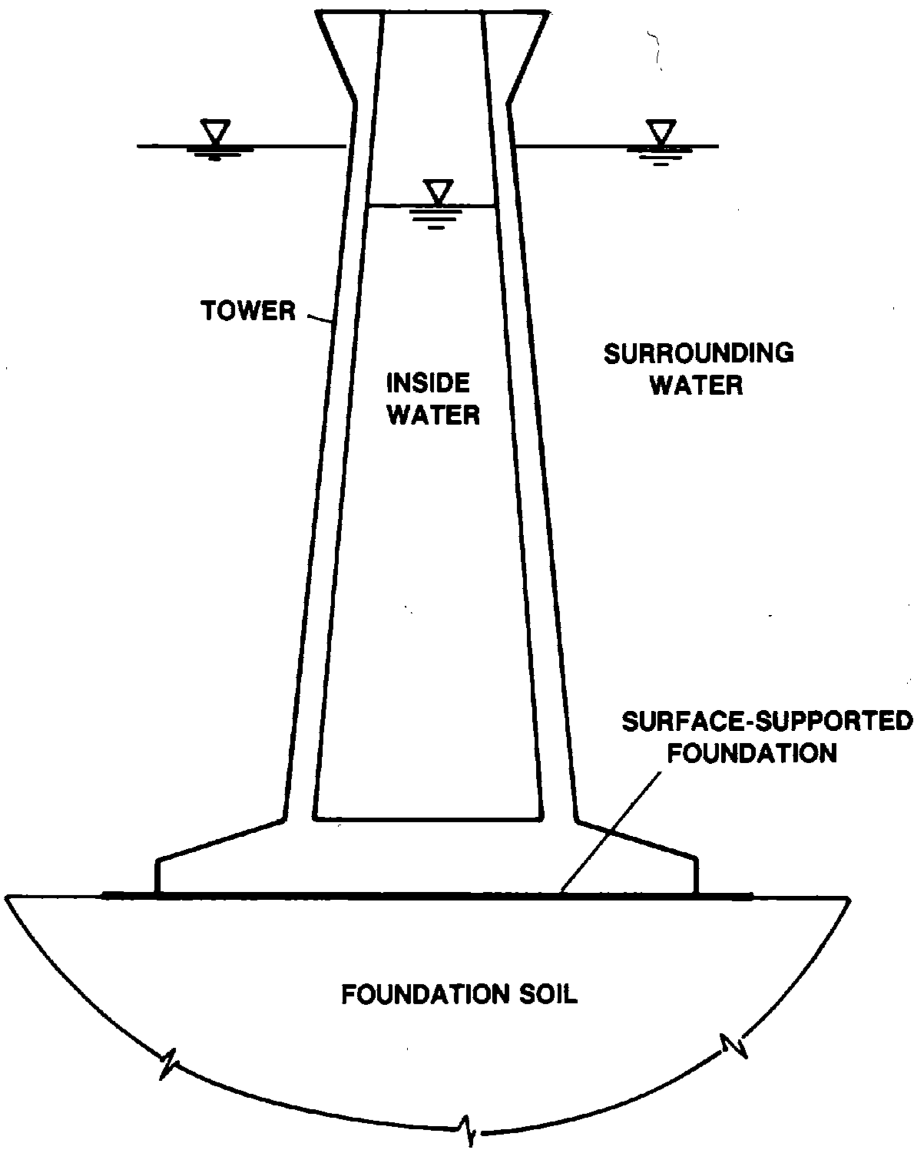

Figure 7.1 Idealized Tower-Water-Foundation-Soil System

homogeneous viscoelastic halfspace (Figure 7.1). This simple idealization is reasonable for the typical situation where the foundation is either surface supported or is at most slightly embedded. The system is analyzed under the assumption of linear behavior for the tower concrete, the surrounding and inside water, and the foundation soil.

The response results are computed for towers with three different geometries : circular cylindrical towers, circular tapered towers, and non-circular uniform towers. For a circular cylindrical tower (Figure 7.2a), three different values for the ratio of tower height to average radius, H_s/r_a= 20, 10, and 5 are considered. The ratio of the inside and outside radii, r_i/r_o, is selected equal to 0.8, i.e. the wall thickness t_w = 0.2 r_o, a value typical of many towers. For a tapered tower with circular cross-section (Figure 7.2b), the inside and outside radii at the top of the tower are taken equal to half of what they are at the base. The inside and outside radii decrease linearly along the height but their ratio $r_i(z)/r_o(z)$ at any location z above the base remains 0.8. Three values of the ratio of the tower height to its average radius r_a at the base, H_s/r_a= 20, 10 and 5, are considered. The responses of a uniform tower with the non-circular cross-section shown in Figure 7.2c, and with H_s/r_a = 20, are computed for ground motion applied separately along two axes of symmetry.

All towers are assumed to be homogeneous and isotropic with linear elastic properties for the concrete : Poisson's ratio = 0.17, unit weight = 155 lb/ft^3 and the Young's modulus of elasticity E_s = 4.5 million psi. The modification in the effective modulus of elasticity due to reinforcing steel is not considered. Energy dissipation in the tower concrete is represented by constant hysteretic damping factor of η_s = 0.10. This value corresponds to a viscous damping ratio of 0.05 in all natural vibration modes of the tower without water on rigid foundation soil.

Tower-foundation-soil interaction effects are investigated only for axisymmetric (both cylindrical and tapered) towers. In both cases, the tower structure is assumed to be supported through a rigid circular foundation on the surface of deformable foundation soil idealized as a homogeneous, isotropic, viscoelastic halfspace. The following material

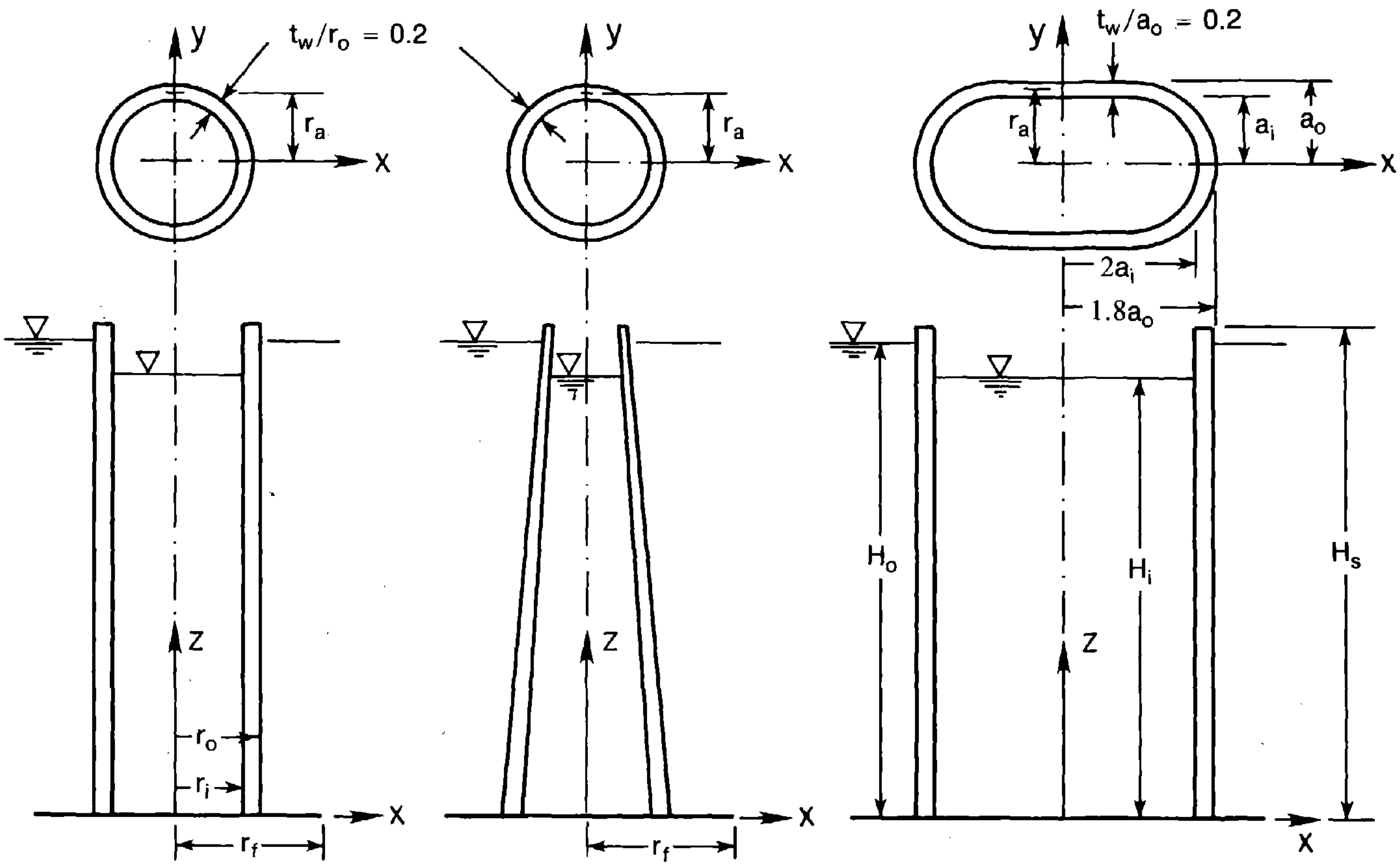

CIRCULAR CYLINDRICAL TOWER

CIRCULAR TAPERED TOWER

NON-CIRCULAR UNIFORM TOWER

Figure 7.2 Three Idealized Towers

properties of the foundation soil are kept constant : Poisson's ratio ν_f = 1/3, and the ratio of the rock mass density to concrete mass density, ρ_f/ρ_s, = 1. Similarly, the ratio of the mass of the foundation to the mass of the superstructure, m_f/m_t, and the ratio of the rotatory inertia of the foundation to the total rotatory inertia of the tower structure about the base, I_f/I_t, are taken equal to 1.0 and 0.2, respectively. The selected values for m_f/m_t and I_f/I_t are more or less representative of many existing towers.

In order to check the accuracy of the simplified representation of the interaction effects for the wide range of tower materials and tower-foundation systems, the wave parameter σ is varied from 20 to ∞, where the latter value represents rigid foundation soil ; the ratio H_s/r_f is varied from 2 to 8 ; constant hysteretic damping factor η_f for the foundation soil is varied from 0.0 to 0.50 ; and two values of parameter γ are considered : 0.15 for circular cylindrical towers without water (Figure 7.2a), and 0.06 for axisymmetric tapered towers without water (Figure 7.2b). This particular choice of dimensionless parameters for the tower-foundation-soil systems is discussed in Section 5.2.2.

The water surrounding (outside) the tower is idealized as a fluid domain of constant depth extending to infinity in radial directions. The unit weight of water is taken equal to 62.4 lb/ft^3. Three values of inside water depth, H_i, and surrounding water depth, H_o, are considered : no water (H_o/H_s = 0, H_i/H_s = 0), full surrounding water only (H_o/H_s = 1, H_i/H_s = 0), and full outside and inside water (H_o/H_s = 1, H_i/H_s = 1).

The earthquake excitation considered for the simplified analysis of intake-outlet towers is the horizontal free-field ground acceleration $\ddot{u}_g(t)$ in a plane of symmetry of the tower plan. Using this simplified procedure, the maximum response of the tower to each horizontal component of ground motion can be evaluated separately and the combined effects of the responses to the two components should be considered in designing a new tower or evaluating the safety of an existing tower.

7.3 Modal Response of Towers

As in the 'exact' analysis procedure (Chapters 2 and 3), the tower is idealized as a one-dimensional Timoshenko beam including the effects of shear deformations and rotatory inertia. The lateral displacements $u(z,t)$ and rotations $\theta(z,t)$ of the tower axis resulting from the deformations of the tower, i.e. excluding the rigid body motions associated with translation and rotation of the foundation due to horizontal ground motion, can be expressed as a linear combination of the fixed-base natural vibration modes :

$$u(z,t) = \sum_{n=1}^{\infty} \phi_n(z)\, Y_n(t) \tag{7.1a}$$

$$\theta(z,t) = \sum_{n=1}^{\infty} \psi_n(z)\, Y_n(t) \tag{7.1b}$$

where $Y_n(t)$ is the generalized (modal) coordinate associated with the n-th vibration mode, defined by two functions $\phi_n(z)$ and $\psi_n(z)$ describing the lateral displacements and rotations of the tower axis in n-th vibration mode. As demonstrated earlier [11], two vibration modes are sufficient to represent the response of intake-outlet towers with their fundamental vibration period in the acceleration or velocity-controlled regions of the earthquake response spectrum ; even the fundamental mode alone is sufficient in the acceleration controlled region of the spectrum. In a simplified analysis, it is therefore appropriate to consider only the contribution of the first two vibration modes to the response of the tower. The displacements of the tower in the n-th vibration mode are :

$$u(z,t) = \phi_n(z)\, Y_n(t) \tag{7.2a}$$

$$\theta(z,t) = \psi_n(z)\, Y_n(t) \tag{7.2b}$$

The equation of motion for a fixed-base tower without water restricted to vibrate in its n-th mode shape due to harmonic free-field ground acceleration $\ddot{u}_g(t) = e^{i\omega t}$ can be written in terms of the frequency response function $\overline{Y}_n(\omega)$ for the associated modal coordinate :

$$[\,-\,\omega^2 M_n + (\,1 + i\ \eta_s\,)\ \omega_n^2\ M_n\,]\ \bar{Y}_n(\omega) = -\ L_n \tag{7.3}$$

in which ω_n is the n-th natural vibration frequency ; η_s is the constant hysteretic damping factor which is related to ξ_n, the fraction of critical damping for the n-th vibration mode, by $\eta_s = 2\ \xi_n$; and the generalized mass term M_n and generalized excitation term L_n are given by :

$$M_n = \int_0^{H_s} m_s(z)\ [\ \phi_n(z)\ ]^2\ dz + \int_0^{H_s} I_s(z)\ [\ \psi_n(z)\ ]^2\ dz \tag{7.4}$$

$$L_n = \int_0^{H_s} m_s(z)\ \phi_n(z)\ dz \tag{7.5}$$

in which $m_s(z)$ and $I_s(z)$ are the mass and the mass moment of inertia, respectively, of the tower per unit of its height; and H_s is the height of the tower.

The frequency response function for the modal coordinates $\bar{Y}_n(\omega)$ is directly obtained from equation (7.3) :

$$\bar{Y}_n(\omega) = \frac{-\ L_n}{M_n\ [\ -\ \omega^2 + (\ 1 + i\eta_s\ )\ \omega_n^2\ ]} \tag{7.6}$$

The response-history of the modal coordinate $Y_n(t)$ due to a specified ground motion then can be computed from its frequency response function, equation (7.6), using standard Fourier synthesis techniques. The displacement response history of the tower is then given by equation (7.2) ; other response quantities (shear forces or bending moments) can be expressed in terms of $Y_n(t)$. Furthermore, the maximum deformations and forces can be directly computed from the response spectrum for an earthquake ground motion [9,14].

As demonstrated in Chapter 4, the influence of shear deformations and rotatory inertia on the fixed-base vibration frequencies of towers without water increases with increasing mode number and for decreasing slenderness ratio, and more than three-fourths of the change in frequencies because of these two effects is due to shear deformations. It was therefore concluded in Chapter 4 that, in the dynamic analysis of towers considering only the first two modes of vibration, while the contributions of shear deformations should be included in the analysis of squat towers, the influence of rotatory inertia may be neglected without introducing significant errors. This approximation has the advantage that it is not necessary to compute the bending slope functions, $\psi_n(z)$, in the simplified analysis. Presented in the following sections of this chapter are extensions to equation (7.3) necessary to include the effects of surrounding and inside water and of tower-foundation-soil interaction in the simplified analysis of the modal response of towers to earthquake ground motion.

7.4 Towers with Water

7.4.1 Exact Individual Mode Response

The governing equation for the response of tower constrained to vibrate in the n-th vibration mode [equation (7.1)] can be modified to include the hydrodynamic interaction effects. The resulting equation is a special case of equation (3.46a), considering N vibration modes and the coupling among them due to hydrodynamic effects :

$$[\ -\ \omega^2\ (\ \tilde{M}_n\ )\ +\ (1+i\eta_s)\ \omega_n^2\ M_n\ ]\ \bar{Y}_n(\omega)\ =\ -\ \tilde{L}_n \tag{7.7}$$

$$\tilde{M}_n\ =\ M_n\ +\ M_{nn}^o\ +\ M_{nn}^i \tag{7.8a}$$

$$\tilde{L}_n\ =\ L_n\ +\ L_n^o\ +\ L_n^i \tag{7.8b}$$

in which M_n and L_n were defined by equations (7.4) and (7.5) ; and M_{nn}^o and L_n^o are the added mass and the added excitation terms, respectively, arising from interaction between the tower and the surrounding water :

$$M_{nn}^o\ =\ \int_0^{H_o} \phi_n(z)\ f_n^o(z)\ dz\ +\ \int_0^{H_o} \psi_n(z)\ m_n^o(z)\ dz \tag{7.9}$$

$$L_n^o = \int_0^{H_o} \phi_n(z)\, f_0^o(z)\, dz + \int_0^{H_o} \psi_n(z)\, m_0^o(z)\, dz \tag{7.10}$$

in which H_o is the depth of surrounding water. In equations (7.9) and (7.10), $f_0^o(z)$ and $m_0^o(z)$ are the hydrodynamic lateral forces and external moments acting in the plane of vibration on the outside surface of the tower when the excitation is a unit horizontal acceleration of the ground and the tower is rigid; and $f_n^o(z)$ and $m_n^o(z)$ represent the corresponding functions when the excitation is the horizontal acceleration $\phi_n(z)$ and rotational acceleration $\psi_n(z)$ of the tower axis with no ground motion. Similarly, the added mass term M_{nn}^i and the added excitation term L_n^i due to inside water in the n-th mode vibration of the tower are evaluated by the following equations:

$$M_{nn}^i = \int_0^{H_i} \phi_n(z)\, f_n^i(z)\, dz + \int_0^{H_i} \psi_n(z)\, m_n^i(z)\, dz \tag{7.11}$$

$$L_n^i = \int_0^{H_i} \phi_n(z)\, f_0^i(z)\, dz + \int_0^{H_i} \psi_n(z)\, m_0^i(z)\, dz \tag{7.12}$$

where H_i is the inside water depth; $f_0^i(z)$ and $m_0^i(z)$ are the hydrodynamic lateral forces and external moments acting in the plane of vibration on the inside surface of the tower when the excitation is unit horizontal acceleration of the ground and the tower is rigid; and $f_n^i(z)$ and $m_n^i(z)$ are the corresponding functions when the excitation is the horizontal acceleration $\phi_n(z)$ and rotational acceleration $\psi_n(z)$ of the tower axis with no ground motion.

The functions $f_0^o(z)$, $m_0^o(z)$, $f_n^o(z)$, and $m_n^o(z)$ for the surrounding water and functions $f_0^i(z)$, $m_0^i(z)$, $f_n^i(z)$, and $m_n^i(z)$ for the inside water can be evaluated by solving the Laplace equation, governing the dynamics of incompressible fluids, subjected to appropriate boundary conditions at the free surface of water, the bottom boundary of the water domain, and the tower water interface. These boundary value problems have been described in Chapter

4, wherein efficient numerical procedures to solve the Laplace equation for surrounding and inside water domains have also been presented.

The external hydrodynamic moment functions $m_0^o(z)$ and $m_n^o(z)$ are zero if the cross-section of the outside surface of the tower is uniform over the height of the tower. Similarly $m_0^i(z)$ and $m_n^i(z)$ are zero for towers with uniform cross-section of the inside surface. In other words, these external hydrodynamic moments are non-zero for tapered towers, in which case they contribute to the hydrodynamic terms through equations (7.9) to (7.12). In order to evaluate the influence of external hydrodynamic moments on the dynamic response of towers, analyses were carried out by the procedure developed in Chapters 3 and 4, using the implementing series of computer programs "TOWERRZ" and "TOWER3D", for the towers described in Section 7.2. Presented in Figure 7.3 is the amplitude of the steady state response of two tapered towers due to harmonic ground motion plotted against the excitation frequency. These results were computed by two methods : (1) exact analyses as described in Chapters 3 and 4, and (2) similar analyses but neglecting external hydrodynamic moments. It is apparent from these results that the effects of hydrodynamic moments, which increase for squat towers, may be neglected in representing the hydrodynamic effects in the dynamic analysis of practical, tapered towers. Neglecting hydrodynamic moments leads to the same advantage as in neglecting rotatory inertia effects that the bending slope function $\psi_n(z)$ need not be computed in the simplified analysis.

If the contribution of hydrodynamic moments to the added hydrodynamic mass and excitation terms [equations (7.9) to (7.12)] is neglected, the effects of surrounding water on the dynamics of towers in the n-th mode of vibration are completely and exactly accounted for by considering

$$m_a^o(z) = \frac{f_n^o(z)}{\phi_n(z)} \tag{7.13}$$

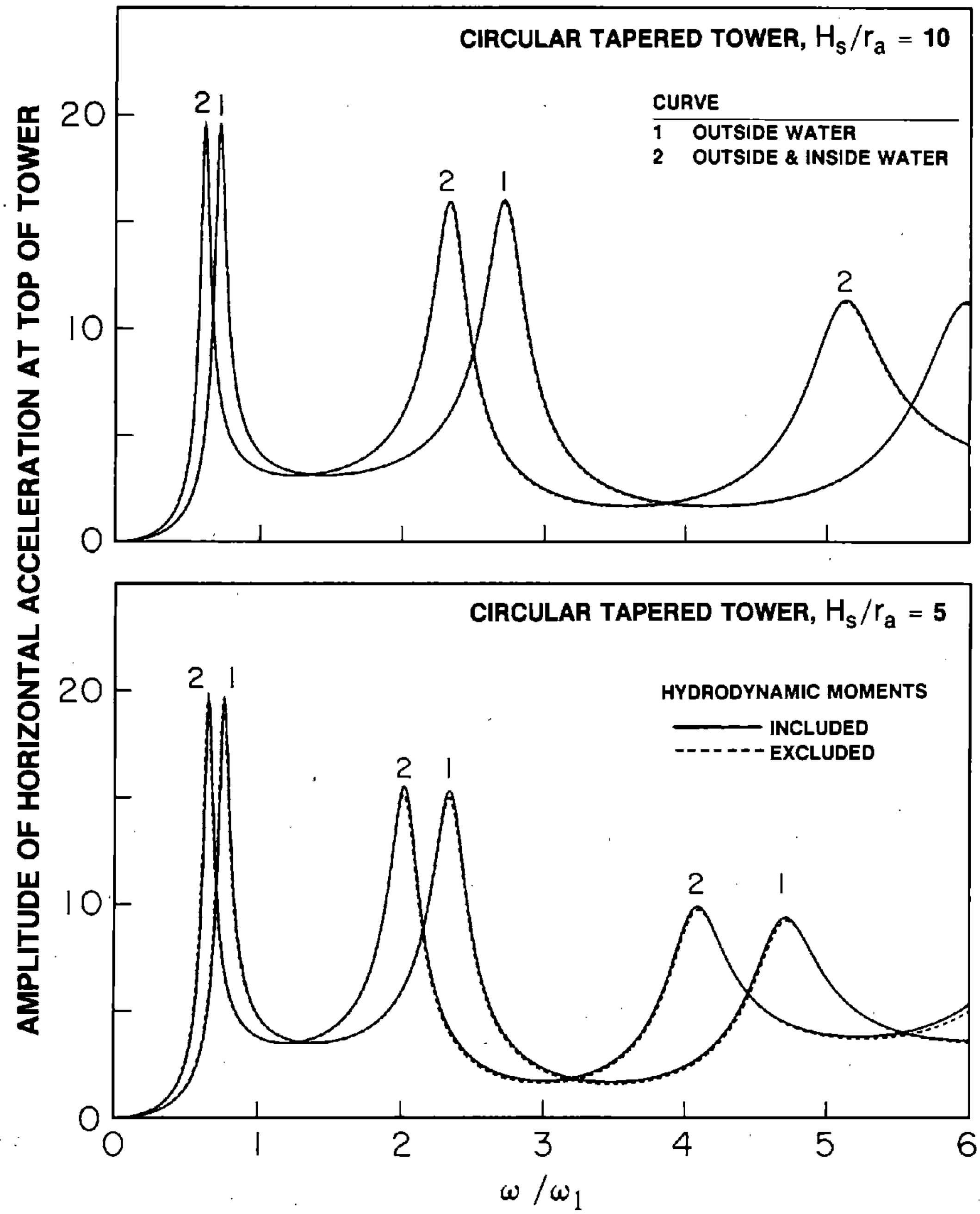

Figure 7.3 Influence of External Hydrodynamic Moments on the Response of Circular Tapered Towers on Rigid Foundation Soil with Full Water due to Harmonic Ground Motion

as an added mass per unit of height of the tower. Similarly, the effects of inside water in the n-th mode of vibration of the tower are completely and exactly accounted for by considering

$$m_a^i(z) = \frac{f_n^i(z)}{\phi_n(z)} \tag{7.14}$$

as an added mass per unit of height of the tower. It can be shown that, in the absence of hydrodynamic moments, equation (7.7) is also the equation of motion for a tower in air with mass distribution

$$\tilde{m}_s(z) = m_s(z) + m_a^o(z) + m_a^i(z) \tag{7.15}$$

constrained to be vibrating in the shape $\phi_n(z)$, with $m_a^o(z)$ and $m_a^i(z)$ given by equations (7.13) and (7.14). The added hydrodynamic mass functions for the surrounding and inside water depend on the shape $\phi_n(z)$ of the vibration mode considered. This, of course, implies that no one function, $m_a^o(z)$ for the surrounding water or $m_a^i(z)$ for the inside water, will be exactly valid for all vibration modes of the tower.

7.4.2 Added Hydrodynamic Mass

On the other hand, for many years the concept of an added hydrodynamic mass to represent the inertial influence of water interacting with a structure has been based on the assumption of a rigid structure. This concept has been applied in different situations, including problems in classical hydrodynamics [31], dams impounding water [49], cylindrical tanks containing water [29], and cylindrical structures surrounded by water [32]. For towers such a concept leads to the following definitions for added hydrodynamic mass, $m_a^o(z)$ and $m_a^i(z)$:

$$m_a^o(z) = f_0^o(z) \tag{7.16}$$

$$m_a^i(z) = f_0^i(z) \tag{7.17}$$

where, as defined earlier, $f_0^o(z)$ and $f_0^i(z)$ are the lateral hydrodynamic forces acting in the plane of vibration on the outside and inside surfaces of a rigid tower, respectively, due to unit horizontal acceleration of the ground. The additional generalized excitation terms in the n-th vibration mode associated with these added masses are $\int_0^{H_o} m_a^o(z)\,\phi_n(z)\,dz$ and $\int_0^{H_i} m_a^i(z)\,\phi_n(z)\,dz$ which can be shown to be equal to L_n^o and L_n^i [equations (7.10) and (7.12)], respectively, if the hydrodynamic moments are neglected [32, Chapter 3]. However, the additional generalized mass terms associated with the added masses of equations (7.16) and (7.17), given by $\int_0^{H_o} m_a^o(z)\,\phi_n^2(z)\,dz$ and $\int_0^{H_i} m_a^i(z)\,\phi_n^2(z)\,dz$, are not equal to M_{nn}^o and M_{nn}^i [equations (7.9) and (7.11)], respectively. Consequently, the added masses defined by equations (7.16) and (7.17) are not exact representations of the hydrodynamic effects. However, they have the advantage that they do not depend on the vibration mode shapes of the tower.

It is thus of interest to investigate whether these added masses, equations (7.16) and (7.17), are adequate as approximate representations of the hydrodynamic effects. The accuracy of these added masses is evaluated for three towers described earlier. For this purpose, the distributions of equivalent lateral forces are examined first. With the added mass representation of equation (7.15), the equivalent lateral forces associated with the maximum response in the n-th vibration mode of the fixed-base towers are [9,11] :

$$f_n(z) = \frac{\tilde{L}_n}{\tilde{M}_n}\, S_a(T_n^r,\xi_n^r)\, \tilde{m}_s(z)\, \phi_n(z) \tag{7.18}$$

where S_a is the ordinate of the pseudo-acceleration response spectrum for the earthquake ground motion evaluated at vibration period T_n^r and damping ratio $\xi_n^r = \xi_n = \eta_s / 2$. The period $T_n^r = 2\pi/\omega_n^r$ is the vibration period of the n-th vibration mode of the tower including the effects of water. The contribution of the surrounding water in the equivalent lateral forces $f_n(z)$ of equation (7.18) for the n-th vibration mode is :

$$[f_n(z)]_{outside} = \frac{\tilde{L}_n}{\tilde{M}_n} S_a(T_n^r, \xi_n^r)\, m_a^o(z)\, \phi_n(z) \tag{7.19}$$

The distributions of these forces over the depth of water is displayed in Figures 7.4 to 7.9 for the first two vibration modes for two definitions of the added hydrodynamic mass $m_a^o(z)$: exact value of equation (7.13) and the approximate value of equation (7.16). Although exact and approximate distributions of added mass differ over the height, their integrals over the height can be shown to be equal using the reciprocity property of hydrodynamic forces [equation (3.28)]. Thus, the discrepancies in the distribution of the associated shearing forces $Q_n(z)$ and bending moments $m_n(z)$ are small enough in circular uniform towers (Figures 7.4 to 7.6) as well as in circular tapered towers (Figures 7.7 to 7.9), over a wide range of H_s/r_a values, to make the approximate added mass suitable for simplified analysis.

Similarly, the contribution of the inside water in the equivalent lateral forces $f_n(z)$ of equation (7.18) for the n-th vibration mode is :

$$[f_n(z)]_{inside} = \frac{\tilde{L}_n}{\tilde{M}_n} S_a(T_n^r, \xi_n^r)\, m_a^i(z)\, \phi_n(z) \tag{7.20}$$

The distribution of these forces, and the associated shears and moments over the depth of water, are displayed in Figures 7.10 to 7.15 for the first two vibration modes for two distributions of the added hydrodynamic mass $m_a^i(z)$: exact value of equation (7.14) and the approximate value of equation (7.17). As in the case of surrounding water, and for similar reasons, the approximate added mass of equation (7.17) provides results that are sufficiently accurate for simplified analysis. The results presented also demonstrate that the approximate added mass concept is better in representing the effects of inside water (Figures 7.10 to 7.15) compared to outside water (Figures 7.4 to 7.9).

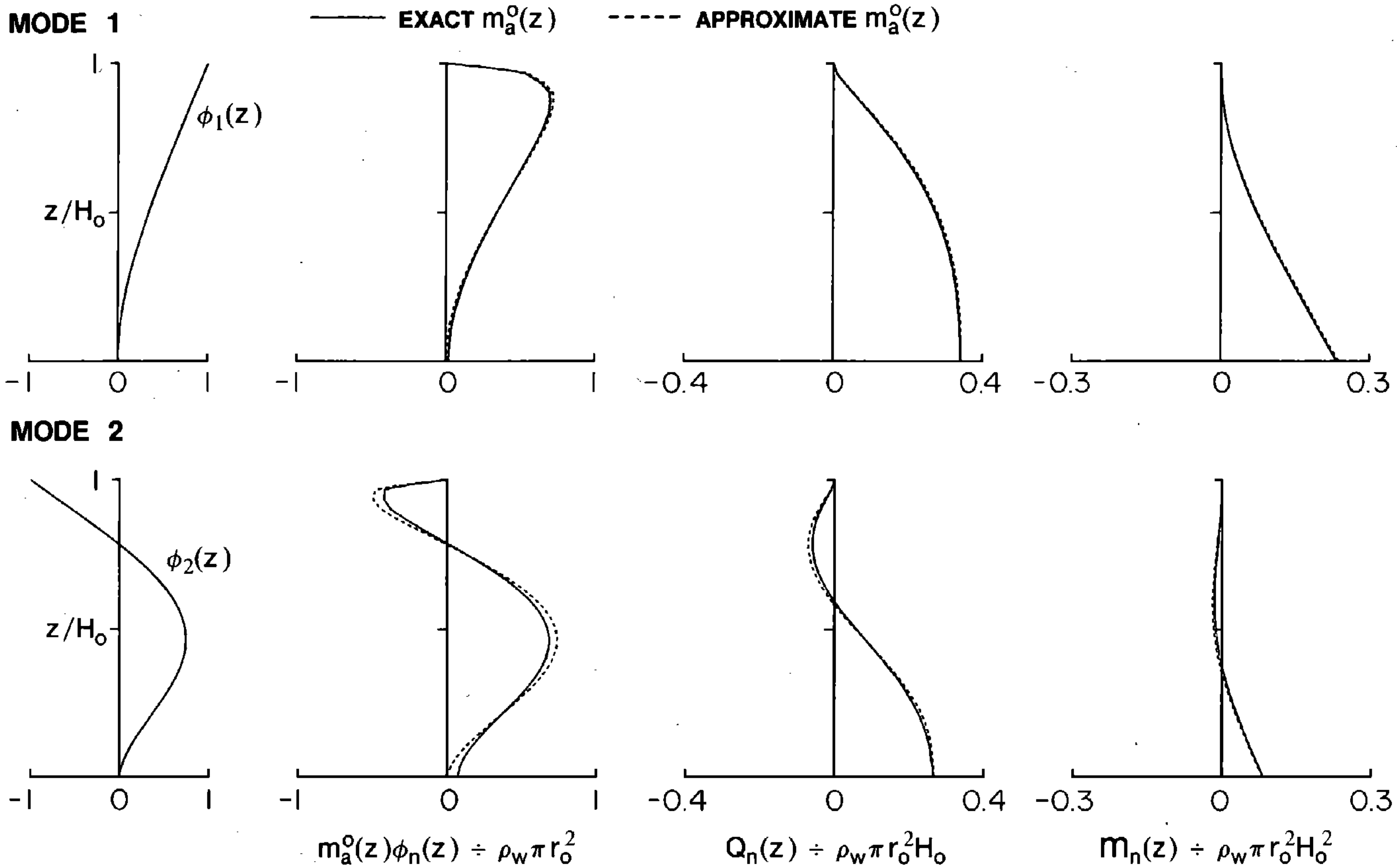

Figure 7.4 Contribution of Surrounding Water to Distribution of Lateral Forces, Shearing Forces and Bending Moments for Circular Cylindrical Tower, $H_s/r_a = 20$

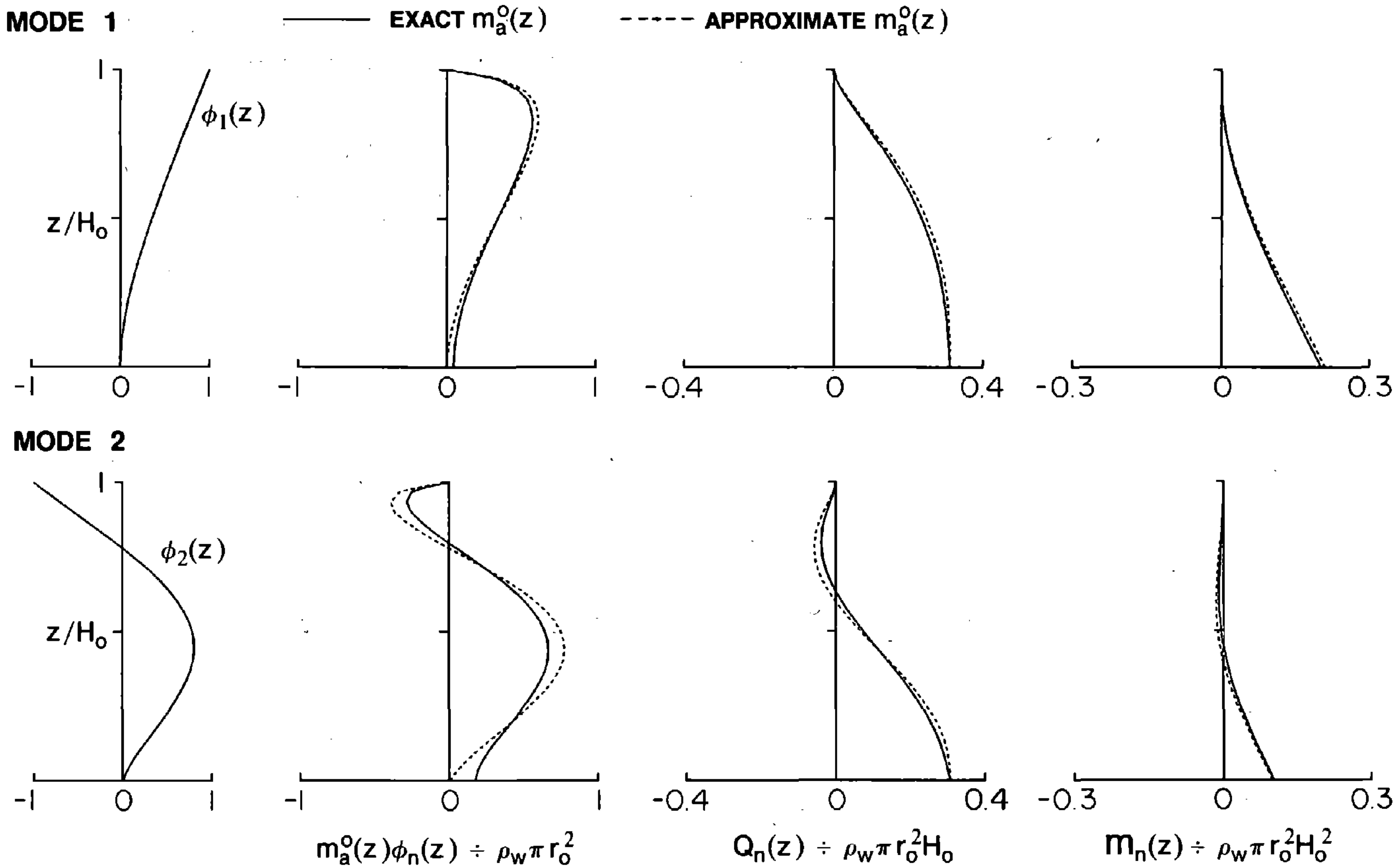

Figure 7.5 Contribution of Surrounding Water to Distribution of Lateral Forces, Shearing Forces and Bending Moments for Circular Cylindrical Tower, $H_s/r_a = 10$

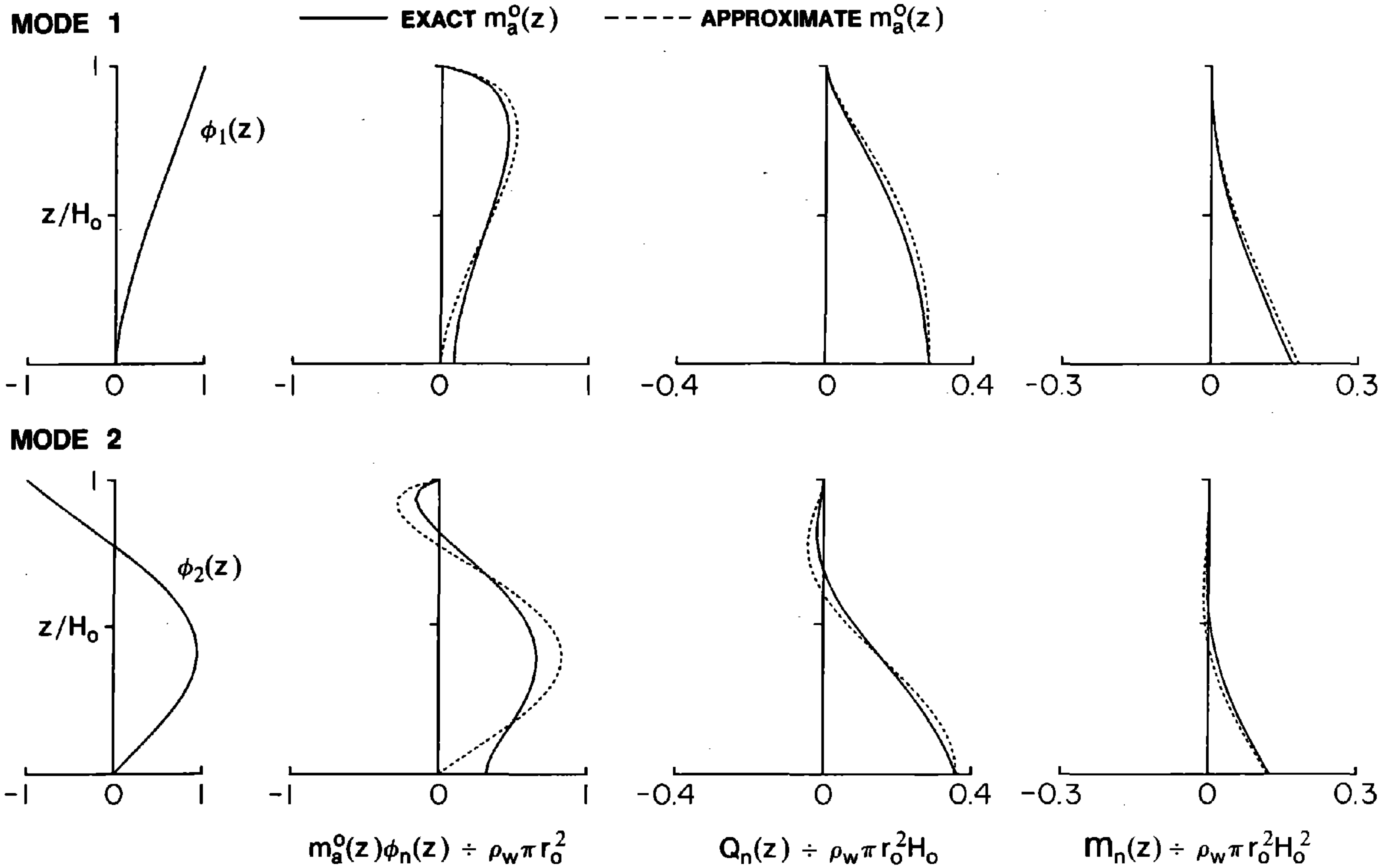

Figure 7.6 Contribution of Surrounding Water to Distribution of Lateral Forces, Shearing Forces and Bending Moments for Circular Cylindrical Tower, $H_s/r_a = 5$

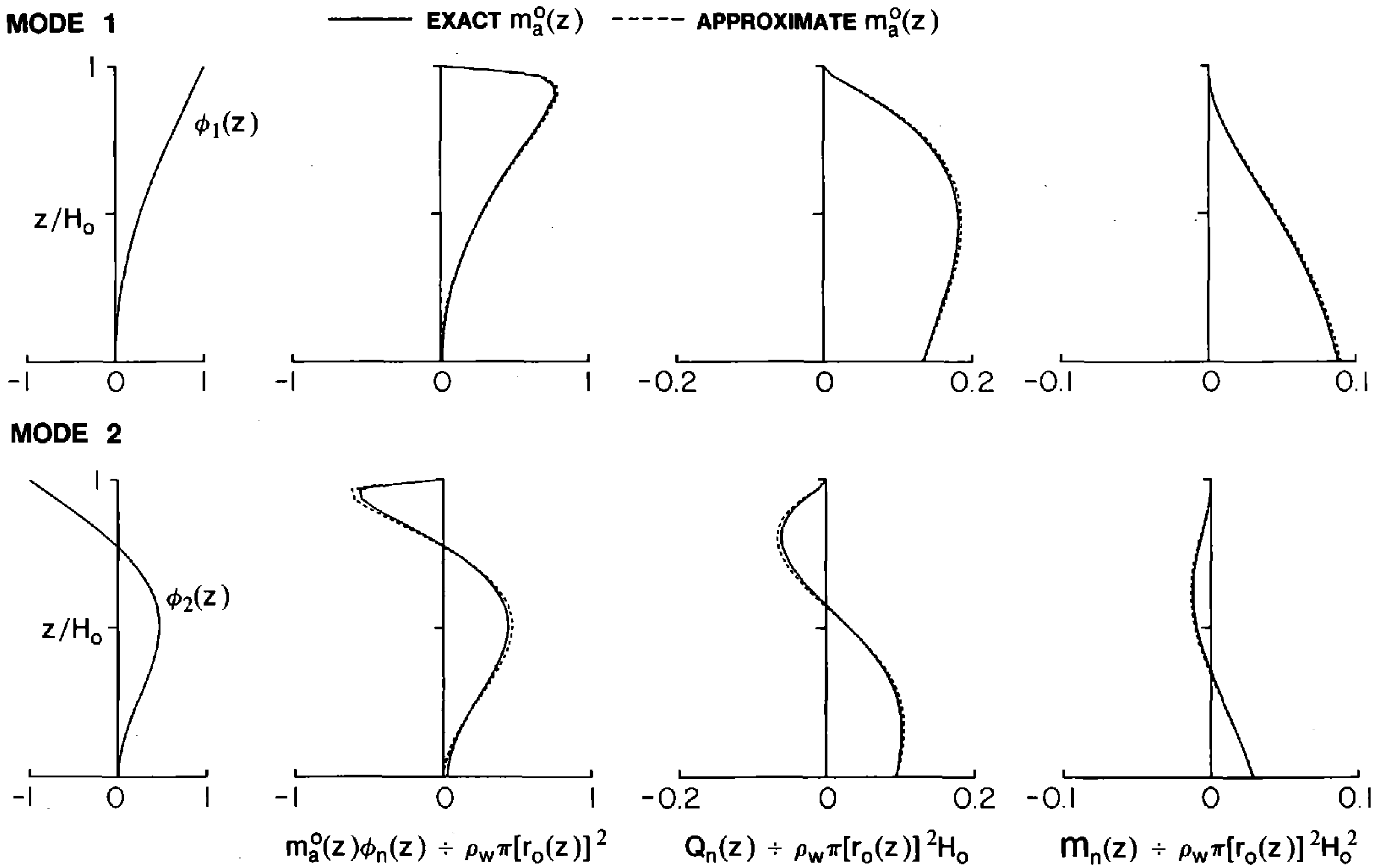

Figure 7.7 Contribution of Surrounding Water to Distribution of Lateral Forces, Shearing Forces and Bending Moments for Circular Tapered Tower, $H_s/r_a = 20$

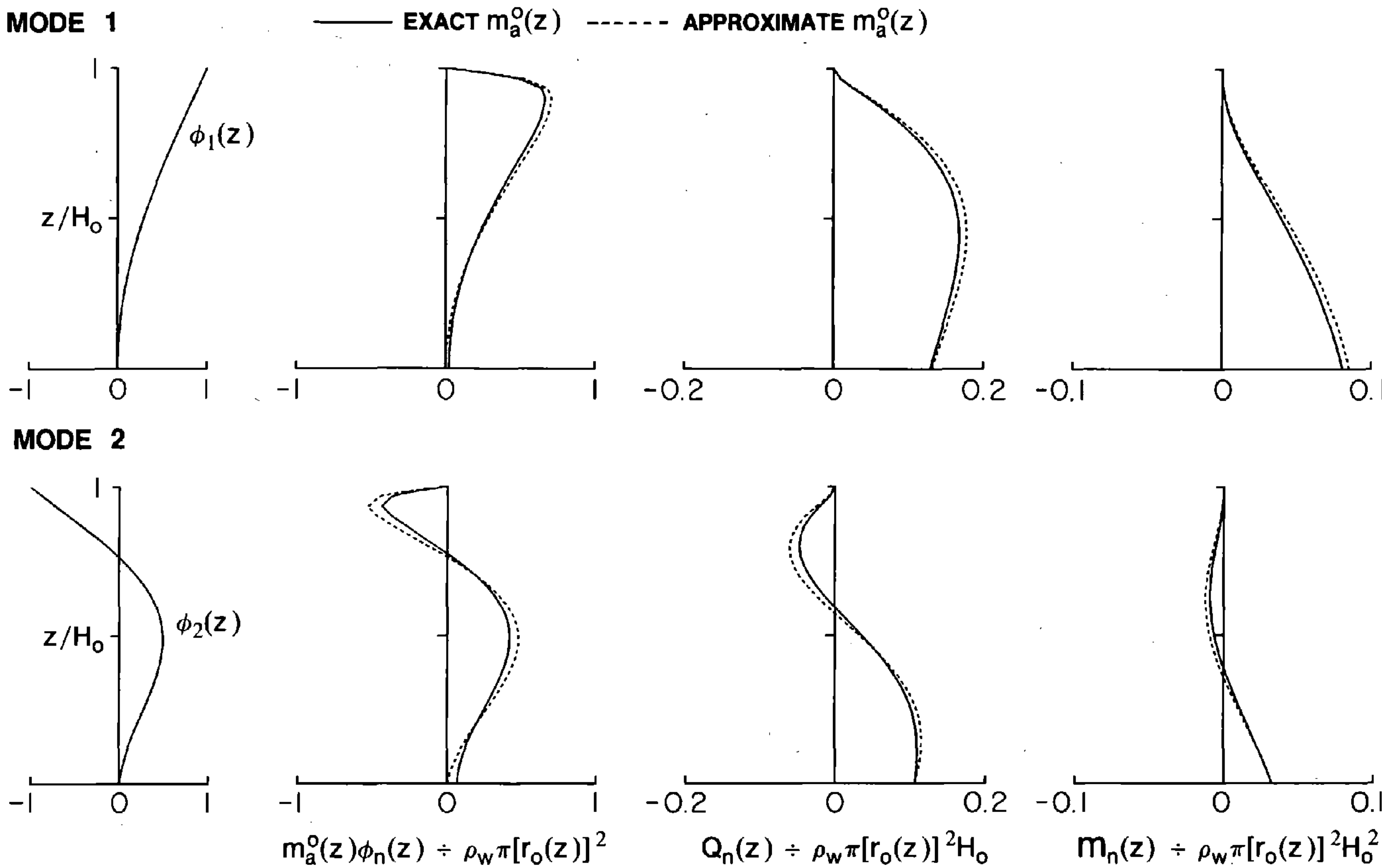

Figure 7.8 Contribution of Surrounding Water to Distribution of Lateral Forces, Shearing Forces and Bending Moments for Circular Tapered Tower, $H_s/r_a = 10$

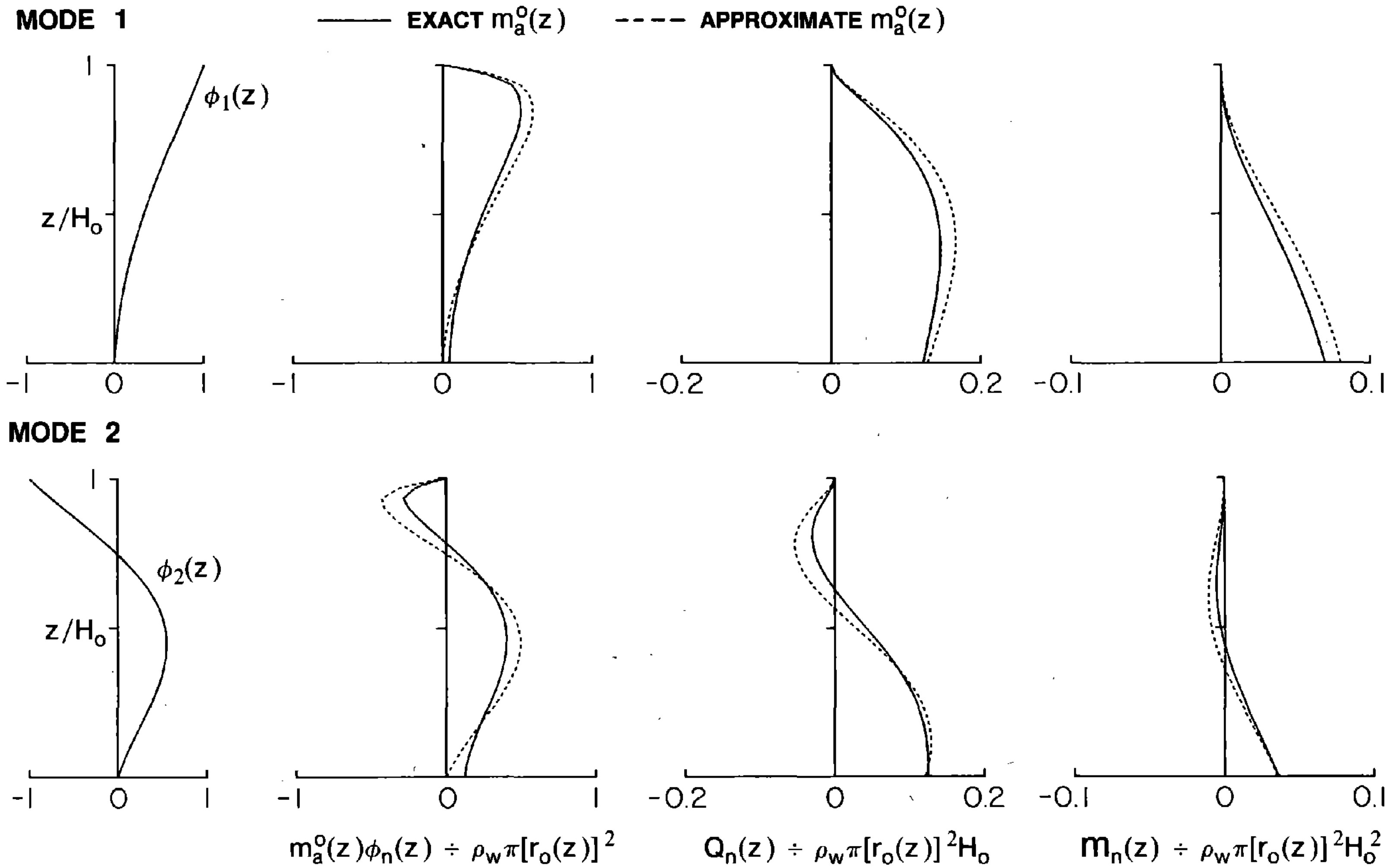

Figure 7.9 Contribution of Surrounding Water to Distribution of Lateral Forces, Shearing Forces and Bending Moments for Circular Tapered Tower, $H_s/r_a = 5$

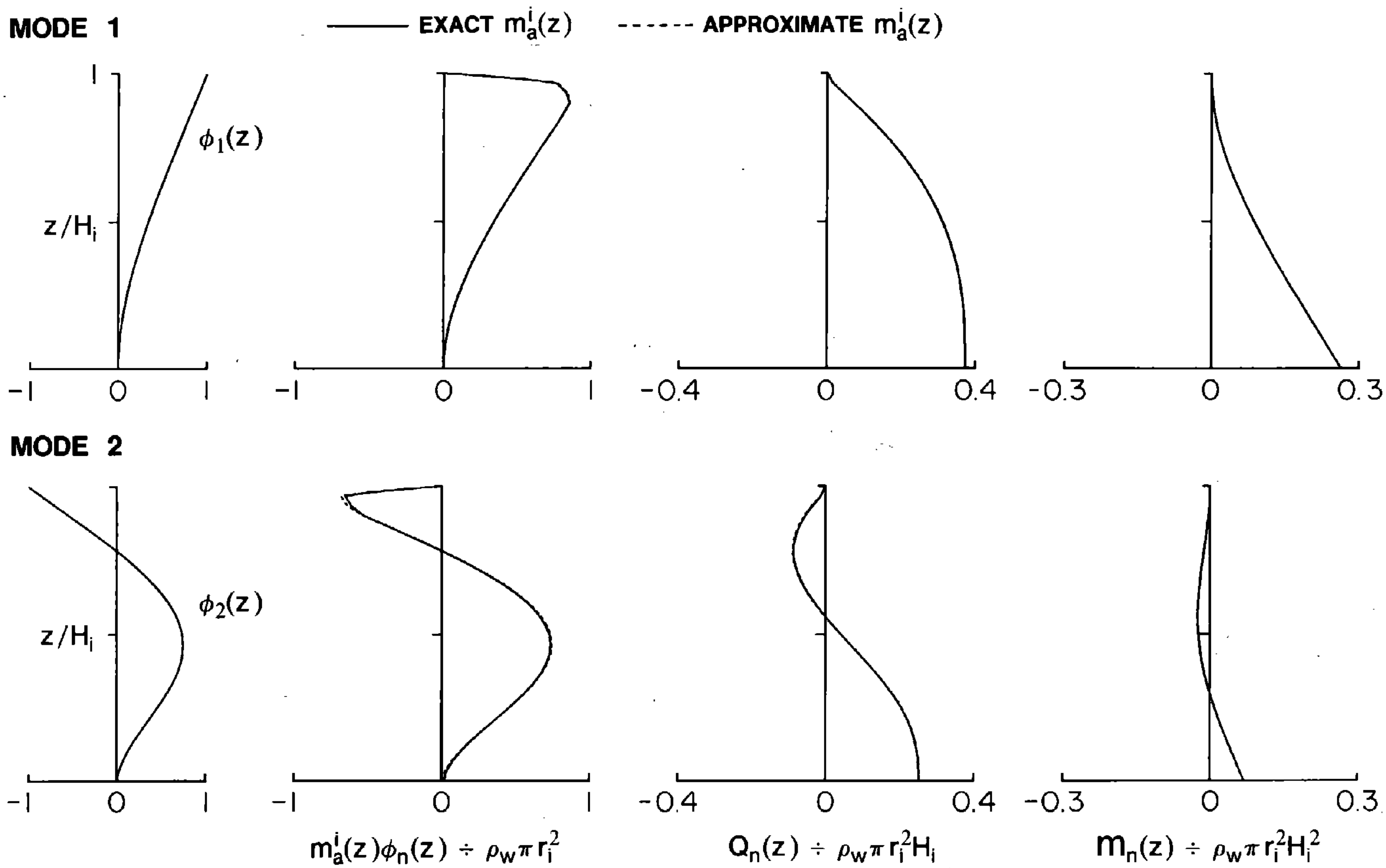

Figure 7.10 Contribution of Inside Water to Distribution of Lateral Forces, Shearing Forces and Bending Moments for Circular Cylindrical Tower, $H_s/r_a = 20$

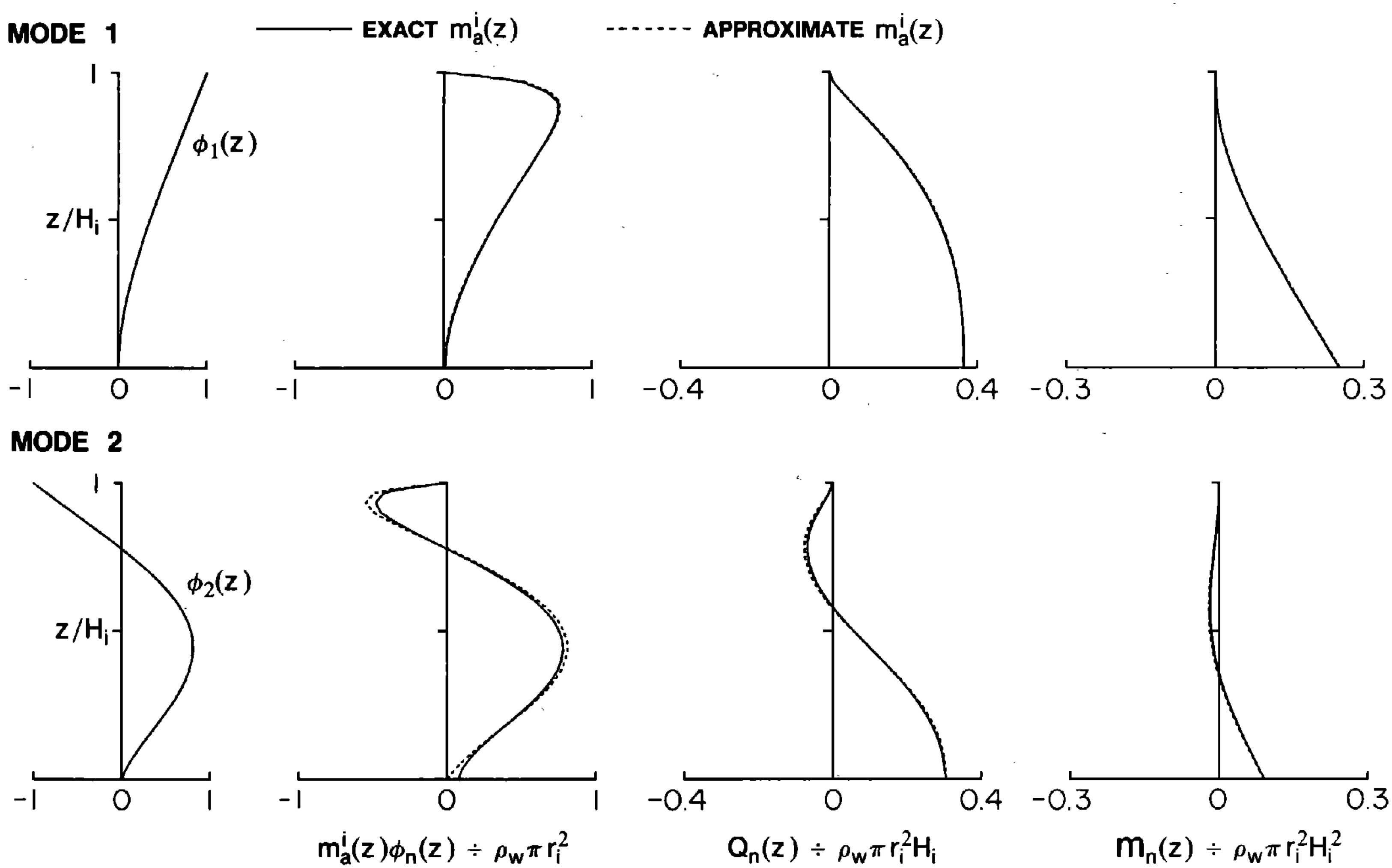

Figure 7.11 Contribution of Inside Water to Distribution of Lateral Forces, Shearing Forces and Bending Moments for Circular Cylindrical Tower, $H_s/r_a = 10$

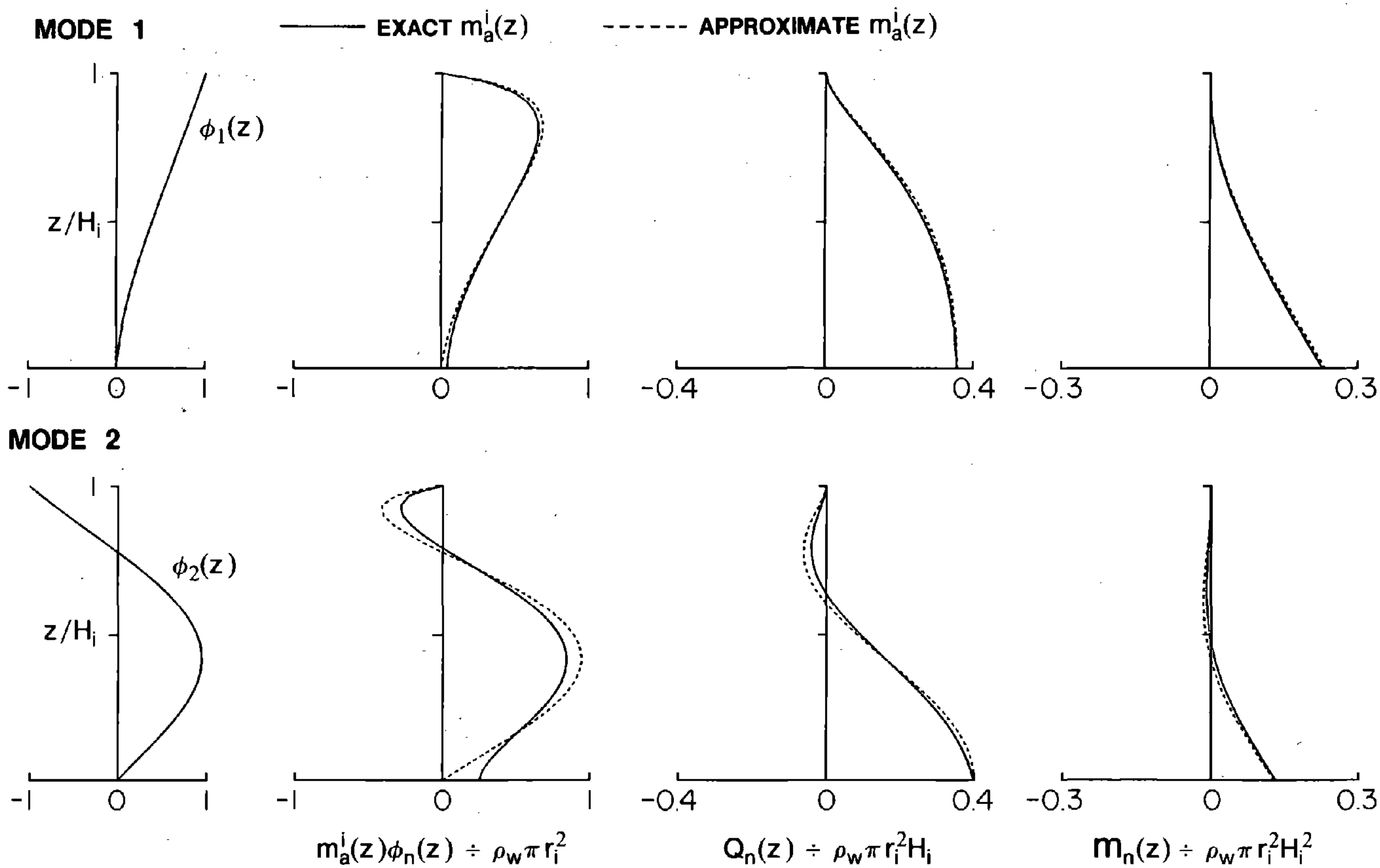

Figure 7.12 Contribution of Inside Water to Distribution of Lateral Forces, Shearing Forces and Bending Moments for Circular Cylindrical Tower, $H_s/r_a = 5$

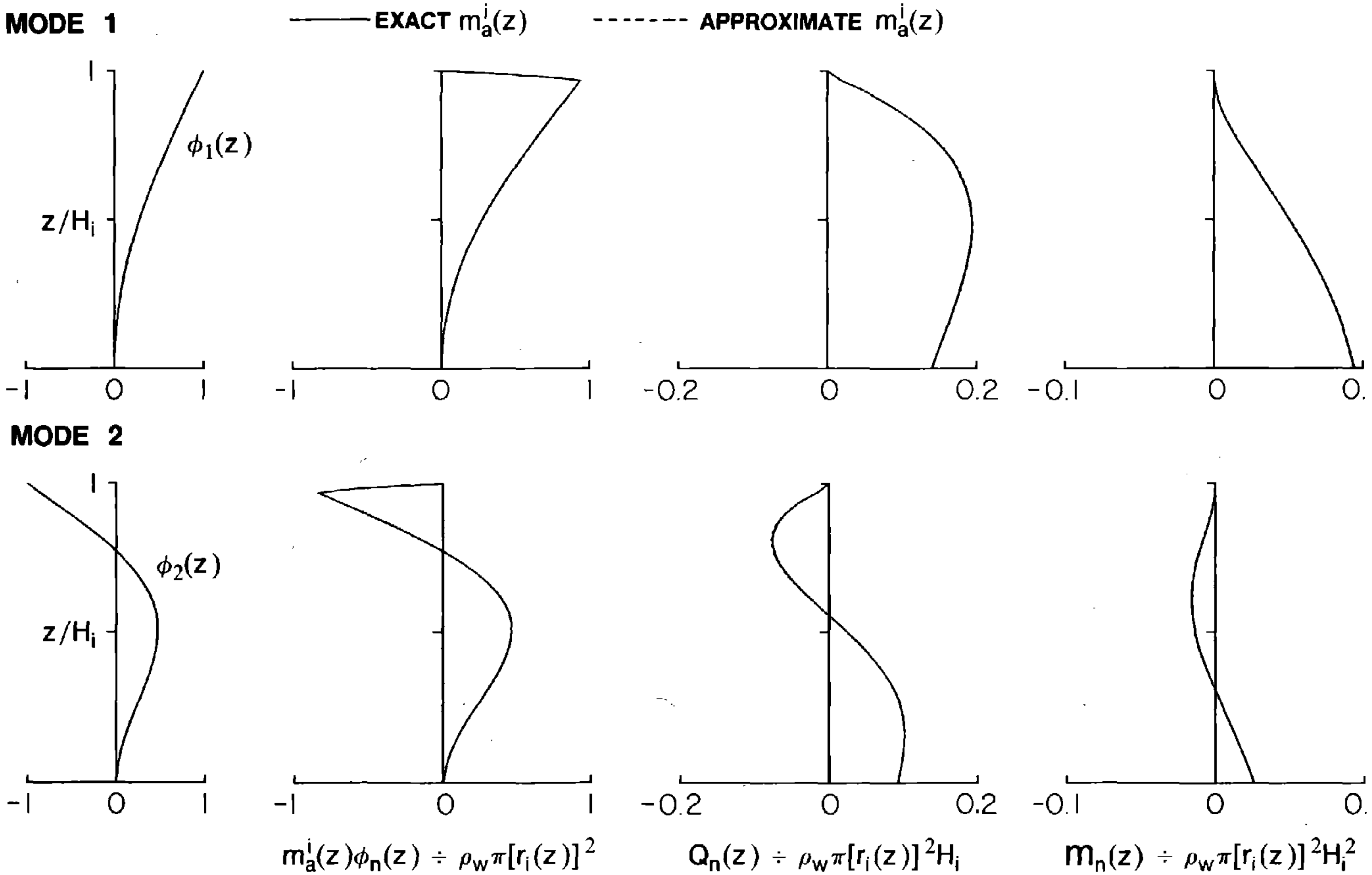

Figure 7.13 Contribution of Inside Water to Distribution of Lateral Forces, Shearing Forces and Bending Moments for Circular Tapered Tower, $H_s/r_a = 20$

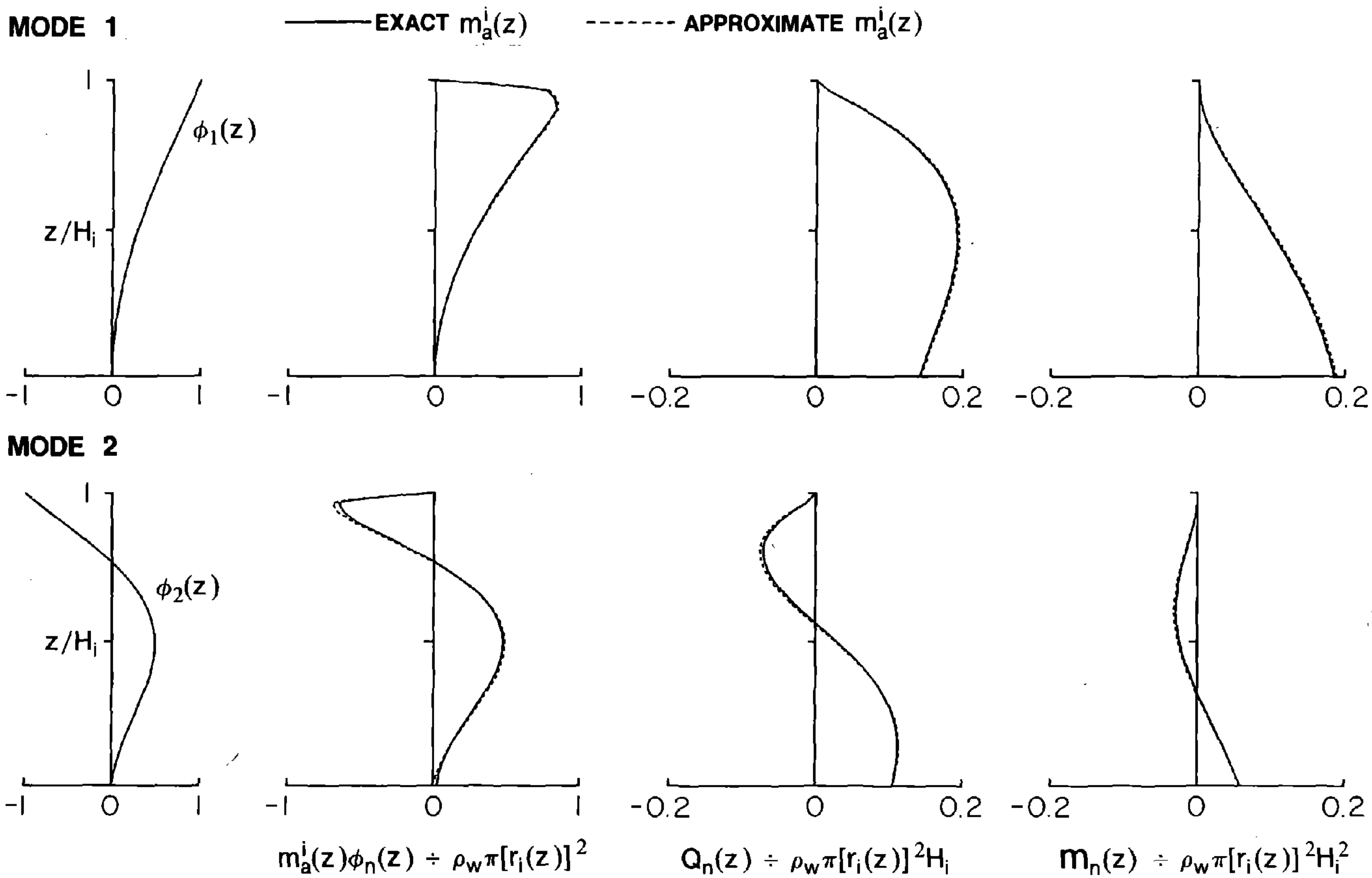

Figure 7.14 Contribution of Inside Water to Distribution of Lateral Forces, Shearing Forces and Bending Moments for Circular Tapered Tower, H_s/r_a = 10

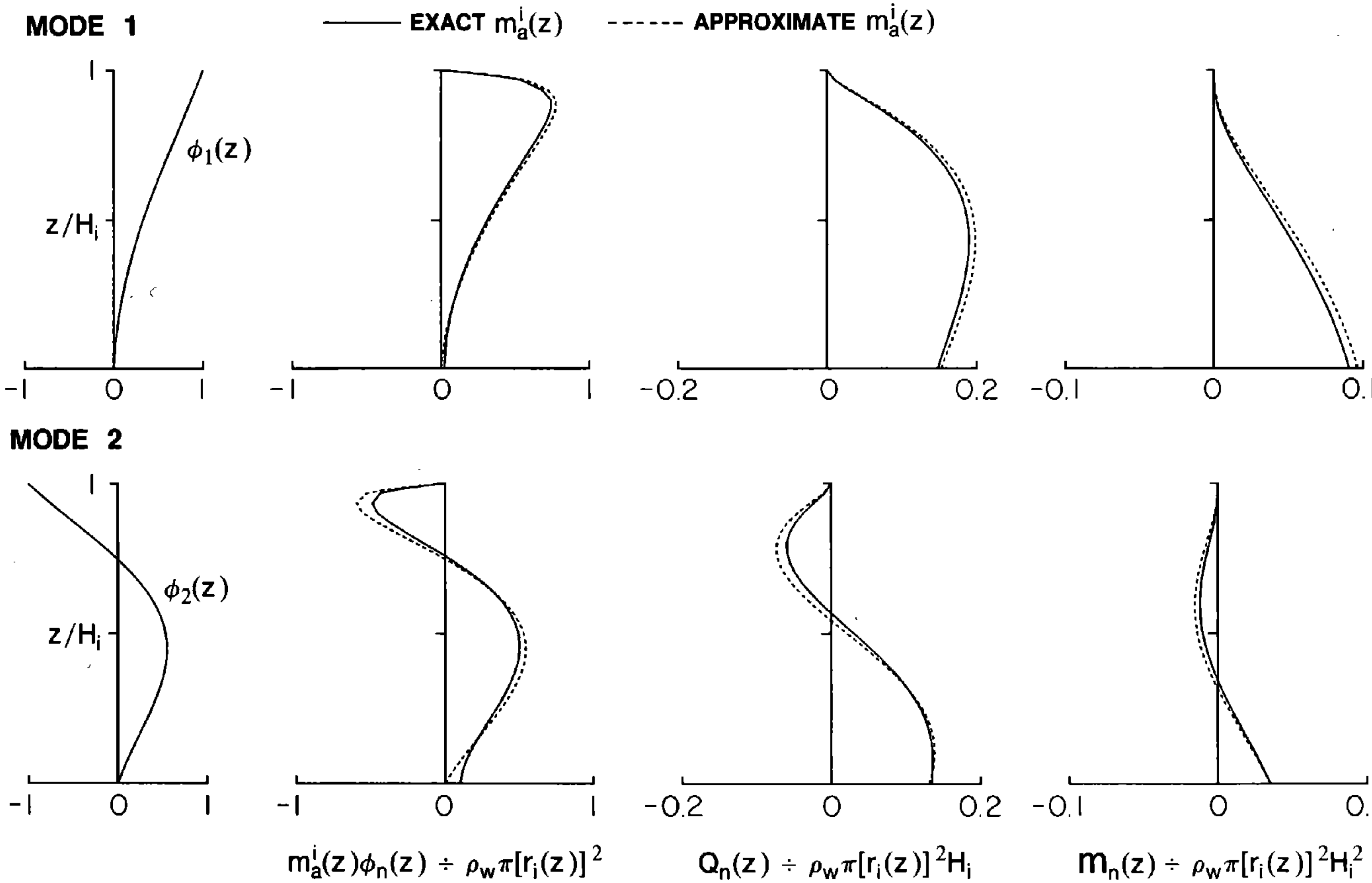

Figure 7.15 Contribution of Inside Water to Distribution of Lateral Forces, Shearing Forces and Bending Moments for Circular Tapered Tower, $H_s/r_a = 5$

7.4.3 Response Results

Presented in Figures 7.16 to 7.18 is the amplitude of the steady state response of towers with full outside water only, and with full outside and inside water, to harmonic ground motion, plotted as a function of the normalized excitation frequency ω/ω_1, ω_1 being the fundamental vibration frequency of the fixed-base tower without water, for three towers described in Section 7.2 for various values of the slenderness ratio. These results were computed by : (1) exact analysis described in Chapter 3 , and (2) analysis of the tower in air with its mass equal to the actual mass plus the added hydrodynamic masses of equations (7.16) and (7.17).

These results demonstrate that the added mass approximation provides accurate responses in the fundamental vibration mode, resulting in accurate values of the fundamental resonant amplitude for towers with a wide range of H_s/r_a values, with the results being most accurate for slender towers. The added mass approximation is not as good in predicting the second mode response and hence the second resonant period, with the errors increasing for squat towers. However, over a wide range of slenderness ratios, the resonant responses and the resonant periods (Figures 7.19 and 7.20) including hydrodynamic effects, are reasonably accurate.

Based on the response results presented in this section, it is apparent that the hydrodynamic interaction effects can most simply be included in the response spectrum analysis of towers by replacing the mass of the tower $m_s(z)$ by the virtual mass $\tilde{m}_s(z)$ [equation (7.15)], with the added hydrodynamic mass distributions given by equation (7.16) for the surrounding water and by equation (7.17) for the inside water. However, the analytical expressions to evaluate the added hydrodynamic mass are available only for circular cylindrical towers [33,40] and for uniform elliptical towers [30]. For towers of arbitrary cross-section in plan and dimensions varying along the height, the computation of the added hydrodynamic mass requires a finite element solution of the boundary value problem for rigid towers (Chapters 3 and 4). In order to avoid this complicated analysis in the

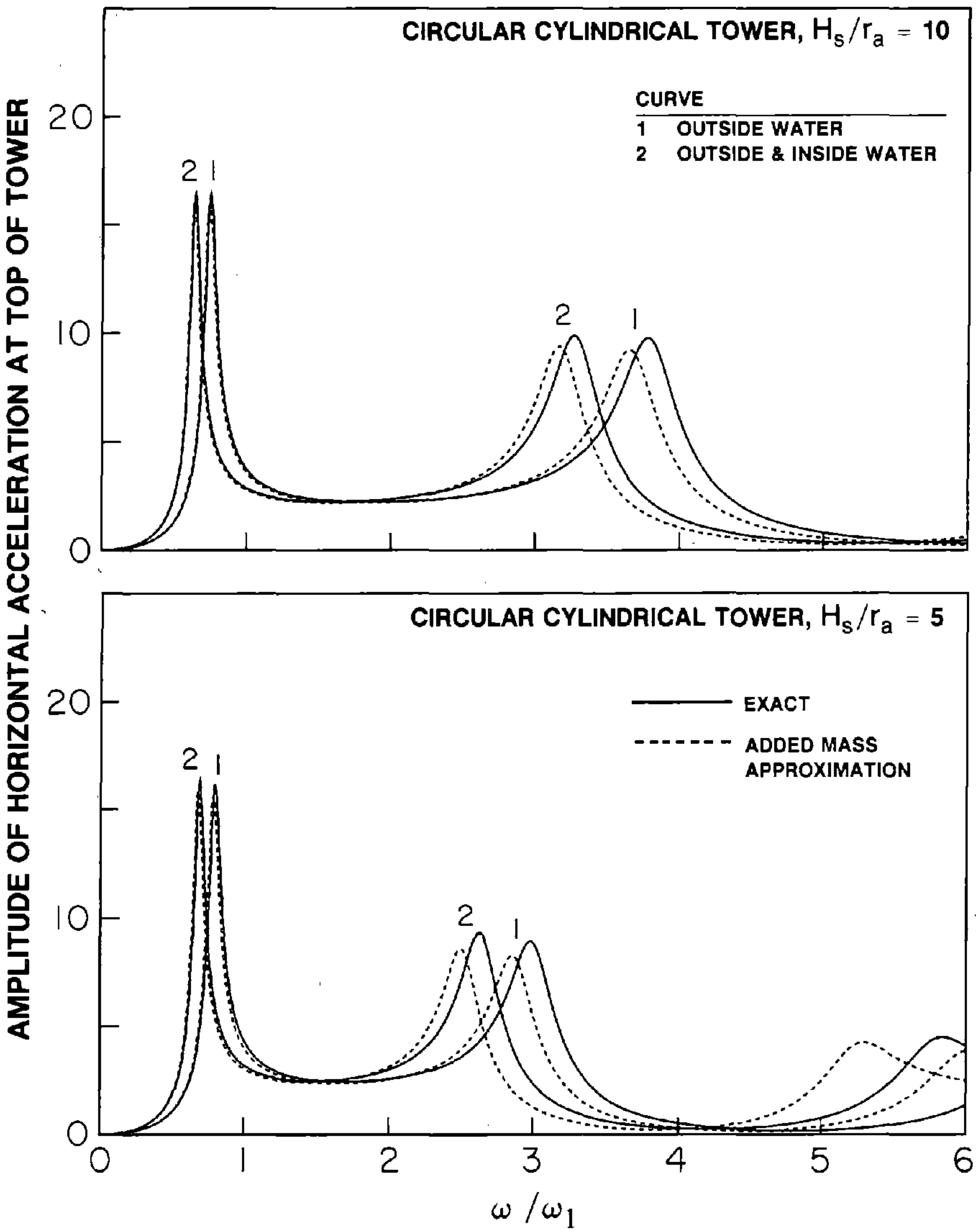

Figure 7.16 Comparison of Exact and Approximate (Added Mass Representation of Hydrodynamic Effects) Response of Circular Cylindrical Towers on Rigid Foundation Soil with Water due to Harmonic Horizontal Ground Motion

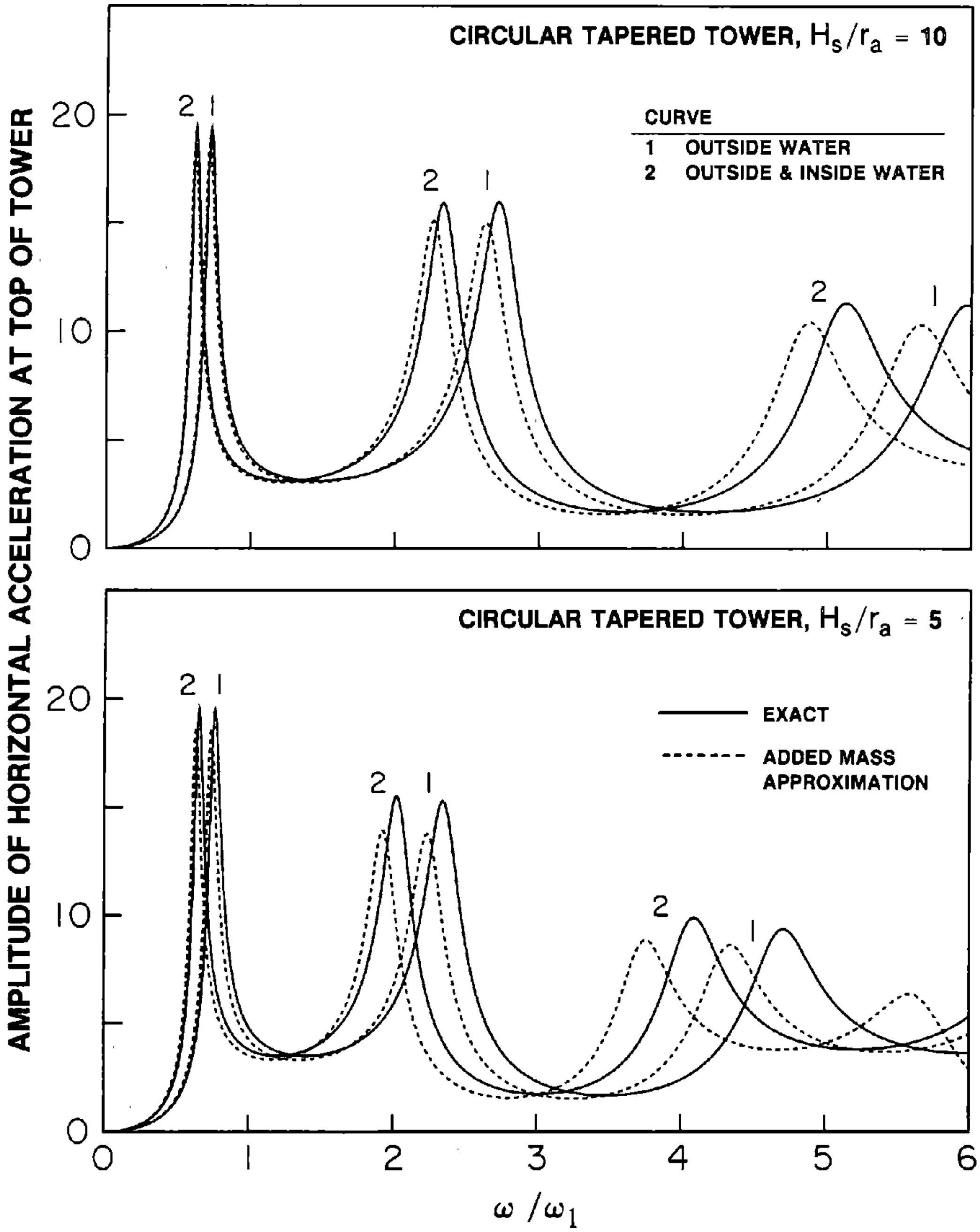

Figure 7.17 Comparison of Exact and Approximate (Added Mass of Representation of Hydrodynamic Effects) Response of Circular Tapered Towers on Rigid Foundation Soil with Water due to Harmonic Horizontal Ground Motion

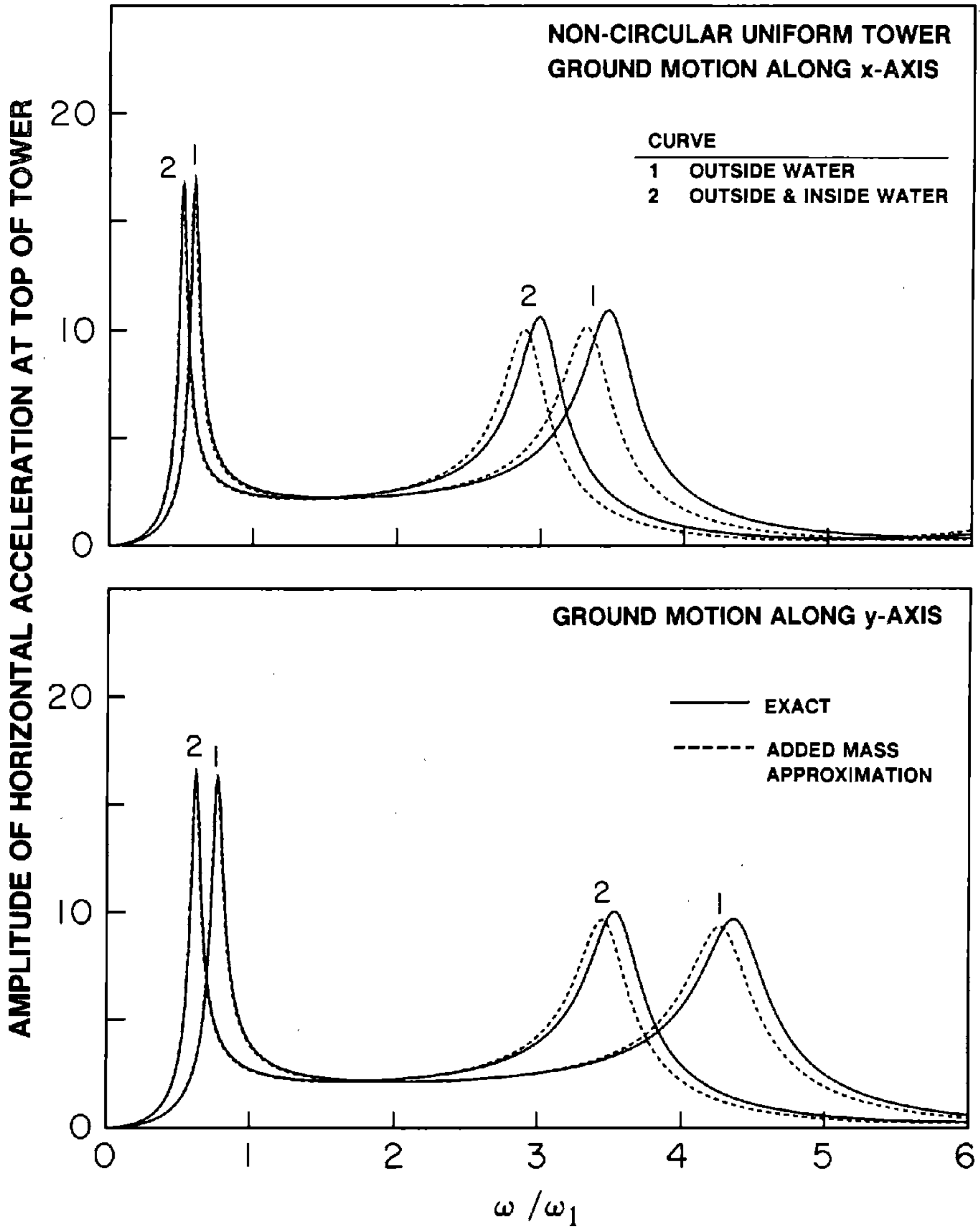

Figure 7.18 Comparison of Exact and Approximate (Added Mass of Representation of Hydrodynamic Effects) Response of Non-Circular Uniform Tower on Rigid Foundation Soil with Water due to Harmonic Horizontal Ground Motion

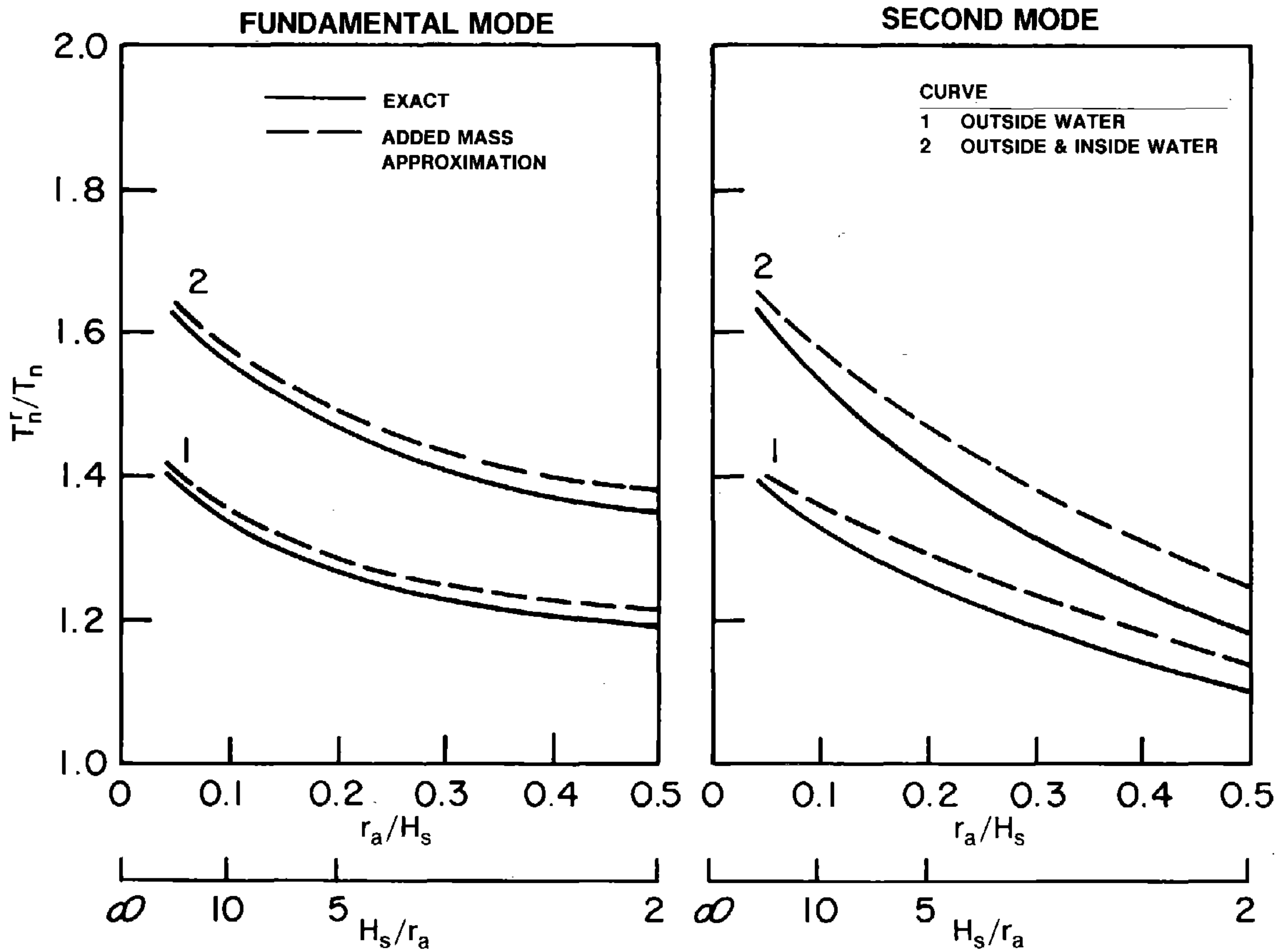

Figure 7.19 Evaluation of Added Mass Representation for Hydrodynamic Effects in the Analysis of Circular Cylindrical Towers; Result Presented is the Period Ratio of Towers with and Without Water on Rigid Foundation Soil

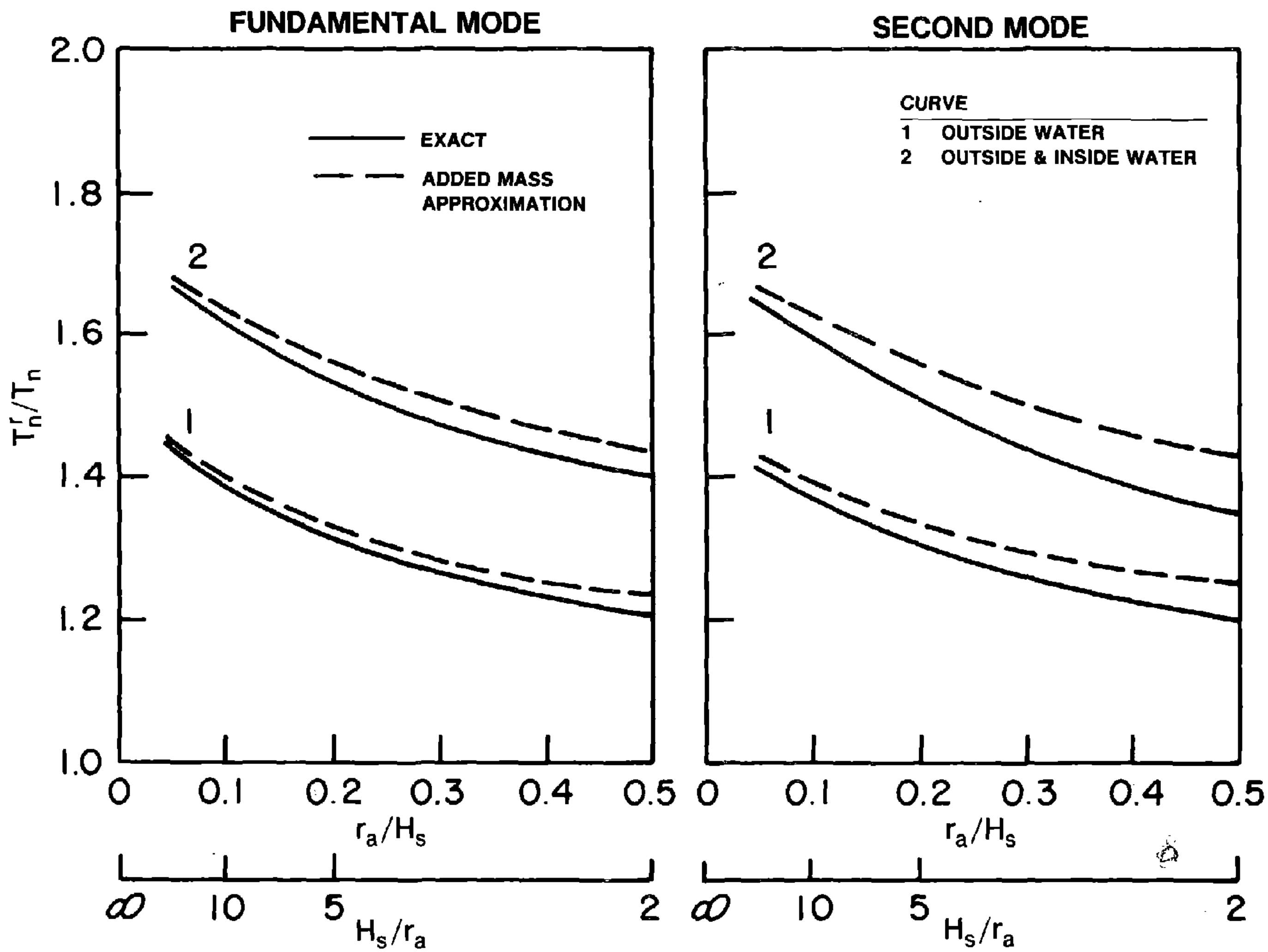

Figure 7.20 Evaluation of Added Mass Representation for Hydrodynamic Effects in the Analysis of Circular Tapered Towers; Result Presented is the Period Ratio of Towers with and Without Water on Rigid Foundation Soil

preliminary design or safety evaluation of towers, an approximate procedure is presented in Chapter 8 to evaluate the added hydrodynamic mass.

7.5 Towers on Flexible Soil

Simplified procedures have been developed to include the effects of soil-structure interaction in the earthquake response analysis of buildings [45,46] and concrete gravity dams [20]. The basic concepts underlying these procedures are : (i) structure-foundation interaction effects in the fundamental vibration mode of the structure can be expressed by changes in the vibration period and damping ratio for the fixed-base mode; and (ii) the contribution of the higher vibration modes to the response may be approximately computed as if the structure was supported on rigid soil. Based on these same concepts, a simplified procedure is developed for the analysis of intake-outlet towers including tower-foundation-soil interaction effects. Although the contribution of the second mode to the base shear and moment is more significant in the response of towers compared to most buildings [15], resulting in increased influence of tower-foundation-soil interaction in the response contribution of this mode (Chapters 5 and 6), the above mentioned approximation is reasonable because, over a wide range of fundamental vibration periods, the tower response is dominated by the fundamental mode.

7.5.1 Exact Fundamental Mode Response

The equation governing the frequency response function $\bar{Y}_1(\omega)$ for the modal coordinate associated with the fundamental vibration mode of the tower on fixed-base, equation (7.1) for $n = 1$, must be modified to include the response functions for the rotation $\bar{\theta}_f(\omega)$ and horizontal translation $\bar{u}_f(\omega)$ of the tower foundation relative to the free-field ground motion, permitted by the soil flexibility [equation (3.17) with $N = 1$] :

$$\begin{bmatrix} [-\omega^2 M_1+(1+i\eta_s)\omega_1^2 M_1] & -\omega^2 L_1^h & -\omega^2 L_1^r \\ -\omega^2 L_1^h & -\omega^2(m_t+m_f)+K_{VV}(\omega) & -\omega^2 L_0^r+K_{VM}(\omega) \\ -\omega^2 L_1^r & -\omega^2 L_0^r+K_{MV}(\omega) & -\omega^2(I_t+I_f)+K_{MM}(\omega) \end{bmatrix} \begin{Bmatrix} \bar{Y}_1(\omega) \\ \bar{u}_f(\omega) \\ \bar{\theta}_f(\omega) \end{Bmatrix}$$

$$= - \begin{Bmatrix} L_1 \\ m_t+m_f \\ L_0^r \end{Bmatrix} \tag{7.21}$$

in which $L_1^h = L_1$; m_t is the total mass of the tower and I_t is the mass moment of inertia of the tower about the base including the contributions of the portion of the foundation above the ground level (Section 7.2) :

$$m_t = \int_0^{H_s} m_s(z)\, dz \tag{7.22}$$

$$I_t = \int_0^{H_s} z^2\, m_s(z)\, dz + \int_0^{H_s} I_s(z)\, dz \tag{7.23}$$

In equation (7.21), m_f and I_f are the mass and mass moment of inertia of the part of the foundation below the ground level (Section 7.2) ; and

$$L_1^r = \int_0^{H_s} z\, m_s(z)\, \phi_1(z)\, dz + \int_0^{H_s} I_s(z)\, \psi_1(z)\, dz \tag{7.24}$$

$$L_0^r = \int_0^{H_s} z\, m_s(z)\, dz \tag{7.25}$$

The frequency-dependent impedance functions, $K_{VV}(\omega)$, $K_{MM}(\omega)$, and $K_{VM}(\omega)$ (since $K_{MV}(\omega) = K_{VM}(\omega)$ by reciprocity property) which appear in the equations of motion for tower-foundation-soil system [equation (7.21)] are obtained from the solution of two boundary value problems for a viscoelastic halfspace, arising from the application of a harmonic horizontal force and a harmonic moment, separately, to the rigid foundation. Procedures to evaluate these impedance functions have been presented in Chapter 4. The frequency response function for the modal coordinate $\overline{Y}_1(\omega)$ can be evaluated by numerically solving equation (7.21) repeatedly for various values of the excitation frequency ω over the range of interest.

The influence of coupling impedances $K_{VM}(\omega)$ and $K_{MV}(\omega)$, which are usually neglected in the analysis of multistory buildings [45,46] but should be included in the analysis of concrete gravity dams [20], is insignificant in the fundamental mode response of towers, as shown in Figure 7.21 for circular cylindrical towers. The additional radiation damping associated with the coupling impedances is small for intake-outlet towers and the resonant response is slightly overestimated by neglecting coupling impedances. Therefore, in the simplified analysis procedure presented next, the coupling impedances are neglected.

7.5.2 Approximate Fundamental Mode Response

The inertia terms m_t, I_t and L_0^r associated with the rigid body motion allowed by foundation-soil flexibility may be approximated by the contributions of the fundamental vibration mode: $m_t \approx m_1^*$, $L_0^r \approx m_1^* h_1^*$, and $I_t \approx m_1^*(h_1^*)^2$, where $m_1^* = (L_1)^2/M_1$ and $h_1^* = L_1^r/L_1$ are the effective mass and effective height, respectively, of the tower in its fundamental vibration mode. With this approximation, equation (7.21) also governs the response of a single degree of freedom (SDF) system with mass m_1^*, height h_1^*, fixed-base frequency ω_1, and constant hysteretic damping factor η_s, supported on the actual foundation-soil system. Therefore, following the procedure developed earlier for building-foundation systems [45,46], the contribution of the fundamental vibration mode of the tower to its earthquake response can be modeled by an equivalent SDF system on fixed base. The properties of the equivalent system are defined to recognize the reduction in stiffness and change in damping of the tower due to soil-structure interaction.

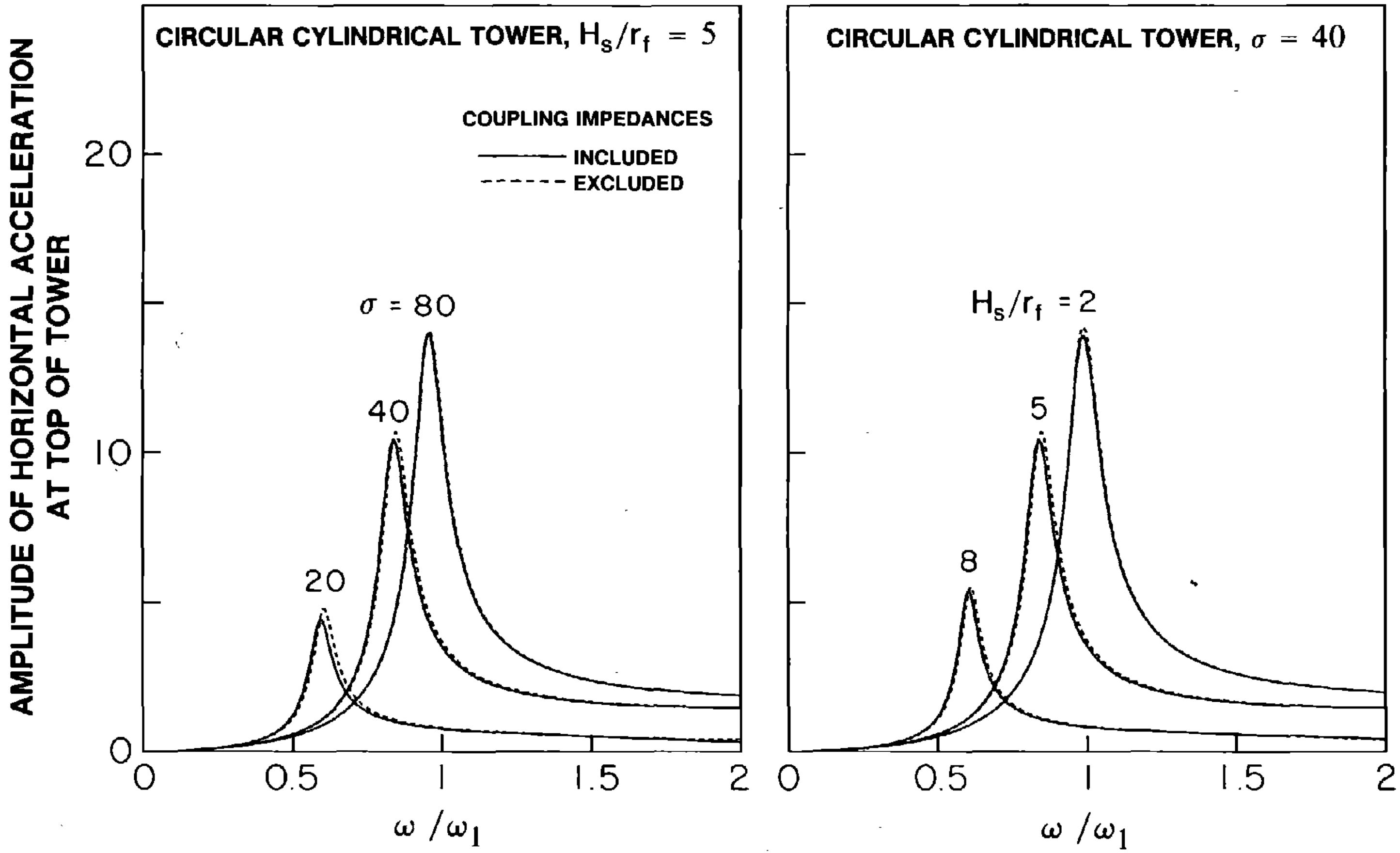

Figure 7.21 Effect of Coupling Impedance on Response of Circular Cylindrical Towers on Flexible Foundation Soil without Water due to Harmonic Horizontal Ground Motion

The natural frequency ω_1^f of the equivalent SDF system that models the fundamental mode response of the tower without water on flexible soil is given by (Appendix F) :

$$\omega_1^f = \frac{\omega_1}{\sqrt{1 + \mathrm{Re}[F(\omega_1^f)]}} \tag{7.26}$$

in which

$$F(\omega) = m_1^* \omega_1^2 \left[\frac{(h_1^*)^2}{K_{MM}(\omega)} + \frac{1}{K_{VV}(\omega)} \right] \tag{7.27}$$

and $\mathrm{Re}[F(\omega)]$ is the real part of the complex-valued function $F(\omega)$. In deriving equations (7.26) and (7.27), the effect of the second order damping term is ignored, and the foundation mass m_f and rotatory inertia I_f are neglected, simplifications which do not introduce significant errors [45]. Equation (7.26) must be solved iteratively to obtain the vibration frequency ω_1^f, which will always be less than ω_1 because $\mathrm{Re}[F(\omega)] > 0$ for all excitation frequencies. By substituting equation (7.27), it can be shown that equation (7.26) is the same as the corresponding expression in Reference [46] for building-foundation systems.

The frequency response function for the equivalent SDF system with natural frequency ω_1^f and constant hysteretic damping factor η_1^f can be shown to have the following form (Appendix F) :

$$\bar{\bar{Y}}_1(\omega) = \left[\frac{\omega_1^f}{\omega_1} \right]^2 \frac{-L_1}{-\omega^2 M_1 + (1 + i\,\eta_1^f)\,(\omega_1^f)^2\, M_1} \tag{7.28}$$

in which the constant hysteretic damping factor η_1^f is (Appendix F) :

$$\eta_1^f = \left[\frac{\omega_1^f}{\omega_1} \right]^2 \eta_s + \eta_a \tag{7.29}$$

where

$$\eta_a = -\left[\frac{\omega_1^f}{\omega_1}\right]^2 \mathrm{Im}[F(\omega_1^f)] \tag{7.30}$$

and $\mathrm{Im}[F(\omega)]$ is the imaginary part of the complex-valued function $F(\omega)$. In equation (7.29), the first term on the right represents the contribution of the structural damping to η_1^f, and the second term represents the added damping due to the contribution of foundation damping. The added damping factor η_a is always positive because $\mathrm{Im}[F(\omega)] < 0$ for all excitation frequencies. The equivalent viscous damping ratio ξ_1^f is, of course, related to the hysteretic damping factor η_1^f by $\xi_1^f = \eta_1^f/2$.

In earlier work on simplified analysis of buildings [45,46] and concrete gravity dams [20], energy dissipation in the structure on fixed-base was modeled by the viscous damping ratio ξ_1. With this damping model, the viscous damping ratio for the equivalent SDF system representing the structure-foundation-soil system was shown to be [20] :

$$\xi_1^f = \left[\frac{\omega_1^f}{\omega_1}\right]^3 \xi_1 + \xi_a \tag{7.31}$$

where the added damping ratio ξ_a due to soil-structure interaction is :

$$\xi_a = -\frac{1}{2}\left[\frac{\omega_1^f}{\omega_1}\right]^2 \mathrm{Im}[F(\omega_1^f)] \tag{7.32}$$

The contribution of foundation damping is unaffected by the damping model for the structure, and consequently equations (7.30) and (7.32) are equivalent. However, the structural damping is reduced proportional to $(\omega_1^f/\omega_1)^2$ -- the same factor as in equation (7.30) or (7.32) -- in case of the frequency-independent hysteretic damping model for the structure but the reduction is proportional to $(\omega_1^f/\omega_1)^3$ if frequency-dependent viscous damping is used to model energy dissipation in the structure. The frequency dependence of viscous damping results in the additional factor (ω_1^f/ω_1) because of the frequency shift due to soil-structure interaction.

7.5.3 Response Results

Figure 7.22 shows the amplitude of the horizontal acceleration at the top of circular cylindrical towers (Figure 7.2a), relative to the tower base, due to horizontal harmonic free-field ground acceleration, computed from equation (7.21) for several values of the wave parameter σ and tower-height-to-footing-radius ratio H_s/r_f with hysteretic damping factors $\eta_s = 0.10$ for the tower and $\eta_f = 0.10$ for the foundation soil. Similar results for circular tapered towers (Figure 7.2b) are also presented in Figure 7.23. As the wave parameter σ decreases or the ratio H_s/r_f increases, the fundamental resonant frequency of the tower decreases and the amplitude of the fundamental resonant peak also decreases. These effects of foundation-soil flexibility and damping, both material and radiation, have been discussed extensively for buildings [46], for concrete gravity dams [18,20], and for intake-outlet towers (Chapters 5 and 6). The frequency response function for the equivalent SDF system, computed from equation (7.28), with the natural frequency ω_1^f and damping ratio η_1^f given by equations (7.26) and (7.29), respectively, is also presented in Figures 7.22 and 7.23. These results demonstrate that, over a wide range of excitation frequencies and tower-foundation-soil system parameters σ, H_s/r_f and γ, the equivalent SDF system accurately represents the fundamental mode response of towers supported on flexible soil.

The lengthening of the fundamental resonant period of the tower due to tower-foundation-soil interaction, determined from the resonant peak of $\bar{Y}_1(\omega)$, obtained by solving equation (7.21), is shown in Figure 7.24 for a range of σ and H_s/r_f values. The vibration period T_1^f of the equivalent SDF system, where $T_1^f = 2\pi/\omega_1^f$ is computed from equation (7.26), is close to the fundamental resonant period of the tower-foundation-soil system for large values of σ and low values of H_s/r_f, but its accuracy decreases as σ decreases or H_s/r_f

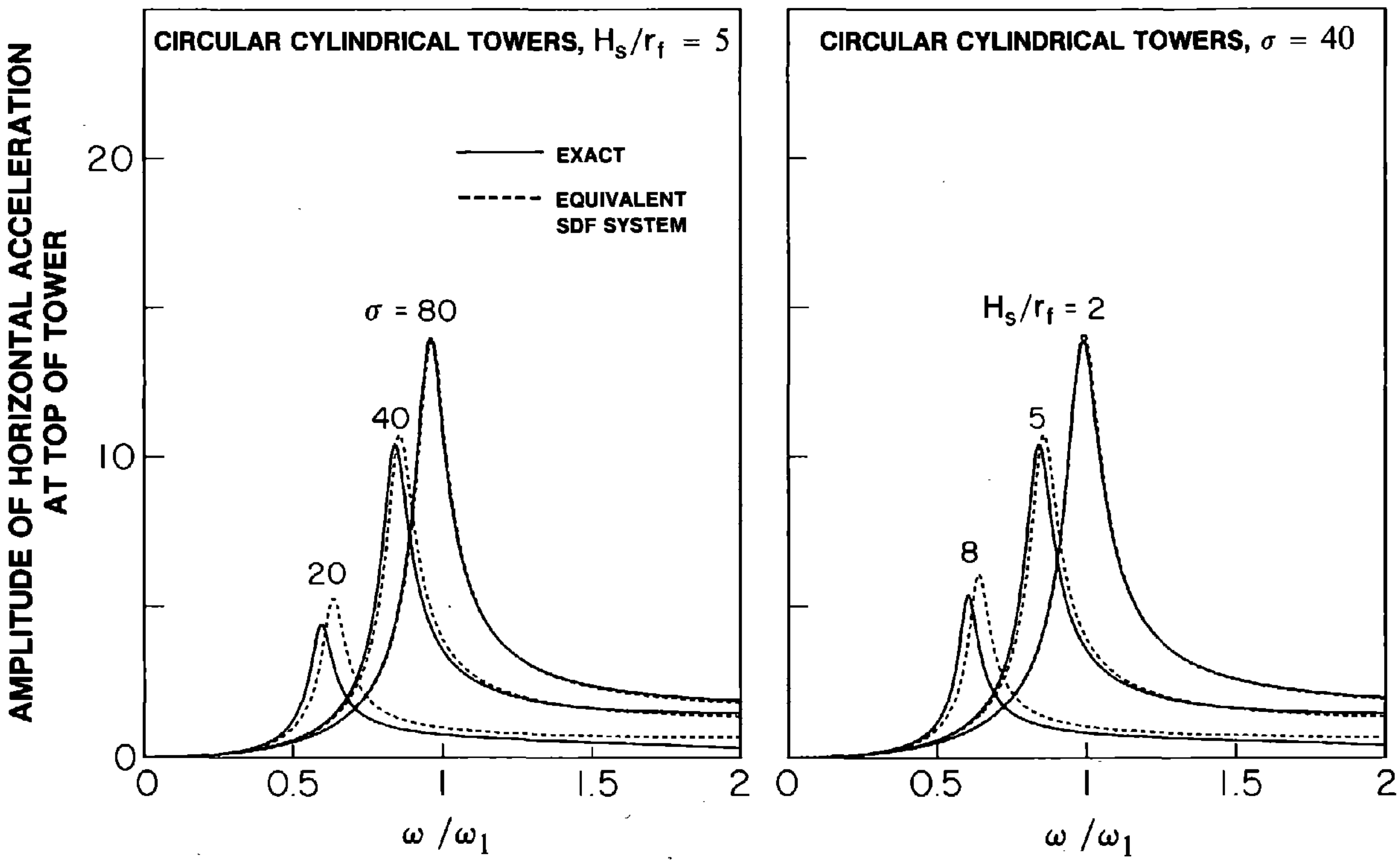

Figure 7.22 Comparison of Exact and Equivalent SDF System Response of Circular Cylindrical Towers on Flexible Foundation Soil without Water due to Harmonic Horizontal Ground Motion

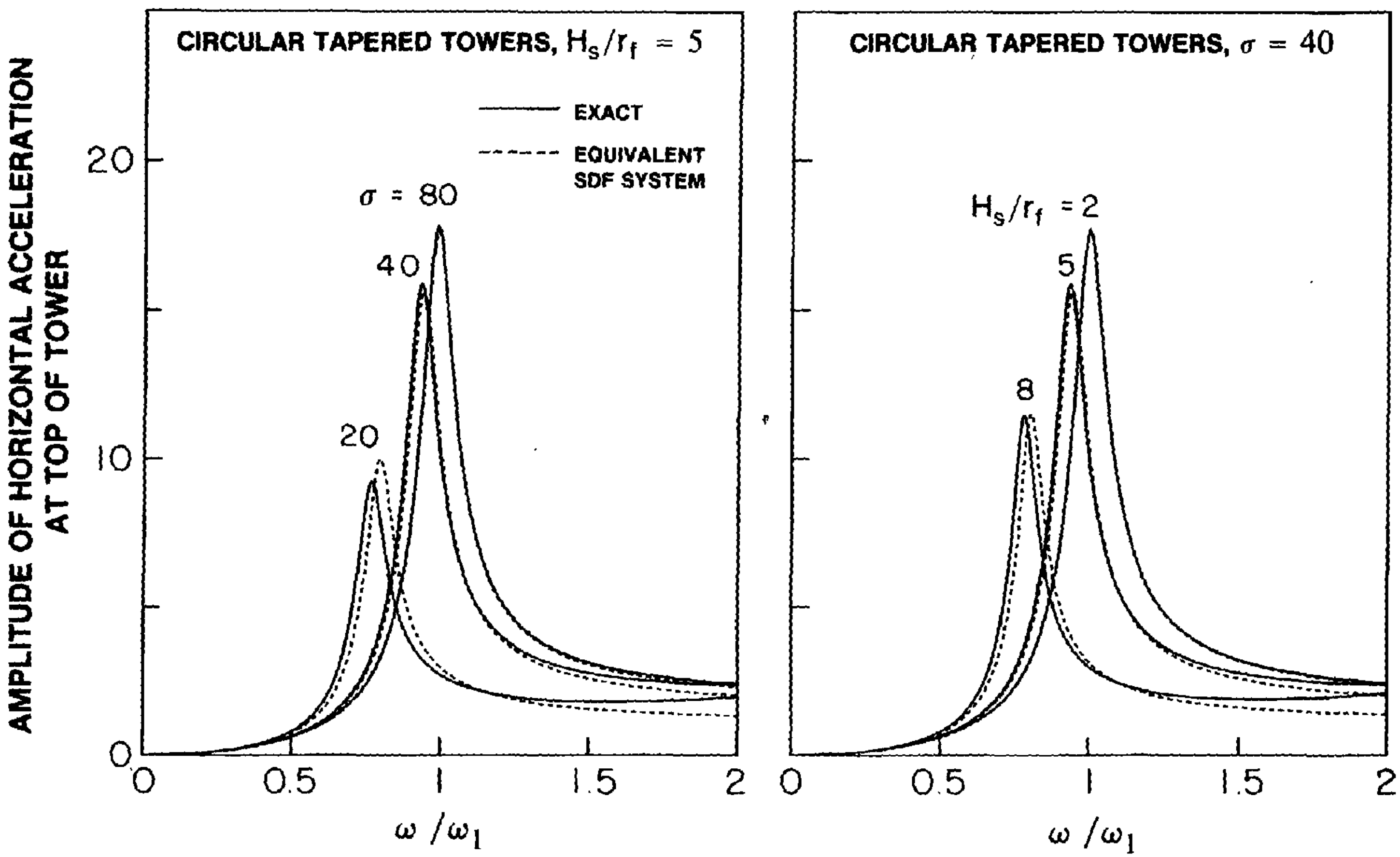

Figure 7.23 Comparison of Exact and Equivalent SDF System Response of Circular Tapered Towers on Flexible Foundation Soil without Water due to Harmonic Horizontal Ground Motion

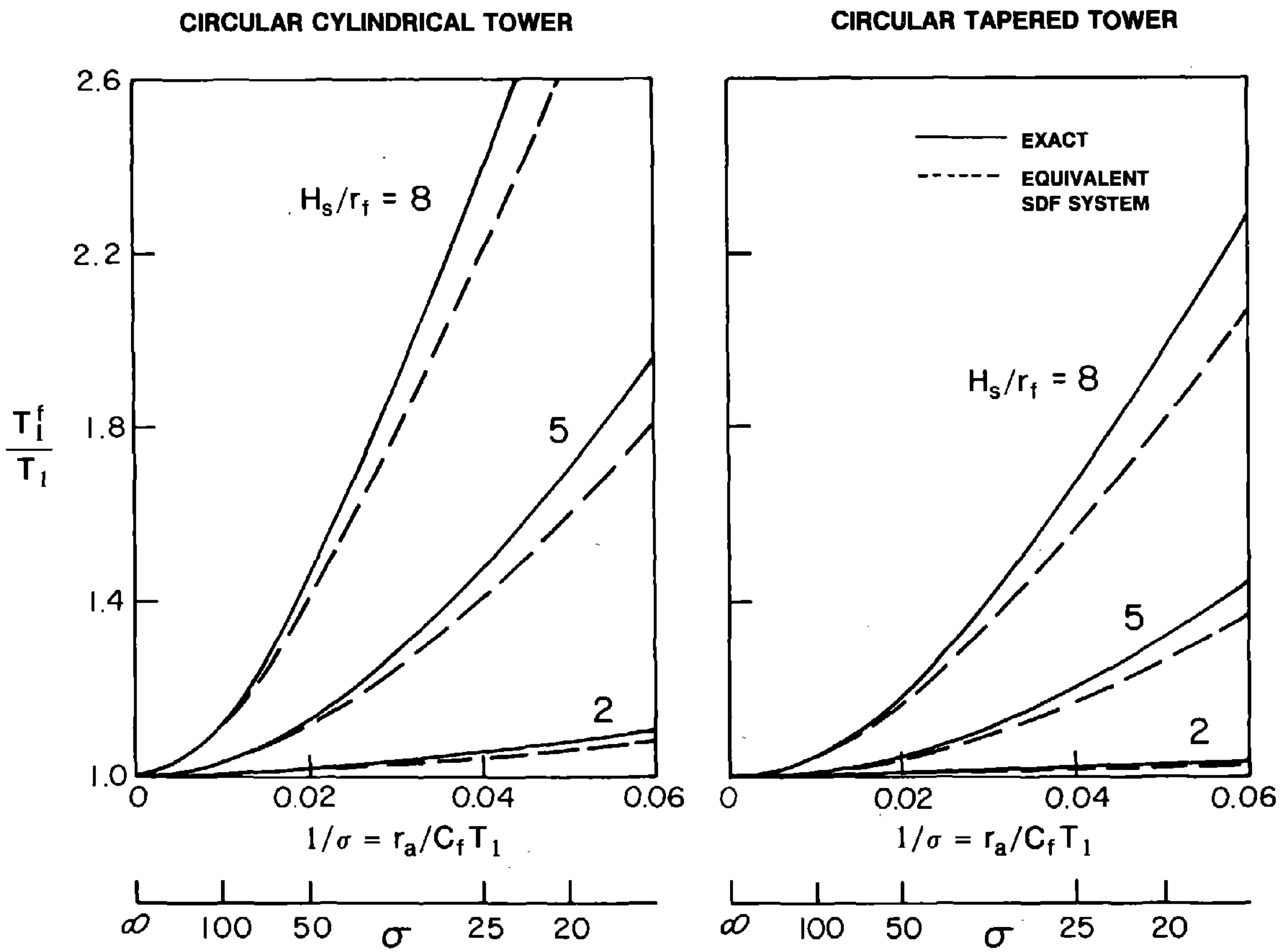

Figure 7.24 Comparison of Exact and Approximate (Equivalent SDF System) Values of the Ratio of Fundamental Vibration Periods of Towers without Water on a Flexible and Rigid Foundation Soil for a Range of Values for σ and H_s/r_f

increases, i.e., as tower-foundation-soil interaction effects become more significant.

The added damping factor η_a due to tower-foundation-soil interaction is presented in Figures 7.25 and 7.26, and the overall damping factor η_1^f of the equivalent SDF system is shown in Figures 7.27 and 7.28 for circular cylindrical and tapered towers with $\eta_s = 0.10$ for a range of values of η_f, σ, and H_s/r_f. Considering that ω_1^f is less than ω_1, equation (7.30) indicates that tower-foundation-soil interaction reduces the effectiveness of structural damping and therefore, the damping ratio in the fundamental vibration mode of the interacting system will be less than the damping ratio of the fixed-base tower unless this reduction is compensated by the increase due to added foundation damping. This is apparent from Figure 7.28 for towers supported on purely elastic soil. In most cases, however, this reduction is more than compensated by the added damping η_a resulting in an increase in the overall damping.

7.6 Towers on Flexible Soil with Water

7.6.1 Exact Fundamental Mode Response

When modified to include the effects of tower-water interaction, the frequency domain equations for the fundamental mode response of towers on flexible foundation soil, equation (7.21), become [equation (3.46) specialized for $N = 1$] :

$$\begin{bmatrix} [-\omega^2\tilde{M}_1+(1+i\eta_s)\omega_1^2M_1] & -\omega^2\tilde{L}_1^h & -\omega^2\tilde{L}_1^r \\ -\omega^2\tilde{L}_1^h & -\omega^2(\tilde{m}_t+m_f)+K_{VV}(\omega) & -\omega^2\tilde{L}_0^r+K_{VM}(\omega) \\ -\omega^2\tilde{L}_1^r & -\omega^2\tilde{L}_0^r+K_{MV}(\omega) & -\omega^2(\tilde{I}_t+I_f)+K_{MM}(\omega) \end{bmatrix} \begin{Bmatrix} \bar{Y}_1(\omega) \\ \bar{u}_f(\omega) \\ \bar{\theta}_f(\omega) \end{Bmatrix}$$

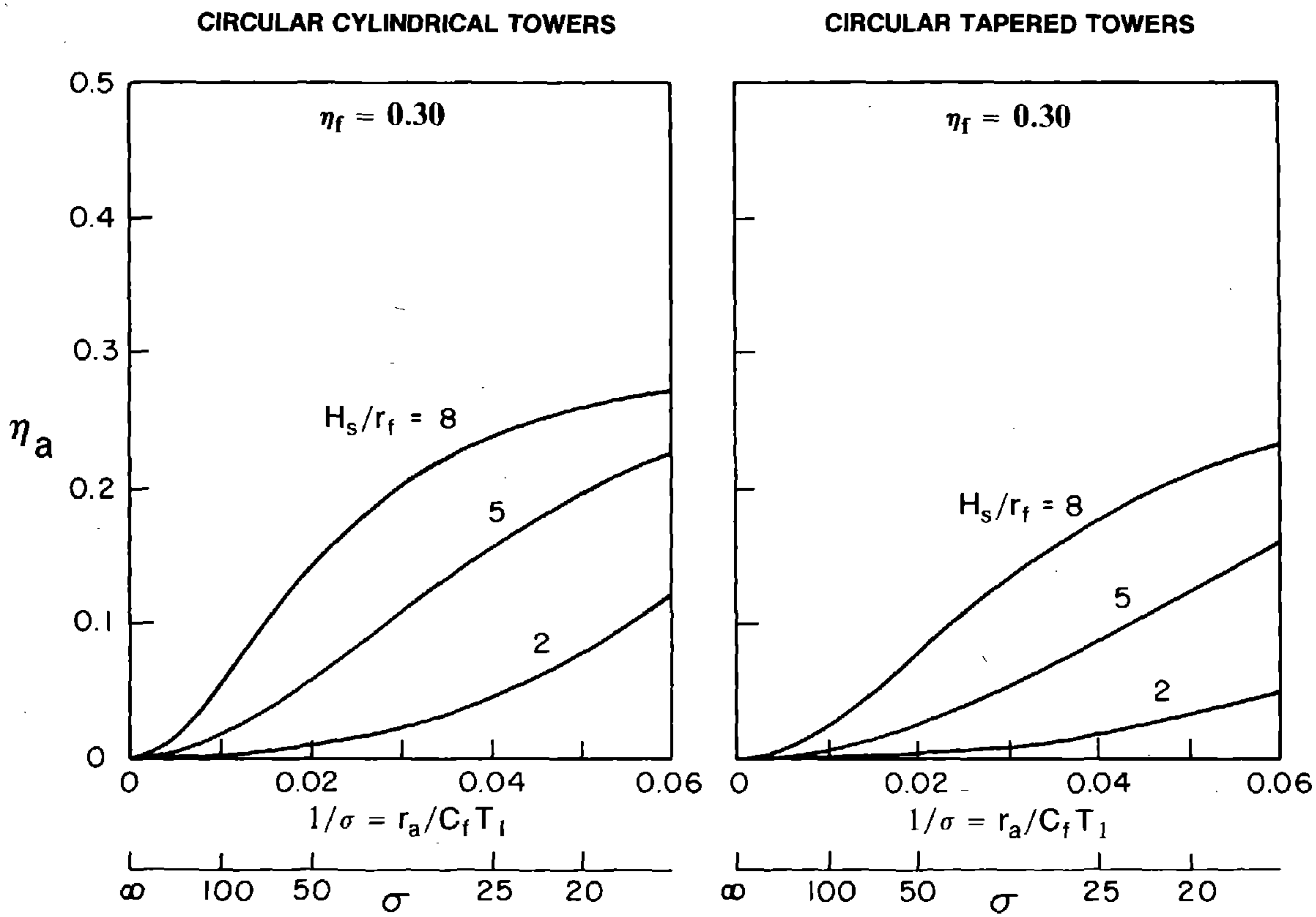

Figure 7.25 Added Constant Hysteretic Damping Factor η_a due to Tower-Foundation-Soil Interaction for a Range of σ Values and Various Values of H_s/r_f; Results Presented for $\eta_f = 0.30$

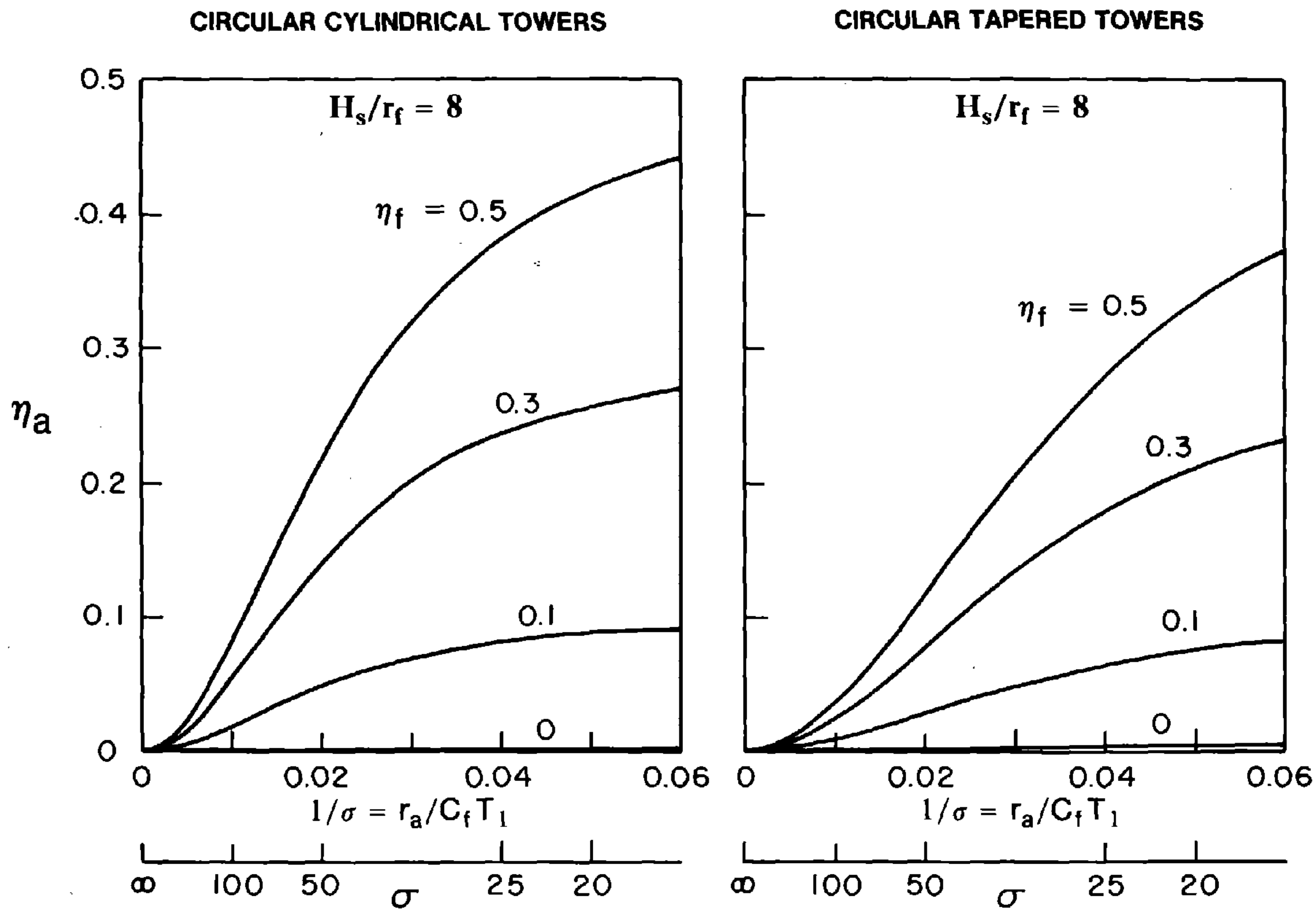

Figure 7.26 Added Constant Hysteretic Damping Factor due to Tower-Foundation-Soil Interaction for a Range of σ Values and Various Values of η_f; Results Presented for $H_s/r_f = 8$

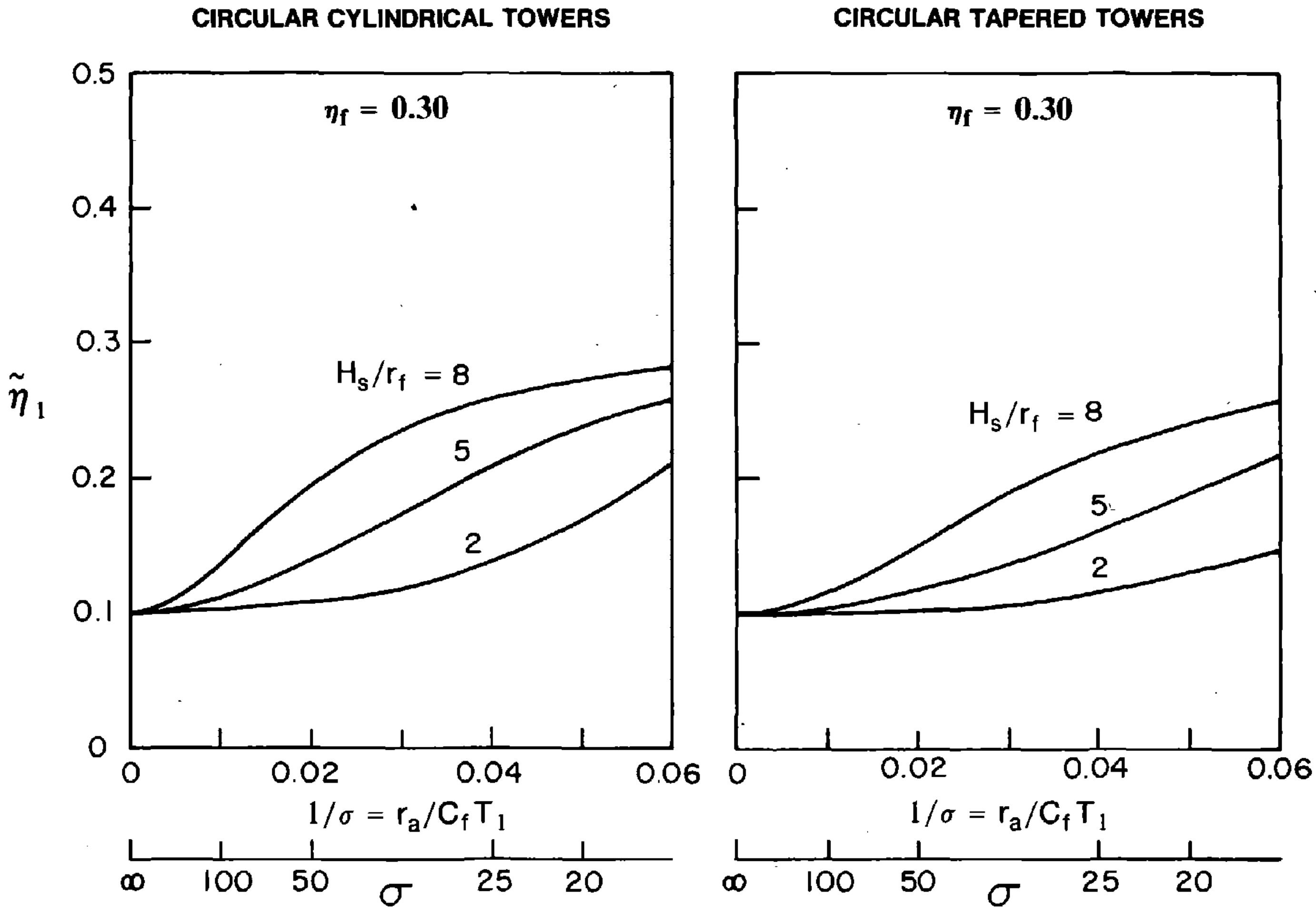

Figure 7.27 Constant Hysteretic Damping Factor $\tilde{\eta}_1$ of the Equivalent SDF System Representing Towers on Flexible Foundation Soil without Water for a Range of σ Values and Various Values of H_s/r_f ; Results Presented for $\eta_f = 0.30$ and $\eta_s = 0.10$

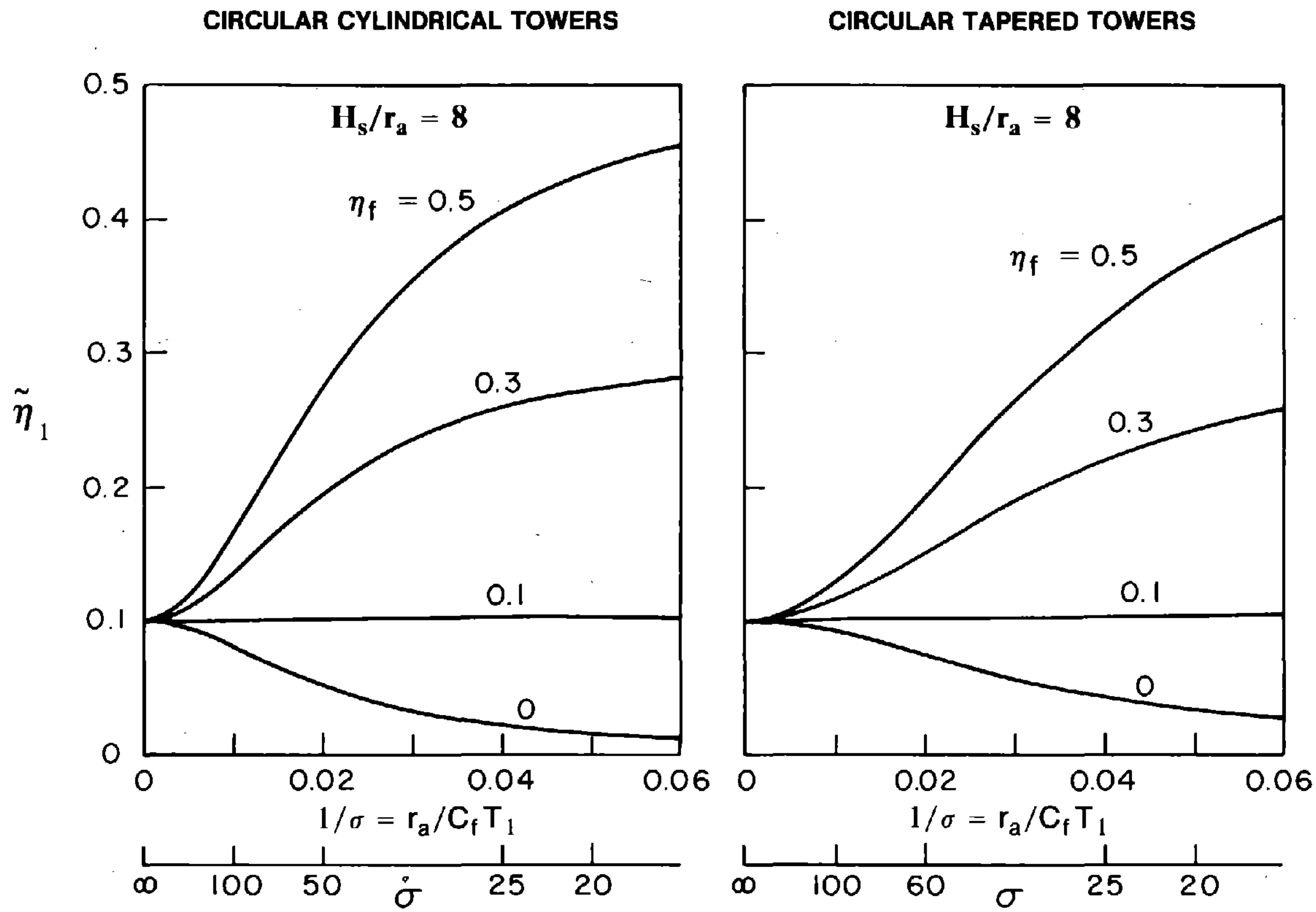

Figure 7.28 Constant Hysteretic Damping Factor $\tilde{\eta}_1$ of the Equivalent SDF System Representing Towers on Flexible Foundation Soil without Water for a Range of σ Values and Various Values of η_f ; Results Presented for $H_s/r_a = 8$ and $\eta_s = 0.10$

$$= - \begin{Bmatrix} \tilde{L}_1 \\ \tilde{m}_t + m_f \\ \tilde{L}_0^r \end{Bmatrix} \tag{7.33}$$

in which

$$\tilde{M}_1 = M_1 + M_{11}^o + M_{11}^i \tag{7.34a}$$

$$\tilde{L}_1 = L_1 + L_1^o + L_1^i \tag{7.34b}$$

$$\tilde{L}_1^h = L_1^h + L_1^{ho} + L_1^{hi} \tag{7.34c}$$

$$\tilde{L}_1^r = L_1^r + L_1^{ro} + L_1^{ri} \tag{7.34d}$$

$$\tilde{m}_t = m_t + m_t^o + m_t^i \tag{7.34e}$$

$$\tilde{I}_t = I_t + I_t^o + I_t^i \tag{7.34f}$$

$$\tilde{L}_0^r = L_0^r + L_0^{ro} + L_0^{ri} \tag{7.34g}$$

where $L_1^h = L_1$; $\tilde{L}_1^h = \tilde{L}_1$; the hydrodynamic terms M_{11}^o and L_1^o due to surrounding water and M_{11}^i, L_1^i due to inside water, all of them associated with the vibration of tower in the fundamental mode, have been defined in equations (7.9) to (7.12). In these equations, the lateral and rotational motions of the foundation result in additional generalized mass terms m_t^o, I_t^o and L_0^{ro} associated with the inertial influence of the surrounding water ; and m_t^i, I_t^i and L_0^{ri} associated with the inertial influence of the inside water :

$$m_t^\alpha = \int_0^{H_a} f_0^\alpha(z)\, dz \quad ; \quad \alpha = o\,,\, i \tag{7.35}$$

$$I_t^\alpha = \int_0^{H_\alpha} z^2 f_r^\alpha(z)\, dz + \int_0^{H_\alpha} m_r^\alpha(z)\, dz \quad ; \quad \alpha = o\,,\, i \tag{7.36}$$

$$L_0^{r\alpha} = \int_0^{H_\alpha} z\, f_r^\alpha(z)\, dz \quad ; \quad \alpha = o\,,\, i \tag{7.37}$$

in which subscript or superscript $\alpha = o$ and i identify the terms for the outside and the inside water, respectively ; and the functions $f_r^\alpha(z)$, $m_r^\alpha(z)$ represent the hydrodynamic lateral forces and moments, respectively, on the outside or inside surface of the rigid tower when the excitation is the unit rotational acceleration of the base. The additional hydrodynamic terms associated with the coupling between the rigid-body motion of the tower permitted by supporting-soil flexibility and the vibration of the tower in its fundamental vibration mode are given by :

$$L_1^{h\alpha} = L_1^\alpha \quad ; \quad \alpha = o\,,\, i \tag{7.38}$$

$$L_1^{r\alpha} = \int_0^{H_\alpha} \phi_1(z)\, f_r^\alpha(z)\, dz + \int_0^{H_\alpha} \psi_1(z)\, m_r^\alpha(z)\, dz \quad ; \quad \alpha = o\,,\, i \tag{7.39}$$

The frequency response function for the modal coordinate $\bar{Y}_1(\omega)$ can be evaluated by numerically solving equation (7.33) repeatedly for varying values of the excitation frequency ω over the range of interest.

7.6.2 Approximate Fundamental Mode Response

It has been demonstrated in Section 7.4 that the influence of tower-water interaction on the response may be approximately represented by the added hydrodynamic mass $m_a^o(z)$ due to outside water [equation (7.16)] and $m_a^i(z)$ due to inside water [equation (7.17)]. Based on this added mass representation, the hydrodynamic forces $f_r^o(z)$ for the surrounding water and $f_r^i(z)$ for the inside water may be approximated by :

$$f_r^o(z) \approx z \; m_a^o(z) \tag{7.40}$$

$$f_r^i(z) \approx z \; m_a^i(z) \tag{7.41}$$

That this is a reasonable approximation is indirectly supported by the results of Figures 7.4 to 7.15 where the added mass approximation was shown to be accurate for the first two modes of vibration of the tower on fixed-base. Similar numerical results have demonstrated that the same added mass representation is satisfactory in rigid body motions of the tower due to foundation rotation.

If the contribution of hydrodynamic moments to the hydrodynamic terms is neglected, which was already shown to be small in Section 7.4.1, and the hydrodynamic effects are represented by the added mass $m_a^o(z)$ and $m_a^i(z)$ of equations (7.16) and (7.17), it can be shown that the equation (7.33) for the tower-water-foundation-soil system is identical to the equation (7.21) for a tower on flexible soil in air but with virtual mass distribution $\tilde{m}_s(z)$ given by equation (7.15). Implicit in the above statement is the fact that $\omega_1^2 M_1 = (\omega_1^r)^2 \tilde{M}_1$, where ω_1^r is the fundamental vibration frequency of the tower-water system on rigid foundation soil.

The amplitude of the steady state acceleration response at the top of the tower to harmonic ground motion is presented in Figure 7.29 for a circular cylindrical tower and for a circular tapered tower, described in Section 7.2, both on flexible foundation soil. These results were computed by two different methods : (1) the exact analysis described in Chapter 3 and (2) analysis of the tower in air with virtual mass $\tilde{m}_s(z)$. It is apparent from these results that, even on flexible foundation soil, the added hydrodynamic mass provides a satisfactory representation of the hydrodynamic effects in the lower vibration mode response of towers. Therefore, the equivalent SDF system defined in Section 7.5 to model the fundamental mode response of towers on flexible foundation soil without water can be extended to include the hydrodynamic effects. To this end, the fundamental mode properties of the

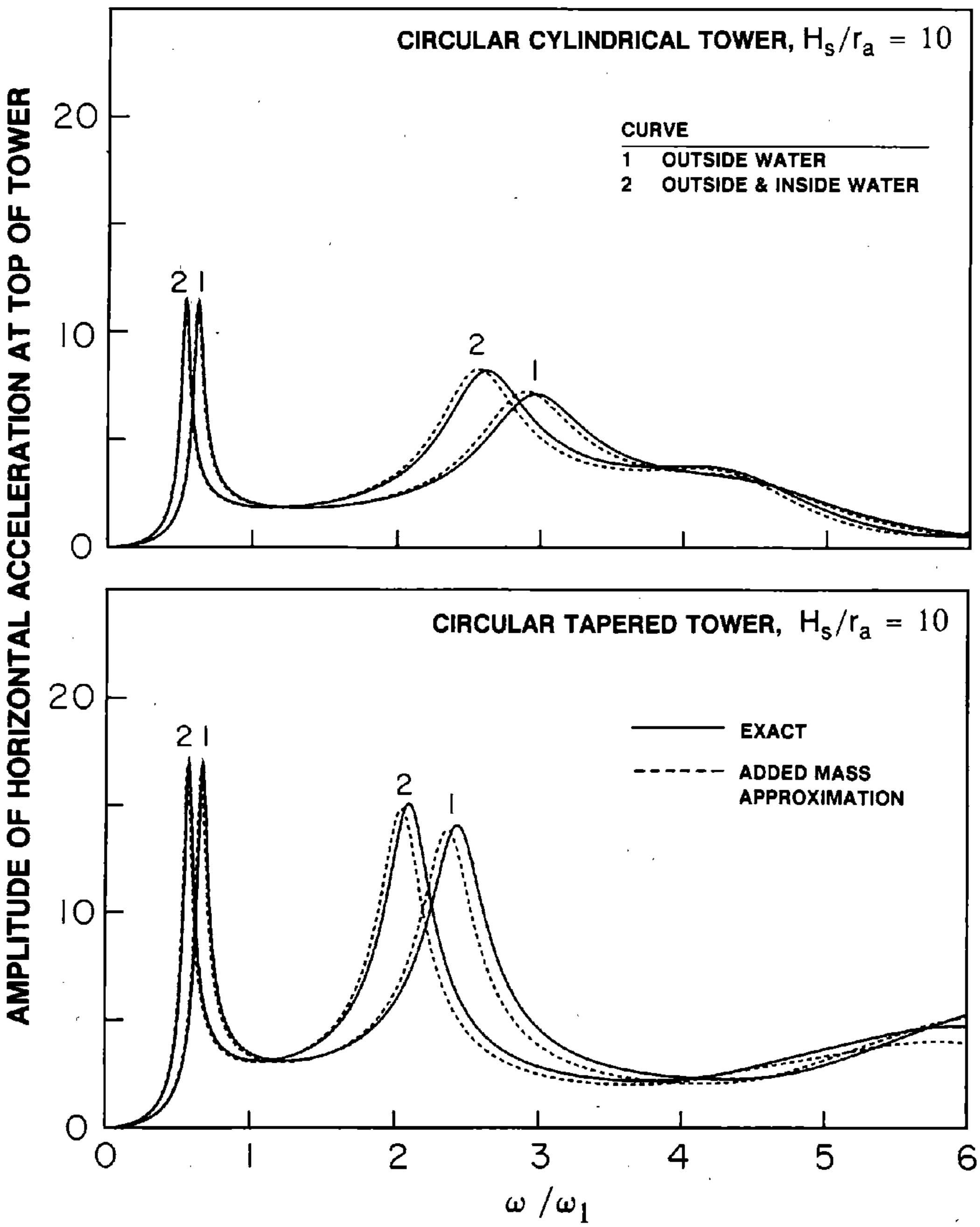

Figure 7.29 Comparison of Exact and Approximate (Added Mass Representation of Hydrodynamic Effects) Response of Towers on Flexible Foundation Soil with Water due to Harmonic Horizontal Ground Motion

tower without water, namely the fundamental vibration frequency ω_1, generalized mass M_1, generalized excitation L_1, effective mass m_1^* and effective height h_1^* are replaced by the corresponding properties of the tower with water, i.e. ω_1^r, $\tilde{M}_1$, $\tilde{L}_1$, $\tilde{m}_1^* = (\tilde{L}_1)^2/\tilde{M}_1$, and $\tilde{h}_1^* = \tilde{L}_1^r/\tilde{L}_1$. The latter set of properties can be determined by vibration analysis of the tower in air but its mass taken as the virtual mass $\tilde{m}_s(z)$ of equation (7.15).

Thus the natural frequency $\tilde{\omega}_1$ of the equivalent SDF system that models the fundamental mode response of the tower with water on flexible soil is given by an extension of equations (7.26) and (7.27) :

$$\tilde{\omega}_1 = \frac{\omega_1^r}{\sqrt{1 + \mathrm{Re}[\tilde{F}(\tilde{\omega}_1)]}} \tag{7.42}$$

where

$$\tilde{F}(\omega) = \tilde{m}_1^* \, (\omega_1^r)^2 \left[\frac{(\tilde{h}_1^*)^2}{K_{MM}(\omega)} + \frac{1}{K_{VV}(\omega)} \right] \tag{7.43}$$

Similarly, the constant hysteretic damping factor $\tilde{\eta}_1$ of the equivalent SDF system that models the fundamental mode response of the tower with water on flexible foundation soil is given by an extension of equations (7.29) and (7.30) :

$$\tilde{\eta}_1 = \left[\frac{\tilde{\omega}_1}{\omega_1^r} \right]^2 \eta_s + \eta_a \tag{7.44}$$

where

$$\eta_a = - \left[\frac{\tilde{\omega}_1}{\omega_1^r} \right]^2 \mathrm{Im}[\tilde{F}(\tilde{\omega}_1)] \tag{7.45}$$

The frequency response function for the equivalent SDF system with natural frequency $\tilde{\omega}_1$ and constant hysteretic damping factor $\tilde{\eta}_1$ is similar to equation (7.28) if the actual mass of the tower is replaced by the virtual mass [equation (7.15)] :

$$\bar{\tilde{Y}}_1(\omega) = \left[\frac{\tilde{\omega}_1}{\omega_1^r} \right]^2 \frac{-\tilde{L}_1}{-\omega^2 \tilde{M}_1 + (1 + i\,\tilde{\eta}_1)\,\tilde{\omega}_1^2\,\tilde{M}_1} \tag{7.46}$$

7.6.3 Response Results

The final results of the series of approximations used to simplify the analysis of the fundamental mode response of the tower-water-foundation-soil systems are shown in Figure 7.30 for circular cylindrical towers and in Figure 7.31 for circular tapered towers. The "exact" fundamental mode response of the tower on flexible foundation soil with full water was computed by solving equation (7.33). The response of the equivalent SDF system was computed using equation (7.46) with natural frequency $\tilde{\omega}_1$ and constant damping factor $\tilde{\eta}_1$ evaluated from equations (7.42) and (7.44) for the tower with virtual mass $\tilde{m}_s(z)$. These response results demonstrate that the equivalent SDF system provides a good approximation of the fundamental mode response of the towers with water for a wide range of values for σ and H_s/r_f. In fact, the quality of approximation is better when the effects of tower-water interaction and of tower-foundation-soil interaction are simultaneously included compared to when these effects are considered individually because the added hydrodynamic mass overestimates the decrease in the resonant frequency due to hydrodynamic effects, whereas the equivalent SDF system underestimates the decrease in resonant frequency due to soil-structure interaction , and thus the errors in the two approximations are partially canceled.

7.7 Equivalent Lateral Forces

It has been shown in this chapter that the hydrodynamic effects in the dynamic response of towers may be represented by the added mass functions $m_a^o(z)$ and $m_a^i(z)$ defined

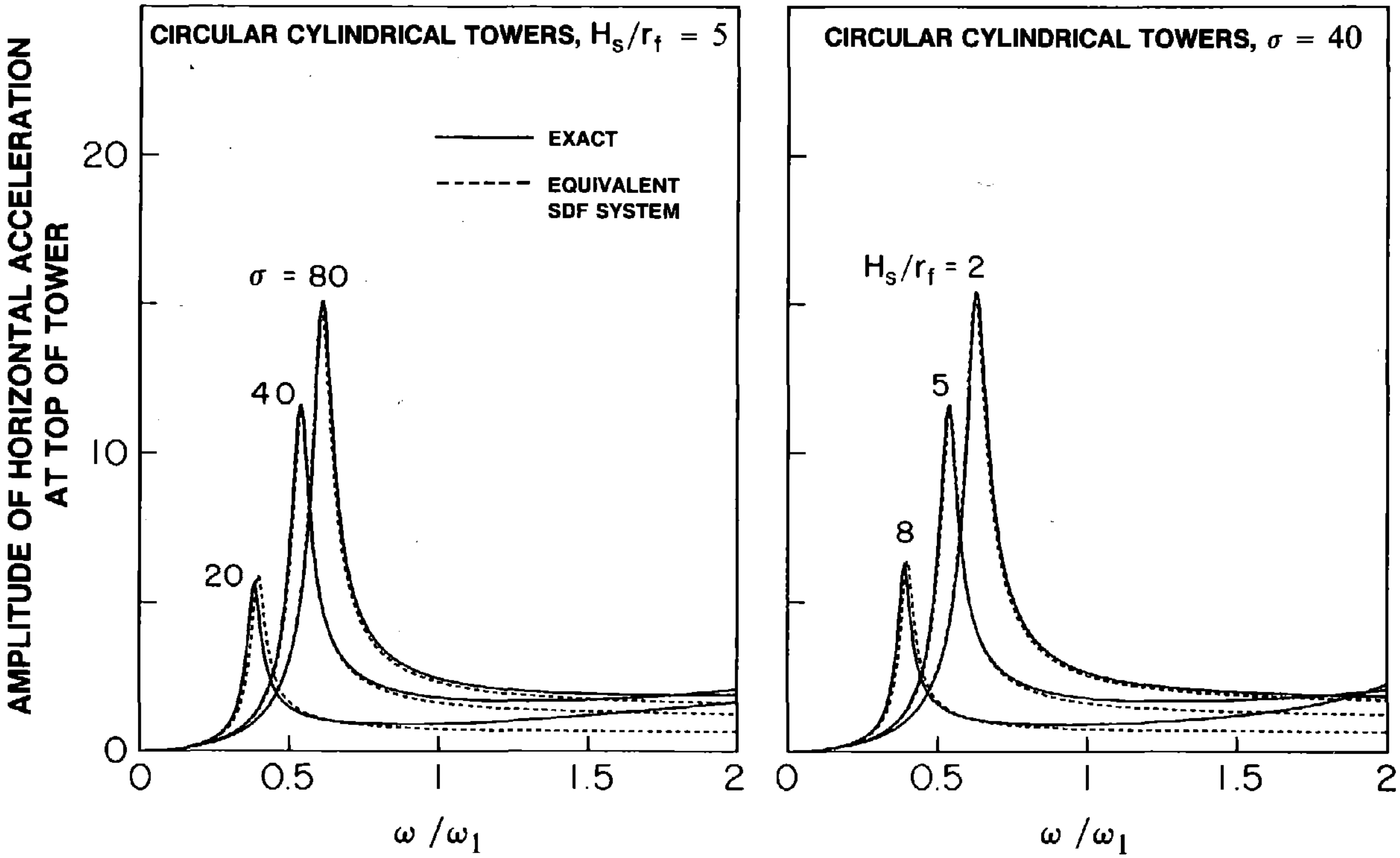

Figure 7.30 Comparison of Exact and Equivalent SDF System Response of Circular Cylindrical Towers on Flexible Foundation Soil with Water due to Harmonic Horizontal Ground Motion

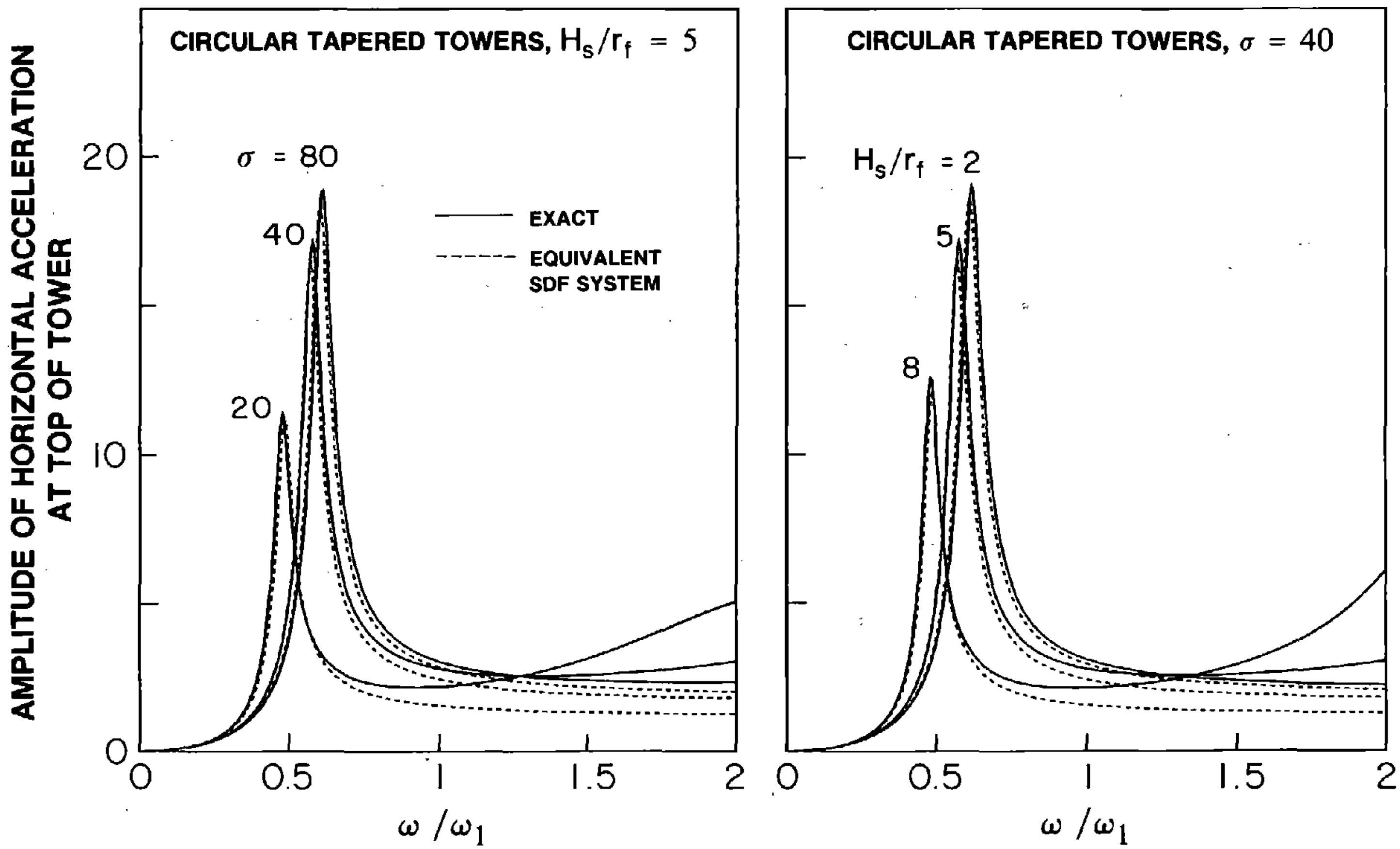

Figure 7.31 Comparison of Exact and Equivalent SDF System Response of Circular Tapered Towers on Flexible Foundation Soil with Water due to Harmonic Horizontal Ground Motion

by equations (7.16) and (7.17), respectively. Thus, the hydrodynamic effects can most simply be considered by replacing the actual mass $m_s(z)$ of the tower by the virtual mass

$$\tilde{m}_s(z) = m_s(z) + m_a^o(z) + m_a^i(z) \tag{7.47}$$

and analyzing the tower. Because such an approximation satisfactorily predicts the response of towers to harmonic ground motion over a complete range of excitation frequencies, it can be used in the analysis of tower response to arbitrary ground motion. In particular, the equivalent lateral forces associated with the maximum response in the n-th mode of vibration of the tower are [9]:

$$f_n(z) = \frac{\tilde{L}_n}{\tilde{M}_n} S_a(\, T_n^r, \xi_n^r \,)\, \tilde{m}_s(z)\, \tilde{\phi}_n(z) \tag{7.48}$$

in which T_n^r and $\tilde{\phi}_n(z)$ are the n-th natural vibration period and mode shape of the tower with virtual mass $\tilde{m}_s(z)$, $S_a(T_n^r, \xi_n^r)$ is the ordinate of the pseudo acceleration response spectrum for the ground motion at vibration period T_n^r and damping ratio $\xi_n^r = \xi_n = \eta_s/2$; note that the hydrodynamic effects do not change the damping ratio. The generalized mass $\tilde{M}_n$ and generalized excitation term $\tilde{L}_n$ is given by equations (7.4) and (7.5) with $m_s(z)$ replaced by $\tilde{m}_s(z)$ and neglecting the effects of rotatory inertia:

$$\tilde{M}_n = \int_0^{H_s} \tilde{m}_s(z)\, [\, \tilde{\phi}_n(z)\,]^2\, dz \tag{7.49}$$

$$\tilde{L}_n = \int_0^{H_s} \tilde{m}_s(z)\, \tilde{\phi}_n(z)\, dz \tag{7.50}$$

Recognizing that the first two vibration modes are usually sufficient for the approximate evaluation of the earthquake design forces [11], it will be necessary to evaluate equation (7.50) for n = 1 and 2. This will require evaluation of (i) the first two vibration frequencies and mode shapes by solving the associated eigenvalue problem for the tower with virtual mass $\tilde{m}_s(z)$; and (ii) the added mass functions $m_a^o(z)$ and $m_a^i(z)$ by solving three-dimensional boundary value problems for the outside and inside water domains respectively. Simplified methods for computing these quantities in practical application are developed in Chapters 8 and 9.

It has also been shown that the fundamental mode response of towers including tower-foundation-soil interaction effects is accurately predicted by an equivalent SDF system with the following properties: natural frequency $\tilde{\omega}_1$ given by equation (7.42) and constant hysteretic damping factor $\tilde{\eta}_1$ given by equation (7.44). Because the equivalent SDF system representation is accurate over a complete range of frequencies, it can be used in the analysis of tower response to arbitrary ground motion. Following the concepts developed earlier for buildings [45] and dams [20], it can be shown that the equivalent lateral forces associated with the maximum response in the fundamental mode of vibration are:

$$f_1(z) = \frac{\tilde{L}_1}{\tilde{M}_1} S_a(\tilde{T}_1, \tilde{\xi}_1)\, \tilde{m}_s(z)\, \tilde{\phi}_1(z) \tag{7.51}$$

where $S_a(\tilde{T}_1, \tilde{\xi}_1)$ is the ordinate of the pseudo acceleration response spectrum for the ground motion at vibration period $\tilde{T}_1 = 2\pi/\tilde{\omega}_1$ and damping ratio $\tilde{\xi}_1 = \tilde{\eta}_1/2$. As mentioned earlier, the equivalent lateral forces associated with the response in the second vibration mode may be computed from equation (7.48) because tower-foundation-soil interaction effects are negligible in higher mode response. Thereafter, the shear and bending moment at any section of the tower are computed by static analysis of the tower subjected to forces $f_n(z)$, n = 1 and 2, and appropriately combining the modal maxima.

Required in the evaluation of equation (7.51) is an iterative solution of the frequency equation (7.42) to determine $\tilde{\omega}_1$ and subsequently $\tilde{\eta}_1$ from equation (7.44). In these equations, the impedance functions $K_{VV}(\omega)$ and $K_{MM}(\omega)$ for the foundation-soil system are also required. Simplified methods for computing these quantities in practical application are developed in Chapter 9.

8. SIMPLIFIED EVALUATION OF ADDED HYDRODYNAMIC MASS

8.1 Introduction

It has been demonstrated in Chapter 7 that the hydrodynamic interaction effects can most simply be included in earthquake response spectrum analysis of an intake-outlet tower, having an arbitrary cross-section with two axes of symmetry, by replacing the mass of the tower $m_s(z)$ by the virtual mass $\tilde{m}_s(z)$ defined as:

$$\tilde{m}_s(z) = m_s(z) + m_a^o(z) + m_a^i(z) \tag{8.1}$$

where the added hydrodynamic masses $m_a^o(z)$ and $m_a^i(z)$ represent the effects of the surrounding (outside) and inside water, respectively, on the dynamic response of the tower. Added mass functions $m_a^o(z)$ and $m_a^i(z)$ have been defined in Chapter 7 to account for hydrodynamic effects in the dynamic response of the tower constrained to be vibrating in the n-th vibration mode shape $\phi_n(z)$ of the tower without water. The hydrodynamic effects in the n-th mode of vibration of the tower are represented exactly by these added mass functions if the tower is uniform and quite accurately (but not exactly) if the cross-sectional dimensions of the tower vary along its height (Chapter 7). Because the added mass functions obviously depend on the shape $\phi_n(z)$ of the vibration mode considered, no one function, $m_a^o(z)$ for the surrounding water or $m_a^i(z)$ for the inside water, will be exactly valid for all vibration modes of the tower.

On the other hand, for many years the concept of an added hydrodynamic mass to represent the inertial influence of water interacting with a structure has been based on the assumption of a rigid structure. This concept has been applied in different situations including problems in classical hydrodynamics [31], dams impounding water [49], cylindrical tanks containing water [29], and on cylindrical towers surrounded by water [33]. Although not exact, this added mass has been shown to account for the hydrodynamic effects to a useful degree of accuracy for preliminary analysis of towers (Chapter 7).

Based on this concept, the added hydrodynamic mass functions $m_a^o(z)$ and $m_a^i(z)$ are the lateral hydrodynamic forces along the plane of vibration acting on the outside and inside surfaces, respectively, of a rigid tower due to unit horizontal ground acceleration. Analytical expressions for these added hydrodynamic mass functions are available only for circular cylindrical towers [32,40] and for uniform elliptical towers [30]. For a uniform tower of arbitrary cross-section or for towers with cross-sectional dimensions varying along the height, computation of the added hydrodynamic mass functions requires a finite element solution of boundary value problems for the outside and inside fluid domains (Chapters 3 and 4). Such analyses may be too complicated in the preliminary stage of design or safety evaluation of towers.

The objective of this chapter is to develop a simplified procedure for evaluating the added hydrodynamic mass which is accurate enough for preliminary earthquake analysis of towers.

8.2 Added Hydrodynamic Mass for Surrounding Water

8.2.1 Uniform Towers

The added mass for circular cylindrical towers associated with hydrodynamic effects of surrounding water, obtained from an analytical solution of the Laplace equation [29,32,40], is :

$$m_a^o(z) = (\rho_w \pi r_o^2) \cdot \left[\frac{16}{\pi^2} \frac{H_o}{r_o} \sum_{m=1}^{\infty} \frac{(-1)^{m-1}}{(2m-1)^2} E_m(\alpha_m r_o/H_o) \cos(\alpha_m z/H_o) \right] \tag{8.2}$$

where z = distance above the base of the tower, H_o = depth of the surrounding water, ρ_w = mass density of water, r_o = radius of the outside surface of the tower, $\alpha_m = (2m-1)\pi/2$, and

$$E_m(\alpha_m r_o/H_o) = \frac{K_1(\alpha_m r_o/H_o)}{K_0(\alpha_m r_o/H_o) + K_2(\alpha_m r_o/H_o)} \tag{8.3}$$

in which K_n is the modified Bessel function of order n of the second kind. For an infinitely long uniform tower with the same circular cross-section, the added mass per unit of height is

$$m_\infty^o = \rho_w \, \pi \, r_o^2 \tag{8.4}$$

which is equal to the mass of the water displaced by the (solid) tower per unit of height. The normalized added mass $m_a^o(z)/m_\infty^o$ for circular cylindrical towers is presented in Figure 8.1 for a range of values of r_o/H_o, the ratio of the outside radius to water depth. It is apparent that the normalized added mass is unity for the limiting case of an infinitely slender cylinder (i.e. $H_o/r_o = \infty$), and it decreases as the tower becomes more squat (i.e. the slenderness ratio H_o/r_o decreases). In case of a finite-length tower, the fluid flows along the height as well as around the circumference, whereas the fluid flow is two dimensional, only around the circumference, for an infinitely long tower. Therefore, the inertial resistance to motion is less in case of a finite tower than that for an infinitely long tower.

For a uniform tower of arbitrary cross-section, the added hydrodynamic mass can also be determined by solving the Laplace equation for the surrounding water domain. In this case, however, analytical solutions are generally not feasible, and discrete methods of Chapter 4 are necessary for computing the added hydrodynamic mass. Solution of a three-dimensional boundary value problem (BVP) is required to evaluate $m_a^o(z)$ [Section 4.3] but m_∞^o can be determined by solving a simpler two-dimensional BVP in the cross-sectional plane of the tower using the semi-analytical process in the finite element procedure of Section 4.3 (Appendix G, Section G.1).

Determined by this procedure, the added mass m_∞^o per unit height of an infinitely-long uniform tower is presented in Table 8.1 for a variety of cross-sections. The cross-section of the outside surface of the tower has an area A_o with a width of $2a_o$ perpendicular to the

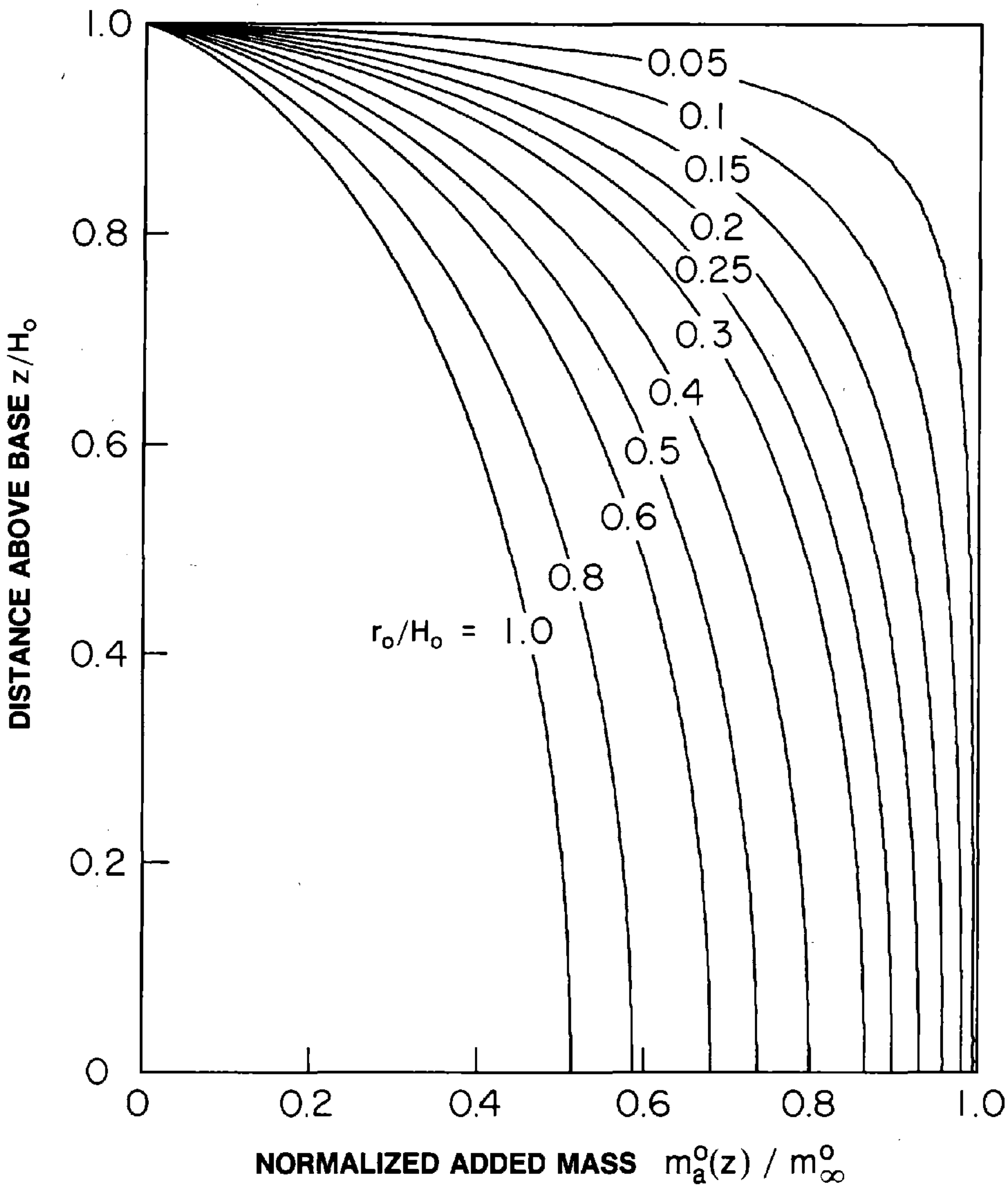

Figure 8.1 Normalized Added Hydrodynamic Mass for Circular Cylindrical Towers Associated with Surrounding Water

Table 8.1 -- Added Hydrodynamic Mass m_∞^o for Infinitely-Long Towers Associated with Surrounding Water*

Cross-Section of the Outside Surface	Direction of Ground Motion	$\frac{a_o}{b_o}$	$\frac{m_\infty^o}{\rho_w A_o}$	$\frac{m_\infty^o}{\rho_w \pi a_o^2}$
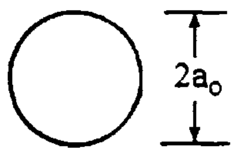	$\longleftrightarrow$	1	1.000	1.000
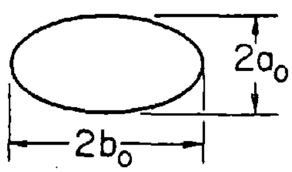	$\longleftrightarrow$	FOR ALL VALUES	a_o/b_o	1.000
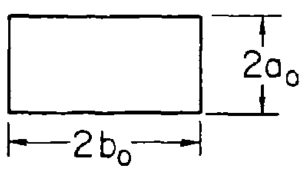	$\longleftrightarrow$	1/5	0.311	1.980
		1/4	0.377	1.920
		1/3	0.480	1.835
		1/2	0.667	1.701
		2/3	0.853	1.630
		1	1.186	1.511
		3/2	1.661	1.411
		2	2.136	1.359
		3	3.038	1.289
		4	3.896	1.242
		5	4.752	1.211

* Values for some cross-sections also presented in Reference [17]

Table 8.1 (Continued)

Cross-Section of the Outside Surface	Direction of Ground Motion	$\frac{a_o}{b_o}$	$\frac{m^o_\infty}{\rho_w A_o}$	$\frac{m^o_\infty}{\rho_w \pi a_o^2}$
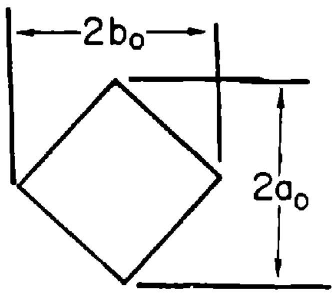	↔	1/2	0.527	0.671
		1	1.189	0.756
		2	2.661	0.847
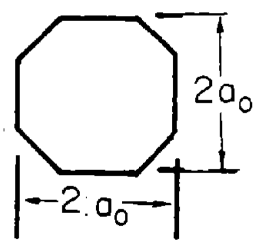	↔	1	1.046	1.165
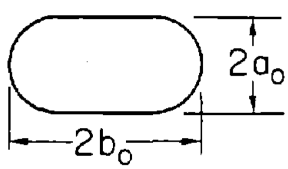	↔	1/5	0.261	1.592
		1/4	0.314	1.511
		1/3	0.397	1.408
		1/2	0.555	1.262
		2/3	0.707	1.157
		1	1.000	1.000
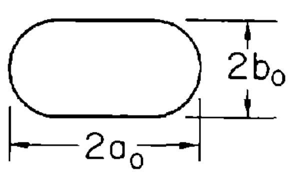	↕	3/2	1.444	1.050
		2	1.896	1.077
		3	2.787	1.098
		4	3.658	1.102
		5	4.516	1.101

Table 8.1 (Continued)

Cross-Section of the Outside Surface	Direction of Ground Motion	$\frac{a_o}{b_o}$	$\frac{m^o_\infty}{\rho_w A_o}$	$\frac{m^o_\infty}{\rho_w \pi a_o^2}$
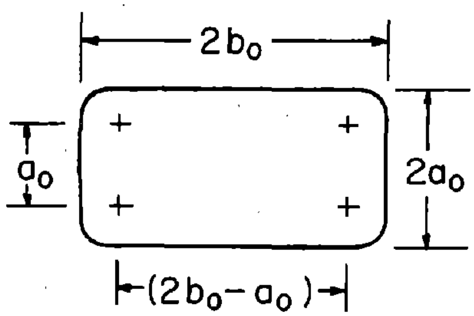	↔	1/5	0.282	1.779
		1/4	0.339	1.704
		1/3	0.429	1.609
		1/2	0.597	1.479
		2/3	0.756	1.392
		1	1.059	1.276
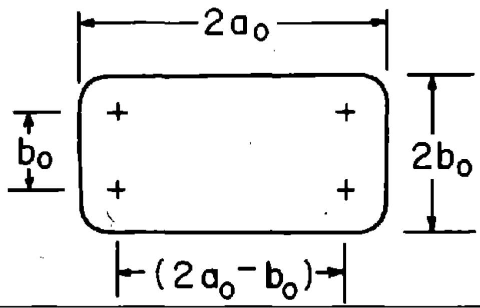	↕	3/2	1.540	1.261
		2	2.007	1.244
		3	2.909	1.213
		4	3.786	1.189
		5	4.646	1.170
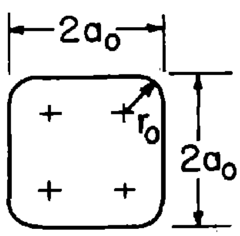 $r/a_o = 1.0$	↔	1	1.000	1.000
$r/a_o = 0.8$			1.009	1.109
$r/a_o = 0.6$			1.037	1.218
$r/a_o = 0.4$			1.080	1.328
$r/a_o = 0.2$			1.135	1.433
$r/a_o = 0.0$			1.186	1.511

direction of ground motion, and its dimension along the direction of ground motion is $2b_o$. The computed added mass has been normalized with respect to (1) $\rho_w A_o$, the mass of the water displaced by the (solid) tower per unit height ; and (2) $\rho_w \pi a_o^2$, the mass per unit height of a circular cylinder of water having diameter equal to $2a_o$. It is apparent that the added mass m_∞^o depends on the shape of the cross-section, and for a given shape, say a rectangle, it varies with the ratio a_o/b_o of the cross-sectional dimensions perpendicular and parallel to the direction of ground motion. Furthermore, contrary to the recommendations of Reference [39], the added mass m_∞^o for a non-circular cross-section with dimension $2a_o$ perpendicular to the direction of ground motion can be much different than that for a circular cross-section of diameter $2a_o$.

Not only does the added mass m_∞^o for an infinitely long tower vary with a_o/b_o, so does the normalized added mass $m_a^o(z)/m_\infty^o$ for a tower of finite height. This is demonstrated in Figure 8.2 where this quantity, determined by the procedure of Section 4.3, is plotted for towers with elliptical cross-section for two values of a_o/H_o and several values of a_o/b_o. It is apparent that the influence of a_o/b_o increases with decrease in slenderness ratio H_o/a_o.

Similarly the normalized added hydrodynamic mass depends on the shape of the cross-section of the tower. This is apparent from Figure 8.3 where $m_a^o(z)/m_\infty^o$ is presented for two towers with different cross-sections, rectangle and ellipse, but with the same slenderness ratio H_o/a_o and the same ratio a_o/b_o of the cross-sectional dimensions. For a fixed a_o/b_o, the area A_o of the cross-section depends on the shape, e.g. A_o is $4a_ob_o$ for a rectangle and πa_ob_o for an ellipse. Thus A_o may be treated as an indicator of the cross-sectional shape. It is only a partial indicator because even if the parameters a_o/H_o, a_o/b_o and A_o are identical for two towers, the normalized added hydrodynamic mass need not be identical if their cross-sectional shapes are different. Thus, the normalized added hydrodynamic mass is influenced by the slenderness ratio H_o/a_o (Figure 8.1), the ratio a_o/b_o of the cross-sectional dimensions

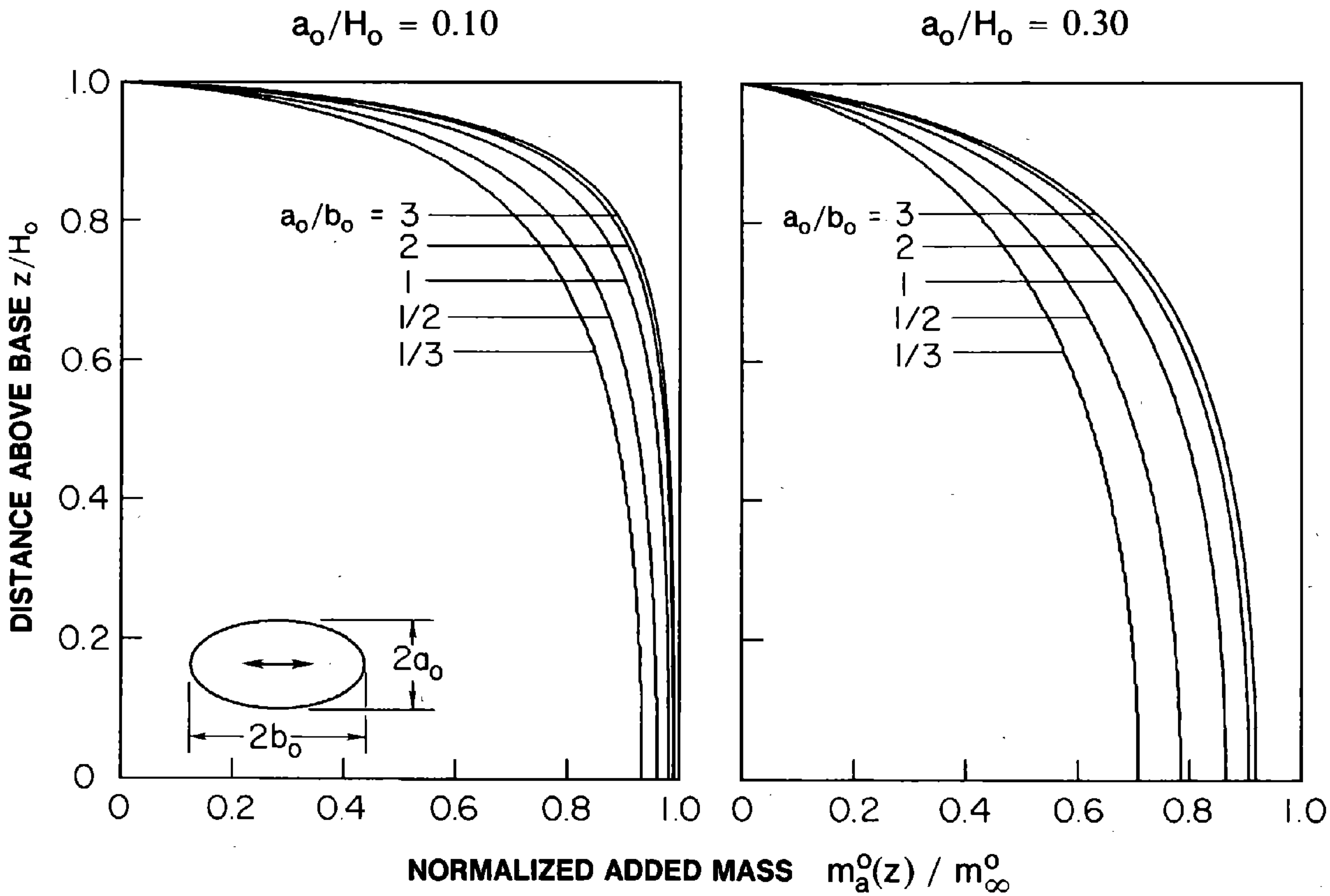

Figure 8.2 Normalized Added Mass for Elliptical Towers Associated with Surrounding Water

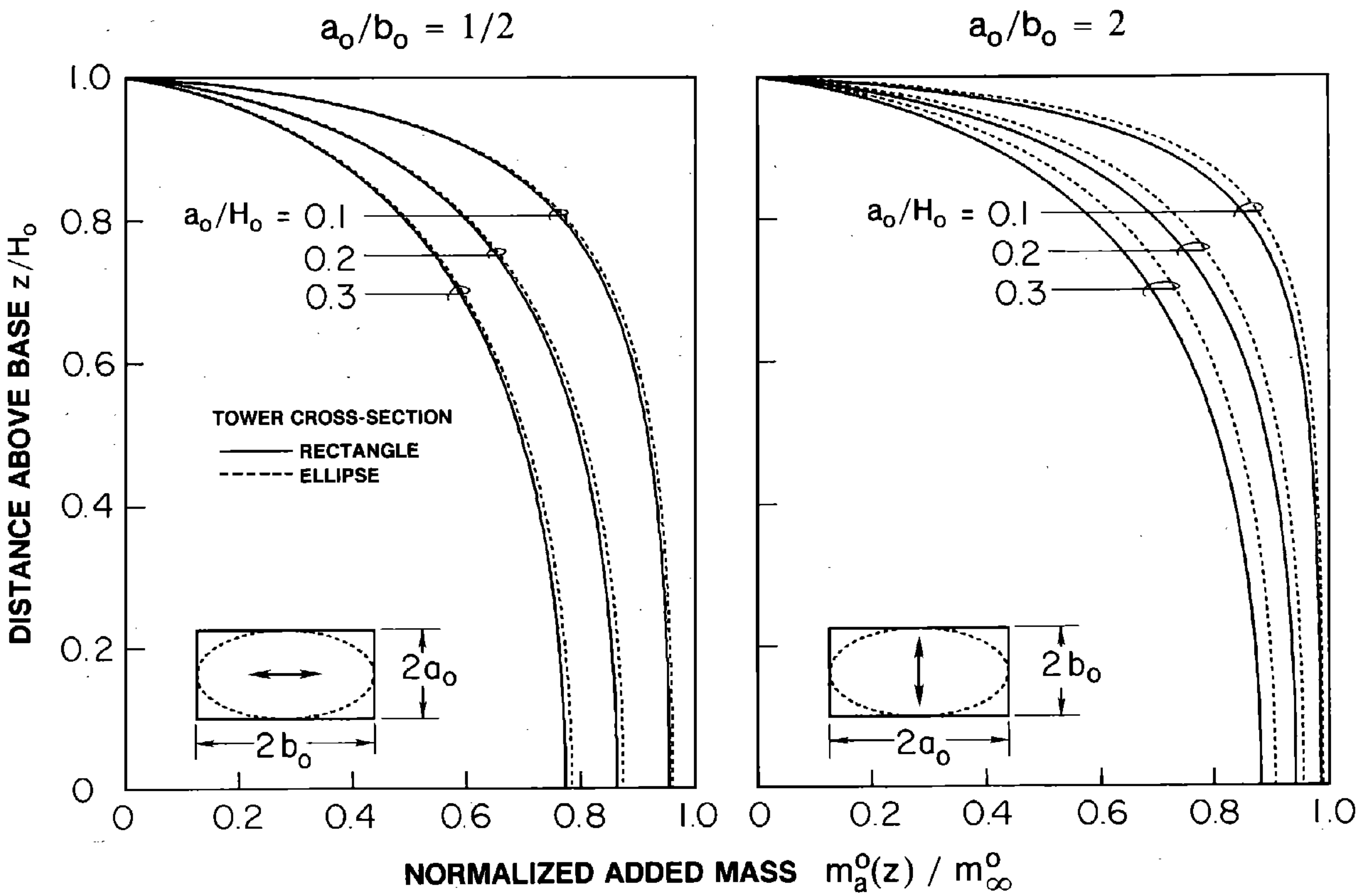

Figure 8.3 Normalized Added Hydrodynamic Mass for Circular Cylindrical Towers Associated with Surrounding Water for Uniform Towers of Elliptical and Rectangular Cross-Sections with the Same Values of Parameters H_o/a_o and a_o/b_o

(Figure 8.2), the cross-sectional area A_o (Figure 8.3), and the cross-sectional shape. In order to identify the conditions under which the normalized added hydrodynamic mass is essentially the same for two towers, this quantity is computed for two towers with different cross-sections, rectangle and ellipse, under two conditions : (i) same H_o, H_o/a_o and A_o, resulting in different values of b_o and hence a_o/b_o (Figure 8.4), and (ii) same H_o, a_o/b_o and A_o, resulting in different values of a_o and hence H_o/a_o (Figure 8.5). Figure 8.6 is similar to the latter figure but shows results for a practical cross-section. It is apparent from these figures that the normalized added hydrodynamic mass for towers with same H_o, a_o/b_o and A_o is essentially independent of the shape of the cross-section. The influence of the cross-sectional shape, however, increases as the slenderness ratio H_o/a_o decreases.

Thus the normalized added hydrodynamic mass for uniform tower of arbitrary cross-section is essentially the same as that for an "equivalent" elliptical tower. The plan dimensions ratio $\tilde{a}_o/\tilde{b}_o$ and the slenderness ratio $H_o/\tilde{a}_o$ of the equivalent elliptical tower are related to a_o/b_o, A_o and H_o for the actual tower by :

$$\frac{H_o}{\tilde{a}_o} = \frac{H_o}{\sqrt{A_o/\pi}} \cdot \sqrt{\frac{b_o}{a_o}} \tag{8.5a}$$

$$\frac{\tilde{a}_o}{\tilde{b}_o} = \frac{a_o}{b_o} \tag{8.5b}$$

These properties of the equivalent elliptical towers corresponding to towers with cross-sections considered in Figures 8.5 and 8.6 are presented in Table 8.2. Therefore, the normalized added hydrodynamic mass for a uniform tower of arbitrary cross-section can be readily determined if this quantity were available for towers of elliptical cross-section for a practical range of values of a_o/b_o and H_o/a_o. Using the discrete methods of Section 4.3, the normalized added mass for uniform towers with elliptical cross-sections can be determined and tabulated for a number of values of the parameters a_o/b_o and H_o/a_o but this will require a large number of graphs and tables, and interpolation for intermediate values of the

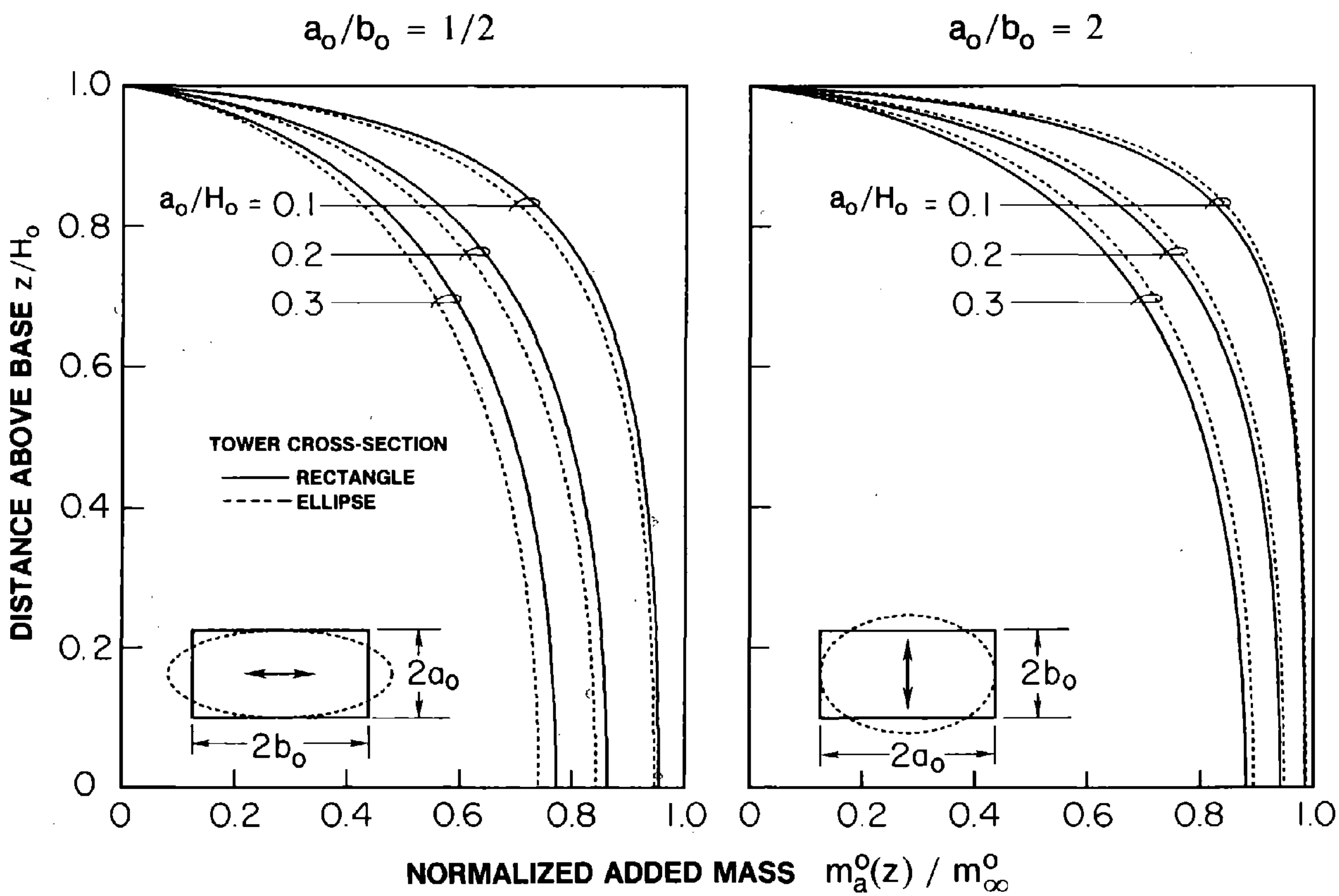

Figure 8.4 Normalized Added Hydrodynamic Mass Associated with Surrounding Water for Uniform Towers of Elliptical and Rectangular Cross-Sections with same Values of Parameters H_o, H_o/a_o, and A_o

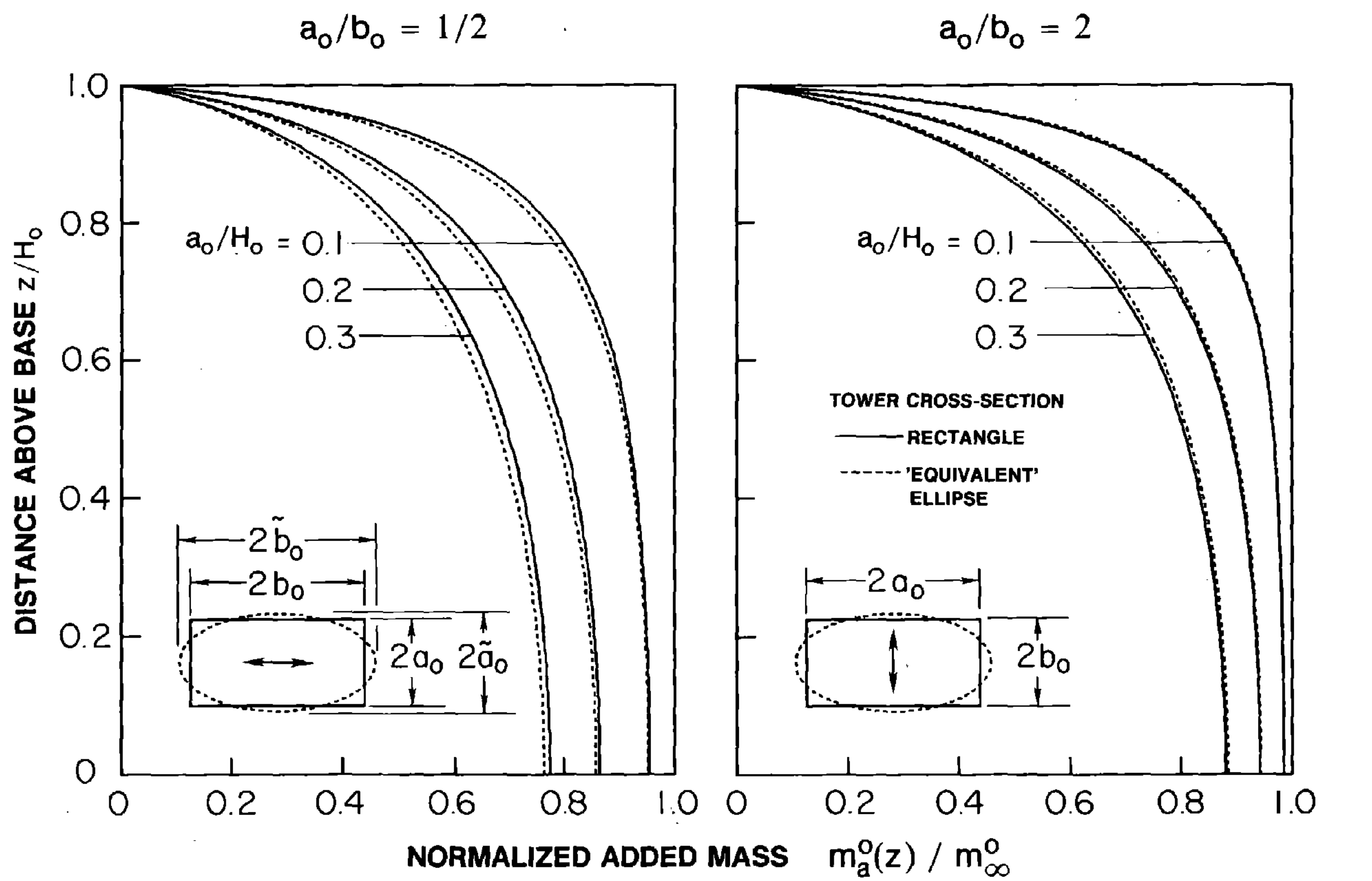

Figure 8.5 Normalized Added Hydrodynamic Mass Associated with Surrounding Water for Uniform Towers of Elliptical and Rectangular Cross-Sections with Same Values of Parameters H_o , a_o/b_o , and A_o

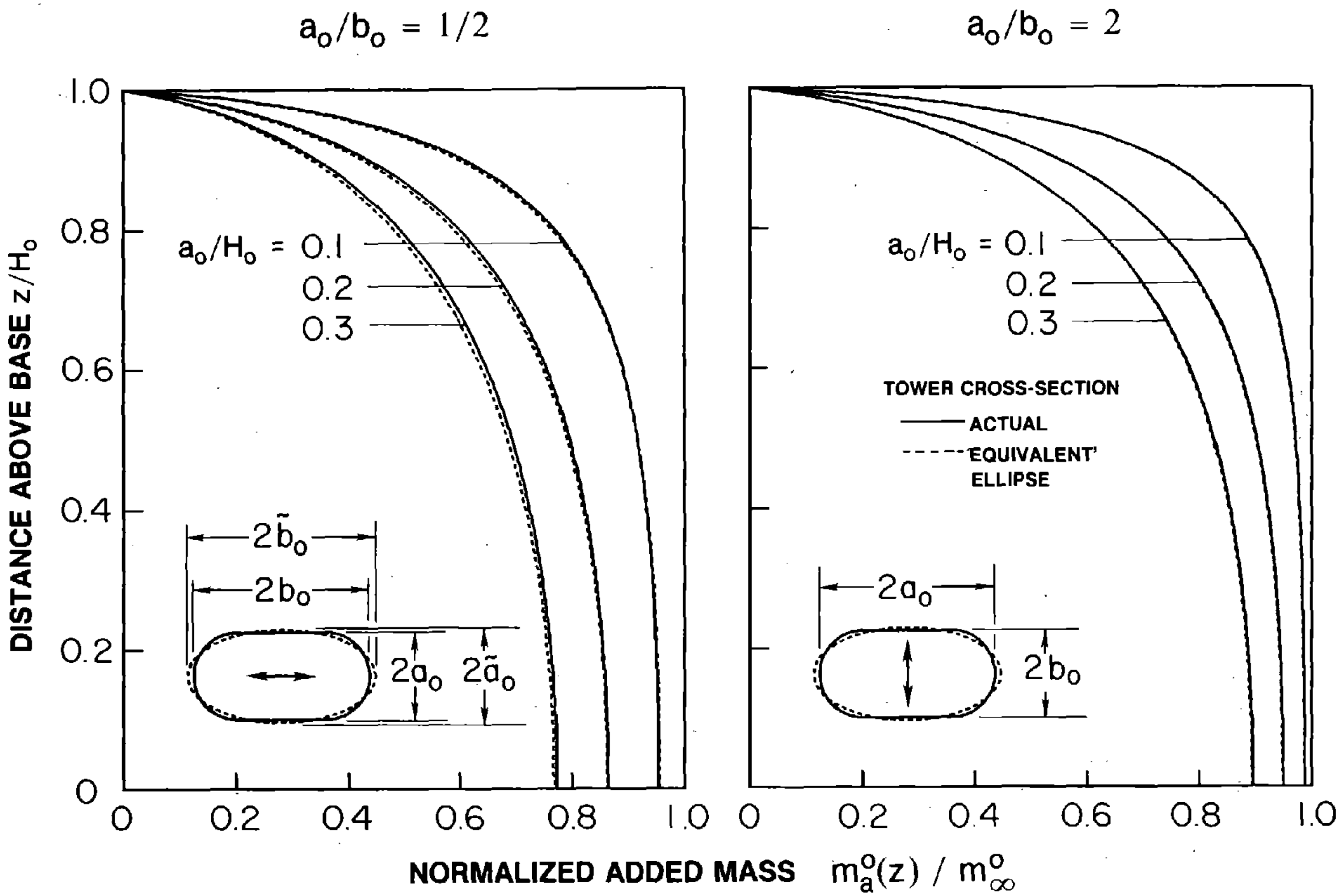

Figure 8.6 Normalized Added Hydrodynamic Mass Associated with Surrounding Water for Uniform Towers of Actual and Equivalent Elliptical Cross-Sections with Same Values of Parameters; H_o , a_o/b_o , and A_o

Table 8.2 -- Properties of 'Equivalent', Uniform Elliptical Towers for Actual Uniform Towers

Cross-Section of the Outside Surface	Direction of Ground Motion	Actual Tower		Equivalent, Elliptical Tower	
		a_o/b_o	a_o/H_o	$\tilde{a}_o/\tilde{b}_o$	$\tilde{a}_o/\tilde{H}_o$
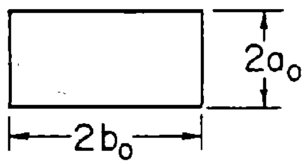	↔	1/2	0.10	1/2	0.113
		1/2	0.20	1/2	0.226
		1/2	0.30	1/2	0.339
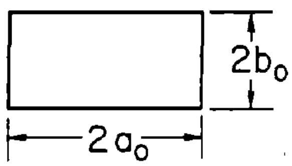	↕	2	0.10	2	0.113
		2	0.20	2	0.226
		2	0.30	2	0.339
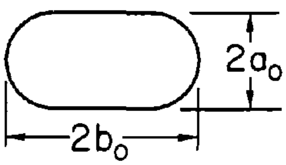	↔	1/2	0.10	1/2	0.107
		1/2	0.20	1/2	0.213
		1/2	0.30	1/2	0.320
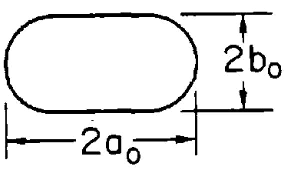	↕	2	0.10	2	0.107
		2	0.20	2	0.213
		2	0.30	2	0.320

parameters.

The approach that is more convenient in practical application is to replace the uniform elliptical tower by an "equivalent" circular cylindrical tower. Thus for fixed values of a_o/b_o and H_o/a_o for an elliptical tower, determined is the radius $\tilde{r}_o$ and hence slenderness ratio $H_o/\tilde{r}_o$ of the equivalent circular cylindrical tower, such that the integrals over water depth of the normalized added hydrodynamic mass $m_a^o(z)/m_\infty^o$ of the two towers are equal. The properties of the equivalent circular cylindrical tower are determined by iterative, numerical techniques wherein $m_a^o(z)/m_\infty^o$ is determined from equation (8.2) for the circular cylindrical tower and by the methods of Section 4.3 for the uniform elliptical tower. The results are summarized in Figure 8.7 wherein $\tilde{r}_o/H_o$, the inverse of the slenderness ratio of the equivalent circular cylindrical tower, is presented against the corresponding quantity a_o/H_o for the elliptical tower for various values of a_o/b_o for the elliptical cross-section. The normalized added mass for elliptical towers determined approximately by evaluating equation (8.2) for the equivalent circular cylindrical tower turns out to be essentially identical to the 'exact' results obtained by the numerical methods of Section 4.3 (Figure 8.8). Although only the integrals over water depth of the normalized added mass for the elliptical and equivalent circular towers were enforced to be equal, the two added mass functions are essentially identical throughout the water depth.

Motivated by the observation from Figure 8.7 that, for a fixed value of a_o/b_o, $\tilde{r}_o/H_o$ is almost a linear function of a_o/H_o, the data of Figure 8.7 is presented in a different form in Figure 8.9. It is apparent that the ratio $\tilde{r}_o/a_o$ is essentially independent of the slenderness ratio H_o/a_o if a_o/b_o is within 1/3 to 3 which would cover most practical cases. However, outside this range of a_o/b_o, H_o/a_o has more influence on the ratio $\tilde{r}_o/a_o$. Therefore, the mean curve presented in Figure 8.9 can be used to determine the ratio $\tilde{r}_o/a_o$ if $1/3 \leq a_o/b_o \leq 3$.

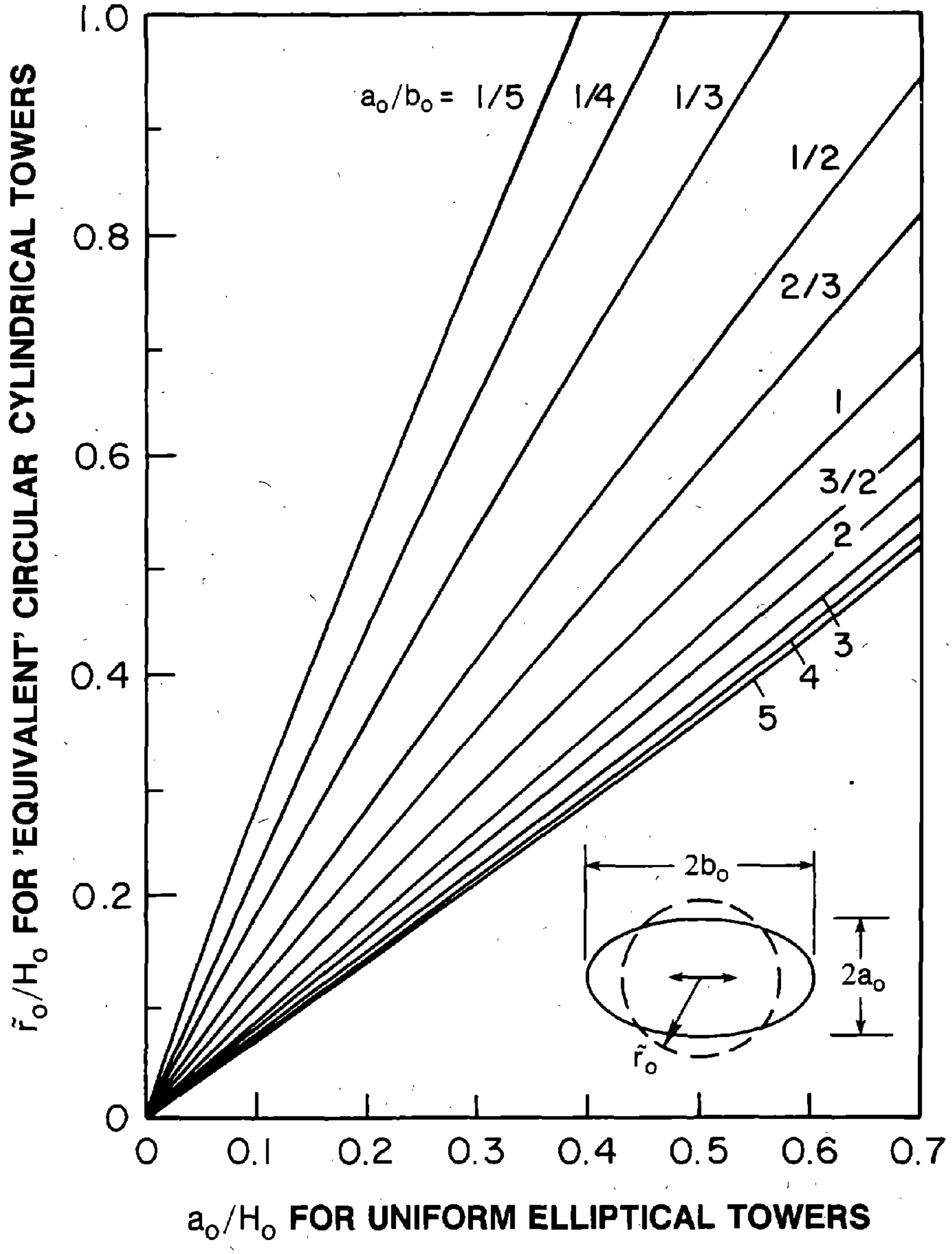

Figure 8.7 Properties of 'Equivalent' Circular Cylindrical Towers for Uniform Elliptical Towers Associated with Added Hydrodynamic Mass due to Surrounding Water

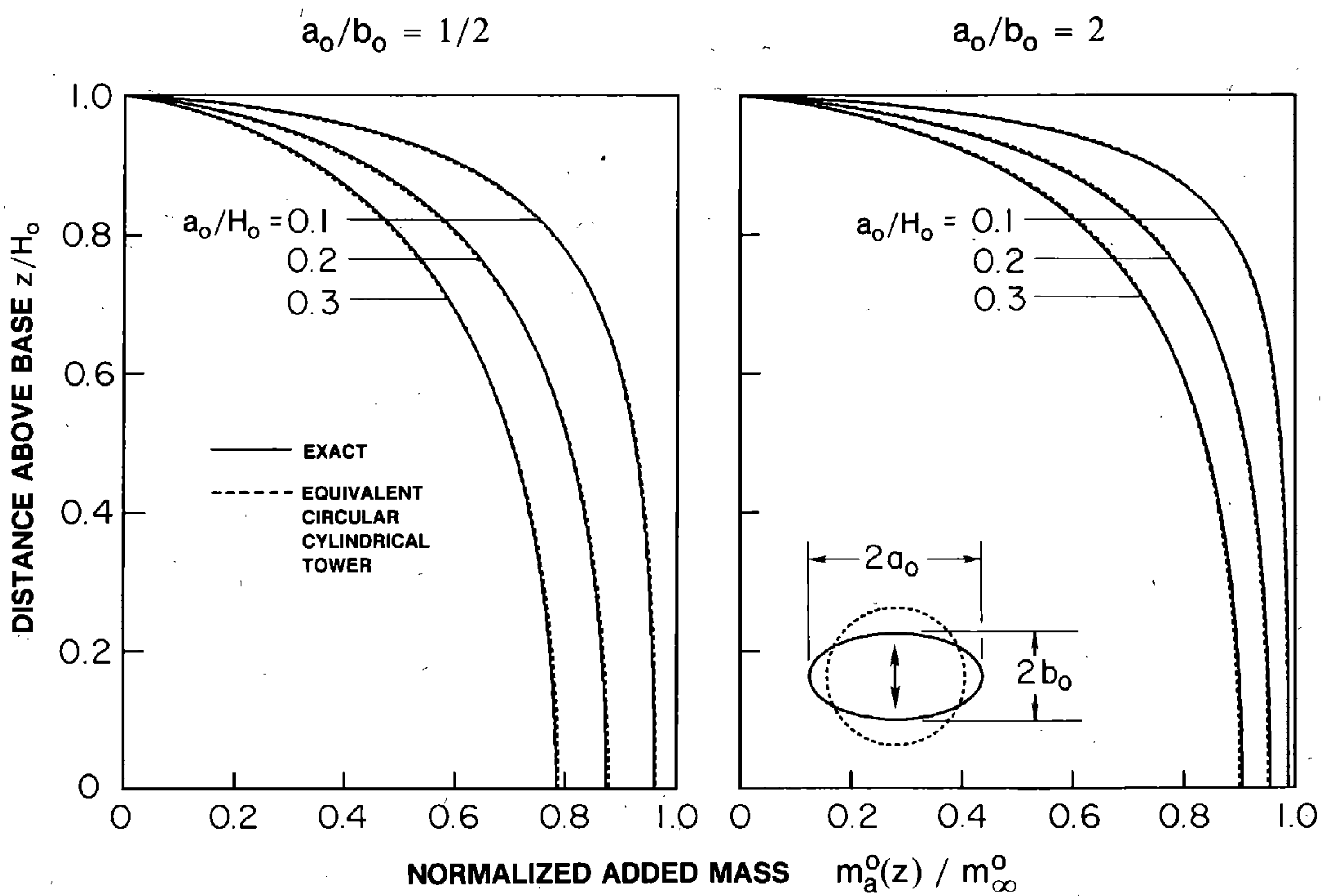

Figure 8.8 Comparison of Exact and Approximate ('Equivalent' Circular Cylindrical Towers) Values of the Normalized Added Hydrodynamic Mass for Uniform Towers Associated with Surrounding Water

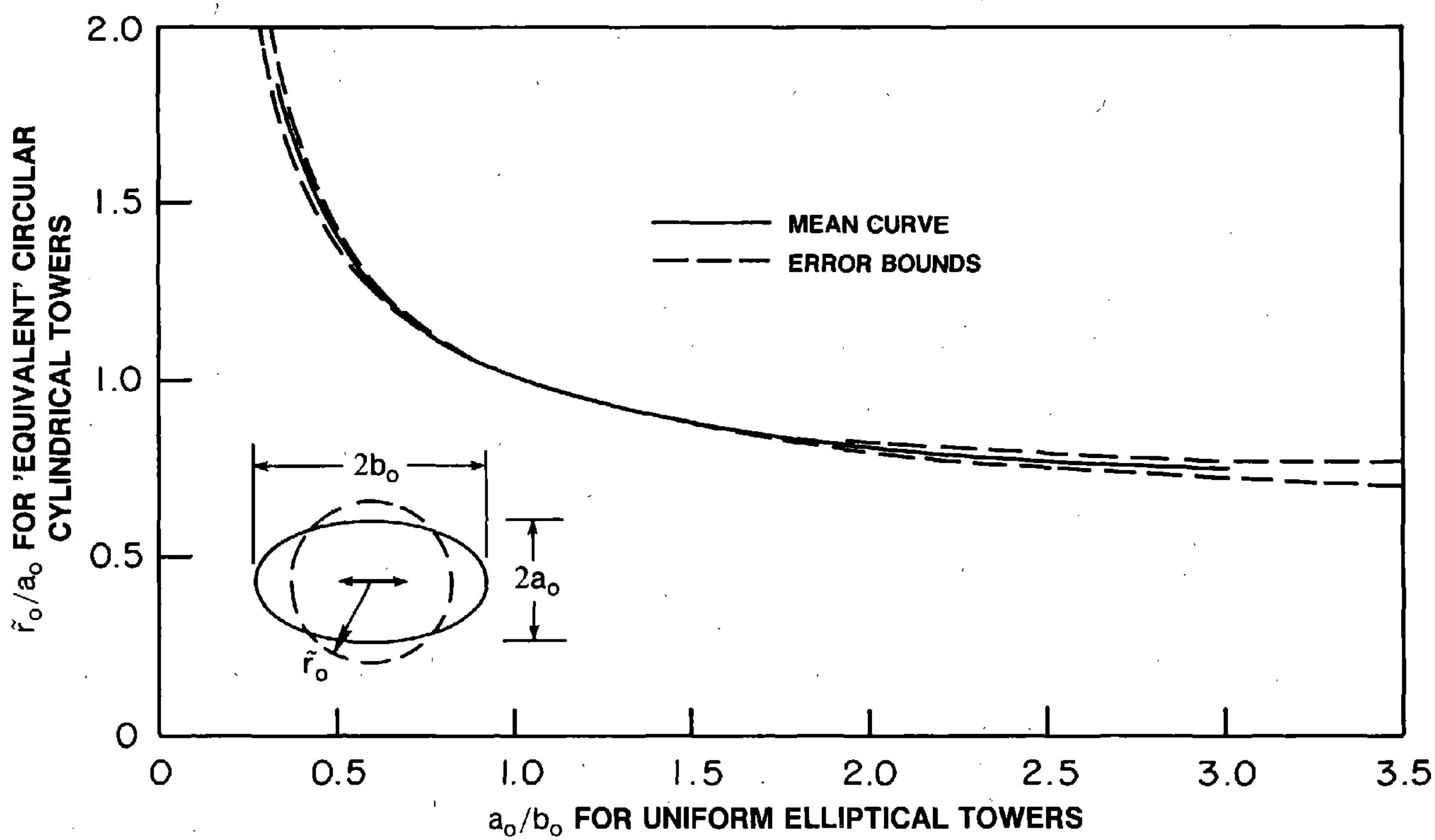

Figure 8.9 Properties of 'Equivalent' Circular Cylindrical Towers for Uniform Elliptical Towers Associated with Added Hydrodynamic Mass due to Surrounding Water

8.2.2 Uniform Towers -- Summary

Based on the analysis and results presented earlier, the added hydrodynamic mass associated with surrounding water for uniform towers of arbitrary cross-section with two axes of symmetry can be determined by the following steps :

1. Evaluate the parameters $\tilde{a}_o/\tilde{b}_o$ and $H_o/\tilde{a}_o$ for the 'equivalent' uniform elliptical tower, using equation (8.5), corresponding to the properties of the actual tower : slenderness ratio H_o/a_o, cross-sectional area A_o, and ratio a_o/b_o of the plan dimensions.

2. Evaluate the slenderness ratio $H_o/\tilde{r}_o$ of the 'equivalent' circular, cylindrical tower from the properties $\tilde{a}_o/\tilde{b}_o$ and $H_o/\tilde{a}_o$ determined in step 1 for the equivalent, elliptical tower using the data of Figure 8.7 or Table 8.3. Use linear interpolation between the curves of Figure 8.7 for intermediate values of $\tilde{a}_o/\tilde{b}_o$. Alternatively, if $1/3 \leq \tilde{a}_o/\tilde{b}_o \leq 3$, $\tilde{r}_o/a_o$ may be determined from the mean curve of Figure 8.9 corresponding to $\tilde{a}_o/\tilde{b}_o$ determined in step 1.

3. Evaluate the normalized added mass $m_a^o(z)/m_\infty^o$ for the circular cylindrical tower with slenderness ratio ratio $H_o/\tilde{r}_o$, determined in step 2, from Figure 8.1 or Table 8.4. Use linear interpolation for intermediate values of $\tilde{r}_o/H_o$.

4. Determine the added hydrodynamic mass m_∞^o for an infinitely long tower with the actual cross-section from Table 8.1 where such results are presented for a few selected cross-sections. For other cross-sections, a two-dimensional solution of the Laplace equation should be carried out for the surrounding water domain. For convenience of the user, the finite element procedure to implement the analysis is presented in Appendix G, and the required series of computer programs 'TOWER-INF', and their user's manuals are presented in Appendix J of this report with a numerical example.

Table 8.3 -- $\tilde{r}_o/H_o$ for 'Equivalent', Circular Cylindrical Tower for a Uniform Elliptical Tower with Plan Dimension Ratio a_o/b_o and Slenderness Ratio H_o/a_o ; Associated with Added Hydrodynamic Mass due to Surrounding water

a_o/H_o	a_o/b_o										
	1/5	1/4	1/3	1/2	2/3	1	3/2	2	3	4	5
0.05	0.146	0.117	0.094	0.071	0.060	0.050	0.043	0.040	0.037	0.036	0.035
0.10	0.279	0.228	0.185	0.141	0.120	0.010	0.087	0.080	0.075	0.072	0.070
0.15	0.408	0.337	0.274	0.211	0.180	0.150	0.131	0.121	0.112	0.108	0.105
0.20	0.536	0.445	0.363	0.280	0.240	0.200	0.175	0.162	0.150	0.144	0.141
0.25	0.661	0.551	0.450	0.348	0.299	0.250	0.219	0.203	0.188	0.181	0.177
0.30	0.785	0.656	0.536	0.416	0.358	0.300	0.263	0.245	0.227	0.218	0.213
0.40	1.026	0.861	0.707	0.551	0.475	0.400	0.352	0.328	0.305	0.294	0.287
0.50	-	1.062	0.875	0.685	0.591	0.500	0.441	0.412	0.385	0.371	0.363
0.60	-	-	1.040	0.817	0.708	0.600	0.531	0.497	0.465	0.449	0.440
0.70	-	-	-	0.949	0.823	0.700	0.621	0.583	0.546	0.528	0.517

Table 8.4 -- Normalized Added Mass $m_a^o(z)/m_\infty^o$ for Circular Cylindrical Towers Associated with Surrounding Water

z/H_o	r_o/H_o										
	0.05	0.10	0.15	0.20	0.25	0.30	0.40	0.50	0.60	0.80	1.00
1.00	0.000	0.000	0.000	0.000	0.000	0.000	0.000	0.000	0.000	0.000	0.000
0.98	0.455	0.306	0.236	0.194	0.166	0.146	0.118	0.099	0.086	0.068	0.056
0.96	0.634	0.459	0.366	0.308	0.267	0.236	0.193	0.164	0.143	0.114	0.095
0.94	0.736	0.561	0.459	0.392	0.343	0.306	0.254	0.217	0.190	0.153	0.128
0.92	0.802	0.636	0.531	0.459	0.405	0.364	0.304	0.262	0.230	0.186	0.156
0.90	0.846	0.693	0.588	0.514	0.457	0.413	0.348	0.301	0.266	0.215	0.181
0.88	0.878	0.737	0.635	0.560	0.502	0.456	0.386	0.336	0.297	0.242	0.204
0.86	0.901	0.773	0.674	0.599	0.541	0.493	0.420	0.367	0.326	0.266	0.225
0.84	0.919	0.802	0.708	0.634	0.574	0.526	0.451	0.395	0.351	0.288	0.244
0.82	0.932	0.826	0.736	0.663	0.604	0.555	0.478	0.421	0.375	0.309	0.262
0.80	0.943	0.846	0.761	0.690	0.631	0.582	0.504	0.444	0.397	0.328	0.279
0.78	0.951	0.863	0.782	0.713	0.655	0.606	0.527	0.466	0.417	0.345	0.294
0.76	0.958	0.878	0.801	0.734	0.676	0.627	0.548	0.486	0.436	0.362	0.309
0.74	0.963	0.890	0.817	0.752	0.696	0.647	0.567	0.504	0.454	0.377	0.323
0.72	0.968	0.901	0.831	0.769	0.713	0.665	0.585	0.521	0.470	0.392	0.335
0.70	0.972	0.910	0.844	0.784	0.729	0.682	0.602	0.537	0.485	0.405	0.347
0.68	0.975	0.918	0.856	0.797	0.744	0.697	0.617	0.552	0.499	0.418	0.359
0.66	0.977	0.925	0.866	0.809	0.757	0.711	0.631	0.566	0.513	0.430	0.370

Table 8.4 (Continued)

z/H_o	r_o/H_o										
	0.05	0.10	0.15	0.20	0.25	0.30	0.40	0.50	0.60	0.80	1.00
0.64	0.980	0.931	0.875	0.820	0.770	0.724	0.644	0.579	0.525	0.441	0.380
0.62	0.982	0.937	0.883	0.830	0.781	0.736	0.657	0.591	0.537	0.452	0.389
0.60	0.983	0.942	0.891	0.840	0.791	0.747	0.668	0.603	0.548	0.462	0.399
0.56	0.986	0.950	0.904	0.856	0.810	0.766	0.689	0.624	0.568	0.481	0.415
0.52	0.988	0.956	0.914	0.869	0.825	0.783	0.707	0.642	0.586	0.497	0.430
0.48	0.990	0.961	0.923	0.881	0.838	0.798	0.723	0.658	0.602	0.512	0.444
0.44	0.991	0.965	0.930	0.890	0.850	0.810	0.736	0.672	0.616	0.525	0.456
0.40	0.992	0.969	0.936	0.898	0.859	0.821	0.748	0.684	0.628	0.536	0.466
0.36	0.993	0.972	0.941	0.905	0.868	0.830	0.759	0.695	0.639	0.546	0.475
0.32	0.993	0.974	0.945	0.911	0.875	0.838	0.768	0.704	0.648	0.555	0.484
0.28	0.994	0.976	0.949	0.916	0.881	0.845	0.775	0.712	0.656	0.563	0.491
0.24	0.994	0.977	0.951	0.920	0.886	0.850	0.782	0.719	0.663	0.569	0.497
0.20	0.994	0.978	0.954	0.923	0.890	0.855	0.787	0.724	0.668	0.575	0.502
0.16	0.995	0.979	0.955	0.926	0.893	0.859	0.791	0.729	0.673	0.579	0.506
0.12	0.995	0.980	0.957	0.928	0.895	0.861	0.795	0.732	0.676	0.582	0.509
0.08	0.995	0.981	0.958	0.929	0.897	0.863	0.797	0.735	0.679	0.585	0.511
0.04	0.995	0.981	0.958	0.930	0.898	0.865	0.798	0.736	0.680	0.586	0.512
0.00	0.995	0.981	0.958	0.930	0.898	0.865	0.799	0.737	0.681	0.587	0.513

5. Determine the added hydrodynamic mass $m_a^o(z)$ for the actual tower by multiplying the normalized added mass determined in step 3 by m_∞^o computed in step 4.

For uniform towers of selected cross-sections, and each with three different values of the slenderness ratio, the added hydrodynamic mass has been determined by two methods : (1) 'exact' analysis procedure presented in Section 4.3, and (2) the simplified analysis procedure presented above. It is apparent from Figures 8.10 to 8.12 that the results obtained by the simplified procedure are satisfactory for a wide range of parameters. The accuracy is more than satisfactory for analyzing towers in their preliminary phase of seismic design or safety evaluation.

8.2.3 Non-Uniform Towers

Although the cross-sectional shape of an intake-outlet tower usually does not change along its height, the cross-sectional dimensions often decrease with increasing height above the base. The procedure described in the preceding section to determine an equivalent circular, cylindrical tower for a uniform tower of arbitrary cross-section can be extended to such a non-uniform tower. Because the cross-sectional dimensions of such a tower vary over its height, this extension results in an equivalent, non-uniform tower with circular plan.

It was demonstrated in the preceding section that an equivalent circular, cylindrical tower can be defined for the purpose of determining the normalized added hydrodynamic mass for a uniform tower of arbitrary cross-section. The slenderness ratio $H_o/\tilde{r}_o$ of the equivalent tower depends on the shape, the area A_o, and ratio a_o/b_o of the actual cross-section of the actual tower. Thus, for a given water depth H_o, the radius $\tilde{r}_o$ of the equivalent circular cross-section can be determined, which depends on the cross-sectional shape and dimensions of the actual tower. This procedure can be successively applied to several cross-sections of a non-uniform tower to determine the radii of the corresponding equivalent circular cross-sections. The result would be an 'equivalent' tower of circular cross-section, or an equivalent axisymmetric tower, with its radius $\tilde{r}_o(z)$ varying with height.

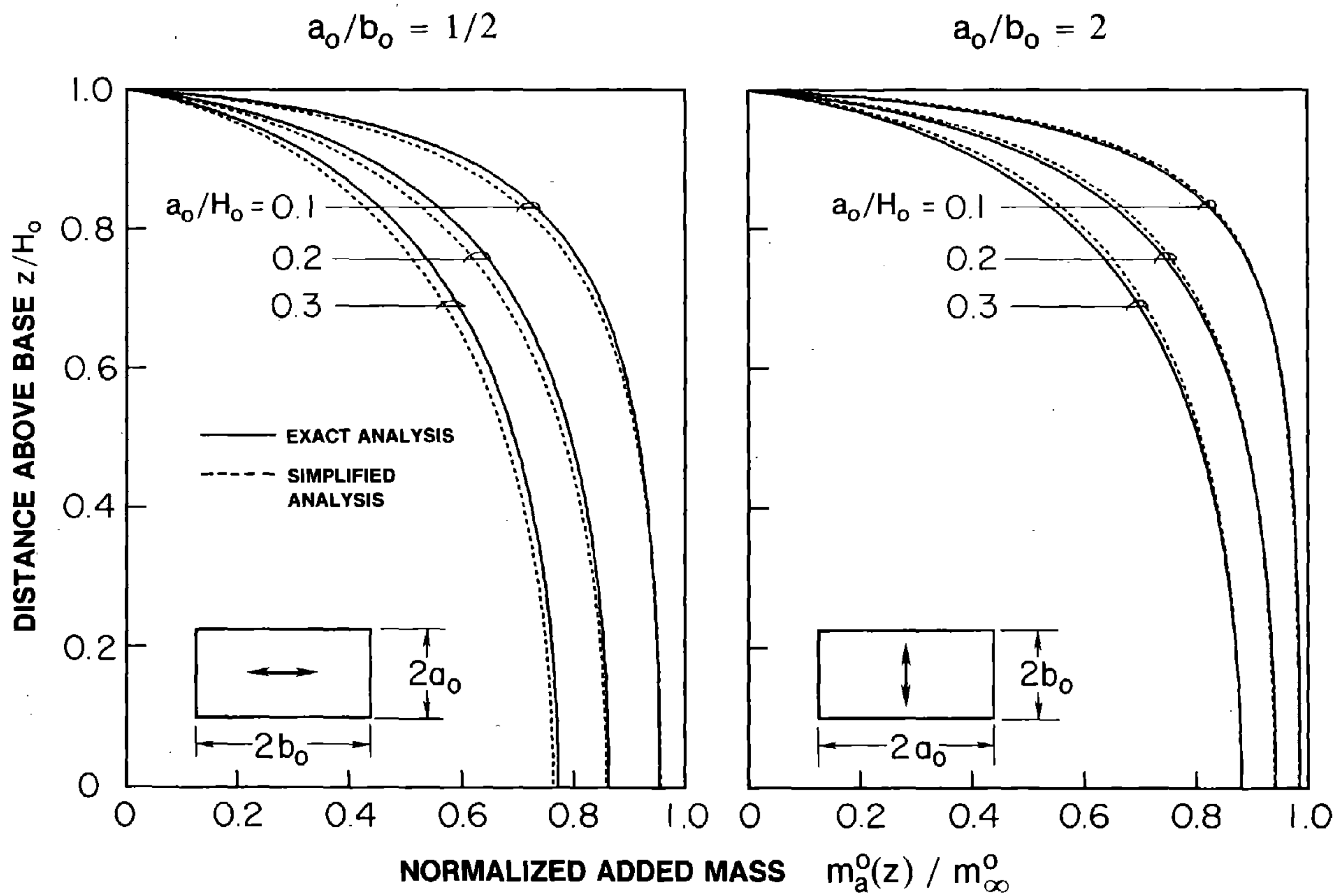

Figure 8.10 Comparison of Exact and Approximate (Simplified Analysis Procedure) Values of the Normalized Added Hydrodynamic Mass for Uniform Towers Associated with Surrounding Water

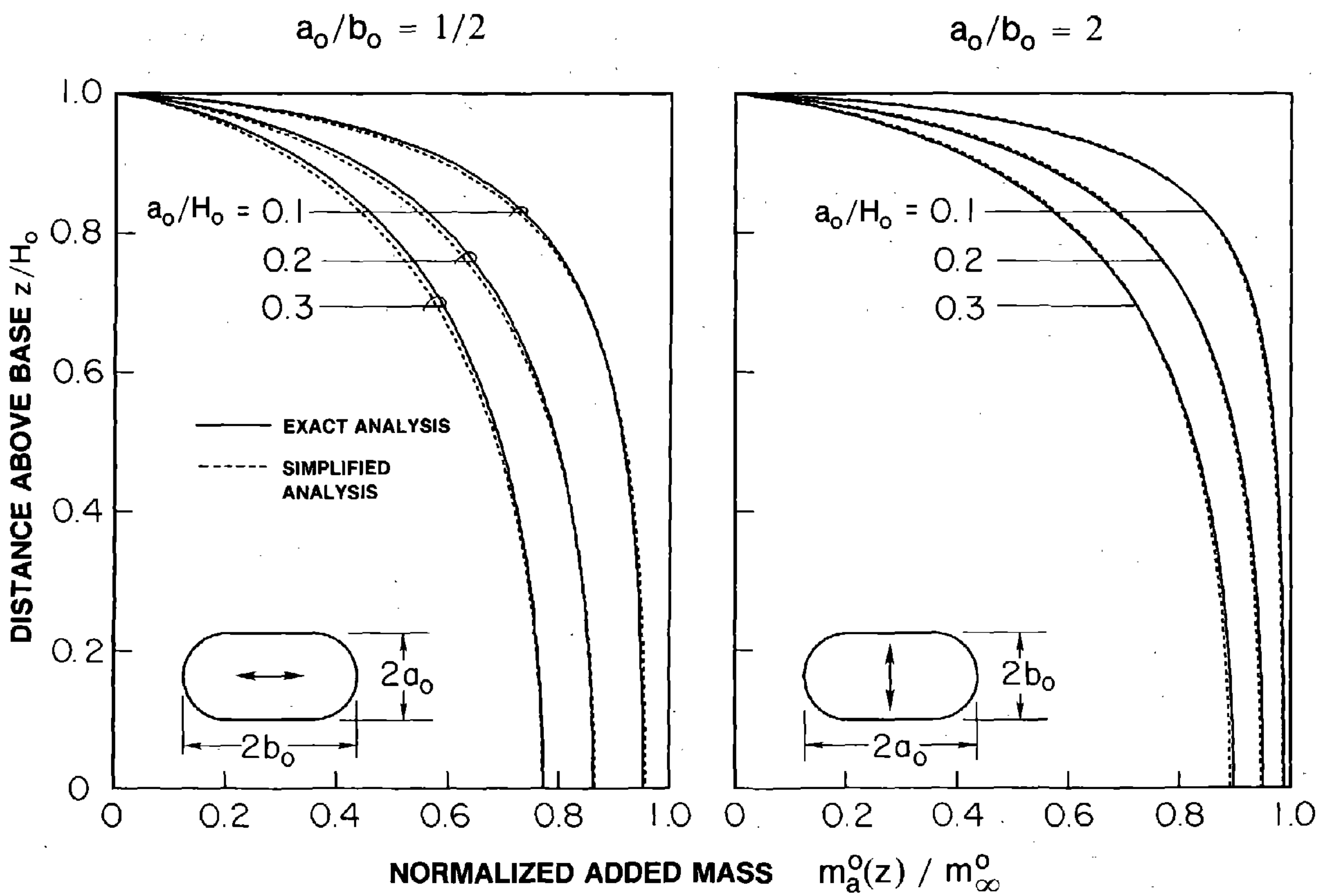

Figure 8.11 Comparison of Exact and Approximate (Simplified Analysis Procedure) Values of the Normalized Added Hydrodynamic Mass for Uniform Towers Associated with Surrounding Water

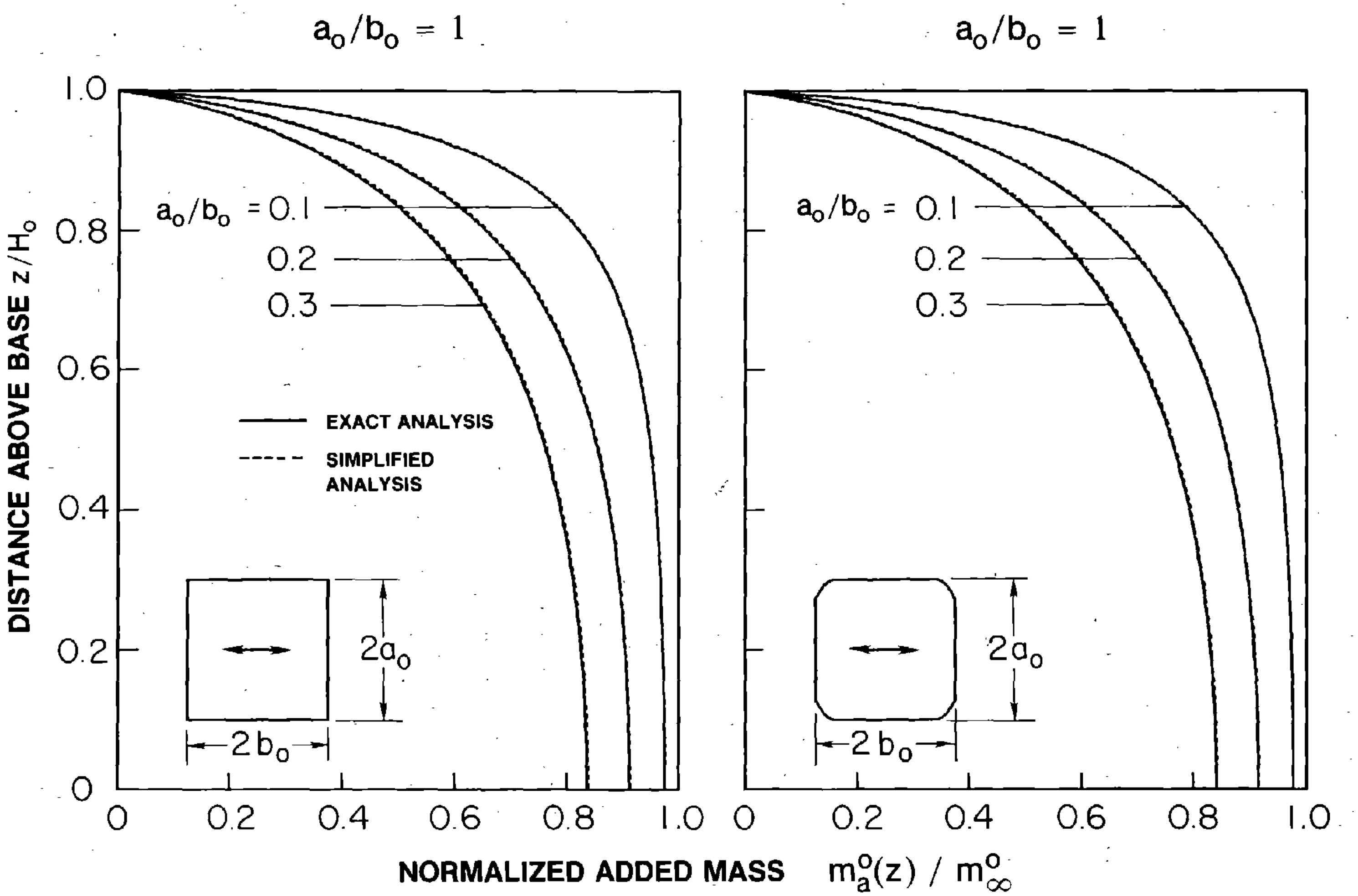

Figure 8.12 Comparison of Exact and Approximate (Simplified Analysis Procedure) Values of the Normalized Added Hydrodynamic Mass for Uniform Towers Associated with Surrounding Water

Such equivalent towers are shown for selected tapered towers in Figure 8.13. Because, as discussed earlier, $\tilde{r}_o/a_o$ is essentially independent of H_o/a_o, $\tilde{r}_o(z)$ is almost a linear function, i.e, if the cross-sectional dimensions of the actual tower decrease linearly with height, the equivalent axisymmetric towers also have close to a linear taper.

The normalized added hydrodynamic mass $m_a^o(z)/m_\infty^o(z)$ for selected non-uniform towers is presented in Figure 8.14 as determined by two methods : (1) exact three-dimensional hydrodynamic analysis of the surrounding water domain for the actual tower using the methods of Sections 4.3.1 to 4.3.3 ; and (2) exact, axisymmetric hydrodynamic analysis of the surrounding water domain for the equivalent axisymmetric tower by the procedures presented in Section 4.3.4. The added mass $m_a^o(z)$ at any location z of the tower has been normalized by $m_\infty^o(z)$, the added mass for the cross-section at the same location, i.e., the added mass per unit height of an infinitely long tower with that cross-section. The latter added mass is determined 'exactly' by a two-dimensional hydrodynamic analysis in the x-y plane (Appendix G). It is apparent that the equivalent axisymmetric tower provide results for normalized added hydrodynamic mass that are quite accurate.

Although, the evaluation of the normalized added hydrodynamic mass is considerably simplified in replacing the three-dimensional hydrodynamic analysis by an axisymmetric analysis, the latter is by no means simple enough or used widely enough in engineering practice to be convenient in practical application. However, it can be shown that, at the expense of some accuracy, a simple procedure can be developed [13]. The normalized added hydrodynamic mass $m_a^o(z)/m_\infty^o(z)$ at any location z of the equivalent axisymmetric tower, where the radius is $\tilde{r}_o(z)$, may be computed from the analytically obtained normalized added mass for a circular cylindrical tower with $r_o/H_o = \tilde{r}_o(z)/H_o$ [equation (8.2), Figure 8.1, or Table 8.4]. The resulting approximate values for the normalized added hydrodynamic mass are compared in Figure 8.15 with 'exact' solutions for axisymmetric tapered towers obtained by the rigorous analysis procedures of Section 4.3.4. It is apparent that the approximate

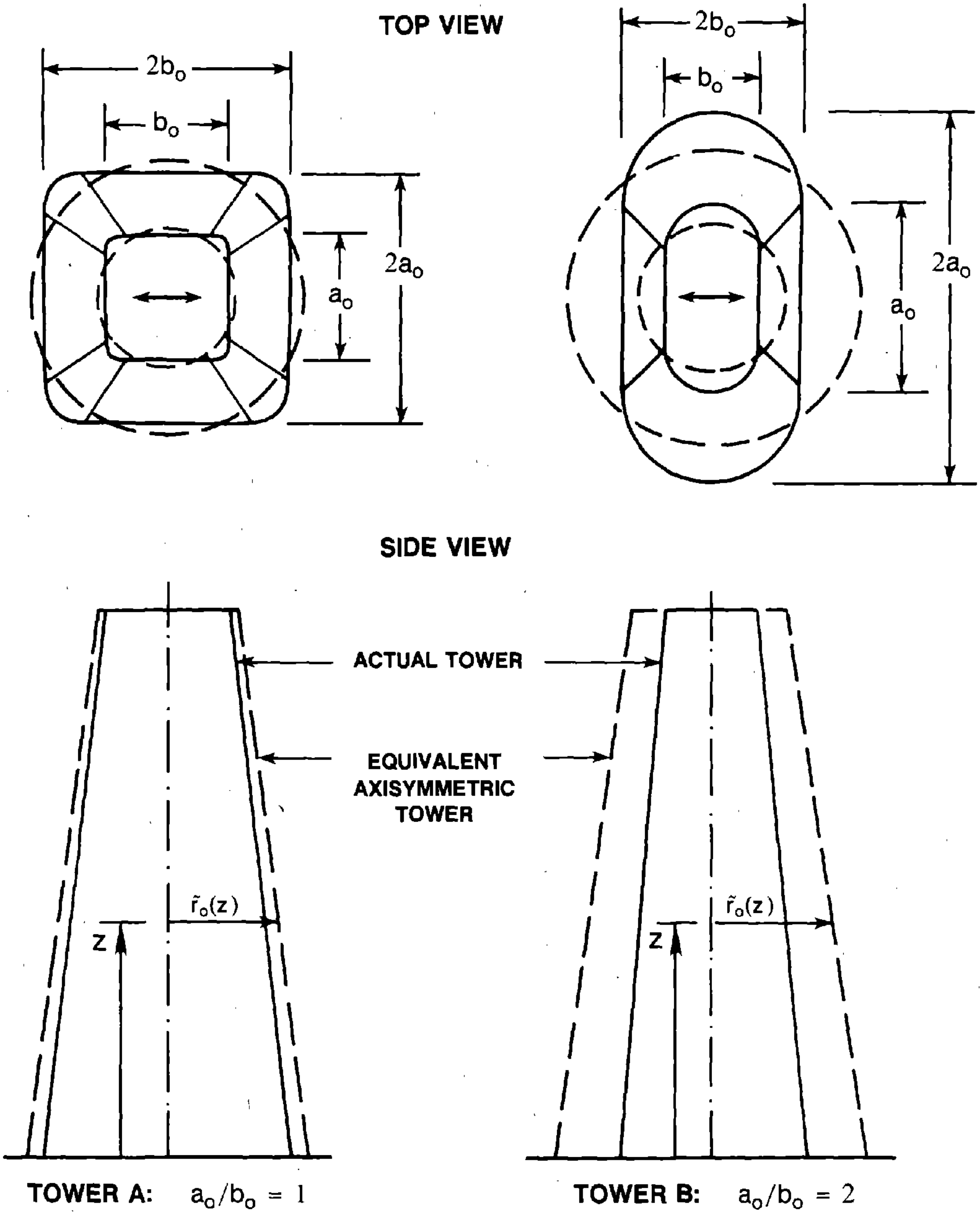

Figure 8.13 Equivalent Axisymmetric Towers for Two Non-Uniform Towers with Outside Surface Cross-Sections As Shown

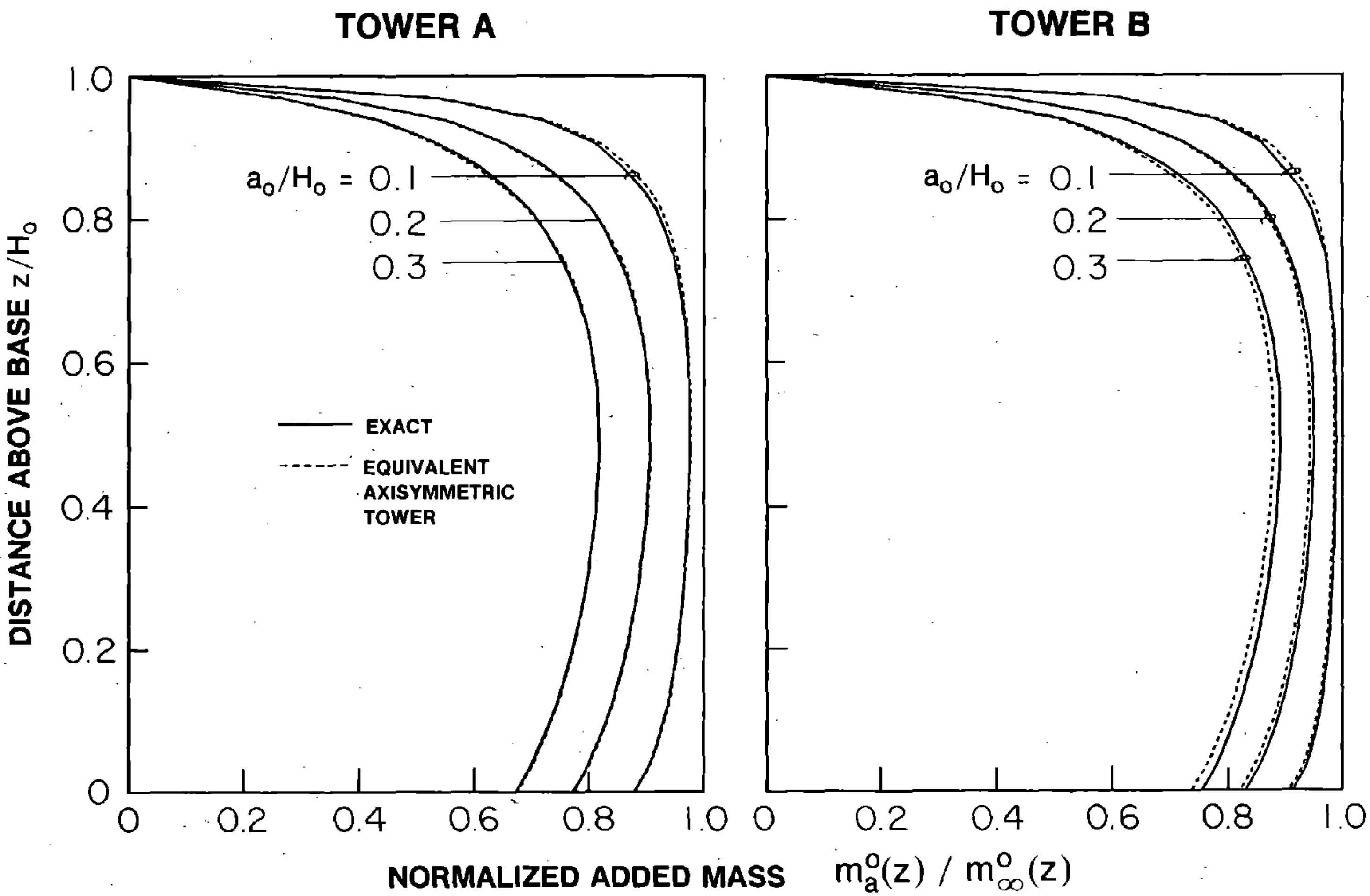

Figure 8.14 Comparison of Exact and Approximate (Equivalent Axisymmetric Tower) Values of the Normalized Added Hydrodynamic Mass for Two Non-Uniform Towers Associated with Surrounding Water

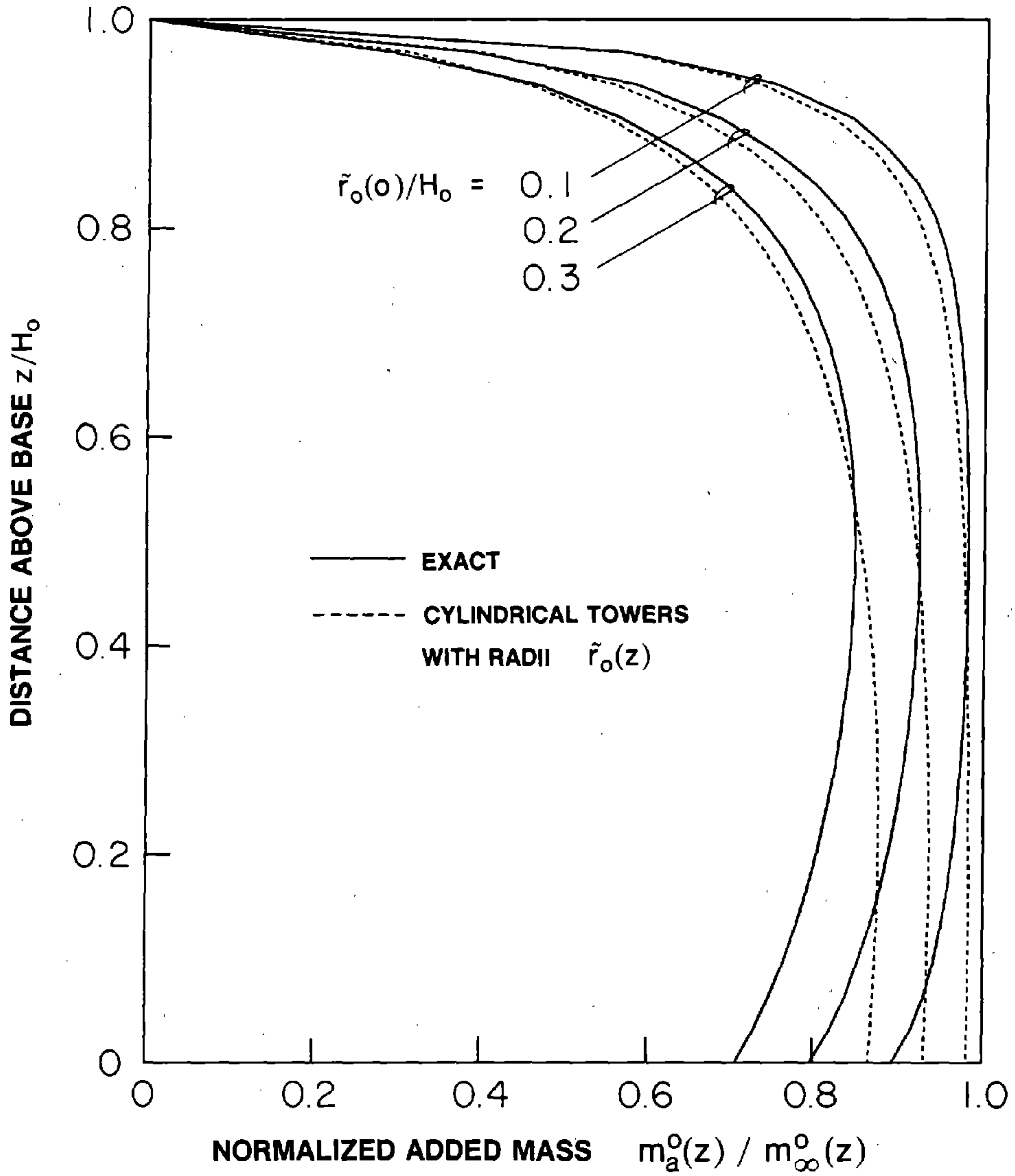

Figure 8.15 Comparison of Exact and Approximate [Circular Cylindrical Towers with Radii $\tilde{r}_0(z)$] Values of the Normalized Added Hydrodynamic Mass for Axisymmetric Tapered Towers Associated with Surrounding Water; $\tilde{r}_0(0)/\tilde{r}_0(H_s)$ = 2

procedure leads to good results for the upper half of the tower. Because the vibration frequencies and mode shapes of the tower would not be much affected by the errors in the added mass near the tower base, this simplified procedure should be accurate enough for the preliminary phase of design and safety evaluation of towers.

8.2.4 Non-Uniform Towers -- Summary

Based on the analysis and results presented earlier, the added hydrodynamic mass associated with surrounding water for non-uniform towers of arbitrary cross-section with two axes of symmetry can be determined by the following steps :

1. Select a sufficient number of locations along the height where the added hydrodynamic mass for the non-uniform tower will be estimated to obtain the the height-wise distribution of added mass $m_a^o(z)$. Compute the height coordinate z for the selected locations.

2. Determine the cross-sectional radius $\tilde{r}_o(z)$ of the equivalent axisymmetric tower at a selected location z. This is achieved by using the procedure for uniform towers (Section 8.2.2) with the cross-section of the uniform tower taken to be the same as the actual cross-section pertaining to that location.

3. Evaluate the normalized added hydrodynamic mass for the equivalent axisymmetric tower at the selected location z as the normalized mass from Figure 8.1 (or Table 8.4) for a circular cylindrical tower corresponding to $r_o/H_o = \tilde{r}_o(z)/H_o$ pertaining to that location, determined in step 2.

4. Compute the added hydrodynamic mass $m_\infty^o(z=0)$ for an infinitely long tower with its cross-section same as at the base of the actual tower from either Table 8.1 or a two-dimensional analysis of the Laplace equation for the surrounding water domain (Appendix G). If the shape of the cross-section of the actual tower is unchanged along its height and only its dimensions vary, determine the added mass $m_\infty^o(z)$ at the selected location z by recognizing that the ratio $m_\infty^o(z)/m_\infty^o(0)$

is equal to the ratio $A_o(z)/A_o(0)$ of the cross-sectional areas at the two locations. If the cross-sectional shape changes, evaluate $m_\infty^o(z)$ directly from the cross-sectional properties of the actual tower at the location z selected in step 2 (Appendix G).

5. Determine the added hydrodynamic mass $m_a^o(z)$ for the actual tower at the location z selected in step 2 by multiplying the normalized added mass, determined in step 3, by $m_\infty^o(z)$ for that location computed in step 4.

6. Repeat steps 2 to 5 for various locations along the tower height, selected in step 1, to obtain the complete distribution of added hydrodynamic mass for a non-uniform tower.

For selected non-uniform towers (Figure 8.13), the added hydrodynamic mass associated with outside water has been determined by two methods : (1) the simplified analysis procedure just summarized, and (2) the 'exact' analysis procedure presented in Sections 4.3.1 to 4.3.3. It is apparent from Figure 8.16 that the simplified procedure leads to results that seem accurate enough for use in preliminary design and safety evaluation of towers, especially for slender towers.

8.3 Added Hydrodynamic Mass for Inside Water

8.3.1 Uniform Towers

The added hydrodynamic mass for circular cylindrical towers associated with hydrodynamic effects of inside water, obtained from an analytical solution of the Laplace equation [29,40], is :

$$m_a^i(z/H_i) = (\rho_w \pi r_i^2) \cdot \left[\frac{16}{\pi^2} \frac{H_i}{r_i} \sum_{m=1}^{\infty} \frac{(-1)^{m-1}}{(2m-1)^2} D_m(\alpha_m r_i/H_i) \cos(\alpha_m z/H_i) \right] \tag{8.6}$$

where z = distance above the base of the tower, H_i = depth of the inside water, ρ_w = mass density of water, r_i = radius of the inside surface of the tower, $\alpha_m = (2m-1)\pi/2$, and

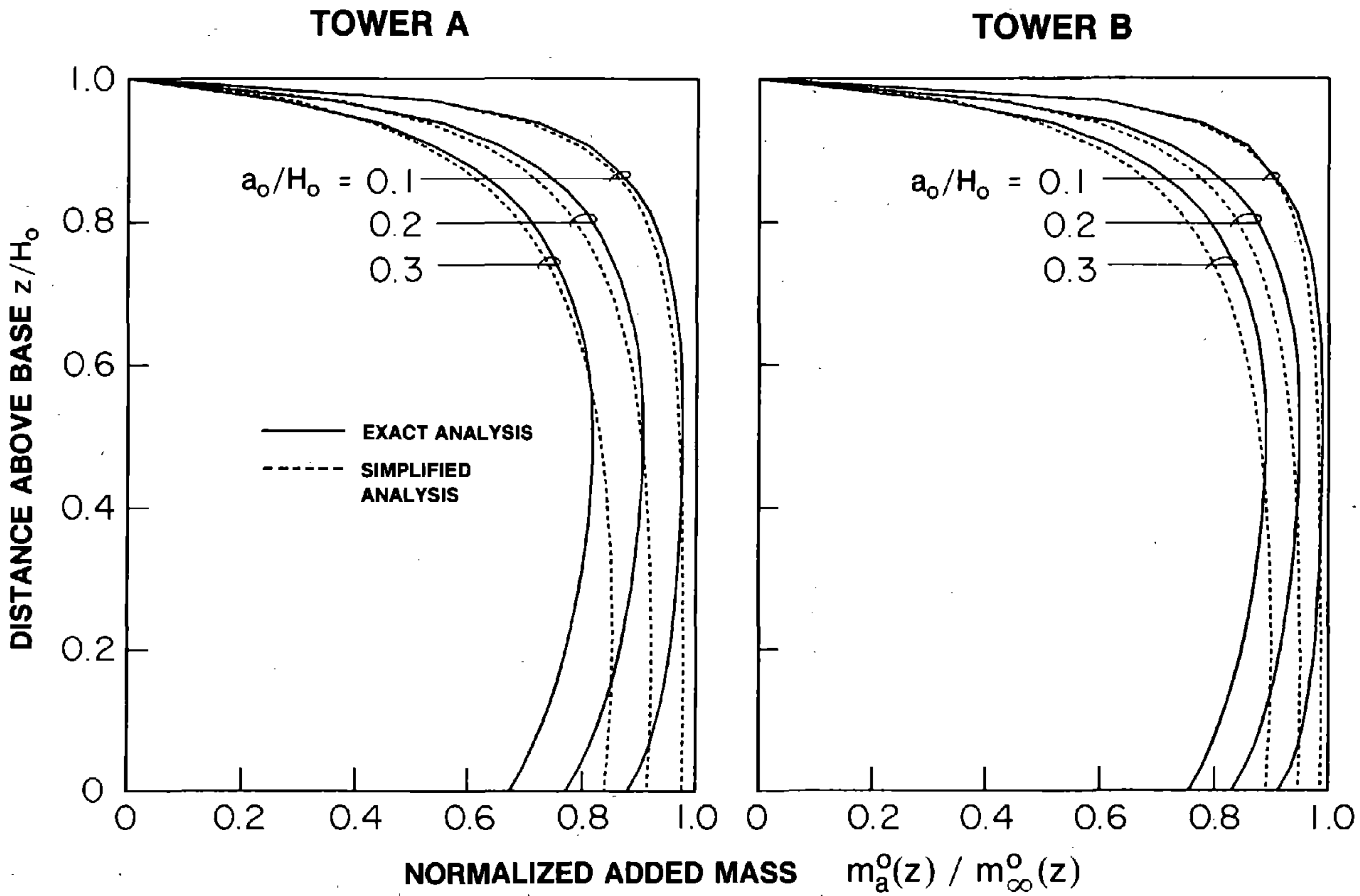

Figure 8.16 Comparison of Exact and Approximate (Simplified Analysis Procedure) Values of the Normalized Added Hydrodynamic Mass for Two Non-Uniform Towers Associated with Surrounding Water

$$D_m(\alpha_m r_i/H_i) = \frac{I_1(\alpha_m r_i/H_i)}{I_0(\alpha_m r_i/H_i) + I_2(\alpha_m r_i/H_i)} \tag{8.7}$$

in which I_n is the modified Bessel function of order n of the first kind. For an infinitely-long tower with the same circular cross-section, the added mass per unit of height is :

$$m_\infty^i = \rho_w \, \pi \, r_i^2 \tag{8.8}$$

which is equal to the mass of the water contained within the hollow tower per unit height. The normalized added mass $m_a^i(z)/m_\infty^i$ for circular cylindrical towers is presented in Figure 8.17 for a range of values of r_i/H_i, the ratio of the inside radius to water depth. It is apparent that the normalized added mass is unity for the limiting case of an infinitely slender tower (i.e. $H_i/r_i = \infty$), and it decreases as the tower becomes more squat, i.e. the slenderness ratio H_i/r_i decreases. When compared with the normalized added mass of surrounding water (Figure 8.1), it is apparent that for the same slenderness ratio, the normalized added mass for the inside water is larger.

For a uniform tower of arbitrary cross-section, the added hydrodynamic mass can also be determined by solving the Laplace equation for the inside water domain. In this case, however, analytical solutions are generally not feasible and discrete methods of Chapter 4 are necessary for computing the added hydrodynamic mass. Solution of a three-dimensional boundary value problem (BVP) is required to evaluate $m_a^i(z)$ [Section 4.4]. However, it can be demonstrated [Appendix G, Section G.2] that for any tower cross-section

$$m_\infty^i = \rho_w \, A_i \tag{8.9}$$

where A_i is the cross-sectional area of the inside surface of the tower (Appendix G, Section G.2). Thus, m_∞^i is simply equal to the mass of the water contained within the hollow, uniform tower per unit of height.

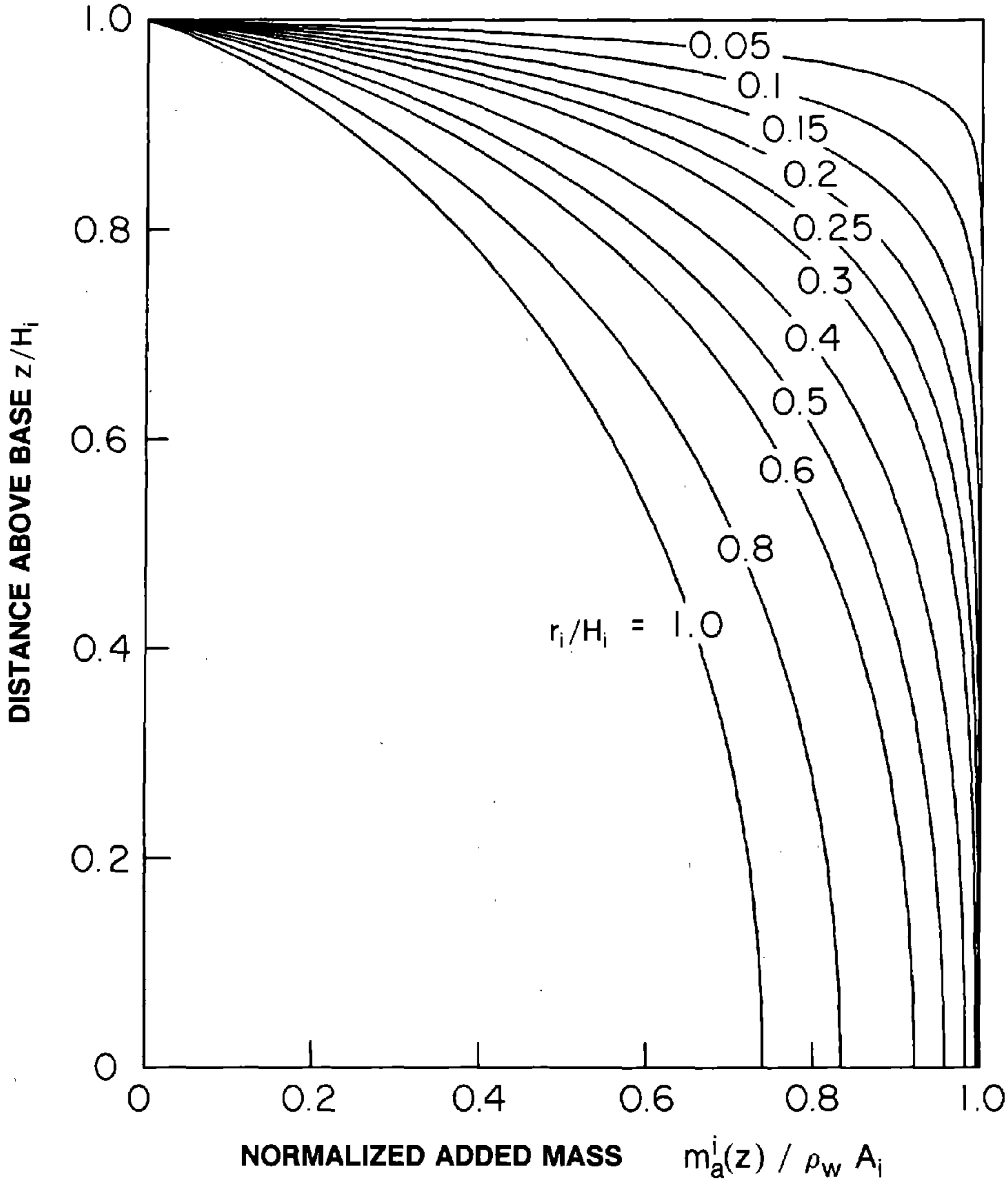

Figure 8.17 Normalized Added Hydrodynamic Mass for Circular Cylindrical Towers Associated with Inside Water

It has been demonstrated in Section 8.2.1 that the normalized added hydrodynamic mass $m_a^o(z)/m_\infty^o$ associated with surrounding water for a uniform tower of arbitrary cross-section is essentially the same as that for an "equivalent" circular cylindrical tower. A procedure to determine the properties of the equivalent tower was summarized in Section 8.2.2. Once these properties have been determined, the normalized added hydrodynamic mass is directly obtained from the analytical results for circular cylindrical towers. These concepts are also applicable to the analysis of the inside water domain, which could have been demonstrated in a manner similar to Section 8.2.1. Without going through the detailed development, a simplified procedure parallel to the presentation of Section 8.2.2 for surrounding water is summarized next for inside water.

8.3.2 Uniform Towers -- Summary

Consider a uniform tower of arbitrary cross-section with two axes of symmetry having an interior cross-section with area A_i, width $2a_i$ perpendicular to the direction of ground motion and interior dimension $2b_i$ along the direction of ground motion , and the interior water depth equal to H_i. The added hydrodynamic mass associated with inside water may be determined by the following steps :

1. Evaluate the properties of the 'equivalent' uniform, elliptical tower with interior cross-sectional dimensions $2\tilde{a}_i$ and $2\tilde{b}_i$ perpendicular and along the direction of ground motion, respectively. The ratio $\tilde{a}_i/\tilde{b}_i$ and the slenderness ratio $H_i/\tilde{a}_i$ are given by

$$\frac{H_i}{\tilde{a}_i} = \frac{H_i}{\sqrt{A_i/\pi}} \cdot \sqrt{\frac{b_i}{a_i}} \tag{8.10a}$$

$$\frac{\tilde{a}_i}{\tilde{b}_i} = \frac{a_i}{b_i} \tag{8.10b}$$

2. Evaluate the slenderness ratio $H_i/\tilde{r}_i$ of the 'equivalent', circular cylindrical tower from the properties $\tilde{a}_i/\tilde{b}_i$ and $H_i/\tilde{a}_i$ determined in step 1 for the equivalent, elliptical tower using the data of Figure 8.18. These data were developed by procedures parallel to those of section 8.2.1. However, when the data of Figure 8.18 is presented in the form of Figure 8.19, it is apparent that, for all values of the ratio $\tilde{a}_i/\tilde{b}_i$, $\tilde{r}_i = \tilde{b}_i$ which after utilizing equation (8.10) becomes :

$$\tilde{r}_i = \sqrt{\frac{A_i}{\pi} \cdot \frac{b_i}{a_i}} \tag{8.11}$$

3. Evaluate the normalized added mass $m_a^i(z)/m_\infty^i$ for the circular cylindrical tower with slenderness ratio $H_i/\tilde{r}_i$, determined in step 2, from Figure 8.17 or Table 8.5. Use linear interpolation for intermediate values of $\tilde{r}_i/H_i$.

4. Determine the added hydrodynamic mass $m_a^i(z)$ for the actual tower by multiplying the normalized added mass determined in step 3 by $m_\infty^i = \rho_w A_i$.

For uniform towers of selected cross-sections and each with three different values of the slenderness ratio H_i/a_i, the added hydrodynamic mass associated with inside water has been determined by two methods : (1) the simplified analysis procedure just summarized, and (2) the 'exact' analysis procedure of Section 4.4. It is apparent from Figures 8.20 to 8.22 that the results obtained by the simplified procedure are excellent indeed for a wide range of parameters. A comparison of Figures 8.20 to 8.22 with Figures 8.10 to 8.12 indicates that the simplified procedure works better for inside water than it does for surrounding water. In both cases, the simplified procedure is accurate enough for analyzing towers in their preliminary phase of design or safety evaluation.

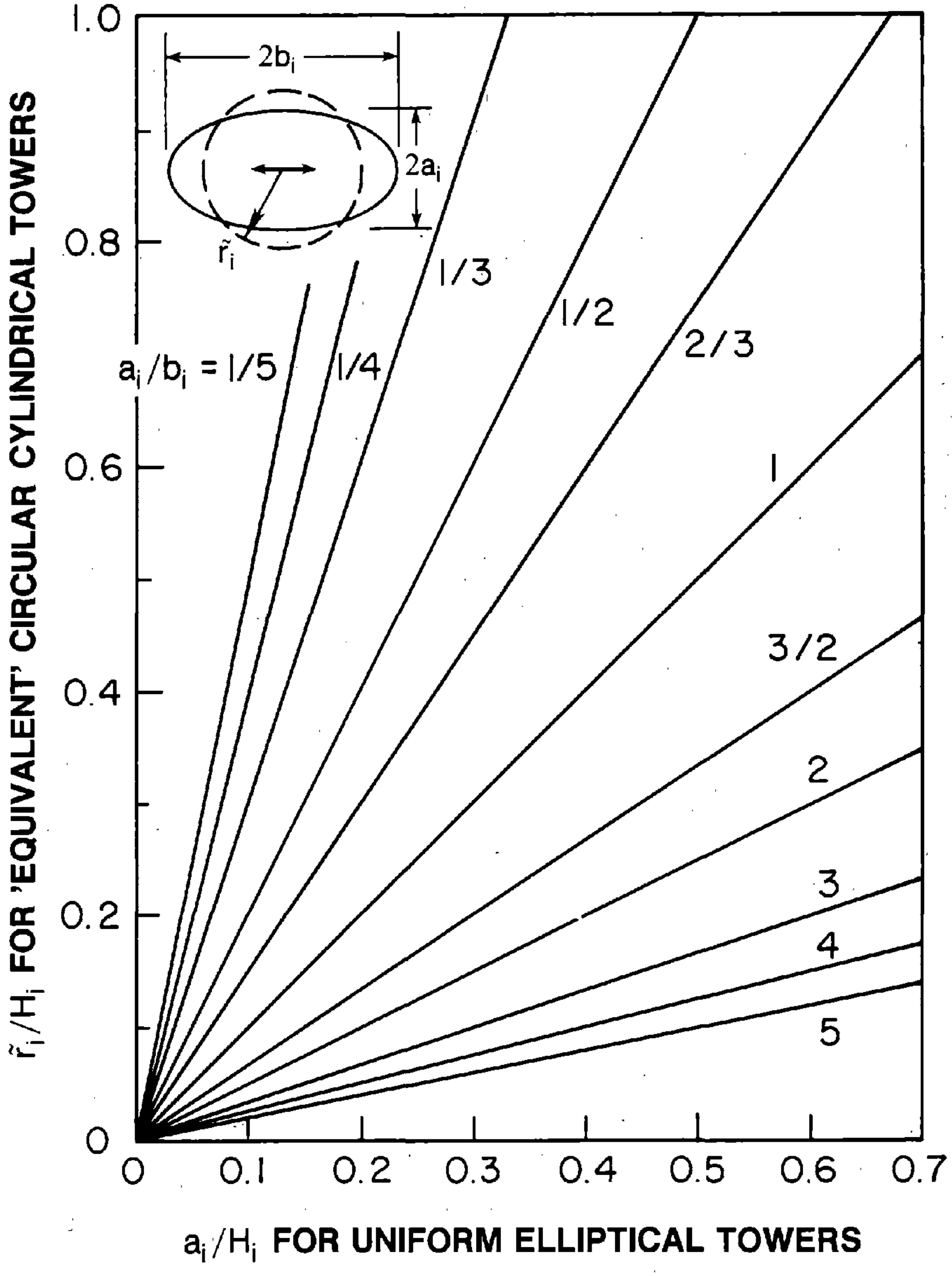

Figure 8.18 Properties of 'Equivalent' Circular Cylindrical Towers for Uniform Elliptical Towers Associated with Added Hydrodynamic Mass due to Inside Water

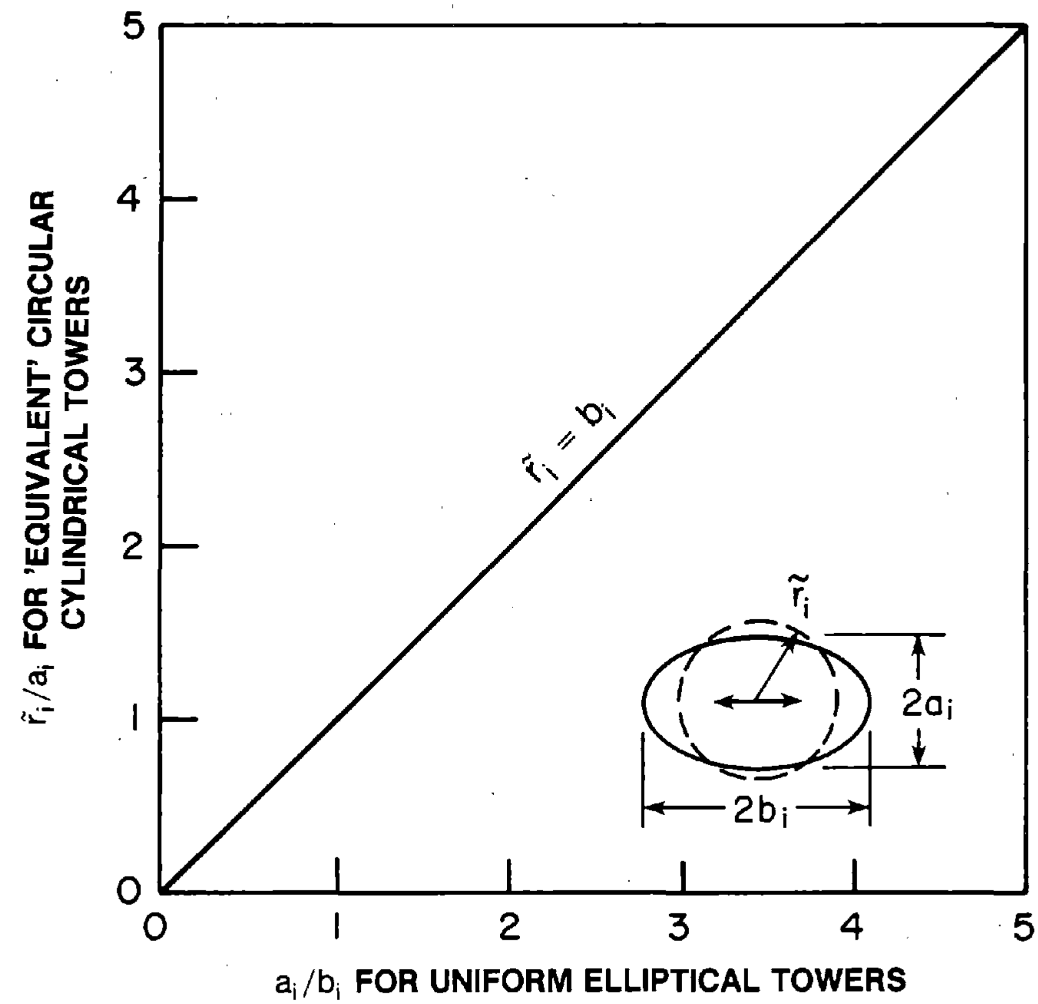

Figure 8.19 Properties of 'Equivalent' Circular Cylindrical Towers for Uniform Elliptical Towers Associated with Hydrodynamic Added Mass due to Inside Water

Table 8.5 -- Normalized Added Mass $m_a^i(z)/\rho_w A_i$ for Circular Cylindrical Towers Associated with Inside Water

z/H_i	r_i/H_i										
	0.05	0.10	0.15	0.20	0.25	0.30	0.40	0.50	0.60	0.80	1.00
1.00	0.000	0.000	0.000	0.000	0.000	0.000	0.000	0.000	0.000	0.000	0.000
0.98	0.588	0.388	0.295	0.240	0.204	0.178	0.143	0.120	0.104	0.082	0.067
0.96	0.806	0.589	0.466	0.388	0.335	0.295	0.240	0.204	0.177	0.141	0.117
0.94	0.907	0.719	0.589	0.501	0.437	0.389	0.320	0.274	0.240	0.192	0.160
0.92	0.956	0.807	0.682	0.589	0.520	0.466	0.389	0.334	0.294	0.237	0.198
0.90	0.979	0.867	0.752	0.661	0.589	0.533	0.448	0.388	0.343	0.278	0.233
0.88	0.990	0.908	0.807	0.719	0.648	0.590	0.501	0.436	0.387	0.316	0.265
0.86	0.995	0.936	0.849	0.767	0.698	0.639	0.548	0.480	0.428	0.350	0.295
0.84	0.997	0.956	0.882	0.807	0.740	0.682	0.589	0.520	0.465	0.382	0.322
0.82	0.999	0.969	0.908	0.840	0.776	0.720	0.627	0.556	0.499	0.412	0.349
0.80	0.999	0.979	0.928	0.867	0.807	0.753	0.661	0.589	0.530	0.440	0.373
0.78	1.000	0.985	0.944	0.889	0.834	0.782	0.692	0.619	0.560	0.467	0.396
0.76	1.000	0.990	0.956	0.908	0.857	0.807	0.719	0.647	0.587	0.491	0.418
0.74	1.000	0.993	0.965	0.923	0.876	0.830	0.744	0.673	0.612	0.514	0.439
0.72	1.000	0.995	0.973	0.936	0.893	0.849	0.767	0.696	0.635	0.536	0.458
0.70	1.000	0.997	0.979	0.947	0.908	0.867	0.788	0.718	0.657	0.557	0.477
0.68	1.000	0.998	0.983	0.956	0.921	0.882	0.807	0.738	0.678	0.576	0.495
0.66	1.000	0.998	0.987	0.963	0.931	0.896	0.824	0.757	0.697	0.595	0.511

Table 8.5 (Continued)

z/H_i	r_i/H_i										
	0.05	0.10	0.15	0.20	0.25	0.30	0.40	0.50	0.60	0.80	1.00
0.64	1.000	0.999	0.990	0.969	0.941	0.908	0.839	0.774	0.715	0.612	0.527
0.62	1.000	0.999	0.992	0.975	0.949	0.919	0.853	0.790	0.731	0.628	0.542
0.60	1.000	0.999	0.994	0.979	0.956	0.928	0.866	0.805	0.747	0.644	0.557
0.56	1.000	1.000	0.996	0.985	0.967	0.944	0.889	0.831	0.775	0.672	0.583
0.52	1.000	1.000	0.998	0.990	0.976	0.956	0.907	0.854	0.800	0.697	0.607
0.48	1.000	1.000	0.998	0.993	0.982	0.965	0.923	0.873	0.821	0.720	0.628
0.44	1.000	1.000	0.999	0.995	0.986	0.973	0.935	0.889	0.840	0.740	0.647
0.40	1.000	1.000	0.999	0.997	0.990	0.979	0.946	0.903	0.856	0.757	0.664
0.36	1.000	1.000	1.000	0.998	0.992	0.983	0.954	0.915	0.870	0.773	0.679
0.32	1.000	1.000	1.000	0.998	0.994	0.987	0.961	0.925	0.882	0.786	0.693
0.28	1.000	1.000	1.000	0.999	0.996	0.990	0.967	0.933	0.892	0.798	0.704
0.24	1.000	1.000	1.000	0.999	0.997	0.992	0.972	0.940	0.900	0.808	0.714
0.20	1.000	1.000	1.000	0.999	0.998	0.993	0.976	0.946	0.907	0.816	0.722
0.16	1.000	1.000	1.000	1.000	0.998	0.994	0.978	0.950	0.913	0.822	0.729
0.12	1.000	1.000	1.000	1.000	0.998	0.995	0.981	0.954	0.917	0.827	0.734
0.08	1.000	1.000	1.000	1.000	0.999	0.996	0.982	0.956	0.920	0.831	0.737
0.04	1.000	1.000	1.000	1.000	0.999	0.996	0.983	0.957	0.922	0.833	0.740
0.00	1.000	1.000	1.000	1.000	0.999	0.996	0.983	0.958	0.922	0.834	0.740

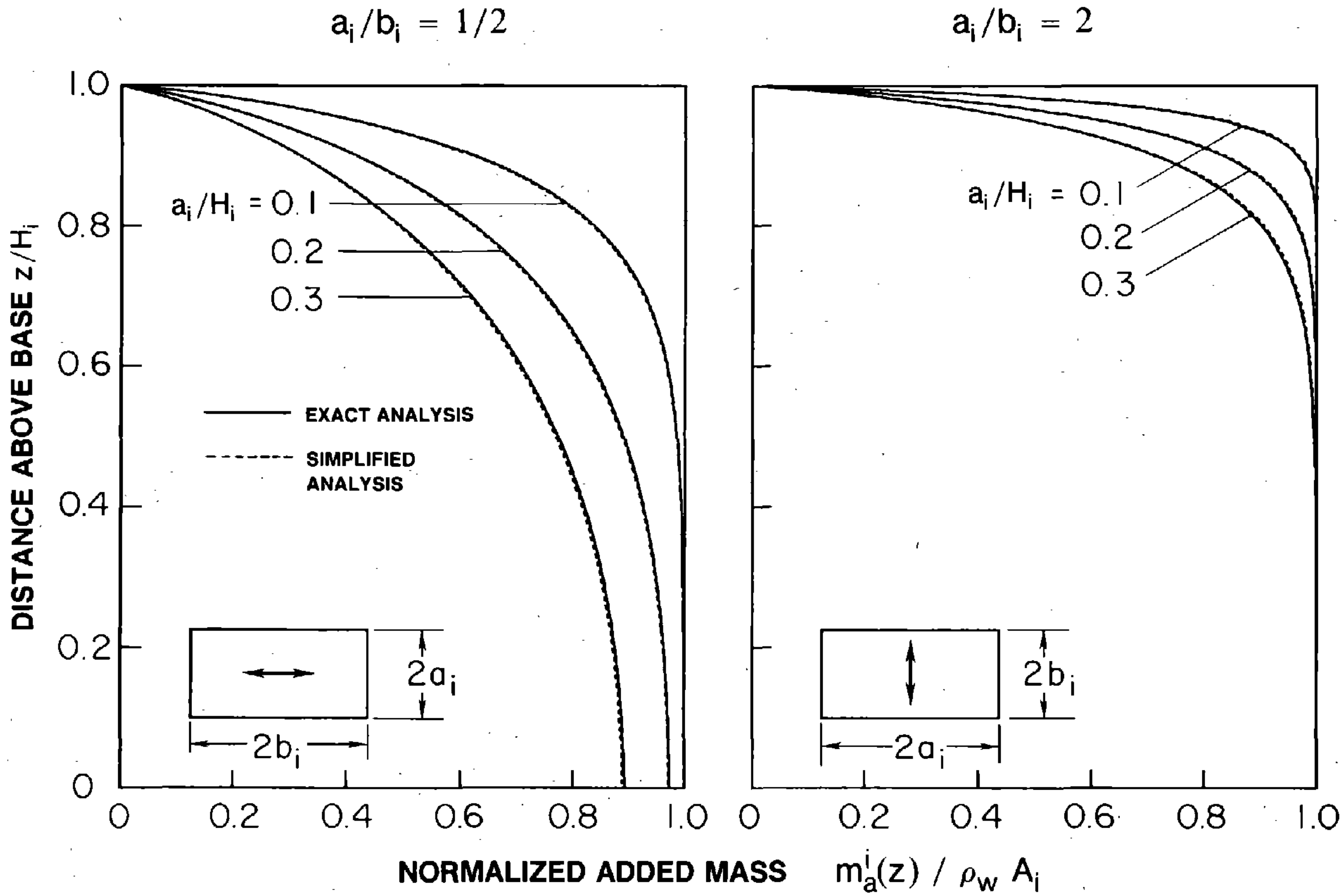

Figure 8.20 Comparison of Exact and Approximate (Simplified Analysis Procedure) Values of the Normalized Added Hydrodynamic Mass for Uniform Towers Associated with Inside Water

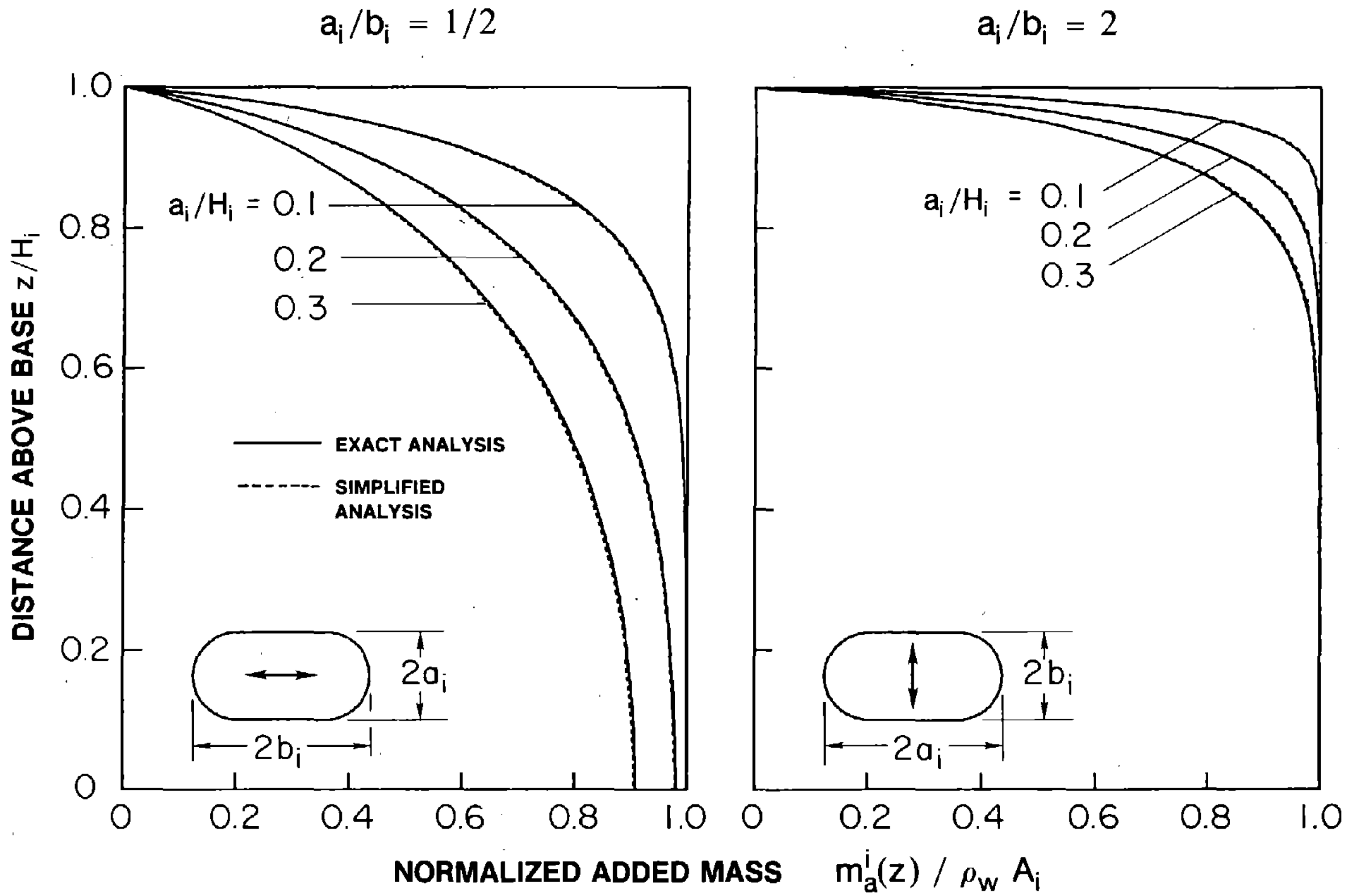

Figure 8.21 Comparison of Exact and Approximate (Simplified Analysis Procedure) Values of the Normalized Added Hydrodynamic Mass for Uniform Towers Associated with Inside Water

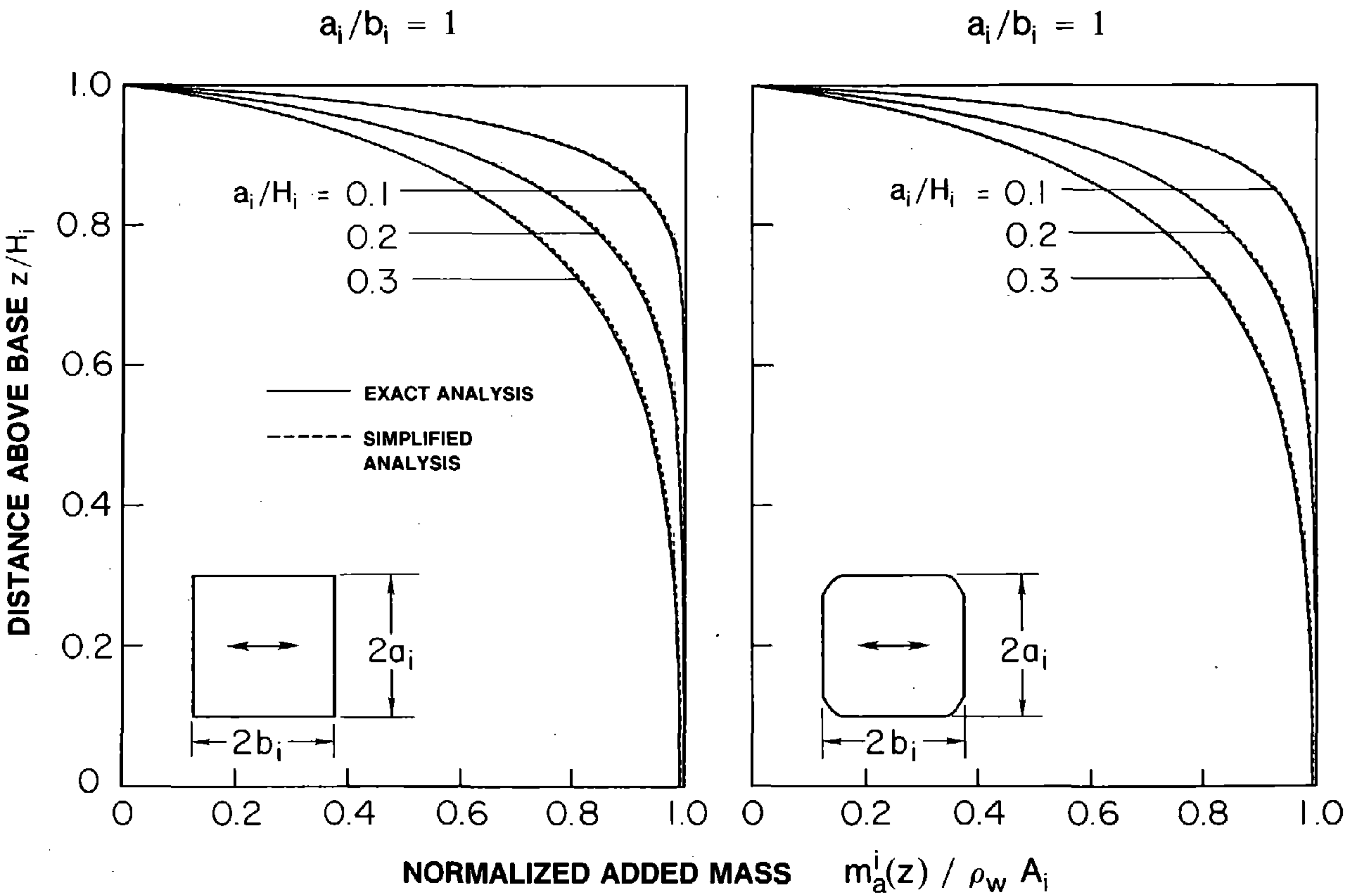

Figure 8.22 Comparison of Exact and Approximate (Simplified Analysis Procedure) Values of the Normalized Added Hydrodynamic Mass for Uniform Towers Associated with Inside Water

8.3.3 Non-Uniform Towers

It has been demonstrated in Section 8.2.3 that, for purposes of evaluating the added hydrodynamic mass associated with water surrounding a non-uniform tower, it is possible to define an 'equivalent' axisymmetric tower, i.e. a tower with its exterior surface having a circular cross-section, with its radius $\tilde{r}_o(z)$ varying with height.

This idea works even better for inside water. The interior radius $\tilde{r}_i(z)$ of the equivalent axisymmetric tower would be determined as in the case of surrounding water, by applying the procedure for uniform towers (steps 1 and 2 of Section 8.3.2) successively for several locations along the height. At each location, the cross-section of the uniform tower is taken as the cross-section at that location of the actual tower. This is demonstrated in Figure 8.24 where the normalized added hydrodynamic mass $m_a^i(z)/m_\infty^i(z)$ is presented for selected towers (Figure 8.23) as determined by two methods : (1) exact three-dimensional analysis of the inside water domain for the actual tower using the methods of Section 4.4.2 ; and (2) exact, axisymmetric hydrodynamic analysis of the inside water domain for the equivalent axisymmetric tower by the procedure presented in Section 4.4.3. It is apparent that the agreement between the results from the two analyses is excellent.

It was also shown in Section 8.2.3 that the normalized added hydrodynamic mass at each cross-section of the equivalent axisymmetric tower could be computed to a satisfactory degree of accuracy from the analytical results for a circular cylindrical tower. It can be shown that this concept is also satisfactory for evaluating the added hydrodynamic mass associated with water contained inside an axisymmetric tower. Thus, the normalized added hydrodynamic mass $m_a^i(z)/m_\infty^i(z)$ at any location z, where the radius is $\tilde{r}_i(z)$, of the equivalent axisymmetric tower may be computed from the analytically obtained results for a circular cylindrical tower with $r_i/H_i = \tilde{r}_i(z)/H_i$ [equation (8.6), Figure 8.17 or Table 8.5]. The resulting approximate values appear to be satisfactory for preliminary analysis of towers (Figure 8.25). Therefore, a simplified procedure, parallel to the presentation of Section 8.2.4

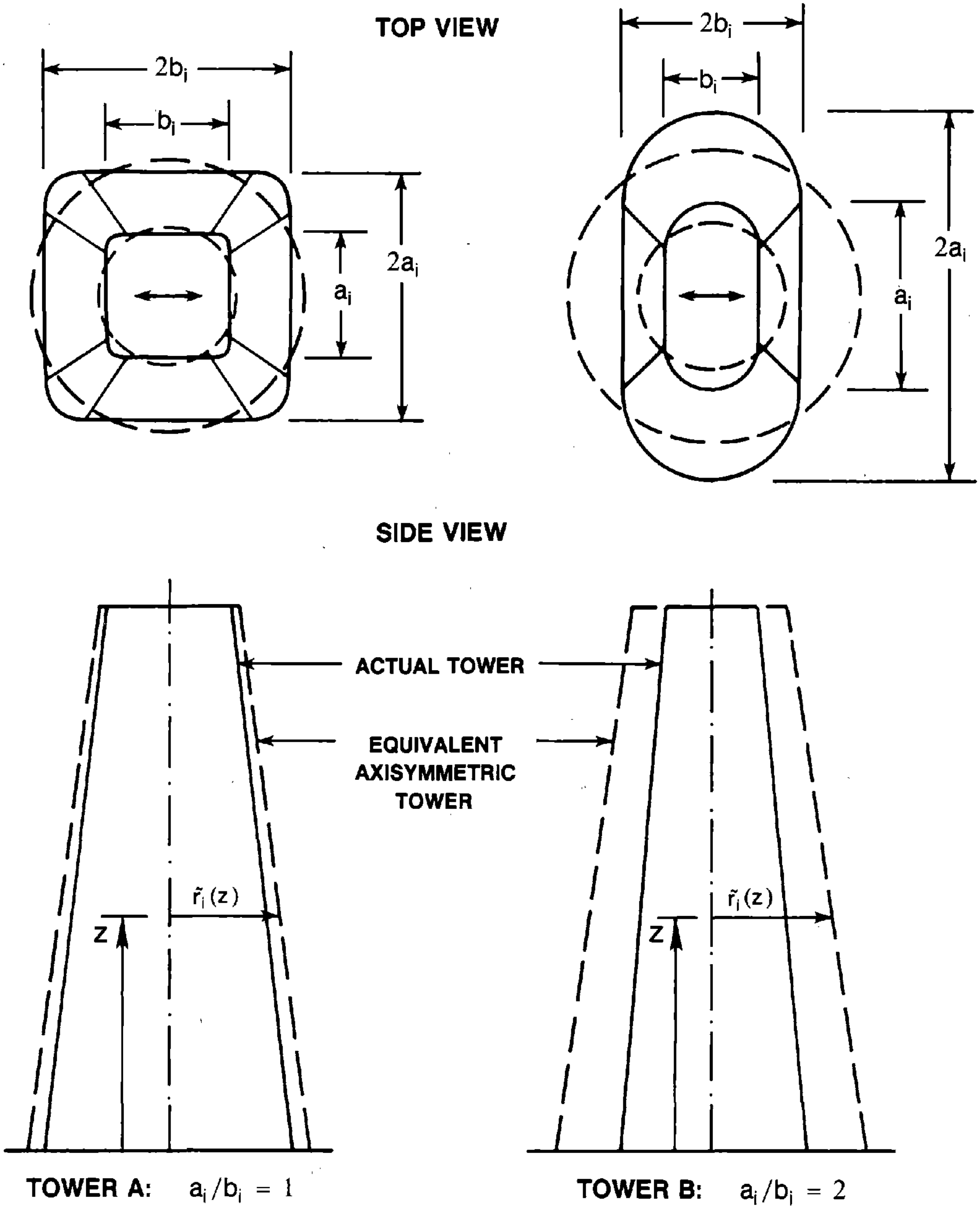

Figure 8.23 Equivalent Axisymmetric Towers for Two Non-Uniform Towers with Inside Surface Cross-Sections As Shown

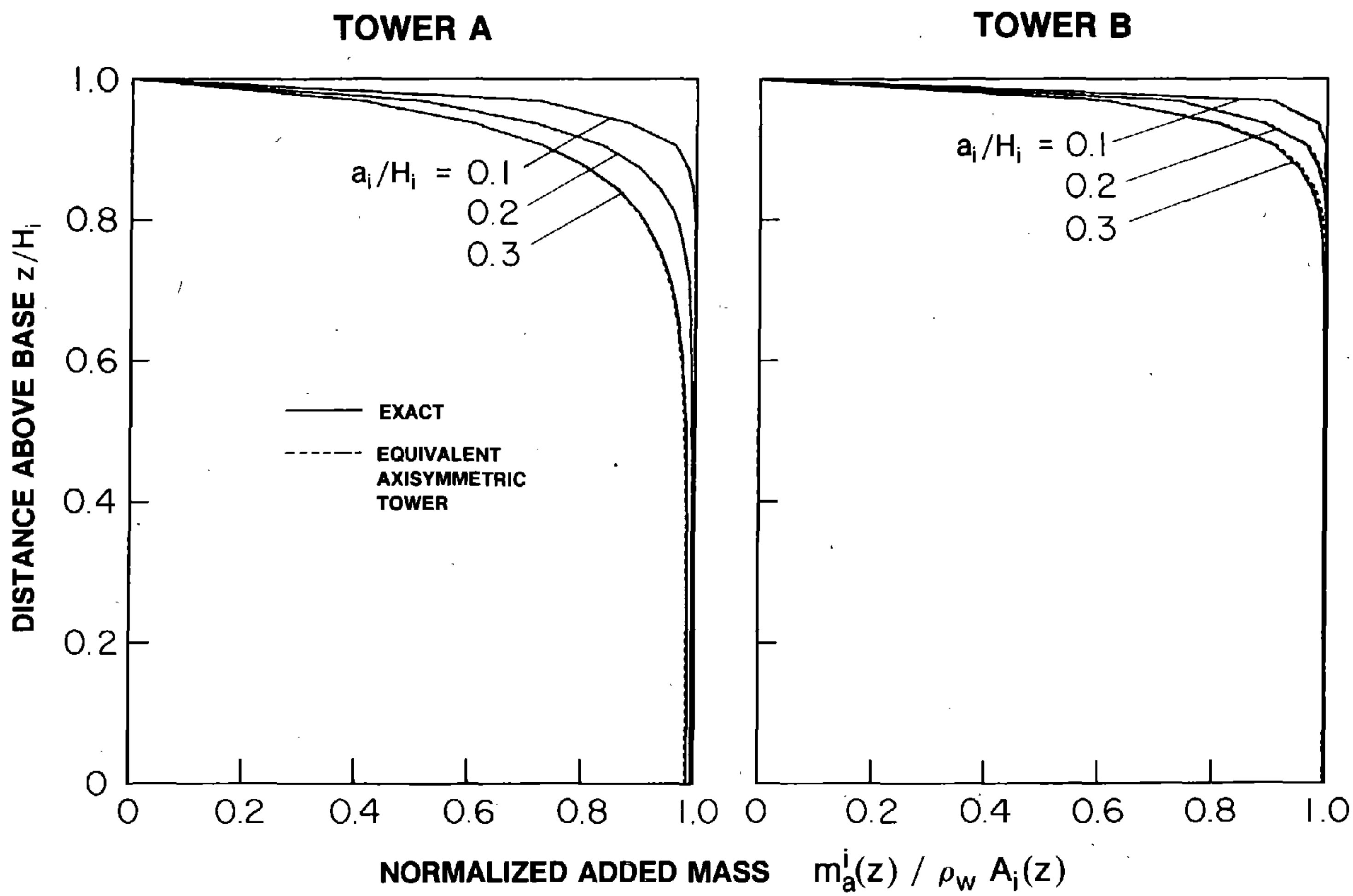

Figure 8.24 Comparison of Exact and Approximate ('Equivalent' Axisymmetric Tower) Values of the Normalized Added Hydrodynamic Mass for Two Non-Uniform Towers Associated with Inside Water

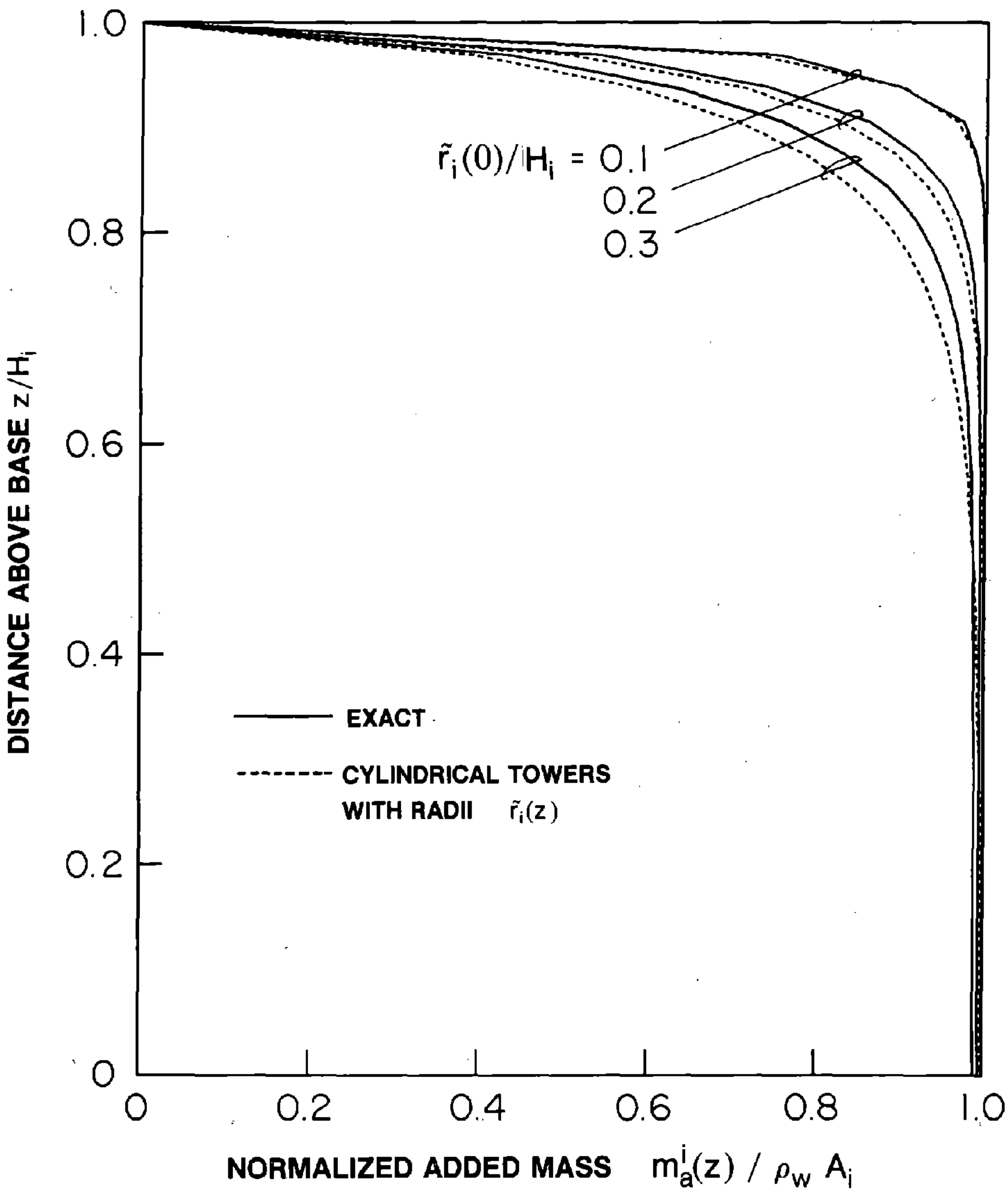

Figure 8.25 Comparison of Exact and Approximate [Circular Cylindrical Towers with Radii $\tilde{r}_i(z)$] Values of the Normalized Added Hydrodynamic Mass for Axisymmetric Tapered Towers Associated with Inside Water; $\tilde{r}_i(0)/\tilde{r}_i(H_s)$ = 2

for surrounding water, is summarized next for inside water.

8.3.4 Non-Uniform Towers -- Summary

Based on the analysis and results presented earlier, the added hydrodynamic mass associated with inside water for non-uniform towers of arbitrary cross-section with two axes of symmetry can be determined by the following steps :

1. Select a sufficient number of locations along the height where the added hydrodynamic mass for the non-uniform tower will be estimated to obtain the height-wise distribution of added mass $m_a^i(z)$. Compute the height coordinate z for the selected locations.

2. Determine the cross-sectional radius $\tilde{r}_i(z)$ of the equivalent axisymmetric tower at a selected location z. This is achieved by using the procedure for uniform towers [equation (8.11)] with the cross-section of the uniform tower taken to be the same as the actual cross-section pertaining to that location.

3. Evaluate the normalized added hydrodynamic mass for the equivalent axisymmetric tower at the selected location z as the normalized mass from Figure 8.17 (or Table 8.5) for a circular cylindrical tower corresponding to $r_i/H_i = \tilde{r}_i(z)/H_i$ pertaining to that location, determined in step 2.

4. Determine the added hydrodynamic mass $m_a^i(z)$ for the actual tower at location z selected in step 2 by multiplying the normalized added mass, determined in step 3, by $m_\infty^i(z)$ for that location. If $A_i(z)$ is the area of the interior cross-section, $m_\infty^i(z) = \rho_w A_i(z)$.

5. Repeat steps 2 to 4 for various locations along the tower height, selected in step 1, to obtain the complete distribution of added hydrodynamic mass $m_a^i(z)$ for a non-uniform tower.

For selected non-uniform towers (Figure 8.23), the added hydrodynamic mass associated with inside water has been determined by two methods : (1) the simplified analysis procedure just summarized, and (2) 'exact' analysis procedure presented in Section 4.4.2. It is apparent from Figure 8.26 that the simplified procedure leads to results that seem accurate enough for use in preliminary design and safety evaluation of towers.

For a non-circular tapered tower, the added hydrodynamic mass due to surrounding and inside water has been computed using the simplified procedure presented in this chapter. Since the added hydrodynamic mass for a non-circular tower usually depends on the direction of ground motion (Chapter 5), the added hydrodynamic mass for the selected tower has been computed for two orthogonal directions of ground motion. The step-by-step computational details for this numerical example are summarized in Appendix H.

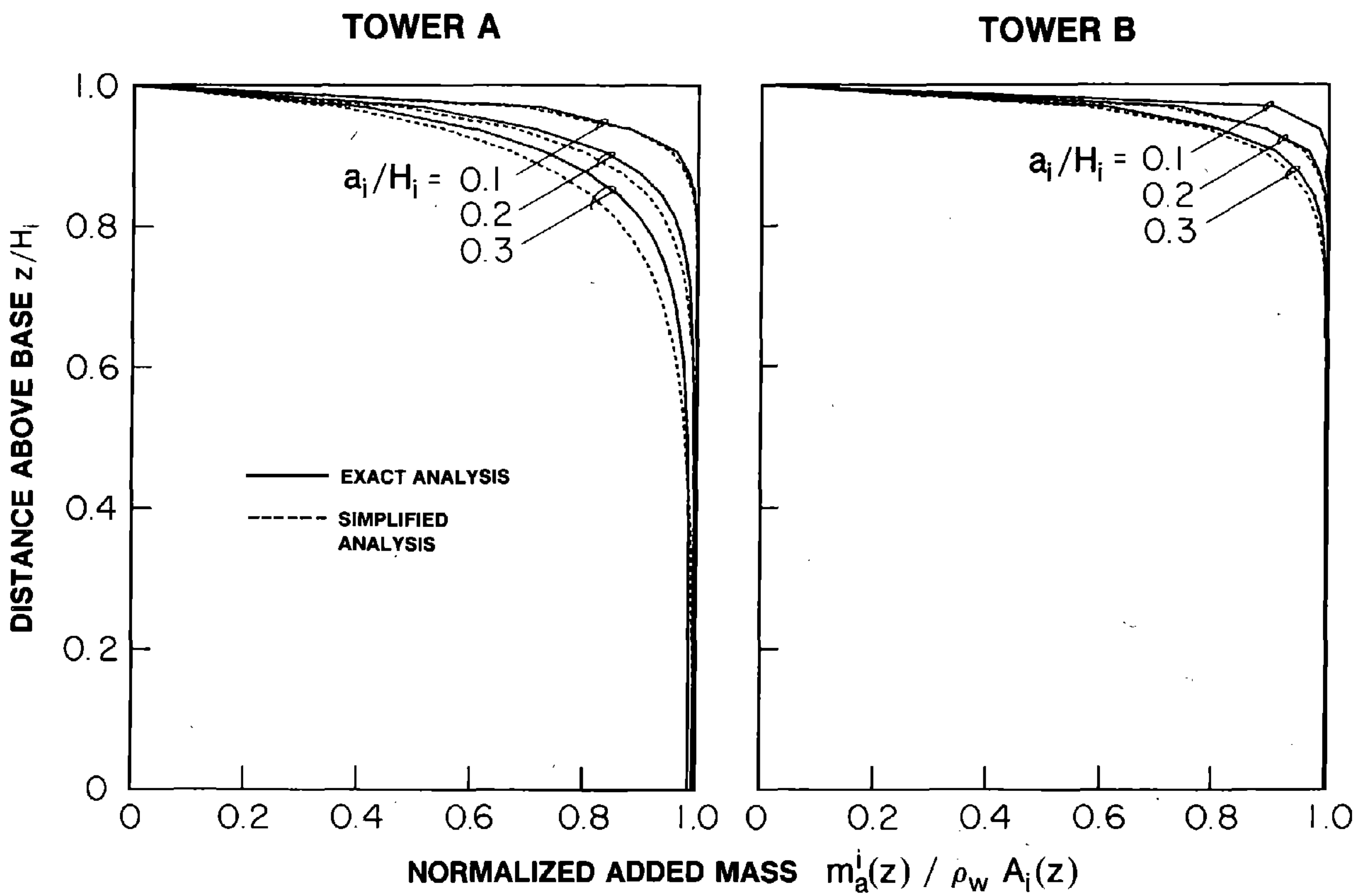

Figure 8.26 Comparison of Exact and Approximate (Simplified Analysis Procedure) Values of the Normalized Added Hydrodynamic Mass for Two Non-Uniform Towers Associated with Inside Water

9. SIMPLIFIED EARTHQUAKE ANALYSIS OF INTAKE-OUTLET TOWERS

9.1 Introduction

A general procedure for analysis of the earthquake response of intake-outlet towers of arbitrary geometry but with two axes of plan symmetry was developed in Chapters 3 and 4. Based on the response results obtained by this procedure, which were presented in Chapters 5 and 6, and the conclusions derived from these results, a simplified representation of the hydrodynamic and foundation interaction effects to approximately model the more significant factors influencing the response of intake-outlet towers, was presented in Chapter 7. In particular, it was demonstrated that : (1) the added mass representation of hydrodynamic effects due to surrounding (outside) and inside water is appropriate and provides sufficiently accurate results ; and (2) tower-foundation-soil interaction effects can be approximately included in the response analysis by simply modifying the fundamental vibration period and the associated damping ratio. Earlier work on buildings suggests that the contribution of the second vibration mode to the response may be computed as if the the tower was supported on rigid foundation soil [45,46]. Similarly it has been demonstrated that the first two vibration modes are usually sufficient for the approximate evaluation of the earthquake design forces in the preliminary phase of design and safety evaluation of towers [11].

However, the procedure presented in Chapter 7 for the approximate earthquake response analysis of intake-outlet towers still requires : (1) evaluation of the first two vibration frequencies and mode shapes by solving the associated eigen value problem for the tower ; (2) evaluation of the added hydrodynamic mass associated with surrounding (outside) and inside water by solving three-dimensional boundary value problems for the outside and inside water domains, respectively ; and (3) computation of the modifications in the vibration period and damping ratio of the fundamental vibration mode due to tower-foundation-soil interaction effects by iterative solution of the frequency equation [equation (7.26)].

The objective of this chapter is to develop a simplified version of the earthquake analysis procedure presented in Chapter 7 for intake-outlet towers, including tower-water interaction and tower-foundation-soil interaction effects, which is easier to implement but still provides sufficiently accurate estimates of the maximum earthquake (design) forces directly from the earthquake design spectrum without the need for a response history analysis. Utilized in the simplified analysis are the procedure and standard data of Chapter 8 for evaluation of the added hydrodynamic mass due to surrounding and inside water. Also included are convenient methods for computing the first two natural frequencies and modes of vibration of the tower, and the modifications to the frequency and damping ratio of the fundamental mode due to tower-foundation-soil interaction. The resulting analysis procedure is intended for the preliminary phase of design and safety evaluation of intake-outlet towers.

9.2 Natural Frequencies and Vibration Modes of Tower

Computation of the natural frequencies and shapes of the first two vibration modes of an intake-outlet tower requires solution of an eigen problem for a one-dimensional finite element idealization of the tower considering flexural and shear deformations. Such solutions can be obtained readily if appropriate computer programs are available. Otherwise, simplified procedures based on Stodola and Rayleigh methods [4,14] that can be readily implemented are recommended. They have been utilized earlier for multistory buildings [16], which are specialized next for intake-outlet towers with distributed mass and stiffness properties. The influence of rotatory inertia on the frequencies and mode shapes, which already has been shown to be small (Chapter 4), is neglected in order to simplify the computational procedure.

9.2.1 Fundamental Mode

The fundamental frequency and mode of vibration can be computed from the following step-by-step procedure :

1. Determine the height-wise distribution of an initial set of inertia forces associated with $\bar{u}_1^0(z)$, an initial estimate of the fundamental mode shape of the tower normalized to unit value at the top ($z = H_s$) :

$$F_1(z) = m_s(z)\, \bar{u}_1^0(z) \tag{9.1}$$

where $m_s(z)$ is the mass of the tower per unit of height. If the tower to be analyzed is an existing tower or is a proposed tower for which a preliminary design is available, then $m_s(z)$ is known and $\bar{u}_1^0(z)$ could be any reasonable deflected shape e.g. the fundamental mode shape of a uniform cantilever, the parabola $(z/H_s)^2$, etc. On the other hand, if the tower to be analyzed is a proposed tower for which a preliminary design is not available, the distribution of lateral forces $F(z)$ may be estimated as specified by the governing design code, and a preliminary design of the tower may be developed to resist the forces and other appropriate design loads specified by the code. The lateral displacements $u_1^0(z)$ may then be computed by static analysis of the tower (see steps 2 and 3) subjected to lateral forces $F(z)$ and normalized to obtain $\bar{u}_1^0(z) = u_1^0(z)/u_1^0(H_s)$.

2. Compute shear forces and bending moments by static analysis of the tower subjected to lateral forces $F_1(z)$:

$$Q_1(z) = \int_z^{H_s} F_1(\zeta)\, d\zeta \tag{9.2}$$

$$m_1(z) = \int_z^{H_s} (\, \zeta - z \,)\, F_1(\zeta)\, d\zeta \tag{9.3}$$

3. Compute lateral displacements of the tower axis due to static forces $F_1(z)$ by the principle of virtual work :

$$u_1(z) = \int_0^z (\zeta - z) \frac{m_1(\zeta)}{E_s I(\zeta)} d\zeta + \int_0^z \frac{Q_1(\zeta)}{G_s k(\zeta) A(\zeta)} d\zeta \tag{9.4}$$

in which E_s is the Young's modulus and G_s the modulus of rigidity for the tower concrete, $A(z)$ is the area, and $I(z)$ is the moment of inertia at a location z above the base. The shape factor $k(z)$ accounts for the shear stress distribution over the cross-section of the tower; e.g. k is 5/6 for a solid rectangular section and 9/10 for a solid circular section [44]. Values of k for typical cross-sections of intake-outlet towers are presented in Table 9.1. Steps 2 and 3 describe just one method for computing deflections. Any standard method, including analysis of a one-dimensional finite element idealization (including flexural and shear deformations) of the tower, may be used.

4. Normalize the computed displacements by the displacement at the top of the tower:

$$\bar{u}_1(z) = u_1(z) \,/\, u_1(H_s) \tag{9.5}$$

5. Compare displacement function $\bar{u}_1(z)$ computed in step 4 with the $\bar{u}_1^0(z)$ used in equation (9.1). If they do not agree to a desired degree of accuracy, replace $\bar{u}_1^0(z)$ in equation (9.1) by $\bar{u}_1(z)$ and compute a new set of forces $F_1(z)$, and repeat steps 2, 3 and 4. After a few such iterative repetitions, the two deflection functions will agree to a sufficient degree of accuracy. Then proceed to the next step.

6. The fundamental mode shape, $\phi_1(z)$, is given by $\bar{u}_1(z)$ computed in the final iteration cycle.

7. Compute the fundamental frequency ω_1 from

$$\omega_1^2 = \frac{\int_0^{H_s} F_1(z)\, u_1(z)\, dz}{\int_0^{H_s} m_s(z)\, [u_1(z)]^2\, dz} \tag{9.6}$$

Table 9.1 -- Shape Factor k For Selected Tower Cross-Sections

Cross-Section of the Tower	Direction of Ground Motion	Shape Factor k
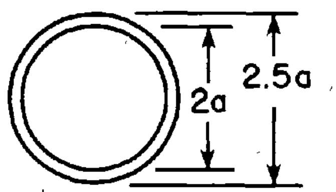	↔	0.680
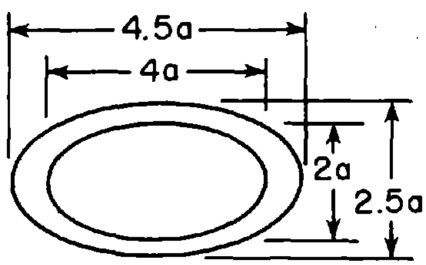	↔ ↕	0.774 0.552
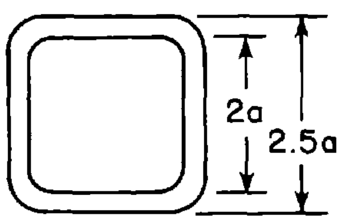	↔	0.442
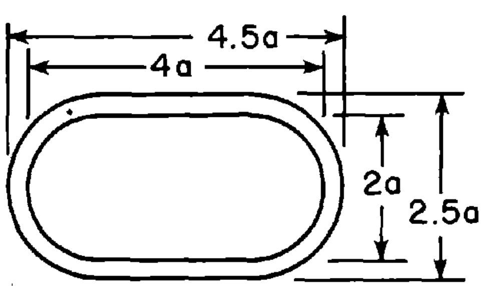	↔ ↕	0.734 0.794

9.2.2 Second Mode

Because the contributions of the second vibration mode to tower response are smaller compared to the fundamental mode, it seems unnecessary to compute the vibration properties of the second mode to a high degree of accuracy. Thus the Stodola method with iteration, described above, is avoided in computing the vibration properties of the second mode. Instead the simple procedure developed for buildings [16] is utilized.

The approximate vibration properties of the second mode are therefore computed by the following step-by-step procedure :

1. Compute the height-wise variation of the remainder (total minus first mode contribution) of the effective forces :

$$F_r(z) = - m_s(z) \left[1 - \frac{L_1}{M_1} \phi_1(z) \right] \tag{9.7}$$

where $\phi_1(z)$ is the fundamental mode shape determined from the procedure of the preceding section and the generalized mass M_1 and excitation term L_1 associated with the fundamental mode are :

$$M_1 = \int_0^{H_s} m_s(z) \, [\phi_1(z)]^2 \, dz \tag{9.8}$$

$$L_1 = \int_0^{H_s} m_s(z) \, \phi_1(z) \, dz \tag{9.9}$$

2. Compute the lateral deflection of the tower axis, $u_2(z)$, by static analysis of tower subjected to lateral forces $F_r(z)$. Any appropriate method may be used, including the one summarized in steps 2 and 3 of Section 9.2.1 with $F_1(z)$ replaced by $F_r(z)$.

3. Determine the approximate second mode shape $\phi_2(z)$ by normalizing the computed deflections, i.e dividing them by a convenient reference value :

$$\phi_2(z) = \frac{u_2(z)}{u_2(H_s)} \tag{9.10}$$

4. Compute the second mode frequency from the mode shape by :

$$\omega_2^2 = \frac{\int_0^{H_s} F_r(z)\, u_2(z)\, dz}{\int_0^{H_s} m_s(z)\, [u_2(z)]^2\, dz} \tag{9.11}$$

Two useful properties of the approximate frequency ω_2 and mode shape $\phi_2(z)$ determined in this manner have been demonstrated [16]: Firstly, the approximate frequency ω_2 is always larger than its exact value. Secondly, the approximate second mode shape is orthogonal to the exact fundamental mode shape; and is a linear combination of higher vibration modes with the combination dominated by the second mode.

9.3 Added Hydrodynamic Mass

The hydrodynamic interaction effects can most simply be included in response spectrum analysis of intake-outlet towers by replacing the mass of the tower $m_s(z)$ by the virtual mass (Chapter 7) :

$$\tilde{m}_s(z) = m_s(z) + m_a^o(z) + m_a^i(z) \tag{9.12}$$

where the added hydrodynamic masses $m_a^o(z)$ and $m_a^i(z)$ represent the effects of the surrounding (outside) and inside water, respectively, on the dynamic response of the tower. It has been demonstrated in Chapter 7 that the earthquake response of towers can be computed to a useful degree of accuracy with the added mass functions $m_a^o(z)$ and $m_a^i(z)$ given by the lateral forces associated with hydrodynamic pressures acting on the tower, assumed to be rigid, due to unit horizontal acceleration of the ground and the tower. Because the analytical expressions for the added hydrodynamic mass for a rigid tower are available only for circular cylindrical towers [32,40] and for uniform elliptical towers [30], a simplified procedure for evaluating the added hydrodynamic mass which is accurate enough for preliminary earthquake analysis of towers was developed in Chapter 8. Presented next is a summary of this simplified procedure.

9.3.1 Added Hydrodynamic Mass for Surrounding Water

Consider a tower of arbitrary cross-section with two axes of symmetry and its outside surface having cross-sections of area $A_o(z)$, width $2a_o(z)$ perpendicular to the direction of ground motion, and dimension $2b_o(z)$ along the direction of ground motion. The depth of the surrounding water is H_o, and z is the height coordinate above the base. The added hydrodynamic mass associated with surrounding water can be determined by the following steps :

1. Select a sufficient number of locations along the height where the added hydrodynamic mass for the tower will be determined to obtain the height-wise distribution of added mass $m_a^o(z)$. Compute the height coordinate z for the selected locations.

2. Determine the cross-sectional radius $\tilde{r}_o(z)$ of the 'equivalent', axisymmetric tower at a selected location z. This is achieved by using the following procedure for uniform towers with the cross-section of the uniform tower taken to be same as the actual cross-section pertaining to that location :

   (a) Evaluate the parameters $\tilde{a}_o(z)/\tilde{b}_o(z)$ and $H_o/\tilde{a}_o(z)$ for the 'equivalent', uniform, elliptical tower, using equation (9.13) along with the properties of the actual tower at the selected location z : slenderness ratio $H_o/a_o(z)$, cross-sectional area $A_o(z)$, and ratio $a_o(z)/b_o(z)$ of the plan dimensions.

$$\frac{H_o}{\tilde{a}_o(z)} = \frac{H_o}{\sqrt{A_o(z)/\pi}} \cdot \sqrt{\frac{b_o(z)}{a_o(z)}} \tag{9.13a}$$

$$\frac{\tilde{a}_o(z)}{\tilde{b}_o(z)} = \frac{a_o(z)}{b_o(z)} \tag{9.13b}$$

(b) Evaluate the slenderness ratio $H_o/\tilde{r}_o(z)$ of the 'equivalent', axisymmetric tower for the selected z location from the properties $\tilde{a}_o(z)/\tilde{b}_o(z)$ and $H_o/\tilde{a}_o(z)$ -- determined in step 2(a) for the equivalent, uniform, elliptical tower pertaining to the selected location z -- using the data of Figure 8.7 or Table 8.3. Alternatively, if $1/3 \leq \tilde{a}_o(z)/\tilde{b}_o(z) \leq 3$, $\tilde{r}_o(z)/a_o(z)$ may be determined from the mean curve of Figure 8.9 corresponding to $\tilde{a}_o(z)/\tilde{b}_o(z)$ determined in step 2(a).

3. Evaluate the normalized added hydrodynamic mass for the 'equivalent', axisymmetric tower at the selected location z as the normalized mass from Figure 8.1 (or Table 8.4) for a circular cylindrical tower corresponding to $r_o/H_o = \tilde{r}_o(z)/H_o$ pertaining to that location, determined in step 2.

4. Compute the added hydrodynamic mass $m_\infty^o(z=0)$ for an infinitely long tower with its cross-section same as at the base of the actual tower from either Table 8.1 or a two-dimensional analysis of the Laplace equation for the surrounding water domain (Appendix G). If the shape of the cross-section of the actual tower is unchanged along its height and only its dimensions vary, determine the added mass $m_\infty^o(z)$ at the location z selected in step 2 by recognizing that the ratio $m_\infty^o(z)/m_\infty^o(0)$ is equal to the ratio $A_o(z)/A_o(0)$ of the cross-sectional areas at the two locations. If the cross-sectional shape changes, evaluate $m_\infty^o(z)$ directly from the cross-sectional properties of the actual tower at the location z selected in step 2 (Appendix G).

5. Determine the added hydrodynamic mass $m_a^o(z)$ for the actual tower at the location z selected in step 2 by multiplying the normalized added mass, determined in

step 3, by $m_{\infty}^{o}(z)$ for that location computed in step 4.

6. Repeat steps 2 to 5 for various locations along the tower height, selected in step 1, to obtain the complete distribution of added hydrodynamic mass for a non-uniform tower.

If the outside surface of the tower is uniform, i.e. $A_o(z)$, $a_o(z)$, and $b_o(z)$ are constants independent of z, the computations required in the procedure just summarized are reduced. In particular, the 'equivalent' axisymmetric tower defined in step 2 will reduce to an 'equivalent', circular cylindrical tower, i.e. $\tilde{r}_o(z) = \tilde{r}_o$, independent of z, and steps 2 and 4 need to be carried out only once and step 3 is much simpler to implement.

9.3.2 Added Hydrodynamic Mass for Inside Water

Consider a tower of arbitrary cross-section with two axes of symmetry and its inside surface having cross-sections of area $A_i(z)$, width $2a_i(z)$ perpendicular to the direction of ground motion, and dimension $2b_i(z)$ along the direction of ground motion. The depth of inside water is H_i, and z is the height coordinate above the base. The added hydrodynamic mass associated with inside water can be determined by the following steps :

1. Select a sufficient number of locations along the height where the added hydrodynamic mass for the non-uniform tower will be determined to obtain the height-wise distribution of added mass $m_a^i(z)$. Compute the height coordinate z for the selected locations.

2. Determine the cross-sectional radius $\tilde{r}_i(z)$ of the 'equivalent' axisymmetric tower at a selected location z. This is achieved by using the procedure for uniform towers with the cross-section of the uniform tower taken to be same as the actual cross-section pertaining to that location, i.e. using equation (9.14) along with the cross-sectional properties of the actual tower, $A_i(z)$, $a_i(z)$ and $b_i(z)$ at the selected location :

$$\tilde{r}_i(z) = \sqrt{\frac{A_i(z)}{\pi} \cdot \frac{b_i(z)}{a_i(z)}} \tag{9.14}$$

3. Evaluate the normalized added hydrodynamic mass for the 'equivalent' axisymmetric tower at the location z selected in step 2 as the normalized mass from Figure 8.17 (or Table 8.5) for a circular cylindrical tower corresponding to $r_i/H_i = \tilde{r}_i(z)/H_i$ pertaining to that location, determined in step 2.

4. Determine the added hydrodynamic mass $m_a^i(z)$ for the actual tower at the location z selected in step 2 by multiplying the normalized added mass, determined in step 3, by $m_\infty^i(z)$ for that location. If $A_i(z)$ is the area of the interior cross-section, and ρ_w is the mass density of water, $m_\infty^i(z) = \rho_w A_i(z)$.

5. Repeat steps 2 to 4 for various locations along the tower height, selected in step 1, to obtain the complete distribution of added hydrodynamic mass for the tower.

If the interior surface of the tower is uniform along the height, i.e. $A_i(z)$, $a_i(z)$ and $b_i(z)$ are constants independent of z, the computations required in the analysis procedure just summarized are reduced. In particular, the 'equivalent', axisymmetric tower defined in step 2 will reduce to an 'equivalent', circular, cylindrical tower, i.e. $\tilde{r}_i(z) = \tilde{r}_i$, independent of z, and step 2 needs to be carried out only once and steps 3 and 4 are much simpler to implement.

9.4 Tower-Foundation-Soil Interaction Effects

As demonstrated in Chapter 7, tower-foundation-soil interaction effects can be approximately included in the response contribution of the fundamental vibration mode of towers by modifying the vibration period and damping ratio for this vibration mode. Standard data and simplified procedures for estimating the modified vibration period and damping ratio without requiring an iterative solution of equation (7.26) are presented in this section.

Earlier work on buildings [46] suggests that the response contribution of the second vibration mode may be determined by standard procedures disregarding the effects of tower-foundation-soil interaction.

9.4.1 System Parameters

The dimensionless parameters chosen in Chapter 5 to characterize tower-foundation-soil interaction are not the most appropriate to present standard data for modifications in the fundamental mode period and damping ratio. For this purpose, the fundamental vibration mode of the tower on fixed base is represented by a singe-degree-of-freedom (SDF) system having the natural vibration period T_1, lumped mass equal to m_1^*, the effective mass for the fundamental vibration mode, located at height h_1^*, the effective height for the fundamental mode. The effective mass m_1^* of the tower in the fundamental mode of vibration (Chapter 7) is :

$$m_1^* = L_1^2 / M_1 \tag{9.15}$$

where M_1 and L_1 are the generalized mass and excitation terms for that mode, defined by equations (9.8) and (9.9), respectively. The effective height of the tower in the fundamental mode of vibration (Chapter 7) is :

$$h_1^* = L_1^r / L_1 \tag{9.16}$$

in which

$$L_1^r = \int_0^{H_s} z \; m_s(z) \; \phi_1(z) \; dz \tag{9.17}$$

The parameters characterizing the-single-degree-of-freedom (SDF) system, representing the fundamental vibration mode of the tower, supported through a rigid foundation on a viscoelastic halfspace, are listed here in order of more or less decreasing importance [45] :

1. The wave parameter

$$\sigma^* = \frac{C_f \, T_1}{h_1^*} \tag{9.18}$$

which is a measure of the relative stiffness of the foundation soil and the SDF system; C_f is the shear wave velocity in the halfspace ; T_1 is the fundamental vibration period of the fixed-base tower;

2. The ratio h_1^*/r_f of the effective height of the tower to the radius of the circular foundation. Since towers are usually slender structures and rocking motion of the foundation is more influential in controlling the tower-foundation-soil interaction effects (Chapter 5), the 'equivalent' radius for a non-circular foundation can be approximately computed from the moment of inertia I_o of the actual foundation (Chapter 4) :

$$r_f \approx \left[\frac{4 I_o}{\pi} \right]^{\frac{1}{4}} \tag{9.19}$$

3. The fixed-base fundamental vibration period of the tower, T_1.

4. The constant hysteretic damping factor η_f for the supporting foundation soil.

5. The damping ratio of the fixed-base tower in its fundamental mode of vibration, ξ_1.

6. The relative mass density for the tower and the supporting foundation soil

$$\gamma^* = \frac{m_1^*}{\rho_f \, \pi \, r_f^2 \, h_1^*} \tag{9.20}$$

in which ρ_f is the mass density of the soil.

7. The ratio m_f/m_1^* of the mass of the foundation to the effective, first-mode mass of the tower.

8. Poisson's ratio for the foundation soil, ν_f.

For the solutions presented in this section, the mass of the foundation below the ground level is neglected and the Poisson's ratio for the foundation soil, ν_f, is taken as 1/3, a value representative for rock. Within the range of values that are of practical applications, the response of the structure is generally insensitive to variations in these particular parameters and therefore, the applicability of the results presented in this section is not limited [45].

Special attention is required in assigning numerical values to the shear wave velocity C_f and damping factor η_f for the foundation soil or rock, because both are strain-dependent quantities [43], and the tower response is influenced by these quantities (Chapters 5 to 7). The strains induced in the foundation soils depend on the properties of the soil and the severity of ground motion. Other things being equal, stronger the ground motion, smaller is the effective value of C_f, and greater is the value of η_f [43]. Therefore, the choice of these values in a given case must be based on an estimate of the magnitude of strains that may be induced in the foundation soil by the design ground motion, and the information of the type presented in Reference [43]. However, these nonlinear considerations are less significant in the case of towers as they are typically founded on rock.

9.4.2 Effective Period of System

The fundamental vibration period, T_1^f, of the tower considering soil-structure interaction is given approximately by the equation

$$T_1^f = T_1 \sqrt{1 + k_1^* \left[\frac{1}{K_x\, k_{VV}} + \frac{[h_1^*]^2}{K_\theta\, k_{MM}} \right]} \tag{9.21}$$

in which $k_1^* = \omega_1^2\, m_1^*$ is the generalized stiffness of the fixed-base tower in its fundamental vibration mode; K_x and K_θ represent the static stiffness of the foundation in translational and rocking directions, defined by

$$K_x = \frac{8\ G_f\ r_f}{2 - \nu_f} \tag{9.22a}$$

$$K_\theta = \frac{8\ G_f\ r_f^3}{3\ (\ 1 - \nu_f\ )} \tag{9.22b}$$

The quantity G_f in these equations represents the shear modulus of elasticity, and k_{VV} and k_{MM} are dimensionless real-valued coefficients that are functions of the Poisson's ratio and the period of vibration. These coefficients may be determined from the information presented in Chapter 4.

Equivalent to the corresponding result for building-foundation systems, equation (9.21) is an approximate version of equation (7.26), obtained by dropping the terms associated with radiation and material damping of the foundation. The resulting errors in T_1^f can be demonstrated to be negligible.

Because of the period-dependence of the coefficients k_{VV} and k_{MM}, equations (9.21) or (7.26) must be evaluated by iteration. This computation may be significantly simplified, however, by the use of static values of the stiffnesses, i.e. by taking $k_{VV} = k_{MM} = 1$. The use of static stiffness values lead to results for the period T_1^f which are sufficiently accurate for practical applications, especially for slender structures such as intake-outlet towers [45].

In Figure 9.1, the ratio T_1^f/T_1 is plotted as a function of the relative flexibility parameter, $1/\sigma^*$, for towers having several different values of the ratio h_1^*/r_f. These 'exact' results were obtained by an iterative solution of equation (7.26) with the mass density parameter, $\gamma^* = 0.10$; Poisson's ratio $\nu_f = 1/3$; and foundation damping factor, $\eta_f = 0$. As shown in Figure 9.2, the influence of η_f on the vibration period is small. Therefore, the results presented in Figure 9.1 are applicable for all values of η_f.

For other values of γ^*, T_1^f/T_1 can be approximately estimated from $(T_1^f/T_1)_{\gamma^*=0.10}$, the value determined for γ^*=0.10 from Figure 9.1, using the following equation :

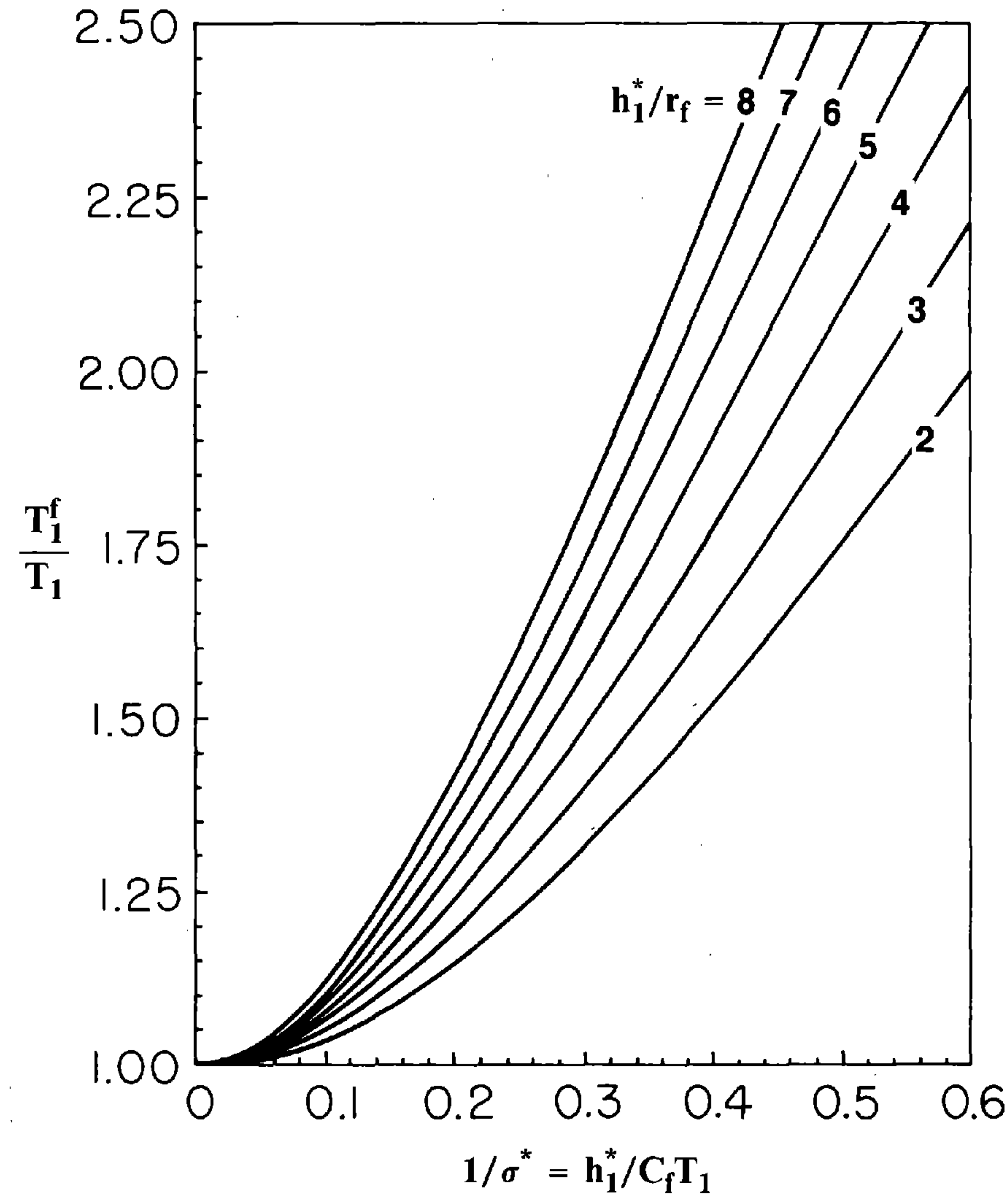

Figure 9.1 Effective Fundamental Vibration Period, T_1^f, for Towers Supported on a Viscoelastic Halfspace for a Range of h_1^*/r_f Values; $\gamma^* = 0.10$, $\eta_f = 0.0$

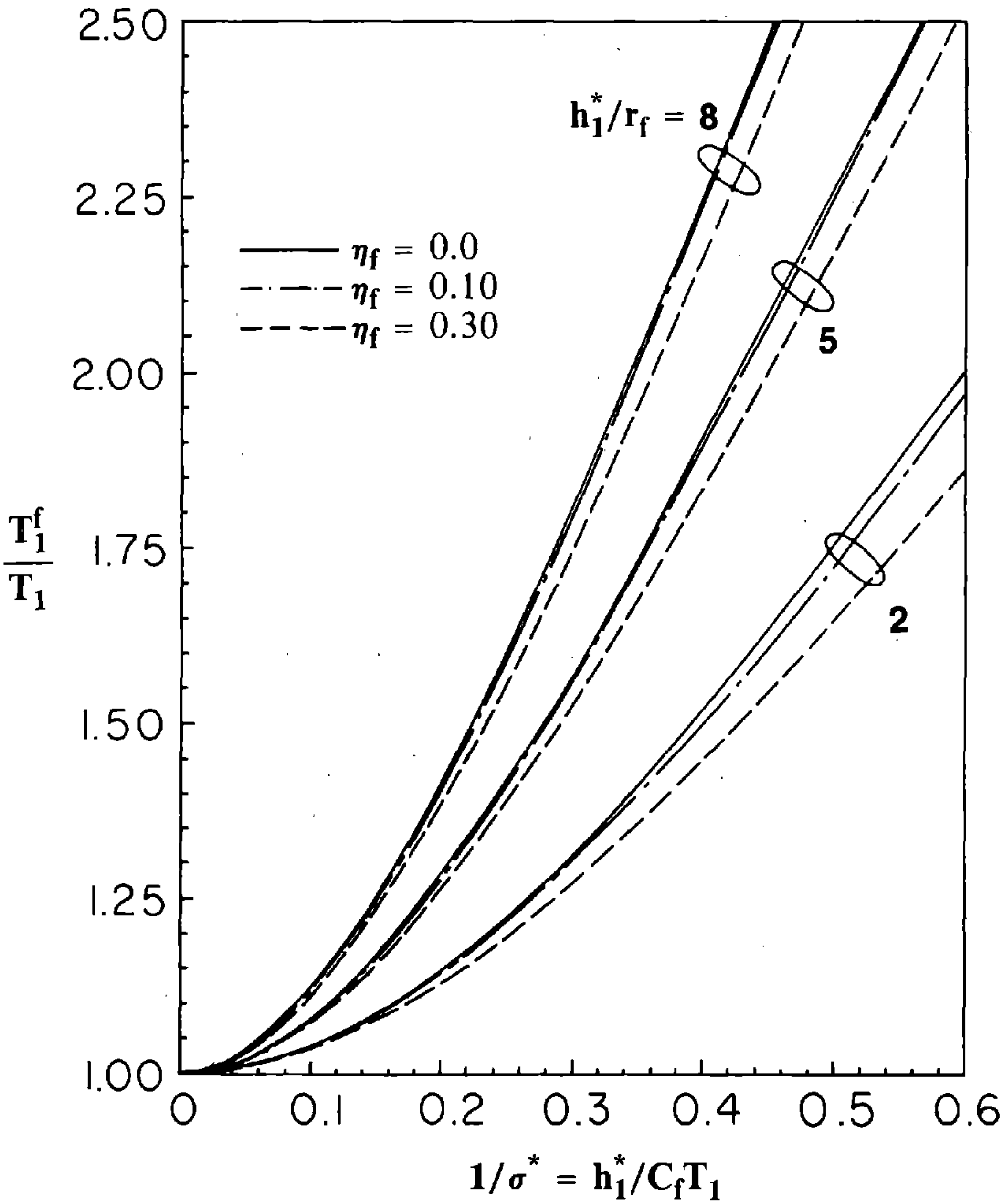

Figure 9.2 Influence of Foundation Damping Factor, η_f, on the Effective Fundamental Vibration Period, T_1^f, for a Range of h_1^*/r_f Values; $\gamma^* = 0.10$, $\eta_f = 0.0$

$$\frac{T_1^f}{T_1} = \sqrt{1 + \frac{\gamma^*}{0.10}\left[\left[\frac{T_1^f}{T_1}\right]^2_{\gamma^*=0.10} - 1\right]} \tag{9.23}$$

As shown in Figure 9.3, the ratio T_1^f/T_1 evaluated from equation (9.23) for $\gamma = 0.05$ and 0.15 is in excellent agreement with the 'exact' results obtained from an iterative solution of equation (7.26).

The exact solutions of Figure 9.1 for $\gamma^* = 0.10$ and similar results for $\gamma^* = 0.05$ and $\gamma^* = 0.15$ are replotted in Figure 9.4 as a function of the dimensionless parameter $\sqrt{\gamma^*}\,\chi$ in which

$$\chi = \frac{1}{\sigma^*}\left[\frac{h_1^*}{r_f}\right]^{1/4} = \frac{h_1^*}{C_f\,T_1}\left[\frac{h_1^*}{r_f}\right]^{1/4} \tag{9.24}$$

An alternative measure of the relative flexibility of the foundation soil and the structure, this parameter was determined by trial and error so that the results would fall within a relatively narrow band, making them especially useful for practical application to building design [45]. For the range of h_1^*/r_f and γ^* relevant to intake-outlet towers, the spread in the results of Figure 9.4 is about 20%, which is about twice of that observed for buildings [45].

In order that the results fall within an even narrower band, additional trials led to the selection of a modified parameter $\sqrt{\gamma^*}\,\tilde{\chi}$ in which

$$\tilde{\chi} = \frac{1}{\sigma^*}\left[\frac{h_1^*}{r_f}\right]^{2/5} = \frac{h_1^*}{C_f\,T_1}\left[\frac{h_1^*}{r_f}\right]^{2/5} \tag{9.25}$$

When the results of Figure 9.4 are replotted in Figure 9.5 as a function of $\sqrt{\gamma^*}\,\tilde{\chi}$, they fall within a narrower band, and the maximum deviation from the mean is about 3%. The value of T_1^f may, therefore, be evaluated readily with good accuracy from the mean curve presented in this figure.

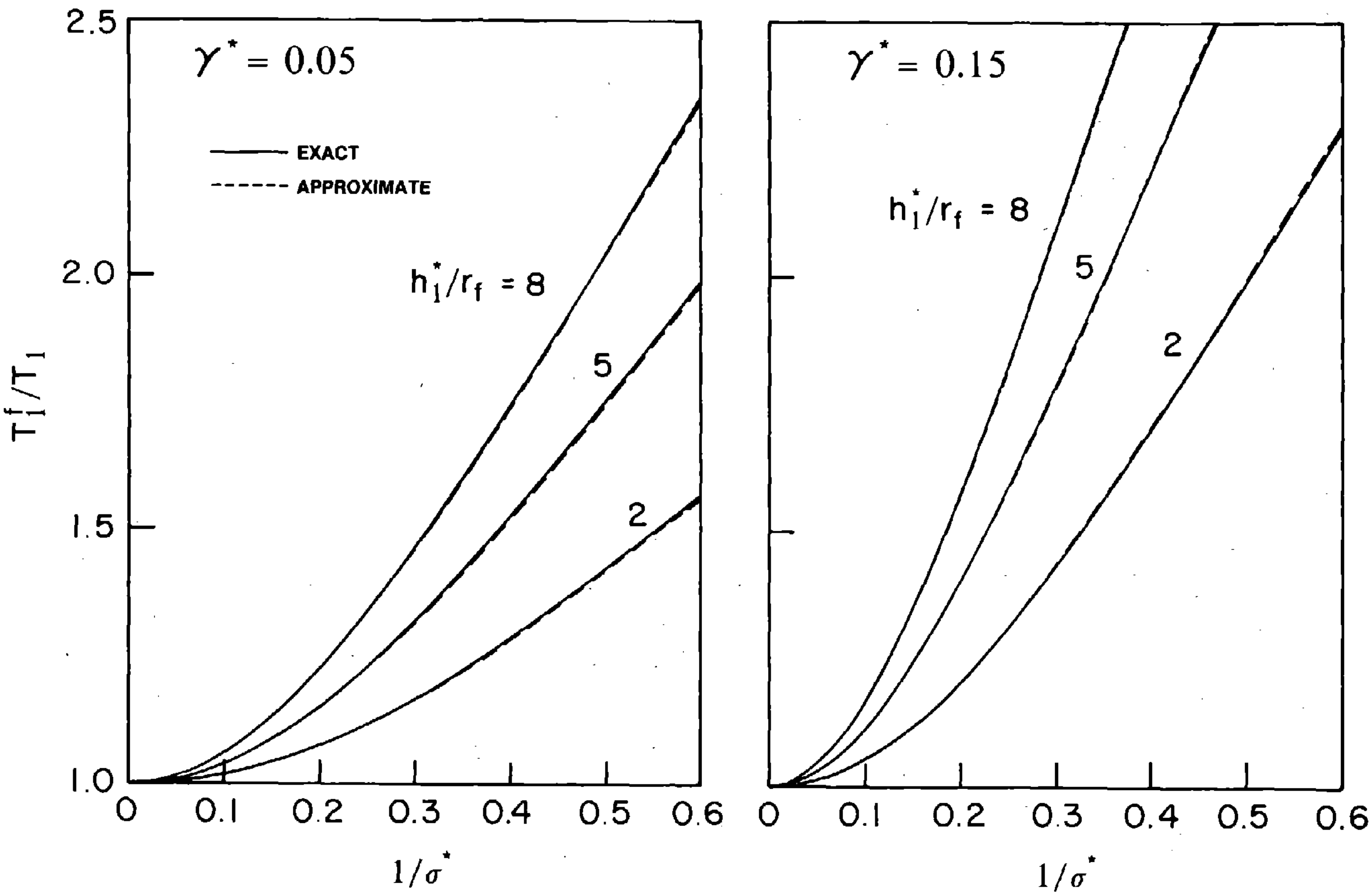

Figure 9.3 Comparison of Exact and Approximate Values of Effective Fundamental Vibration Period, T_1^f for Towers Supported on a Viscoelastic Halfspace with $\eta_f = 0.10$

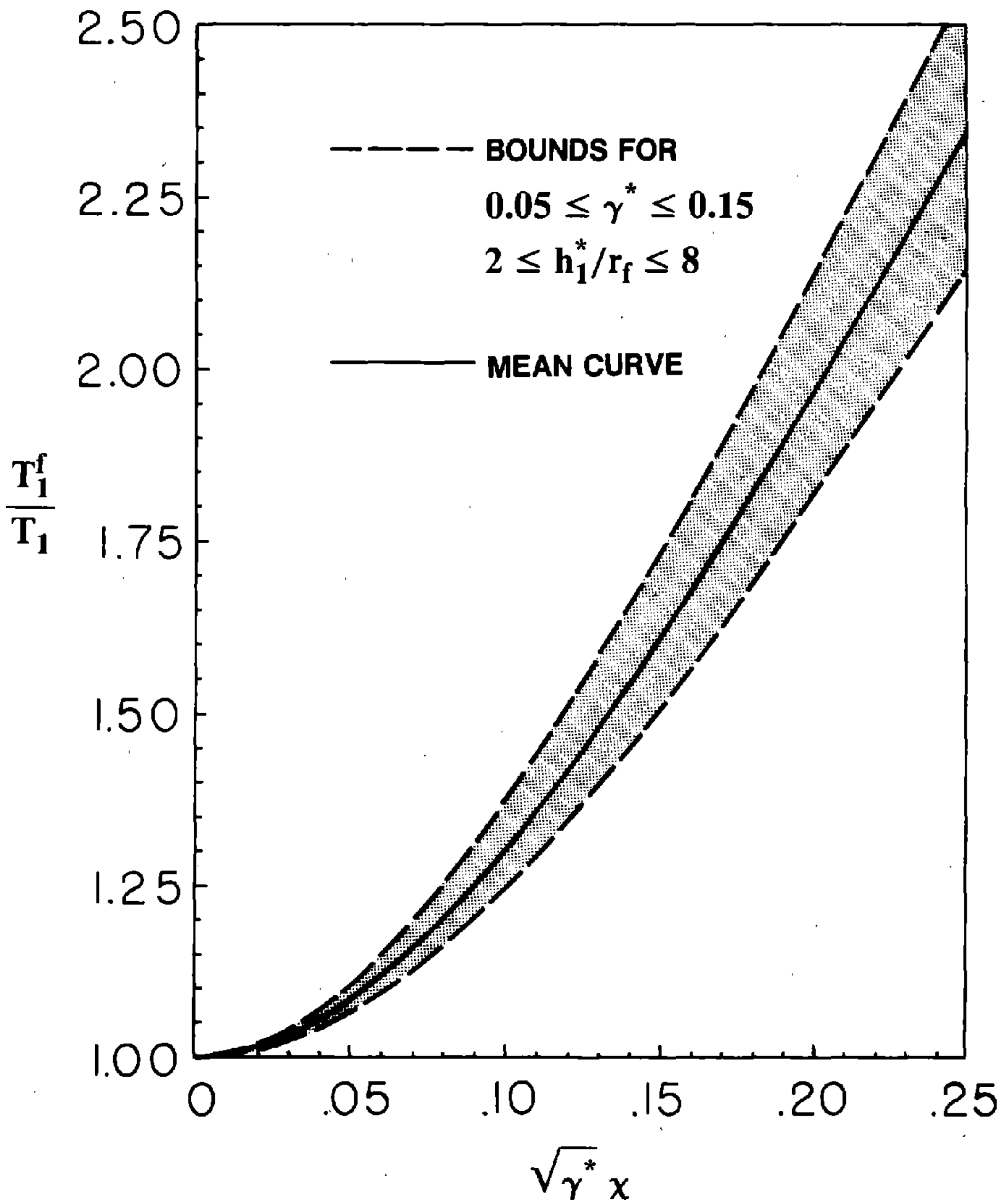

Figure 9.4 Effective Fundamental Vibration Period, T_1^f , for Towers Supported on a Viscoelastic Halfspace for a Range of h_1^*/r_f and γ^* Values; η_f = 0.0, η_s =0.0

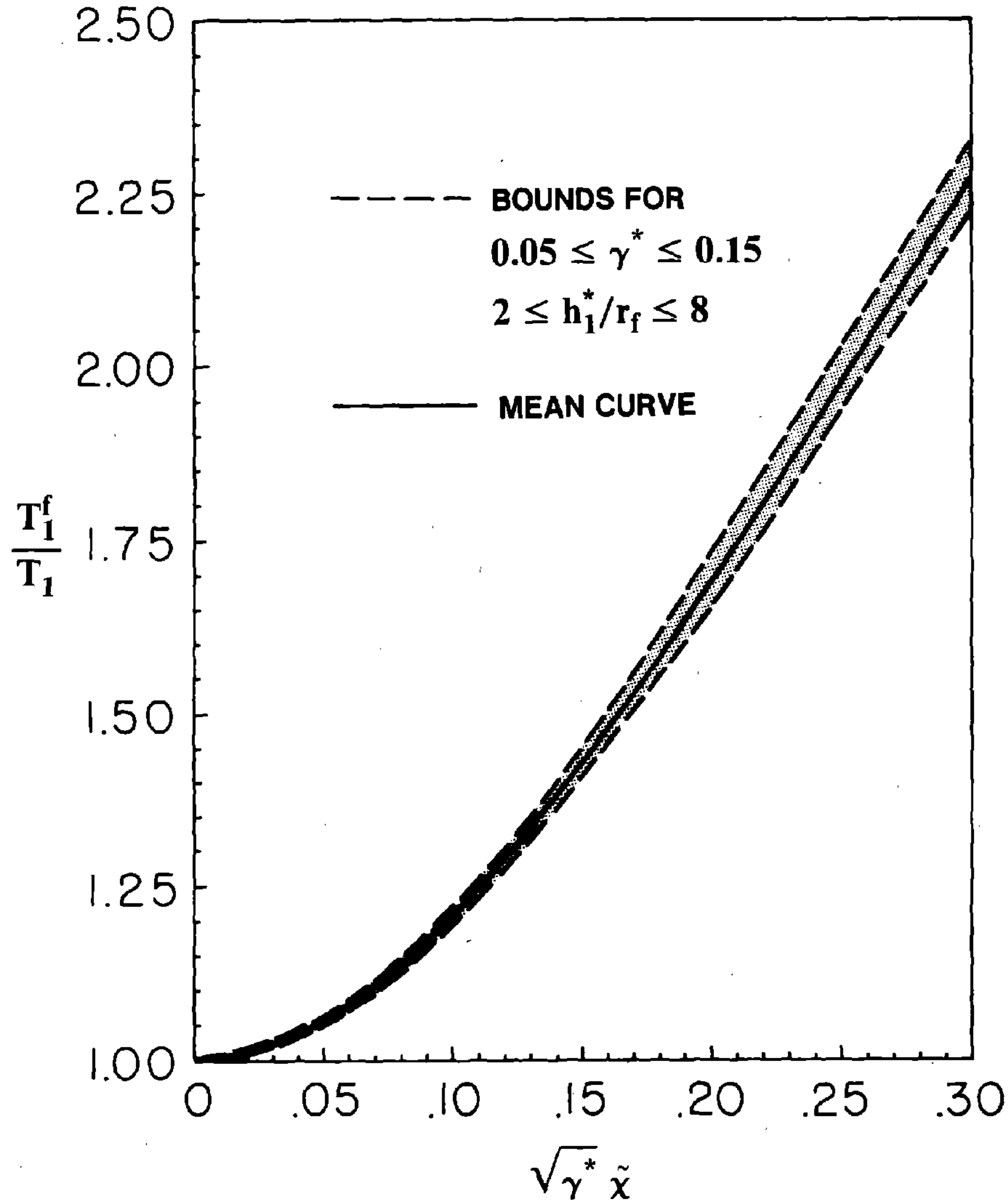

Figure 9.5 Effective Fundamental Vibration Period, T_1^f, for Towers Supported on a Viscoelastic Halfspace for a Range of h_1^*/r_f and γ^* Values; $\eta_f = 0.0$, $\eta_s = 0.0$

9.4.3 Effective Damping of System

The effective damping ratio of the interacting system, ξ_1^f, is given approximately (Chapter 7) by :

$$\xi_1^f = \frac{\xi_1}{(T_1^f / T_1)^3} + \xi_a \tag{9.26}$$

in which the first term represents the contribution of structural damping and the second term represents the damping arising from soil-structure interaction including both material and radiation damping effects.

Considering that T_1^f is greater than T_1, it is apparent that soil-structure interaction reduces the effectiveness of structural damping. The contribution of structural damping is inversely proportional to the square of the period ratio T_1^f / T_1 if the damping mechanism in the structure is characterized as constant hysteretic, and is inversely proportional to the cube of T_1^f / T_1 for viscously damped structures (Chapter 7). Since the actual damping mechanism for the structure is usually unknown, the latter mechanism is selected for presenting equation (9.26) as it leads to smaller damping ξ_1^f and hence to conservative estimates of earthquake response.

The foundation damping factor ξ_a, obtained by evaluating equation (7.32), is shown in Figures 9.6 to 9.10 for various values of η_f and h_1^* / r_f. For convenience in practical application, following Reference [45], the results are plotted as a function of the period ratio T_1^f / T_1 instead of the flexibility parameter $1/\sigma^*$ used in Figure 9.1.

It is apparent from these figures that the foundation damping may be a significant contributor to the overall damping of the system. Considering that intake-outlet towers usually are slender structures, the contribution of soil material damping would be particularly significant because the contribution of radiation damping is known to be small for such

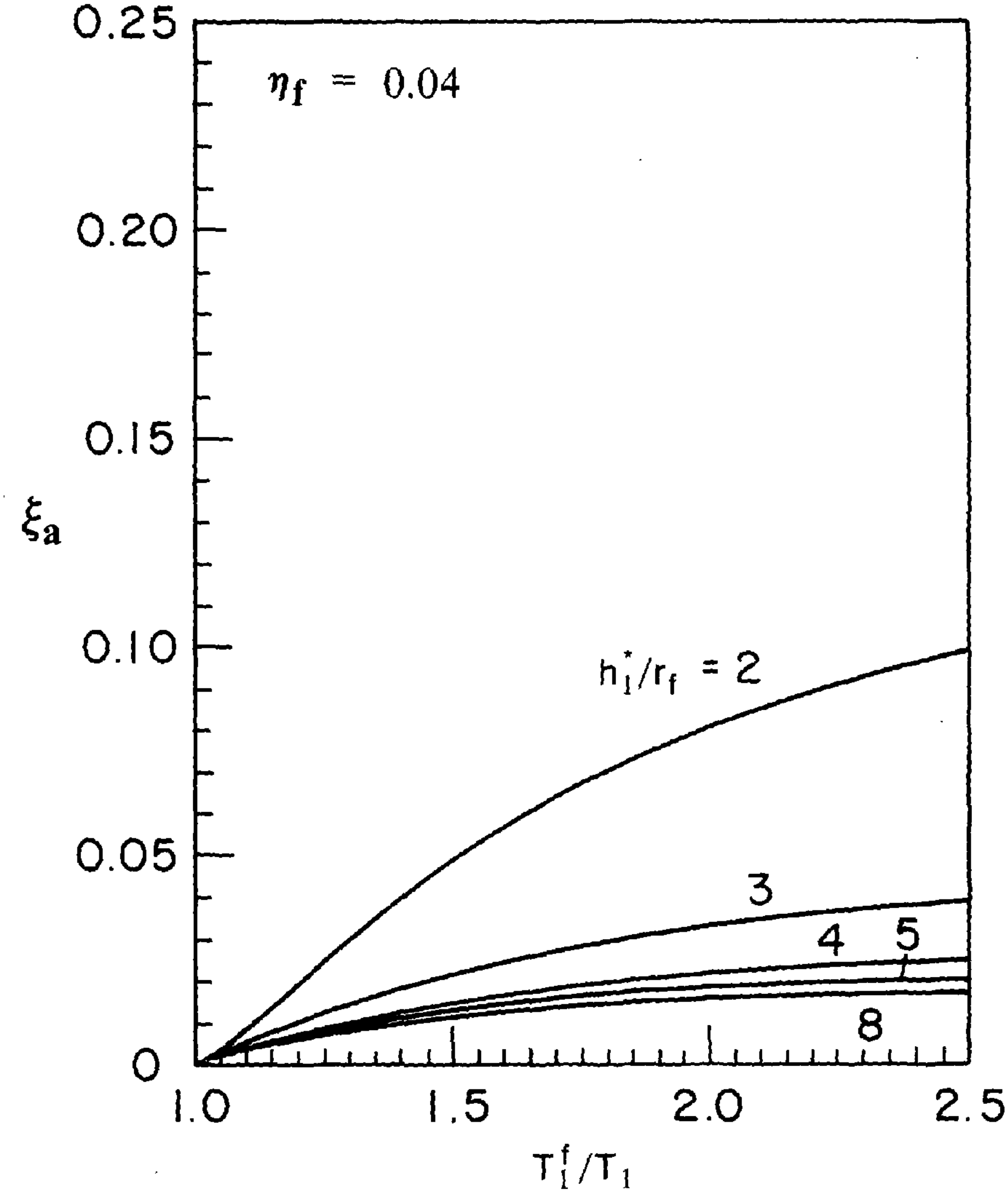

Figure 9.6 Added Foundation Damping, ξ_a , for Towers Supported on a Viscoelastic Halfspace with η_f = 0.04; γ^* = 0.10

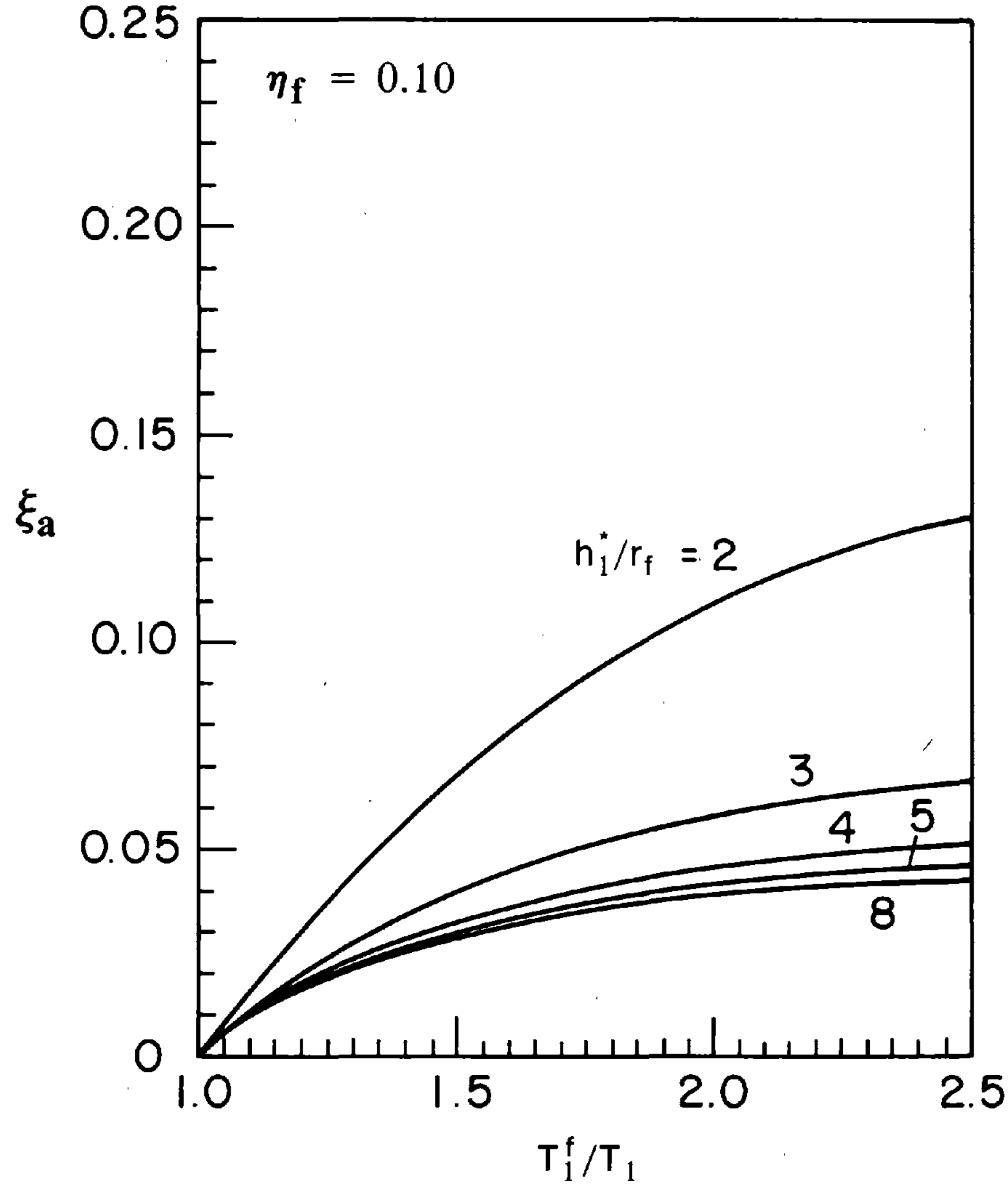

Figure 9.7 Added Foundation Damping, ξ_a, for Towers Supported on a Viscoelastic Halfspace with η_f = 0.10; γ^* = 0.10

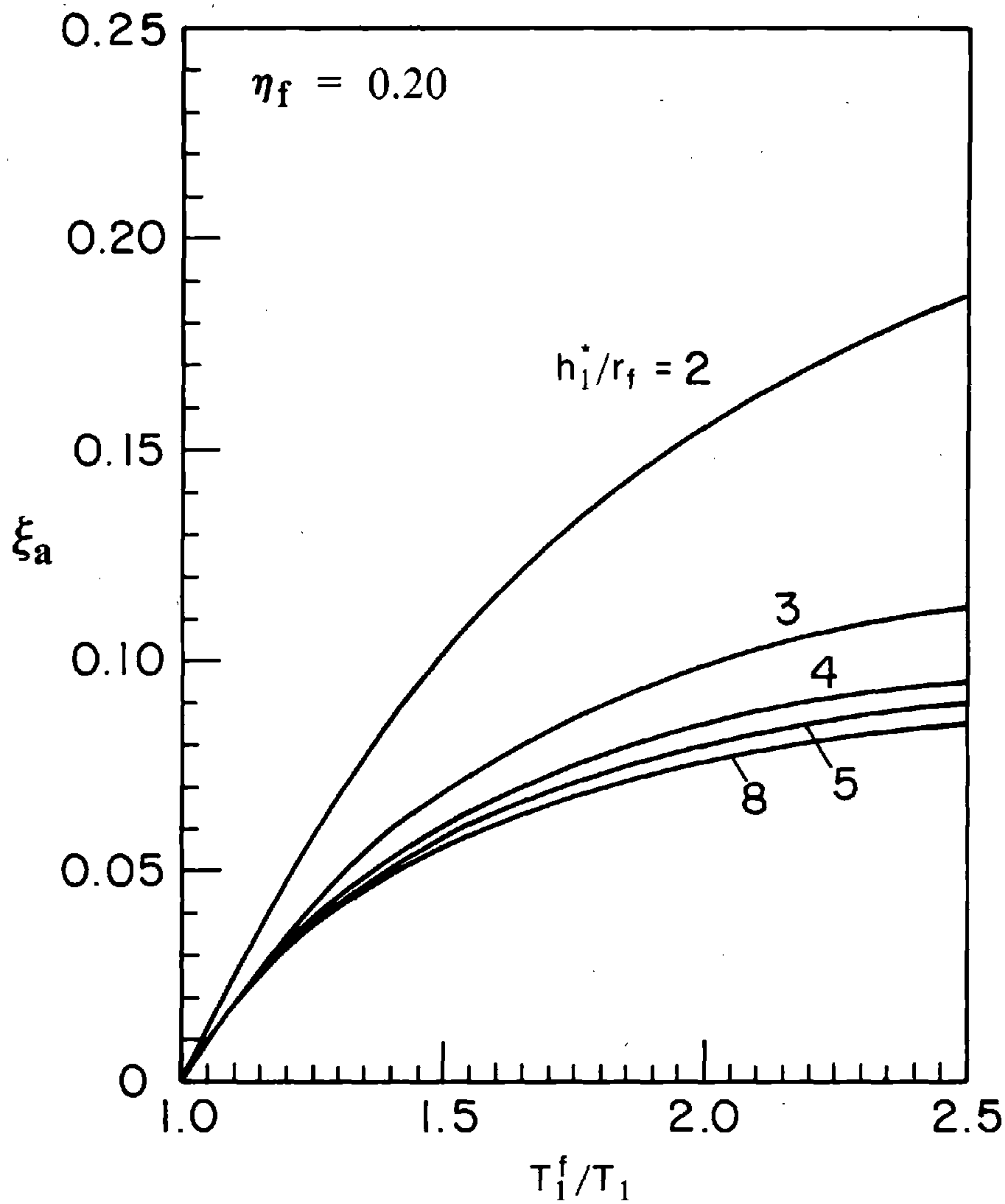

Figure 9.8 Added Foundation Damping, ξ_a , for Towers Supported on a Viscoelastic Halfspace with η_f = 0.20; γ^* = 0.10

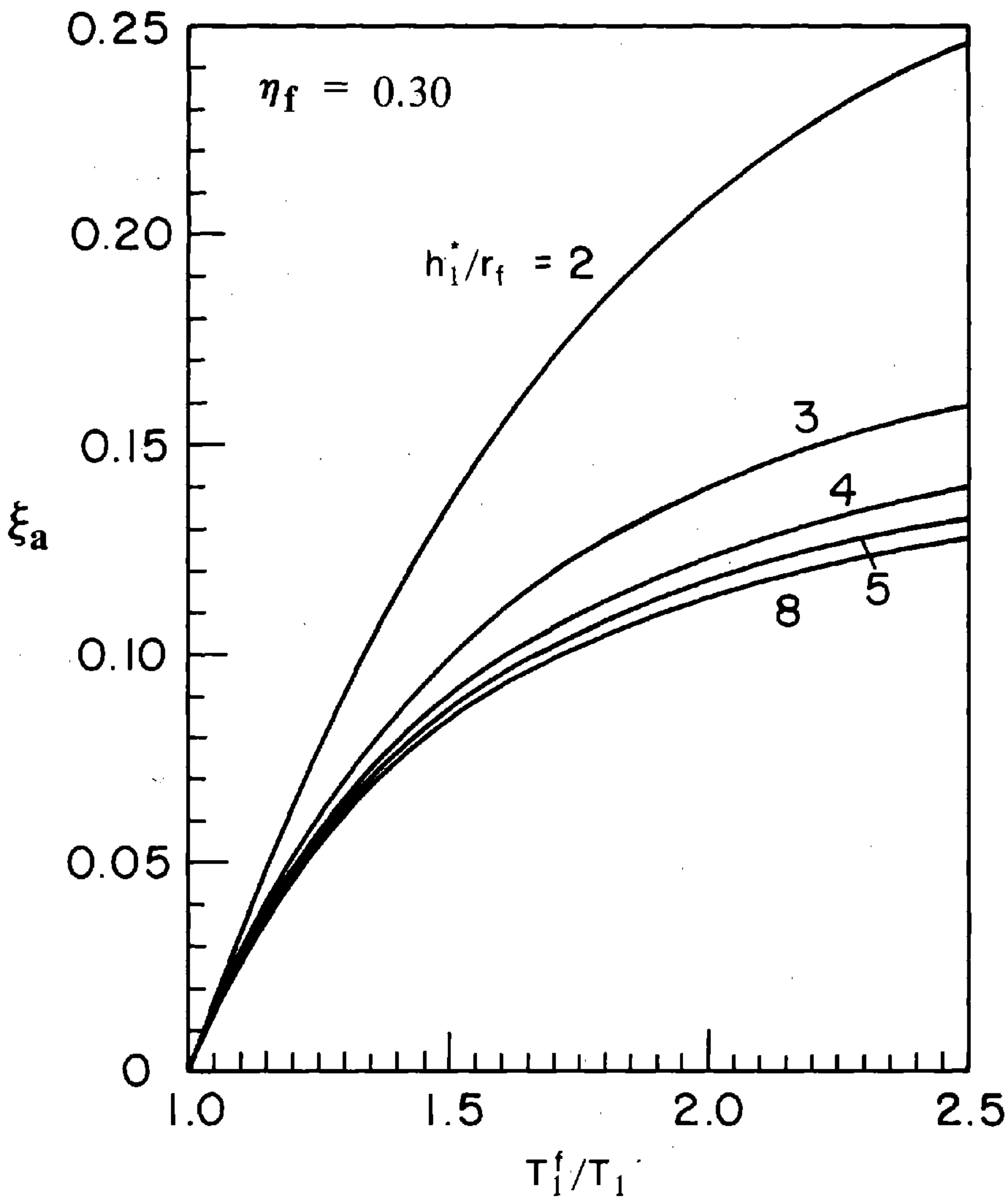

Figure 9.9 Added Foundation Damping, ξ_a , for Towers Supported on a Viscoelastic Halfspace with η_f = 0.30; γ^* = 0.10

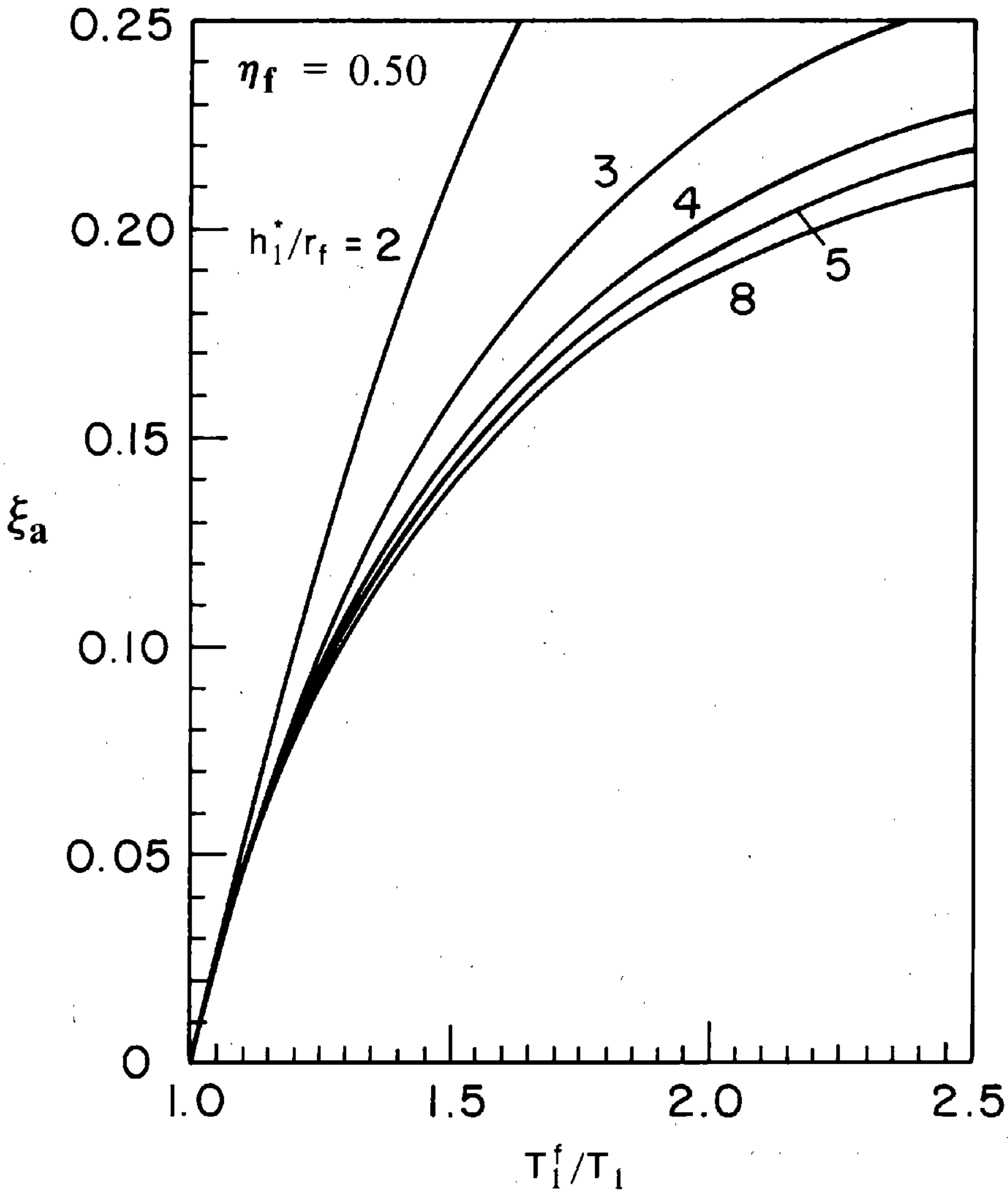

Figure 9.10 Added Foundation Damping, ξ_a , for Towers Supported on a Viscoelastic Halfspace with $\eta_f = 0.50$; $\gamma^* = 0.10$

structures [45].

The data presented in Figures 9.6 to 9.10 are for systems with $\gamma^* = 0.10$. For systems having any value of γ^* between 0.05 to 0.15, ξ_a may be estimated by multiplying the results obtained from Figures 9.6 to 9.10 by the factor C_γ determined by trial and error [45]:

$$C_\gamma = \sqrt{\frac{0.10}{\gamma^*}} \tag{9.27}$$

If this correction factor exactly accounted for the effect of γ^*, the three curves for any fixed value of h_1^*/r_f in Figure 9.11 would be coincident. Clearly this is not the case for the range of h_1^*/r_f and γ^* relevant to intake-outlet towers, whereas much better agreement was obtained for the range of parameters considered for buildings [45].

Noting that the agreement among the curves in Figure 9.11 for various γ^* deteriorate with increasing h_1^*/r_f, it seemed that better results could be obtained by modifying C_γ to be dependent on r_f/h_1^* leading to

$$\tilde{C}_\gamma = \left[\frac{0.10}{\gamma^*}\right]^{r_f/h_1^*} \tag{9.28}$$

This correction factor is adopted for towers as it reduces the spread in the results (Figure 9.12) compared to the factor of equation (9.27).

Having determined T_1^f/T_1 and ξ_a, the effective damping ratio ξ_1^f can be computed from equation (9.26). If the computed value turns out to be less than the damping ratio ξ_1 of the fixed-base tower, in design applications it is appropriate to take $\xi_1^f = \xi_1$ [45].

9.4.4 Criterion for Assessing Importance of Interaction

The ratio T_1^f/T_1 may be used as a basis for assessing the importance of tower-foundation-soil interaction; e.g. these interaction effects may be considered negligible if

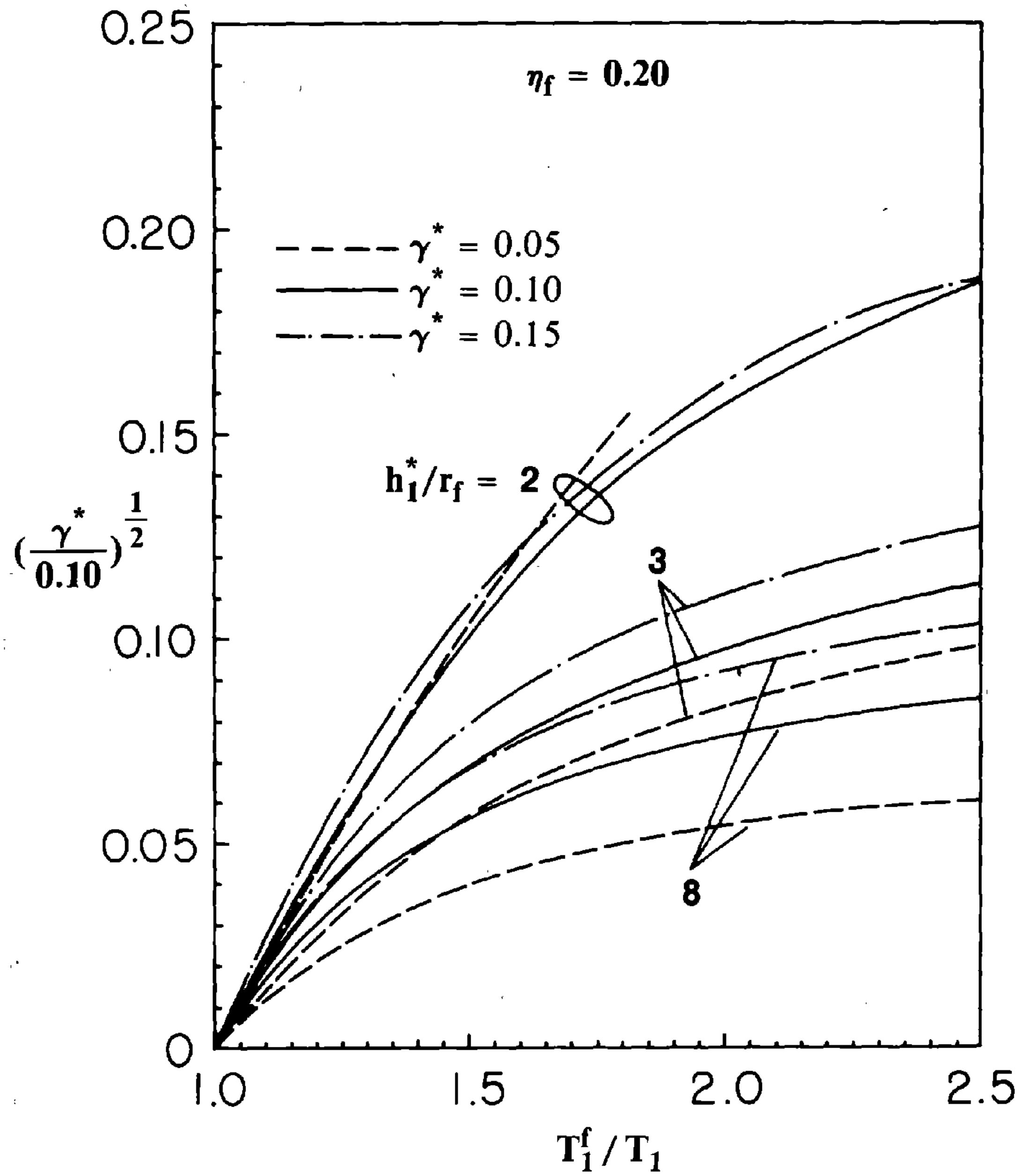

ıre 9.11 Added Foundation Damping, ξ_a, for Towers Supported on a Viscoelas-
Halfspace with a Range of Values of γ^*; η_f = 0.20

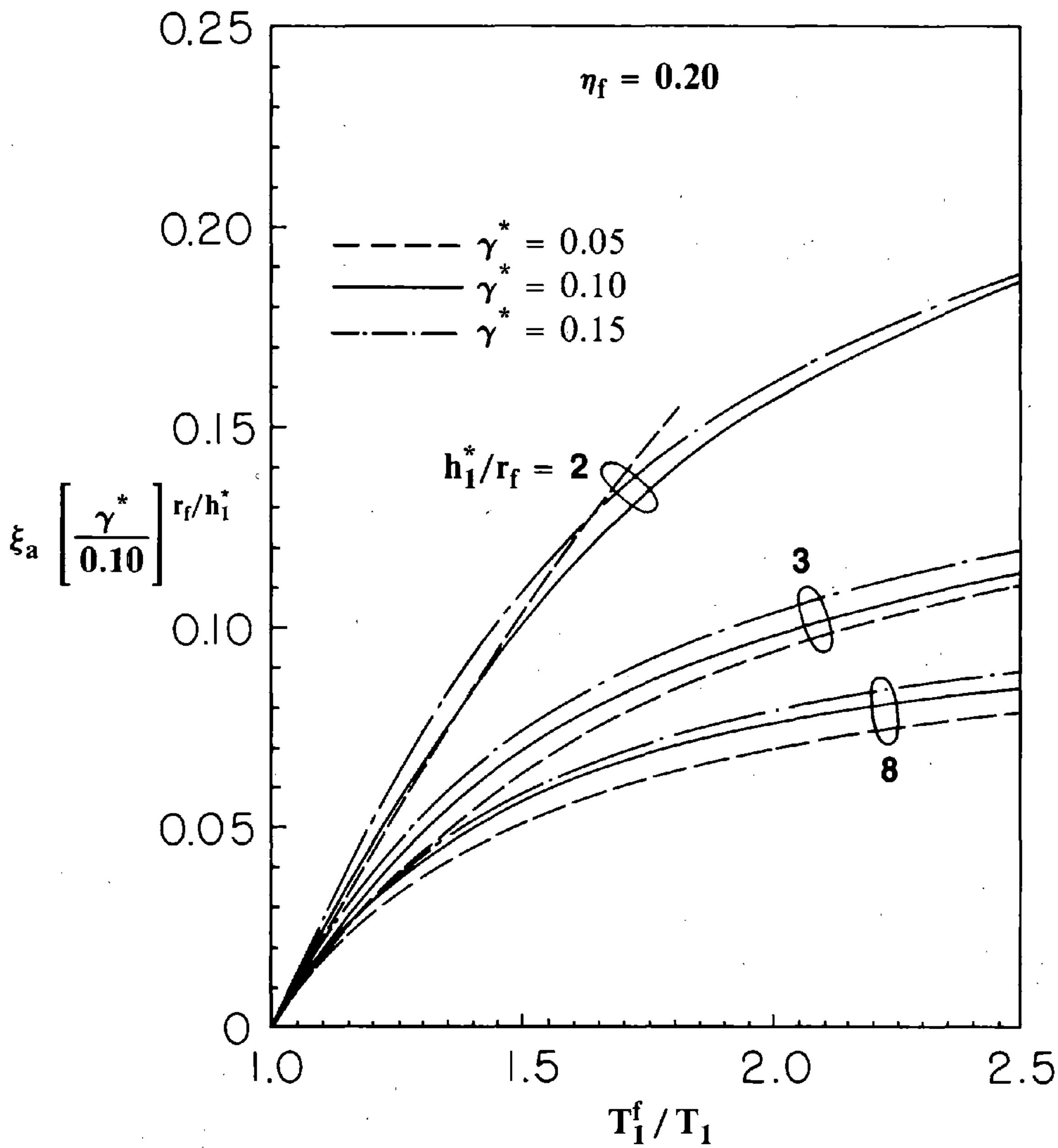

Figure 9.12 Added Foundation Damping, ξ_a, for Towers Supported on a Viscoelastic Halfspace with a Range of Values of γ^*; η_f = 0.20

T_1^f/T_1 is less than about 1.05. Although it is not difficult to compute T_1^f from equation (9.21), especially if it is evaluated using the static values of the foundation stiffnesses, it may be more convenient to assess the importance of interaction by a criterion based on the parameter $\tilde{\chi}$. Based on the results for T_1^f/T_1 and ξ_a presented earlier, it has been concluded that the interaction effects are generally of negligible importance for design applications when the dimensionless parameter defined by equation (9.25) is less than 0.20, i.e.

$$\tilde{\chi} \leq 0.20 \tag{9.29}$$

This inequality corresponds approximately to values of $T_1^f/T_1 \leq 1.10$ for $\gamma^* = 0.10$, a reasonable average value for intake-outlet towers with added hydrodynamic mass.

9.4.5 Summary of the Procedure

Based on the information presented in the preceding sections, the vibration period T_1^f and the damping ratio ξ_1^f for the fundamental vibration mode of the tower, considering the effects of tower-foundation-soil interaction, can be estimated as follows :

1. Evaluate the fixed-base natural period, T_1, and mode shape, $\phi_1(z)$, of the fundamental vibration mode of the tower by the procedure of Section 9.2.1. Use structural properties which are consistent with the severity of the design ground motion.

2 Determine the effective mass m_1^* and the effective height h_1^* for the fundamental vibration mode by equations (9.15) and (9.16) respectively.

3 Evaluate the dimensionless flexibility parameters $\tilde{\chi}$, defined by equation (9.25), and γ^*, defined by equation (9.20). Use soil properties which are consistent with the severity of the design ground motion. The parameter r_f is the radius of the circular foundation. For a non-circular foundation, use equation (9.19) to determine the radius of the 'equivalent' circular foundation. If $\tilde{\chi} \leq 0.20$, ignore the effects of interaction and analyze the structure as if it were fixed at the base. Otherwise, proceed with the

following steps.

4 Determine the effective natural vibration period $\tilde{T}_1^f$ of the system from the mean curve presented in Figure 9.5. If desired, a more accurate estimate may be obtained by iteration from equation (9.21), recognizing that stiffnesses k_{VV} and k_{MM} depend on the vibration period.

5. Estimate the values of η_f and ξ_1 which would be appropriate for the severity of the design ground motion, and evaluate the added foundation damping, ξ_a, from Figures 9.6 to 9.10 and by use of equation (9.28).

6. Compute the effective damping ratio $\tilde{\xi}_1^f$ of the interacting system from equation (9.26). If $\tilde{\xi}_1^f$ turns out to be less than ξ_1, take $\tilde{\xi}_1^f = \xi_1$.

9.5 Simplified Analysis Procedure

Utilizing the procedures presented earlier to compute the first two vibration periods and mode shapes (Section 9.2), the added hydrodynamic mass associated with surrounding and inside water (Section 9.3), the modifications to the vibration period and damping ratio for the fundamental vibration mode (Section 9.4), a simplified procedure is presented next to compute, directly from the earthquake design spectrum, the maximum shear forces and bending moments in an intake-outlet tower. The procedure is presented as a sequence of computational steps :

1. Define the smooth design spectrum for the tower at the particular site. This may be an elastic design spectrum or a reduced inelastic design spectrum to account for the effects of ductility. The design ductility of towers generally should not exceed 2, which is much smaller than typically selected for building design for reasons discussed earlier [13].

2. Compute the added hydrodynamic mass $m_a^o(z)$ associated with the surrounding (outside) water, using the procedure of Section 9.3.1.

3. Compute the added hydrodynamic mass $m_a^i(z)$ associated with the inside water, using the procedure of Section 9.3.2.

4. Define structural properties of the tower :

   (a) Virtual mass, $\tilde{m}_s(z)$, per unit of height is given by the equation

$$\tilde{m}_s(z) = m_s(z) + m_a^o(z) + m_a^i(z) \tag{9.30}$$

   where $m_s(z)$ is the mass of the tower by itself, $m_a^o(z)$ is computed in step 2, and $m_a^i(z)$ in step 3.

   (b) Flexural stiffness, $E_s I(z)$, and shear stiffness, $G_s k(z) A(z)$, per unit of height.

   (c) Modal damping ratios, ξ_n.

5. Compute the periods $T_n^r = 2\pi/\omega_n^r$ and mode shapes $\tilde{\phi}_n(z)$ for the first two modes of vibration (i.e. $n = 1,2$) by the simplified procedure of Section 9.2 with mass $m_s(z)$ replaced by the virtual mass $\tilde{m}_s(z)$. The superscript r in ω_n is included to be consistent with earlier notation as ω_n^r includes the effects of water on the vibration frequencies, and the notation $\tilde{\phi}_n(z)$ is used to indicate that these are mode shapes of the tower with mass $\tilde{m}_s(z)$.

6. Compute the vibration period $\tilde{T}_1$ and damping ratio $\tilde{\xi}_1$ for the fundamental vibration mode of the tower including the hydrodynamic effects and the tower-foundation-soil interaction effects. For this purpose, the period ratio $\tilde{T}_1/T_1^r$ and damping ratio $\tilde{\xi}_1$ are given by T_1^f/T_1 and ξ_1^f, respectively, determined by the procedure of Section 9.4.5 with $m_s(z)$ replaced by the virtual mass $\tilde{m}_s(z)$.

7. The vibration period $\tilde{T}_2$ and damping ratio $\tilde{\xi}_2$ for the second vibration mode are determined by standard procedures disregarding the effects of tower-foundation-soil interaction. Thus :

$$\tilde{T}_2 = T_2^r \tag{9.31}$$

where T_2^r was determined in step 5, and

$$\tilde{\xi}_2 = \xi_2 \tag{9.32}$$

where the damping ratio ξ_2 was estimated in step 4(c).

8. Compute the maximum response (shears and moments) in individual modes of vibration by repeating the following steps for the first two modes of vibration (i.e. $n = 1 , 2$):

   (a) Corresponding to period $\tilde{T}_n$ and damping ratio $\tilde{\xi}_n$, read the ordinate S_a of the pseudo-acceleration from the design spectrum.

   (b) Compute equivalent lateral forces $f_n(z)$ associated with vibration of the tower in its n-th mode from:

$$f_n(z) = \frac{\tilde{L}_n}{\tilde{M}_n} S_a(\tilde{T}_n,\tilde{\xi}_n)\, \tilde{m}_s(z)\, \tilde{\phi}_n(z) \tag{9.33}$$

   in which the generalized mass $\tilde{M}_n$ and generalized excitation $\tilde{L}_n$ terms, including the added hydrodynamic mass, are :

$$\tilde{M}_n = \int_0^{H_s} \tilde{m}_s(z)\, [\, \tilde{\phi}_n(z)\,]^2\, dz \tag{9.34}$$

$$\tilde{L}_n = \int_0^{H_s} \tilde{m}_s(z)\, \tilde{\phi}_n(z)\, dz \tag{9.35}$$

(c) Compute the shear $Q_n(z)$ and bending moment $\mathcal{M}_n(z)$ at any section by static analysis of the tower subjected to equivalent lateral forces $f_n(z)$:

$$Q_n(z) = \int_z^{H_s} f_n(\zeta)\, d\zeta \tag{9.36}$$

$$\mathcal{M}_n(z) = \int_z^{H_s} (\zeta - z)\, f_n(\zeta)\, d\zeta \tag{9.37}$$

9. Determine an estimate of the maximum shear $Q(z)$ and bending moment $\mathcal{M}(z)$ at any section by combining the modal maxima $Q_n(z)$ and $\mathcal{M}_n(z)$ in accordance with the equations :

$$Q(z) \approx \sqrt{Q_1^2(z) + Q_2^2(z)} \tag{9.38}$$

$$\mathcal{M}(z) \approx \sqrt{\mathcal{M}_1^2(z) + \mathcal{M}_2^2(z)} \tag{9.39}$$

This square-root-of-the-sum-of-squares (SRSS) combination rule is appropriate because the vibration periods $\tilde{T}_1$ and $\tilde{T}_2$ of towers are well separated. Essentially no improvement in accuracy will result by including correlation of modal responses in equations (9.38) or (9.39).

For the special case of rigid foundation soil, $\tilde{T}_n = T_n^r$, and $\xi_a = 0$ leading to $\tilde{\xi}_n = \xi_n$. If there is no water, use $\tilde{m}_s(z) = m_s(z)$ throughout the above analysis.

In practical applications, it would be necessary to determine the total response considering the combined effects of the two horizontal components of ground motion. With the selected design spectrum, taken to be the same for both components of ground motion, the procedure described above should be implemented for each component, using tower properties appropriate for vibration in that direction. The peak value of any response quantity R, due to the combined effects of the gravity loads and ground motion components, can be obtained by combining the peak responses R_x due to the x-component of ground motion, and R_y due to the y-component of ground motion, and the response R_o due to gravity loads. The design value of R is approximately equal to the largest of the values obtained from the following equations:

$$R = R_o \pm R_x \pm \alpha R_y \tag{9.40a}$$

$$R = R_o \pm \alpha R_x \pm R_y \tag{9.40b}$$

In particular, this procedure is applicable to the computation of an individual stress component at a point in the tower.

For reinforced concrete towers, however, it is more useful to compute the shearing force and bending moment at each section of the tower instead of evaluating the stress distribution across the section. For a tower with plan symmetric about x and y axes, at any section the x component of ground motion will cause shear only in the x direction, Q_x, and bending moment only about the y-axis, $\mathcal{M}_x$, and the y-component of ground motion will produce shear only in the y direction, Q_y, and bending moment only about the x-axis, $\mathcal{M}_y$.

In designing a reinforced concrete tower, with its plan being symmetrical in geometry as well as reinforcement about the x and y axes, it would be sufficient to consider at each section the following combinations of shears: (1) Q_x and $\alpha\, Q_y$, and (2) $\alpha\, Q_x$ and Q_y. Similarly, the combinations of bending moments that need to be considered are: (1) $\mathcal{M}_x$ and $\alpha\, \mathcal{M}_y$, and (2) $\alpha\, \mathcal{M}_x$ and $\mathcal{M}_y$. The gravity loads will not contribute to the shearing forces or bending moments in a symmetrical tower.

In the case of towers with hollow circular cross-sections, $Q_x = Q_y$ and $\mathcal{M}_x = \mathcal{M}_y$ because the tower properties for vibration in x and y directions are the same, and the design spectrum is taken to be the same for the two components of ground motion. Therefore, the tower section should be designed for shearing force $= Q_x \sqrt{1 + \alpha^2}$ and bending moment $=$ $\mathcal{M}_x \sqrt{1 + \alpha^2}$.

Based on Reference [42], it is appropriate to take $\alpha = 0.5$ for towers which is significantly larger than the value of 0.3 recommended for buildings.

9.6 Evaluation of Simplified Analysis Procedure

As mentioned in Chapters 7 and 8, and in the preceding sections of this chapter, various approximations were introduced to develop the simplified analysis procedure and these were individually checked to ensure that they would lead to acceptable results. In order to provide an overall evaluation of the simplified analysis procedure, earthquake-induced shear forces and bending moments computed by this procedure were compared with those obtained from the refined response history analysis, rigorously including effects of tower-water interaction and tower-foundation-soil interaction (Chapters 3 and 4).

9.6.1 System and Ground Motion

The system considered is a tapered tower with circular cross-section supported through a rigid circular foundation on the horizontal surface of a homogeneous viscoelastic halfspace (Figure 9.13). The inside and outside radii at the top of the tower are taken equal to half of their respective values at the base. The inside and outside radii decrease linearly along the height but their ratio $r_i(z)/r_o(z)$ at any location z above the base remains 0.8. Three values of the ratio of the tower height to its average radius at the base, $H_s/r_a = 20$, 10 and 5, are considered. The foundation radius r_f is taken as twice of the average radius of the tower at the base.

All towers are assumed to be homogeneous and isotropic with linear elastic properties for the concrete : Poisson's ratio $\nu_s = 0.17$, unit weight $= 155$ lb/ft^3 and the Young's modulus of elasticity $E_s = 4.5$ million psi. Energy dissipation in the tower is represented by constant hysteretic damping factor of $\eta_s = 0.10$ in the refined analysis but by viscous damping in the simplified analysis with damping ratios $\xi_n = 0.05$ in all the natural vibration modes of the tower on rigid foundation soil. The properties of the viscoelastic halfspace

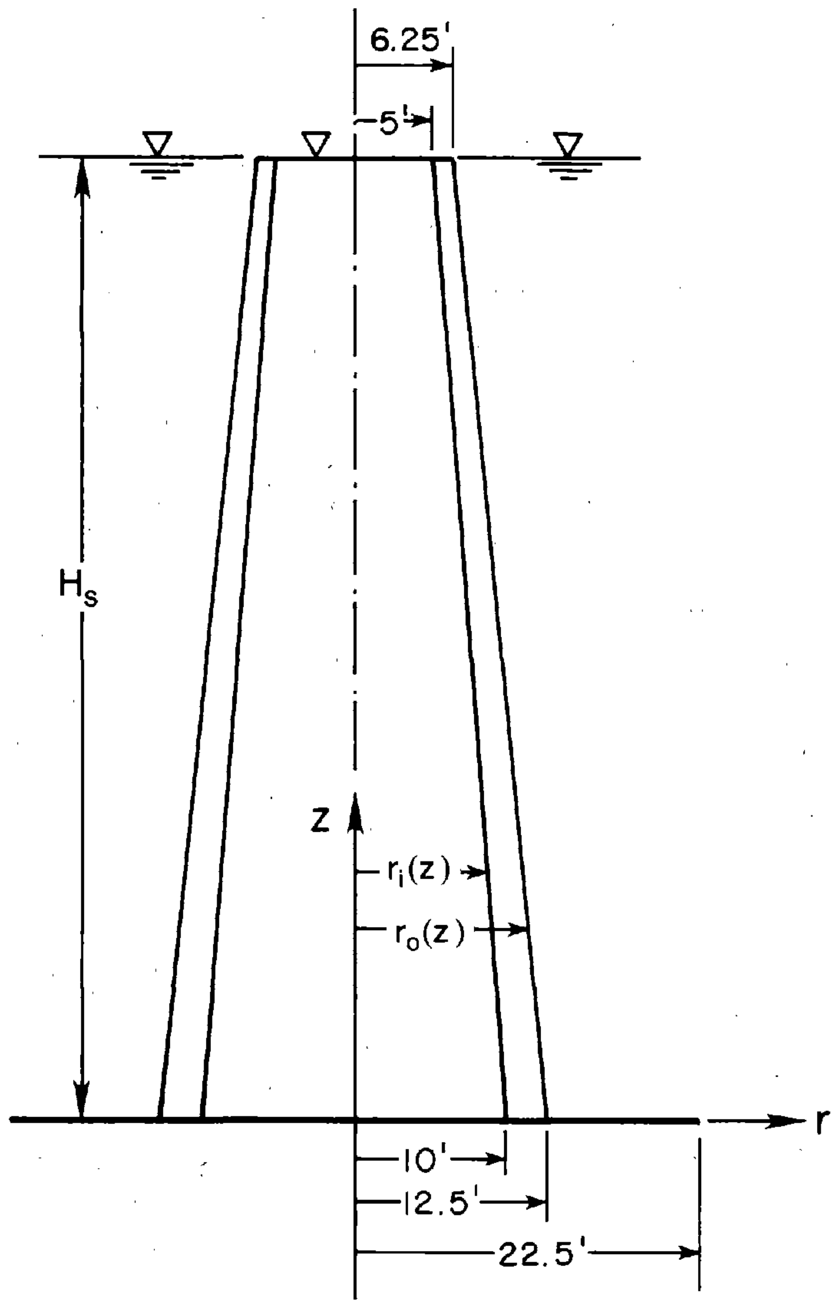

Figure 9.13 Idealized Axisymmetric Tapered Tower

material are : Poisson's ratio ν_f = 1/3, unit weight = 165 lb/ft^3, elastic shear wave velocity C_f = 1000 ft/sec, and the constant hysteretic damping coefficient of η_f = 0.10. The depths of the surrounding (outside) and inside water are taken equal to the height of the tower.

The ground motion for which the selected towers are analyzed is the S69E component of the ground motion recorded at the Taft Lincoln School Tunnel during the Kern County, California, earthquake of July 21, 1952. The response spectrum for this ground motion is shown in Figure 9.14. Such an irregular spectrum of an individual ground motion is inappropriate in conjunction with the simplified procedure, wherein a smooth design spectrum is recommended, but is used here to provide direct comparison with the results obtained from the refined analysis procedure.

9.6.2 Vibration Frequencies and Mode Shapes

In the simplified analysis procedure, the natural frequency and shape of the fundamental mode of vibration are computed by the Stodola method. By performing a sufficient number of iterations, these vibration properties can be computed almost exactly. On the other hand, the natural vibration frequency and shape of the second vibration mode is computed approximately -- without any iteration and neglecting rotatory inertia (Section 9.2.2). In Figure 9.15, the approximate results obtained by this procedure for the selected towers on rigid soil without water are compared with the exact frequency and shape of the second vibration mode obtained by computer analysis of the eigen-problem, including rotatory inertia (Chapter 4). Considering the simplicity of the approximate procedure, the results from this procedure are very good, which indicates that this procedure to evaluate the frequencies and mode shapes should be useful in practical applications.

9.6.3 Simplified Analysis Procedure

The earthquake induced forces for each of the 12 cases of Table 9.2 are computed by the simplified response spectrum analysis (SRSA) procedure, in which the maximum response in each of the first two vibration modes of the tower are determined from equations (9.33), (9.36) and (9.37) with n = 1 and 2, and the modal maxima are combined in

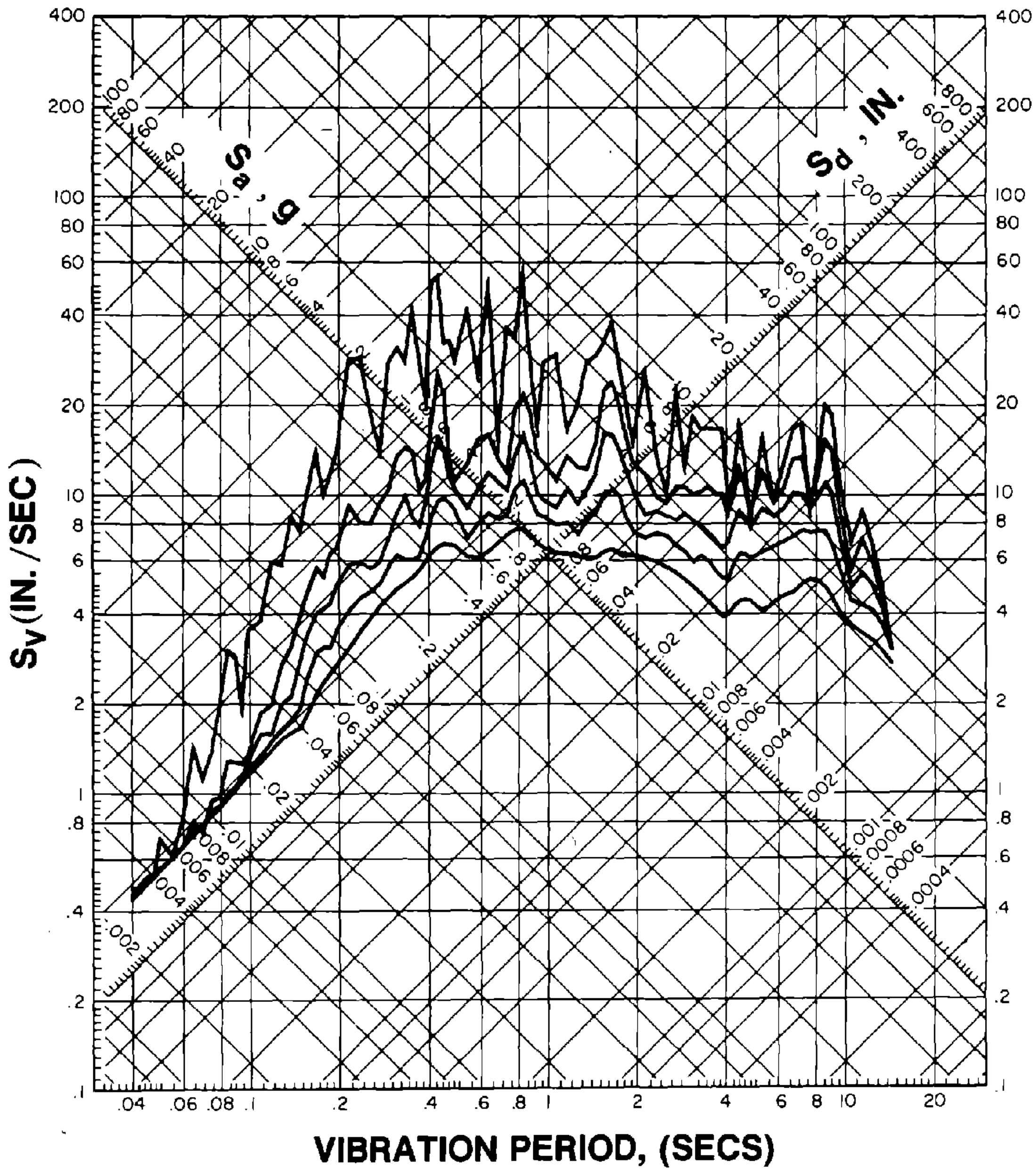

Figure 9.14 Response Spectrum for the S69E Component of Taft Ground Motion; Damping Ratios = 0, 2, 5, 10 and 20 Percent

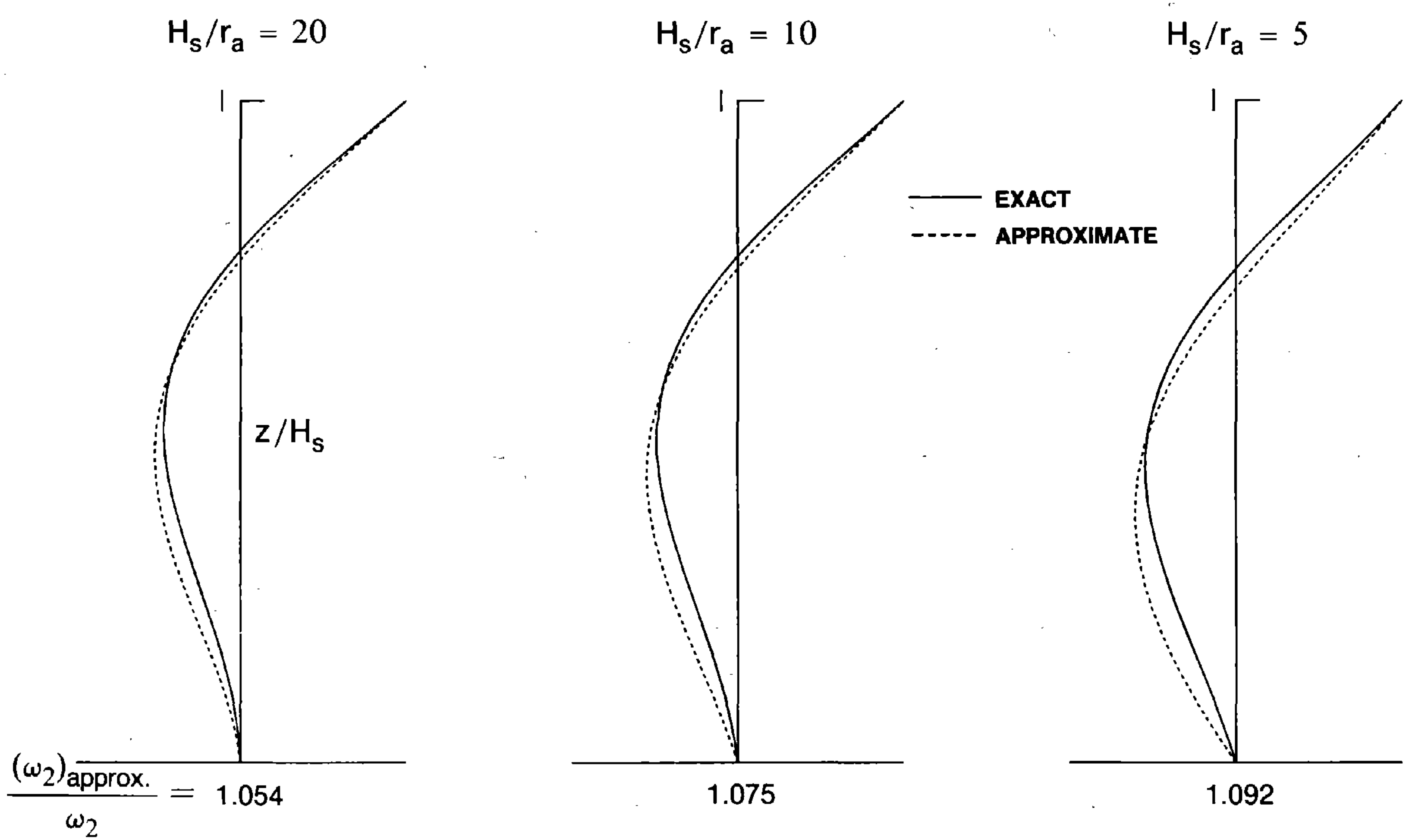

Figure 9.15 Comparison of Exact and Approximate Values of the Frequency and Shape for the Second Vibration Mode of Circular Tapered Towers

Table 9.2 -- Circular Tapered Tower Analysis Cases, and Fundamental Mode Properties from Simplified and Refined Analyses

Case	$\frac{H_s}{r_a}$	Water	Foundation Soil	Exact Analysis			Simplified Analysis		
				$\tilde{T}_1$ (sec.)	$\tilde{\xi}_1$ (percent)	$\frac{S_a(\tilde{T}_1, \tilde{\xi}_1)}{g}$	$\tilde{T}_1$ (sec.)	$\tilde{\xi}_1$ (percent)	$\frac{S_a(\tilde{T}_1, \tilde{\xi}_1)}{g}$
1	20	none	rigid	0.722	5.00	0.238	0.720	5.00	0.240
2	20	none	flexible	0.870	4.96	0.293	0.852	4.49	0.325
3	20	full	rigid	1.203	5.00	0.145	1.210	5.00	0.143
4	20	full	flexible	1.444	4.89	0.125	1.433	4.45	0.127
5	10	none	rigid	0.187	5.00	0.380	0.186	5.00	0.387
6	10	none	flexible	0.267	6.22	0.352	0.251	5.44	0.356
7	10	full	rigid	0.304	5.00	0.426	0.305	5.00	0.430
8	10	full	flexible	0.425	5.25	0.533	0.414	4.77	0.487
9	5	none	rigid	0.053	5.00	0.188	0.052	5.00	0.186
10	5	none	flexible	0.106	21.28	0.198	0.080	24.81	0.192
11	5	full	rigid	0.081	5.00	0.195	0.082	5.00	0.198
12	5	full	flexible	0.152	13.94	0.206	0.137	12.11	0.210

accordance with equations (9.38) and (9.39) to obtain an estimate of the total values of the earthquake induced forces. Contained in these results are the errors associated with the approximate evaluation of the frequency and shape of the second vibration mode, the approximate representation of hydrodynamic and foundation interaction effects, neglecting response contributions of higher vibration modes (i.e. higher than second mode), and with the usual procedures of combining the peak modal responses. Computational details of the steps concerned with tower-foundation-soil interaction effects are presented in Appendix I as an example.

In order to eliminate the errors associated with combining modal maxima, the response of each tower was also determined by a variation of the simplified analysis procedure. Instead of computing the modal maxima from equation (9.33), the modal response-history is obtained by replacing $S_a(\tilde{T}_n,\tilde{\xi}_n)$ by the time-history of pseudo-acceleration for a single-degree-of-freedom system with vibration period $\tilde{T}_n$ and damping ratio $\tilde{\xi}_n$ due to the selected ground motion. At any instant of time, the shear and bending moment at any section of the tower is then obtained by static analysis of the tower subjected to the equivalent lateral forces $f_n(z,t)$ at that time. The instantaneous values of the modal contributions are combined exactly and the peak value of the combined value is then determined. The results of this simplified response history analysis (SRHA) procedure are not affected by the approximations involved in the procedures for combining peak values of modal responses.

9.6.4 Comparison with Refined Analysis Procedure

The earthquake response of towers is computed for each of the 12 cases of Table 9.2 by the 'exact' analysis procedure in which the hydrodynamic and foundation interaction effects are rigorously considered (Chapter 3). In this procedure the deformations of the tower are expressed as a linear combination of the fixed-base natural vibration modes of the tower. Two separate 'exact' analyses were implemented in each case, considering two and five modes, respectively. The responses were essentially unaffected by the contributions of vibration modes higher than the 5-th mode.

Before examining the response results, the effective period and damping ratio for the fundamental vibration mode obtained from the refined and simplified analysis procedures are presented in Table 9.2 along with the corresponding values of the ordinate of the pseudo-acceleration response spectrum of the Taft ground motion. It is apparent that the simplified procedure leads to acceptable estimates of the vibration period and the damping ratio for the fundamental mode. Since for some towers the response is dominated by the fundamental vibration mode, this comparison provides a confirmation that the simplified analysis procedure is able to represent the important effects of tower-water interaction and tower-foundation-soil interaction. The underestimation of the damping ratio in the simplified analysis of some towers on flexible foundation soil (Table 9.2) is the result, in part, of the assumption of viscous damping mechanism for the tower in the simplified analysis in contrast to the constant hysteretic damping mechanism used in the refined analysis.

The accuracy of the simplified response history analysis (SRHA) is illustrated in Figures 9.16 to 9.18 and Table 9.3 in which are presented the computed shears and bending moments in the tower and compared with those obtained from the 'exact' analysis considering two fixed-base modes. The agreement is satisfactory implying that the errors arising from approximations in the vibration properties of the second mode and in the simplified representation of hydrodynamic and foundation interaction effects are acceptably small.

In the SRSA procedure, the peak value of each of the the first two modal responses is computed directly from the response spectrum without a response history analysis. The accuracy of combining the peak modal responses is evaluated in Figures 9.19 to 9.21 and Table 9.3 in which the combined value is compared with the results obtained by the SRHA in which the instantaneous values of the modal contributions were combined exactly. It is apparent that significant errors can result from the usual procedure for combining modal maxima when the results are based on response to a single ground motion. These errors are inherent in response spectrum analysis (RSA) procedures and are well known. However,

Table 9.3 Maximum Values of Base Shear and Base Moment for Circular Tapered Towers due to S69E Component of Taft Ground Motion

Case	H_s/r_a	Water	Found. Soil	Base Shear / $(m_t g)$				Base Moment / $(m_t g H_s)$			
				Exact Analysis		Simplified Analysis		Exact Analysis		Simplified Analysis	
				2 Mode	5 Mode	RHA	RSA	2 Mode	5 Mode	RHA	RSA
1	20	none	rigid	0.182	0.193	0.206	0.153	0.088	0.090	0.094	0.079
2	20	none	flexible	0.168	0.193	0.187	0.182	0.098	0.099	0.100	0.098
3	20	full	rigid	0.297	0.381	0.325	0.347	0.152	0.149	0.156	0.147
4	20	full	flexible	0.313	0.399	0.348	0.335	0.141	0.141	0.131	0.134
5	10	none	rigid	0.193	0.216	0.207	0.191	0.124	0.125	0.128	0.125
6	10	none	flexible	0.208	0.241	0.189	0.177	0.123	0.126	0.118	0.115
7	10	full	rigid	0.669	0.746	0.713	0.618	0.402	0.409	0.417	0.394
8	10	full	flexible	0.900	0.974	0.810	0.694	0.528	0.534	0.474	0.446
9	5	none	rigid	0.139	0.164	0.150	0.111	0.073	0.075	0.073	0.066
10	5	none	flexible	0.145	0.173	0.151	0.114	0.077	0.079	0.075	0.068
11	5	full	rigid	0.399	0.469	0.436	0.332	0.203	0.205	0.207	0.187
12	5	full	flexible	0.394	0.453	0.433	0.347	0.205	0.207	0.213	0.198

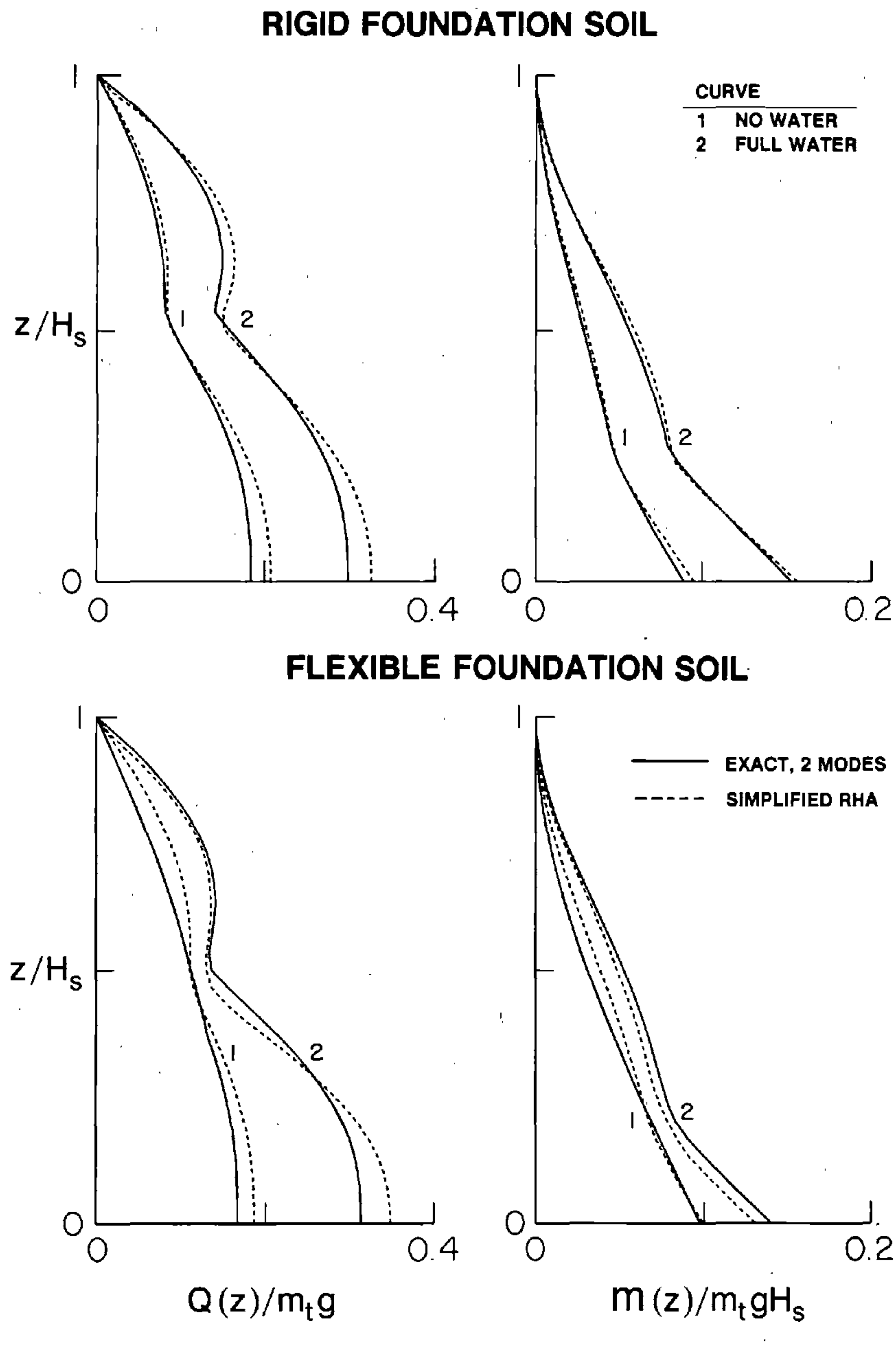

Figure 9.16 Comparison of Exact (2 Modes) and Simplified Response History Analysis Results for Envelope Values of Maximum Shear Forces and Bending Moments in Circular Tapered Tower with $H_s/r_a = 20$ due to S69E Component of Taft Ground Motion; Cases 1 to 4

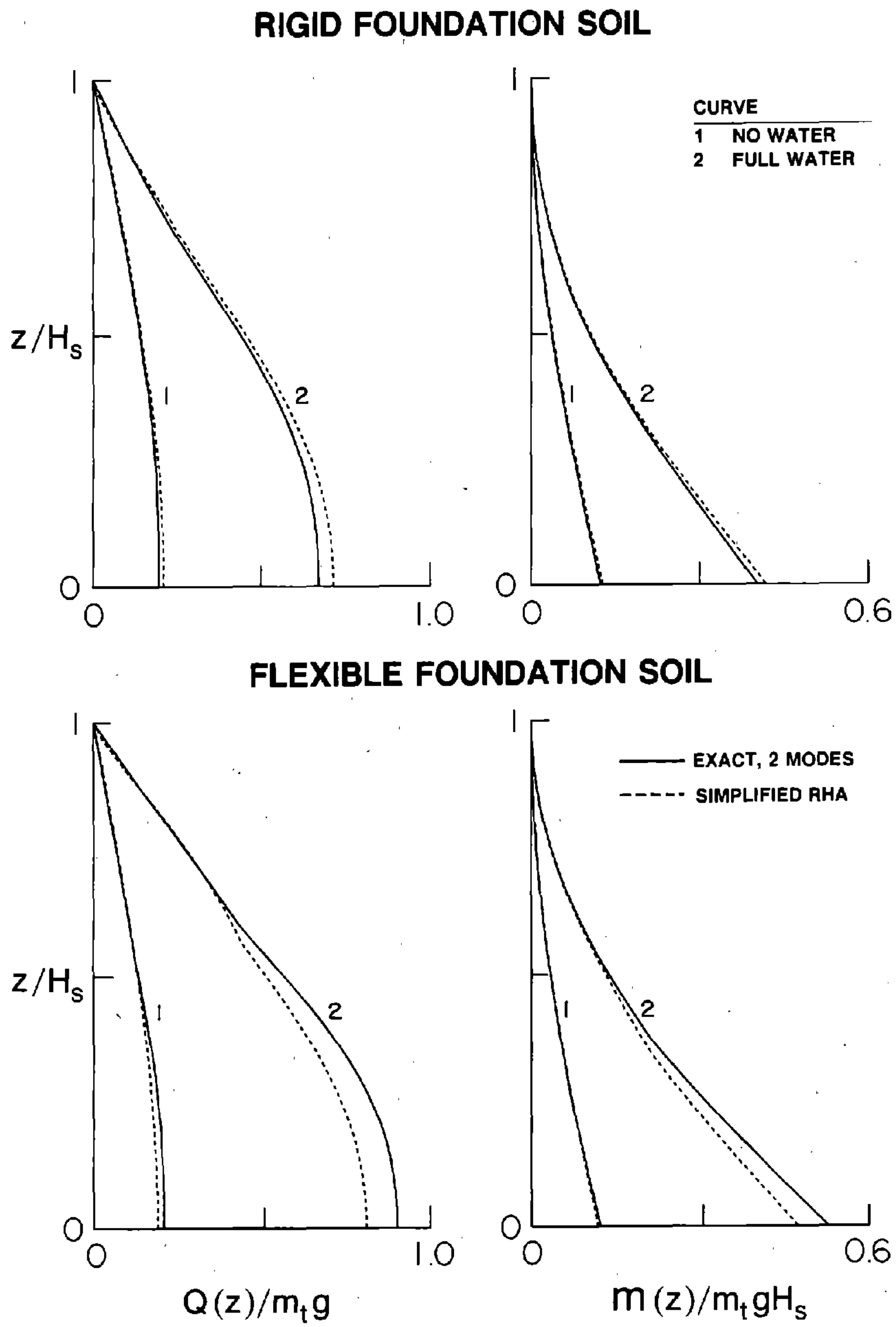

Figure 9.17 Comparison of Exact (2 Modes) and Simplified Response History Analysis Results for Envelope Values of Maximum Shear Forces and Bending Moments in Circular Tapered Tower with H_s/r_a = 10 due to S69E Component of Taft Ground Motion; Cases 5 to 8

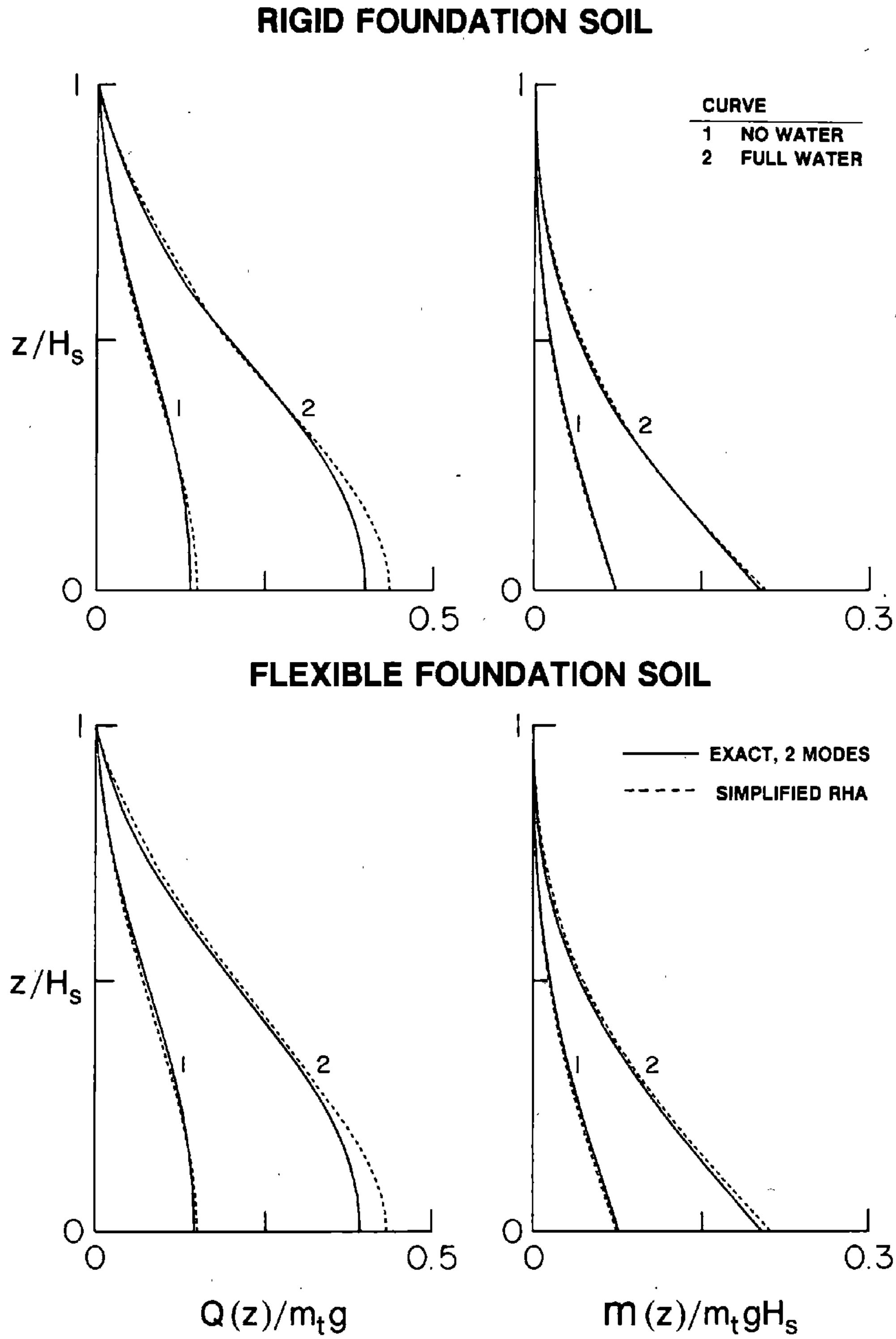

Figure 9.18 Comparison of Exact (2 Modes) and Simplified Response History Analysis Results for Envelope Values of Maximum Shear Forces and Bending Moments in Circular Tapered Tower with $H_s/r_a = 5$ due to S69E Component of Taft Ground Motion; Cases 9 to 12

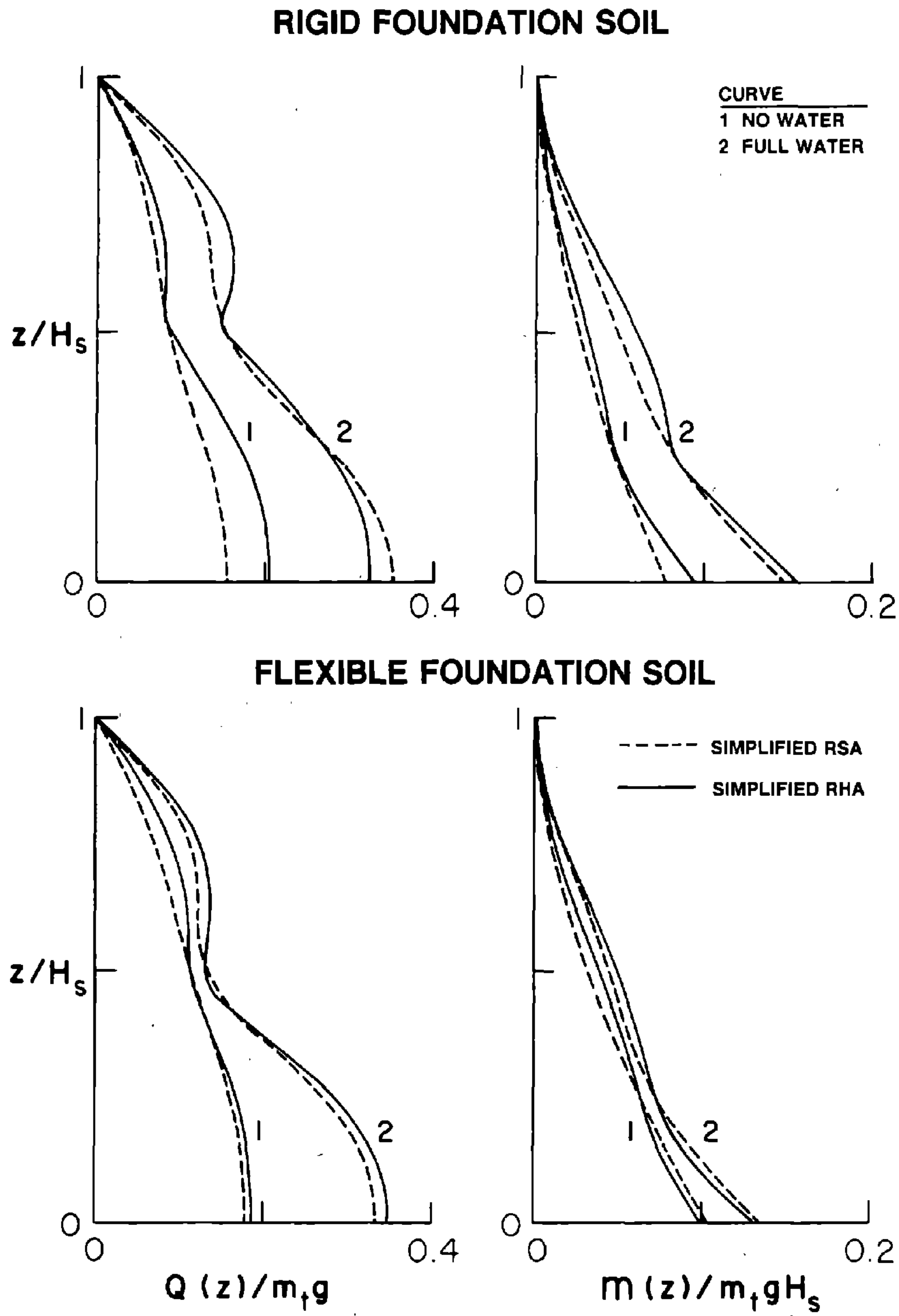

Figure 9.19 Comparison of Simplified Response Spectrum and Simplified Response History Analysis Results for Envelope Values of Maximum Shear Forces and Bending Moments in Circular Tapered Tower with H_s/r_a = 20 due to S69E Component of Taft Ground Motion; Cases 1 to 4

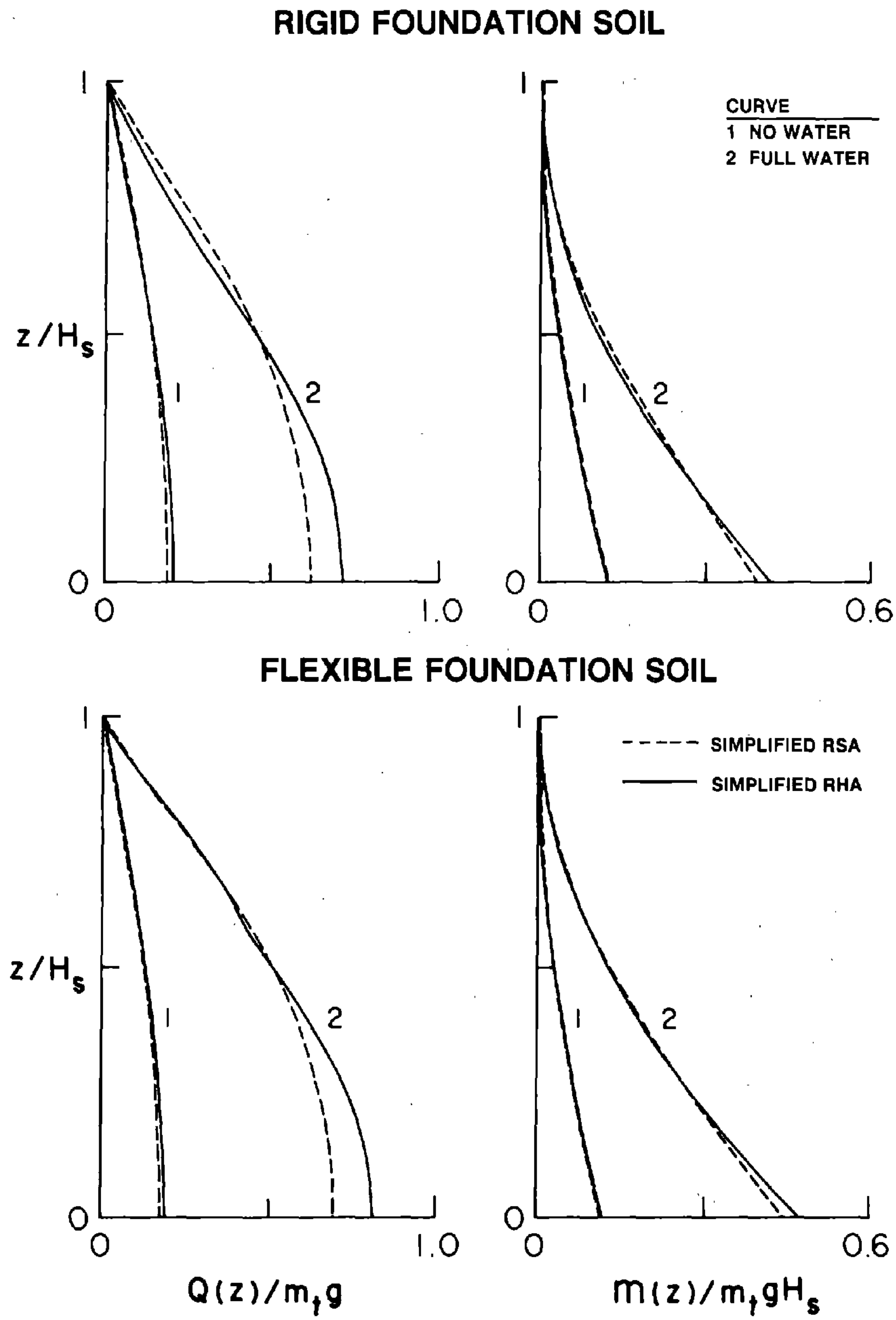

Figure 9.20 Comparison of Simplified Response Spectrum and Simplified Response History Analysis Results for Envelope Values of Maximum Shear Forces and Bending Moments in Circular Tapered Tower with $H_s/r_a = 10$ due to S69E Component of Taft Ground Motion; Cases 5 to 8

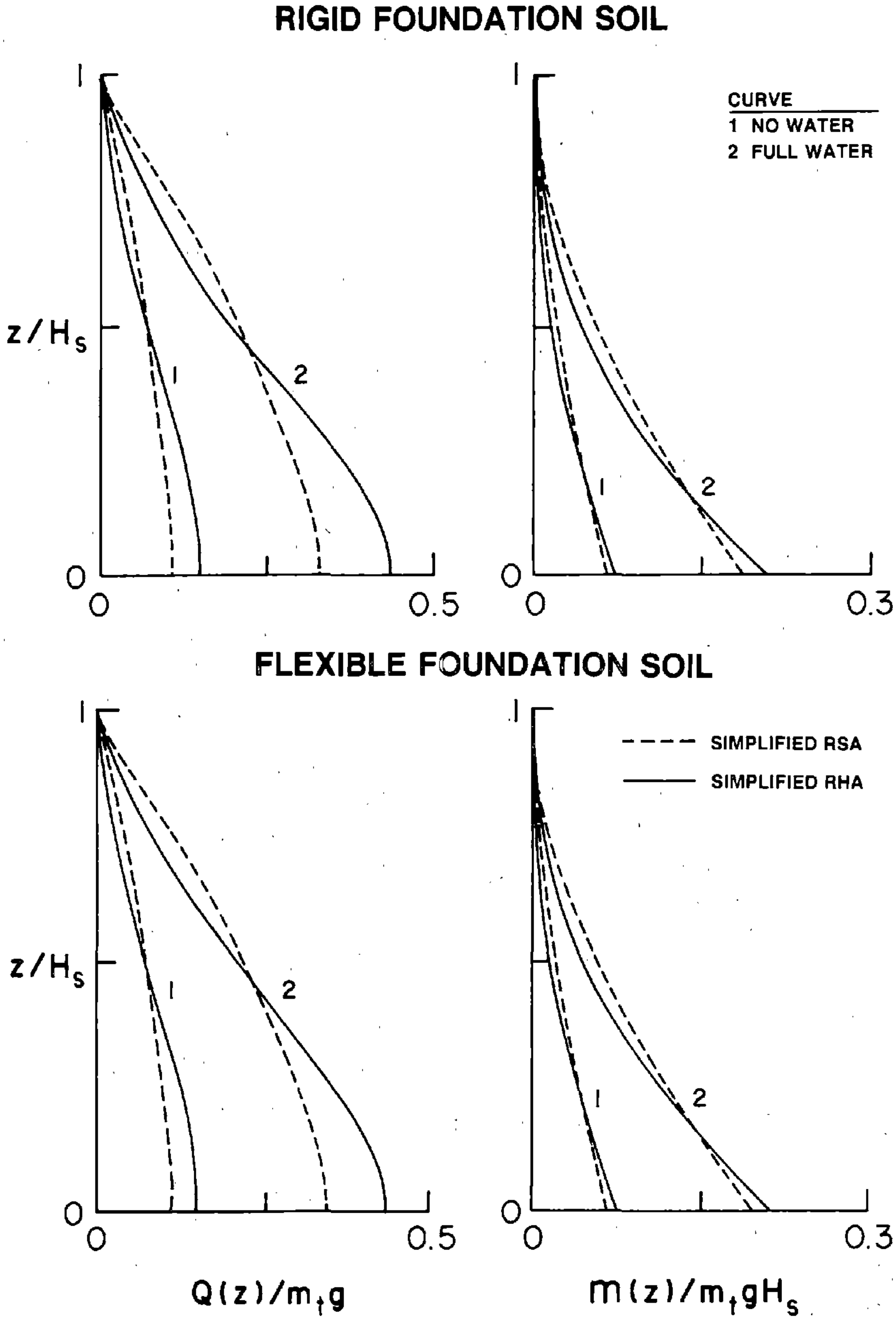

Figure 9.21 Comparison of Simplified Response Spectrum and Simplified Response History Analysis Results for Envelope Values of Maximum Shear Forces and Bending Moments in Circular Tapered Tower with $H_s/r_a = 5$ due to S69E Component of Taft Ground Motion; Cases 9 to 12

they become smaller when the RSA procedure is used in conjunction with a smooth design spectrum. Although the peak modal responses were combined by the SRSS procedure to obtain the results of Figure 9.19 to 9.21 and Table 9.3, the results would have been essentially unaffected by using any procedure, such as CQC, that considers correlation of modal responses because the modal vibration periods of towers are well separated.

The response contributions of the vibration modes higher than the second mode are illustrated in Figures 9.22 to 9.24 and Table 9.3 where the results from the two 'exact' analyses are compared. The higher mode contributions vary with slenderness ratio, among other parameters, being more significant in the response of slender towers. Such towers are usually long-period structures (Table 9.2) and, as is well known, the higher mode contributions are relatively more significant in the responses of such structures.

Finally, In Figures 9.25 to 9.27 and Table 9.3, the results obtained from the SRSA procedure are compared with the 'exact' analysis considering five vibration modes. As mentioned earlier, contained in the SRSA results are the errors arising from approximations in evaluating the frequency and shape of the second vibration mode, representing hydrodynamic and foundation interaction effects, neglecting response contributions of higher vibration modes (i.e. higher than second mode) and in the usual procedures of combining the peak modal responses. Because of these approximations, significant errors can be noted in the SRSA results for some cases in these figures. However, these errors will become significantly smaller when the SRSA procedure is used in conjunction with a smooth design spectrum instead of the irregular spectrum (Figure 9.14), typical of an individual ground motion.

It is apparent from the comparisons presented above that the accuracy of the response results obtained by the simplified analysis procedure is satisfactory for the preliminary phase in the design of new towers and in the safety evaluation of existing towers, considering the complicated effects of tower-water and tower-foundation-soil interactions, and the number of approximations necessary to develop the procedure. The simplified analysis procedure

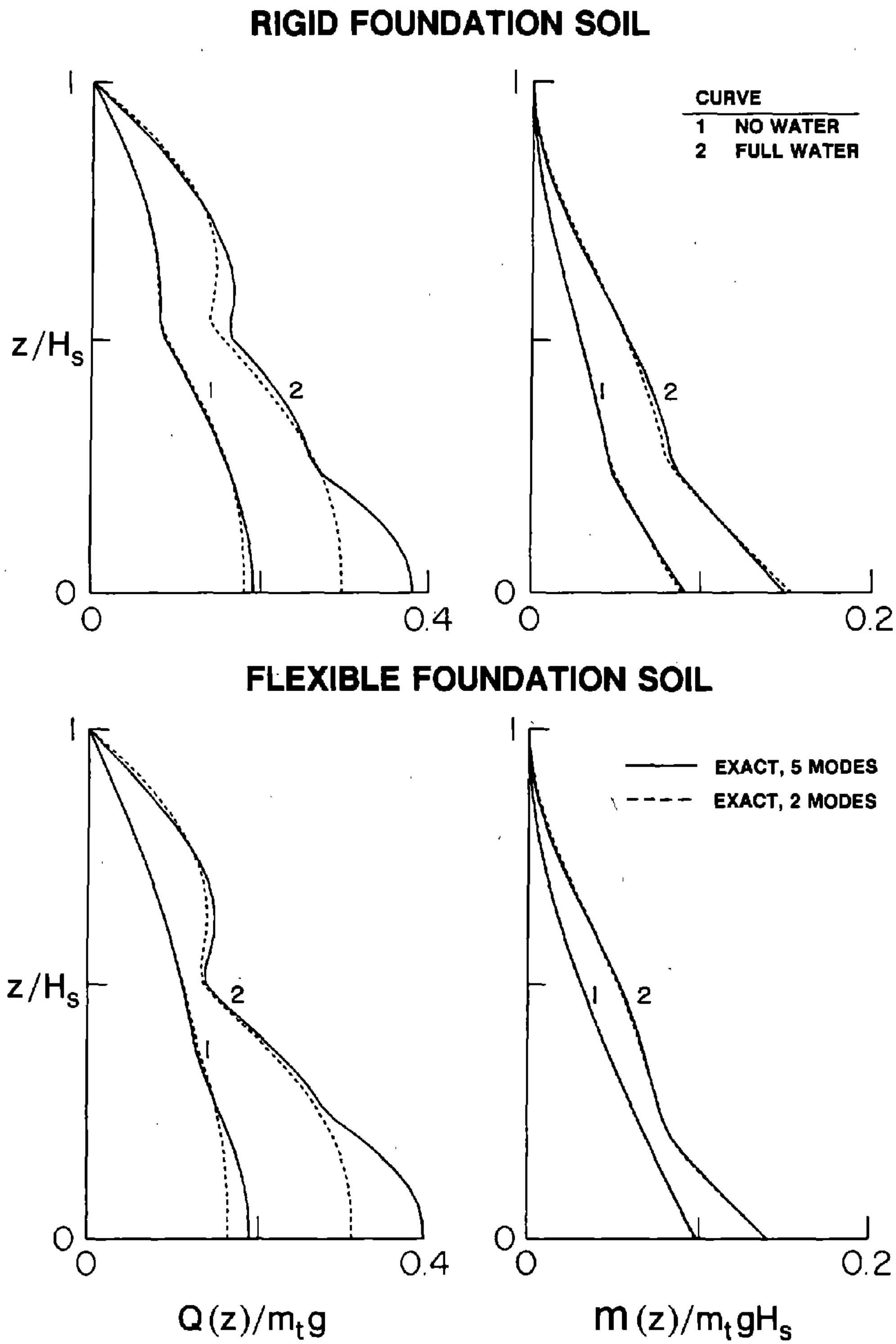

Figure 9.22 Influence of Higher Vibration Modes on the Envelope Values of Maximum Shear Forces and Bending Moments in Circular Tapered Towers with H_s/r_a = 20 due to S69E Component of Taft Ground Motion; Cases 1 to 4

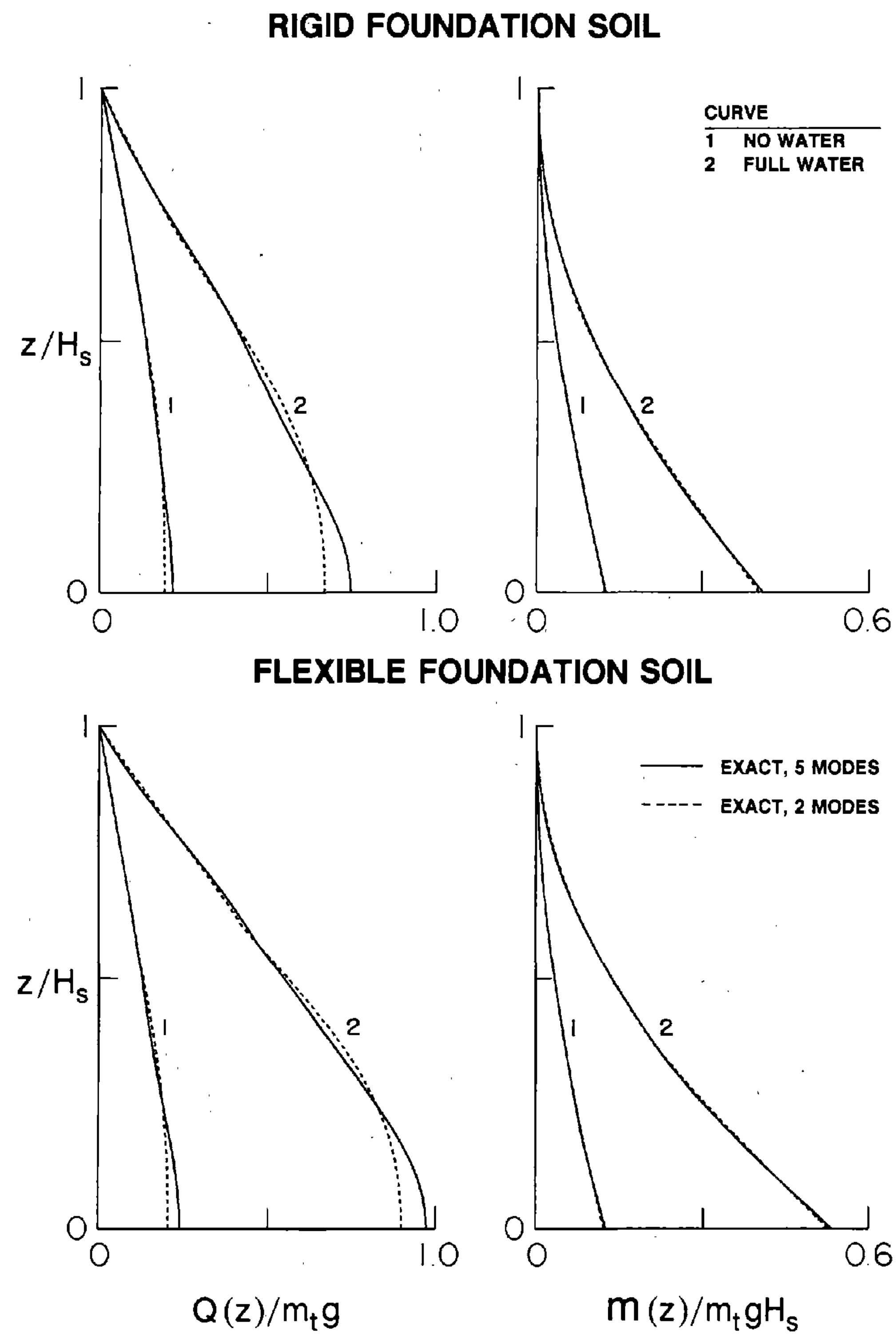

Figure 9.23 Influence of Higher Vibration Modes on the Envelope Values of Maximum Shear Forces and Bending Moments in Circular Tapered Towers with H_s/r_a = 10 due to S69E Component of Taft Ground Motion; Cases 5 to 8

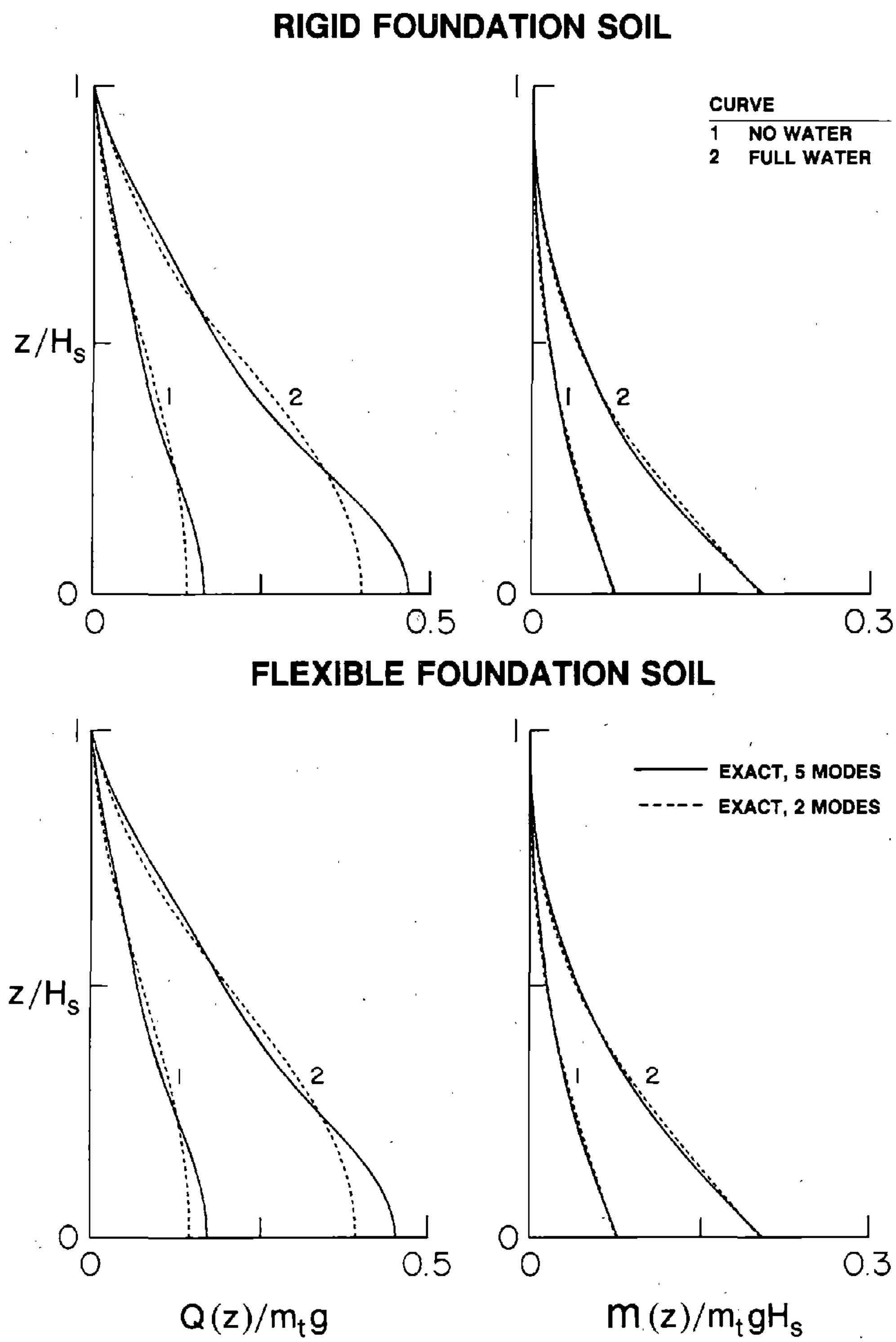

Figure 9.24 Influence of Higher Vibration Modes on the Envelope Values of Maximum Shear Forces and Bending Moments in Circular Tapered Towers with H_s/r_a = 5 due to S69E Component of Taft Ground Motion; Cases 9 to 12

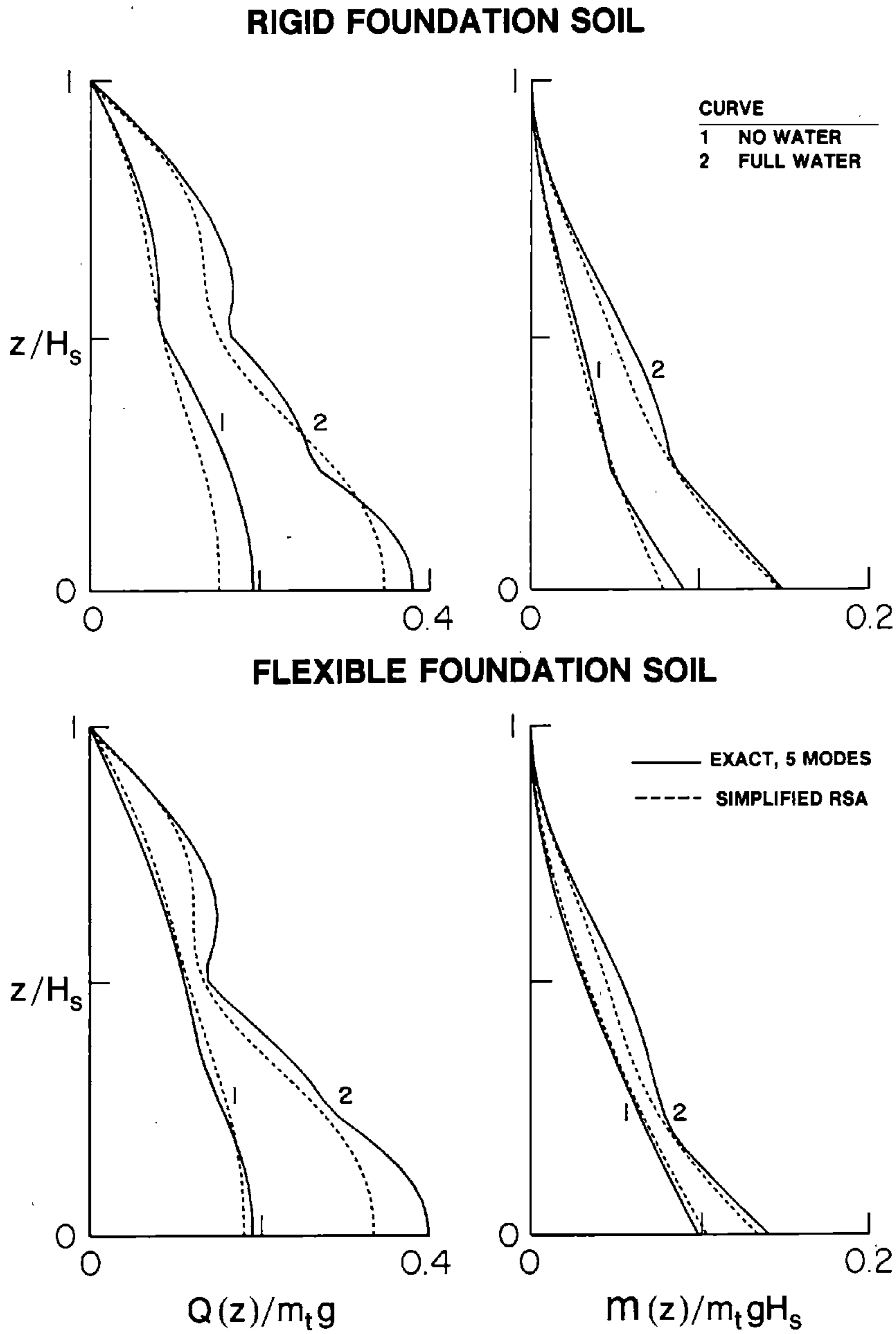

Figure 9.25 Comparison of Exact (5 Modes) and Simplified Analysis Results for Envelope Values of Maximum Shear Forces and Bending Moments in Circular Tapered Tower with H_s/r_a = 20 due to S69E Component of Taft Ground Motion; Cases 1 to 4

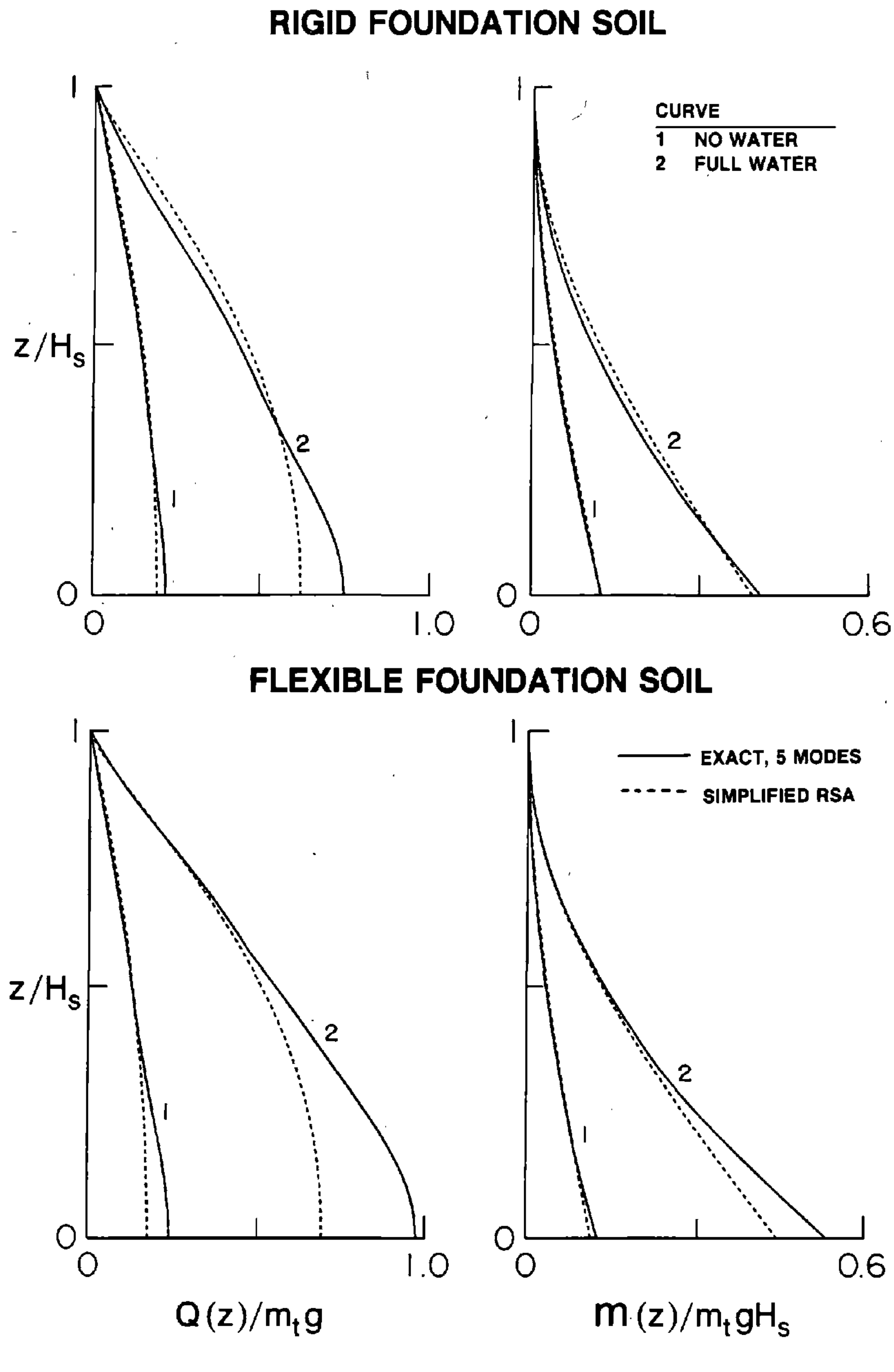

Figure 9.26 Comparison of Exact (5 Modes) and Simplified Analysis Results for Envelope Values of Maximum Shear Forces and Bending Moments in Circular Tapered Tower with H_s/r_a = 10 due to S69E Component of Taft Ground Motion; Cases 5 to 8

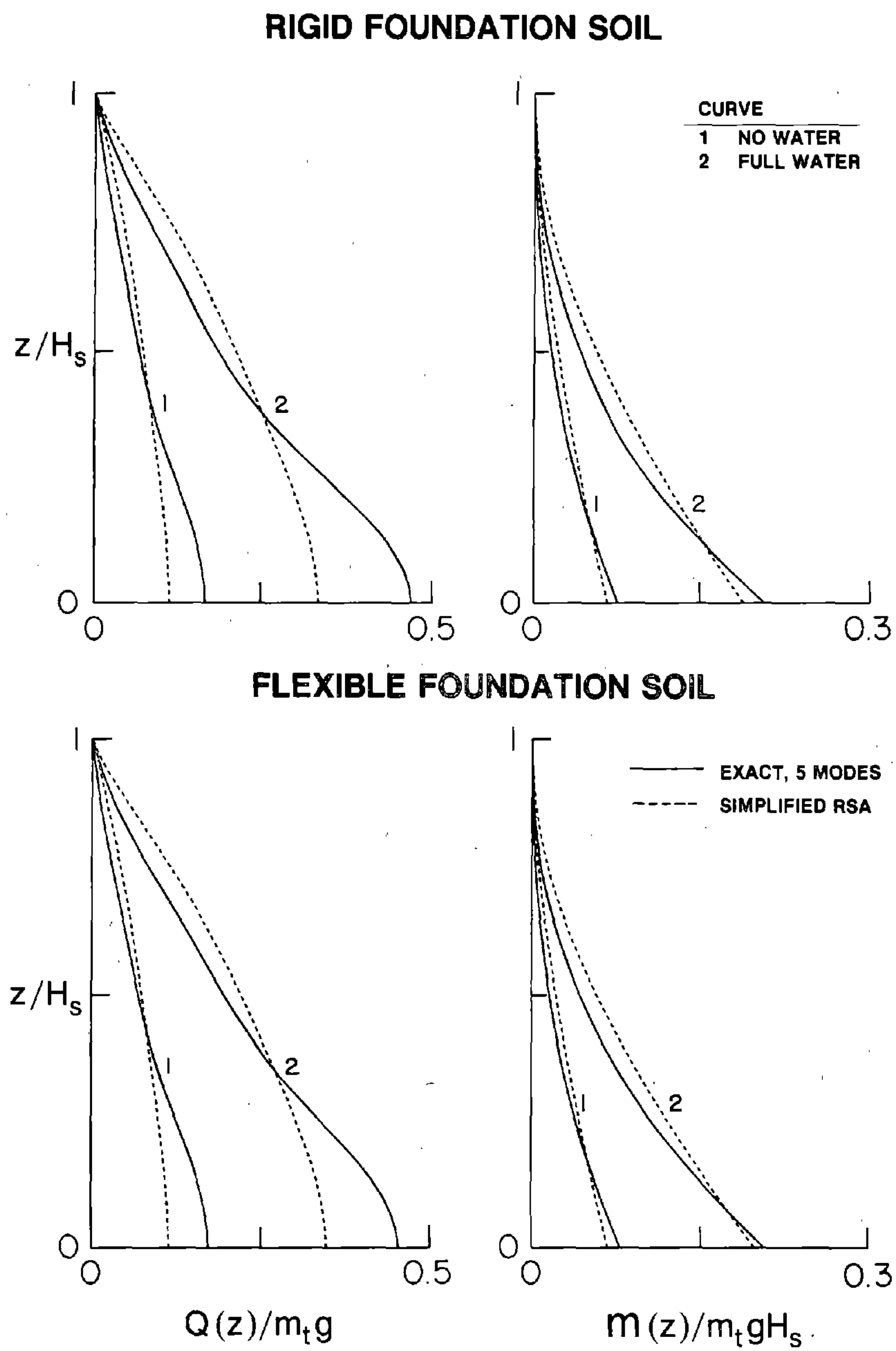

Figure 9.27 Comparison of Exact (5 Modes) and Simplified Analysis Results for Envelope Values of Maximum Shear Forces and Bending Moments in Circular Tapered Tower with H_s/r_a = 5 due to S69E Component of Taft Ground Motion; Cases 9 to 12

should be used only in conjunction with a "smooth" earthquake design spectrum in order to obtain reliable results by minimizing the errors associated with the simplified computation of effective vibration periods of the two modes, and of the effective damping in the fundamental mode (Table 9.2), and with the usual procedures of combining peak modal responses.

10. CONCLUSIONS

A general procedure for the earthquake analysis of linear response of intake-outlet towers of arbitrary cross-section, having two axes of symmetry, including the effects of tower-water interaction and tower-foundation-soil interaction, has been developed in Chapter 3. The idealized tower-water-foundation-soil system is treated as four interacting substructures : the tower by itself, the foundation and supporting soil, the surrounding water domain, and the inside water domain. Efficient numerical solution procedures have been developed in Chapter 4 for evaluating the dynamic properties of each substructure : natural vibration frequencies and mode shapes of the tower, impedance functions for the foundation, and the added hydrodynamic mass and excitation terms, associated with fluid domains surrounding the tower and contained within the tower, in the equations of motion for the tower.

Evaluation of the added hydrodynamic mass and excitation terms due to surrounding water require solutions of the Laplace equation over the three-dimensional, unbounded fluid domain exterior to the tower. Efficient numerical techniques have been developed to solve the boundary value problems for towers of arbitrary geometry. In this mixed approach, the fluid domain exterior to the tower but contained within a hypothetical circular-cylindrical surface is discretized by finite elements, whereas analytical solutions for the fluid domain exterior to the hypothetical cylinder are utilized in a boundary integral procedure for this sub domain. The resulting procedure is advantageous compared to the standard finite element procedure in that it leads to accurate results with much less computational effort and core-storage requirements.

Utilizing the analytical and computational procedures developed in Chapters 3 and 4, the responses of idealized intake-outlet towers to harmonic ground motion have been presented in Chapter 5 for a wide range of system parameters. Based on the frequency response functions, it has been shown that tower-water interaction and tower-foundation-soil interaction may have a significant effect on the dynamic response of intake-outlet towers.

Specifically, the response results lead to the following conclusions :

1. Water, inside or outside, has the effect of lengthening the vibration periods of the tower because of the added hydrodynamic mass. The vibration periods of slender towers are lengthened to a greater degree than for squat towers. However, the effective damping is unchanged because energy dissipation in the towers is modeled as frequency-independent hysteretic damping and water compressibility effects are negligible.

2. For full reservoir (i.e. $H_o/H_s = 1$ or $H_i/H_s = 1$), the percentage lengthening of the first two vibration periods is about the same ; however, for partially filled reservoir, specially when $0.2 \leq H_o/H_s$ or $H_i/H_s \leq 0.8$, the percentage increase in the second vibration period is substantially larger than that in the fundamental vibration period.

3. The increases in a resonant period due to surrounding and inside water are cumulative. The individual effects can be combined by equation (5.1).

4. The frequency response functions for a tower having unequal plan dimensions in two orthogonal directions with surrounding water, in particular the lengthening of vibration period due to surrounding water, may be significantly influenced by the direction of ground motion. The resulting differences in the response are the result of different values for the added hydrodynamic mass, for vibration in the two directions. On the contrary, frequency response functions for a tower with inside water are essentially independent of the direction of excitation because the added hydrodynamic mass is close to the total mass of the contained water.

5. Tower-foundation-soil interaction lengthens the fundamental resonant period of the tower and increases the effective damping at this period because of the radiation and material damping in the foundation-soil region. Similarly the higher resonant periods are lengthened, although to a lesser degree, but the effective damping at these periods is substantially larger.

6. Tower-foundation-soil interaction effects are stronger for towers with short fundamental vibration period (i.e. stiff structures) and with large tower-height-to-footing-radius ratio. The interaction effects depend, in part, on the relative flexibility of the foundation soil and the tower, and on the height-wise mass distribution of the tower.

7. The effects of tower-foundation-soil interaction on the period and amplitude of the fundamental resonant peak are qualitatively similar, whether hydrodynamic interaction effects are included in the analysis or not. In particular, percentage lengthening of the fundamental resonant period due to tower-water-foundation soil interaction is almost independent of hydrodynamic effects. The influence of tower-foundation interaction is however smaller in the presence of water.

Utilizing the analytical and numerical procedures of Chapters 3 and 4, the earthquake response of Briones Dam Intake Tower to Taft ground motion has been presented in Chapter 6 for various assumptions of the water and the foundation soil. These response results lead to the following conclusions :

1. The earthquake response of Briones Dam Intake Tower is increased because of hydrodynamic interaction effects and decreased as a result of tower-foundation-soil interaction. These interaction effects in the response of a tower to a specified earthquake ground motion are controlled, in part, by the changes in response spectrum ordinates corresponding to the fundamental and second (and higher) resonant peaks associated with the changes in the resonant periods and effective damping because of interaction.

2. The response of this tower to typical ground motion can be computed to a satisfactory degree of accuracy by considering only the contributions of only the first two natural vibration modes of the tower on fixed base without water in the analysis procedure of Chapter 3.

The effects of tower-water interaction and tower-foundation-soil interaction on the response of an intake-outlet tower depend, in part, on the particular tower and earthquake ground motion, so that the conclusions deduced in Chapter 6 from the computed response of Briones Dam Intake Tower to Taft ground motion would not apply in their entirety to all towers and ground motions. Whereas the detailed observations may be problem dependent, the broad conclusions should be valid for many cases.

The response results presented in this investigation have demonstrated that the response of intake-outlet towers to earthquake ground motion is affected by tower- water interaction, and by tower-foundation-soil interaction. These effects can be efficiently included in practical analysis of towers utilizing the analytical and numerical procedures developed in Chapters 3 and 4.

In Chapter 7, it was demonstrated that the hydrodynamic interaction effects can be represented to a useful degree of accuracy in the response spectrum analysis of towers by replacing the mass of the towers $m_s(z)$ by the virtual mass, $\tilde{m}_s(z)$:

$$\tilde{m}_s(z) = m_s(z) + m_a^o(z) + m_a^i(z)$$

where the added hydrodynamic mass distributions $m_a^o(z)$ and $m_a^i(z)$ for outside and inside water, respectively, are determined from hydrodynamic analyses with the assumption of rigid tower. In order to avoid these complicated hydrodynamic analyses in practical applications, a simplified procedure is presented in Chapter 8.

Following earlier work on buildings and dams, an equivalent single-degree-of-freedom (SDF) system is developed to represent approximately the response of towers in their fundamental vibration mode including the effects of tower-foundation-soil interaction. Because the equivalent SDF system accurately predicts the response of towers to harmonic ground motion over the complete range of excitation frequencies, it can be used in response analysis of towers to arbitrary ground motion. Thus the equivalent lateral forces associated with the maximum response in the fundamental vibration mode are given by equation (7.51).

A simplified procedure has been presented in Chapter 8 to evaluate the magnitude and height-wise distribution of added hydrodynamic mass for a tower of arbitrary cross-section having two axes of symmetry, and its dimensions varying along the height. It has been demonstrated that the added mass associated with surrounding water or inside water can be determined accurately without rigorous three-dimensional analyses of the fluid domains. In particular, the added mass can be determined as the product of (1) the normalized added mass for an "equivalent" axisymmetric tower which can be determined by two-dimensional hydrodynamic analysis ; and (2) the added mass for an infinitely-long tower with cross-section same as that at the base of the actual tower, which also requires a two-dimensional analysis. The computational effort required in this approximate procedure is an order of magnitude less that required for the rigorous three-dimensional analysis.

Both of these two-dimensional analyses can be avoided, as shown in Chapter 8, at the expense of some accuracy. The normalized added hydrodynamic mass for the equivalent axisymmetric tower can be determined to a useful degree of accuracy as the normalized mass from analytical solutions for circular cylindrical towers. These analytical solutions have been computed and presented in the form of standard data. Similarly, for convenience of the user, the added mass values for infinitely-long towers have been presented for several different cross-sections.

In Chapter 9, a simplified analysis procedure for intake-outlet towers, including tower-water and tower-foundation-soil interaction effects, is presented to compute the maximum earthquake forces directly from the earthquake design spectrum without the need for a response history analysis. This presentation utilizes the procedure and standard data of Chapter 8 for simplified evaluation of the added hydrodynamic mass. Also included are convenient methods for (1) computing the natural periods and shapes of the first two modes of vibration of the tower, which are shown to be sufficient for approximate evaluation of the design forces ; and (2) the modifications to the vibration period and damping ratio of the fundamental mode due to tower-foundation-soil interaction. Following the earlier work on buildings, the contribution of the second vibration mode to the response can be computed as if the tower was supported on rigid foundation soil. This simplified procedure is presented as a sequence of computational steps along with all the standard data necessary for convenient implementation. It is shown that this procedure leads to solutions that are sufficiently accurate for the preliminary phase of design and safety evaluation of intake-outlet towers.

REFERENCES

1. Abramowitz, M. and Stegun, I.A., "Handbook of Mathematical Functions," Chapter 9, Dover Publication, Inc., New York, November 1972, pp. 355-434.
2. Bathe, K.J. and Wilson, E.L., "Numerical Methods in Finite Element Analysis," Printice Hall, Inc., Englewood Cliffs, New Jersey, 1976.
3. Beredugo, Y.O., and Novak, M., "Coupled Horizontal and Rocking Vibration of Embedded Footings," Canadian Geotechnical Journal, 9, 1972, pp. 477-497.
4. Biggs, J.M., "Introduction to Structural Dynamics," McGraw Hill Inc., New York, 1964.
5. Bland, D.R., "The Theory of Linear Viscoelasticity," Pergamon Press, Oxford, 1960.
6. Brigham, E.O., "The Fast Fourier Transform," Prentice Hall, Englewood Cliffs, N.J., 1974.
7. Chen, H.S. and Mei, C.C., "Oscillations and Wave Forces in a Man Made Harbor in Open Sea," Proceedings 10th Naval Hydrodynamics Symposium, June 1974, pp. 573-594.
8. Cheung, Y.K., Cao, Z-Y and Wu, S.Y., "Dynamic Analysis of Prismatic Structures Surrounded by an Infinite Fluid Medium," International Journal of Earthquake Engineering and Structural Dynamics, Vol. 13, 1985, pp. 351-360.
9. Chopra, A.K., "Dynamics of Structures, A Primer," Earthquake Engineering Research Institute, Berkeley, CA, 1980.
10. Chopra, A.K. and Chakarbarti, P., "Earthquake Analysis of Concrete Gravity Dams Including Dam-Water-Foundation Rock Interaction," International Journal of Earthquake Engineering and Structural Dynamics, Vol. 9, No. 4, July-August 1981, pp. 363-383.
11. Chopra, A.K. and Fok, K.L., "Evaluation of Simplified Earthquake Analysis Procedures for Intake-Outlet Towers," Proceedings of the 8-th World Conference on Earthquake Engineering, San Francisco, July 1984, Vol. VII, pp. 467-474.
12. Chopra, A.K. and Gutierrez, J.A., "Earthquake Response Analysis of Multistory Buildings Including Foundation Interaction," International Journal of Earthquake Engineering and Structural Dynamics, Vol. 3, 1974, pp. 65-77.
13. Chopra, A.K. and Liaw, C-Y, "Earthquake Resistant Design of Intake-Outlet Towers," Journal of Structural Division, ASCE, Vol. 101, No. ST7, July 1975, pp. 1349-1366.
14. Clough, R.W. and Penzien, J., "Dynamics of Structures," McGraw Hill Book Co., New York, N.Y., 1975.
15. Cruz, E.F., and Chopra, A.K., "Elastic Earthquake Response of Building Frames," J. Struct. Eng., ASCE, Vol. 112, No. 3, Mar. 1986, pp. 443-459.
16. Cruz, E.F., and Chopra, A.K., "Simplified Procedures for Earthquake Analysis of Buildings," J. Struct. Eng., ASCE, Vol. 112, No. 3, Mar. 1986, pp. 461-480.
17. Dong, R.G., "Effective Mass and Damping of Submerged Structures," Report No. UCRL-52342, Lawrence Livermore Laboratory, University of California, Livermore, April 1, 1978.
18. Fenves, G. and Chopra, A.K., "Earthquake Analysis and Response of Concrete Gravity Dams," Report No. UCB/EERC-84/10, Earthquake Engineering Research Center, University of California, Berkeley, August 1984.
19. Fenves, G., and Chopra, A.K., "Earthquake Analysis of Concrete Gravity Dams Including Reservoir Bottom Absorption and Dam-Water-Foundation Rock Interaction," Eartquake Engineering and Structural Dynamics, Vol. 12, No. 5, Sept.-Oct. 1984, pp. 663-680.

20. Fenves, G., and Chopra, A.K., "Simplified Eartquake Analysis of Concrete Gravity Dams: Separate Hydrodynamic and Foundation Interaction Effects," Journal of Engineering Mechanics, American Society of Civil Engineers, Vol. III, No. 6, June 1985, pp. 715-735.

21. Fenves, G., and Chopra, A.K., "Simplified Earthquake Analysis of Concrete Gravity Dams: Combined Hydrodynamic and Foundation Interaction effects," Journal of Engineering Mechanics, American Society of Civil Engineers, Vol. III, No. 6, June 1985, pp. 736-756.

22. Fok, K-L, and Chopra, A.K., "Earthquake Analysis of Arch Dams Including Dam-Water Interaction, Reservoir Boundary Absorption and Foundation Flexibility," Earthquake Engineering Structural Dynamics, Vol. 14, 1986, pp. 155-184.

23. Hall, J.F., "An FFT Algorithm for Structural Dynamics," International Journal of Earthquake Engineering and Structural Dynamics, Vol. 10, No. 6, November-December 1982, pp. 797-811.

24. Hall, J.F. and Chopra, A.K., "Dynamic Response of Embankment, Cocrete Gravity and Arch Dams," Report No. UCB/EERC-80/39, Earthquake Engineering Research Center, University of California, Berkeley, October 1980, 220 pp.

25. Herrera, I., "Boundary Methods for Fluids," Chapter 9, in Finite Elements in Fluids, Vol. 4, (Editors: R.H. Gallaghar, D.H. Norrie, J.T. Oden, and O.C. Zienkiewicz), John Wiley & Sons Ltd., 1982, pp. 403-432.

26. Herrmann, G., "Forced Motions of Timoshenko Beam," Transactions of the ASME, Journal of Applied Mechanics, March 1955, pp. 53-56.

27. Huang, T.C., "Effects of Rotatory Inertia and Shear on the Vibration of Beams Treated by the Approximate Methods of Ritz and Galerkin," Proceedings of the Third U.S. National Congress of Applied Mechanics, ASME, 1958, pp. 189-194.

28. Huang, T.C., "The Effects of Rotatory Inertia and of Shear Deformation on the Frequency and Normal Mode Equations of Uniform Beams With Simple End Conditions," Transactions of the ASME, Journal of Applied Mechanics, December 1961, pp. 579-584.

29. Jacobson, L.S., "Impulsive Hydrodynamics of Fluids inside a Cylindrical Tank and of Fluid surrounding a Cylindrical Pier," Bulletin, Seismological Society of America, Vol. 39, 1949, pp. 189-204.

30. Kotsubo, S., "Seismic Force Effect on Submerged Pier with Elliptical Cross-Sections," Proceedings 3rd World Conference on Earthquake Engineering, New Zealand, 1965, Vol. II, pp. 342-356.

31. Lamb, H., "Hydrodynamics," 6-th edition, Cambridge University Press, 1932.

32. Liaw, C-Y and Chopra, A.K., "Earthquake Response of Axisymmetric Tower Structures Surrounded by Water," Report No. EERC 73-25, Earthquake Engineering Reasearch Center, University of California Berkeley, October 1973, 161 pages.

33. Liaw, C-Y and Chopra, A.K., "Dynamics of Towers Surrounded by Water," International Journal of Earthquake Engineering and Structural Dynamics, Vol. 3, No. 1, July-Sept. 1974, pp. 33-49.

34. Liaw, C-Y and Chopra, A.K., "Earthquake Analysis of Axisymmetric Towers Partially Submerged in Water," International Journal of Earthquake Engineering and Structural Dynamics, Vol. 3, No. 3, Jan-March 1975, pp. 233-248.

35. Luco, J.E., "Soil-Structure Interaction Effects on the Seismic Response of Tall Chimneys," Soil Dynamics and Earthquake Engineering, Vol. 5, No. 3, 1986, pp. 170-177.

36. Luco, J.E. and Westmann, R.A., "Dynamic Response of Circular Footings," Journal of Engineering Mechanics Division, ASCE, 97:EM5, 1971, pp. 1381-1395.

37. Mikhlin, S.G., "Variational Methods in Mathematical Physics," English Translation by T. Boddington, Pergamon, 1964.

38. Mlakar, P.F., and Jones, P.S., "Seismic Analysis of Intake Towers," Technical Report SL-82-8, Structures Laboratory, U.S. Army Engineer Waterways Experiment Station, Vicksburg, Miss., October, 1982.

39. Newmark, N.M., and Rosenblueth, E., "Fundamentals of Earthquake Engineering," Chapter 6, Prentice Hall Inc., Englewood Cliffs, N.J., 1971.

40. Rashed, A., "Dynamic Analysis of Fluid-Structure Systems," Report No. EERL82-03, Earthquake Engineering Research Laboratory, California Institute of Technology, Pasadena, 1982.

41. Rea, D., Liaw, C-Y and Chopra, A.K., "Dynamic Properties of San Bernardino Intake Tower," Report No. EERC 75-7, Earthquake Engineering Research Center, University of California, Berkeley, Februry 1975.

42. Rosenblueth, E. and Contreas, H., "Approximate Design for Multicomponent Earthquakes", Journal of the Engineering Mechanics Division, ASCE, Vol. 103, No. EM5, October 1977, pp. 881-893.

43. Seed, H.B. and Idriss, I.M., "Soil Moduli and Damping Factors for Dynamic Response Analysis," Report No. EERC 70-10, Eartquake Engineering Research Center, University of California, Berkeley, 1970.

44. Timoshenko, S.P., "Vibration Problems in Engineering," Third Edition, D. Van Nostrand Company, Inc., New York, N.Y., 1955.

45. Veletsos, A.S., "Dynamics of Structure Foundation Systems," Structural and Geotechnical Mechanics, A Volume Honoring N.M. Newmark (W.J. Hall, Editor), Prentice Hall, Inc., Englewood, Cliffs, N.J., 1977, pp. 333-361.

46. Veletsos, A.S. and Meek, J.W., "Dynamic Behavior of Building-Foundation Systems," International Journal of Earthquake Engineering and Structural Dynamics, Vol. 3, No. 2, 1974, pp. 121-138.

47. Veletsos, A.S. and Verbic, B., "Vibration of Viscoelastic Foundations," International Journal of Earthquake Engineering and Structural Dynamics, Vol. 2, 1973, pp. 87-102.

48. Veletsos, A.S. and Wei, Y.T., "Lateral and Rocking Vibration of Footings," Proceedings ASCE, 97, SM9, 1971, pp. 1227-1248.

49. Westergard, H.M., "Water Presuures on Dams during Earthquakes," Transactions ASCE, Vol. 98, 1933, pp. 418-433.

50. Wong, H.L. and Luco, J.E., "Dynamic Response of Rigid Foundations of Arbitrary Shape," International Journal of Earthquake Engineering and Structural Dynamics, 4:6, 1976, pp. 579-587.

51. Wong, H.L. and Luco, J.E., "Tables of Impedance Functions and Input Motions for Rectangular Foundations," Report No. CE-78-15, Department of Civil Engineering, University of Southern California, Los Angeles, California, December 1978.

52. Wood, W.L., "On the Finite Element Solution of an Exterior Boundary Value Problem," International Journal of Numerical Methods in Engineering, Vol. 10, 1976, pp. 885-891.

53. Zienkiewicz, O.C., "The Finite Element Method," McGraw Hill Book Company, 1982.

54. Zienkiewicz, O.C., Kelly, D.W. and Bettess, P., "The Coupling of the Finite Element Method and Boundary Solution Procedures," International Journal of Numerical Methods in Engineering, Vol. 11, 1977, pp. 355-375

55. "Tentative Provisions for the Development of Seismic Regulations for Buildings," prepared by Applied Technology Council, NBS Special Publication 510, U.S. Government Printing Office, Washington, D.C., 1978.

NOTATIONS

a_n^o , a_n^i	outside/inside surface acceleration in its normal direction
a_f	frequency parameter for foundation
a_o , a_i	cross-sectional dimension of the outside/inside surface of a non-circular tower in the perpendicular direction of ground motion
$\tilde{a}_o$, $\tilde{a}_i$	cross-sectional dimension of the outside/inside surface of an equivalent elliptical tower for a non-circular tower in the perpendicular direction of ground motion
A	cross-sectional area for tower structure
A_f	cross-sectional area of the foundation
A_i	area enclosed by the cross-section of the inside surface
A_o	area enclosed by the cross-section of the outside surface
b	distance of inside water bottom from ground level
b_o , b_i	cross-sectional dimension of the outside/inside surface of a non-circular tower in the direction of ground motion
$\tilde{b}_o$, $\tilde{b}_i$	cross-sectional dimension of the outside/inside surface of an equivalent elliptical tower for a non-circular tower in the direction of ground motion
b_n^o , b_n^i	outside/inside acceleration of reservoir bottom
c_{VV} , c_{MM} , c_{VM}	damping coefficients for elastic foundation
c_{VV}^v , c_{MM}^v , c_{VM}^v	damping coefficients for viscoelastic foundation
C_f	shear wave velocity for foundation medium
C_γ	factor defined by equation (9.27)
$\tilde{C}_\gamma$	factor defined by equation (9.28)
d	duration of ground motion
E_s	elastic modulus for tower material
f_0^o , f_0^i	lateral hydrodynamic force functions of outside/inside water for rigid towers subjected to horizontal acceleration at base

f_n^o , f_n^i	lateral hydrodynamic force functions of outside/inside water for vibration shape $\phi_n(z)$, $\psi_n(z)$.
f_r^o , f_r^i	lateral hydrodynamic force functions of outside/inside water due to rocking motion of rigid towers
$\bar{f}^o$, $\bar{f}^i$	frequency response functions for lateral hydrodynamic forces on the outside/inside surface
f_n	equivalent lateral forces in n-th vibration mode
G_f	elastic shear modulus for foundation
$\tilde{G}_f$	viscoelastic shear modulus for foundation
G_s	elastic shear modulus for tower material
h_1^*	effective height of tower without water in the fundamental mode of vibration
$\tilde{h}_1^*$	effective height of tower with water in the fundamental mode of vibration
H_o , H_i	outside/inside water depth
H_s	Height of the tower
i	$\sqrt{-1}$
I	moment of inertia for tower cross-section
I_f	mass moment of inertia for footing
I_o	moment of inertia for the foundation
I_s	$= \rho_s I$, mass moment of inertia for tower cross-section
I_n	modified Bessell function of order n of the first kind
I_t	integral defined by equation (3.11)
I_t^o , I_t^i	integral defined by equation (3.36) for outside/inside water
k	shape factor of cross-section for shear stress distribution
k_{VV} , k_{MM} , k_{VM}	stiffness coefficient for elastic foundation
k_{VV}^v , k_{MM}^v , k_{VM}^v	stiffness coefficients for viscoelastic foundation

K_n	modified Bessell function of order n of the second kind
K_x	static stiffness of the foundation in translation [equation (9.22a)]
K_θ	static stiffness of the foundation in rocking [equation (9.22b)]
K_{VV} , K_{MM} , K_{VM}	foundation impedance functions
$\boldsymbol{K}_o$, $\boldsymbol{K}_i$	finite element matrices for outside/inside water domain
$\boldsymbol{K}_s$	stiffness matrix for tower structure
$\bar{l}_n^o$, $\bar{l}_n^i$	integrals defined by equation (3.13) for outside/inside water
$\bar{l}_h^o$, $\bar{l}_h^i$	integrals defined by equation (3.14) for outside/inside water
$\bar{l}_r^o$, $\bar{l}_r^i$	integrals defined by equation (3.15) for outside/inside water
L_n	generalized excitation due to structure mass
L_n^o , L_n^i	generalized excitations due to outside/inside water
L_n^h , L_n^r , L_0^r	generalized mass terms due to tower-foundation-soil interaction
L_n^{ho} , L_n^{ro} , L_0^{ro}	generalized mass terms due to outside water-foundation-soil interaction
L_n^{hi} , L_n^{ri} , L_0^{ri}	generalized mass terms due to inside water-foundation-soil interaction
m_f	mass of the footing
$m_s(z)$	mass of the tower per unit of height
m_a^o , m_a^i	added hydrodynamic mass for outside/inside water
m_t	total structural mass
m_1^*	effective mass of tower without water in the fundamental mode of vibration
$\tilde{m}_1^*$	effective mass of tower with water in the fundamental mode of vibration
m_t^o , m_t^i	integral defined by equation (3.35) for outside/inside water
M_n	generalized mas term for tower structure
M_z	number of $\cos(\alpha_m z/H_o)$ functions in equation (4.43)

M_{nj}^o , M_{nj}^i	generalized mass term due to outside/inside water
$M_j(\vec{x})$	three-dimensional trial functions for boundary integral domain
$M_j^\Gamma(\vec{x})$	trial functions on hypothetical cylinder
$\overline{M}_j(r,z)$	axi-symmetric trial functions
$m(z)$	bending moment along the height
m_x	bending moment due to x component of ground motion
m_y	bending moment due to y component of ground motion
$m_n(z)$	bending moment distribution in n-th mode
$\overline{m}_f$	response function of interaction moment at the base
$\overline{m}^o$, $\overline{m}^i$	response functions for hydrodynamic moments due to outside/inside water
m_0^o , m_0^i	hydrodynamic moments due to outside/inside water for rigid towers subjected to horizontal acceleration at base
m_n^o , m_n^i	hydrodynamic moments due to outside/inside water for towers vibrating in shape $\phi_n(z)$, $\psi_n(z)$.
m_r^o , m_r^i	hydrodynamic moments due to outside/inside water for rigid towers in rocking motion
$\boldsymbol{M}_s$	mass matrix for tower structure
n^o , n^i	direction of normal to outside/inside surfaces
n_x^o , n_z^o	direction cosines of normal to outside surface
n_x^i , n_z^i	direction cosines of normal to inside surface
N	number of modes considered
$N_i(z)$	one-dimensional interpolation functions
$N_i(\vec{x})$	three-dimensional interpolation functions
$\overline{N_i}(r,z)$	axi-symmetric interpolation functions
N_S	number of nodes in finite element system for tower structure

N_θ	number of $\cos(2n-1)\theta$ functions in equation (4.43)
N_A	number of nodal points in finite element system for fluid domains
N_B	number of trial functions in boundary integral procedure
$\bar{p}^o$, $\bar{p}^i$	frequency response functions of hydrodynamic pressure in outside/inside water domain
p_0^o , p_0^i	hydrodynamic pressure functions of outside/inside water for rigid towers subjected to horizontal acceleration at base
p_n^o , p_n^i	pressure functions of outside/inside water vibrating in shape $\phi_n(z)$, $\psi_n(z)$
p_r^o , p_r^i	pressure functions of outside/inside water for rigid towers in rocking motion
$Q(z)$	shear force along the height
Q_x	shear force due to x component of ground motion
Q_y	shear force due to y component of ground motion
$Q_n(z)$	shear force distribution in n-th mode of vibration
$\boldsymbol{Q}_o$, $\boldsymbol{Q}_i$	finite element vectors for outside/inside domains
r,z,θ	cylindrical coordinates
r_c	radius of hypothetical cylindrical surface
$\tilde{r}_o$, $\tilde{r}_i$	radius of equivalent cylindrical tower for added mass computation for outside/inside water
r_f	radius of circular footing
r_o , r_i	outside/inside radius of axisymmetric towers
R	$= \sqrt{1 + \eta_f^2}$ (Chapter 4, Section 4.2.3)
R	peak value of any response quantity
R_o	peak value of any response quantity due to gravity loads in equation (9.40)
R_x	peak value of any response quantity due to ground motion along x axis in equation (9.40)

R_y	peak value of any response quantity due to ground motion along y axis in equation (9.40)
s_1^o , s_1^i	local co-ordinate along the perimeter of the outside/inside surface
t	time
T_n	n-th mode vibration period of fixed-base tower without water
T_n^o	n-th mode vibration period of fixed-base tower with surrounding water
T_n^i	n-th mode vibration period of fixed-base tower with inside water
T_n^r	n-th mode vibration period of fixed-base tower with surrounding and inside water
T_n^f	n-th mode vibration period of tower without water on flexible foundation soil
$\tilde{T}_n$	n-th mode vibration period of tower on flexible foundation soil with surrounding and inside water
u	transverse displacement of neutral axis
$\bar{u}$	frequency response function of u
u_f	relative displacement of footing
$\ddot{u}_g$	ground acceleration
$\bar{V}_f$	frequency response function of interaction shear force at base
$\Delta W/W$	specific loss factor for viscoelastic medium
x,y,z	cartesian coordinate
$\vec{x}$	co-ordinate vector
Y_n	generalized coordinates
$\bar{Y}_n$	frequency response function for Y_n
$\alpha = o,i$	subscript or superscript to identify parameter for outside and inside water (Chapter 3)
α 1.5i	coefficient used for combining responses of x and y ground motion components (equation 9.40)
α_m	$=(2m-1)\pi/2$

$\beta_1, \ldots, \beta_4$	numerical coefficients
γ	tower-foundation-soil interaction parameter defined in Table 5.1
$\gamma_1, \ldots, \gamma_4$	numerical coefficients
γ^*	interaction parameter for equivalent SDF system defined by equation (9.20)
Γ_a^o , Γ_a^i	surface of anti-symmetry for outside/inside water domain
Γ_b^o , Γ_b^i	reservoir bottom for outside/inside water domain
Γ_c^o	hypothetical cylindrical surface
Γ_e^o	portion of footing exposed to outside water
Γ_f^o , Γ_f^i	free surface for outside/inside water domain
Γ_s^o , Γ_s^i	surface of symmetry for outside/inside water domain
Γ_t^o , Γ_t^i	tower-water interface for outside/inside water domain
$\delta(z)$	Dirac-delta function
δ_{ij}	Kronecker delta function
ϵ	belongs to
η_f	hysteretic damping factor for foundation material
η_s	hysteretic damping factor for tower
η_a	added damping factor in the fundamental vibration mode due to foundation damping
η_1^f	effective damping factor in the fundamental vibration mode of tower-foundation-soil system
$\tilde{\eta}_1$	effective damping factor in the fundamental vibration mode of tower-water-foundation-soil system
$\bar{\theta}$	frequency response function for slope of neutral axis due to bending deformations only
θ_f	rocking of the footing
Λ_b^o , Λ_b^i	axisymmetric reservoir bottom for outside/inside water domain

Λ_c^o	axisymmetric hypothetical surface
Λ_e^o	axisymmetric exposed surface of footing to outside water
Λ_t^o , Λ_t^i	axisymmetric tower-water interface for outside/inside water domain
ν_f	Poisson's ratio for foundation material
ξ_1	damping ratio for tower in fundamental vibration mode
ξ_a	added damping ratio in the fundamental vibration mode due to foundation damping
ξ_1^f	effective damping ratio in the fundamental vibration mode of tower-foundation-soil system
$\tilde{\xi}_1$	effective damping ratio in the fundamental vibration mode of tower-water-foundation-soil system
ξ_n	damping ratio for tower in n-th vibration mode without water
ξ_n^r	damping ratio for tower in n-th vibration mode with water
ρ_s	mass density of tower material
ρ_f	mass density of foundation material
ρ_w	mass density of water
σ	tower-foundation-soil interaction parameter defined in Table 5.1
σ^*	interaction parameter for equivalent SDF system defined by equation (9.18)
τ^o , τ^i	three-dimensional outside/inside water domain
$\phi_n(z)$	transverse deflection in n-th mode of vibration
χ	interaction parameter for equivalent SDF system defined by equation (9.24)
$\tilde{\chi}$	interaction parameter for equivalent SDF system defined by equation (9.25)
$\psi_n(z)$	slope due to bending in n-th mode of vibration
ω	excitation frequency
ω_n	n-th mode vibration frequency of fixed-base tower without water

ω_n^o	n-th mode vibration frequency of fixed-base tower with surrounding water
ω_n^i	n-th mode vibration frequency of fixed-base tower with inside water
ω_n^r	n-th mode vibration frequency of fixed-base tower with surrounding and inside water
ω_n^f	n-th mode vibration frequency of tower without water on flexible foundation soil
$\tilde{\omega}_n$	n-th mode vibration frequency of tower on flexible foundation soil with surrounding and inside water
ω_{bn}	natural vibration frequency of n-th mode of tower by Euler's bending theory
Ω^o , Ω^i	axisymmetric outside/inside water domain

APPENDIX A
RECIPROCITY PROPERTY OF HYDRODYNAMIC FORCES

A.1 Surrounding Water

If the distribution of lateral and rotational accelerations of the tower axis is characterized by the mode shape functions $\phi_\beta(z)$ and $\psi_\beta(z)$, respectively, β being the shape identifier, then the spatial distribution of the acceleration, $a^o_{n\beta}(\vec{x})$, of the tower-water interface Γ^o_t in its normal direction is [equation (3.20)] :

$$a^o_{n\beta}(\vec{x}) = n^o_x(\vec{x})\, \phi_\beta(z) - x\, n^o_z(\vec{x})\, \psi_\beta(z) \qquad \vec{x} \in \Gamma^o_t \tag{A.1}$$

where $n^o_x(\vec{x})$ and $n^o_z(\vec{x})$ are the direction cosines of the normal at a point $\vec{x}$ on the outside surface with respect to x and z axes respectively. If Γ^o_e represents the exposed part of the foundation at reservoir bottom Γ^o_b, the spatial distribution of the accelerations, $b^o_{n\beta}(\vec{x})$, at the reservoir bottom Γ^o_b is [equation (3.22)] :

$$b^o_{n\beta}(\vec{x}) = \begin{cases} -x & \vec{x} \in \Gamma^o_e \\ 0 & otherwise \end{cases} \tag{A.2}$$

As mentioned in Section 3.2.4, the resulting hydrodynamic pressure function $p^o_\beta(\vec{x})$ satisfies the Laplace equation :

$$\nabla^2\, p^o_\beta(\vec{x}) = 0 \tag{A.3}$$

for the surrounding water domain along with the following boundary conditions :

$$\frac{\partial}{\partial n^o} p^o_\beta(\vec{x}) = -\, \rho_w\, a^o_{n\beta}(\vec{x}) \qquad \vec{x} \in \Gamma^o_t \tag{A.4a}$$

$$\frac{\partial}{\partial z} p^o_\beta(\vec{x}) = \begin{Bmatrix} -\, \rho_w\, b^o_{n\beta}(\vec{x}) & \vec{x} \in \Gamma^o_e \\ 0 & otherwise \end{Bmatrix} \qquad \vec{x} \in \Gamma^o_b \tag{A.4b}$$

$$p^o_\beta(\vec{x}) = 0 \qquad \vec{x} \in \Gamma^o_f \tag{A.4c}$$

in which Γ^o_f is the free surface of the surrounding water domain and ρ_w is the mass density of water. The resulting hydrodynamic lateral forces $f^o_\beta(z)$ and external moments $m^o_\beta(z)$ are computed at any location z along the height by integrating pressure function $p_\beta^o(\vec{x})$ along the perimeter of the tower-water interface Γ_t^o pertaining to that location [equation (3.29)] :

$$f_\beta^o(z) = \int_{\Gamma_t^o} n_x^o(\vec{x})\, p_\beta^o(\vec{x})\, ds_1^o \tag{A.5a}$$

$$m_\beta^o(z) = -\int_{\Gamma_t^o} x\, n_z^o(\vec{x})\, p_\beta^o(\vec{x})\, ds_1^o - \delta(z) \int_{\Gamma_e^o} x\, p_\beta^o(\vec{x})\, d\Gamma \tag{A.5b}$$

in which s_1^o defines the local coordinate along the perimeter of the outside surface for any fixed location z along the height such that

$$d\Gamma_t^o = ds_1^o\, dz \tag{A.6}$$

Similarly, if $\phi_\gamma(z)$ and $\psi_\gamma(z)$ characterize the accelerations of the tower axis, the accelerations of the tower-water interface are given by :

$$a_{n\gamma}^o(\vec{x}) = n_x^o(\vec{x})\, \phi_\gamma(z) - x\, n_z^o(\vec{x})\, \psi_\gamma(z) \qquad \vec{x} \in \Gamma_t^o \tag{A.7}$$

and the accelerations of the reservoir bottom by :

$$b_{n\gamma}^o(\vec{x}) = \begin{cases} -x & \vec{x} \in \Gamma_e^o \\ 0 & otherwise \end{cases} \tag{A.8}$$

The resulting hydrodynamic pressure $p_\gamma^o(\vec{x})$ also satisfies :

$$\nabla^2 p_\gamma^o(\vec{x}) = 0 \tag{A.9}$$

for the surrounding water domain along with the following boundary conditions :

$$\frac{\partial}{\partial n^o} p_\gamma^o(\vec{x}) = -\rho_w\, a_{n\gamma}^o(\vec{x}) \qquad \vec{x} \in \Gamma_t^o \tag{A.10a}$$

$$\frac{\partial}{\partial z} p_\gamma^o(\vec{x}) = \left\{ \begin{array}{ll} -\rho_w\, b_{n\gamma}^o(\vec{x}) & \vec{x} \in \Gamma_e^o \\ 0 & otherwise \end{array} \right\} \qquad \vec{x} \in \Gamma_b^o \tag{A.10b}$$

$$p_\gamma^o(\vec{x}) = 0 \qquad \vec{x} \in \Gamma_f^o \tag{A.10c}$$

and the resulting hydrodynamic lateral forces and external moments are computed by the following equations :

$$f_\gamma^o(z) = \int_{\Gamma_i^o} n_x^o(\vec{x})\, p_\gamma^o(\vec{x})\, ds_1^o \tag{A.11a}$$

$$m_\gamma^o(z) = -\int_{\Gamma_i^o} x\, n_z^o(\vec{x})\, p_\gamma^o(\vec{x})\, ds_1^o - \delta(z)\int_{\Gamma_e^o} x\, p_\gamma^o(\vec{x})\, d\Gamma \tag{A.11b}$$

Substituting equation (A.11) into the left hand side of equation (3.29), the reciprocity property of hydrodynamic forces, using the definition of s_1^o [equation (A.6)], and then substituting equations (A.1) and (A.2) lead to :

$$\int_0^{H_o} \phi_\beta(z)\, f_\gamma^o(z)\, dz + \int_0^{H_o} \psi_\beta(z)\, m_\gamma^o(z)\, dz = \int_{\Gamma_i^o} a_{n\beta}^o(\vec{x})\, p_\gamma^o(\vec{x})\, d\Gamma + \int_{\Gamma_e^o} b_{n\beta}^o(\vec{x})\, p_\gamma^o(\vec{x})\, d\Gamma \tag{A.12}$$

Using the boundary conditions of equation (A.4), the equation (A.12) can be written as

$$\int_0^{H_o} \phi_\beta(z)\, f_\gamma^o(z)\, dz + \int_0^{H_o} \psi_\beta(z)\, m_\gamma^o(z)\, dz = -\frac{1}{\rho_w}\int_{\Gamma^o} [\frac{\partial}{\partial n^o} p_\beta^o(\vec{x})]\, p_\gamma^o(\vec{x})\, d\Gamma \tag{A.13}$$

in which Γ^o represents the entire surface of the surrounding water domain.

Similarly, it can be shown that

$$\int_0^{H_o} \phi_\gamma(z)\, f_\beta^o(z)\, dz + \int_0^{H_o} \psi_\gamma(z)\, m_\beta^o(z)\, dz = -\frac{1}{\rho_w}\int_{\Gamma^o} [\frac{\partial}{\partial n^o} p_\gamma^o(\vec{x})]\, p_\beta^o(\vec{x})\, d\Gamma \tag{A.14}$$

Since $p_\beta^o(\vec{x})$ and $p_\gamma^o(\vec{x})$ satisfy Laplace equation for the same domain, Green's theorem implies that

$$\int_{\Gamma^o} [\frac{\partial}{\partial n^o} p_\beta^o(\vec{x})]\, p_\gamma^o(\vec{x})\, d\Gamma - \int_{\Gamma^o} [\frac{\partial}{\partial n^o} p_\gamma^o(\vec{x})]\, p_\beta^o(\vec{x})\, d\Gamma = 0 \tag{A.15}$$

which leads to

$$\int_0^{H_o} \phi_\beta(z)\, f_\gamma^o(z)\, dz + \int_0^{H_o} \psi_\beta(z)\, m_\gamma^o(z)\, dz = \int_0^{H_o} \phi_\gamma(z)\, f_\beta^o(z)\, dz + \int_0^{H_o} \psi_\gamma(z)\, m_\beta^o(z)\, dz \tag{A.16}$$

the reciprocity property for hydrodynamic forces due to surrounding water.

A.2 Inside Water

Since the accelerations of the inside surface, $a_{n\beta}^i(\vec{x})$, $b_{n\beta}^i(\vec{x})$, $a_{n\gamma}^i(\vec{x})$, and $b_{n\gamma}^i(\vec{x})$, are related to the accelerations of the tower axis, $\phi_\beta(z)$, $\psi_\beta(z)$, $\phi_\gamma(z)$, $\psi_\gamma(z)$, through direction cosines $n_x^i(\vec{x})$ and $n_z^i(\vec{x})$ in a manner similar to that for the surrounding water, and the pressure functions $p^i_\beta(\vec{x})$ and $p^i_\gamma(\vec{x})$ also satisfy the similar equations and boundary conditions, except $\Gamma^i_b = \Gamma^i_e$ for the inside water domain, it can be shown that

$$\int_0^{H_i} \phi_\beta(z)\, f^i_\gamma(z)\, dz + \int_0^{H_i} \psi_\beta(z)\, m^i_\gamma(z)\, dz = -\frac{1}{\rho_w} \int_{\Gamma^i} [\frac{\partial}{\partial n^i} p^i_\beta(\vec{x})]\, p^i_\gamma(\vec{x})\, d\Gamma \tag{A.17}$$

and

$$\int_0^{H_i} \phi_\gamma(z)\, f^i_\beta(z)\, dz + \int_0^{H_i} \psi_\gamma(z)\, m^i_\beta(z)\, dz = -\frac{1}{\rho_w} \int_{\Gamma^i} [\frac{\partial}{\partial n^i} p^i_\gamma(\vec{x})]\, p^i_\beta(\vec{x})\, d\Gamma \tag{A.18}$$

in which Γ^i represents the entire surface of the inside water domain. Application of Green's theorem leads to

$$\int_0^{H_i} \phi_\beta(z)\, f^i_\gamma(z)\, dz + \int_0^{H_i} \psi_\beta(z)\, m^i_\gamma(z)\, dz = \int_0^{H_i} \phi_\gamma(z)\, f^i_\beta(z)\, dz + \int_0^{H_i} \psi_\gamma(z)\, m^i_\beta(z)\, dz \tag{A.19}$$

the reciprocity property for hydrodynamic forces due to inside water.

APPENDIX B

COMPUTATION OF SHEAR FORCES AND BENDING MOMENTS

The shear force $Q(z,t)$ and bending moment $\mathcal{M}(z,t)$ along the height of the tower can be determined by static force-displacement relationship, i.e. using the cross-sectional stiffnesses -- $G_s k(z) A(z)$ in shear and $E_s I$ in bending -- and the response history of lateral displacements, $u(z,t)$, and bending slopes, $\theta(z,t)$, of the tower axis :

$$Q(z,t) = G_s k(z) A(z) \left[\frac{\partial}{\partial z} u(z,t) - \theta(z,t) \right] \tag{B.1a}$$

$$\mathcal{M}(z,t) = E_s I \frac{\partial}{\partial z} \theta(z,t) \tag{B.1b}$$

Since the lateral displacements and bending slopes of the tower axis are obtained by superposing modal responses [equation (3.50)] :

$$u(z,t) = \sum_{j=1}^{N} \phi_j(z) \, Y_j(t) \tag{B.2a}$$

$$\theta(z,t) = \sum_{j=1}^{N} \psi_j(z) \, Y_j(t) \tag{B.2b}$$

Consequently, the shear force $Q(z,t)$ and bending moment $\mathcal{M}(z,t)$ along the height of the tower can be determined as :

$$Q(z,t) = \sum_{n=1}^{N} Q_n(z) \, Y_n(t) \tag{B.3a}$$

$$\mathcal{M}(z,t) = \sum_{n=1}^{N} \mathcal{M}_n(z) \, Y_n(t) \tag{B.3b}$$

in which $Q_n(z)$ and $\mathcal{M}_n(z)$ represent the height wise distribution of shear forces and bending moments associated with deflection of the tower in the n-th mode of vibration, described by lateral displacements $\phi_n(z)$ and bending slopes $\psi_n(z)$ of the tower axis. They are defined as :

$$Q_n(z) = G_s k(z) A(z) \left[\frac{d}{dz} \phi_n(z) - \psi_n(z) \right] \tag{B.4a}$$

$$\mathcal{M}_n(z) = E_s I \frac{d}{dz} \psi_n(z) \tag{B.4b}$$

In undamped free vibration of the tower in its n-th mode shape, the lateral displacement $u(z,t)$ and bending slope $\theta(z,t)$ of the tower axis varies as

$$u(z,t) = \phi_n(z)\, e^{i\omega_n t} \tag{B.5a}$$

$$\theta(z,t) = \psi_n(z)\, e^{i\omega_n t} \tag{B.5b}$$

where ω_n is the n-th vibration frequency of the fixed-base tower without water. Since the shear forces and bending moment also varies as

$$Q(z,t) = Q_n(z)\, e^{i\omega_n t} \tag{B.6a}$$

$$\mathcal{M}(z,t) = \mathcal{M}_n(z)\, e^{i\omega_n t} \tag{B.6b}$$

it is possible to compute the functions $Q_n(z)$ and $\mathcal{M}_n(z)$ by direct integration of the equations of motion for the undamped free vibration of the tower.

The equation of motion for the undamped free vibration of the tower, restricted to vibrate in its n-th mode shape, can be written as a special case of equation (3.1) which after substitution of equation (B.4) becomes :

$$-\,\omega_n^2\, m_s(z)\, \phi_n(z) - \frac{d}{dz} Q_n(z) = 0 \tag{B.7a}$$

$$-\,\omega_n^2\, I_s(z)\, \psi_n(z) - \frac{d}{dz} \mathcal{M}_n(z) - Q_n(z) = 0 \tag{B.7b}$$

Integration of equation (B.7a) and using the boundary condition $Q_n(H_s) = 0$ leads to :

$$Q_n(z) = \omega_n^2 \int_z^{H_s} m_s(\xi)\, \phi_n(\xi)\, d\xi \tag{B.8}$$

Substitution of equation (B.8) into equation (B.7b), use of boundary condition $\mathcal{M}_n(H_s) = 0$, and integration of equation (B.7b) leads to :

$$\mathcal{M}_n(z) = \omega_n^2 \left[\int_z^{H_s} (\xi - z)\, m_s(\xi)\, \phi_n(\xi)\, d\xi + \int_z^{H_s} I_s(\xi)\, \psi_n(\xi)\, d\xi \right] \tag{B.9}$$

in which the second term comes from the contributions of rotatory inertia.

APPENDIX C

DERIVATION OF EULER-LAGRANGE EQUATIONS

C.1 Surrounding Water Domain

Let $p^o(\vec{x})$ be the function in domain τ^o of the following form :

$$p^o(\vec{x}) = \begin{cases} p_A^o(\vec{x}) & \vec{x} \in \tau_A^o \\ p_B^o(\vec{x}) & \vec{x} \in \tau_B^o \end{cases} \tag{C.1}$$

and the function $p_B^o(\vec{x})$ is restricted to the form of equation (4.35). If the function $p_A^o(\vec{x})$ and the unknown coefficients in function $p_B^o(\vec{x})$ are selected in such a way that the function $p^o(\vec{x})$ renders the following localized functional stationary:

$$\Pi(p) = \frac{1}{2} \int_{\tau_A^o} \nabla p^o \cdot \nabla p^o \, d\tau + \frac{1}{2} \int_{\Gamma_c^o} p_B^o(\vec{x}) \left[\frac{\partial}{\partial n_A^o} p_B^o(\vec{x}) \right] d\Gamma + \int_{\Gamma_c^o} p_A^o(\vec{x}) \left[- \frac{\partial}{\partial n_A^o} p_B^o(\vec{x}) \right] d\Gamma$$

$$- \rho_w \int_{\Gamma_t^o} p_A^o(\vec{x}) \, a_n^o(\vec{x}) \, d\Gamma - \rho_w \int_{\Gamma_e^o} p_A^o(\vec{x}) \, b_n^o(\vec{x}) \, d\Gamma \tag{C.2}$$

Then the first variation of the functional of equation (C.2) evaluated for the function $p^o(\vec{x})$ must be zero, i.e.

$$\int_{\tau_A^o} [- \nabla^2 p^o] \, \delta p_A^o(\vec{x}) \, d\tau + \int_{\Gamma^o} \frac{\partial}{\partial n_A^o} p_A^o(\vec{x}) \, \delta p_A^o(\vec{x}) \, d\Gamma + \frac{1}{2} \int_{\Gamma_c^o} \delta p_B^o(\vec{x}) \left[\frac{\partial}{\partial n_A^o} p_B^o(\vec{x}) \right] d\Gamma$$

$$+ \frac{1}{2} \int_{\Gamma_c^o} p_B^o(\vec{x}) \, \delta\left[\frac{\partial}{\partial n_A^o} p_B^o(\vec{x}) \right] d\Gamma + \int_{\Gamma_c^o} \delta p_A^o(\vec{x}) \left[- \frac{\partial}{\partial n_A^o} p_B^o(\vec{x}) \right] d\Gamma + \int_{\Gamma_c^o} p_A^o(\vec{x}) \, \delta\left[- \frac{\partial}{\partial n_A^o} p_B^o(\vec{x}) \right] d\Gamma$$

$$- \rho_w \int_{\Gamma_t^o} \delta p_A^o(\vec{x}) \, a_n^o(\vec{x}) \, d\Gamma - \rho_w \int_{\Gamma_e^o} \delta p_A^o(\vec{x}) \, b_n^o(\vec{x}) \, d\Gamma = 0 \tag{C.3}$$

in which Γ^o represents the entire surface of domain τ_A^o, i.e.

$$\Gamma^o = \Gamma_t^o \cup \Gamma_e^o \cup (\Gamma_b^o - \Gamma_e^o) \cup \Gamma_f^o \cup \Gamma_c^o \tag{C.4}$$

In equation (C.4), Γ_t^o is the tower-water interface, Γ_e^o is the exposed surface of the footing, Γ_b^o is the bottom boundary of the surrounding water domain, Γ_c^o is the hypothetical cylindrical surface, and Γ_f^o is the free surface of the surrounding water domain.

Using

$$\frac{\partial}{\partial n^o} = - \frac{\partial}{\partial n_A^o} \qquad on \;\; \Gamma_t^o \tag{C.5a}$$

$$\frac{\partial}{\partial n^o} = - \frac{\partial}{\partial z} \qquad on \;\; \Gamma_b^o \tag{C.5b}$$

$$\frac{\partial}{\partial n^o} = \frac{\partial}{\partial n_A^o} \qquad on \;\; \Gamma_c^o \tag{C.5c}$$

$$\frac{\partial}{\partial n^o} = \frac{\partial}{\partial z} \qquad on \;\; \Gamma_f^o \tag{C.5d}$$

and the following special property of function $p_B^o(\vec{x})$ on surface Γ_c^o :

$$\int_{\Gamma_c^o} \delta p_B^o(\vec{x}) \, [\, \frac{\partial}{\partial n_A^o} p_B^o(\vec{x}) \,] \, d\Gamma = \int_{\Gamma_c^o} p_B^o(\vec{x}) \, \delta [\, \frac{\partial}{\partial n_A^o} p_B^o(\vec{x}) \,] \, d\Gamma \tag{C.6}$$

equation (C.3) can be written in the following form :

$$\begin{aligned} &\int_{\tau_A^o} [\, - \nabla^2 p_A^o(\vec{x}) \,] \, \delta p_A^o(\vec{x}) \, d\tau + \int_{\Gamma_t^o} [\, - \frac{\partial}{\partial n^o} p_A^o(\vec{x}) - \rho_w \, a_n^o(\vec{x}) \,] \, \delta p_A^o(\vec{x}) \, d\Gamma \\ &+ \int_{\Gamma_c^o} [\, - \frac{\partial}{\partial z} p_A^o(\vec{x}) - \rho_w \, b_n^o(\vec{x}) \,] \, \delta p_A^o(\vec{x}) \, d\Gamma + \int_{\Gamma_b^o - \Gamma_c^o} [\, - \frac{\partial}{\partial z} p_A^o(\vec{x}) \,] \, \delta p_A^o(\vec{x}) \, d\Gamma \\ &+ \int_{\Gamma_f^o} [\, \frac{\partial}{\partial z} p_A^o(\vec{x}) \,] \, \delta p_A^o(\vec{x}) \, d\Gamma + \int_{\Gamma_c^o} [\, \frac{\partial}{\partial n_A^o} p_A^o(\vec{x}) - \frac{\partial}{\partial n_A^o} p_B^o(\vec{x}) \,] \, \delta p_A^o(\vec{x}) \, d\Gamma \\ &+ \int_{\Gamma_c^o} [\, p_B^o(\vec{x}) - p_A^o(\vec{x}) \,] \, \delta [\, \frac{\partial}{\partial n_A^o} p_B^o(\vec{x}) \,] \, d\Gamma = 0 \end{aligned} \tag{C.7}$$

This implies that if the function $p_A^o(\vec{x})=0$ on the free surface Γ_f^o, then the function $p^o(\vec{x})$ of the form of equation (C.1), which makes the functional of equation (C.3) stationary, will also be the solution of the following boundary value problem :

$$\nabla^2 p^o(\vec{x}) = 0 \qquad \vec{x} \in \tau^o \tag{C.8}$$

$$\frac{\partial}{\partial n^o} p^o(\vec{x}) = - \rho_w \, a_n^o(\vec{x}) \qquad \vec{x} \in \Gamma_t^o \tag{C.9a}$$

$$\frac{\partial}{\partial z} p^o(\vec{x}) = \left\{ \begin{array}{ll} -\rho_w \, b_n^o(\vec{x}) & \vec{x} \in \Gamma_e^o \\ 0 & otherwise \end{array} \right\} \quad \vec{x} \in \Gamma_b^o \tag{C.9b}$$

$$p^o(\vec{x}) = 0 \qquad \vec{x} \in \Gamma_f^o \tag{C.9c}$$

Additionally, the function $p^o(\vec{x})$ will also satisfy the constraints on the hypothetical cylindrical surface :

$$p_A^o(\vec{x}) = p_B^o(\vec{x}) \qquad \vec{x} \in \Gamma_c^o \tag{C.10a}$$

$$\frac{\partial}{\partial n_A^o} p_A^o(\vec{x}) = \frac{\partial}{\partial n_A^o} p_B^o(\vec{x}) \qquad \vec{x} \in \Gamma_c^o \tag{C.10b}$$

Therefore, the function $p^o(\vec{x})$ which renders the functional of equation (C.2) stationary, is the required solution of the boundary value problem for the surrounding water domain.

C.2 Inside Water Domain

Let $p^i(\vec{x})$ be the function which renders the following functional [equation (4.78)] stationary :

$$\Pi(p) = \frac{1}{2} \int_{\tau^i} \nabla p^i \cdot \nabla p^i \, d\tau - \rho_w \int_{\Gamma_l^i} p^i(\vec{x}) \, a_n^i(\vec{x}) \, d\Gamma - \rho_w \int_{\Gamma_b^i} p^i(\vec{x}) \, b_n^i(\vec{x}) \, d\Gamma \tag{C.11}$$

Then setting the first variation of this functional equal to zero leads to

$$\int_{\tau^i} [-\nabla^2 p^i] \, \delta p^i(\vec{x}) \, d\tau + \int_{\Gamma^i} [\frac{\partial}{\partial n} p^i(\vec{x})] \, \delta p^i(\vec{x}) \, d\Gamma$$

$$- \rho_w \int_{\Gamma_l^i} \delta p^i(\vec{x}) \, a_n^i(\vec{x}) \, d\Gamma - \rho_w \int_{\Gamma_b^i} \delta p^i(\vec{x}) \, b_n^i(\vec{x}) \, d\Gamma = 0 \tag{C.12}$$

Using

$$\Gamma^i = \Gamma_l^i \cup \Gamma_b^i \cup \Gamma_f^i \tag{C.13}$$

and

$$\frac{\partial}{\partial n} p^i(\vec{x}) = - \frac{\partial}{\partial n^i} p^i(\vec{x}) \qquad \vec{x} \in \Gamma_l^i \tag{C.14a}$$

$$\frac{\partial}{\partial n} p^i(\vec{x}) = -\frac{\partial}{\partial z} p^i(\vec{x}) \qquad \vec{x} \in \Gamma_b^i \tag{C.14b}$$

$$\frac{\partial}{\partial n} p^i(\vec{x}) = \frac{\partial}{\partial z} p^i(\vec{x}) \qquad \vec{x} \in \Gamma_f^i \tag{C.14c}$$

equation (C.12) can be written in the following form :

$$\int_{\tau^i} [\, -\nabla^2 p^i(\vec{x})\,]\, \delta p^i(\vec{x})\, d\tau + \int_{\Gamma_t^i} [\, -\frac{\partial}{\partial n^i} p^i(\vec{x}) - \rho_w\, a_n^i(\vec{x})\,]\, \delta p^i(\vec{x})\, d\Gamma$$

$$+ \int_{\Gamma_b^i} [\, -\frac{\partial}{\partial z} p^i(\vec{x}) - \rho_w\, b_n^i(\vec{x})\,]\, \delta p^i(\vec{x})\, d\Gamma + \int_{\Gamma_f^i} [\, \frac{\partial}{\partial z} p^i(\vec{x})\,]\, \delta p^i(\vec{x})\, d\Gamma = 0 \tag{C.15}$$

This implies that if $p^i(\vec{x})$ is restricted to be zero on surface Γ_f^i, and if $p^i(\vec{x})$ renders the functional of equation (C.11) stationary, it is also the solution of the following boundary value problem:

$$\nabla^2 p^i(\vec{x}) = 0 \qquad \vec{x} \in \tau^i \tag{C.16}$$

$$\frac{\partial}{\partial n^i} p^i(\vec{x}) = -\rho_w\, a_n^i(\vec{x}) \qquad \vec{x} \in \Gamma_t^i \tag{C.17a}$$

$$\frac{\partial}{\partial z} p^i(\vec{x}) = -\rho_w\, b_n^i(\vec{x}) \qquad \vec{x} \in \Gamma_b^i \tag{C.17b}$$

$$p^i(\vec{x}) = 0 \qquad \vec{x} \in \Gamma_f^i \tag{C.17c}$$

Thus, the function $p^i(\vec{x})$, which renders the functional of equation (C.11) stationary, is also the solution of the boundary value problem associated with hydrodynamic pressures due to inside water.

APPENDIX D

HYDRODYNAMIC ANALYSIS OF AXISYMMETRIC FLUID DOMAINS

D.1 Surrounding Water Domain

As mentioned in Section 4.3.5, the functions $\bar{p}_A^o(r,z)$ and $\bar{p}_B^o(r,z)$ which render the following functional

$$\Pi(\bar{p}^o) = \frac{1}{2} \int_{\Omega_A^o} [\frac{\partial}{\partial r}\bar{p}_A^o \cdot \frac{\partial}{\partial r}\bar{p}_A^o + \frac{\partial}{\partial z}\bar{p}_A^o \cdot \frac{\partial}{\partial z}\bar{p}_A^o] \, r \, dr \, dz + \frac{1}{2} \int_{\Omega_A^o} \frac{1}{r} \, \bar{p}_A^o \cdot \bar{p}_A^o \, dr \, dz$$

$$+ \frac{1}{2} \int_{\Lambda_c^o} \bar{p}_B^o [\frac{\partial}{\partial r}\bar{p}_B^o] \, r \, dz - \int_{\Lambda_c^o} \bar{p}_A^o [\frac{\partial}{\partial r}\bar{p}_B^o] \, r \, dz$$

$$- \rho_w \int_{\Lambda_i^o} \bar{p}_A^o \, \bar{a}_n^o(r,z) \, r \, d\Lambda - \rho_w \int_{\Lambda_e^o} \bar{p}_A^o \, \bar{b}_n^o(r,z) \, r \, d\Lambda \qquad \text{(D.1)}$$

stationary, are also the solution of the boundary value problem for the fluid domain surrounding the axisymmetric tower.

Let N_A be the number of nodal points for the finite element system in r-z plane, then the pressure function $\bar{p}_A^o(r,z)$ in domain Ω_A^o is approximated by

$$\bar{p}_A^o(r,z) \approx \sum_{i=1}^{N_A} \bar{N}_i(r,z) \, p_i \qquad (r,z) \in \Omega_A^o \qquad \text{(D.2)}$$

Similarly, the pressure function $\bar{p}_B^o(r,z)$ in domain Ω_B^o is approximated by the linear combination of the first N_B normalized functions :

$$\bar{p}_B^o(r,z) \approx \sum_{i=1}^{N_B} \bar{M}_i(r,z) \, q_i \qquad (r,z) \in \Omega_B^o \qquad \text{(D.3)}$$

in which q_i's are the unknown coefficients and

$$\bar{M}_i(r,z) = [\frac{K_1(\alpha_i r/H_o)}{K_1(\alpha_i r_c/H_o)}] \cos(\alpha_i z/H_o) \qquad ; \quad i=1,2, \ldots, N_B \qquad \text{(D.4)}$$

Since function $\bar{p}_B^o(r,z)$ and its derivatives appear in the functional of equation (D.1) only under the integral of Λ_c^o, (i.e $r=r_c$), it is sufficient to compute $\bar{p}_B^o(r,z)$ and its derivatives on Λ_c^o :

$$\bar{p}_B^o(r,z) \approx \sum_{i=1}^{N_B} \overline{M}_i^\Gamma(r,z)\, q_i \qquad (r,z) \in GCI \tag{D.5}$$

$$\frac{\partial}{\partial r}\bar{p}_B^o(r,z) \approx \sum_{i=1}^{N_B} \bar{B}_i\, \overline{M}_i^\Gamma(r,z)\, q_i \qquad (r,z) \in GCI \tag{D.6}$$

in which functions $\overline{M}_i^\Gamma(r,z)$ and constants $\bar{B}_i$ are defined as

$$\overline{M}_i^\Gamma(r,z) = \cos(\alpha_i z/H_o) \qquad ; \quad i=1,2,\ldots,N_B \tag{D.7}$$

$$\bar{B}_i = -\frac{1}{2}\,\frac{\alpha_i}{H_o}\,\frac{K_0(\alpha_i r_c/H_o) + K_2(\alpha_i r_c/H_o)}{K_1(\alpha_i r_c/H_o)} \qquad ; \quad i=1,2,\ldots,N_B \tag{D.8}$$

Substitution of equations (D.2), (D.5) and (D.6) into equation (D.1) leads to a functional in vectors $\boldsymbol{p}$ and $\boldsymbol{q}$ containing the unknowns p_i, $i=1,2,\ldots,N_A$ and q_i, $i=1,2,\ldots,N_B$ respectively:

$$\Pi(\,\boldsymbol{p},\boldsymbol{q}\,) = \frac{1}{2}\boldsymbol{p}^T\boldsymbol{K}_I\boldsymbol{p} + \frac{1}{2}\boldsymbol{q}^T\boldsymbol{K}_{III}\boldsymbol{q} + \frac{1}{2}[\,\boldsymbol{p}^T\boldsymbol{K}_{II}\boldsymbol{q} + \boldsymbol{q}^T\boldsymbol{K}_{II}^T\boldsymbol{p}\,] - \boldsymbol{p}^T\boldsymbol{Q}_I - \boldsymbol{p}^T\boldsymbol{Q}_{II} \tag{D.9}$$

which is similar to equation (4.49) for a general three-dimensional fluid domain.

In equation (D.9), $\boldsymbol{K}_I$ is $N_A \times N_A$ symmetric matrix with its jk- element given by

$$(\boldsymbol{K}_I)_{j,k} = \int_{\Omega_A^o} [\,\frac{\partial}{\partial r}\overline{N}_j(r,z)\cdot\frac{\partial}{\partial r}\overline{N}_k(r,z) + \frac{\partial}{\partial z}\overline{N}_j(r,z)\cdot\frac{\partial}{\partial z}\overline{N}_k(r,z)\,]\, r\, dr\, dz$$

$$+ \int_{\Omega_A^o} \overline{N}_j(r,z)\cdot\overline{N}_k(r,z)\,\frac{1}{r}\,dr\,dz \qquad ; \quad j,k=1,2,\ldots,N_A \tag{D.10}$$

The zero pressure boundary condition on surface Λ_f^o is satisfied by assigning zeros to the rows and columns in the matrix $\boldsymbol{K}_I$ corresponding to the nodes on this surface.

Since $\overline{M}_i^\Gamma$, $i=1,2,\ldots,N_B$ is a set of orthogonal functions on surface Λ_c^o, the matrix $\boldsymbol{K}_{III}$ in equation (D.9) is a diagonal matrix of order N_B with its jj- elements given by :

$$(\boldsymbol{K}_{III})_{j,j} = \bar{B}_j\, r_c \int_{\Lambda_c^o} \overline{M}_j^\Gamma(r_c,z)\,\overline{M}_j^\Gamma(r_c,z)\,dz \qquad ; \quad j=1,2,\ldots,N_B \tag{D.11}$$

If the nodal points in the finite element mesh for domain Ω_A^o are numbered in a special way, assigning the first N_T numbers to the tower-water interface and the last N_C numbers to the hypothetical surface between domains Ω_A^o and Ω_B^o, the matrix defining the coupling between the pressures in domains Ω_A^o and Ω_B^o is of size $N_C \times N_B$ and its jk- element is given by

$$(\boldsymbol{K}_{II})_{j,k} = -\,\overline{B}_k\, r_c \int_{\Lambda_c^o} \overline{N}_j(r_c,z)\, \overline{M}_k^{\Gamma}(r_c,z)\, dz \quad ; \quad j=N_A-N_c+1, \ldots, N_A \;\; ; \;\; k=1,2, \ldots \tag{D.12}$$

The vectors $\boldsymbol{Q}_I$ and $\boldsymbol{Q}_{II}$ appearing in the functional [equation (D.1)] are of order N_A and their jj-terms are given by :

$$(\boldsymbol{Q}_I)_j = \int_{\Lambda_i^o} \overline{N}_j(r,z)\, \overline{a}_n^o(r,z)\, r\, d\Lambda \quad ; \; j=1,2, \ldots, N_A \tag{D.13}$$

$$(\boldsymbol{Q}_{II})_j = \int_{\Lambda_e^o} \overline{N}_j(r,z)\, \overline{b}_n^o(r,z)\, r\, d\Lambda \quad ; \; j=1,2, \ldots, N_A \tag{D.14}$$

In vector $\boldsymbol{Q}_I$, only the first N_T terms are non-zero which correspond to the nodes on the tower-water interface. Similarly, in vector $\boldsymbol{Q}_{II}$, only those terms which correspond to the nodes on the exposed portion of the foundation surface in contact with water are non-zero.

Similar to the procedure presented in Section 4.3.4, stationarity of the functional of equation (D.9) leads to N_A+N_B linear algebraic equations in unknowns p_i, $i=1,2, \ldots, N_A$ and q_i, $i=1,2, \ldots, N_B$. Solution of these equations leads to unknowns p_i's and q_i's. The pressure functions $\overline{p}_A^o(r,z)$ and $\overline{p}_B^o(r,z)$ then can be approximated from equations (D.2) and (D.3). The hydrodynamic pressures, their equivalent lateral forces and external moments are then evaluated by equations (4.63), (4.64) and (4.70).

D.2 Inside Water Domain

As mentioned in Section 4.4.3, the functions $\overline{p}^i(r,z)$ which renders the following functional [equation (4.88)]

$$\Pi(\overline{p}^i) = \frac{1}{2} \int_{\Omega^i} \left[\frac{\partial}{\partial r}\overline{p}^i \cdot \frac{\partial}{\partial r}\overline{p}^i + \frac{\partial}{\partial z}\overline{p}^i \cdot \frac{\partial}{\partial z}\overline{p}^i \right] r\, dr\, dz + \frac{1}{2} \int_{\Omega^i} \frac{1}{r}\, \overline{p}^i \cdot \overline{p}^i\, dr\, dz$$
$$- \rho_w \int_{\Lambda_i^i} \overline{p}^i\, \overline{a}_n^i(r,z)\, r\, d\Lambda - \rho_w \int_{\Lambda_b^i} \overline{p}^i\, \overline{b}_n^i(r,z)\, r\, d\Lambda \tag{D.15}$$

stationary, is also the solution of the boundary value problem for the fluid domain contained within the axisymmetric tower.

Similar to equation (D.2) for the surrounding water domain, pressure in domain Ω^i is expressed in terms of the unknown pressure p_i at i-th node for N_A nodal points by the following equation :

$$\bar{p}^i(r,z) \approx \sum_{i=1}^{N_A} \bar{N}_i(r,z)\, p_i \qquad (r,z) \in \Omega^i \tag{D.16}$$

Substitution of equation (D.16) into equation (D.15) leads to a functional in vector $\boldsymbol{p}$ containing the unknowns p_i, $i=1,2,\ldots,N_A$:

$$\Pi(\,\boldsymbol{p}\,) = \frac{1}{2}\boldsymbol{p}^T \boldsymbol{K}_I \boldsymbol{p} - \boldsymbol{p}^T \boldsymbol{Q}_I - \boldsymbol{p}^T \boldsymbol{Q}_{II} \tag{D.17}$$

in which $\boldsymbol{K}_I$ is $N_A \times N_A$ symmetric matrix with its jk- element given by

$$(\boldsymbol{K}_I)_{j,k} = \int_{\Omega^i} [\, \frac{\partial}{\partial r}\bar{N}_j(r,z) \cdot \frac{\partial}{\partial r}\bar{N}_k(r,z) + \frac{\partial}{\partial z}\bar{N}_j(r,z) \cdot \frac{\partial}{\partial z}\bar{N}_k(r,z)\,]\; r\, dr\, dz$$

$$+ \int_{\Omega^i} \bar{N}_j(r,z) \cdot \bar{N}_k(r,z)\, \frac{1}{r}\, dr\, dz \quad ; \quad j,k=1,2,\ldots,N_A \tag{D.18}$$

The zero pressure boundary condition on surface Λ_f^i is satisfied by assigning zeros to the rows and columns in the matrix $\boldsymbol{K}_I$ corresponding to the nodes on this surface. The vectors $\boldsymbol{Q}_I$ and $\boldsymbol{Q}_{II}$ appearing in the functional [equation (D.15)] are of order N_A and their jj-terms are given by :

$$(\boldsymbol{Q}_I)_j = \int_{\Lambda_t^i} \bar{N}_j(r,z)\, \bar{a}_n^i(r,z)\, r\, d\Lambda \quad ; \quad j=1,2,\ldots,N_A \tag{D.19}$$

$$(\boldsymbol{Q}_{II})_j = \int_{\Lambda_b^i} \bar{N}_j(r,z)\, \bar{b}_n^i(r,z)\, r\, d\Lambda \quad ; \quad j=1,2,\ldots,N_A \tag{D.20}$$

In vector $\boldsymbol{Q}_I$, only first N_T terms are non-zero which correspond to the nodes on the tower-water interface. Similarly, in matrix $\boldsymbol{Q}_{II}$, only those terms which correspond to the nodes on the reservoir bottom are non-zero.

Similar to the procedure presented in Section 4.4.2, stationarity of the functional of equation (D.17) leads to N_A linear algebraic equations in unknowns p_i, $i=1,2,\ldots,N_A$. Solution of these equations leads to unknowns p_i's. The pressure functions $\bar{p}^i(r,z)$ then can be approximated from equation (D.16). The hydrodynamic pressures, their equivalent lateral forces and external moments are then evaluated by equations (4.87) and (4.92).

APPENDIX E

COMBINED EFFECTS OF SURROUNDING AND INSIDE WATER ON TOWER VIBRATION PROPERTIES

The equation of motion for a fixed-base tower without water, restricted to vibrate in its n-th mode shape, due to harmonic ground acceleration $\ddot{u}_g(t) = e^{i\omega t}$ is

$$[\ -\ \omega^2 M_n + (\ 1 + i\ \eta_s\ )\ \omega_n^2 M_n\ ]\ \bar{Y}_n(\omega) = -\ L_n \tag{E.1}$$

in which ω_n is the n-th natural vibration frequency, η_s is the constant hysteretic damping factor; and the generalized mass M_n, and the generalized excitation term L_n are given by equations (7.4) and (7.5).

As shown in Chapter 3, the surrounding (outside) water introduces an added mass term M_{nn}^o and an added excitation term L_n^o in equation (E.1), leading to:

$$[\ -\ \omega^2\ (\ M_n + M_{nn}^o\ ) + (\ 1 + i\ \eta_s\ )\ \omega_n^2 M_n\ ]\ \bar{Y}_n(\omega) = -\ L_n - L_n^o \tag{E.2}$$

From this equation, the natural frequency of the tower with surrounding water may be expressed as

$$\omega_n^o = \omega_n \sqrt{M_n\ /\ (\ M_n + M_{nn}^o\ )} \tag{E.3}$$

which can be rewritten in terms of the corresponding vibration periods as:

$$T_n^o = T_n \sqrt{1 + (\ M_{nn}^o\ /\ M_n\ )} \tag{E.4}$$

Similarly, as shown in Chapter 3, the inside water introduces an added mass term M_{nn}^i and an added excitation term L_n^i in equation (E.1), leading to:

$$[\ -\ \omega^2\ (\ M_n + M_{nn}^i\ ) + (\ 1 + i\ \eta_s\ )\ \omega_n^2 M_n\ ]\ \bar{Y}_n(\omega) = -\ L_n - L_n^i \tag{E.5}$$

From this equation, T_n^i, the n-th vibration period of the tower with inside water is given by:

$$T_n^i = T_n \sqrt{1 + (\ M_{nn}^i\ /\ M_n\ )} \tag{E.6}$$

When the effects of surrounding and inside water are considered together, the equation of motion becomes :

$$[\,-\,\omega^2\,(\,M_n + M_{nn}^o + M_{nn}^i\,) + (\,1 + i\;\eta_s\,)\,\omega_n^2\,M_n\,]\,\overline{Y}_n(\omega) = -\,L_n - L_n^o - L_n^i \qquad \text{(E.7)}$$

From this equation, T_n^r, the n-th vibration period of the tower with surrounding and inside water can be expressed as:

$$T_n^r = T_n \sqrt{1 + (\,M_{nn}^o \,/\, M_n\,) + (\,M_{nn}^i \,/\, M_n\,)} \qquad \text{(E.8)}$$

Elimination of $M_{nn}^o \,/\, M_n$ and $M_{nn}^i \,/\, M_n$ from equation (E.8) by substituting equations (E.4) and (E.6) respectively, leads to :

$$\left[\frac{T_n^r}{T_n}\right]^2 = \left[\frac{T_n^o}{T_n}\right]^2 + \left[\frac{T_n^i}{T_n}\right]^2 - 1 \qquad \text{(E.9)}$$

APPENDIX F

PROPERTIES OF EQUIVALENT SINGLE-DEGREE-OF-FREEDOM SYSTEM WITH CONSTANT HYSTERETIC DAMPING

The frequency domain equations for the fundamental mode response of towers on flexible foundation soil with impounded water are [equation (7.21)]:

$$\begin{bmatrix} [-\omega^2 M_1 + (1+i\eta_s)\omega_1^2 M_1] & -\omega^2 L_1^h & -\omega^2 L_1^r \\ -\omega^2 L_1^h & -\omega^2(m_t+m_f)+K_{VV}(\omega) & -\omega^2 L_0^r + K_{VM}(\omega) \\ -\omega^2 L_1^r & -\omega^2 L_0^r + K_{MV}(\omega) & -\omega^2(I_f+I_t)+K_{MM}(\omega) \end{bmatrix} \begin{Bmatrix} \overline{Y}_1(\omega) \\ \overline{u}_f(\omega) \\ \overline{\theta}_f(\omega) \end{Bmatrix}$$

$$= - \begin{Bmatrix} L_1 \\ m_f + m_t \\ L_0^r \end{Bmatrix} \tag{F.1}$$

This system of three complex-valued equations can be solved for $\overline{Y}_1(\omega)$, the frequency response function for the modal coordinate corresponding to the fundamental mode of vibration of the tower.

Solution of equation (F.1) for the frequency response function $\overline{Y}_1(\omega)$ for the fundamental mode coordinate is complicated by the implicit contributions of the higher vibration modes of the tower to the three terms, m_t, I_t and L_0^r representing the inertial influence of the tower mass due to rigid-body motions allowed by foundation-soil flexibility. It can be shown from numerical results that the influence of m_f and I_f on the tower response is small, and that the tower response is accurately predicted with the assumption that these inertia terms are approximated by the contribution of the fundamental vibration mode :

$$m_t \approx m_1^* \tag{F.2a}$$

$$L_0^r \approx m_1^* \, h_1^* \tag{F.2b}$$

$$I_t \approx m_1^* \, (h_1^*)^2 \tag{F.2c}$$

in which $m_1^* = (L_1)^2 / M_1$ and $h_1^* = L_1^r / L_1$ are the effective mass and effective height, respectively, of the tower in its fundamental mode of vibration [20,46]. Similarly, the influence of coupling impedances $K_{VM}(\omega)$ and $K_{MV}(\omega)$ can be neglected (Chapter 7). Substitution of equation (F.2) into equation (F.1) and neglecting m_f, I_f, and the coupling impedances leads to :

$$\begin{bmatrix} [-\omega^2 M_1+(1+i\eta_s)\omega_1^2 M_1] & -\omega^2 L_1 & -\omega^2 L_1^r \\ -\omega^2 L_1 & -\omega^2 m_1^* + K_{VV}(\omega) & -\omega^2 m_1^* \ h_1^* \\ -\omega^2 L_1^r & -\omega^2 m_1^* \ h_1^* & -\omega^2 m_1^* \ (h_1^*)^2 + K_{MM}(\omega) \end{bmatrix} \begin{Bmatrix} \overline{Y}_1(\omega) \\ \overline{u}_f(\omega) \\ \overline{\theta}_f(\omega) \end{Bmatrix}$$

$$= - \begin{Bmatrix} L_1 \\ m_1^* \\ m_1^* \ h_1^* \end{Bmatrix} \tag{F.3}$$

Solving equation (F.3) for $\overline{Y}_1(\omega)$ using Cramer's rule gives :

$$\overline{Y}_1(\omega) = \frac{-\ L_1}{[-\omega^2 M_1+(1+i\eta_s)\omega_1^2 M_1] \ - \ \omega^2 M_1(1+i\eta_s) \ F(\omega)} \tag{F.4}$$

where

$$F(\omega) = m_1^* \ \omega_1^2 \left[\frac{(\ h_1^*\ )^2}{K_{MM}(\omega)} + \frac{1}{K_{VV}(\omega)} \right] \tag{F.5}$$

The natural vibration frequency ω_1^f of the equivalent single-degree-of-freedom (SDF) system that models the fundamental mode response of the tower on flexible foundation soil without water is given by the excitation frequency that makes the real valued component of the denominator in equation (F.4) zero :

$$-\ (\ \omega_1^f\ )^2 + \omega_1^2 - (\ \omega_1^f\ )^2 \ \mathrm{Re}[F(\omega_1^f)] + (\ \omega_1^f\ )^2 \ \eta_s \ \mathrm{Im}[F(\omega_1^f)] = 0 \tag{F.6}$$

Neglecting the effect of the second order damping terms leads to

$$\omega_1^f = \frac{\omega_1}{\sqrt{1 + \mathrm{Re}[F(\omega_1^f)]}} \tag{F.7}$$

which must be evaluated iteratively. The vibration frequency ω_1^f will always be less than ω_1 because $\mathrm{Re}[F(\omega)] > 0$ for all excitation frequencies.

The frequency response function $\tilde{\overline{Y}}_1(\omega)$ for the equivalent SDF system can be obtained from the frequency response function $\overline{Y}_1(\omega)$ for the fundamental mode response of the tower, equation (F.4). Evaluating the frequency dependent terms at excitation frequency ω_1^f, using equation (F.6) and (F.7) for the real valued terms in the denominator of equation (F.4), and grouping the imaginary valued terms, gives the frequency response function $\bar{\bar{Y}}_1(\omega)$ for the equivalent SDF system :

$$\bar{\bar{Y}}_1(\omega) = \left[\frac{\omega_1^f}{\omega_1} \right]^2 \frac{-L_1}{-\omega^2 M_1 + (1 + i\eta_1^f)\,(\omega_1^f)^2 M_1} \tag{F.8}$$

in which the constant hysteretic damping factor η_1^f is

$$\eta_1^f = \left[\frac{\omega_1^f}{\omega_1} \right]^2 \eta_s + \eta_a \tag{F.9}$$

where

$$\eta_a = - \left[\frac{\omega_1^f}{\omega_1} \right]^2 \mathrm{Im}[F(\omega_1^f)] \tag{F.10}$$

The two terms on the right side of equation (F.9) represent the contributions of structural damping and foundation damping, respectively. The damping factor η_a is always positive because $\mathrm{Im}[F(\omega)] < 0$ for all excitation frequencies. This added damping due to soil-structure interaction is the combined effects of soil material damping and radiation damping.

APPENDIX G

ADDED HYDRODYNAMIC MASS FOR INFINITELY-LONG UNIFORM TOWERS

G.1 Added Mass for Surrounding Water

The geometry of the fluid domain surrounding an infinitely-long uniform tower does not vary with the z coordinate defined along its length, and the normal to the outside surface remains in x-y plane. These special geometric properties allow the distribution of surface acceleration for a rigid tower to be written in the following form :

$$a_n^o(\vec{x}) = n_x^o(s_1^o) \tag{G.1}$$

in which s_1^o is the local coordinate defined along the perimeter of the outside surface in the x-y plane, as shown in Figure G.1, and n_x^o is the direction cosine of the normal to the outside surface with respect to the direction of ground motion. Consequently, the solution for the hydrodynamic pressure is sought independent of z coordinate :

$$p^o(\vec{x}) = \bar{p}^o(x,y) \tag{G.2}$$

and it is sufficient only to solve the two-dimensional Laplace equation in the x-y plane. For this purpose, the domains τ_A^o and Γ_b^o in Section 4.3.4 are replaced by domains Ω_A^o and Ω_B^o, both in x-y plane (Figure G.1), and surfaces Γ_t^o and Γ_c^o are replaced by contours Λ_t^o and Λ_c^o, also in x-y plane. Thus, similar to the procedure of Sections 4.3.3 and 4.3.4, the pressure function $\bar{p}^o(x,y)$ is computed by making the following functional stationary :

$$\Pi(\bar{p}^o) = \frac{1}{2} \int_{\Omega_A^o} \nabla\bar{p}^o \cdot \nabla\bar{p}^o \, d\Omega + \frac{1}{2} \int_{\Lambda_c^o} \bar{p}_B^o \left[\frac{\partial}{\partial n_A^o} \bar{p}_B^o \right] d\Lambda + \int_{\Lambda_c^o} \bar{p}_A^o \left[- \frac{\partial}{\partial n_A^o} \bar{p}_B^o \right] d\Lambda$$

$$- \rho_w \int_{\Lambda_t^o} \bar{p}_A^o \, a_n^o(s_1^o) \, d\Lambda \tag{G.3}$$

The functions $\bar{p}_A^o$ and $\bar{p}_B^o$ in domains Ω_A^o and Ω_B^o, respectively, are approximated by interpolating them in x-y plane using the special forms of equations (4.40) and (4.42):

$$\bar{p}_A^o(x,y) \approx \sum_{i=1}^{N_A} \bar{N}_i(x,y)\, p_i \qquad (x,y) \in \Omega_A^o \tag{G.4}$$

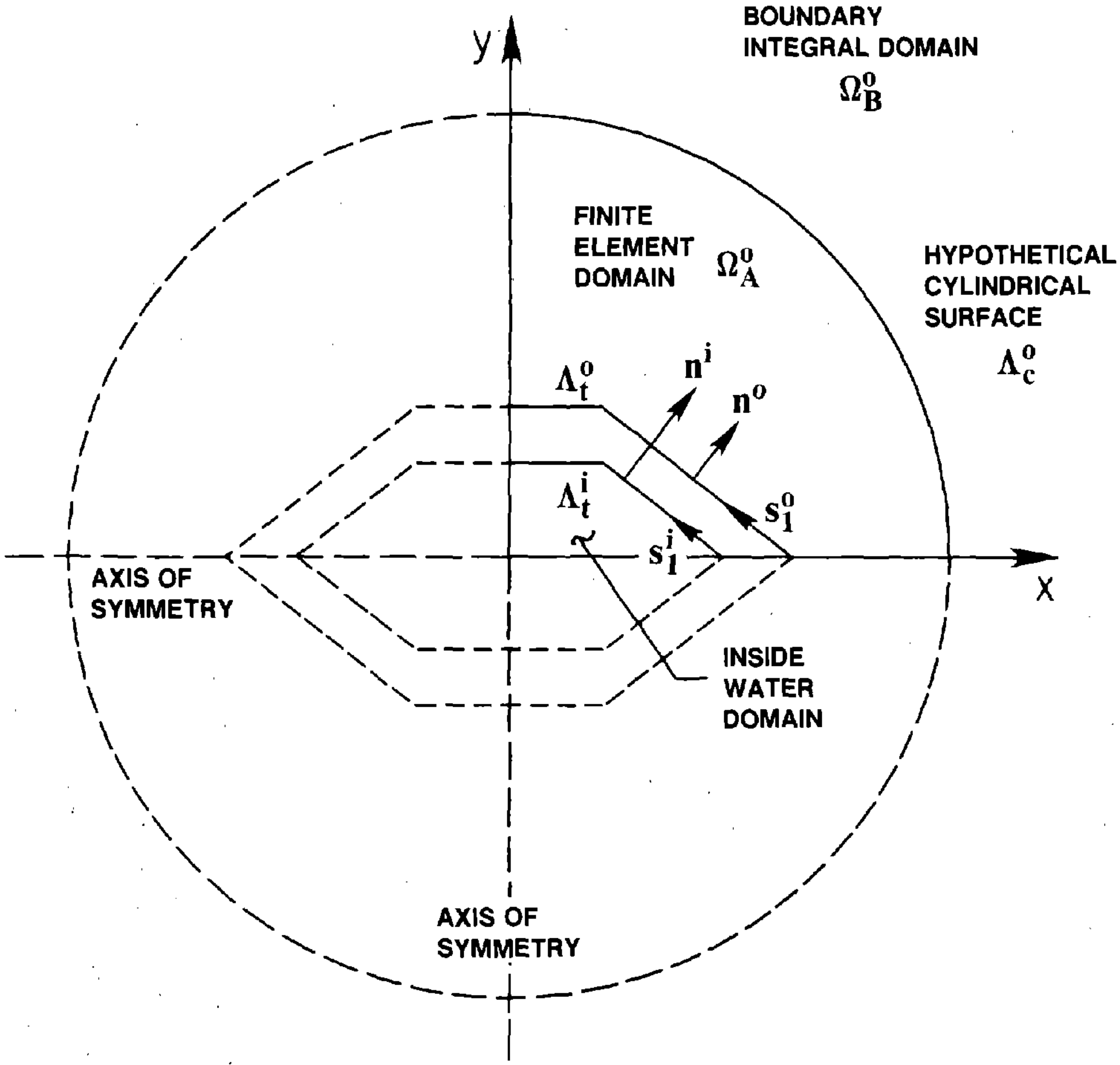

Figure G.1 Surrounding and Inside Water Domains for an Infinitely-Long Uniform Tower

$$\bar{p}_B^o(x,y) \approx \sum_{i=1}^{N_B} \overline{M}_i(x,y)\, q_i \qquad (x,y) \in \Omega_B^o \tag{G.5}$$

In these equations, $\overline{N}_i(x,y)$, $i=1,2,\ldots,N_A$ are the interpolation functions in the x-y plane and $\overline{M}_i(x,y)$, $i=1,2,\ldots,N_B$ are general solutions of the Laplace equation for the fluid domain exterior to a hypothetical, infinitely-long, circular cylinder. If r_c is the radius of the hypothetical cylinder, $\overline{M}_i(x,y)$ can be written in cylindrical coordinates in the following form :

$$\overline{M}_i(x,y) = [\, r/r_c \,]^{-(2i-1)} \cos(2i-1)\theta \qquad ; \qquad i=1,2,\ldots,N_B \tag{G.6}$$

This form of the solution of the Laplace equation comes from the lack of boundary conditions at the free surface and at the horizontal base of an infinitely-long tower. It should also be noted that the symmetry of pressure functions about the plane of motion, and the antisymmetry of pressure functions about the plane normal to the direction of motion have been used to obtain this form of the general solution.

Because Λ_c^o is a circle, its outward normal always satisfies the following equation:

$$\frac{\partial}{\partial n_A^o} = \frac{\partial}{\partial r} \qquad along \;\; \Lambda_c^o \tag{G.7}$$

Therefore, due to the special structure of $\overline{M}_i(x,y)$, the pressure function $\bar{p}_B^o(x,y)$ and its gradient on the contour Λ_c^o can be represented in the following form by using equation (G.7) and substituting $r=r_c$ in equation (G.6):

$$\bar{p}_B^o(x,y) \approx \sum_{i=1}^{N_B} \overline{M}_i^{\Gamma}(x,y)\, q_i \qquad (x,y) \in \Lambda_c^o \tag{G.8}$$

$$\frac{\partial}{\partial n_A^o}\bar{p}_B^o(x,y) \approx \sum_{i=1}^{N_B} \overline{B}_i\, \overline{M}_i^{\Gamma}(x,y)\, q_i \qquad (x,y) \in \Lambda_c^o \tag{G.9}$$

in which functions $\overline{M}_i^{\Gamma}(x,y)$ and constants $\overline{B}_i$ are defined as

$$\overline{M}_i^{\Gamma}(x,y) = \cos(2i-1)\theta \qquad ; \qquad i=1,2,\ldots,N_B \tag{G.10}$$

$$\overline{B}_i = -\,(2i-1)\,/\,r_c \qquad ; \qquad i=1,2,\ldots,N_B \tag{G.11}$$

Substitution of equations (G.4), (G.8) and (G.9) into equation (G.3) leads to a functional in vectors $\boldsymbol{p}$ and $\boldsymbol{q}$ containing the unknowns p_i, $i=1,2,\ldots,N_A$ and q_i, $i=1,2,\ldots,N_B$

respectively:

$$\Pi(\, \boldsymbol{p},\boldsymbol{q}\,) = \frac{1}{2}\boldsymbol{p}^T \boldsymbol{K}_I \boldsymbol{p} + \frac{1}{2}\boldsymbol{q}^T \boldsymbol{K}_{III} \boldsymbol{q} + \frac{1}{2}[\, \boldsymbol{p}^T \boldsymbol{K}_{II} \boldsymbol{q} + \boldsymbol{q}^T \boldsymbol{K}_{II}^T \boldsymbol{p}\,] - \boldsymbol{p}^T \boldsymbol{Q}_I \tag{G.12}$$

which is similar to equation (4.49) for a general three-dimensional fluid domain.

In equation (G.12), $\boldsymbol{K}_I$ is $N_A \times N_A$ symmetric matrix with its jk- element given by

$$(\boldsymbol{K}_I)_{j,k} = \int_{\Omega_A^o} \nabla \overline{N}_j(x,y) \cdot \nabla \overline{N}_k(x,y)\, d\Omega \quad ; \; j,k=1,2,\ldots,N_A \tag{G.13}$$

Since $\overline{M}_i^\Gamma$, $i=1,2,\ldots,N_B$ is a set of orthogonal functions on surface Λ_c^o, the matrix $\boldsymbol{K}_{III}$ in equation (G.12) is a diagonal matrix of order N_B with its jj- element given by :

$$(\boldsymbol{K}_{III})_{j,j} = \overline{B}_j \int_{\Lambda_c^o} \overline{M}_j^\Gamma(x,y) \cdot \overline{M}_j^\Gamma(x,y)\, d\Lambda \quad ; \; j=1,2,\ldots,N_B \tag{G.14}$$

If the nodal points in the finite element mesh for domain Ω_A^o are numbered in a special way, assigning the first N_T numbers to the tower-water interface and the last N_C numbers to the hypothetical surface between domains Ω_A^o and Ω_B^o, the matrix defining the coupling between the pressures in domains Ω_A^o and Ω_B^o is of size $N_C \times N_B$ and its jk- element is given by :

$$(\boldsymbol{K}_{II})_{j,k} = -\,\overline{B}_k \int_{\Lambda_c^o} \overline{N}_j(x,y)\, \overline{M}_k^\Gamma(x,y)\, d\Lambda \quad ; \; j=N_A-N_C+1,\ldots,N_A \; ; \; k=1,2,\ldots,N_B \tag{G.15}$$

The vector $\boldsymbol{Q}_I$ appearing in the functional [equation (G.3)] is of order N_A and its j-term is given by :

$$(\boldsymbol{Q}_I)_j = \int_{\Lambda_t^o} \overline{N}_j(x,y)\, a_n^o(s_1^o)\, d\Lambda \quad ; \; j=1,2,\ldots,N_A \tag{G.16}$$

in which $a_n^o(s_1^o) = n_x^o(s_1^o)$ [equation (G.1)] for the ground motion along x-axis. In vector $\boldsymbol{Q}_I$, only the first N_T terms are non-zero which correspond to the nodes on the tower-water interface.

Only matrix $\boldsymbol{K}_{III}$ can be evaluated analytically and therefore, all other matrices are evaluated by numerical integration. Since the interpolation functions $\overline{N}_i(x,y)$, $i=1,2,\ldots,N_A$ are locally supported, integration is not performed over the full domain or the entire surface for each element of these matrices. The domain Ω_A^o is discretized into two-dimensional elements and contours Λ_t^o and Λ_c^o into one-dimensional elements.

Integration in equations (G.13) to (G.16) is done at element level and the element matrices are assembled by standard procedures [53].

Stationarity of the functional of equation (G.12) with respect to p_i's and q_i's leads to N_A+N_B simultaneous, linear algebraic equations [Section 4.3.4]. Solution of these equations results in p_i's and q_i's. The pressure function $\bar{p}^o(x,y)$ then can be obtained using equations (G.4) and (G.5), and the conditions of symmetry and antisymmetry for pressure function along the direction of ground motion, and normal to the direction of ground motion, respectively.

The added hydrodynamic mass per unit of length, m^o_∞, which is equal to the hydrodynamic force computed by integrating the component of pressure function $\bar{p}^o(x,y)$ in the direction of ground motion along the perimeter of the tower-water interface is then given by

$$m^o_\infty = \int_{\Lambda^o_t} \bar{p}^o(x,y)\, n^o_x(s^o_1)\, d\Lambda \tag{G.17}$$

G.2 Added Mass for Inside Water

The hydrodynamic pressure function $p^i(\vec{x})$ for the water domain contained inside an infinitely-long uniform tower is also independent of z coordinate :

$$p^i(\vec{x}) = \bar{p}^i(x,y) \tag{G.18}$$

The pressure function $\bar{p}^i(x,y)$ is the solution of the two-dimensional Laplace equation :

$$\frac{\partial^2}{\partial x^2}\bar{p}^i(x,y) + \frac{\partial^2}{\partial y^2}\bar{p}^i(x,y) = 0 \tag{G.19}$$

subjected to the following boundary conditions on the tower-water interface, Λ^i_t, if the ground motion is assumed to act along the x-axis :

$$\frac{\partial}{\partial x}\bar{p}^i(x,y) = -\rho_w \tag{G.20a}$$

$$\frac{\partial}{\partial y}\bar{p}^i(x,y) = 0 \tag{G.20b}$$

If the origin of the coordinates is selected at the point of intersection for the two axes of the symmetry of the cross-section, the solution

$$\bar{p}^i(x,y) = -\rho_w\, x \tag{G.21}$$

satisfies equation (G.19) and the boundary conditions of equation (G.20). The added hydrodynamic mass per unit of length, m_{∞}^{i} is given by an equation similar to equation (G.17) :

$$m_{\infty}^{i} = \int_{\Lambda_i} \bar{p}^{i}(x,y)\, n_x^{i}(s_1^{i})\, d\Lambda \tag{G.22}$$

in which n_x^{i} is the direction cosine of the normal of a point on the tower-water interface with respect to the direction of ground motion. Substitution of equation (G.21) into equation (G.22) and using Stoke's theorem leads to :

$$m_{\infty}^{i} = \rho_w A_i \tag{G.23}$$

in which A_i is the area enclosed by the curve defining the cross-section of the inside surface of the tower. Equation (G.23) implies that the added mass per unit of length for an infinitely-long uniform tower associated with hydrodynamic effects of the inside water is equal to the mass of water per unit of length contained inside the hollow tower.

APPENDIX H
SIMPLIFIED EVALUATION OF ADDED HYDRODYNAMIC MASS -- NUMERICAL EXAMPLE

The objective of this appendix is to illustrate the use of the simplified procedure of Chapter 8 to compute the added hydrodynamic mass for a selected non-circular tapered tower. This example tower is shown in Figure H.1 and its geometric properties are summarized in Tables H.1 and H.2. Since, as shown in Chapter 5, the added hydrodynamic mass for a non-circular tower may depend on the direction of ground motion, the added mass for the selected tower is evaluated for ground motion acting separately in x and y directions.

The added hydrodynamic mass is computed at selected locations along the height of the tower. More specifically, the added hydrodynamic mass due to surrounding water is computed at nodes 1 to 12 while the added mass due to inside water is computed at nodes 3 to 11 (Figure H.1). Nodes 2 and 3 are defined at the same location because the cross-section of the tower changes abruptly. The added mass is computed using both the cross-sections at this location. Since the bottom boundaries of the outside and inside fluid domain may not be at the level of the tower base, two new coordinates, z_o and z_i, measured from the bottom boundaries of the outside and inside fluid domains, respectively, have been introduced along the height of the tower.

The added hydrodynamic mass is computed by implementing the simplified procedure described in Sections 8.2.4 and 8.3.4, and the computational details are presented in Tables H.3 to H.6.

H.1 Added Hydrodynamic Mass for Surrounding Water

The detailed step-by-step computations of added hydrodynamic mass due to surrounding water for the ground motion along x - axis are summarized next for one location along the height corresponding to node 7 (Figure H.1).

1. The addeded hydrodynamic mass for surrounding water has been computed for twelve locations along the height, identified by node numbers 1 to 12 (Figure H.1). The z_o coordinate for node 7 is 100.0 ft.

2a. For $a_o/b_o = 1/2$, $A_o = 457.1$ ft^2, and $H_o = 200.0$ ft, equation (8.5a) gives $H_o/\tilde{a}_o = 23.47$ implying $\tilde{a}_o/H_o = 0.043$. For $a_o/b_o = 1/2$, from equation (8.5b), $\tilde{a}_o/\tilde{b}_o = 1/2$

2b. From Table 8.3 (or Figure 8.7), corresponding to $\tilde{a}_o/\tilde{b}_o = 1/2$ (Step 2a), $\tilde{r}_o/H_o = 0.071$ for $\tilde{a}_o/H_o = 0.05$, and $\tilde{r}_o/H_o = 0.0$ for $\tilde{a}_o/H_o = 0.0$. For $\tilde{a}_o/H_o = 0.043$ (Step 2a), linear interpolation gives $\tilde{r}_o/H_o = 0.060$.

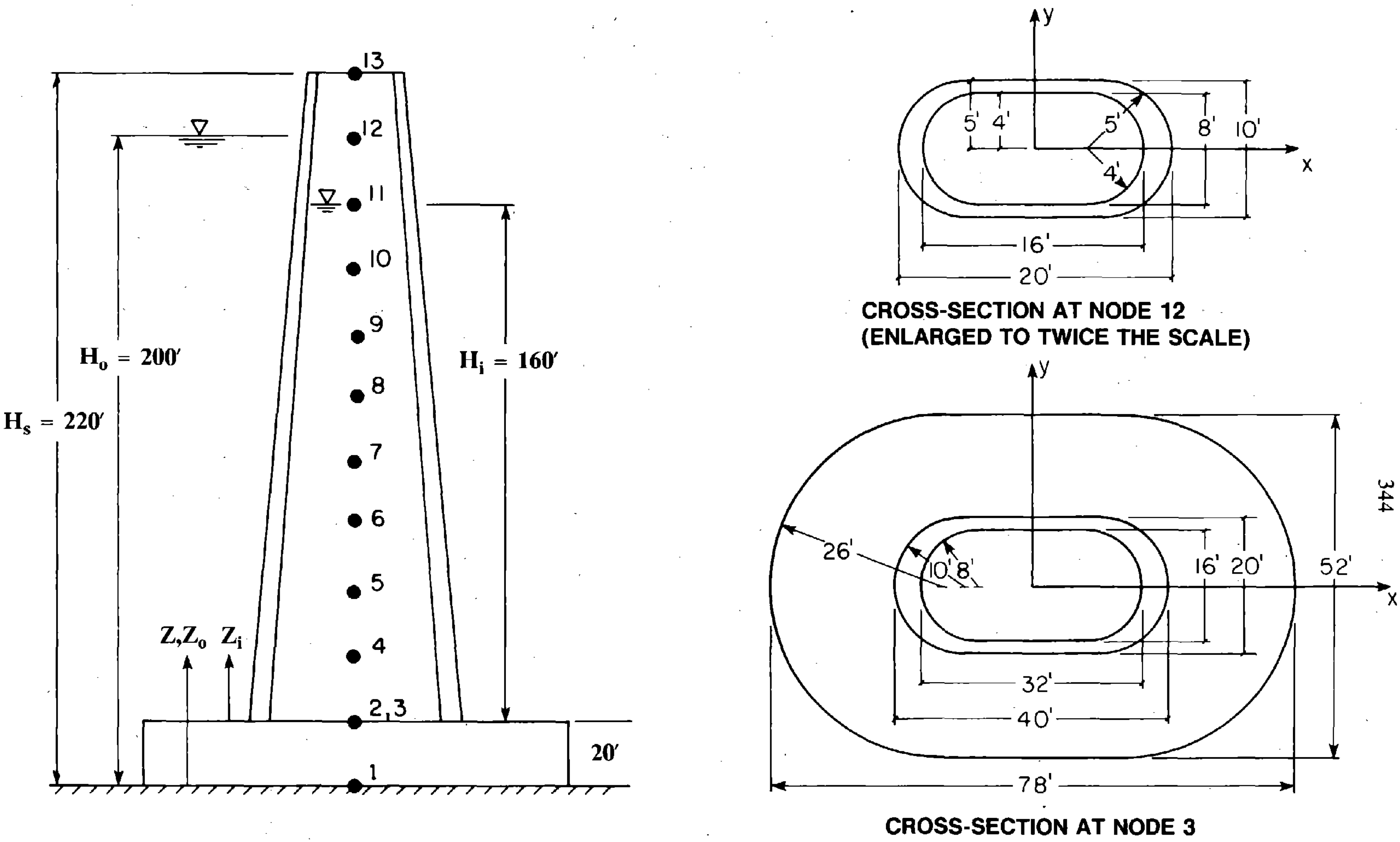

Figure H.1 Selected Intake-Outlet Tower

Table H.1 -- Geometric Properties of Tower for Ground Motion along x-Axis

Node		Outside Surface						Inside Surface					
#	z (ft)	z_o (ft)	a_o (ft)	b_o (ft)	z_o/H_o	a_o/b_o	A_o (ft^2)	z_i (ft)	a_i (ft)	b_i (ft)	z_i/H_i	a_i/b_i	A_i (ft^2)
1	0	0	26.0	39	0.00	2/3	3475.7	-	-	-	-	-	-
2	20	20	26.0	39	0.10	2/3	3475.7	-	-	-	-	-	-
3	20	20	10.0	20	0.10	1/2	714.2	0	8.0	16.0	0.00	1/2	457.1
4	40	40	9.5	19	0.20	1/2	644.5	20	7.6	15.2	0.125	1/2	412.5
5	60	60	9.0	18	0.30	1/2	578.5	40	7.2	14.4	0.25	1/2	370.2
6	80	80	8.5	17	0.40	1/2	516.0	60	6.8	13.6	0.375	1/2	330.2
7	100	100	8.0	16	0.50	1/2	457.1	80	6.4	12.8	0.50	1/2	292.5
8	120	120	7.5	15	0.60	1/2	401.7	100	6.0	12.0	0.625	1/2	257.1
9	140	140	7.0	14	0.70	1/2	349.9	120	5.6	11.2	0.75	1/2	224.0
10	160	160	6.5	13	0.80	1/2	301.7	140	5.2	10.4	0.875	1/2	193.1
11	180	180	6.0	12	0.90	1/2	257.1	160	4.8	9.6	1.00	1/2	164.5
12	200	200	5.5	11	1.00	1/2	216.0	-	4.4	8.8	-	-	138.3
13	220	-	5.0	10	-	1/2	178.5	-	4.0	8.0	-	-	114.3

Table H.2 -- Geometric Properties of Tower for Ground Motion along y-Axis

Node #	z (ft)	Outside Surface z_o (ft)	a_o (ft)	b_o (ft)	z_o/H_o	a_o/b_o	A_o (ft^2)	Inside Surface z_i (ft)	a_i (ft)	b_i (ft)	z_i/H_i	a_i/b_i	A_i (ft^2)
1	0	0	39	26.0	0.00	3/2	3475.7	-	-	-	-	-	-
2	20	20	39	26.0	0.10	3/2	3475.7	-	-	-	-	-	-
3	20	20	20	10.0	0.10	2	714.2	0	16.0	8.0	0.00	2	475.1
4	40	40	19	9.5	0.20	2	644.5	20	15.2	7.6	0.125	2	412.5
5	60	60	18	9.0	0.30	2	578.5	40	14.4	7.2	0.25	2	370.2
6	80	80	17	8.5	0.40	2	516.0	60	13.6	6.8	0.375	2	330.2
7	100	100	16	8.0	0.50	2	457.1	80	12.8	6.4	0.50	2	292.5
8	120	120	15	7.5	0.60	2	401.7	100	12.0	6.0	0.625	2	257.1
9	140	140	14	7.0	0.70	2	349.9	120	11.2	5.6	0.75	2	224.0
10	160	160	13	6.5	0.80	2	301.7	140	10.4	5.2	0.875	2	193.1
11	180	180	12	6.0	0.90	2	257.1	160	9.6	4.8	1.00	2	164.5
12	200	200	11	5.5	1.00	2	216.0	-	8.8	4.4	-	-	138.3
13	220	-	10	5.0	-	2	178.5	-	8.0	4.0	-	-	114.3

Table H.3 -- Computation of Added Hydrodynamic Mass for Surrounding Water -- Computational Details for Ground Motion along x-Axis

Node		Outside Geometry			Equivalent Ellipse		Equivalent Cylinder			Infinitely-Long Tower			
#	z_o (ft)	$\frac{a_o}{b_o}$	$\frac{a_o}{H_o}$	A_o (ft^2)	$\frac{\tilde{a}_o}{\tilde{b}_o}$	$\frac{\tilde{a}_o}{H_o}$	$\frac{\tilde{r}_o}{H_o}$	$\frac{z_o}{H_o}$	$\frac{m_a^o(z)}{m_\infty^o}$	$\rho_w A_o$ ($ks^{-2}f^{-1}/ft$)	$\frac{m_\infty^o}{\rho_w A_o}$	m_∞^o ($ks^{-2}f^{-1}/ft$)	$m_a^o(z)$ ($ks^{-2}f^{-1}/ft$)
1	0	2/3	0.130	3475.7	2/3	0.136	0.163	0.0	0.951	6.739	0.707	4.765	4.531
2	20	2/3	0.130	3475.7	2/3	0.136	0.163	0.10	0.949	6.739	0.707	4.765	4.522
3	20	1/2	0.050	714.2	1/2	0.053	0.075	0.10	0.988	1.385	0.555	0.768	0.759
4	40	1/2	0.048	644.5	1/2	0.051	0.071	0.20	0.987	1.250	0.555	0.694	0.685
5	60	1/2	0.045	578.5	1/2	0.048	0.068	0.30	0.987	1.122	0.555	0.622	0.614
6	80	1/2	0.042	516.0	1/2	0.045	0.064	0.40	0.986	1.000	0.555	0.555	0.548
7	100	1/2	0.040	457.1	1/2	0.043	0.060	0.50	0.983	0.886	0.555	0.492	0.484
8	120	1/2	0.038	401.7	1/2	0.040	0.056	0.60	0.978	0.779	0.555	0.432	0.423
9	140	1/2	0.035	349.9	1/2	0.037	0.053	0.70	0.968	0.678	0.555	0.377	0.364
10	160	1/2	0.032	301.7	1/2	0.935	0.049	0.80	0.945	0.585	0.555	0.325	0.307
11	180	1/2	0.030	257.1	1/2	0.032	0.045	0.90	0.861	0.500	0.555	0.277	0.238
12	200	1/2	0.028	216.0	1/2	0.029	0.041	1.00	0.0	0.420	0.555	0.232	0.00

Table H.4 -- Computation of Added Hydrodynamic Mass for Surrounding Water -- Computational Details for Ground Motion along y-Axis

Node		Outside Geometry			Equivalent Ellipse		Equivalent Cylinder			Infinitely-Long Tower		m_∞^o	$m_a^o(z)$
#	z_o (ft)	$\frac{a_o}{b_o}$	$\frac{a_o}{H_o}$	A_o (ft^2)	$\frac{\tilde{a}_o}{\tilde{b}_o}$	$\frac{\tilde{a}_o}{H_o}$	$\frac{\tilde{r}_o}{H_o}$	$\frac{z_o}{H_o}$	$\frac{m_a^o(z)}{m_\infty^o}$	$\rho_w A_o$ ($ks^{-2}f^{-1}/ft$)	$\frac{m_\infty^o}{\rho_w A_o}$	($ks^{-2}f^{-1}/ft$)	($ks^{-2}f^{-1}/ft$)
1	0	3/2	0.195	3475.7	3/2	0.204	0.179	0.0	0.942	6.739	1.444	9.732	9.167
2	20	3/2	0.195	3475.7	3/2	0.204	0.173	0.10	0.941	6.739	1.444	9.732	9.158
3	20	2	0.100	714.2	2	0.107	0.086	0.10	0.985	1.385	1.896	2.626	2.586
4	40	2	0.095	644.5	2	0.101	0.081	0.20	0.984	1.250	1.896	2.369	2.330
5	60	2	0.090	578.5	2	0.096	0.077	0.30	0.984	1.122	1.896	2.127	2.093
6	80	2	0.085	516.0	2	0.091	0.073	0.40	0.981	1.000	1.896	1.896	1.861
7	100	2	0.080	457.1	2	0.085	0.068	0.50	0.978	0.886	1.896	1.680	1.643
8	120	2	0.075	401.7	2	0.080	0.064	0.60	0.972	0.779	1.896	1.477	1.435
9	140	2	0.070	349.9	2	0.075	0.060	0.70	0.960	0.687	1.896	1.286	1.235
10	160	2	0.065	301.7	2	0.069	0.055	0.80	0.933	0.585	1.896	1.109	1.035
11	180	2	0.060	257.1	2	0.064	0.051	0.90	0.843	0.498	1.896	0.945	0.797
12	200	2	0.055	216.0	2	0.059	0.047	1.00	0.00	0.419	1.896	0.794	0.00

Table H.5 -- Computation of Added Hydrodynamic Mass for Inside Water -- Computational Details for Ground Motion along x-Axis

Node		Inside Geometry			Equivalent Cylinder			m^i_∞	$m^i_a(z)^*$
#	z_i (ft)	a_i/b_i	a_i/H_i	A_i (ft^2)	$\tilde{r}_i/H_i$	z_i/H_i	$m^i_a(z)/m^i_\infty$	$=\rho_w A_i$ ($ks^{-2}f^{-1}/ft$)	($ks^{-2}f^{-1}/ft$)
3	20	1/2	0.050	457.1	0.107	0.000	1.000	0.886	0.886
4	40	1/2	0.048	412.5	0.101	0.125	1.000	0.800	0.800
5	60	1/2	0.045	370.2	0.096	0.250	1.000	0.718	0.718
6	80	1/2	0.042	330.2	0.091	0.375	1.000	0.640	0.640
7	100	1/2	0.040	292.5	0.085	0.500	1.000	0.567	0.567
8	120	1/2	0.038	257.1	0.080	0.625	0.999	0.498	0.498
9	140	1/2	0.035	224.0	0.075	0.750	0.996	0.434	0.433
10	160	1/2	0.032	193.1	0.069	0.875	0.961	0.374	0.360
11	180	1/2	0.030	164.5	0.064	1.000	0.00	0.319	0.00

Table H.6 -- Computation of Added Hydrodynamic Mass for Inside Water --

Computational Details for Ground Motion along y-Axis

Node		Inside Geometry			Equivalent Cylinder			m^i_∞	$m^i_a(z)$
#	z_i (ft)	a_i/b_i	a_i/H_i	A_i (ft^2)	$\tilde{r}_i/H_i$	z_i/H_i	$m^i_a(z)/m^i_\infty$	$=\rho_w A_i$ ($ks^{-2}f^{-1}/ft$)	($ks^{-2}f^{-1}/ft$)
3	20	2	0.100	457.1	0.053	0.00	1.000	0.886	0.886
4	40	2	0.095	412.5	0.051	0.125	1.000	0.800	0.800
5	60	2	0.090	370.2	0.048	0.25	1.000	0.718	0.718
6	80	2	0.085	330.2	0.045	0.375	1.000	0.640	0.640
7	100	2	0.080	292.5	0.043	0.50	1.000	0.567	0.567
8	120	2	0.075	257.1	0.040	0.625	1.000	0.498	0.498
9	140	2	0.070	224.0	0.037	0.750	1.000	0.434	0.434
10	160	2	0.065	193.1	0.035	0.875	0.993	0.374	0.372
11	180	2	0.060	164.5	0.032	1.000	0.000	0.319	0.000

3. For node 6, $z_o = 100$ ft, $H_o = 200$ ft, which give $z_o/H_o = 0.50$ From Table 8.4 (or Figure 8.1), for $\tilde{r}_o/H_o = 0.05$, $z_o/H_o = 0.52$, $m_a^o(z)/m_\infty^o(z) = 0.988$, and for $\tilde{r}_o/H_o = 0.05$, $z_o/H_o = 0.48$, $m_a^o(z)/m_\infty^o(z) = 0.990$. Linear interpolation gives $m_a^o(z)/m_\infty^o(z) = 0.989$ for $\tilde{r}_o/H_o = 0.05$ and $z_o/H_o = 0.50$. Similarly from Table 8.4 (or Figure 8.1), for $\tilde{r}_o/H_o = 0.10$, $z_o/H_o = 0.52$, $m_a^o(z)/m_\infty^o(z) = 0.956$, and for $\tilde{r}_o/H_o = 0.10$, $z_o/H_o = 0.48$, $m_a^o(z)/m_\infty^o(z) = 0.961$. Linear interpolation gives $m_a^o(z)/m_\infty^o(z) = 0.958$ for $\tilde{r}_o/H_o = 0.10$ and $z_o/H_o = 0.50$. Linear interpolation for $m_a^o(z)/m_\infty^o(z)$ corresponding to $z_o/H_o = 0.50$ and $\tilde{r}_o/H_o = 0.06$ (Step 3) from the two calculated values gives $m_a^o(z)/m_\infty^o(z) = 0.983$ for $\tilde{r}_o/H_o = 0.06$ and $z_o/H_o = 0.50$.
4. For unit weight of water 62.4 lb / ft^3, acceleration due to gravity $g = 32.18$ ft / Sec^2, mass density of water $\rho_w = 0.001939$ Kips Sec^2 / ft^4. For $A_o = 457.062$ ft^2 corresponding to location for node 7, $\rho_w A_o = 0.8862$ Kips Sec^2 / ft^2. From Table 8.1 for the cross-sectional shape of the tower corresponding to $a_o/b_o = 1/2$, $m_\infty^o(z)/\rho_w A_o = 0.555$, which multiplied by the value of $\rho_w A_o$ computed earlier gives $m_\infty^o(z) = 0.492$ Kips Sec^2 / ft^2.
5. For $m_a^o(z)/m_\infty^o(z) = 0.983$ (computed in Step 3) and $m_\infty^o(z) = 0.492$ Kips Sec^2 / ft^2 (computed in Step 4), multiplication of both values gives $m_a^o(z) = 0.484$ Kips Sec^2 ft^{-1} / ft, the added hydrodynamic mass per unit height due to surrounding water at the location of node 7 for the ground motion along x - axis.
6. Steps 2 to 5 for various locations along the heigh, selected in step 1, have been repeated and the results are summarized in Table H.3.

H.2 Added Hydrodynamic Mass for Inside Water

The detailed step-by-step computations of added hydrodynamic mass due to inside water for the ground motion along x - axis are summarized next for one location along the height corresponding to node 7.

1. The addeded hydrodynamic mass for inside water has been computed for nine locations along the height, identified by node numbers 3 to 11 (Figure H.1). The z_i coordinate for node 7 is 80.0 ft.

2. For $a_i/b_i = 1/2$, $A_i = 292.520\ ft^2$. from equation (8.11), $\tilde{r}_i = 13.65$ ft.
3. For $H_i = 160.0$ ft, $\tilde{r}_i/H_i = 0.085$ and for $z_i = 80.0$ ft, $H_i = 160.0$ ft, $z_i/H_i = 0.50$. From Table 8.5 (or Figure 8.17), $m_a^i(z)/m_\infty^i(z) = 1.000$ for $0.48 \le z_i/H_i \le 0.52$ and $0.05 \le \tilde{r}_i/H_i \le 0.10$. Therefore, for $z_i/H_i = 0.50$, and $\tilde{r}_i/H_i = 0.085$ (computed earlier), $m_a^i(z)/m_\infty^i(z) = 1.000$.
4. For $\rho_w = 0.001939$ Kips Sec^2 / ft^4 (Section H.1), $A_i = 292.520\ ft^2$, equation (8.9) gives $m_\infty^i(z) = 0.567$ Kips Sec^2 / ft^2. For $m_a^i(z)/m_\infty^i(z) = 1.000$ (computed in Step 3) and $m_\infty^i(z) = 0.5672$ Kips Sec^2 / ft^2 (computed above), multiplication of both values gives $m_a^i(z) = 0.567$ Kips Sec^2 ft^{-1} / ft, the added hydrodynamic mass per unit height due to inside water at the location of node 7 for the ground motion along x - axis.
5. Steps 2 to 4 for various locations along the heigh, selected in step 1, have been repeated and the results are summarized in Table H.5.

APPENDIX I
SIMPLIFIED EVALUATION OF TOWER-FOUNDATION-SOIL INTERACTION EFFECTS -- NUMERICAL EXAMPLE

It has been demonstrated in Chapter 7 that the tower-foundation-soil interaction effects can be approximately included in the response analysis of towers by modifying the vibration period and damping ratio for the fundamental mode. The objective of this appendix is to illustrate the use of the simplified procedure presented in Chapter 9, Section 9.4, to compute the vibration period T_1^f and the damping ratio ξ_1^f for the fundamental mode of the tower, considering the effects of tower-foundation-soil interaction. The tower is supported through a circular footing of radius r_f = 25 ft. on the viscoelastic halfspace. The following values are selected for various parameters of the halfspace: shear wave velocity C_f = 1000.0 ft./ Sec. ; constant hysteretic damping factor η_f =0.10 ; unit weight = 165 lb/ft^3 ; and Poisson's ratio ν_f = 0.33. The computational details of the step-by-step procedure of Section 9.4.5 are summarized next.

1. The following vibration properties have been selected for the numerical example: Vibration period for the fundamental mode = T_1 = 0.3 Sec. generalized mass M_1 for the fundamental mode M_1 = 19.6 kips Sec^2 / ft ; generalized excitation L_1 for the fundamental mode = L_1 = 37.4 kips Sec^2 / ft ; and L_1^r = 2829.1 kips Sec^2. These values are taken from the numerical example of Chapter 5 for a tapered circular tower.

2. For L_1 = 37.4 kips Sec^2 / ft, M_1 = 19.6 kips Sec^2 / ft, using equation (9.15), the effective mass m_1^* = 37.4 × 37.4 / 19.6 = 71.4 kips Sec^2 / ft. The effective height h_1^* from equation (9.16) is h_1^* = 2829.1 / 37.4 = 75.6 ft.

3. For the shear wave velocity, C_f, of the foundation soil equal to 1000 ft / Sec., from equation (9.18), the wave parameter σ^* = 1000 × 0.3 / 75.6 = 4.03, leading to 1/ σ^* = 0.25. For r_f = 22.5 ft, the ratio of the effective height of the tower to the radius of the footing is h_1^*/r_f = 75.6 / 22.5 = 3.36. Using equation (9.25), $\tilde{\chi}$ = 0.25 × (3.36)$^{2/5}$ = 0.40. For mass density of soil ρ_f = 0.165 / 32.18 = 0.005127 kips Sec^2 / ft^4, m_1^* = 71.4 kips Sec^2 / ft, h_1^* = 75.6 ft, and r_f = 22.5 ft, from equation (9.20), the relative mass density parameter γ^* = 71.4 / (0.005127 × 3.14 × 22.5 × 22.5 × 75.6) = 0.116. Since $\tilde{\chi} \geq 0.20$, proceed to next step.

4. Corresponding to $\sqrt{\gamma^* \tilde{\chi}} = \sqrt{0.116 \times 0.40} = 0.137$, from Figure 9.5, $T_1^f \,/\, T_1 = 1.36$. Thus, $T_1^f = 1.36 \times 0.3 = 0.418$ Sec.

5. In this numerical example, damping in the fundamental vibration mode of the tower on rigid foundation-soil is selected as 5%, i.e. $\xi_1 = 0.05$. For $\eta_f = 0.10$, and $T_1^f / T_1 = 1.36$, computed in step 4, from Figure 9.7, added damping ratio ξ_a is 3.2% for $h_1^* / r_f = 3$ and 2.6% for $h_1^* / r_f = 4$. Interpolating linearly for $h_1^* / r_f = 3.36$ leads to $\xi_a = 3.0$ %. Modifying this damping ratio for $\gamma^* = 0.116$ using equation (9.28) leads to $\xi_a = 3.0 \times (0.10 \,/\, 0.116\,)^{1/3.361} = 2.9\%$.

6. From equation (9.26), for $\xi_1 = 5\%$, $T_1^f / T_1 = 1.36$ and $\xi_a = 2.92$ %, the effective damping ratio $\xi_1^f = (\,1 \,/\, 1.36\,)^3 \times 0.05 + 0.029 = 0.492$ %. Since ξ_1^f is less than ξ_1, ξ_1^f is taken equal to $\xi_1 = 0.05$ or 5%.

APPENDIX J
TOWERINF SERIES OF PROGRAMS : USERS MANUAL

J.1 Introduction

The TOWERINF series of computer programs implements the procedure presented in Appendix G, Section G.1 to evaluate the added mass associated with the hydrodynamic effects of the water surrounding an infinitely-long, uniform tower. The tower is restricted to cross-sections with two axes of symmetry, and the added mass is computed for motion along an axis of symmetry.

The added mass is determined by solving the Laplace equation in a cross-sectional (x-y) plane with the tower subjected to unit acceleration in the x direction. The surrounding fluid domain up to a hypothetical cylindrical surface is discretized in the x-y plane by a finite element system (Figure J.1) and the effects of the unbounded extent of the fluid outside the hypothetical cylinder are treated by the boundary integral procedures utilizing classical solutions for domains exterior to a circular cylinder. Because of two axes of plan symmetry, only one quadrant of the fluid domain needs to be discretized (Figure J.1).

J.2 Organization of TOWERINF Series of Programs

The TOWERINF series of programs contains the following two modules:

1. TOWERINF — This program reads the information about the mathematical model from the input file **TOWERINF.DAT** in free-field type of input and create a data base for the second module.

2. AMASSINF — This program computes the added hydrodynamic mass per unit of length for an infinitely-long uniform tower of the specified cross-section. The results are written on a file named **TOWERINF.OUT** and it contains : (a) Normalized added hydrodynamic mass; (b) Nodal coordinates and equation numbers; (c) Connectivity of elements; (d) Connectivity of segments on tower-water interface; and (e) Connectivity of segments on hypothetical cylindrical surface.

The source listings of both the modules are available in FORTRAN-77 programming language.

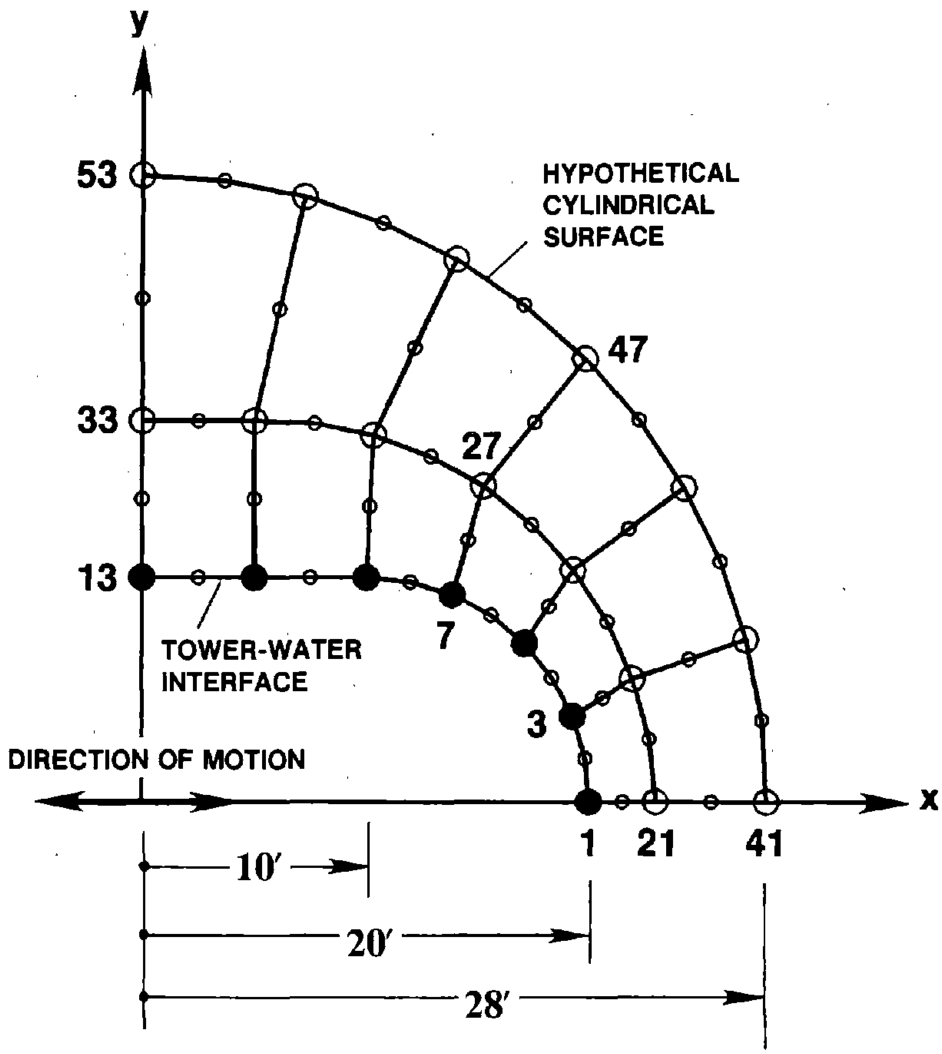

Figure J.1 Finite Element Idealization of Surrounding Fluid Domain in Example

J.3 Execution of Programs

Both the program segments can be compiled and linked independently using commonly available FORTRAN compilers. TOWERINF should be executed first to create a data base for the program AMASSINF. The program AMASSINF should be executed after TOWERINF has been executed. It is recommended that the user should check the file TOWERINF.OUT for possible errors in input data file.

Whenever the data file TOWERINF.DAT is modified, it is necessary to execute TOWERINF first and then run the module AMASSINF.

J.4 Idealization of Surrounding Water Domain

The boundary value problem associated with surrounding water domain is solved using finite elements coupled with boundary integral procedure. The fluid domain between the outside surface of tower and a hypothetical cylindrical surface is discretized by finite elements and the effects of the fluid domain exterior to this surface are treated by boundary integral procedures. The user should follow the instructions listed below:

1. **The nodes on the hypothetical cylindrical surface should be numbered last at the end of the sequence.**
2. The connectivity of eight-node elements should be provided in the order shown in Figure J.2b.
3. The connectivity of the three-node segments on the interface of the tower and the outside water should be provided in the order shown in Figure J.2a.
4. The connectivity of the three-node segments on the hypothetical cylindrical surface should be provided in the order shown in Figure J.2a.
5. **No node should be common to the tower-outside water interface and the hypothetical cylindrical surface.**

J.5 Input Data File (TOWERINF.DAT)

The free-field input data format is similar to that introduced by E.L. Wilson, and M. Hoit, at the University of California, Berkeley for SAP-80 series of programs.

In this system, "separator lines" are used to subdivide the data into logical groups. The data group can be in any order with each group being terminated with a line having colon ':' in "column 1". **The name on the separator line must be in CAPITAL LETTERS and must start in "column 1".** The program identifies the separator only by its first four characters. Rest of the characters are optional and used only for user's own understanding.

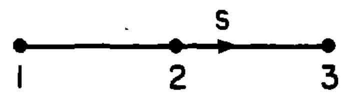

(a) 3-NODE SEGMENT

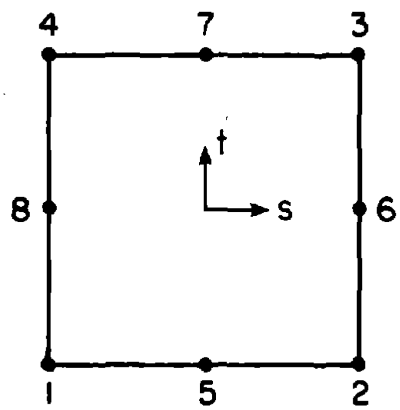

(b) 8-NODE ELEMENT

Figure J.2 Order of Node Numbering for Elements and Segments in the Finite Element Idealization

All lines of numerical data are entered in the following free field form:

N1,N2,N3,-- R=R1,R2,R3,--- Z=Z1,Z2,---

where the input data is designated by Ni, Ri or Zi. Numerical data lists must be separated by a single comma or by one blank. A numerical data list without identification, such as N1,N2,N3,---, must be the first information on the line. A data list of the form R=R1,R2,R3,--- can be in any order or location on the line. The data list is identified by "R=" only; therefore additional symbolic data must be entered between data lists.

A colon ":", which is optional, indicates the end of information on a line. Information entered to the right of the colon is ignored by the program; therefore, it can be used to provide additional information or comments within the input file.

A "C" in column 1 of any line will cause the line to be ignored by the program. Such lines can be used as comment lines to identify the data.

Simple arithmetic statements are possible when entering floating point real numbers. For example, the following type of data can be entered:

D=200+12/3.5-2,4.5*34

The statement 200+12/3.5-2 is evaluated as (((200+12)/3.5)-2).

In this manual, the values given in [?] are the default values of the parameters, i.e. the values adopted by the program if they are not provided or if the required identifier is missing.

The following sections provide the user with the necessary information to generate the TOWERINF.DAT input file.

J.5.1 **CONTROL** *Information*

The line of data which follows the CONTROL separator is used to supply general data about the finite element system used to idealize the surrounding (outside) water domain.

This line contains the following information:

N=? E=? T=? H=? M=? R=? W=? A=?

where

N= Number of nodes required in the idealization of water domain surrounding the tower.

E= Number of elements in the idealization of the fluid domain surrounding the tower. Eight-node isoparametric elements are used for the finite element idealization of the surrounding water.

T= Number of three-node segments defining the tower-water interface.

H= Number of three-node segments defining the hypothetical cylindrical surface for boundary integral procedure.

M= Number of trial functions to be used in the boundary integral procedure. [5]

R= Radius of the hypothetical cylindrical surface.

W= Mass density of water, i.e. unit weight divided by the acceleration due to gravity.

A= Constant with the dimensions of area used for the normalization of added hydrodynamic mass, e.g. area enclosed by the curve defining the cross-section. [1.0]

This data group must be terminated by a line with a colon ':' in the first column.

J.5.2 **ONODES** *Information*

The lines which follow the ONODES separator define the location of the nodes of the idealized fluid domain surrounding the uniform infinitely-long tower. These lines contain the following information:

Nid X=? Y=? I=? G=---- R=---- C=----

where

Nid= Node identification number to be selected by the user. The node number Nid must be less than or equal to the total number of nodes specified after the CONTROL separator.

X= x-ordinate

Y= y-ordinate

I= 1 for node on tower-water interface. For other nodes, need not be specified. [0]

The data may be automatically generated using the **linear generation option**, which can be activated by the addition of the following information on any line which contains the information about a nodal point:

G=Nf,Nl,Inc

where

Nf= The first node number in the sequence

Nl= The last node number in the sequence

Inc= Increment used to define generated node numbers. [1]

The generated nodes will be at equal interval along a straight line between nodes Nf and Nl.

The data may be automatically generated using the **radial generation option**, which can be activated by the addition of the following information on any line which contains the information about a nodal point:

R=Nf,Nl,Inc,Nc

where

Nf=	The first node number in the sequence
Nl=	The last node number in the sequence
Inc=	Increment used to define generated node numbers. [1]
Nc=	The node number for the center of the radial arc. If Nc=0, the center of the radial arc can be specified by adding the following information on the same line where radial generation is requested: C=Cx,Cy

where

Cx=	x-ordinate of the center of the radial arc
Cy=	y-ordinate of the center of the radial arc

The generated nodes will be at equal interval along a radial arc with the specified center between nodes Nf and Nl.

Alternatively, the location of a node not on the tower-water interface may be specified in terms of two nodes already defined. The program will place this node in the middle of the specified nodes. This information can be provided in a separate line in the following form:

Nid M=M1,M2 L=Nad,Nidinc,M1inc,M2inc

where

Nid=	Node identification number to be selected by the user.
M1=	First node number to be used in generation.
M2=	Second node number to be used in generation.
Nad=	Number of additional nodes to be generated using similar option.
Nidinc	Increment of Nid in generated nodes.
M1inc=	Increment of M1 in generated nodes.

M2inc= Increment of M2 in generated nodes.

This sequence of lines must be terminated by a line with colon ':' in the first column.

J.5.3 **OELEMENTS** *Information*

The sequence of lines which follow OELEMENTS separator define the connectivity of eight-node isoparametric elements used to idealize surrounding water domain in x-y plane. **No dummy nodes are allowed.**

These lines contain the following information:

Nid,J1,J2,J3,J4,J5,J6,J7,J8 G=------

where

Nid= Identification (ID) number for the element. Must be less than or equal to the total number of elements specified under CONTROL separator.

J1 to J8= Node numbers defining the connectivity of the element

The option to automatically generate element connectivity data is activated by the addition of the following information on any line:

G=Nad,Nidinc,J1inc,J2inc,J3inc,J4inc,J5inc,J6inc,J7inc,J8inc

where

Nad= Number of additional elements to be generated.

Nidinc= Increment of ID number in generated elements.[1]

J1inc= Increment of J1 in generated elements. [2]

J2inc= Increment of J2 in generated elements. [2]

J3inc= Increment of J3 in generated elements. [2]

J4inc= Increment of J4 in generated elements. [2]

J5inc= Increment of J5 in generated elements. [1]

J6inc= Increment of J6 in generated elements. [2]

J7inc= Increment of J7 in generated elements. [1]

J8inc= Increment of J8 in generated elements. [2]

This group of data lines must be terminated by a line having colon ':' in the first column.

J.5.4 **OTOWER-WATER INTERFACE** *Information*

The sequence of lines which follow OTOWER-WATER separator define the connectivity of three-node segments of the fluid elements in the surrounding water domain on the tower-water interface. These lines contain the following information:

Nid,J1,J2,J3 G=------

where

Nid= Identification (ID) number for the segment on the tower-outside water interface. Must be less than or equal to the total number of segments specified under CONTROL separator.

J1,J2,J3 = Node numbers defining the connectivity of the segment on the tower-outside water interface.

The option to automatically generate segment connectivity data is activated by the addition of the following information on any line:

G=Nad,Nidinc,J1inc,J2inc,J3inc

where

Nad= Number of additional segments to be generated.

Nidinc= Increment of ID number in generated segments.[1]

J1inc= Increment of J1 in generated segments. [2]

J2inc= Increment of J2 in generated segments. [2]

J3inc= Increment of J3 in generated segments. [2]

This group of data lines must be terminated by a line having colon ':' in the first column.

J.5.5 **OHYPOTHETICAL CYLINDER** *Information*

The sequence of lines which follow OHYPOTHETICAL separator define the connectivity of three-node segments of fluid elements in the outside water domain on the hypothetical cylindrical surface. These lines contain the following information:

Nid,J1,J2,J3 G=------

where

Nid= Identification (ID) number for the segment on the hypothetical cylindrical surface. Must be less than or equal to the total number of segments specified under CONTROL separator.

J1,J2,J3= Node numbers defining the connectivity of the segment on hypothetical cylindrical surface

The option to automatically generate segment connectivity data is activated by the addition of the following information on any line:

G=Nad,Nidinc,J1inc,J2inc,J3inc

where

Nad=	Number of additional segments to be generated.
Nidinc=	Increment of ID number in generated segments.[1]
J1inc=	Increment of J1 in generated segments. [2]
J2inc=	Increment of J2 in generated segments. [2]
J3inc=	Increment of J3 in generated segments. [2]

This group of data lines must be terminated by a line having colon ':' in the first column.

J.6 Numerical Example

For the convenience of the user, the input data file **TOWERINF.DAT** used for analysis of a infinitely-long uniform tower with a non-circular cross-section is presented. The mathematical model and the numbering schemes used in the finite element idealization of the fluid domain surrounding the tower in x-y plane are also presented in Figure J.1. The output file **AMASSINF.OUT** for the example case is also provided on the diskette with the source codes.

```
C.......EXAMPLE DATA FOR PROGRAM TOWERINF SERIES
CONTROL
N=53  E=12  T=6  H=6   M=5  R=28.0  W=1.0   A=714.159265
:
ONODES
   1    X=20.000      Y=.000     I=1
   9    X=10.000    Y=10.000     I=1  R=1,9,1  C=10.0,0.0
   13     X=0.000     Y=10.000     I=1  G=9,13,1
   21     X=23.0      Y=0.0
   31     X=5.0       Y=17.0     R=21,31,1     C=5.0,0.0
   33     X=0.0       Y=17.0     G=31,33,1
   14   M=1,21    L=6,1,2,2
   41    X=28.0    Y=0.0
   53    X=0.0     Y=28.0     R=41,53,1    C=0.0,0.0
   34    M=21,41    L=6,1,2,2
:
OELEMENTS
1,1,21,23,3,14,22,15,2          G=5,1,2,2,2,2,1,2,1,2
7,21,41,43,23,34,42,35,22       G=5,1,2,2,2,2,1,2,1,2
:
OTOWER-WATER
1,1,2,3   G=5,1,2,2,2
:
OHYPOTHETICAL
1,41,42,43     G=5,1,2,2,2
:
```

APPENDIX K
TOWERRZ SERIES OF PROGRAMS : USERS MANUAL

K.1 Introduction

The TOWERRZ series of programs were specifically developed for the earthquake response analysis of axisymmetric intake-outlet towers; i.e. towers with hollow circular cross-section with radius varying arbitrarily over height, subjected to one or two components of ground motion. The effects of tower-water interaction, due to water surrounding the tower and contained inside the tower, and tower-foundation-soil interaction can be included independently or simultaneously.

The output of the computer program consists of the maximum responses -- lateral displacement, shear force, and bending moment -- at selected locations along the height of the tower. The time variation of each response quantity due to one ground motion component is computed from which the maximum value is determined. Denoting any response quantity as $R(t)$, its time variation due to the x-component of ground motion, $R_x(t)$, and due to y-component of ground motion, $R_y(t)$, is determined by the computer program using the analytical procedure developed in Chapters 3 and 4 but specialized for axisymmetric towers. The resultant value of the two responses is given by the equation

$$R(t) = \sqrt{R_x(t)^2 + R_y(t)^2}$$

The program prints the maximum values (over time) of $R(t)$, $R_x(t)$, and $R_y(t)$.

K.2 Organization of TOWERRZ Series of Programs

The TOWERRZ series of programs are divided into six modules. The major advantage of the modular organization is that the modules can be restarted at certain points after data changes without starting other modules. The separate program segments interact by communication with a common file data base. So, the user has to prepare only one input data file **TOWERRZ.DAT**. The TOWERRZ series of programs contain the following six modules:

1. TOWERRZ — This program reads the information about the mathematical model from the input file **TOWERRZ.DAT** in free-field type of input and create a data base for various modules.

2. OUTPUTRZ — This program writes the information about the mathematical model in a file **TOWERRZ.OUT** and is used to check the correctness of the input data.

3. EIGENRZ This program computes the frequencies and mode shapes of the tower without water, generates generalized mass and excitation matrices and computes modal shears and moment transformation vectors. The generated section properties of the tower, its natural frequencies and mode shapes are written on a file **TOWERRZ.VEC** .

4. OUTWRZ This program computes the generalized added mass matrix and excitation vector due to water surrounding the tower.

5. INWRZ This program computes the generalized added mass matrix and excitation vector due to water inside the tower.

6. RESPRZ This program evaluates the impedance functions of the foundation footing, computes the frequency response functions of modal coordinates; the maximum displacement, shear force and bending moment at specified locations, and displacement time history at specified locations. The amplitudes of the frequency response functions for the first two modal coordinates only are written on a file **TOWERRZ.FRF**, the maximum responses are written on a file **TOWERRZ.MAX**, and response history on a file named **TOWERRZ.HIS**.

The source listings of all these modules are available in FORTRAN-77 programming language.

K.3 Execution of Programs

All the program segments can be compiled and linked independently using commonly available FORTRAN compilers. The sequence in which the programs should be executed is summarized in Figure K.1. TOWERRZ should be executed first. EIGENRZ comes next. RESPRZ should be executed in the end. Programs OUTWRZ should be executed after EIGENRZ only when interaction effects due to surrounding water need be included. Similarly, INWRZ should be executed after EIGENRZ but before RESPRZ if the effects of inside water need be included. The programs OUTWRZ and INWRZ can be executed in any order. The program OUTPUTRZ can be executed any time after TOWERRZ has been executed. It is recommended that the user should check the file TOWERRZ.OUT for possible errors in input data file before executing the subsequent program segments.

Whenever the data file TOWERRZ.DAT is modified, it is necessary to execute TOWERRZ and then run the module for which data has been changed. The other modules need not be executed if input data for them is not changed.

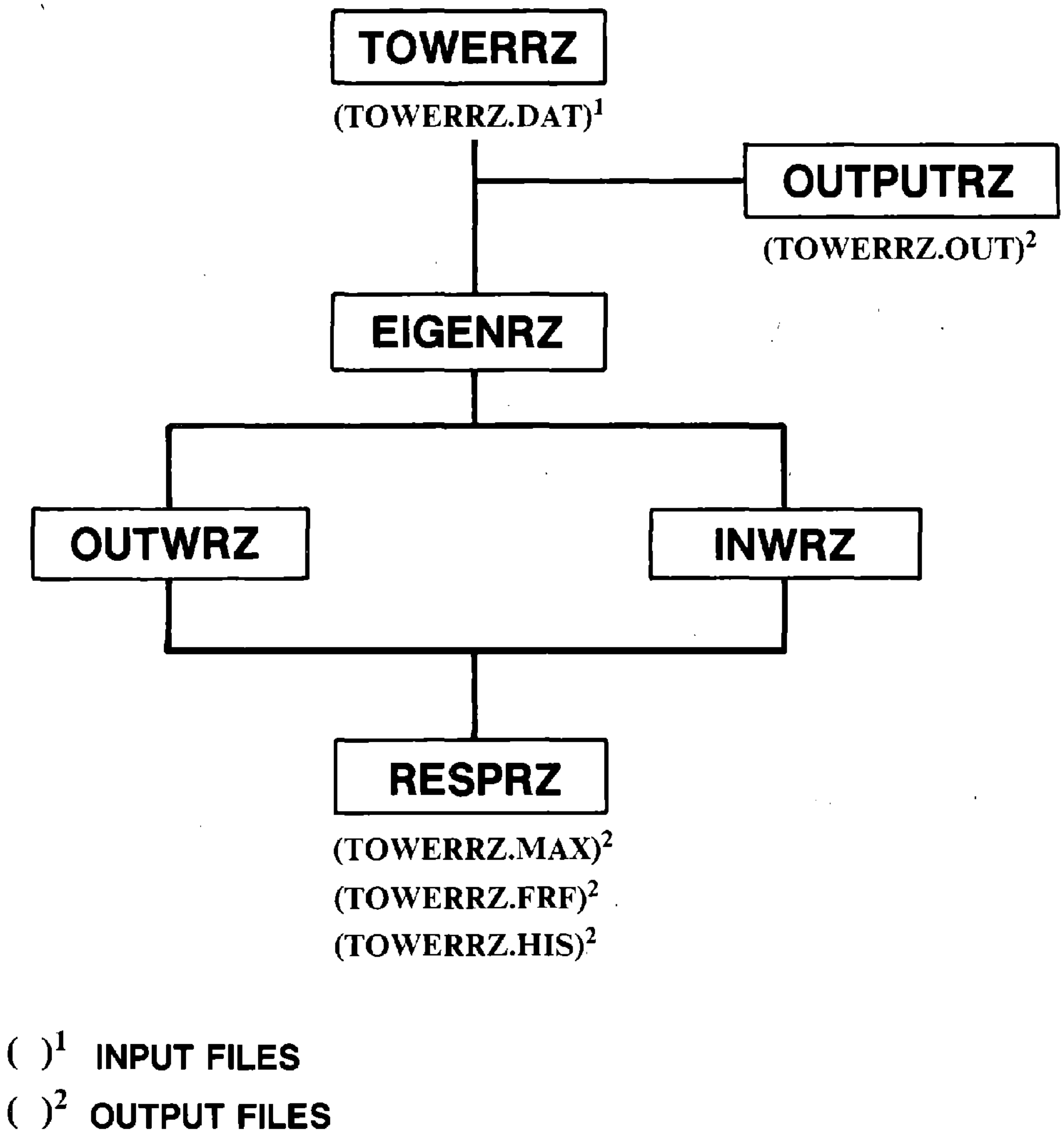

Figure K.1 Order of Execution for TOWERRZ Series of Programs

K.4 Idealization of Tower-Water-Foundation Soil System

The tower, the surrounding water domain, the inside water domain, and the foundation-soil system are idealized independently as substructures. The user should follow these instructions carefully in idealizing each substructure:

K.4.1 Tower Substructure

1. The numbering of the nodes should always start from the base to the top. Each node has two degrees of freedom, translational and rotational displacements.
2. The program uses a three-node Timoshenko beam element for which the connectivity should be provided from bottom to top in the order shown in Figure K.2a.
3. At any location above the base where the cross-section is discontinuous, two nodes need be specified with consecutive numbers and different section properties. The lower numbered node should define the section just below the node and the higher numbered node should define the section just above the node. The equation numbers for the degrees of freedom of the higher numbered node should be equal to that of lower numbered node. This is obtained by setting restraint code for higher numbered node to '-1' (see under TRESTRAINT separator). **The two nodes defining a discontinuous sections must belong to different elements,** i.e. the lower numbered node will be the third node of one element and the higher numbered node will be the first node of a different element.

K.4.2 Outside Water Domain Substructure

The boundary value problem associated with surrounding water domain is solved using finite elements coupled with boundary integral procedure. The fluid domain between the outside surface of tower and a hypothetical cylindrical surface is discretized by finite elements and the effects of the fluid domain exterior to this surface are treated by boundary integral procedures. The user should follow the instructions listed below:

1. The radius r_c of the hypothetical cylindrical surface should be selected as the smallest value sufficient to contain the tower (Figure 4.5), and the nodes on this surface should numbered last at the end of the sequence.
2. The connectivity of eight-node elements should be provided in the order shown in Figure K.2b.
3. The connectivity of the three-node segments on the interface of the tower and the outside water should be provided in the order shown in Figure K.2a.
4. The connectivity of the three-node segments on the hypothetical cylindrical surface should be provided in the order shown in Figure K.2a.

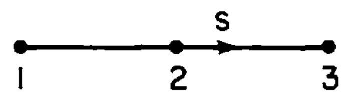

(a) 3-NODE ELEMENT OR SEGMENT

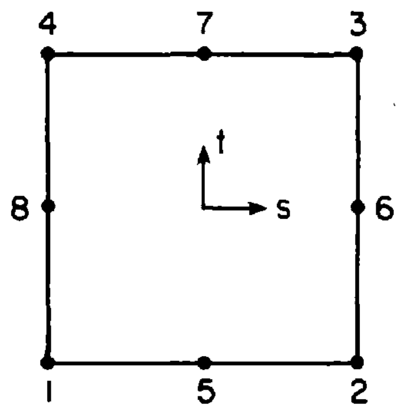

(b) 8-NODE ELEMENT

Figure K.2 Order of Node Numbering for Elements and Segments in the Finite Element Idealization

5. No node should be common to the tower-outside water interface and the hypothetical cylindrical surface.

K.4.3 Inside Water Domain Substructure

1. The connectivity of eight-node elements should be in the same order as shown in Figure K.2b for the elements of surrounding water domain.
2. The connectivity of three-node segments on the interface between the tower and the inside water should be in the same order as shown in Figure K.2a for the segments of the surrounding water domain.

K.4.4 Foundation-Soil Substructure

1. The program uses analytical functions to compute the frequency-dependent foundation impedances for surface-supported circular foundation (Chapter 4). The program selects the necessary constants, already provided in the program, based on the selected Poisson's ratio for foundation rock or soil. These constants are provided only for Poisson's ratio 0.0, 0.33, 0.45 and 0.5. For intermediate values, it interpolates the constants linearly. However, it is recommended to use one of these four values, as the tower response is not sensitive to the Poisson's ratio values within a practical range.
2. **The location of the footing must be at z=0.**
3. The program will use user's defined impedance functions if the radius of the footing is set equal to 0.0. Details are provided in section K.5.17 under FOUNDATION separator.

K.5 Input Data File (TOWERRZ.DAT)

The free-field input data format is similar to that introduced by Wilson, E.L. and Hoit, M. at University of California, Berkeley for SAP-80 series of programs.

In this system, "separator lines" are used to subdivide the data into logical groups. The data group can be in any order with each group being terminated with a line having colon ':' in "column 1". **The name on the separator line must be in CAPITAL LETTERS and must start in "column 1".** The program identifies the separator only by its first four characters. Rest of the characters are optional and used only for user's own understanding.

All lines of numerical data are entered in the following free field form:

N1,N2,N3,--   R=R1,R2,R3,---   Z=Z1,Z2,---

where the input data is designated by Ni, Ri or Zi. Numerical data lists must be separated by a single comma or by one blank. A numerical data list without identification, such as N1,N2,N3,---, must be the first information on the line. A data list of the form

R=R1,R2,R3,--- can be in any order or location on the line. The data list is identified by "R=" only; therefore additional symbolic data must be entered between data lists.

A colon ":", which is optional, indicates the end of information on a line. Information entered to the right of the colon is ignored by the program; therefore, it can be used to provide additional information or comments within the input file.

A "C" in column 1 of any line will cause the line to be ignored by the program. Such lines can be used as comment lines to identify the data.

Simple arithmetic statements are possible when entering floating point real numbers. For example, the following type of data can be entered:

D=200+12/3.5-2,4.5*34

The statement 200+12/3.5-2 is evaluated as (((200+12)/3.5)-2).

In this manual, the values given in [?] are the default values of the parameters, i.e. the values adopted by the program if they are not provided or if the required identifier is missing.

The following sections provide the user with the necessary information to generate the TOWERRZ.DAT input file.

K.5.1 **CONTROL** *Information*

The line of data which follows the **CONTROL** separator is used to supply general data required by the program and contains the following information:

V=? D=? M=? T=?

where

V=	Number of natural vibration modes to be included. In most cases, 5 modes are sufficient.
D=	Hysteretic damping coefficient for tower concrete. A value of 0.10 implies 5% modal damping in all vibration modes of the tower without water on rigid foundation soil.
M=	Number of iterations in computing the natural frequencies and mode shapes. [20]
T=	Tolerance in frequency. [0.001]

This data group must be terminated by a line with colon ':' in the first column.

K.5.2 **TOWER STRUCTURE** *Information*

The line of data which follows the TOWER STRUCTURE separator is used to supply general data about tower substructure and contains the following information:

N=?   E=?   M=?   A=?

where

N= Number of nodes in the idealization of tower. This must be equal to the maximum node number. Extra nodes without any unknown degrees of freedom attached can be used. However, they should be properly identified.

E= The number of elements in the idealization of tower. The program uses three-node quadrilateral Timoshenko-beam element.

M= Number of material types used in tower structure.

A= Number of nodes where extra concentrated or lumped mass is specified. From the mass density of tower materials, program itself computes the mass of tower structure. This option is useful in considering the mass of machinery etc.[0]

This data group must be terminated by a line with colon ':' in the first column.

K.5.3 **TGEOMETRY** *Information*

The sequence of lines which follow the TGEOMETRY separator define the tower geometry, and the location of nodes in the finite element idealization of the tower. These lines contain the following information:

Nid   Z=?   R=Ri,Ro   G=-------

where

Nid= Node identification number to be selected by the user. The node number Nid must be less than or equal to the total number of nodes specified after the TOWER separator.

Z= z-ordinate.

Ri= Inside radius of the tower at node Nid

Ro= Outside radius of the tower at node Nid

The part of the finite element system may be automatically generated using the linear generation option, which can be activated by the addition of the following information on any line which contains the information about tower geometry at a nodal point:

G=Nf,Nl,Inc

where

Nf= The first node number in the sequence

Nl= The last node number in the sequence

Inc= Increment used to define generated node numbers. [1]

The generated nodes will be at equal interval along a straight line between nodes Nf and Nl.

This sequence of lines must be terminated by a line with colon ':' in the first column.

K.5.4 **TRESTRAINT** *Information*

The sequence of lines which follow the TRESTRAINT separator define the unknown displacements which exist at the nodes of the structural system of tower. Unless a restraint is specified at a node, it is assumed that the node has two unknown displacements (one translation and one rotation). These lines contain the following information:

N1,N2,Inc R=Ux,Rx

where

N1= Node number for first node in a series of nodes which have identical displacement specification.

N2= Node number for last node in series. [N1]

Inc= Node number increment which is used to define the nodes in the series. [1]

Ux= Lateral displacement specification = 0 or 1 or -1

Rx= Rotation specification = 0 or 1 or -1

A specification of 0 allows the unknown displacement to exist. If the specification Ux and Rx is set to "1" the displacement and rotation is restrained to zero. The restraint specification "-1" for translation or rotation for any node, say Nth node, will specify the equation number of (N-1)th node to that of node N. This option is used to specify two nodes at the same location of the tower having discontinuity in the geometry at that location.

This data group must be terminated by a line having colon ':' in the first column.

K.5.5 **TMATERIALS** *Information*

The sequence of lines which follow the TMATERIALS separator define the material properties of the tower concrete. For each material type, one data line is required. The number of lines, so specified under this data group must be equal to the number of material types specified earlier under TOWER separator. These lines contain the following information:

Nid E=? G=? W=?

where

Nid= Material identification number. This must be less than or equal to the total number of material types specified earlier under TOWER separator.

E= Elastic modulus of tower concrete.

G= Shear modulus of tower concrete. [E/2.34]

W= Mass density of tower concrete, i.e. unit weight divided by the acceleration due to gravity.

This sequence of data lines must be terminated by a line having colon ':' in the first column.

K.5.6 **TELEMENTS** *Information*

The sequence of lines which follow TELEMENTS separator define the connectivity of three-node, quadrilateral Timoshenko beam elements used to idealize the tower. The material type of the element is also specified under this data group. These lines contain the following information:

Nid,J1,J2,J3 M=? G=-------

where

Nid= Identification (ID) number for the element. Must be less than or equal to the total number of elements specified under TOWER separator.

J1,J2,J3= Node numbers defining the connectivity of the element

M= Material property identification number.

The option to automatically generate element connectivity data is activated by the addition of the following information on any line:

G=Nad,Nidinc,J1inc,J2inc,J3inc,Minc

where

Nad= Number of additional elements to be generated.

Nidinc= Increment of ID number in generated elements.[1]

J1inc= Increment of J1 in generated elements. [2]

J2inc= Increment of J2 in generated elements. [2]

J3inc= Increment of J3 in generated elements. [2]

Minc= Increment of material ID number in generated elements. [0]

This group of data lines must be terminated by a line having colon ':' in the first column.

K.5.7 **TEXTRA MASS** *Information*

For actual towers, it may be necessary to specify concentrated lumped masses at the nodes, or distributed mass along the height of the tower, in addition to the element mass which is automatically calculated by the program. This data is specified after the TEXTRA MASS separator. This group of data is required only if the number of nodes with extra mass specified by identifier "A=" under TOWER separator is non-zero. If for a node, this data is not specified, zero is assumed for both concentrated and distributed mass. Each line of this sequence contains the following information:

N1,N2,Inc   C=?   D=?

where

N1=	Node number for first node in a series of nodes which have identical concentrated and distributed extra mass.
N2=	Node number for last node in series. [N1]
Inc=	Node number increment which is used to define the nodes in the series. [1]
C=	Concentrated (Lumped) mass at that node. [0.0]
D=	Distributed mass at that node. [0.0]

This data group must be terminated by a line having colon ':' in the first column.

K.5.8 **OUTSIDE WATER DOMAIN** *Information*

The line of data which follows the OUTSIDE WATER DOMAIN separator is used to supply general data about surrounding (outside) water domain. **If this separator is missing, the program will not include the intercation effects due to surrounding water. Any information for the surrounding water domain, if provided, will be disregarded in that case.**

This line contains the following information:

N=?   E=?   T=?   H=?   M=?   R=?   W=?

where

N=	Number of nodes required in the idealization of water domain surrounding the tower. **No dummy nodes are allowed.**
E=	Number of elements in the idealization of the fluid domain surrounding the tower. Eight-node isoparametric, axisymmetric elements are used for the finite element idealization of the surrounding water.
T=	Number of three-node segments defining the tower-water interface.
H=	Number of three-node segments defining the hypothetical cylindrical surface for boundary integral procedure.

M= Number of trial functions to be used in the boundary integral procedure. [12]

R= Radius of the hypothetical cylindrical surface. This may be the smallest radius such that the cylindrical surface contains the tower (Figure 4.5).

W= Mass density of water, i.e. unit weight divided by the acceleration due to gravity.

This data group must be terminated by a line with a colon ':' in the first column.

K.5.9 **ONODES** *Information*

The lines which follow the ONODES separator define the location of the nodes of the idealized fluid domain surrounding the tower. These lines contain the following information:

Nid R=? Z=? I=? G=-----

where

Nid= Node identification number to be selected by the user. The node number Nid must be less than or equal to the total number of nodes specified after the OUTSIDE separator.

R= r-ordinate

Z= z-ordinate

I= 1 for node on tower-water interface. Need not be specified for other nodes. [0]

The data may be automatically generated using the linear generation option, which can be activated by the addition of the following information on any line which contains the information about a nodal point:

G=Nf,Nl,Inc

where

Nf= The first node number in the sequence

Nl= The last node number in the sequence

Inc= Increment used to define generated node numbers. [1]

The generated nodes will be at equal interval along a straight line between nodes Nf and Nl.

This sequence of lines must be terminated by a line with colon ':' in the first column.

K.5.10 **OELEMENTS** *Information*

The sequence of lines which follow OELEMENTS separator define the connectivity of eight-node isoparametric elements used to idealize surrounding water domain in r-z plane. These lines contain the following information:

Nid,J1,J2,J3,J4,J5,J6,J7,J8 G=------

where

Nid= Identification (ID) number for the element. Must be less than or equal to the total number of elements specified under OUTSIDE separator.

J1 to J8= Node numbers defining the connectivity of the element

The option to automatically generate element connectivity data is activated by the addition of the following information on any line:

G=Nad,Nidinc,J1inc,J2inc,J3inc,J4inc,J5inc,J6inc,J7inc,J8inc

where

Nad= Number of additional elements to be generated.

Nidinc= Increment of ID number in generated elements.[1]

J1inc= Increment of J1 in generated elements. [2]

J2inc= Increment of J2 in generated elements. [2]

J3inc= Increment of J3 in generated elements. [2]

J4inc= Increment of J4 in generated elements. [2]

J5inc= Increment of J5 in generated elements. [1]

J6inc= Increment of J6 in generated elements. [2]

J7inc= Increment of J7 in generated elements. [1]

J8inc= Increment of J8 in generated elements. [2]

This group of data lines must be terminated by a line having colon ':' in the first column.

K.5.11 **OTOWER-WATER INTERFACE** *Information*

The sequence of lines which follow OTOWER-WATER separator define the connectivity of three-node segments of the fluid elements in the surrounding water domain on the tower-water interface. These lines contain the following information:

Nid,J1,J2,J3 G=------

where

Nid= Identification (ID) number for the segment on the tower-outside water interface. Must be less than or equal to the total number of segments specified under OUTSIDE separator.

J1,J2,J3 = Node numbers defining the connectivity of the segment on the tower-outside water interface.

The option to automatically generate segment connectivity data is activated by the addition of the following information on any line:

G=Nad,Nidinc,J1inc,J2inc,J3inc

where

Nad= Number of additional segments to be generated.

Nidinc= Increment of ID number in generated segments.[1]

J1inc= Increment of J1 in generated segments. [2]

J2inc= Increment of J2 in generated segments. [2]

J3inc= Increment of J3 in generated segments. [2]

This group of data lines must be terminated by a line having colon ':' in the first column.

K.5.12 **OHYPOTHETICAL CYLINDER** *Information*

The sequence of lines which follow OHYPOTHETICAL separator define the connectivity of three-node segments of fluid elements in the outside water domain on the hypothetical cylindrical surface. These lines contain the following information:

Nid,J1,J2,J3 G=------

where

Nid= Identification (ID) number for the segment on the hypothetical cylindrical surface. Must be less than or equal to the total number of segments specified under OUTSIDE separator.

J1,J2,J3= Node numbers defining the connectivity of the segment on hypothetical cylindrical surface

The option to automatically generate segment connectivity data is activated by the addition of the following information on any line:

G=Nad,Nidinc,J1inc,J2inc,J3inc

where

Nad= Number of additional segments to be generated.

Nidinc= Increment of ID number in generated segments.[1]

J1inc= Increment of J1 in generated segments. [2]

J2inc= Increment of J2 in generated segments. [2]

J3inc= Increment of J3 in generated segments. [2]

This group of data lines must be terminated by a line having colon ':' in the first column.

K.5.13 **INSIDE WATER DOMAIN** *Information*

The line of data which follows the INSIDE WATER DOMAIN separator is used to supply general data about inside water domain. **If this separator is missing, the program will not include the intercation effects due to water contained inside the tower. Any information for the inside water domain, if provided, will be disregarded in that case.**

This line contains the following information:

N=? E=? T=? W=?

where

N= Number of nodes required in the finite element idealization of water domain contained inside the hollow tower. **No dummy nodes are allowed.**

E= Number of elements in the idealization of the fluid domain contained inside the tower. Eight-node isoparametric, axisymmetric elements are used for the finite element idealization of the inside water.

T= Number of three-node segments defining the tower-water interface.

W= Mass density of water, i.e. unit weight divided by the acceleration due to gravity.

This data group must be terminated by a line with a colon ':' in the first column.

K.5.14 **INODES** *Information*

The lines which follow the INODES separator define the location of the nodes of the idealized fluid domain contained inside the tower. These lines contain the following information:

Nid R=? Z=? I=? G=-----

where

Nid= Node identification number to be selected by the user. The node number Nid must be less than or equal to the total number of nodes specified after the

INSIDE separator.

R= r-ordinate

Z= z-ordinate

I= 1 for node on tower-water interface. Need not be specified for other nodes. [0]

The data may be automatically generated using the linear generation option, which can be activated by the addition of the following information on any line which contains the information about a nodal point:

G=Nf,Nl,Inc

where

Nf= The first node number in the sequence

Nl= The last node number in the sequence

Inc= Increment used to define generated node numbers. [1]

The generated nodes will be at equal interval along a straight line between nodes Nf and Nl.

This sequence of lines must be terminated by a line with colon ':' in the first column.

K.5.15 **IELEMENTS** *Information*

The sequence of lines which follow IELEMENTS separator define the connectivity of eight-node isoparametric elements used to idealize inside water domain in r-z plane. These lines contain the following information:

Nid,J1,J2,J3,J4,J5,J6,J7,J8 G=------

where

Nid= Identification (ID) number for the element. Must be less than or equal to the total number of elements specified under INSIDE separator.

J1 to J8= Node numbers defining the connectivity of the element

The option to automatically generate element connectivity data is activated by the addition of the following information on any line:

G=Nad,Nidinc,J1inc,J2inc,J3inc,J4inc,J5inc,J6inc,J7inc,J8inc

where

Nad= Number of additional elements to be generated.

Nidinc= Increment of ID number in generated elements.[1]

J1inc=	Increment of J1 in generated elements. [2]
J2inc=	Increment of J2 in generated elements. [2]
J3inc=	Increment of J3 in generated elements. [2]
J4inc=	Increment of J4 in generated elements. [2]
J5inc=	Increment of J5 in generated elements. [1]
J6inc=	Increment of J6 in generated elements. [2]
J7inc=	Increment of J7 in generated elements. [1]
J8inc=	Increment of J8 in generated elements. [2]

This group of data lines must be terminated by a line having colon ':' in the first column.

K.5.16 **ITOWER-WATER INTERFACE** *Information*

The sequence of lines which follow ITOWER-WATER separator define the connectivity of three-node segments of the fluid elements in the inside water domain on the tower-water interface. These lines contain the following information:

Nid,J1,J2,J3 G=------

where

Nid=	Identification (ID) number for the segment on the tower-outside water interface. Must be less than or equal to the total number of segments specified under INSIDE separator.
J1,J2,J3 =	Node numbers defining the connectivity of the segment on the tower-inside water interface.

The option to automatically generate segment connectivity data is activated by the addition of the following information on any line:

G=Nad,Nidinc,J1inc,J2inc,J3inc

where

Nad=	Number of additional segments to be generated.
Nidinc=	Increment of ID number in generated segments.[1]
J1inc=	Increment of J1 in generated segments. [2]
J2inc=	Increment of J2 in generated segments. [2]
J3inc=	Increment of J3 in generated segments. [2]

This group of data lines must be terminated by a line having colon ':' in the first column.

K.5.17 **FOUNDATION-SOIL SYSTEM** *Information*

The line of data which follows the FOUNDATION-SOIL SYSTEM separator is used to supply the information about the foundation soil system. **If this separator is missing, foundation-soil interaction effects will not be considered in the analysis. This line contains the following information:**

M=? I=? R=? C=? P=? W=? D=?

where

M= Mass of the foundation footing below the ground level. [0.0]

I= Mass moment of inertia of the foundation footing below ground level. [0.0]

R= Radius of the footing.

If the radius of the footing is set to 0.0, user must provide the impedance functions for the foundation-soil system. The program reads the foundation impedance functions from the file FOUNDIMP.DAT. If 'N' points are used to define the acceleration time history, including the "quiet zone", then the impedance functions should be available at the interval of $\Delta\omega=2\pi/N\Delta t$, in which Δt is the time interval between consecutive data points in acceleration time history. A total (N/2+1) lines of data, corresponding to 0, $\Delta\omega$, $2\Delta\omega$, ..., frequencies are required in the file FOUNDIMP.DAT. Each line of data contains the following four values separated by a ',' (comma) or a blank space:

KVVR,KVVI,KMMR,KMMI

where

KVVR= Real part of impedance function K_{VV}.

KVVI Imaginary part of impedance function K_{VV}.

KMMR Real part of impedance function K_{MM}.

KMMI Imaginary part of impedance function K_{MM}.

C= Shear wave velocity of foundation-soil.

P= Poisson's ratio of foundation soil. [0.33]

W= Mass density of foundation soil, i.e. unit weight divided by the acceleration due to gravity.

D= Hysteretic damping factor for foundation soil. [0.10]

This data group must be terminated by a line with colon ':' in the first column.

K.5.18 GROUND MOTION *Information*

The sequence of lines which follow the GROUND MOTION separator provide information about the earthquake acceleration data. The first line contains the following information:

N=Nx,Ny   T=?   S=?   M=?

where

Nx= The number of data points in the ground motion along x-axis. This number must be a multiple of 8.

Ny= The number of data points in the ground motion along y-axis. This number must be a multiple of 8. If only one component of ground motion is used, Ny should be set to zero.

T= The uniform time interval between consecutive data points in the ground motion records. Both the ground motion components must be digitized at the same time interval.

S= Scale factor for the ground motion. acceleration units.

M= The control parameter to select the number of points ($=2^M$) to be used in the discrete Fast Fourier Transform (DFFT) computations. The selected value of M should be large enough to provide sufficient 'quiet zone' to ensure accurate DFFT computations.*

After this line, the ground motion data is provided. EIGHT data points are provided in each line in FORMAT 8F9.5, standard FORTRAN formats. First Nx/8 lines are for the ground motion along x-axis. Next Ny/8 lines are for the ground motion along y-axis. Comment lines however can be provided between the two sets of data to distinguish them from each other.

This data group must be terminated by a line with colon ':' in the first column.

K.5.19 OUTPUT CONTROL *Information*

The FOUR lines which follow the OUTPUT CONTROL separator identify the nodes where displacement, shear force and bending moment response is required. The FIRST line of this data group contains the information about the nodes where the **maximum displacement** over the duration of the earthquake is to be determined. This data is presented in the following form:

*G. Fenves and A. K. Chopra, EAGD-84, "A Computer Program for Earthquake Analysis of Concrete Gravity Dams", Report No. UCB/EERC-84/11, University of California, Berkeley, Calif., August 1984, 92pp.

D=Nt   L=L1,L2,.......,LNt   N=Nf,Ninc

where

Nt= Total number of nodes where maximum lateral displacement should be computed.

The list of nodes can be specified either by N= or by L=. If the response is required at less than twenty nodes, and they are not regularly distributed in numbers, option L= can be used to just list those nodes. The option N= should be used if the nodes are regularly distributed, or the response at all the nodes is required. The program looks for the L= option only if it does not find the N= option. So, both the options can not be used simultaneously. In option N=, the terms have the following meaning:

Nf= The first node number where information is requested.

Ninc= The increment in the sequence of nodes. The last node number is automatically determined by the program using Nt, the total number of nodes where information is requested.

The SECOND line of this data group contains the information about the nodes where the **maximum shear force** is to be determined. This data is presented in the following form:

S=Nt   L=L1,L2,.......,LNt   N=Nf,Ninc

where

Nt= Total number of nodes where maximum shear force should be computed.

All other parameters carry the same meaning as in the FIRST line.

The THIRD line of this data group contains the information about the nodes where the **maximum bending moment** is to be determined. This data is presented in the following form:

M=Nt   L=L1,L2,.......,LNt   N=Nf,Ninc

where

Nt= Total number of nodes where maximum bending moment should be computed.

All other parameters carry the same meaning as in the FIRST line.

The FOURTH line of this data group contains the information about the nodes where the **lateral displacement history** is to be included in the output. This data is presented in the following form:

H=Nt   L=L1,L2,.......,LNt   N=Nf,Ninc

where

Nt= Total number of nodes where displacement history need be computed.

All other parameters carry the same meaning as in the FIRST line.

This data group must be terminated by a line with colon ':' in the first column.

K.6 Numerical Example

For the convenience of the user, the input data file **TOWERRZ.DAT** used for analysis of the SANBERNADINO TOWER is presented. Figures K.3 to K.5 provide the information about the mathematical model and the numbering schemes used in the earthquake response analysis of this tower. The output files, mentioned in Figure K.1, for thsi numerical example are also provided on the diskette with the source codes.

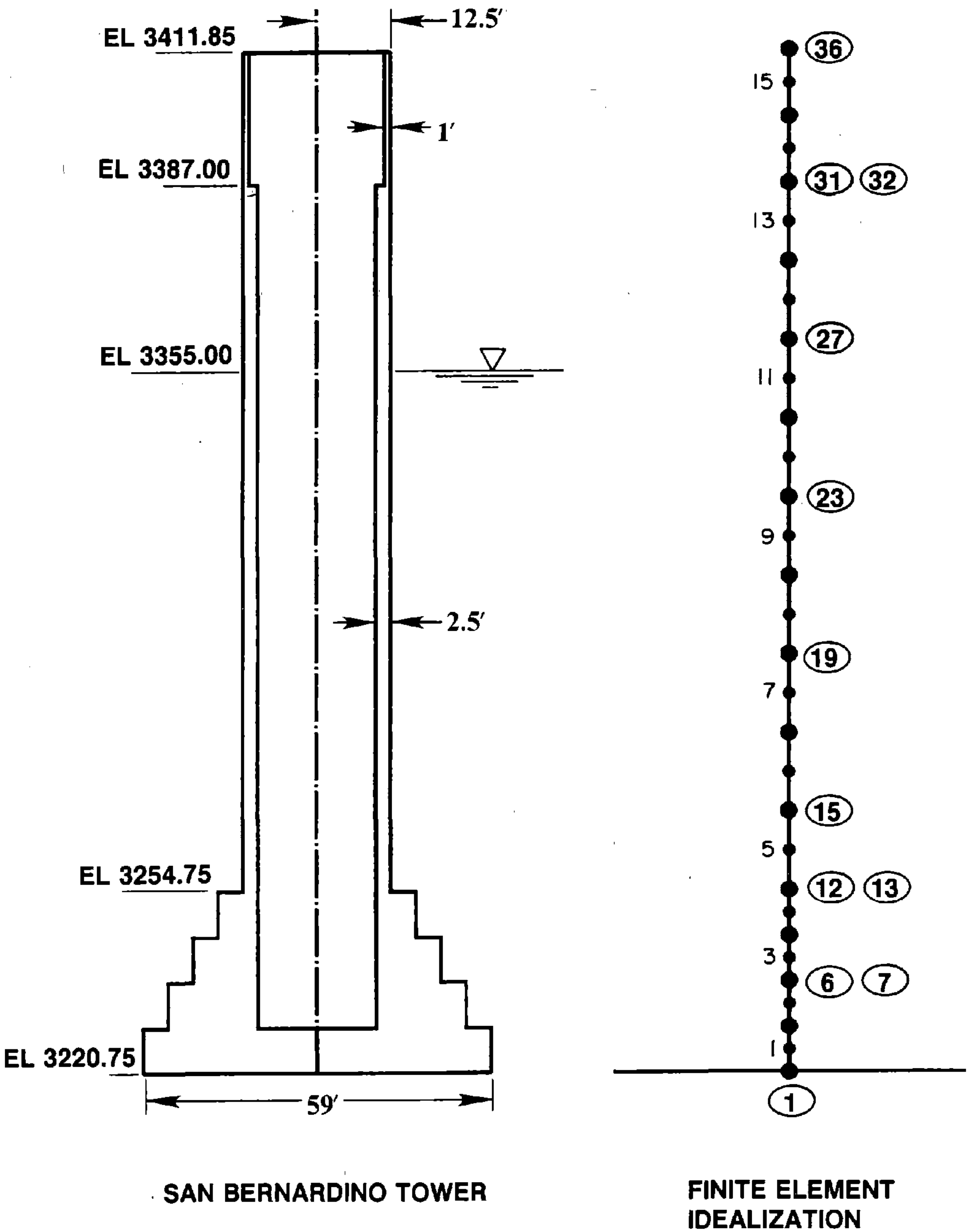

Figure K.3 Finite Element Idealization of San Bernardino Intake Tower

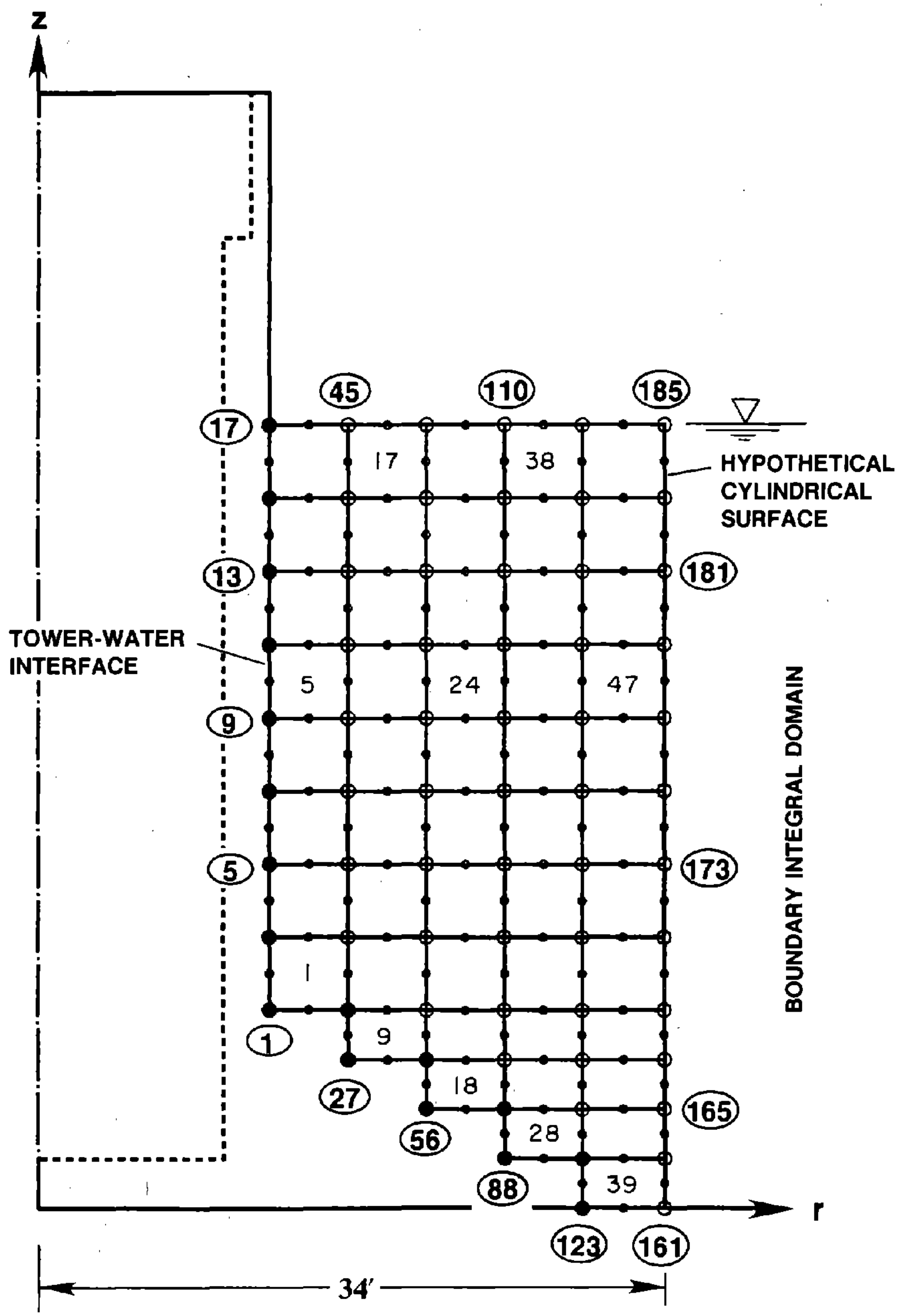

Figure K.4 Finite Element Idealization of Surrounding Water Domain

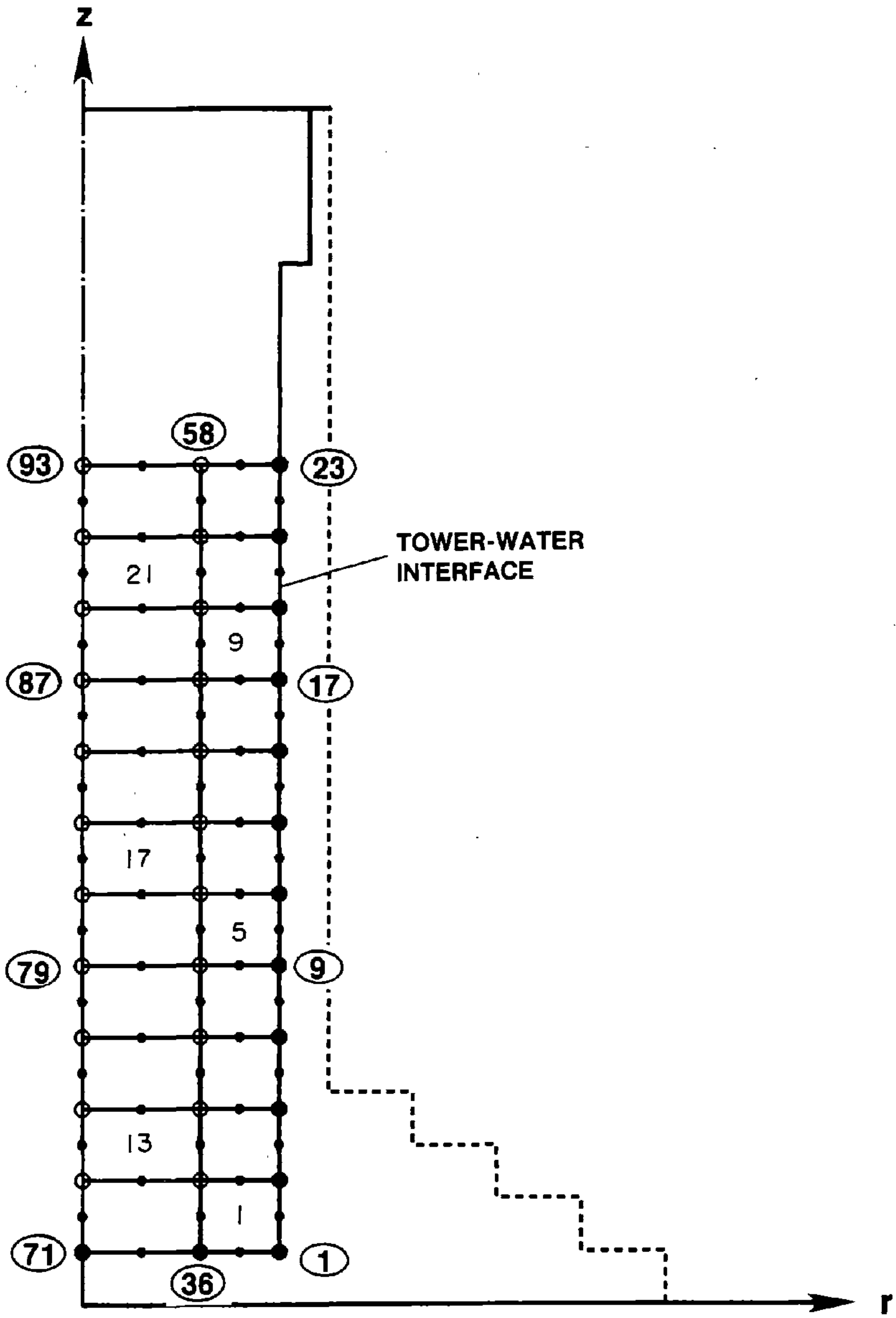

Figure K.5 Finite Element Idealization of Inside Water Domain

```
C......EXAMPLE DATA FOR TOWERRZ SERIES, SAN BERNARDINO TOWER
CONTROL
 V=2  D=0.10   M=20  T=0.01  :
:
TOWER STRUCTURE
 N=36   E=15   M=1   A=0  :
:
TGEOMETRY
1    R=0.,29.5   Z=0.
3    R=0.,29.5   Z=8.5   G=1,3,1
4    R=10.,25.25   Z=8.5
6    R=10.,25.25   Z=17.  G=4,6,1
7    R=10.,21.0    Z=17.
9    R=10.,21.0    Z=25.5   G=7,9,1
10   R=10.,16.75   Z=25.5
12   R=10.,16.75   Z=34.    G=10,12,1
13   R=10.,12.5    Z=34.
31   R=10.,12.5    Z=166.25   G=13,31,1
32   R=11.5,12.5   Z=166.25
36   R=11.5,12.5   Z=191.10   G=32,36,1
:
TRESTRAINTS
1    R=1,1
4,13,3  R=-1,-1
32       R=-1,-1
:
TELEMENTS
1,1,2,3  M=1    G=3,1,3,3,3,0
5,13,14,15  M=1   G=8,1,2,2,2,0
14,32,33,34  M=1   G=1,1,2,2,2,0
:
TMATERIALS
1  E=648000.   G=276923.   W=.004817
:
OUTSIDE WATER DOMAIN
 N=185  E=50  T=16  H=12  M=12  R=34.0  W=0.001939
:
ONODES
1    R=12.5     Z=34.0       I=1
17   R=12.5     Z=134.25     I=1       G=1,17,1
18   R=14.625   Z=34.0       I=1
26   R=14.625   Z=134.25               G=18,26,1
27   R=16.75    Z=25.5       I=1
29   R=16.75    Z=34.0                 G=27,29,1
45   R=16.75    Z=134.25               G=29,45,1
46   R=18.875   Z=25.5       I=1
47   R=18.875   Z=34.0
55   R=18.875   Z=134.25               G=47,55,1
56   R=21.0     Z=17.0       I=1
58   R=21.0     Z=25.5       I=1       G=56,58,1
60   R=21.0     Z=34.0                 G=58,60,1
76   R=21.0     Z=134.25               G=60,76,1
77   R=23.125   Z=17.0       I=1
79   R=23.125   Z=34.0                 G=77,79,1
87   R=23.125   Z=134.25               G=79,87,1
88   R=25.25    Z=8.5        I=1
90   R=25.25    Z=17.0       I=1       G=88,90,1
94   R=25.25    Z=34.0                 G=90,94,1
110   R=25.25   Z=134.25               G=94,110,1
111   R=27.375  Z=8.5        I=1
114   R=27.375  Z=34.0                 G=111,114,1
122   R=27.375  Z=134.25               G=114,122,1
123   R=29.5    Z=0.0        I=1
125   R=29.5    Z=8.5        I=1       G=123,125,1
131   R=29.5    Z=34.0                 G=125,131,1
147   R=29.5    Z=134.25               G=131,147,1
148   R=31.75   Z=0.0        I=1
152   R=31.75   Z=34.0                 G=148,152,1
160   R=31.75   Z=134.25               G=152,160,1
161   R=34.0    Z=0.         I=1
169   R=34.0    Z=34.0                 G=161,169,1
185   R=34.0    Z=134.25               G=169,185,1
:
OELEMENTS
1,1,29,31,3,18,30,19,2                 G=7,1,2,2,2,2,1,2,1,2
9,27,58,60,29,46,59,47,28              G=8,1,2,2,2,2,1,2,1,2
18,56,90,92,58,77,91,78,57             G=9,1,2,2,2,2,1,2,1,2
28,88,125,127,90,111,126,112,89        G=10,1,2,2,2,2,1,2,1,2
39,123,161,163,125,148,162,149,124     G=11,1,2,2,2,2,1,2,1,2
:
OTOWER-WATER INTERFACE
1,17,16,15       G=7,1,-2,-2,-2
9,1,18,29
10,29,28,27
11,27,46,58
12,58,57,56
13,56,77,90
14,90,89,88
15,88,111,125
16,125,124,123
:
OHYPOTHETICAL CYLINDRICAL SURFACE
1,161,162,163    G=11,1,2,2,2
:
INSIDE WATER DOMAIN
 N=93  E=22  T=13  W=0.001939
:
INODES
1    R=10.      Z=8.5      I=1
23   R=10.      Z=134.25   I=1      G=1,23,1
24   R=8.       Z=8.5      I=1
35   R=8.       Z=134.25            G=24,35,1
36   R=6.       Z=8.5      I=1
58   R=6.       Z=134.25            G=36,58,1
59   R=3.       Z=8.5      I=1
70   R=3.       Z=134.25            G=59,70,1
71   R=0.       Z=8.5      I=1
93   R=0.       Z=134.25            G=71,93,1
:
IELEMENTS
1,36,1,3,38,24,2,25,37       G=10,1,2,2,2,2,1,2,1,2
12,71,36,38,73,59,37,60,72   G=10,1,2,2,2,2,1,2,1,2
:
ITOWER-WATER INTERFACE
1,71,59,36
2,36,24,1
3,1,2,3  G=10,1,2,2,2
:
FOUNDATION-SOIL SYSTEM
 M=0.  I=0.  R=29.5  C=1000.  P=1./3.  W=0.005127  D=0.10
:
GROUND MOTION
 N=1000,0   M=11  T=0.02   S=32.18
C.........GROUND MOTION COMPONENET ALONG X-AXIS; TAFT S69E
  -.00632  -.00194   .00408   .01010   .00530  -.00031  -.00428  -.00286
   .00122   .00541   .00398  -.00306  -.00867  -.00867  -.00612  -.00082
  -.00031  -.00020   .00408   .01071   .01163   .00663   .00449   .00235
   .00214   .00194  -.00398  -.00755  -.00112   .00592   .00286  -.01040
```

```
-.01153  -.00479   .00500   .00102  -.00408  -.00255   .00592   .00734
-.00663  -.01091   .00326   .01724   .01010  -.00490  -.00663   .00367
 .00459  -.00286   .00357   .01459   .02325   .01816   .01867   .01255
-.00133  -.00867  -.00683  -.00479   .00408   .00561  -.00143  -.00408
-.00010  -.00224  -.00867  -.01132  -.01530  -.01877  -.01601  -.00806
-.00031   .00826   .00428  -.00785  -.01836  -.01163   .00092   .01071
 .00867   .00755   .00898   .00979   .00163  -.00530  -.00082   .00683
 .01714   .01989   .01377   .00510   .00316   .01193   .02387   .02417
 .00632  -.00694  -.01142  -.00867  -.00388   .00224   .00235  -.01612
-.02652  -.00918   .01632   .02234   .01703   .02142   .02478   .01877
 .00428  -.01061  -.02387  -.00898   .01418   .03692   .03090   .01601
 .01153   .00734  -.00806  -.01346  -.01275  -.00775   .00683   .02264
 .02295   .01989   .02591   .02366   .01204  -.00102  -.00867  -.01142
-.01459  -.02081  -.01999  -.01693  -.01856  -.01785  -.00898  -.00153
-.00500  -.00530  -.00408  -.00928  -.00796  -.00214   .00347  -.00510
-.02223  -.03631  -.03264  -.02448  -.03284  -.04926  -.05783  -.06211
-.07221  -.06640  -.05457  -.05263  -.04977  -.05079  -.05283  -.05722
-.04906  -.03539  -.02601  -.01724  -.01479  -.02611  -.04029  -.04590
-.04406  -.02407   .00337   .03274   .05569   .07588   .09424   .12056
 .14932   .17941   .16391   .11954   .06946   .01877  -.03509  -.06528
-.06232  -.05640  -.04600  -.04773  -.05640  -.06599  -.05742  -.03774
-.01652   .00469   .00469  -.00877  -.02274  -.04029  -.04671  -.02142
 .01367   .05079   .08506   .06885   .03733  -.00153  -.00153   .03060
 .06650   .07639   .07068   .06303   .03417   .00326  -.03233  -.04569
-.04498  -.01663   .03570   .09394   .12352   .08384   .03417  -.02203
-.03774  -.05406  -.05651  -.03733  -.01459   .01112   .03488   .06211
 .06956   .04651   .02142   .00051  -.03182  -.08639  -.11342  -.08853
-.05100  -.00979   .03141   .03998   .02815   .01122   .00510   .00061
-.01877  -.04049  -.05263  -.04263  -.02907  -.01826  -.02764  -.04110
-.05753  -.06823  -.04641  -.01530   .01928   .05314   .08843   .11097
 .11423   .10475   .08965   .06324   .02774  -.00847  -.04396  -.05069
-.04192  -.03743  -.04814  -.06273  -.07854  -.09302  -.07405  -.03560
 .00714   .04314   .03050   .00194  -.01520   .00755   .03682   .07313
 .09057   .06405   .02988  -.01193  -.02172   .00459   .02438   .03284
 .04192   .03682   .02336   .00806  -.00673  -.01540  -.01499   .00092
 .02937   .03294   .01652  -.00694  -.00214   .03427   .07619   .09577
 .07323   .06324   .03243  -.00796  -.05253  -.09669  -.13963  -.14932
-.14616  -.14116  -.13657  -.13678  -.13698  -.11117  -.07762  -.04172
-.00530   .03029   .06823   .08476   .05875   .02937  -.00949  -.02254
-.00877   .00887   .02846   .04916   .05620   .03692   .01438  -.01173
-.03672  -.05997  -.05202  -.03325  -.01163   .01071   .03243   .05508
 .07619   .10057   .10301   .07078   .03509  -.00683  -.03264  -.01285
 .00092  -.01581  -.03957  -.05926  -.03866  -.01683  -.02254  -.03988
-.03886  -.01387   .01193   .04223   .06915   .10006   .11250   .10873
 .10138   .09853   .10342   .10414   .07425   .03641  -.00581  -.04559
-.09067  -.09700  -.04172  -.01581  -.03692  -.06946  -.08353  -.04549
-.03713  -.02060   .02234   .06783   .08496   .05671   .01377  -.03060
-.07782  -.08027  -.04386  -.00745  -.00357  -.01499  -.01397  -.01010
-.01397  -.02234  -.00755   .01734   .04437   .03866   .00938  -.01846
-.03723  -.05345  -.07313  -.08945  -.08976  -.06028  -.01469   .03784
 .06364   .05436   .04223   .03060   .03019   .02376   .01387   .01408
 .03182   .05508   .06324   .04396   .02152  -.00418  -.02886  -.03274
-.01459   .00265   .02927   .06354   .10658   .11423   .08496   .05008
 .00928  -.03131  -.07191  -.11148  -.10495  -.06568  -.03396  -.01795
 .01275   .04926   .09241   .10301   .07956   .05161   .02570   .01469
 .00571  -.00204  -.01550  -.02988  -.04559  -.05742  -.04835  -.03254
-.02162  -.02733  -.01561   .01499   .04906   .07721   .06762   .05253
 .04243   .03182   .00265  -.02958  -.04896  -.06609  -.07160  -.05936
-.04631  -.02876  -.02529  -.04029  -.06028  -.06772  -.04784  -.02438
 .00000  -.01000  -.03519  -.05120  -.02703   .00377   .04284   .05691
 .03488   .00683  -.02172  -.01693  -.00479  -.01163  -.02958  -.02295
-.00122   .01489   .01000   .00082  -.00938  -.00347   .00653   .01540
 .01622   .02458   .03519   .04875   .05406   .04192   .02693   .02744
 .03131   .02458   .00836   .00663   .02580   .04518   .04110   .02489
 .02264   .03060   .03447   .02060   .00337  -.01693  -.03376  -.04926
-.06364  -.08598  -.08302  -.05151  -.01601   .02101   .06099   .07099
 .03458  -.00337  -.05120  -.06987  -.06650  -.05875  -.03396  -.00734
 .02285   .04335   .05375   .05987   .04019   .01244  -.01428  -.02478
-.02132  -.00979   .00153  -.00082   .00000   .01285   .02540   .04049
 .03478   .01510  -.00714  -.03029  -.05273  -.05661  -.05059  -.05100
-.05528  -.04845  -.02693  -.00510   .02050   .03315   .03580   .03243
 .02682   .02091   .01408   .01081   .02376   .04223   .05314   .03570
 .01295  -.01306  -.02846  -.03876  -.04835  -.05151  -.03866  -.02264
-.00826  -.01112  -.01765  -.02591  -.01673   .00694   .03111   .05651
 .04284   .00938  -.03009  -.04590  -.03651  -.02682  -.01581  -.00133
 .01642   .02336   .01897   .02580   .03641   .04549   .04518   .04202
 .02652   .00714  -.01520  -.02774  -.02672  -.02591  -.03274  -.04161
-.03417  -.01979  -.00357   .01285   .02917   .03886   .04080   .03651
 .03009   .02438   .03478   .04835   .02784  -.00245  -.03713  -.06701
-.08292  -.09333  -.10546  -.09955  -.06966  -.03662  -.00163   .03458
 .05477   .04345   .02856   .00908  -.00867  -.02540  -.01499   .00153
 .02203   .02621   .01714   .00643  -.00571  -.00745  -.00245   .00061
 .00520   .00949   .01357   .01224   .01581   .03264   .04243   .02856
 .01091  -.01112  -.01948  -.01408  -.00826  -.00571   .00031   .01295
 .02835   .03090   .00275  -.02886  -.06640  -.07762  -.06589  -.05090
-.04141  -.03600  -.01499   .00439   .01632   .01030  -.00602  -.00979
-.00306   .00745   .00357  -.01214  -.01805  -.02529  -.03345  -.03631
-.03386  -.03213  -.02754  -.01040   .00979   .03162   .04314   .04559
 .04631   .03998   .03539   .04223   .05447   .05559   .04641   .03009
 .00357  -.02274  -.05171  -.07374  -.07109  -.06069  -.04896  -.03284
-.01071   .01234   .03611   .05814   .05916   .05090   .04070   .02999
 .01938   .00877   .00275   .00122  -.00867  -.01734  -.02489  -.02733
-.02050  -.01336  -.02030  -.03366  -.05090  -.04121  -.01540   .01295
 .04100   .03998   .02387   .00775  -.00367  -.01234  -.02183  -.01642
 .00418   .02550   .04957   .06477   .07109   .07721   .07476   .05793
 .03917   .01856  -.00163  -.02009  -.01448  -.00265   .01265   .02305
 .01938   .01153   .00785   .00082  -.01561  -.03284  -.05273  -.06242
-.04896  -.03029  -.01244  -.00694  -.00061   .00418   .00612   .00826
 .01193   .01550   .02172   .02591   .02815   .02693   .01989   .01326
 .00949   .00133  -.00938  -.02009  -.02948  -.03315  -.02642  -.01795
-.01071  -.00643   .00255   .01377   .02132   .01275   .00020  -.01071
-.01397  -.01724  -.02223  -.03182  -.02937  -.01795  -.00632  -.00877
-.01581  -.02285  -.02009  -.01510  -.00867  -.00275   .00388   .00918
 .00959   .00714   .01000   .01469   .02070   .01765   .00683  -.00347
 .00428   .02285   .04223   .06222   .05895   .04314   .02468   .00561
-.01316  -.01968  -.01775  -.01805  -.02213  -.02366  -.02081  -.02019
-.02560  -.02805  -.02733  -.02744  -.03162  -.01724   .00204   .02540
 .03927   .04212   .03488   .01958   .00357  -.00306  -.00082   .00092
-.00418  -.01204  -.00796   .00173   .01244   .01244   .00755   .01102
 .01652   .02193   .02682   .03203   .03437   .02356   .00918  -.00571
-.01234  -.01703  -.01877  -.01642  -.01387  -.01010  -.01102  -.01591
-.02223  -.02254  -.01469  -.00643   .00224   .00031  -.00581  -.01316
-.01928  -.01142   .00173   .01091   .01958   .03192   .04580   .05528
 .05202   .04294   .02438   .00418  -.01703  -.03662  -.03274  -.01663
 .00173   .01795   .01295   .00265  -.01030  -.01754  -.01989  -.02417
-.03315  -.03651  -.02234  -.00235   .01805   .03957   .03682   .01693
-.00653  -.02295  -.02693  -.02764  -.02295  -.01459   .00051   .01632
 .03427   .03988   .03172   .02570   .02244   .01836   .01193   .00581
 .00479   .00796   .00806   .00510   .00255  -.00041  -.00500  -.01153
-.01336  -.00826  -.00500  -.00296   .00224   .01122   .01061   .00449
-.00296  -.01091  -.01724  -.01418  -.00765  -.00643  -.01754  -.02642
:
OUTPUT
 D=3   N=26,5    :
 S=3   N=1,6      :
 M=3   L=1,7,13    :
 H=1    L=36
:
```

APPENDIX L
TOWER3D SERIES OF PROGRAMS : USERS MANUAL

L.1 Introduction

The TOWER3D series of programs were specifically developed for the earthquake response analysis of intake-outlet towers, with arbitrary cross-section but having two axes of symmetry, subjected to one component of ground motion. The effects of tower-water interaction, due to water surrounding the tower and contained inside the tower, and tower-foundation-soil interaction can be included independently or simultaneously.

The output of the computer program consists of the maximum responses -- lateral displacement, shear force, and bending moment -- at selected locations along the height of the tower. The time variation of each response quantity due to one ground motion component is computed from which the maximum value is determined. These response quantities are computed by the computer program using the analytical procedure developed in Chapters 3 and 4.

L.2 Organization of TOWER3D Series of Programs

The TOWER3D series of programs are divided into six modules. The major advantage of the modular organization is that the modules can be restarted at certain points after data changes without starting other modules. The separate program segments interact by communication with a common file data base. So, the user has to prepare only one input data file **TOWER3D.DAT**. The TOWER3D series of programs contain the following six modules:

1. TOWER3D — This program reads the information about the mathematical model from the input file **TOWER3D.DAT** in free-field type of input and create a data base for various modules.

2. OUTPUT3D — This program writes the information about the mathematical model in a file **TOWER3D.OUT** and is used to check the correctness of the input data.

3. EIGEN3D — This program computes the frequencies and mode shapes of the tower without water, generates generalized mass and excitation matrices and computes modal shear and moment transformation vectors. The generated section properties of the tower, its natural frequencies and mode shapes are written on a file **TOWER3D.VEC** .

4. OUTW3D — This module computes the generalized added mass matrix and excitation vector due to water surrounding the tower. This module consists

of three programs, OUTW3D, OMAT3D and OMASS3D which must be executed in order.

5. INW3D — This program computes the generalized added mass matrix and excitation vector due to water inside the tower. This module consists of three programs, INW3D, IMAT3D and IMASS3D which must be executed in order.

6. RESP3D — This program evaluates the impedance functions of the foundation footing, computes the frequency response functions of modal coordinates; the maximum displacement, shear force and bending moment at specified locations, and displacement time history at specified locations. The amplitudes of the frequency response functions for the first two modal coordinates only are written on a file **TOWER3D.FRF**, the maximum responses are written on a file **TOWER3D.MAX**, and response history on a file named **TOWER3D.HIS**.

The source listings of all these modules are available in FORTRAN-77 programming language.

L.3 Execution of Programs

All the program segments can be compiled and linked independently using commonly available FORTRAN compilers. The sequence in which the programs should be executed is summarized in Figure L.1. TOWER3D should be executed first. EIGEN3D comes next. RESP3D should be executed in the end. Programs OUTW3D, OMAT3D, and OMASS3D should be executed after EIGEN3D only when interaction effects due to surrounding water need be included. Similarly, programs INW3D, IMAT3D, and IMASS3D should be executed after EIGEN3D but before RESP3D if the effects of inside water need be included. The modules (set of three programs) OUTW3D and INW3D can be executed in any order. The program OUTPUT3D can be executed any time after TOWER3D has been executed. It is recommended that the user should check the file TOWER3D.OUT for possible errors in input data file before executing the subsequent program segments.

Whenever the data file TOWER3D.DAT is modified, it is necessary to execute TOWER3D and then run the module for which data has been changed. The other modules need not be executed if input data for them is not changed.

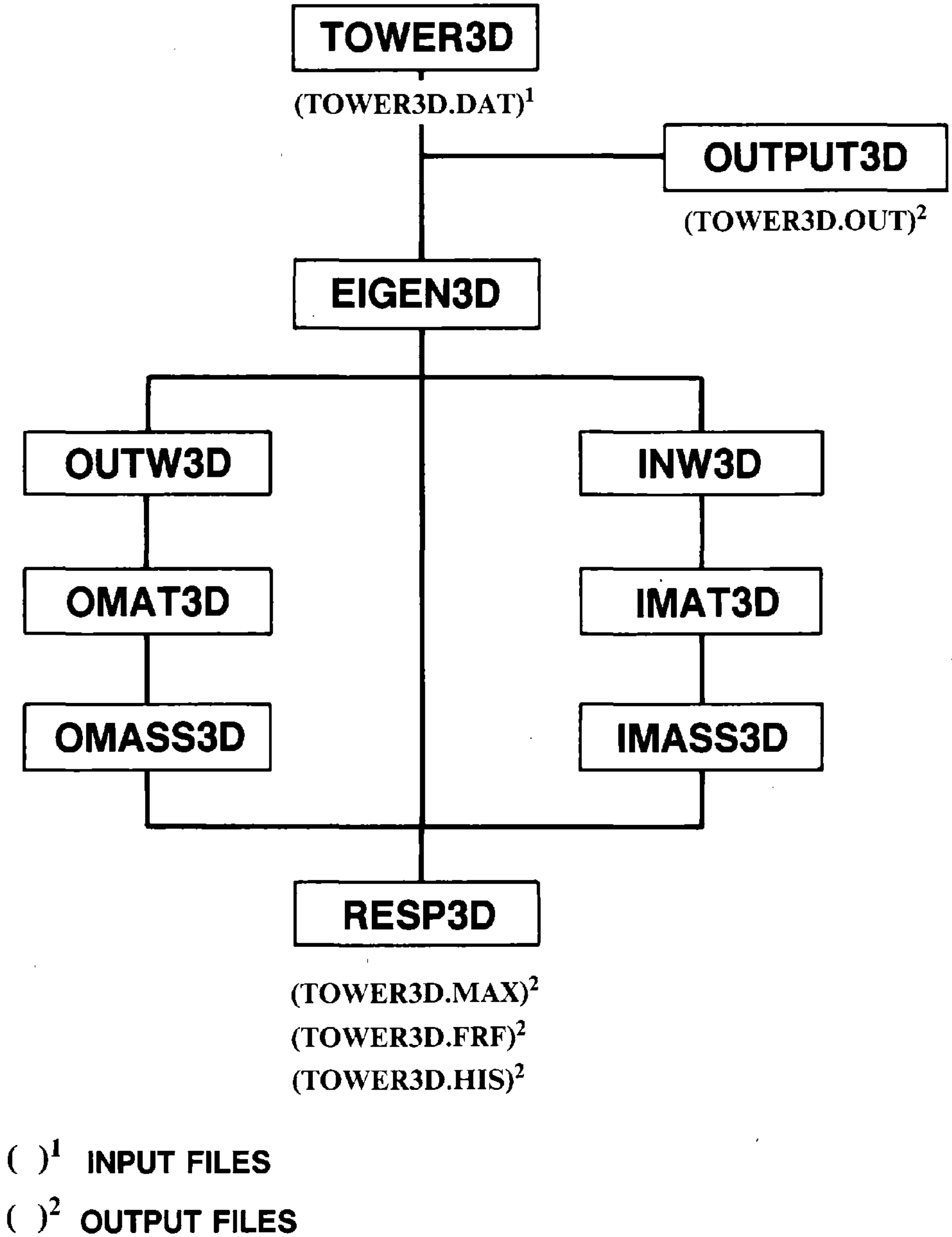

Figure L.1 Order of Execution for TOWER3D Series of Programs

L.4 Idealization of Tower-Water-Foundation Soil System

The tower, the surrounding water domain, the inside water domain, and the foundation-soil system are idealized independently as substructures. Only one quarter of the system with two axes of plan symmetry is analyzed. The user should follow these instructions carefully in idealizing each substructure:

L.4.1 Tower Substructure

1. The numbering of the nodes should always start from the base to the top. Each node has two degrees of freedom, translational and rotational displacements.
2. The program uses a three-node Timoshenko beam element for which the connectivity should be provided from bottom to top in the order shown in Figure L.2a.
3. At any location above the base where the cross-section is discontinuous, two nodes need be specified with consecutive numbers and different section properties. The lower numbered node should define the section just below the node and the higher numbered node should define the section just above the node. The equation numbers for the degrees of freedom of the higher numbered node should be equal to that of lower numbered node. This is obtained by setting restraint code for higher numbered node to '-1' (see under TRESTRAINT separator). **The two nodes defining a discontinuous sections must belong to different elements,** i.e. the lower numbered node will be the third node of one element and the higher numbered node will be the first node of a different element.

L.4.2 Outside Water Domain Substructure

The boundary value problem associated with surrounding water domain is solved using finite elements coupled with boundary integral procedure. The fluid domain between the outside surface of tower and a hypothetical cylindrical surface is discretized by finite elements and the effects of the fluid domain exterior to this surface are treated by boundary integral procedures. The user should follow the instructions listed below:

1. The radius r_c of the hypothetical cylindrical surface should be selected as the smallest value sufficient to contain the tower (Figure 4.5), and the nodes and the elements on this surface should be numbered in the sequence as shown in Figure L.7.
2. The connectivity of twenty-node elements should be provided in the order shown in Figure L.2c.
3. The connectivity of the eight-node segments on the interface of the tower and the outside water should be provided in the order shown in Figure L.2b.

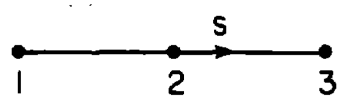

(a) 3-NODE ELEMENT

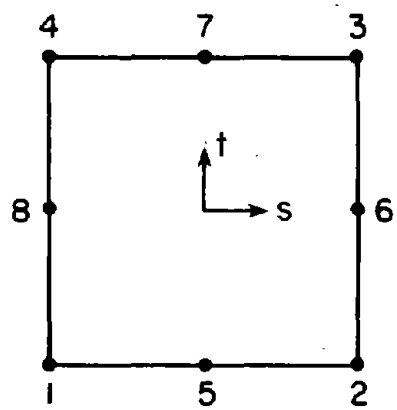

(b) 8-NODE SEGMENT

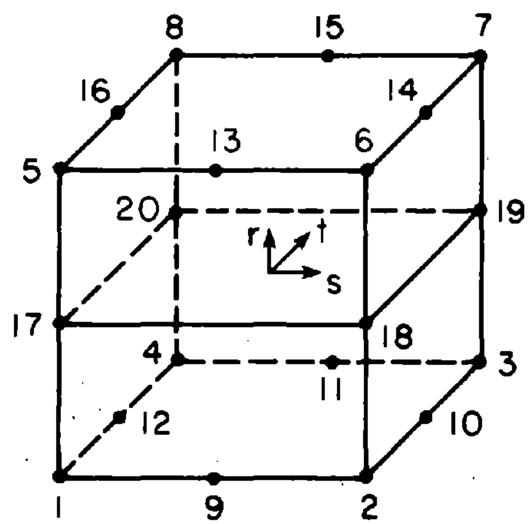

(C) 20-NODE ELEMENT

Figure L.2 Order of Node Numbering for Elements and Segments in the Finite Element Idealization

4. The connectivity of the eight-node segments on the hypothetical cylindrical surface should be provided in the order shown in Figure L.2b.

5. No node should be common to the tower-outside water interface and the hypothetical cylindrical surface.

L.4.3 Inside Water Domain Substructure

1. The connectivity of twenty-node elements should be in the same order as shown in Figure L.2c for the elements of surrounding water domain.

2. The connectivity of eight-node segments on the interface between the tower and the inside water should be in the same order as shown in Figure L.2b for the segments of the surrounding water domain.

L.4.4 Foundation-Soil Substructure

1. The program uses analytical functions to compute the frequency-dependent foundation impedances for surface-supported circular foundation (Chapter 4). The program selects the necessary constants, already provided in the program, based on the selected Poisson's ratio for foundation rock or soil. These constants are provided only for Poisson's ratio 0.0, 0.33, 0.45 and 0.5. For intermediate values, it interpolates the constants linearly. However, it is recommended to use one of these four values, as the tower response is not sensitive to the Poisson's ratio values within a practical range.

2. **The location of the footing must be at z=0.**

3. The program will use user's defined impedance functions if the radius of the footing is set equal to 0.0. The details are given in Section L.5.17 under FOUNDATION separator.

L.5 Input Data File (TOWER3D.DAT)

The free-field input data format is similar to that introduced by Wilson, E.L. and Hoit, M. at University of California, Berkeley for SAP-80 series of programs.

In this system, "separator lines" are used to subdivide the data into logical groups. The data group can be in any order with each group being terminated with a line having colon ':' in "column 1". **The name on the separator line must be in CAPITAL LETTERS and must start in "column 1".** The program identifies the separator only by its first four characters. Rest of the characters are optional and used only for user's own understanding.

All lines of numerical data are entered in the following free field form:

N1,N2,N3,--   R=R1,R2,R3,---   Z=Z1,Z2,---

where the input data is designated by Ni, Ri or Zi. Numerical data lists must be separated by a single comma or by one blank. A numerical data list without identification, such as N1,N2,N3,---, must be the first information on the line. A data list of the form R=R1,R2,R3,--- can be in any order or location on the line. The data list is identified by "R=" only; therefore additional symbolic data must be entered between data lists.

A colon ":", which is optional, indicates the end of information on a line. Information entered to the right of the colon is ignored by the program; therefore, it can be used to provide additional information or comments within the input file.

A "C" in column 1 of any line will cause the line to be ignored by the program. Such lines can be used as comment lines to identify the data.

Simple arithmetic statements are possible when entering floating point real numbers. For example, the following type of data can be entered:

D=200+12/3.5-2,4.5*34

The statement 200+12/3.5-2 is evaluated as (((200+12)/3.5)-2).

In this manual, the values given in [?] are the default values of the parameters, i.e. the values adopted by the program if they are not provided or if the required identifier is missing.

The following sections provide the user with the necessary information to generate the TOWER3D.DAT input file.

L.5.1 **CONTROL** *Information*

The line of data which follows the **CONTROL** separator is used to supply general data required by the program and contains the following information:

V=? D=? M=? T=?

where

V=	Number of natural vibration modes to be included. In most cases, 5 modes are sufficient.
D=	Hysteretic damping coefficient for tower concrete. A value of 0.10 implies 5% modal damping in all vibration modes of the tower without water on rigid foundation soil.
M=	Number of iterations in computing the natural frequencies and mode shapes. [20]
T=	Tolerance in frequency. [0.001]

This data group must be terminated by a line with colon ':' in the first column.

L.5.2 **TOWER STRUCTURE** *Information*

The line of data which follows the TOWER STRUCTURE separator is used to supply general data about tower substructure and contains the following information:

N=? E=? M=? A=?

where

N= Number of nodes in the idealization of tower. This must be equal to the maximum node number. Extra nodes without any unknown degrees of freedom attached can be used. However, they should be properly identified.

E= The number of elements in the idealization of tower. The program uses three-node quadrilateral Timoshenko-beam element.

M= Number of material types used in tower structure.

A= Number of nodes where extra concentrated or lumped mass is specified. From the mass density of tower materials, program itself computes the mass of tower structure. This option is useful in considering the mass of machinery etc.[0]

This data group must be terminated by a line with colon ':' in the first column.

L.5.3 **TGEOMETRY** *Information*

The sequence of lines which follow the TGEOMETRY separator define the tower geometry, and the location of nodes in the finite element idealization of the tower. These lines contain the following information:

Nid Z=? A=? I=? K=?

where

Nid= Node identification number to be selected by the user. The node number Nid must be less than or equal to the total number of nodes specified after the TOWER separator.

Z= z-ordinate.

A= Cross-sectional area of the tower at node Nid

I= Moment of inertia of the tower cross-section at node Nid

K= Shape factor for the cross-section to account for shear stress distribution. For some cross-sections, these factors are given in Table 9.1.

For some special cross-sections (Figure L.3), program can generate the cross-sectional properties. This option is activated by providing the following information on a line instead of "A=? I=? K=?", as mentioned above:

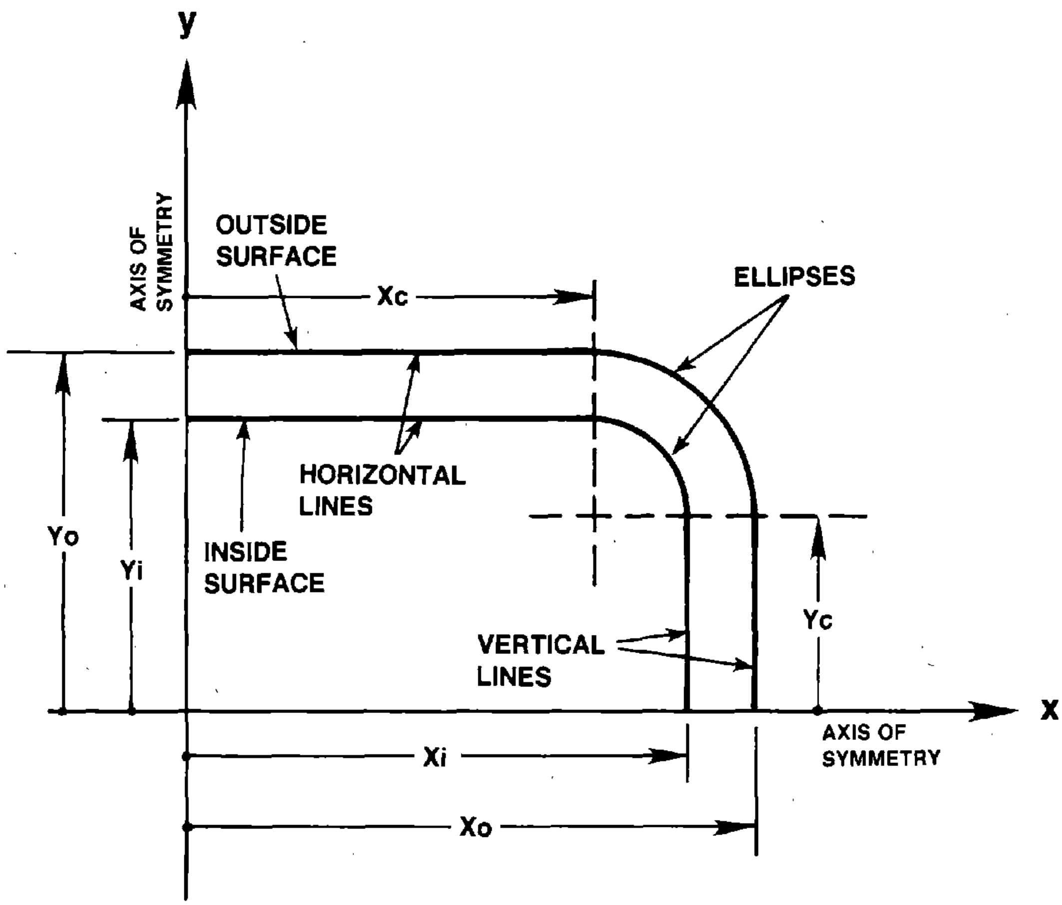

Figure L.3 General Geometry of One Quadrant of Tower Cross-Section for which Cross-Sectional Properties Generation Option is Available

S=Xo,Yo,Xi,Yi,Xc,Yc

For special cross-sections, the section parameters **Xo, Yo, Xi, Yi, Xc, and Yc** are defined in Figure L.3.

This sequence of lines must be terminated by a line with colon ':' in the first column.

L.5.4 **TRESTRAINT** *Information*

The sequence of lines which follow the TRESTRAINT separator define the unknown displacements which exist at the nodes of the structural system of tower. Unless a restraint is specified at a node, it is assumed that the node has two unknown displacements (one translation and one rotation). These lines contain the following information:

N1,N2,Inc   R=Ux,Rx

where

N1=	Node number for first node in a series of nodes which have identical displacement specification.
N2=	Node number for last node in series. [N1]
Inc=	Node number increment which is used to define the nodes in the series. [1]
Ux=	Lateral displacement specification = 0 or 1 or -1
Rx=	Rotation specification = 0 or 1 or -1

A specification of 0 allows the unknown displacement to exist. If the specification Ux and Rx is set to "1" the displacement and rotation is restrained to zero. The restraint specification "-1" for translation or rotation for any node, say N-th node, will specify the equation number of (N-1)th node to that of node N. This option is used to specify two nodes at the same location of the tower having discontinuity in the geometry at that location.

This data group must be terminated by a line having colon ':' in the first column.

L.5.5 **TMATERIALS** *Information*

The sequence of lines which follow the TMATERIALS separator define the material properties of the tower concrete. For each material type, one data line is required. The number of lines, so specified under this data group must be equal to the number of material types specified earlier under TOWER separator. These lines contain the following information:

Nid   E=?   G=?   W=?

where

Nid= Material identification number. This must be less than or equal to the total number of material types specified earlier under TOWER separator.

E= Elastic modulus of tower concrete.

G= Shear modulus of tower concrete. [E/2.34]

W= Mass density of tower concrete, i.e. unit weight divided by the acceleration due to gravity.

This sequence of data lines must be terminated by a line having colon ':' in the first column.

L.5.6 **TELEMENTS** *Information*

The sequence of lines which follow TELEMENTS separator define the connectivity of three-node, quadrilateral Timoshenko beam elements used to idealize the tower. The material type of the element is also specified under this data group. These lines contain the following information:

Nid,J1,J2,J3 M=? G=-------

where

Nid= Identification (ID) number for the element. Must be less than or equal to the total number of elements specified under TOWER separator.

J1,J2,J3= Node numbers defining the connectivity of the element

M= Material property identification number.

The option to automatically generate element connectivity data is activated by the addition of the following information on any line:

G=Nad,Nidinc,J1inc,J2inc,J3inc,Minc

where

Nad= Number of additional elements to be generated.

Nidinc= Increment of ID number in generated elements.[1]

J1inc= Increment of J1 in generated elements. [2]

J2inc= Increment of J2 in generated elements. [2]

J3inc= Increment of J3 in generated elements. [2]

Minc= Increment of material ID number in generated elements. [0]

This group of data lines must be terminated by a line having colon ':' in the first column.

L.5.7 **TEXTRA MASS** *Information*

For actual towers, it may be necessary to specify concentrated lumped masses at the nodes, or distributed mass along the height of the tower, in addition to the element mass which is automatically calculated by the program. This data is specified after the TEXTRA MASS separator. This group of data is required only if the number of nodes with extra mass specified by identifier "A=" under TOWER separator is non-zero. If for a node, this data is not specified, zero is assumed for both concentrated and distributed mass. Each line of this sequence contains the following information:

N1,N2,Inc C=? D=?

where

N1=	Node number for first node in a series of nodes which have identical concentrated and distributed extra mass.
N2=	Node number for last node in series. [N1]
Inc=	Node number increment which is used to define the nodes in the series. [1]
C=	Concentrated (Lumped) mass at that node. [0.0]
D=	Distributed mass at that node. [0.0]

This data group must be terminated by a line having colon ':' in the first column.

L.5.8 **OUTSIDE WATER DOMAIN** *Information*

The line of data which follows the OUTSIDE WATER DOMAIN separator is used to supply general data about surrounding (outside) water domain. **If this separator is missing, the program will not include the intercation effects due to surrounding water. Any information for the surrounding water domain, if provided, will be disregarded in that case.**

This line contains the following information:

N=? E=? T=? H=? M=Mz,Nt R=? W=? B=?

where

N=	Number of nodes required in the idealization of water domain surrounding the tower. **No dummy nodes are allowed.**
E=	Number of elements in the idealization of the fluid domain surrounding the tower. 20-node isoparametric elements are used for the finite element idealization of the surrounding water.
T=	Number of 8-node segments defining the tower-water interface.
H=	Number of 8-node segments defining the hypothetical cylindrical surface for boundary integral procedure.

Mz= Number of trial functions along the height to be used in the boundary integral procedure. [12]

Nt= Number of trial functions along the circumference to be used in the boundary integral procedure. [5]

R= Radius of the hypothetical cylindrical surface. This may be the smallest radius such that the cylindrical surface contains the tower (Figure 4.5).

W= Mass density of water, i.e. unit weight divided by the acceleration due to gravity.

B= Number of segments in the circumferential direction at the base of hypothetical cylindrical surface (Figure L.2).

This data group must be terminated by a line with a colon ':' in the first column.

L.5.9 **ONODES** *Information*

The lines which follow the ONODES separator define the location of the nodes of the idealized fluid domain surrounding the tower. These lines contain the following information:

Nid X=? Y=? Z=? I=? G=--- R=--- C=---

where

Nid= Node identification number to be selected by the user. The node number Nid must be less than or equal to the total number of nodes specified after the OUTSIDE separator.

X= x-ordinate

Y= y-ordinate

Z= z-ordinate

I= 1 for node on tower-water interface. Need not be specified for other nodes. [0]

The data may be automatically generated using the **linear generation option**, which can be activated by the addition of the following information on any line which contains the information about a nodal point:

G=Nf,Nl,Inc

where

Nf= The first node number in the sequence

Nl= The last node number in the sequence

Inc= Increment used to define generated node numbers. [1]

The generated nodes will be at equal interval along a straight line between nodes Nf and Nl.

The data may be automatically generated using the **radial generation option**, which can be activated by the addition of the following information on any line which contains the information about a nodal point:

R=Nf,Nl,Inc,Nc

where

Nf= The first node number in the sequence

Nl= The last node number in the sequence

Inc= Increment used to define generated node numbers. [1]

Nc= The node number for the center of the radial arc. If Nc=0, the center of the radial arc can be specified by adding the following information on the same line where radial generation is requested:

C=Cx,Cy,Cz

where

Cx= x-ordinate of the center of the radial arc

Cy= y-ordinate of the center of the radial arc

Cz= z-ordinate of the center of the radial arc

The generated nodes will be at equal interval along a radial arc with the specified center between nodes Nf and Nl. **The nodes generated by the radial generation option will be in x-y plane and will be assigned the value of z-ordinate same as that of the center of the radial arc.**

Alternatively, the location of a node not on the tower-water interface may be specified in terms of two nodes already defined. The program will place this node in the middle of the specified nodes. This information can be provided in a separate line in the following form:

Nid M=M1,M2 L=Nad,Nidinc,M1inc,M2inc I=?

where

Nid= Node identification number to be selected by the user.

M1= First node number to be used in generation.

M2= Second node number to be used in generation.

Nad= Number of additional nodes to be generated using similar option.

Nidinc Increment of Nid in generated nodes.

M1inc= Increment of M1 in generated nodes.

M2inc= Increment of M2 in generated nodes.

I= 1 for node on tower-water interface. Need not be specified for other nodes. [0]

This sequence of lines must be terminated by a line with colon ':' in the first column.

L.5.10 **OELEMENTS** *Information*

The sequence of lines which follow OELEMENTS separator define the connectivity of twenty-node isoparametric elements used to idealize surrounding water domain. **The connectivity data is provided in FORMAT 20I4, standard FORTRAN formats. Each element requires one line of data in terms of twenty node numbers defining the connectivity of the element. Since element numbering is not important, the program will assign the element identification number in the same order in which data is provided. The number of lines for element connectivity data should be equal to the number of elements specified after OUTSIDE separator with E= identifier.**

This group of data lines must be terminated by a line having colon ':' in the first column.

L.5.11 **OTOWER-WATER INTERFACE** *Information*

The sequence of lines which follow OTOWER-WATER separator define the connectivity of eight-node segments of the fluid elements in the surrounding water domain on the tower-water interface. These lines contain the following information:

Nid,J1,J2,J3,J4,J5,J6,J7,J8 G=------

where

Nid= Identification (ID) number for the segment. Must be less than or equal to the total number of segments on the tower-water interface specified under OUTSIDE separator.

J1 to J8= Node numbers defining the connectivity of the segment.

The option to automatically generate segment connectivity data is activated by the addition of the following information on any line:

G=Nad,Nidinc,J1inc,J2inc,J3inc,J4inc,J5inc,J6inc,J7inc,J8inc

where

Nad= Number of additional segments to be generated.

Nidinc= Increment of ID number in generated segments.[1]

J1inc= Increment of J1 in generated segments. [2]

J2inc= Increment of J2 in generated segments. [2]

J3inc= Increment of J3 in generated segments. [2]

J4inc= Increment of J4 in generated segments. [2]

J5inc= Increment of J5 in generated segments. [1]

J6inc= Increment of J6 in generated segments. [2]

J7inc= Increment of J7 in generated segments. [1]

J8inc= Increment of J8 in generated segments. [2]

This group of data lines must be terminated by a line having colon ':' in the first column.

L.5.12 **OHYPOTHETICAL CYLINDER** *Information*

The sequence of lines which follow OHYPOTHETICAL separator define the connectivity of eight-node segments of fluid elements in the outside water domain on the hypothetical cylindrical surface. These lines contain the following information:

Nid,J1,J2,J3,J4,J5,J6,J7,J8 G=------

where

Nid= Identification (ID) number for the segment. Must be less than or equal to the total number of segments on the hypothetical cylindrical surface specified under OUTSIDE separator.

J1 to J8= Node numbers defining the connectivity of the segment.

The option to automatically generate segment connectivity data is activated by the addition of the following information on any line:

G=Nad,Nidinc,J1inc,J2inc,J3inc,J4inc,J5inc,J6inc,J7inc,J8inc

where

Nad= Number of additional segments to be generated.

Nidinc= Increment of ID number in generated segments.[1]

J1inc= Increment of J1 in generated segments. [2]

J2inc= Increment of J2 in generated segments. [2]

J3inc= Increment of J3 in generated segments. [2]

J4inc= Increment of J4 in generated segments. [2]

J5inc= Increment of J5 in generated segments. [1]

J6inc= Increment of J6 in generated segments. [2]

J7inc= Increment of J7 in generated segments. [1]

J8inc= Increment of J8 in generated segments. [2]

This group of data lines must be terminated by a line having colon ':' in the first column.

L.5.13 **INSIDE WATER DOMAIN** *Information*

The line of data which follows the INSIDE WATER DOMAIN separator is used to supply general data about inside water domain. **If this separator is missing, the program will not include the intercation effects due to water contained inside the tower. Any information for the inside water domain, if provided, will be disregarded in that case.**

This line contains the following information:

N=? E=? T=? W=?

where

N= Number of nodes required in the idealization of water domain contained inside the hollow tower. **No dummy nodes are allowed.**

E= Number of elements in the idealization of the fluid domain contained inside the tower. Twenty-node isoparametric elements are used for the finite element idealization of the inside water.

T= Number of eight-node segments defining the tower-water interface.

W= Mass density of water, i.e. unit weight divided by the acceleration due to gravity.

This data group must be terminated by a line with a colon ':' in the first column.

L.5.14 **INODES** *Information*

The lines which follow the INODES separator define the location of the nodes of the idealized fluid domain contained inside the tower. These lines contain the following information:

Nid X=? Y=? Z=? I=? G=--- R=--- C=---

where

Nid= Node identification number to be selected by the user. The node number Nid must be less than or equal to the total number of nodes specified after the

INSIDE separator.

X= x-ordinate

Y= y-ordinate

Z= z-ordinate

I= 1 for node on tower-water interface. Need not be specified for other nodes. [0]

The data may be automatically generated using the **linear generation option**, which can be activated by the addition of the following information on any line which contains the information about a nodal point:

G=Nf,Nl,Inc

where

Nf= The first node number in the sequence

Nl= The last node number in the sequence

Inc= Increment used to define generated node numbers. [1]

The generated nodes will be at equal interval along a straight line between nodes Nf and Nl.

The data may be automatically generated using the **radial generation option**, which can be activated by the addition of the following information on any line which contains the information about a nodal point:

R=Nf,Nl,Inc,Nc

where

Nf= The first node number in the sequence

Nl= The last node number in the sequence

Inc= Increment used to define generated node numbers. [1]

Nc= The node number for the center of the radial arc. If Nc=0, the center of the radial arc can be specified by adding the following information on the same line where radial generation is requested:

C=Cx,Cy,Cz

where

Cx= x-ordinate of the center of the radial arc

Cy= y-ordinate of the center of the radial arc

Cz= z-ordinate of the center of the radial arc

The generated nodes will be at equal interval along a radial arc with the specified center between nodes Nf and Nl. **The nodes generated by the radial generation option will be in x-y plane and will be assigned the value of z-ordinate same as that of the center of the radial arc.**

Alternatively, the location of a node not on the tower-water interface may be specified in terms of two nodes already defined. The program will place this node in the middle of the specified nodes. This information can be provided in a separate line in the following form:

Nid M=M1,M2 L=Nad,Nidinc,M1inc,M2inc I=?

where

Nid= Node identification number to be selected by the user.

M1= First node number to be used in generation.

M2= Second node number to be used in generation.

Nad= Number of additional nodes to be generated using similar option.

Nidinc Increment of Nid in generated nodes.

M1inc= Increment of M1 in generated nodes.

M2inc= Increment of M2 in generated nodes.

I= 1 for node on tower-water interface. Need not be specified for other nodes. [0]

This sequence of lines must be terminated by a line with colon ':' in the first column.

L.5.15 **IELEMENTS** *Information*

The sequence of lines which follow IELEMENTS separator define the connectivity of twenty-node isoparametric elements used to idealize inside water domain. **The connectivity data is provided in FORMAT 20I4, standard FORTRAN formats. Each element requires one line of data in terms of twenty node numbers defining the connectivity of the element. Since element numbering is not important, the program will assign the element identification number in the same order in which data is provided. The number of lines for element connectivity data should be equal to the number of elements specified after INSIDE separator with E= identifier.**

This group of data lines must be terminated by a line having colon ':' in the first column.

L.5.16 **ITOWER-WATER INTERFACE** *Information*

The sequence of lines which follow ITOWER-WATER separator define the connectivity of eight-node segments of the fluid elements in the inside water domain on the tower-water interface. These lines contain the following information:

Nid,J1,J2,J3,J4,J5,J6,J7,J8 G=------

where

Nid=	Identification (ID) number for the segment. Must be less than or equal to the total number of segments on the tower-water interface specified under INSIDE separator.
J1 to J8=	Node numbers defining the connectivity of the segment.

The option to automatically generate segment connectivity data is activated by the addition of the following information on any line:

G=Nad,Nidinc,J1inc,J2inc,J3inc,J4inc,J5inc,J6inc,J7inc,J8inc

where

Nad=	Number of additional segments to be generated.
Nidinc=	Increment of ID number in generated segments.[1]
J1inc=	Increment of J1 in generated segments. [2]
J2inc=	Increment of J2 in generated segments. [2]
J3inc=	Increment of J3 in generated segments. [2]
J4inc=	Increment of J4 in generated segments. [2]
J5inc=	Increment of J5 in generated segments. [1]
J6inc=	Increment of J6 in generated segments. [2]
J7inc=	Increment of J7 in generated segments. [1]
J8inc=	Increment of J8 in generated segments. [2]

This group of data lines must be terminated by a line having colon ':' in the first column.

L.5.17 **FOUNDATION-SOIL SYSTEM** *Information*

The line of data which follows the FOUNDATION-SOIL SYSTEM separator is used to supply the information about the foundation soil system. **If this separator is missing, foundation-soil interaction effects will not be considered in the analysis. This line contains the following information:**

M=? I=? R=R1,R2 C=? P=? W=? D=?

where

M= Mass of the foundation footing below the ground level. [0.0]

I= Mass moment of inertia of the foundation footing below ground level. [0.0]

R1= Equivalent radius of the footing in translation.

R2= Equivalent radius of the footing in rocking. [R1]

If the equivalent radius of the footing in translation, R1, is set to 0.0, user must provide the impedance functions for the foundation-soil system. The program reads the foundation impedance functions from the file FOUNDIMP.DAT. If 'N' points are used to define the acceleration time history, including the "quiet zone", then the impedance functions should be available at the interval of $\Delta\omega=2\pi/N\Delta t$, in which Δt is the time interval between consecutive data points in acceleration time history. A total (N/2+1) lines of data, corresponding to 0, $\Delta\omega$, $2\Delta\omega$, ..., frequencies are required in the file FOUNDIMP.DAT. Each line of data contains the following four values separated be a ',' (comma) or a blank space:

KVVR,KVVI,KMMR,KMMI

where

KVVR= Real part of impedance function K_{VV}.

KVVI Imaginary part of impedance function K_{VV}.

KMMR Real part of impedance function K_{MM}.

KMMI Imaginary part of impedance function K_{MM}.

C= Shear wave velocity of foundation-soil.

P= Poisson's ratio of foundation soil. [0.33]

W= Mass density of foundation soil, i.e. unit weight divided by the acceleration due to gravity.

D= Hysteretic damping factor for foundation soil. [0.10]

This data group must be terminated by a line with colon ':' in the first column.

L.5.18 **GROUND MOTION** *Information*

The sequence of lines which follow the GROUND MOTION separator provide information about the earthquake acceleration data. The first line contains the following information:

N=Nx T=? S=? M=?

where

Nx= The number of data points in the ground motion along x-axis. This number must be a multiple of 8.

T= The uniform time interval between consecutive data points in the ground motion record.

S= Scale factor for the ground motion. The record may be normalized by g, the acceleration due to gravity, so S= can be specified to bring ground motion to acceleration units.

M= The control parameter to select the number of points ($=2^M$) to be used in the discrete Fast Fourier Transform (DFFT) computations. The selected value of M should be large enough to provide sufficient 'quiet zone' to ensure accurate DFFT computations.

After this line, the ground motion data is provided. EIGHT data points are provided in each line in FORMAT 8F9.5, standard FORTRAN formats. Nx/8 lines are required for the ground motion along x-axis.

This data group must be terminated by a line with colon ':' in the first column.

L.5.19 **OUTPUT CONTROL** *Information*

The FOUR lines which follow the OUTPUT CONTROL separator identify the nodes where displacement, shear force and bending moment response is required. The FIRST line of this data group contains the information about the nodes where the **maximum displacement** over the duration of the earthquake is to be determined. This data is presented in the following form:

D=Nt L=L1,L2,.......,LNt N=Nf,Ninc

where

Nt= Total number of nodes where maximum lateral displacement should be computed.

The list of nodes can be specified either by N= or by L=. If the response is required at less than twenty nodes, and they are not regularly distributed in numbers, option L= can be used to just list those nodes. The option N= should be used if the nodes are regularly distributed, or the response at all the nodes is required. The program looks for the L= option only if it does not find the N= option. So, both the options can not be used simultaneously. In option N=, the terms have the following meaning:

Nf= The first node number where information is requested.

Ninc= The increment in the sequence of nodes. The last node number is automatically determined by the program using Nt, the total number of nodes where information is requested.

The SECOND line of this data group contains the information about the nodes where the **maximum shear force** is to be determined. This data is presented in the following form:

S=Nt L=L1,L2,.......,LNt N=Nf,Ninc

where

Nt= Total number of nodes where maximum shear force should be computed.

All other parameters carry the same meaning as in the FIRST line.

The THIRD line of this data group contains the information about the nodes where the **maximum bending moment** is to be determined. This data is presented in the following form:

M=Nt L=L1,L2,.......,LNt N=Nf,Ninc

where

Nt= Total number of nodes where maximum bending moment should be computed.

All other parameters carry the same meaning as in the FIRST line.

The FOURTH line of this data group contains the information about the nodes where the **lateral displacement history** is to be included in the output. This data is presented in the following form:

H=Nt L=L1,L2,.......,LNt N=Nf,Ninc

where

Nt= Total number of nodes where displacement history need be computed.

All other parameters carry the same meaning as in the FIRST line.

This data group must be terminated by a line with colon ':' in the first column.

L.6 Numerical Example

For the convenience of the user, the input data file **TOWER3D.DAT** used for analysis of a non-circular tapered tower is presented. Figures L.4 to L.9 provide the information about the mathematical model and the numbering schemes used in the earthquake response analysis of this tower. The output files, mentioned in Figure L.1, for this numerical example are also provided on the diskette with the source codes.

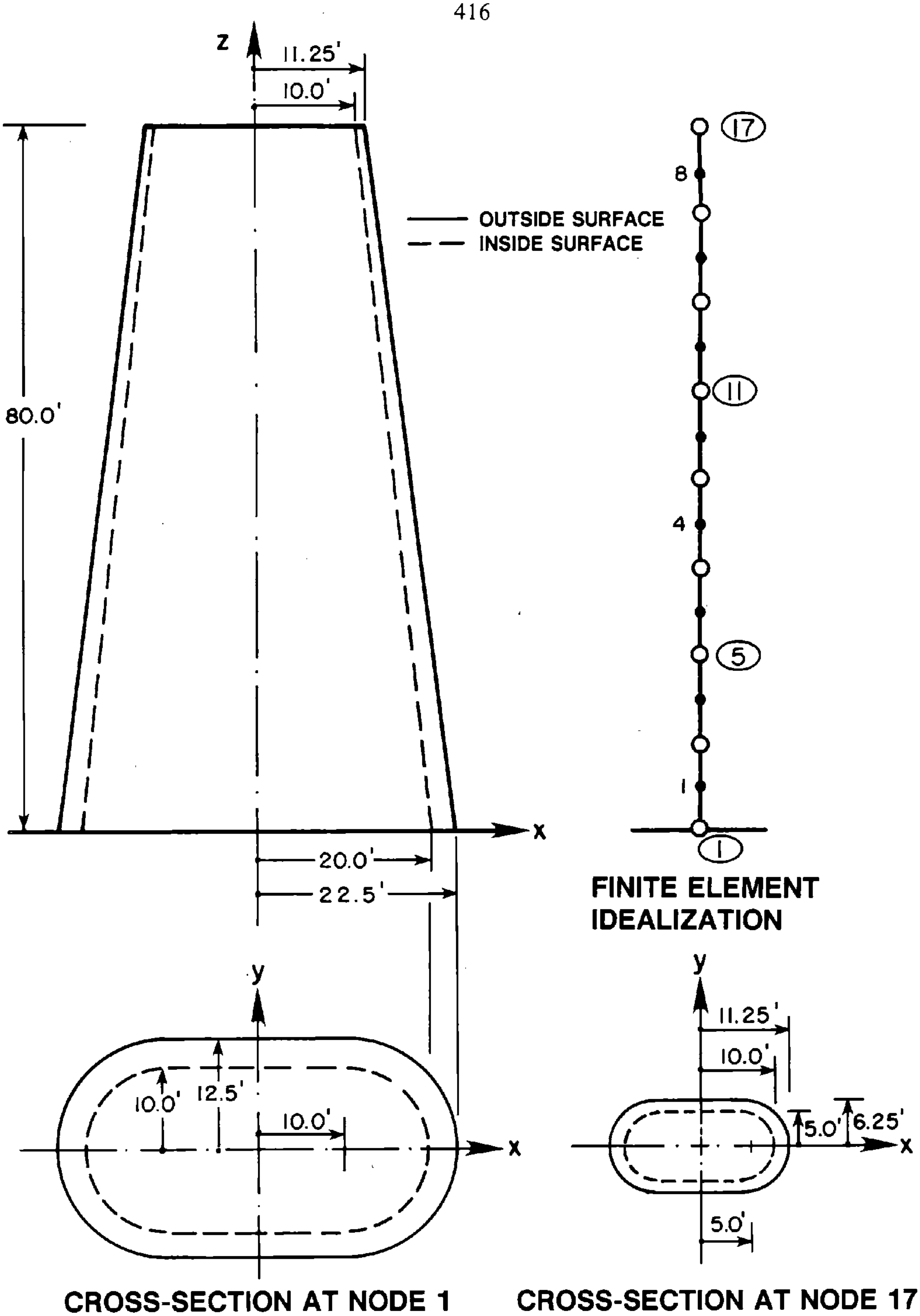

Figure L.4 Finite Element Idealization of the Tower in Example

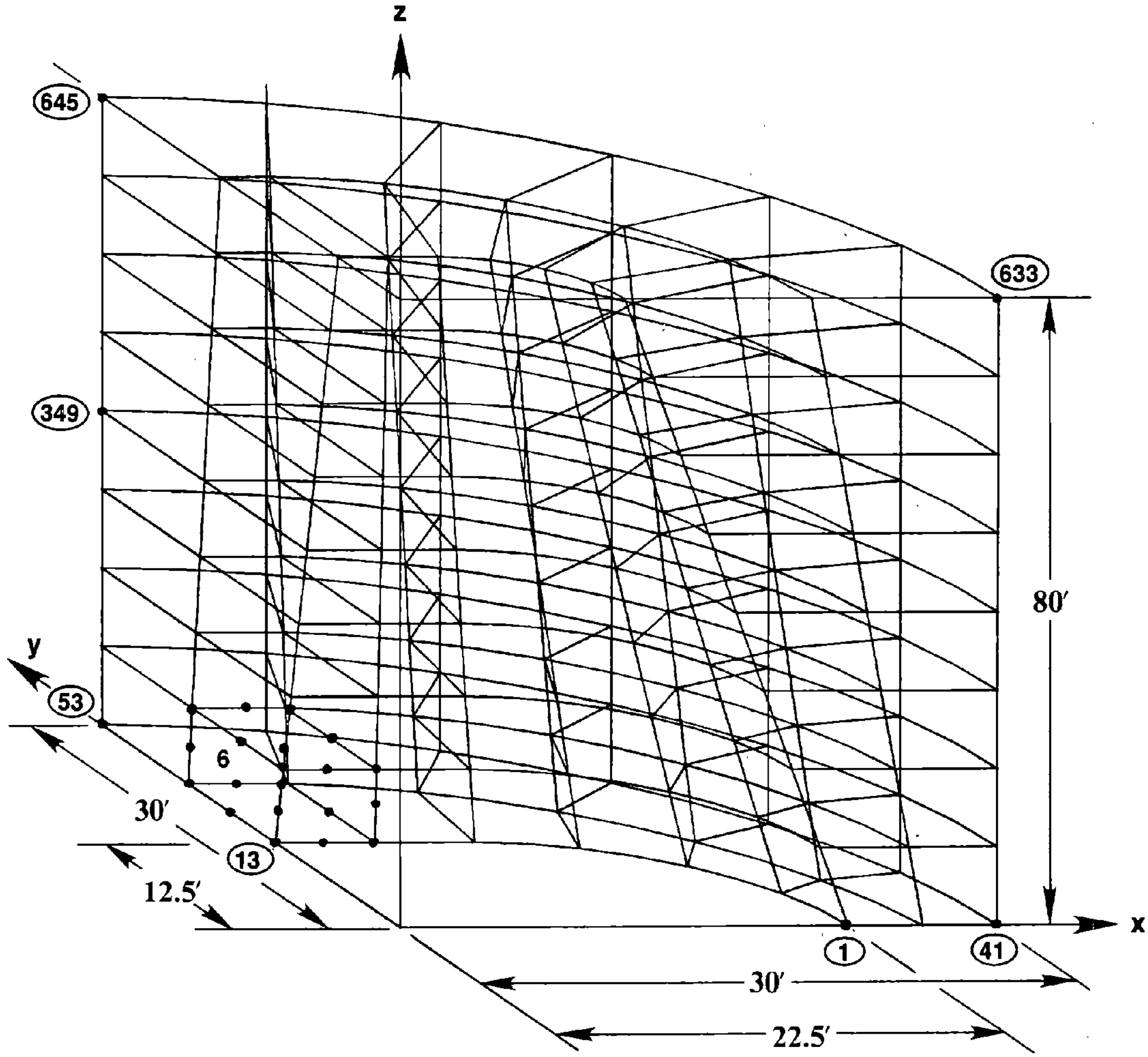

Figure L.5 Finite Element Idealization of Surrounding Water Domain

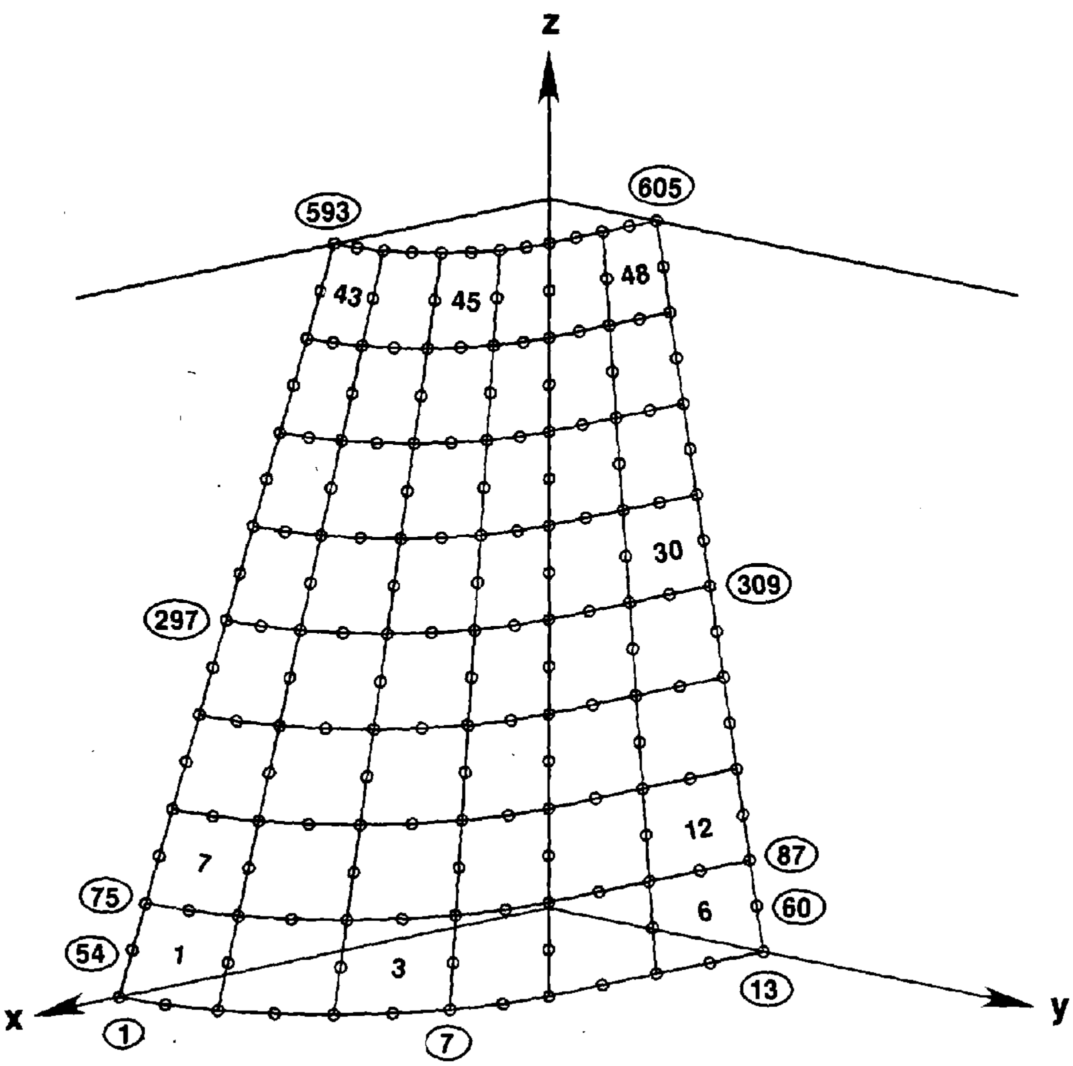

Figure L.6 Finite Element System on Tower-Outside Water Interface

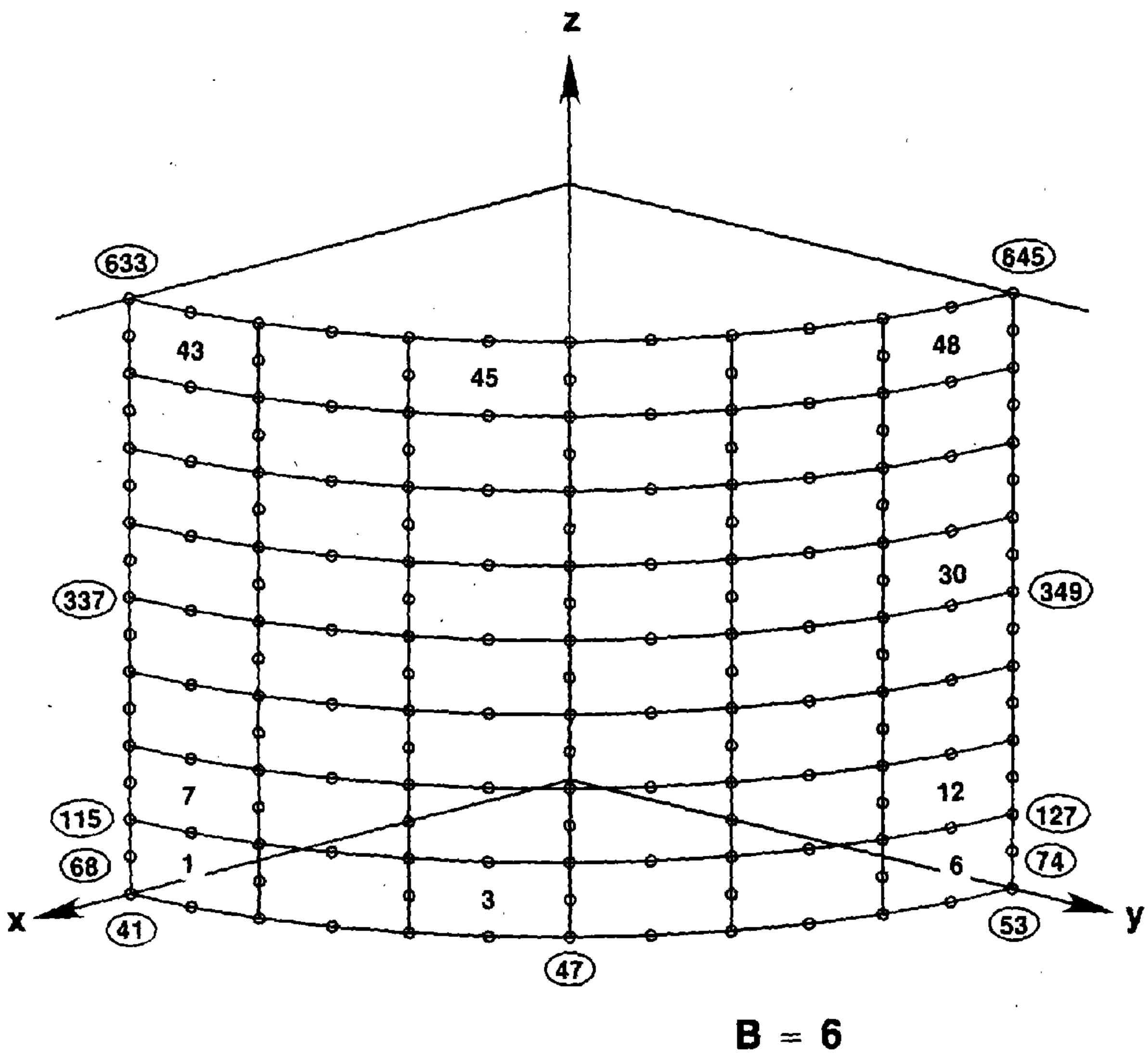

Figure L.7 Finite Element Idealization of Outside Water Domain Showing Nodes on the Hypothetical Cylindrical Surface

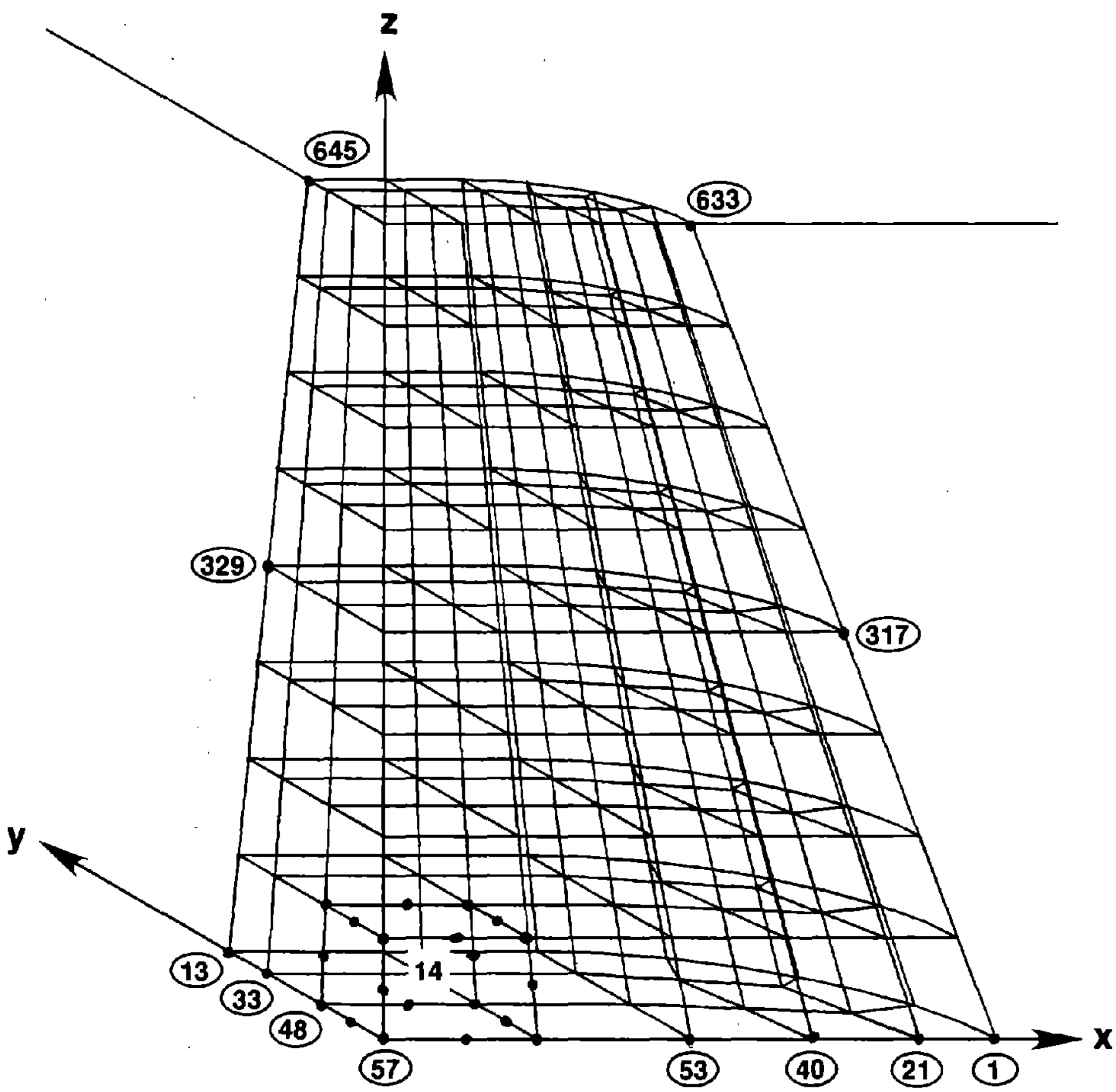

Figure L.8 Finite Element Idealization of Inside Water Domain

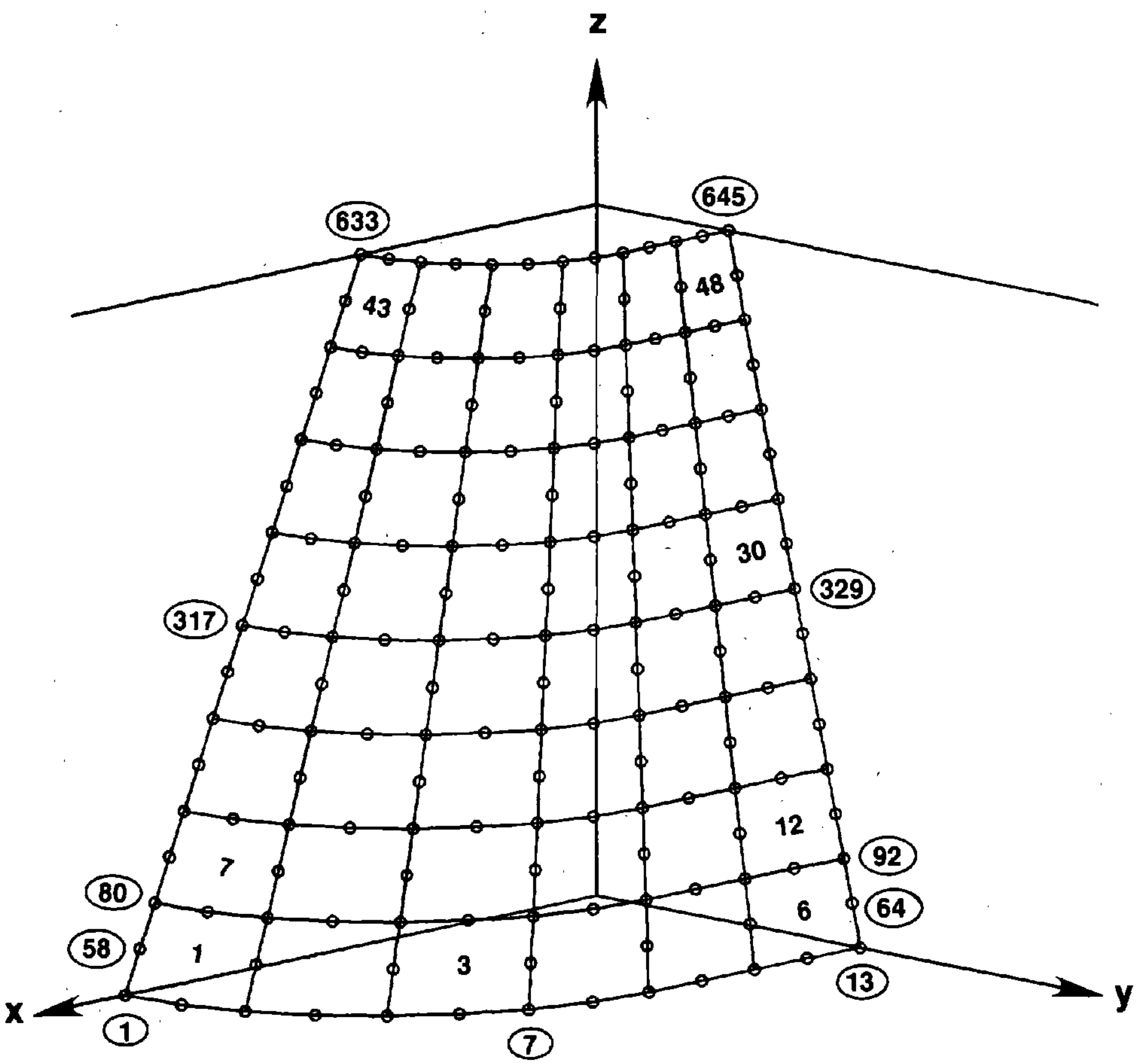

Figure L.9 Finite Element System on Tower-Inside Water Interface

```
C......EXAMPLE DATA FOR TOWER3D SERIES
CONTROL
V=5  D=0.10°  M=20  T=0.001  :
:
TOWER STRUCTURE
N=17  E=8  M=1  A=0  :
:
TGEOMETRY
  1   Z=0.     S=22.5,12.5,20.0,10.0,10.0,0.0
  2   Z= 5.00  A=259.6902  I=28470.3672  K=0.7340
  3   Z=10.00  A=243.2062  I=24970.7344  K=0.7340
  4   Z=15.00  A=227.2627  I=21804.1055  K=0.7340
  5   Z=20.00  A=211.8596  I=18948.6563  K=0.7340
  6   Z=25.00  A=196.9970  I=16383.2988  K=0.7340
  7   Z=30.00  A=182.6749  I=14087.6865  K=0.7340
  8   Z=35.00  A=168.8932  I=12042.2139  K=0.7340
  9   Z=40.00  A=155.6520  I=10228.0127  K=0.7340
 10   Z=45.00  A=142.9512  I=8626.9570  K=0.7340
 11   Z=50.00  A=130.7909  I=7221.6602  K=0.7340
 12   Z=55.00  A=119.1710  I=5995.4727  K=0.7340
 13   Z=60.00  A=108.0916  I=4932.4907  K=0.7340
 14   Z=65.00  A=97.5527  I=4017.5444  K=0.7340
 15   Z=70.00  A=87.5542  I=3236.2073  K=0.7340
 16   Z=75.00  A=78.0962  I=2574.7910  K=0.7340
 17   Z=80.00       S=11.25,6.25,10.0,5.0,5.0,0.0
:
TRESTRAINTS
1   R=1,1
:
TELEMENTS
1,1,2,3  M=1   G=7,1,2,2,2,0
:
TMATERIALS
1  E=648000.   G=276923.  W=.004817
:
OUTSIDE WATER DOMAIN
N=645  E=96  T=48  H=48  M=12,5  R=30.0  W=0.001939  B=6
:
ONODES
1    X=22.5    Y=0.     Z=0.   I=1
9    X=10.0    Y=12.5   Z=0.   I=1    R=1,9,1  C=10.0,0.0,0.0
13   X=0.0     Y=12.5   Z=0.0  I=1    G=9,13,1
21   X=26.25   Y=0.0    Z=0.0
31   X=5.0     Y=21.25  Z=0.0  R=21,31,1   C=0.0,0.0,0.0
33   X=0.0     Y=21.25  Z=0.0  G=31,33,1
41   X=30.0    Y=0.0   Z=0.0
53   X=0.0     Y=30.0  Z=0.0   R=41,53,1   C=0.0,0.0,0.0
14   M=1,21  L=6,1,2,2
34   M=21,41 L=6,1,2,2
593   X=11.25    Y=0.     Z=80.   I=1
601   X=5.0      Y=6.25   Z=80.   I=1    R=593,601,1  C=5.0,0.0,80.0
605   X=0.0      Y=6.25   Z=80.0  I=1    G=601,605,1
613   X=20.625   Y=0.0    Z=80.0
623   X=2.5      Y=18.125 Z=80.0  R=613,623,1 C=0.0,0.0,80.0
625   X=0.0      Y=18.125 Z=80.0   G=623,625,1
633   X=30.0     Y=0.0   Z=80.0
645   X=0.0      Y=30.0  Z=80.0   R=633,645,1   C=0.0,0.0,80.0
606   M=593,613  L=6,1,2,2
626   M=613,633 L=6,1,2,2
1   X=22.5    Y=0.0    Z=0.0  I=1  G=1,593,74
1   X=22.5    Y=0.0    Z=0.0  I=1  G=2,594,74
1   X=22.5    Y=0.0    Z=0.0  I=1  G=3,595,74
1   X=22.5    Y=0.0    Z=0.0  I=1  G=4,596,74
1   X=22.5    Y=0.0    Z=0.0  I=1  G=5,597,74
```

```
1    X=22.5    Y=0.0    Z=0.0  I=1  G=6,598,74
1    X=22.5    Y=0.0    Z=0.0  I=1  G=7,599,74
1    X=22.5    Y=0.0    Z=0.0  I=1  G=8,600,74
1    X=22.5    Y=0.0    Z=0.0  I=1  G=9,601,74
1    X=22.5    Y=0.0    Z=0.0  I=1  G=10,602,74
1    X=22.5    Y=0.0    Z=0.0  I=1  G=11,603,74
1    X=22.5    Y=0.0    Z=0.0  I=1  G=12,604,74
1    X=22.5    Y=0.0    Z=0.0  I=1  G=13,605,74
41   X=30.0    Y=0.0    Z=0.0  G=14,606,74
41   X=30.0    Y=0.0    Z=0.0  G=15,607,74
41   X=30.0    Y=0.0    Z=0.0  G=16,608,74
41   X=30.0    Y=0.0    Z=0.0  G=17,609,74
41   X=30.0    Y=0.0    Z=0.0  G=18,610,74
41   X=30.0    Y=0.0    Z=0.0  G=19,611,74
41   X=30.0    Y=0.0    Z=0.0  G=20,612,74
41   X=30.0    Y=0.0    Z=0.0  G=21,613,74
41   X=30.0    Y=0.0    Z=0.0  G=22,614,74
41   X=30.0    Y=0.0    Z=0.0  G=23,615,74
41   X=30.0    Y=0.0    Z=0.0  G=24,616,74
41   X=30.0    Y=0.0    Z=0.0  G=25,617,74
41   X=30.0    Y=0.0    Z=0.0  G=26,618,74
41   X=30.0    Y=0.0    Z=0.0  G=27,619,74
41   X=30.0    Y=0.0    Z=0.0  G=28,620,74
41   X=30.0    Y=0.0    Z=0.0  G=29,621,74
41   X=30.0    Y=0.0    Z=0.0  G=30,622,74
41   X=30.0    Y=0.0    Z=0.0  G=31,623,74
41   X=30.0    Y=0.0    Z=0.0  G=32,624,74
41   X=30.0    Y=0.0    Z=0.0  G=33,625,74
41   X=30.0    Y=0.0    Z=0.0  G=34,626,74
41   X=30.0    Y=0.0    Z=0.0  G=35,627,74
41   X=30.0    Y=0.0    Z=0.0  G=36,628,74
41   X=30.0    Y=0.0    Z=0.0  G=37,629,74
41   X=30.0    Y=0.0    Z=0.0  G=38,630,74
41   X=30.0    Y=0.0    Z=0.0  G=39,631,74
41   X=30.0    Y=0.0    Z=0.0  G=40,632,74
41   X=30.0    Y=0.0    Z=0.0  G=41,633,74
41   X=30.0    Y=0.0    Z=0.0  G=42,634,74
41   X=30.0    Y=0.0    Z=0.0  G=43,635,74
41   X=30.0    Y=0.0    Z=0.0  G=44,636,74
41   X=30.0    Y=0.0    Z=0.0  G=45,637,74
41   X=30.0    Y=0.0    Z=0.0  G=46,638,74
41   X=30.0    Y=0.0    Z=0.0  G=47,639,74
41   X=30.0    Y=0.0    Z=0.0  G=48,640,74
41   X=30.0    Y=0.0    Z=0.0  G=49,641,74
41   X=30.0    Y=0.0    Z=0.0  G=50,642,74
41   X=30.0    Y=0.0    Z=0.0  G=51,643,74
41   X=30.0    Y=0.0    Z=0.0  G=52,644,74
41   X=30.0    Y=0.0    Z=0.0  G=53,645,74
54   M=1,75      L=6,1,2,2      I=1
61   M=21,95     L=6,1,2,2
68   M=41,115    L=6,1,2,2
128  M=75,149    L=6,1,2,2    I=1
135  M=95,169    L=6,1,2,2
142  M=115,189   L=6,1,2,2
202  M=149,223   L=6,1,2,2    I=1
209  M=169,243   L=6,1,2,2
216  M=189,263   L=6,1,2,2
276  M=223,297   L=6,1,2,2    I=1
283  M=243,317   L=6,1,2,2
290  M=263,337   L=6,1,2,2
350  M=297,371   L=6,1,2,2   I=1
357  M=317,391   L=6,1,2,2
364  M=337,411   L=6,1,2,2
424  M=371,445   L=6,1,2,2      I=1
```

```
431  M=391,465  L=6,1,2,2
438  M=411,485  L=6,1,2,2
498  M=445,519  L=6,1,2,2      I=1
505  M=465,539  L=6,1,2,2
512  M=485,559  L=6,1,2,2
572  M=519,593  L=6,1,2,2     I=1
579  M=539,613  L=6,1,2,2
586  M=559,633  L=6,1,2,2
:
OELEMENT
  1  21  23   3  75  95  97  77  14  22  15   2  88  96  89  76  54  61  62  55
  3  23  25   5  77  97  99  79  15  24  16   4  89  98  90  78  55  62  63  56
  5  25  27   7  79  99 101  81  16  26  17   6  90 100  91  80  56  63  64  57
  7  27  29   9  81 101 103  83  17  28  18   8  91 102  92  82  57  64  65  58
  9  29  31  11  83 103 105  85  18  30  19  10  92 104  93  84  58  65  66  59
 11  31  33  13  85 105 107  87  19  32  20  12  93 106  94  86  59  66  67  60
 21  41  43  23  95 115 117  97  34  42  35  22 108 116 109  96  61  68  69  62
 23  43  45  25  97 117 119  99  35  44  36  24 109 118 110  98  62  69  70  63
 25  45  47  27  99 119 121 101  36  46  37  26 110 120 111 100  63  70  71  64
 27  47  49  29 101 121 123 103  37  48  38  28 111 122 112 102  64  71  72  65
 29  49  51  31 103 123 125 105  38  50  39  30 112 124 113 104  65  72  73  66
 31  51  53  33 105 125 127 107  39  52  40  32 113 126 114 106  66  73  74  67
 75  95  97  77 149 169 171 151  88  96  89  76 162 170 163 150 128 135 136 129
 77  97  99  79 151 171 173 153  89  98  90  78 163 172 164 152 129 136 137 130
 79  99 101  81 153 173 175 155  90 100  91  80 164 174 165 154 130 137 138 131
 81 101 103  83 155 175 177 157  91 102  92  82 165 176 166 156 131 138 139 132
 83 103 105  85 157 177 179 159  92 104  93  84 166 178 167 158 132 139 140 133
 85 105 107  87 159 179 181 161  93 106  94  86 167 180 168 160 133 140 141 134
 95 115 117  97 169 189 191 171 108 116 109  96 182 190 183 170 135 142 143 136
 97 117 119  99 171 191 193 173 109 118 110  98 183 192 184 172 136 143 144 137
 99 119 121 101 173 193 195 175 110 120 111 100 184 194 185 174 137 144 145 138
101 121 123 103 175 195 197 177 111 122 112 102 185 196 186 176 138 145 146 139
103 123 125 105 177 197 199 179 112 124 113 104 186 198 187 178 139 146 147 140
105 125 127 107 179 199 201 181 113 126 114 106 187 200 188 180 140 147 148 141
149 169 171 151 223 243 245 225 162 170 163 150 236 244 237 224 202 209 210 203
151 171 173 153 225 245 247 227 163 172 164 152 237 246 238 226 203 210 211 204
153 173 175 155 227 247 249 229 164 174 165 154 238 248 239 228 204 211 212 205
155 175 177 157 229 249 251 231 165 176 166 156 239 250 240 230 205 212 213 206
157 177 179 159 231 251 253 233 166 178 167 158 240 252 241 232 206 213 214 207
159 179 181 161 233 253 255 235 167 180 168 160 241 254 242 234 207 214 215 208
169 189 191 171 243 263 265 245 182 190 183 170 256 264 257 244 209 216 217 210
171 191 193 173 245 265 267 247 183 192 184 172 257 266 258 246 210 217 218 211
173 193 195 175 247 267 269 249 184 194 185 174 258 268 259 248 211 218 219 212
175 195 197 177 249 269 271 251 185 196 186 176 259 270 260 250 212 219 220 213
177 197 199 179 251 271 273 253 186 198 187 178 260 272 261 252 213 220 221 214
179 199 201 181 253 273 275 255 187 200 188 180 261 274 262 254 214 221 222 215
223 243 245 225 297 317 319 299 236 244 237 224 310 318 311 298 276 283 284 277
225 245 247 227 299 319 321 301 237 246 238 226 311 320 312 300 277 284 285 278
227 247 249 229 301 321 323 303 238 248 239 228 312 322 313 302 278 285 286 279
229 249 251 231 303 323 325 305 239 250 240 230 313 324 314 304 279 286 287 280
231 251 253 233 305 325 327 307 240 252 241 232 314 326 315 306 280 287 288 281
233 253 255 235 307 327 329 309 241 254 242 234 315 328 316 308 281 288 289 282
243 263 265 245 317 337 339 319 256 264 257 244 330 338 331 318 283 290 291 284
245 265 267 247 319 339 341 321 257 266 258 246 331 340 332 320 284 291 292 285
247 267 269 249 321 341 343 323 258 268 259 248 332 342 333 322 285 292 293 286
249 269 271 251 323 343 345 325 259 270 260 250 333 344 334 324 286 293 294 287
251 271 273 253 325 345 347 327 260 272 261 252 334 346 335 326 287 294 295 288
253 273 275 255 327 347 349 329 261 274 262 254 335 348 336 328 288 295 296 289
297 317 319 299 371 391 393 373 310 318 311 298 384 392 385 372 350 357 358 351
299 319 321 301 373 393 395 375 311 320 312 300 385 394 386 374 351 358 359 352
301 321 323 303 375 395 397 377 312 322 313 302 386 396 387 376 352 359 360 353
303 323 325 305 377 397 399 379 313 324 314 304 387 398 388 378 353 360 361 354
305 325 327 307 379 399 401 381 314 326 315 306 388 400 389 380 354 361 362 355
307 327 329 309 381 401 403 383 315 328 316 308 389 402 390 382 355 362 363 356
317 337 339 319 391 411 413 393 330 338 331 318 404 412 405 392 357 364 365 358
319 339 341 321 393 413 415 395 331 340 332 320 405 414 406 394 358 365 366 359
321 341 343 323 395 415 417 397 332 342 333 322 406 416 407 396 359 366 367 360
323 343 345 325 397 417 419 399 333 344 334 324 407 418 408 398 360 367 368 361
325 345 347 327 399 419 421 401 334 346 335 326 408 420 409 400 361 368 369 362
327 347 349 329 401 421 423 403 335 348 336 328 409 422 410 402 362 369 370 363
371 391 393 373 445 465 467 447 384 392 385 372 458 466 459 446 424 431 432 425
373 393 395 375 447 467 469 449 385 394 386 374 459 468 460 448 425 432 433 426
375 395 397 377 449 469 471 451 386 396 387 376 460 470 461 450 426 433 434 427
377 397 399 379 451 471 473 453 387 398 388 378 461 472 462 452 427 434 435 428
379 399 401 381 453 473 475 455 388 400 389 380 462 474 463 454 428 435 436 429
381 401 403 383 455 475 477 457 389 402 390 382 463 476 464 456 429 436 437 430
391 411 413 393 465 485 487 467 404 412 405 392 478 486 479 466 431 438 439 432
393 413 415 395 467 487 489 469 405 414 406 394 479 488 480 468 432 439 440 433
395 415 417 397 469 489 491 471 406 416 407 396 480 490 481 470 433 440 441 434
397 417 419 399 471 491 493 473 407 418 408 398 481 492 482 472 434 441 442 435
399 419 421 401 473 493 495 475 408 420 409 400 482 494 483 474 435 442 443 436
401 421 423 403 475 495 497 477 409 422 410 402 483 496 484 476 436 443 444 437
445 465 467 447 519 539 541 521 458 466 459 446 532 540 533 520 498 505 506 499
447 467 469 449 521 541 543 523 459 468 460 448 533 542 534 522 499 506 507 500
449 469 471 451 523 543 545 525 460 470 461 450 534 544 535 524 500 507 508 501
451 471 473 453 525 545 547 527 461 472 462 452 535 546 536 526 501 508 509 502
453 473 475 455 527 547 549 529 462 474 463 454 536 548 537 528 502 509 510 503
455 475 477 457 529 549 551 531 463 476 464 456 537 550 538 530 503 510 511 504
465 485 487 467 539 559 561 541 478 486 479 466 552 560 553 540 505 512 513 506
467 487 489 469 541 561 563 543 479 488 480 468 553 562 554 542 506 513 514 507
469 489 491 471 543 563 565 545 480 490 481 470 554 564 555 544 507 514 515 508
471 491 493 473 545 565 567 547 481 492 482 472 555 566 556 546 508 515 516 509
473 493 495 475 547 567 569 549 482 494 483 474 556 568 557 548 509 516 517 510
475 495 497 477 549 569 571 551 483 496 484 476 557 570 558 550 510 517 518 511
519 539 541 521 593 613 615 595 532 540 533 520 606 614 607 594 572 579 580 573
521 541 543 523 595 615 617 597 533 542 534 522 607 616 608 596 573 580 581 574
523 543 545 525 597 617 619 599 534 544 535 524 608 618 609 598 574 581 582 575
525 545 547 527 599 619 621 601 535 546 536 526 609 620 610 600 575 582 583 576
527 547 549 529 601 621 623 603 536 548 537 528 610 622 611 602 576 583 584 577
529 549 551 531 603 623 625 605 537 550 538 530 611 624 612 604 577 584 585 578
539 559 561 541 613 633 635 615 552 560 553 540 626 634 627 614 579 586 587 580
541 561 563 543 615 635 637 617 553 562 554 542 627 636 628 616 580 587 588 581
543 563 565 545 617 637 639 619 554 564 555 544 628 638 629 618 581 588 589 582
545 565 567 547 619 639 641 621 555 566 556 546 629 640 630 620 582 589 590 583
547 567 569 549 621 641 643 623 556 568 557 548 630 642 631 622 583 590 591 584
549 569 571 551 623 643 645 625 557 570 558 550 631 644 632 624 584 591 592 585
:
OTOWER-WATER INTERFACE
1,1,3,77,75,2,55,76,54     G=5,1,2,2,2,2,2,1,2,1
7,75,77,151,149,76,129,150,128          G=5,1,2,2,2,2,2,1,2,1
13,149,151,225,223,150,203,224,202    G=5,1,2,2,2,2,2,1,2,1
19,223,225,299,297,224,277,298,276    G=5,1,2,2,2,2,2,1,2,1
25,297,299,373,371,298,351,372,350    G=5,1,2,2,2,2,2,1,2,1
31,371,373,447,445,372,425,446,424    G=5,1,2,2,2,2,2,1,2,1
37,445,447,521,519,446,499,520,498    G=5,1,2,2,2,2,2,1,2,1
43,519,521,595,593,520,573,594,572    G=5,1,2,2,2,2,2,1,2,1
:
OHYPOTHETICAL CYLINDRICAL SURFACE
1,41,43,117,115,42,69,116,68          G=5,1,2,2,2,2,2,1,2,1
7,115,117,191,189,116,143,190,142     G=5,1,2,2,2,2,2,1,2,1
13,189,191,265,263,190,217,264,216    G=5,1,2,2,2,2,2,1,2,1
19,263,265,339,337,264,291,338,290    G=5,1,2,2,2,2,2,1,2,1
25,337,339,413,411,338,365,412,364    G=5,1,2,2,2,2,2,1,2,1
31,411,413,487,485,412,439,486,438    G=5,1,2,2,2,2,2,1,2,1
37,485,487,561,559,486,513,560,512    G=5,1,2,2,2,2,2,1,2,1
43,559,561,635,633,560,587,634,586    G=5,1,2,2,2,2,2,1,2,1
:
INSIDE WATER DOMAIN
```

```
 N=689   E=112  T=48  W=0.001939
:
INODES:
53   X=10.    Y=0.     Z=0.
1    X=20.0    Y=0.     Z=0.   I=1
9    X=10.     Y=10.    Z=0.    I=1    R=1,9,1,53
13   X=0.      Y=10.    Z=0.    I=1    G=9,13,1
21   X=17.5    Y=0.     Z=0.
25   X=16.0    Y=6.0    Z=0.    G=21,25,1
29   X=10.     Y=7.5    Z=0.    G=25,29,1
33   X=0.      Y=7.5    Z=0.    G=29,33,1
14   M=21,1   L=6,1,2,2
42   X=13.5    Y=3.5    Z=0.
40   X=14.0    Y=0.    Z=0.   G=40,42,1
44   X=10.     Y=4.0   Z=0.   G=42,44,1
48   X=0.0     Y=4.0   Z=0.   G=44,48,1
34   M=40,21  L=1,1,2,2
36   M=42,27  L=3,1,2,2
57   X=0.      Y=0.    Z=0.   G=53,57,1
49   M=53,40
50   M=53,44  L=2,1,2,2
685   X=5.    Y=0.     Z=80.
633   X=10.0    Y=0.     Z=80.   I=1
641   X=5.     Y=5.    Z=80.    I=1    R=633,641,1,685
645   X=0.      Y=5.    Z=80.    I=1    G=641,645,1
653   X=8.75    Y=0.     Z=80.
657   X=8.0     Y=3.0    Z=80.    G=653,657,1
661   X=5.      Y=3.75   Z=80.    G=657,661,1
665   X=0.      Y=3.75   Z=80.     G=661,665,1
646   M=653,633   L=6,1,2,2
674   X=6.75    Y=1.75    Z=80.
672   X=7.0     Y=0.    Z=80.    G=672,674,1
676   X=5.0     Y=2.0   Z=80.    G=674,676,1
680   X=0.0     Y=2.0   Z=80.    G=676,680,1
666   M=672,653  L=1,1,2,2
668   M=674,659  L=3,1,2,2
689   X=0.      Y=0.    Z=80.    G=685,689,1
681   M=685,672
682   M=685,676  L=2,1,2,2
1    X=20.0    Y=0.     Z=0.    I=1     G=1,633,79
1    X=20.0    Y=0.     Z=0.    I=1     G=2,634,79
1    X=20.0    Y=0.     Z=0.    I=1     G=3,635,79
1    X=20.0    Y=0.     Z=0.    I=1     G=4,636,79
1    X=20.0    Y=0.     Z=0.    I=1     G=5,637,79
1    X=20.0    Y=0.     Z=0.    I=1     G=6,638,79
1    X=20.0    Y=0.     Z=0.    I=1     G=7,639,79
1    X=20.0    Y=0.     Z=0.    I=1     G=8,640,79
1    X=20.0    Y=0.     Z=0.    I=1     G=9,641,79
1    X=20.0    Y=0.     Z=0.    I=1     G=10,642,79
1    X=20.0    Y=0.     Z=0.    I=1     G=11,643,79
1    X=20.0    Y=0.     Z=0.    I=1     G=12,644,79
1    X=20.0    Y=0.     Z=0.    I=1     G=13,645,79
21   X=17.5    Y=0.     Z=0.    G=14,646,79
21   X=17.5    Y=0.     Z=0.    G=15,647,79
21   X=17.5    Y=0.     Z=0.    G=16,648,79
21   X=17.5    Y=0.     Z=0.    G=17,649,79
21   X=17.5    Y=0.     Z=0.    G=18,650,79
21   X=17.5    Y=0.     Z=0.    G=19,651,79
21   X=17.5    Y=0.     Z=0.    G=20,652,79
21   X=17.5    Y=0.     Z=0.    G=21,653,79
21   X=17.5    Y=0.     Z=0.    G=22,654,79
21   X=17.5    Y=0.     Z=0.    G=23,655,79
21   X=17.5    Y=0.     Z=0.    G=24,656,79
21   X=17.5    Y=0.     Z=0.    G=25,657,79
21   X=17.5    Y=0.     Z=0.    G=26,658,79
21   X=17.5    Y=0.     Z=0.    G=27,659,79
21   X=17.5    Y=0.     Z=0.    G=28,660,79
21   X=17.5    Y=0.     Z=0.    G=29,661,79
21   X=17.5    Y=0.     Z=0.    G=30,662,79
21   X=17.5    Y=0.     Z=0.    G=31,663,79
21   X=17.5    Y=0.     Z=0.    G=32,664,79
21   X=17.5    Y=0.     Z=0.    G=33,665,79
21   X=17.5    Y=0.     Z=0.    G=34,666,79
21   X=17.5    Y=0.     Z=0.    G=35,667,79
21   X=17.5    Y=0.     Z=0.    G=36,668,79
21   X=17.5    Y=0.     Z=0.    G=37,669,79
21   X=17.5    Y=0.     Z=0.    G=38,670,79
21   X=17.5    Y=0.     Z=0.    G=39,671,79
21   X=17.5    Y=0.     Z=0.    G=40,672,79
21   X=17.5    Y=0.     Z=0.    G=41,673,79
21   X=17.5    Y=0.     Z=0.    G=42,674,79
21   X=17.5    Y=0.     Z=0.    G=43,675,79
21   X=17.5    Y=0.     Z=0.    G=44,676,79
21   X=17.5    Y=0.     Z=0.    G=45,677,79
21   X=17.5    Y=0.     Z=0.    G=46,678,79
21   X=17.5    Y=0.     Z=0.    G=47,679,79
21   X=17.5    Y=0.     Z=0.    G=48,680,79
21   X=17.5    Y=0.     Z=0.    G=49,681,79
21   X=17.5    Y=0.     Z=0.    G=50,682,79
21   X=17.5    Y=0.     Z=0.    G=51,683,79
21   X=17.5    Y=0.     Z=0.    G=52,684,79
21   X=17.5    Y=0.     Z=0.    G=53,685,79
21   X=17.5    Y=0.     Z=0.    G=54,686,79
21   X=17.5    Y=0.     Z=0.    G=55,687,79
21   X=17.5    Y=0.     Z=0.    G=56,688,79
21   X=17.5    Y=0.     Z=0.    G=57,689,79
58   M=1,80      L=6,1,2,2    I=1
65   M=21,100    L=6,1,2,2
72   M=40,119    L=4,1,2,2
77   M=53,132    L=2,1,2,2
137  M=80,159    L=6,1,2,2    I=1
144  M=100,179   L=6,1,2,2
151  M=119,198   L=4,1,2,2
156  M=132,211   L=2,1,2,2
216  M=159,238   L=6,1,2,2    I=1
223  M=179,258   L=6,1,2,2
230  M=198,277   L=4,1,2,2
235  M=211,290   L=2,1,2,2
295  M=238,317   L=6,1,2,2    I=1
302  M=258,337   L=6,1,2,2
309  M=277,356   L=4,1,2,2
314  M=290,369   L=2,1,2,2
374  M=317,396    L=6,1,2,2    I=1
381  M=337,416    L=6,1,2,2
388  M=356,435    L=4,1,2,2
393  M=369,448    L=2,1,2,2
453  M=396,475    L=6,1,2,2    I=1
460  M=416,495    L=6,1,2,2
467  M=435,514    L=4,1,2,2
472  M=448,527    L=2,1,2,2
532  M=475,554    L=6,1,2,2    I=1
539  M=495,574    L=6,1,2,2
546  M=514,593    L=4,1,2,2
551  M=527,606    L=2,1,2,2
611  M=554,633    L=6,1,2,2    I=1
618  M=574,653    L=6,1,2,2
625  M=593,672    L=4,1,2,2
630  M=606,685    L=2,1,2,2
```

```
:
IELEMENTS
   1  21  23   3  80 100 102  82  14  22  15   2  93 101  94  81  58  65  66  59
   3  23  25   5  82 102 104  84  15  24  16   4  94 103  95  83  59  66  67  60
   5  25  27   7  84 104 106  86  16  26  17   6  95 105  96  85  60  67  68  61
   7  27  29   9  86 106 108  88  17  28  18   8  96 107  97  87  61  68  69  62
   9  29  31  11  88 108 110  90  18  30  19  10  97 109  98  89  62  69  70  63
  11  31  33  13  90 110 112  92  19  32  20  12  98 111  99  91  63  70  71  64
  21  40  42  23 100 119 121 102  34  41  35  22 113 120 114 101  65  72  73  66
  23  42  27  25 102 121 106 104  35  36  26  24 114 115 105 103  66  73  68  67
  27  42  44  29 106 121 123 108  36  43  37  28 115 122 116 107  68  73  74  69
  29  44  46  31 108 123 125 110  37  45  38  30 116 124 117 109  69  74  75  70
  31  46  48  33 110 125 127 112  38  47  39  32 117 126 118 111  70  75  76  71
  42  40  53  44 121 119 132 123  41  49  50  43 120 128 129 122  73  72  77  74
  44  53  55  46 123 132 134 125  50  54  51  45 129 133 130 124  74  77  78  75
  46  55  57  48 125 134 136 127  51  56  52  47 130 135 131 126  75  78  79  76
  80 100 102  82 159 179 181 161  93 101  94  81 172 180 173 160 137 144 145 138
  82 102 104  84 161 181 183 163  94 103  95  83 173 182 174 162 138 145 146 139
  84 104 106  86 163 183 185 165  95 105  96  85 174 184 175 164 139 146 147 140
  86 106 108  88 165 185 187 167  96 107  97  87 175 186 176 166 140 147 148 141
  88 108 110  90 167 187 189 169  97 109  98  89 176 188 177 168 141 148 149 142
  90 110 112  92 169 189 191 171  98 111  99  91 177 190 178 170 142 149 150 143
 100 119 121 102 179 198 200 181 113 120 114 101 192 199 193 180 144 151 152 145
 102 121 106 104 181 200 185 183 114 115 105 103 193 194 184 182 145 152 147 146
 106 121 123 108 185 200 202 187 115 122 116 107 194 201 195 186 147 152 153 148
 108 123 125 110 187 202 204 189 116 124 117 109 195 203 196 188 148 153 154 149
 110 125 127 112 189 204 206 191 117 126 118 111 196 205 197 190 149 154 155 150
 121 119 132 123 200 198 211 202 120 128 129 122 199 207 208 201 152 151 156 153
 123 132 134 125 202 211 213 204 129 133 130 124 208 212 209 203 153 156 157 154
 125 134 136 127 204 213 215 206 130 135 131 126 209 214 210 205 154 157 158 155
 159 179 181 161 238 258 260 240 172 180 173 160 251 259 252 239 216 223 224 217
 161 181 183 163 240 260 262 242 173 182 174 162 252 261 253 241 217 224 225 218
 163 183 185 165 242 262 264 244 174 184 175 164 253 263 254 243 218 225 226 219
 165 185 187 167 244 264 266 246 175 186 176 166 254 265 255 245 219 226 227 220
 167 187 189 169 246 266 268 248 176 188 177 168 255 267 256 247 220 227 228 221
 169 189 191 171 248 268 270 250 177 190 178 170 256 269 257 249 221 228 229 222
 179 198 200 181 258 277 279 260 192 199 193 180 271 278 272 259 223 230 231 224
 181 200 185 183 260 279 264 262 193 194 184 182 272 273 263 261 224 231 226 225
 185 200 202 187 264 279 281 266 194 201 195 186 273 280 274 265 226 231 232 227
 187 202 204 189 266 281 283 268 195 203 196 188 274 282 275 267 227 232 233 228
 189 204 206 191 268 283 285 270 196 205 197 190 275 284 276 269 228 233 234 229
 200 198 211 202 279 277 290 281 199 207 208 201 278 286 287 280 231 230 235 232
 202 211 213 204 281 290 292 283 208 212 209 203 287 291 288 282 232 235 236 233
 204 213 215 206 283 292 294 285 209 214 210 205 288 293 289 284 233 236 237 234
 238 258 260 240 317 337 339 319 251 259 252 239 330 338 331 318 295 302 303 296
 240 260 262 242 319 339 341 321 252 261 253 241 331 340 332 320 296 303 304 297
 242 262 264 244 321 341 343 323 253 263 254 243 332 342 333 322 297 304 305 298
 244 264 266 246 323 343 345 325 254 265 255 245 333 344 334 324 298 305 306 299
 246 266 268 248 325 345 347 327 255 267 256 247 334 346 335 326 299 306 307 300
 248 268 270 250 327 347 349 329 256 269 257 249 335 348 336 328 300 307 308 301
 258 277 279 260 337 356 358 339 271 278 272 259 350 357 351 338 302 309 310 303
 260 279 264 262 339 358 343 341 272 273 263 261 351 352 342 340 303 310 305 304
 264 279 281 266 343 358 360 345 273 280 274 265 352 359 353 344 305 310 311 306
 266 281 283 268 345 360 362 347 274 282 275 267 353 361 354 346 306 311 312 307
 268 283 285 270 347 362 364 349 275 284 276 269 354 363 355 348 307 312 313 308
 279 277 290 281 358 356 369 360 278 286 287 280 357 365 366 359 310 309 314 311
 281 290 292 283 360 369 371 362 287 291 288 282 366 370 367 361 311 314 315 312
 283 292 294 285 362 371 373 364 288 293 289 284 367 372 368 363 312 315 316 313
 317 337 339 319 396 416 418 398 330 338 331 318 409 417 410 397 374 381 382 375
 319 339 341 321 398 418 420 400 331 340 332 320 410 419 411 399 375 382 383 376
 321 341 343 323 400 420 422 402 332 342 333 322 411 421 412 401 376 383 384 377
 323 343 345 325 402 422 424 404 333 344 334 324 412 423 413 403 377 384 385 378
 325 345 347 327 404 424 426 406 334 346 335 326 413 425 414 405 378 385 386 379
 327 347 349 329 406 426 428 408 335 348 336 328 414 427 415 407 379 386 387 380
 337 356 358 339 416 435 437 418 350 357 351 338 429 436 430 417 381 388 389 382
 339 358 343 341 418 437 422 420 351 352 342 340 430 431 421 419 382 389 384 383
 343 358 360 345 422 437 439 424 352 359 353 344 431 438 432 423 384 389 390 385
 345 360 362 347 424 439 441 426 353 361 354 346 432 440 433 425 385 390 391 386
 347 362 364 349 426 441 443 428 354 363 355 348 433 442 434 427 386 391 392 387
 358 356 369 360 437 435 448 439 357 365 366 359 436 444 445 438 389 388 393 390
 360 369 371 362 439 448 450 441 366 370 367 361 445 449 446 440 390 393 394 391
 362 371 373 364 441 450 452 443 367 372 368 363 446 451 447 442 391 394 395 392
 396 416 418 398 475 495 497 477 409 417 410 397 488 496 489 476 453 460 461 454
 398 418 420 400 477 497 499 479 410 419 411 399 489 498 490 478 454 461 462 455
 400 420 422 402 479 499 501 481 411 421 412 401 490 500 491 480 455 462 463 456
 402 422 424 404 481 501 503 483 412 423 413 403 491 502 492 482 456 463 464 457
 404 424 426 406 483 503 505 485 413 425 414 405 492 504 493 484 457 464 465 458
 406 426 428 408 485 505 507 487 414 427 415 407 493 506 494 486 458 465 466 459
 416 435 437 418 495 514 516 497 429 436 430 417 508 515 509 496 460 467 468 461
 418 437 422 420 497 516 501 499 430 431 421 419 509 510 500 498 461 468 463 462
 422 437 439 424 501 516 518 503 431 438 432 423 510 517 511 502 463 468 469 464
 424 439 441 426 503 518 520 505 432 440 433 425 511 519 512 504 464 469 470 465
 426 441 443 428 505 520 522 507 433 442 434 427 512 521 513 506 465 470 471 466
 437 435 448 439 516 514 527 518 436 444 445 438 515 523 524 517 468 467 472 469
 439 448 450 441 518 527 529 520 445 449 446 440 524 528 525 519 469 472 473 470
 441 450 452 443 520 529 531 522 446 451 447 442 525 530 526 521 470 473 474 471
 475 495 497 477 554 574 576 556 488 496 489 476 567 575 568 555 532 539 540 533
 477 497 499 479 556 576 578 558 489 498 490 478 568 577 569 557 533 540 541 534
 479 499 501 481 558 578 580 560 490 500 491 480 569 579 570 559 534 541 542 535
 481 501 503 483 560 580 582 562 491 502 492 482 570 581 571 561 535 542 543 536
 483 503 505 485 562 582 584 564 492 504 493 484 571 583 572 563 536 543 544 537
 485 505 507 487 564 584 586 566 493 506 494 486 572 585 573 565 537 544 545 538
 495 514 516 497 574 593 595 576 508 515 509 496 587 594 588 575 539 546 547 540
 497 516 501 499 576 595 580 578 509 510 500 498 588 589 579 577 540 547 542 541
 501 516 518 503 580 595 597 582 510 517 511 502 589 596 590 581 542 547 548 543
 503 518 520 505 582 597 599 584 511 519 512 504 590 598 591 583 543 548 549 544
 505 520 522 507 584 599 601 586 512 521 513 506 591 600 592 585 544 549 550 545
 516 514 527 518 595 593 606 597 515 523 524 517 594 602 603 596 547 546 551 548
 518 527 529 520 597 606 608 599 524 528 525 519 603 607 604 598 548 551 552 549
 520 529 531 522 599 608 610 601 525 530 526 521 604 609 605 600 549 552 553 550
 554 574 576 556 633 653 655 635 567 575 568 555 646 654 647 634 611 618 619 612
 556 576 578 558 635 655 657 637 568 577 569 557 647 656 648 636 612 619 620 613
 558 578 580 560 637 657 659 639 569 579 570 559 648 658 649 638 613 620 621 614
 560 580 582 562 639 659 661 641 570 581 571 561 649 660 650 640 614 621 622 615
 562 582 584 564 641 661 663 643 571 583 572 563 650 662 651 642 615 622 623 616
 564 584 586 566 643 663 665 645 572 585 573 565 651 664 652 644 616 623 624 617
 574 593 595 576 653 672 674 655 587 594 588 575 666 673 667 654 618 625 626 619
 576 595 580 578 655 674 659 657 588 589 579 577 667 668 658 656 619 626 621 620
 580 595 597 582 659 674 676 661 589 596 590 581 668 675 669 660 621 626 627 622
 582 597 599 584 661 676 678 663 590 598 591 583 669 677 670 662 622 627 628 623
 584 599 601 586 663 678 680 665 591 600 592 585 670 679 671 664 623 628 629 624
 595 593 606 597 674 672 685 676 594 602 603 596 673 681 682 675 626 625 630 627
 597 606 608 599 676 685 687 678 603 607 604 598 682 686 683 677 627 630 631 628
 599 608 610 601 678 687 689 680 604 609 605 600 683 688 684 679 628 631 632 629
:
ITOWER-WATER INTERFACE
1,1,3,82,80,2,59,81,58    G=5,1,2,2,2,2,2,1,2,1
7,80,82,161,159,81,138,160,137        G=5,1,2,2,2,2,2,1,2,1
13,159,161,240,238,160,217,239,216    G=5,1,2,2,2,2,2,1,2,1
19,238,240,319,317,239,296,318,295    G=5,1,2,2,2,2,2,1,2,1
25,317,319,398,396,318,375,397,374    G=5,1,2,2,2,2,2,1,2,1
31,396,398,477,475,397,454,476,453    G=5,1,2,2,2,2,2,1,2,1
37,475,477,556,554,476,533,555,532    G=5,1,2,2,2,2,2,1,2,1
43,554,556,635,633,555,612,634,611    G=5,1,2,2,2,2,2,1,2,1
:
FOUNDATION-SOIL SYSTEM
 M=0.  I=0.  R=29.5,29.5  C=1000.  P=1./3.  W=0.005127  D=0.10
:
```

```
GROUND MOTION
 N=1000   M=11  T=0.02   S=32.18
C.........GROUND MOTION COMPONENET ALONG X-AXIS; TAFT S69E
  -.00632  -.00194   .00408   .01010   .00530  -.00031  -.00428  -.00286
   .00122   .00541   .00398  -.00306  -.00867  -.00867  -.00612  -.00082
  -.00031  -.00020   .00408   .01071   .01163   .00663   .00449   .00235
   .00214   .00194  -.00398  -.00755  -.00112   .00592   .00286  -.01040
  -.01153  -.00479   .00500   .00102  -.00408  -.00255   .00592   .00734
  -.00663  -.01091   .00326   .01724   .01010  -.00490  -.00663   .00367
   .00459  -.00286   .00357   .01459   .02325   .01816   .01867   .01255
  -.00133  -.00867  -.00683  -.00479   .00408   .00561  -.00143  -.00408
  -.00010  -.00224  -.00867  -.01132  -.01530  -.01877  -.01601  -.00806
  -.00031   .00826   .00428  -.00785  -.01836  -.01163   .00092   .01071
   .00867   .00755   .00898   .00979   .00163  -.00530  -.00082   .00683
   .01714   .01989   .01377   .00510   .00316   .01193   .02387   .02417
   .00632  -.00694  -.01142  -.00867  -.00388   .00224   .00235  -.01612
  -.02652  -.00918   .01632   .02234   .01703   .02142   .02478   .01877
   .00428  -.01061  -.02387  -.00898   .01418   .03692   .03090   .01601
   .01153   .00734  -.00806  -.01346  -.01275  -.00775   .00683   .02264
   .02295   .01989   .02591   .02366   .01204  -.00102  -.00867  -.01142
  -.01459  -.02081  -.01999  -.01693  -.01856  -.01785  -.00898  -.00153
  -.00500  -.00530  -.00408  -.00928  -.00796  -.00214   .00347  -.00510
  -.02223  -.03631  -.03264  -.02448  -.03284  -.04926  -.05783  -.06211
  -.07221  -.06640  -.05457  -.05263  -.04977  -.05079  -.05283  -.05722
  -.04906  -.03539  -.02601  -.01724  -.01479  -.02611  -.04029  -.04590
  -.04406  -.02407   .00337   .03274   .05569   .07588   .09424   .12056
   .14932   .17941   .16391   .11954   .06946   .01877  -.03509  -.06528
  -.06232  -.05640  -.04600  -.04773  -.05640  -.06599  -.05742  -.03774
  -.01652   .00469   .00469  -.00877  -.02274  -.04029  -.04671  -.02142
   .01367   .05079   .08506   .06885   .03733  -.00153  -.00153   .03060
   .06650   .07639   .07068   .06303   .03417   .00326  -.03233  -.04569
  -.04498  -.01663   .03570   .09394   .12352   .08384   .03417  -.02203
  -.03774  -.05406  -.05651  -.03733  -.01459   .01112   .03488   .06211
   .06956   .04651   .02142   .00051  -.03182  -.08639  -.11342  -.08853
  -.05100  -.00979   .03141   .03998   .02815   .01122   .00510   .00061
  -.01877  -.04049  -.05263  -.04263  -.02907  -.01826  -.02764  -.04110
  -.05753  -.06823  -.04641  -.01530   .01928   .05314   .08843   .11097
   .11423   .10475   .08965   .06324   .02774  -.00847  -.04396  -.05069
  -.04192  -.03743  -.04814  -.06273  -.07854  -.09302  -.07405  -.03560
   .00714   .04314   .03050   .00194  -.01520   .00755   .03682   .07313
   .09057   .06405   .02988  -.01193  -.02172   .00459   .02438   .03284
   .04192   .03682   .02336   .00806  -.00673  -.01540  -.01499   .00092
   .02937   .03294   .01652  -.00694  -.00214   .03427   .07619   .09577
   .07323   .06324   .03243  -.00796  -.05253  -.09669  -.13963  -.14932
  -.14616  -.14116  -.13657  -.13678  -.13698  -.11117  -.07762  -.04172
  -.00530   .03029   .06823   .08476   .05875   .02937  -.00949  -.02254
  -.00877   .00887   .02846   .04916   .05620   .03692   .01438  -.01173
  -.03672  -.05997  -.05202  -.03325  -.01163   .01071   .03243   .05508
   .07619   .10057   .10301   .07078   .03509  -.00683  -.03264  -.01285
   .00092  -.01581  -.03957  -.05926  -.03866  -.01683  -.02254  -.03988
  -.03886  -.01387   .01193   .04223   .06915   .10006   .11250   .10873
   .10138   .09853   .10342   .10414   .07425   .03641  -.00581  -.04559
  -.09067  -.09700  -.04172  -.01581  -.03692  -.06946  -.08353  -.04549
  -.03713  -.02060   .02234   .06783   .08496   .05671   .01377  -.03060
  -.07782  -.08027  -.04386  -.00745  -.00357  -.01499  -.01397  -.01010
  -.01397  -.02234  -.00755   .01734   .04437   .03866   .00938  -.01846
  -.03723  -.05345  -.07313  -.08945  -.08976  -.06028  -.01469   .03784
   .06364   .05436   .04223   .03060   .03019   .02376   .01387   .01408
   .03182   .05508   .06324   .04396   .02152  -.00418  -.02886  -.03274
  -.01459   .00265   .02927   .06354   .10658   .11423   .08496   .05008
   .00928  -.03131  -.07191  -.11148  -.10495  -.06568  -.03396  -.01795
   .01275   .04926   .09241   .10301   .07956   .05161   .02570   .01469
   .00571  -.00204  -.01550  -.02988  -.04559  -.05742  -.04835  -.03254
  -.02162  -.02733  -.01561   .01499   .04906   .07721   .06762   .05253
   .04243   .03182   .00265  -.02958  -.04896  -.06609  -.07160  -.05936
  -.04631  -.02876  -.02529  -.04029  -.06028  -.06772  -.04784  -.02438
   .00000  -.01000  -.03519  -.05120  -.02703   .00377   .04284   .05691
   .03488   .00683  -.02172  -.01693  -.00479  -.01163  -.02958  -.02295
  -.00122   .01489   .01000   .00082  -.00938  -.00347   .00653   .01540
   .01622   .02458   .03519   .04875   .05406   .04192   .02693   .02744
   .03131   .02458   .00836   .00663   .02580   .04518   .04110   .02489
   .02264   .03060   .03447   .02060   .00337  -.01693  -.03376  -.04926
  -.06364  -.08598  -.08302  -.05151  -.01601   .02101   .06099   .07099
   .03458  -.00337  -.05120  -.06987  -.06650  -.05875  -.03396  -.00734
   .02285   .04335   .05375   .05987   .04019   .01244  -.01428  -.02478
  -.02132  -.00979   .00153  -.00082   .00000   .01285   .02540   .04049
   .03478   .01510  -.00714  -.03029  -.05273  -.05661  -.05059  -.05100
  -.05528  -.04845  -.02693  -.00510   .02050   .03315   .03580   .03243
   .02682   .02091   .01408   .01081   .02376   .04223   .05314   .03570
   .01295  -.01306  -.02846  -.03876  -.04835  -.05151  -.03866  -.02264
  -.00826  -.01112  -.01765  -.02591  -.01673   .00694   .03111   .05651
   .04284   .00938  -.03009  -.04590  -.03651  -.02682  -.01581  -.00133
   .01642   .02336   .01897   .02580   .03641   .04549   .04518   .04202
   .02652   .00714  -.01520  -.02774  -.02672  -.02591  -.03274  -.04161
  -.03417  -.01979  -.00357   .01285   .02917   .03886   .04080   .03651
   .03009   .02438   .03478   .04835   .02784  -.00245  -.03713  -.06701
  -.08292  -.09333  -.10546  -.09955  -.06966  -.03662  -.00163   .03458
   .05477   .04345   .02856   .00908  -.00867  -.02540  -.01499   .00153
   .02203   .02621   .01714   .00643  -.00571  -.00745  -.00245   .00061
   .00520   .00949   .01357   .01224   .01581   .03264   .04243   .02856
   .01091  -.01112  -.01948  -.01408  -.00826  -.00571   .00031   .01295
   .02835   .03090   .00275  -.02886  -.06640  -.07762  -.06589  -.05090
  -.04141  -.03600  -.01499   .00439   .01632   .01030  -.00602  -.00979
  -.00306   .00745   .00357  -.01214  -.01805  -.02529  -.03345  -.03631
  -.03386  -.03213  -.02754  -.01040   .00979   .03162   .04314   .04559
   .04631   .03998   .03539   .04223   .05447   .05559   .04641   .03009
   .00357  -.02274  -.05171  -.07374  -.07109  -.06069  -.04896  -.03284
  -.01071   .01234   .03611   .05814   .05916   .05090   .04070   .02999
   .01938   .00877   .00275   .00122  -.00867  -.01734  -.02489  -.02733
  -.02050  -.01336  -.02030  -.03366  -.05090  -.04121  -.01540   .01295
   .04100   .03998   .02387   .00775  -.00367  -.01234  -.02183  -.01642
   .00418   .02550   .04957   .06477   .07109   .07721   .07476   .05793
   .03917   .01856  -.00163  -.02009  -.01448  -.00265   .01265   .02305
   .01938   .01153   .00785   .00082  -.01561  -.03284  -.05273  -.06242
  -.04896  -.03029  -.01244  -.00694  -.00061   .00418   .00612   .00826
   .01193   .01550   .02172   .02591   .02815   .02693   .01989   .01326
   .00949   .00133  -.00938  -.02009  -.02948  -.03315  -.02642  -.01795
  -.01071  -.00643   .00255   .01377   .02132   .01275   .00020  -.01071
  -.01397  -.01724  -.02223  -.03182  -.02937  -.01795  -.00632  -.00877
  -.01581  -.02285  -.02009  -.01510  -.00867  -.00275   .00388   .00918
   .00959   .00714   .01000   .01469   .02070   .01765   .00683  -.00347
   .00428   .02285   .04223   .06222   .05895   .04314   .02468   .00561
  -.01316  -.01968  -.01775  -.01805  -.02213  -.02366  -.02081  -.02019
  -.02560  -.02805  -.02733  -.02744  -.03162  -.01724   .00204   .02540
   .03927   .04212   .03488   .01958   .00357  -.00306  -.00082   .00092
  -.00418  -.01204  -.00796   .00173   .01244   .01244   .00755   .01102
   .01652   .02193   .02682   .03203   .03437   .02356   .00918  -.00571
  -.01234  -.01703  -.01877  -.01642  -.01387  -.01010  -.01102  -.01591
  -.02223  -.02254  -.01469  -.00643   .00224   .00031  -.00581  -.01316
  -.01928  -.01142   .00173   .01091   .01958   .03192   .04580   .05528
   .05202   .04294   .02438   .00418  -.01703  -.03662  -.03274  -.01663
   .00173   .01795   .01295   .00265  -.01030  -.01754  -.01989  -.02417
  -.03315  -.03651  -.02234  -.00235   .01805   .03957   .03682   .01693
  -.00653  -.02295  -.02693  -.02764  -.02295  -.01459   .00051   .01632
   .03427   .03988   .03172   .02570   .02244   .01836   .01193   .00581
   .00479   .00796   .00806   .00510   .00255  -.00041  -.00500  -.01153
  -.01336  -.00826  -.00500  -.00296   .00224   .01122   .01061   .00449
  -.00296  -.01091  -.01724  -.01418  -.00765  -.00643  -.01754  -.02642
```

```
:
OUTPUT
 D=9   N=1,2   :
 S=9   N=1,2     :
 M=9   L=1,3,5,7,9,11,13,15,17:
 H=1    L=25
:
```